

New Strategies for Stereoselective Preparation of Densely Functionalized Cyclobutanes

Xinyu Yang

A dissertation
submitted to the Faculty of
the department of Chemistry
in partial fulfillment
of the requirements for the degree of
Doctor of Philosophy

Boston College
Morrissey College of Arts and Sciences
Graduate School

June 2022

New Strategies for Stereoselective Preparation of Densely Functionalized Cyclobutanes

Xinyu Yang

Advisor: Professor Shih-Yuan Liu

Abstract: This dissertation describes the utility of 1,2-azaborine motif as a 4C+1B+1N synthon in organic synthesis, especially for the preparation of densely-functionalized cyclobutanes based on the framework of the 1,2-azaborine photoisomerization. The substitution of a CC unit with a BN unit in benzenes significantly modifies the properties of classic benzenoid compounds, leading to new reactivities and functionalities. In this vein, Chapter 1 discloses photoisomerization of 1,2-azaborines to selectively form BN-analogues of the Dewar benzene. Three applications of the Dewar photoisomers are described herein: 1) a rhodium-catalyzed ring-opening reaction to form 1,2-azaborines; 2) furnishing *cis* aminoborylated cyclobutanes with the boron unit as a further functionalization handle; 3) a stereospecific ring-opening reaction to afford diene which can engage in Diels-Alder reaction. Chapter 2 elaborates on a modular and stereoselective strategy to access a variety of cyclobutane β -amino alcohols. Discussed herein are regioselective functionalizations and di-functionalizations of the 1,2-azaborine core and a tandem photoisomerization-hydrogenation-oxidation protocol to translate the functionalized azaborine core to cyclobutane amino alcohols. Also examined herein are the scope of azaborine photoisomerization and Dewar hydrogenation.

ACKNOWLEDGEMENTS

First of all, I would like to express my deepest appreciation to my research supervisor, Prof. Shih-Yuan Liu, for his continuous guidance and support during my graduate study at Boston College. Prof. Liu is a great research supervisor: his broad chemistry knowledge, critical thinking, meticulous attitude and creative ideas benefit me a lot over the course of my PhD study. Prof. Liu is also a passionate teacher who loves to share his passion of chemistry and knowledge to his students: I learn new knowledge from every single group meeting, and I know that the knowledge I have acquired will serve me well in the future.

I would like to thank Prof. James P. Morken and Prof. Masayuki Wasa for serving as my oral committee and thesis committee, offering invaluable insights and constructive advice. I am also deeply grateful to Prof. Morken and Prof. Wasa for their support and help in my job-hunting process. Prof. X. Peter Zhang's synthesis course and organometallic course as well as Prof. Wasa's mechanistic organic chemistry course were foundational to my graduate study.

I am grateful to all of those with whom I have had the pleasure to work for the past five years at Boston college. I appreciate the mentorship and helpful discussions from Dr. Zachary X. Giustra. The completion of my dissertation would not have been possible without the collaborative work with my fellow colleagues Zachary X. Giustra, Tomoya Ozaki, Nicole Wei, and Prof. Holger F. Bettinger group. My sincere thanks also go to Jacob Ishibashi, Cameron McConnell, Yuanzhe Zhang, Ricky Alvarado, Ziyong Wang, Kevin Byrne, Jiangpeng Liu, and the rest of the Liu group for the stimulating discussions and their love and support that make my graduate research enjoyable.

My research at BC would be impossible without the instrumentation and administration support from the department and university. I greatly appreciate Dr. Bo Li, Dr. Thusitha Jayasundera (TJ), Dr. Jing Jin, Marek Domin, Dale Mahoney, Lynne Houlihan, and Dr. Ian Parr, whose commitment and contribution is crucial for my graduate research.

During the course of my graduate study, I am blessed to get to know a group of amazing people. Specials thanks to Min Cao, Jessica Chan, Yejin Chang, Ahmet Yesilcimen, Chenlong Zhang, Yan Meng, Yong Wang, Xavier Riart-Ferrer, Xin Wen, Arghya Deb, Connie Zhang, Yuebiao Zhou, Chaochen Zhang, Yucheng Mu, Ellen Wang, Jia Li for their support and encouragement.

Finally, I offer my earnest and heartfelt thanks to my family, especially my parents, Yujing Zhu and Aichun Yang for their unconditional love and support, my grandparents, whom I look up to the most, and my wife, Xiaoxu Wang for walking beside me each step of the way on this long and meaningful journey.

LIST OF ABBREVIATIONS

Ac: acetyl	Cy: cyclohexyl
AIBN: 1,1'-azobisisobutyronitrile	DART: direct analysis in real time
aq: aqueous	dba: dibenzylideneacetone
Ar: aryl	DBU: 1,8-diazabicyclo[5.4.0]undec-7-
atm: atmosphere	ene
azaborine: monocyclic 1,2-dihydro-1,2-azaborine	DDQ: 2,3-dichloro-5,6-dicyano-1,4-benzoquinone
B ₂ pin ₂ : bispinacolatodiboron	DEA: diethanolamine
BDE: bond dissociation energy	dFbpy: difluoro-2,2'-bipyridyl
BINAP: 2,2'-bis(diphenylphosphino)-1,1'-binaphthyl	dFCF ₃ ppy: 2-(2,4-difluorophenyl)-5-(trifluoromethyl)pyridine
Bn: benzyl	DFT: density functional theory
Boc: <i>tert</i> -butyloxycarbonyl	DMF: <i>N,N</i> -dimethylformamide
bp: boiling point	DMSO: dimethylsulfoxide
Bu: <i>n</i> -butyl	DIPEA: <i>N,N</i> -diisopropylethylamine
Bz: benzoyl	DPPF: bis(diphenylphosphino)ferrocene
CAM: Cerium ammonium molybdate	dr: diastereomeric ratio
cod: 1,5-cyclooctadiene	dtbbpy: di- <i>tert</i> -butyl-2,2'-bipyridyl
Cp: cyclopentadienyl	<i>E_a</i> : activation energy
Cp*: pentamethylcyclopentadienyl	ee: enantiomeric excess
CV: cyclic voltammetry	<i>E_{ox}</i> : oxidation potential
	equiv.: equivalents

er: enantiomeric ratio
Et: ethyl
E_{red}: reduction potential
ESI: electrospray ionization
ESP: electrostatic potential
eV: electron volts
FT: Fourier transform
h: hour(s)
Het: hetero
HOMO: highest occupied molecular orbital
HPLC: high-performance liquid chromatography
HRMS: high resolution mass spectrometry
HRMS: high-resolution mass spectrometry
ID: inner diameter
ⁱPr: isopropyl
IR: infrared
KHMDS: Potassium bis(trimethylsilyl) amide
LDA: Lithium diisopropylamide
LED: light emitting diode
LUMO: lowest unoccupied molecular orbital
MAS: magic angle spinning
m-CPBA: meta-Chloroperoxybenzoic acid
Me: methyl
Mes: mesityl
mesityl: 2,4,6-trimethylphenyl
MIDA: *N*-methyliminodiacetic acid
mp: melting point
MS: molecular sieves
MTBE: methyl *tert*-butyl ether
ⁿBu: *n*-butyl
nbd: norbornadiene
NBS: *N*-bromosuccinimide
nd: not determined
NHC: *N*-heterocyclic carbene
NMO: *N*-methylmorpholine
NMR: nuclear magnetic resonance
OMe: methoxyl
Ph: phenyl
PG: protecting group

pin: pinacol

PMA: phosphomolybdic acid

PMB: *para*-methoxybenzyl

PPh₃: triphenylphosphosphine

ppm: parts per million

Pr: *n*-propyl

psi: pounds per square inch

p-tol: *para*-tolyl

pyr: pyridine

RCM: ring closing metathesis

Red-Al: Sodium bis(2-methoxyethoxy)aluminium hydride

RSE: resonance stabilization energy

RT: room temperature

S_EAr: electrophilic aromatic substitution

S_NAr: nucleophilic aromatic substitution

*t*_{1/2}: half-life

^tAm: tert-amyl

TBAF: tetra(*n*-butyl)ammonium fluoride

TBS: *tert*-butyldimethylsilyl

TBSCl: *tert*-butyldimethylsilyl chloride

TMSCl: trimethylsilyl chloride

^tBu: *tert*-butyl

THF: tetrahydrofuran

Ts: *para*-toluenesulfonyl

UV: ultraviolet

UV-PES: ultra violet photoelectron spectroscopy

TABLE OF CONTENTS

Chapter 1: Photoisomerization of 1,2-Azaborines: Energy Storage and Synthetic Applications

1.1 Introduction.....	1
1.1.1 1,2-Azaborines: Synthesis and Properties.....	2
1.1.2 Photoisomerization of 1,2-Azaborines.....	9
1.1.3 Valence Isomer Pairs as Potential Molecular Solar Thermal Systems (MOST) .	17
1.1.4 1,2-Azaborines as 4C+1B+1N Synthons	19
1.1.5 Stereoselective Synthesis of Cyclobutanes	20
1.2 Rhodium-catalyzed Ring-opening Reaction of the Dewar Photoisomer to Form 1,2-Azaborines	25
1.2.1 Potential Utility of 1,2-Azaborine Valence Isomer Pairs in Solar Energy Storage	25
1.2.1.2 Reaction Calorimetry Study.....	27
1.2.2 Accessing Enantioenriched Dewar Photoisomers via Kinetic Resolution	28
1.2.2.1 Proposed Mechanisms and Discussion	28
1.3 Accessing <i>cis</i> -Aminoborylated Cyclobutanes and Further Derivatizations	32
1.3.1 Modifications of 1,2-Azaborines and Photoisomerization in Flow	32
1.3.2 Diastereoselective Synthesis of Highly Substituted Aminoborylated Cyclobutanes.....	34
1.3.3 Summary	41
1.4 Stereospecific Ring-opening of the Dewar Photoisomer to Afford Dienes and Tandem Diels-Alder Reactions.....	41
1.5 Conclusions and Future Outlook	44
1.6 Experimental Section.....	45
1.6.1 General Considerations.....	45

1.6.2 Experimental Procedures of Chapter 1.2	46
1.6.2.1 Experimental Procedure.....	46
1.6.2.2 Analytical Data	50
1.6.3 Experimental Procedures of Chapter 1.3	54
1.6.3.1 Details of Photoreactor Assembly	54
1.6.3.2 Synthetic Procedures and Characterizations of New Compounds.....	54
1.6.3.3 X-ray Crystallographic Data.....	85
1.6.3.4 Analytical Data	87
1.6.4 Experimental Procedures of Chapter 1.4	136
1.6.4.1 Procedure and Characterization for New Compounds.....	136
1.6.4.1 Analytic Data	138
Chapter 2: A Modular and Stereoselective Approach to Furnish β-Amino Cyclobutanols	
2.1 Introduction.....	147
2.1.1 Chapter Overview	147
2.1.2 Regioselective Functionalization of 1,2-Azaborines	154
2.2 Strategic Choice of Substituent on Boron.....	163
2.3 Modular Synthesis of <i>Mono</i> - and <i>Di</i> -functionalized 1,2-Azaborines.....	166
2.4 Investigations of the Substrate Scope of Photoisomerization.....	173
2.5 Stereoselective Hydrogenation and Stereospecific Oxidation.....	180
2.6 Summary	186
2.7 Experimental Section.....	187
2.7.1 General Considerations.....	187
2.7.2 Experimental Procedures for Synthesis of New Compounds	189
2.7.2.1 Experimental Procedures for Synthesis of <i>Mono</i> - and <i>Di</i> -Functionalized 1,2- Azaborines (Table 2.1 and Table 2.2).....	189
2.7.2.2 General Procedure for 1,2-Azaborine Photoisomerization (Dewar Substrates in Table 2.3).....	226

2.7.2.3 General Procedure for Sequential Hydrogenation and Oxidation towards the Cyclobutane β -amino alcohol in Table 2.5.....	245
2.7.2.4 X-ray Crystallographic Data.....	261
2.7.3 Analytical Data	265

Chapter 1

Photoisomerization of 1,2-Azaborines: Energy Storage and Synthetic Applications

1.1 Introduction

Isosterism¹ represents an attractive strategy to create and optimize chemical space in disparate applications.² One emerging research area involves the replacement of a C=C bond with an isoelectronic and isosteric BN bond known as BN/CC isosterism.³ Perhaps the most exciting subset of BN/CC isosterism is exemplified by the 1,2-azaborines⁴ (substitution of a CC bond unit with a BN bond unit in benzenes), considering that benzene is a ubiquitous, versatile structural motif found across material science, organic synthesis and biomedical research (Figure 1.1).⁵ The introduction of the BN unit significantly modifies the properties of classic benzenoid compounds, leading to new reactivities and functionalities. The main focus of studies disclosed herein is to leverage the unique

¹ For definitions of isosterism, see: a) Langmuir, I. *J. Am. Chem. Soc.* **1919**, *41*, 1543–1559. b) Grimm, H. *G. Z. Electrochem.* **1925**, *31*, 474–480. c) Erlenmeyer, H.; Berger, E. *Biochem. Z.* **1932**, *252*, 22–36.

² For representative examples, see: a) Nagase, S.; Teramae, H.; Kudo, T. *J. Chem. Phys.* **1987**, *86*, 4513–3517. b) Fink, W. H.; Richards, J. C. *J. Am. Chem. Soc.* **1991**, *113*, 3393–3398. c) Driess, M.; Grützmacher, H. *Angew. Chem. Int. Ed. Engl.* **1996**, *35*, 828–856. (d) Patani, G. A.; LaVoie, E. J. *Chem. Rev.* **1996**, *96*, 3147–3176. e) Kira, B.; Phukan, A. K.; Jemmis, E. D. *Inorg. Chem.* **2001**, *40*, 3615–3618. f) Golberg, D.; Bando, Y.; Huang, Y.; Terao, T.; Mitome, M.; Tang, C.; Zhi, C. *ACS Nano.* **2010**, *4*, 2979–2993. g) Kar, T.; Scheiner, S.; Roy, A. K. *J. Phys. Chem. C* **2015**, *119*, 15541–15546. h) Wu, J.; Zhu, J. *ChemPhysChem* **2015**, *16*, 3806–3813. i) Rivard, E. *Chem. Soc. Rev.* **2016**, *45*, 989–1003.

³ Liu, Z.; Marder, T. B. *Angew. Chem. Int. Ed.* **2008**, *47*, 242–244.

⁴ For reviews of BN/CC isosterism in benzenes and other aromatic systems, see: a) Bosdet, M. J. D.; Piers, W. E. *Can. J. Chem.* **2009**, *87*, 8–29. b) Campbell, P. G.; Marwitz, A. J. V.; Liu, S.-Y. *Angew. Chem. Int. Ed.* **2012**, *51*, 6074–6092. c) Wang, X.-Y.; Wang, J.-Y.; Pei, J. *Chem. Eur. J.* **2015**, *21*, 3528–3539. d) Morgan, M. M.; Piers, W. E. *Dalton Trans.* **2016**, *45*, 5920–5924. e) Helten, H. *Chem. Eur. J.* **2016**, *22*, 12972–12982. f) Bhattacharjee, A.; Davies, G. H. M.; Saeednia, B.; Wisniewski, S. R.; Molander, G. A. *Adv. Synth. Catal.*, **2020**, *363*, 1–19.

⁵ For representative perspectives, see: a) Bonifazi, D.; Fasano, F.; Lorenzo-Garcia, M. M.; Marinelli, D.; Oubaha, H.; Tasseroul, J. *Chem. Commun.* **2015**, *51*, 15222–15236. b) Giustra, Z. X.; Liu, S.-Y. *J. Am. Chem. Soc.* **2018**, *140*, 1184–1194.

reactivities of 1,2-azaborines and explore their potential as useful synthons for accessing important building blocks in organic synthesis.

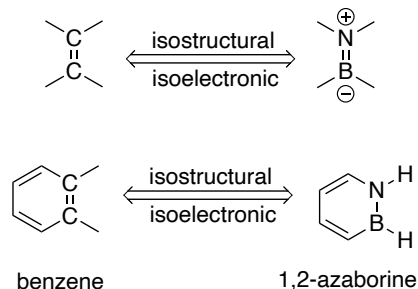


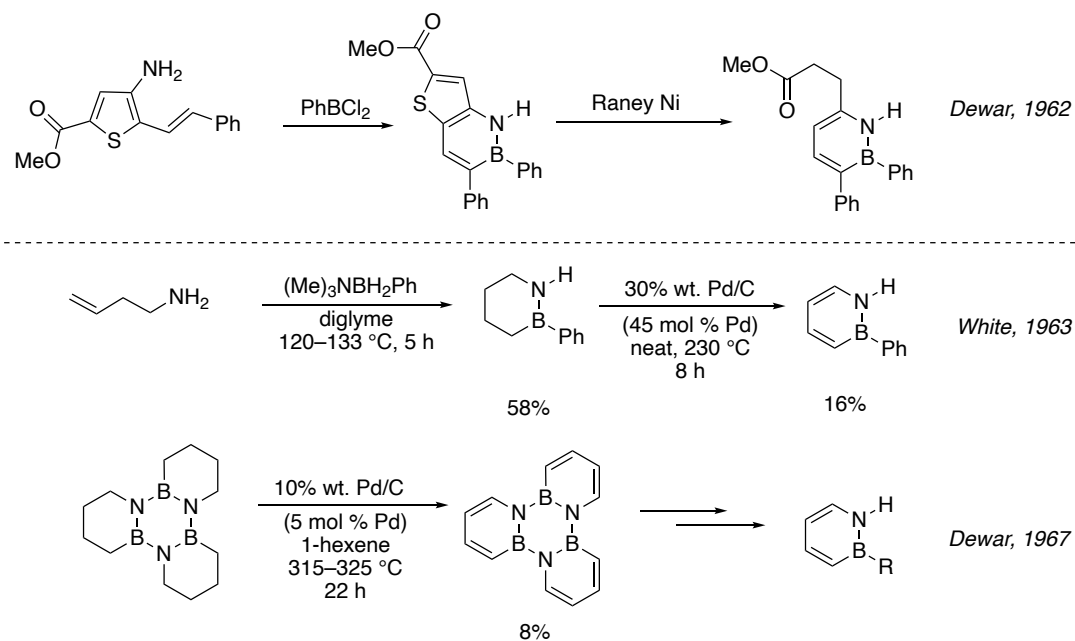
Figure 1.1. BN/CC isosterism and its application in benzene

1.1.1 1,2-Azaborines: Synthesis and Properties

Although conceptually intriguing, the studies of 1,2-azaborines would not be possible without the accomplishment of constructing 1,2-azaborines in the first place. Early efforts to synthesize monocyclic 1,2-azaborine derivatives can be traced back to Dewar and White in 1960s. Among the three protocols, one requires specific substituents at C(3) and C(6),⁶ while the other two involve dehydrogenation under forcing conditions that proceed in low efficiency (Scheme 1.1).⁷ Due to a lack of general and efficient strategy to access 1,2-azaborines, the study of these species has been largely hampered.

⁶ Dewar, J. S.; Marr, P. A. *J. Am. Chem. Soc.* **1962**, *84*, 3782.

⁷ a) White, D. G. *J. Am. Chem. Soc.* **1963**, *85*, 3634–3636. b) Davies, K. M.; Dewar, M. J. S.; Rona, P. J. *Am. Chem. Soc.* **1967**, *89*, 6294–6297.

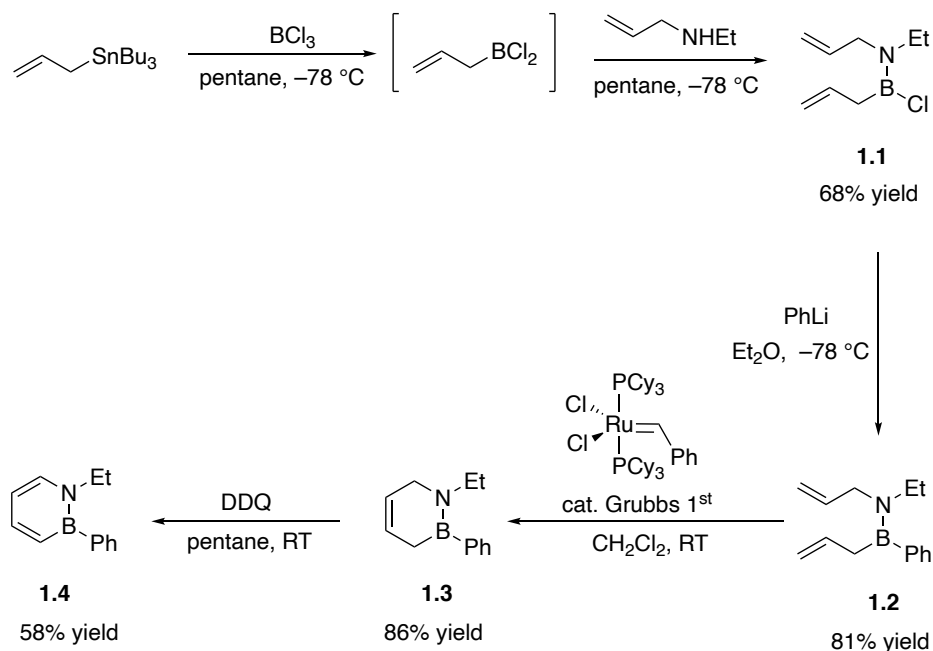


Scheme 1.1. Early synthetic routes to monocyclic 1,2-azaborines

At the beginning of the new millennium (2000), a much-improved approach was reported by Ashe⁸ which benefited from the development of olefin metathesis chemistry (Scheme 1.2).⁹ The route starts with allyltributyltin, which undergoes transmetalation with BCl_3 and condensation with allylamine to afford the B–N adduct **1.1**. Substitution of the boron position with phenyl-lithium results in compound **1.2**, which then undergoes RCM (ring-closing metathesis) with Grubbs 1st generation catalyst. The final step involving 2e oxidation with DDQ is significantly milder compared with 4e oxidation reported previously with Pd/C, delivering the N–Et–B–Ph 1,2-azaborine **1.4** with good yield.

⁸ Ashe, A. J.; Fang. *Org. Lett.* **2000**, *2*, 2089–2091.

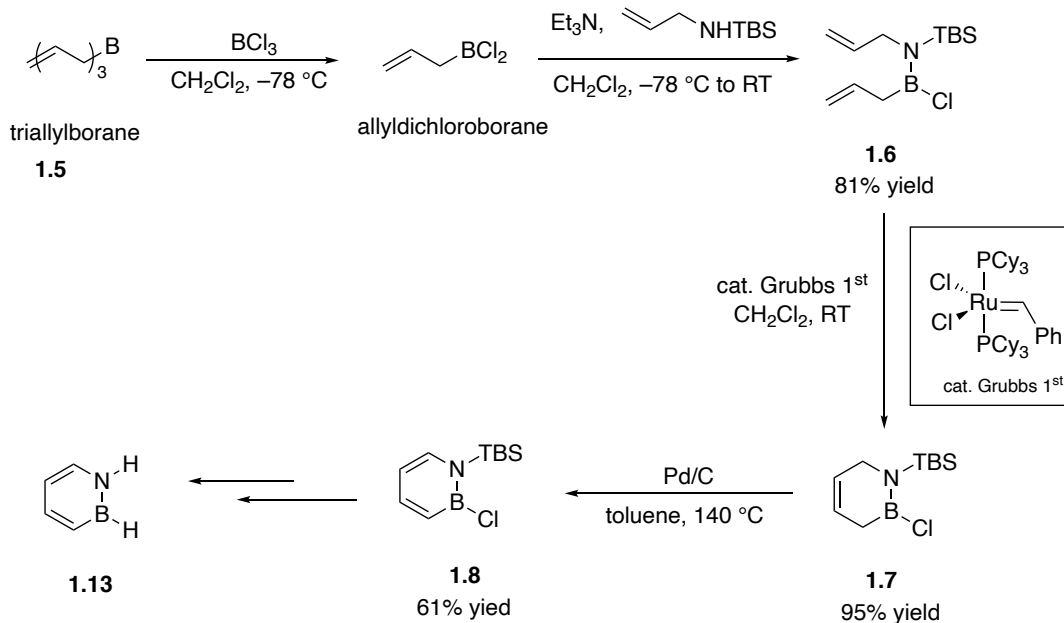
⁹ a) Fu, G. C.; Grubbs, R. H. *J. Am. Chem. Soc.* **1992**, *114*, 7324–7325. b) Fu, G. C.; Nguyen, S. T.; Grubbs, R. H. *J. Am. Chem. Soc.* **1993**, *115*, 9856–9857. For recent reviews on olefin metathesis, see: c) Fürstner, A. *Angew. Chem. Int. Ed.* **2000**, *39*, 3012–3043. d) Schrock, R. R.; Hoveyda, A. H. *Angew. Chem. Int. Ed.* **2003**, *42*, 4592–4633 e) Ogba, O. M.; Warner, N. C.; O’Leary, D. J.; Grubbs, R. H. *Chem. Soc. Rev.* **2018**, *47*, 4510–4544.



Scheme 1.2. Ashe's synthesis of 1,2-azaborine via RCM (ring-closing metathesis) and oxidation approach

In 2009, the Liu group further utilized the metathesis/oxidation approach to access a more versatile *N*-TBS-*B*-Cl 1,2-azaborine synthon **1.8** (Scheme 1.3).¹⁰ Triallylborane **1.5** comproportionates with BCl₃ to deliver allyldichloroborane intermediate, which then condenses with *N*-TBS (tert-butyldimethylsilyl) allylamine to afford the B-N adduct **1.6**. The adduct undergoes smooth RCM reaction followed by oxidation to generate 1,2-azaborine **1.8**. Notably, **1.8** features an easily removable TBS protecting group as well as a chloride leaving-group on the boron, paving the way for the landmark discovery of parent 1,2-azaborine **1.13** synthesis.¹⁰

¹⁰ Marwitz, A. J. V.; Matus, M. H.; Zakharov, L. N.; Dixon, D. A.; Liu, S.-Y. *Angew. Chem. Int. Ed.* **2009**, *48*, 973-977.

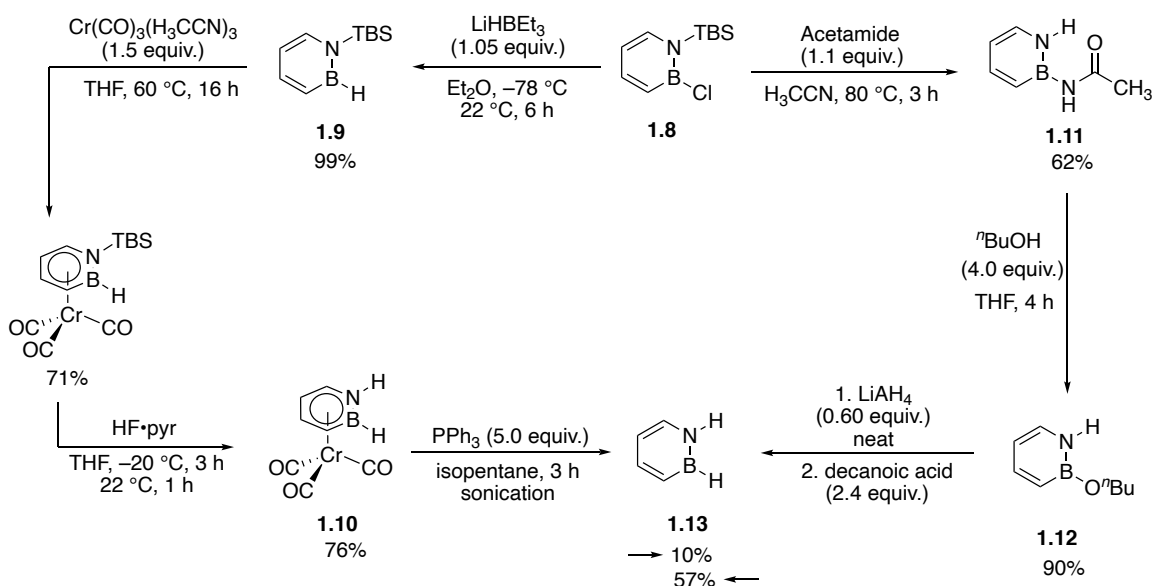


Scheme 1.3. Liu's synthesis of a versatile 1,2-azaborine synthon

The preparation of **1.13** starts with B–Cl reduction, followed by a three-step sequence involving first coordination to $\text{Cr}(\text{CO})_3(\text{H}_3\text{CCN})_3$, then desilylation with $\text{HF}\cdot\text{pyridine}$, and finally decomplexation (Scheme 1.4). Later on, a more efficient route was developed upon the discovery that addition of acetamide to **1.8** results in desilylation to produce amide-substituted **1.11**; the amide group readily exchanges with alcohols to generate **1.12**, which can be reduced to afford **1.13** (Scheme 1.4).^{11,12}

¹¹ a) Lamm, A. N. Fundamental Chemistry of 1,2-Dihydro-1,2-Azaborines. Ph.D. Dissertation, University of Oregon, Eugene, OR, 2012. b) Baggett, A. W. New Strategies Enabling Diverse Functionalization of Aromatic 1,2-Azaborine Motifs. Ph.D. Dissertation, Boston College, Boston, MA, 2016.

¹² Abbey, E. R.; Lamm, A. N.; Baggett, A. W.; Zakharov, L. N.; Liu, S.-Y. *J. Am. Chem. Soc.* **2013**, *135*, 12908-12913.



Scheme 1.4. Routes to parent 1,2-azaborine (**1.13**)

With the successful synthesis and isolation of **1.13**, Liu and others aimed to unveil its fundamental properties, more importantly to provide experimental quantification of the aromatic nature of 1,2-azaborines.^{10,13} Table 1.1 compares several key values measured for **1.13** with those determined for benzene. Compound **1.13** appears to be remarkably distinct from its all-carbon isostere based on some of the key parameters (e.g., mp, bp, $E_{\text{T}}(30)$,¹⁴ E_{ox} ¹⁵). However, X-ray crystallographic analysis of a $\text{Cr}(\text{CO})_3$ adduct shows **1.13** binding to the metal center in the same η^6 fashion as benzene,^{10,16} with essentially no deviation

¹³ a) Chrostowska, A.; Xu, S.; Lamm, A. N.; Mazurek, A.; Weber, C. D.; Dargelos, A.; Baylère, P.; Graciaa, A.; Liu, S.-Y. *J. Am. Chem. Soc.* **2012**, *134*, 10279–10285. b) Abbey, E. R.; Lamm, A. N.; Baggett, A. W.; Zakharov, L. N.; Liu, S.-Y. *J. Am. Chem. Soc.* **2013**, *135*, 12908–12913.

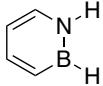
¹⁴ The $E_{\text{T}}(30)$ polarity scale is based on the λ_{max} of absorptions of Reichardt's dye in various solvents. The $E_{\text{T}}(30)$ scale is defined by equation: $E_{\text{T}}(30)(\text{kcal/mol}) = \frac{28591}{\lambda_{\text{max}}(\text{nm})}$, where λ_{max} is the wavelength at the maximum of the longest-wavelength intramolecular charge-transfer $\pi-\pi^*$ absorption band of Reichardt's dye. For related references, see: Reichardt, C. *Chem. Rev.* **1994**, *94*, 2319–2358.

¹⁵ $E_{\text{ox}}(\text{V})$ is the oxidation potential measured via cyclic voltammetry vs Ag/Ag^+ .

¹⁶ Wang, Y.; Angermund, K.; Goddard, R.; Krüger, C. *J. Am. Chem. Soc.* **1987**, *109*, 587–589.

from planarity evident in the parent 1,2-azaborine ring (Figure 1.2). The CO IR stretching frequencies of the two $\text{Cr}(\text{CO})_3$ adducts were also nearly identical.¹⁰

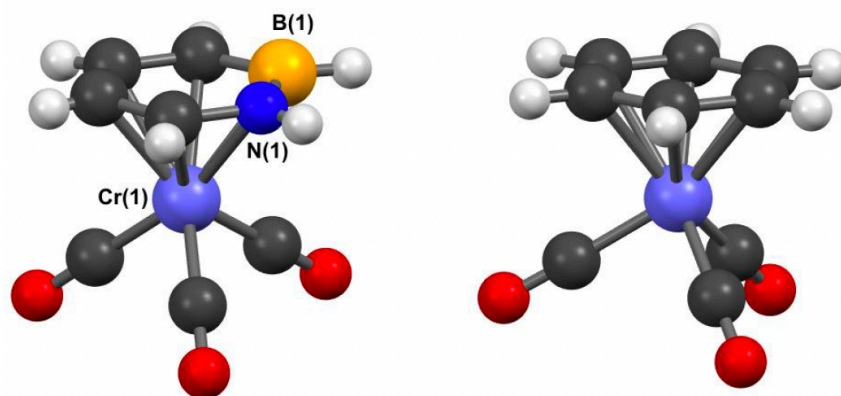
Table 1.1. Measured values for physical and chemical properties of **1.13**^a and benzene^b

		
density	0.904 g·mL ⁻¹	0.879 g·mL ⁻¹
n_D	1.528	1.501
mp	-45 °C	5.5 °C
bp	117 °C	80 °C
$E_T(30)$	47.8 kcal·mol ⁻¹	34.3 kcal·mol ⁻¹
IE(1 st)	8.6 eV	9.25 eV
E_{ox}	1.4 V	2.35 V

^aFrom Ref. 10,12

^bFrom Ref. 12 and the CRC Handbook of Chemistry and Physics, 98th Ed.

Figure 1.2. Ball-and-stick representations of $\text{Cr}(\text{CO})_3(\eta^6\text{-1.13})$ (left) and $\text{Cr}(\text{CO})_3(\eta^6\text{-C}_6\text{H}_6)$ (right) generated from the program Mercury using crystallographic data (Refcodes COPKAU and FETVUV, Cambridge Crystal Structure Database)



$\text{Cr}(\text{CO})_3 \cdot \mathbf{1.13}$
 $\nu \text{ CO} = 1898, 1975 \text{ cm}^{-1}$

$\text{Cr}(\text{CO})_3 \cdot (\eta^6\text{-C}_6\text{H}_6)$
 $\nu \text{ CO} = 1892, 1972 \text{ cm}^{-1}$

A planar ring geometry was also observed for free **1.13** in the gas phase through microwave spectroscopy ($\Delta_0 = 0.02 \text{ amu}\cdot\text{\AA}^2$).¹⁷ Additional analysis of the measured rotational constants revealed the B–N bond length in **1.13** (1.45(3) Å) to be slightly longer than that for aminoborane bond length (H₂B–NH₂; 1.391 Å),¹⁸ but significantly shorter than that for amine borane bond length (H₃B–NH₃; 1.657 Å).¹⁹ Aside from aforementioned structural parameters, study of NMR spectra of various 1,2-azaborines by Ashe reveals ¹H NMR chemical shifts consistent with the presence of aromatic ring current effects.²⁰ Nucleus independent chemical shift (NICS) calculations are also supporting the aromatic character of 1,2-azaborine.^{4b}

Taken together, these results demonstrate **1.13** to fulfill the formal requirements for aromaticity, as classically exemplified by benzene. The question remains to be “how aromatic” **1.13** should be considered.²¹ One classic method to quantitatively evaluate aromaticity is to determine the resonance stabilization energy (RSE) of a given aromatic compound.²² Kistiakowsky and co-workers employed the technique to measure the RSE of benzene to be 36 kcal/ mol.²³ The Liu group undertook an similar approach to experimentally determine the RSE of 1,2-azaborine to be around 16.6 kcal/mol.²⁴ While

¹⁷ Daly, A. M.; Tanjaron, C.; Marwitz, A. J. V.; Liu, S.-Y.; Kukolich, S. G. *J. Am. Chem. Soc.* **2010**, *132*, 5501–5506.

¹⁸ Sugie, M.; Takeo, H.; Matsumura, C. *J. Mol. Spectrosc.* **1987**, *123*, 286–292.

¹⁹ Thorne, L. R.; Suenram, R. D.; Lovas, F. J. *J. Chem. Phys.* **1983**, *78*, 167–171.

²⁰ Ashe, A. J.; Fang, X.; Fang, X.; Kampf, J. W. *Organometallics* **2001**, *20*, 5413–5418.

²¹ For representative theoretical studies, see: a) Kranz, M.; Clark, T. *J. Org. Chem.* **1992**, *57*, 5492–5500. b) Ghosh, D.; Periyasamy, G.; Pati, S. K. *Phys. Chem. Chem. Phys.* **2011**, *13*, 20627–20636. c) Baranac-Stojanović, M. *Chem. Eur. J.* **2014**, *20*, 16558–16565. d) Papadopoulos, A. G.; Charistos, N. D.; Kyriakidou, K.; Sigalas, M. P. *J. Phys. Chem.* **2015**, *119*, 10091–10100.

²² RSE is a measure of the additional energetic stabilization engendered by the cyclic arrangement of a conjugated system compared to the corresponding number of isolated double bonds.

²³ Kistiakowsky, G. B.; Ruhoff, J. R.; Smith, H. A.; Vaughan, W. E. *J. Am. Chem. Soc.* **1936**, *58*, 146–153.

²⁴ Campbell, P. G.; Abbey, E. R.; Neiner, D.; Grant, D. J.; Dixon, D. A.; Liu, S.-Y. *J. Am. Chem. Soc.* **2010**, *132*, 18048–18050.

significantly less than that of benzene, the RSE value for azaborine is on par with those of other heterocycles such as pyrrole (RSE around 21 kcal/mol) and furan (RSE around 15 kcal/mol).²⁵

In addition to aromatic properties of 1,2-azaborine, electronic properties have also drawn researchers' particular interests as they are closely related to the reactivity and functionality.^{10,12,13a,26} Detailed introduction of electronic properties of 1,2-azaborine and how they correlate with the reactivity and selectivity will be discussed in the second chapter of this dissertation.

1.1.2 Photoisomerization of 1,2-Azaborines

Photoisomerization reactions of aromatic molecules have been extensively studied over the past six decades, and their valence isomers have attracted vast interest from both synthetic and theoretical chemists.²⁷ Benzene has received the most attention, and four of its valence isomers are now well-known after extensive investigation experimentally and theoretically.²⁸ Wilzbach discovered that fulvene **1.14** and benzvalene **1.15** are produced during benzene photolysis at 254 nm in solution,²⁹ while fulvene is the predominant isomer produced in the gas phase.³⁰ Ward established that photolysis of benzene at 204 nm in

²⁵ Burford, R. J.; Li, B.; Vasiliu, M.; Dixon, D. A.; Liu, S.-Y. *Angew. Chem. Int. Ed.* **2015**, *54*, 7823–7827.

²⁶ Baggett, A. W.; Vasiliu, M.; Li, B.; Dixon, D. A.; Liu, S. -Y. *J. Am. Chem. Soc.* **2015**, *137*, 5536–5541.

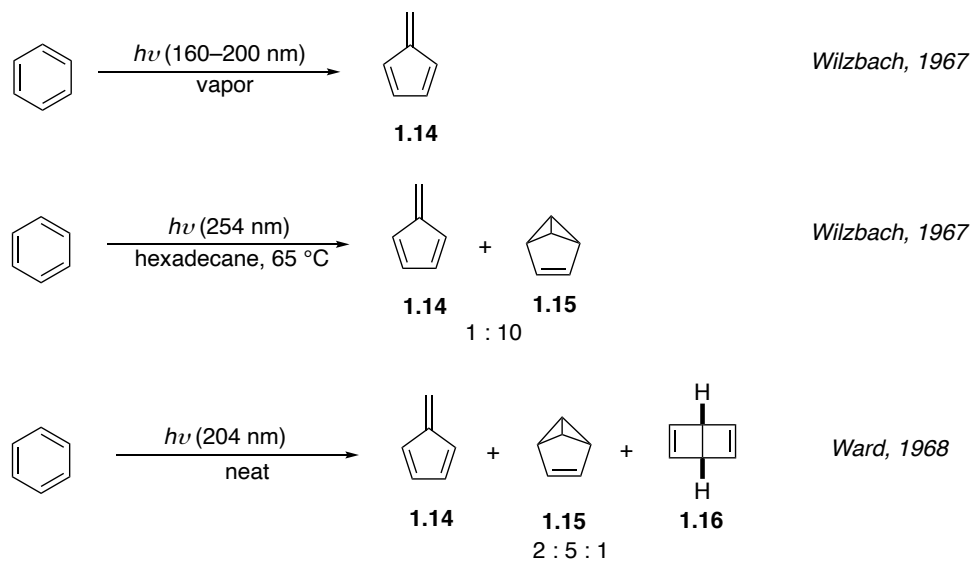
²⁷ a) Harman, P. J.; Kent, J. E.; O'Dwyer, M. F.; Griffith, D. W. T. *J. Phys. Chem.* **1981**, *85*, 2731–2733. b) Noyes, W. A.; Al-Ani, K. E. *Chem. Rev.* **1974**, *74*, 29–43. c) Gilbert, A. *photochemistry*, Vol.36, RSC Publishing, Cambridge, **2007**, pp.91–132.

²⁸ a) Van Tamelen, E. E.; Pappas, S. P. *J. Am. Chem. Soc.* **1963**, *85*, 3297–3298. b) Katz, T. J.; Acton, N. *J. Am. Chem. Soc.* **1973**, *95*, 2738–2739. c) Billups, W. E.; Haley, M. M. *Angew. Chem. Int. Ed. Engl.* **1989**, *28*, 1711–1712. d) Priyakumar, U. D.; Dinadayalane, T. C.; Sastry, G. N. *New J. Chem.* **2002**, *26*, 347–353. e) Li, Z.; Rogers, D. W.; McLafferty, F. J.; Mandziuk, M.; Podosenin, A. V. *J. Phys. Chem. A* **1999**, *103*, 426–430. f) Schulman, J. M.; Disch, R. L. *J. Am. Chem. Soc.* **1985**, *107*, 5059–5061. g) Newton, M. D.; Schulman, J. M.; Manus, M. M. *J. Am. Chem. Soc.* **1974**, *96*, 17–23.

²⁹ Wilzbach, K. E.; Ritscher, J. S.; Kaplan, L. *J. Am. Chem. Soc.* **1967**, *89*, 1031–1032.

³⁰ Kaplan, L.; Wilzbach, K. E. *J. Am. Chem. Soc.* **1967**, *89*, 1030–1031.

liquid phase yields a mixture of fulvene, benzvalene and Dewar benzene **1.16** (Scheme 1.5).³¹



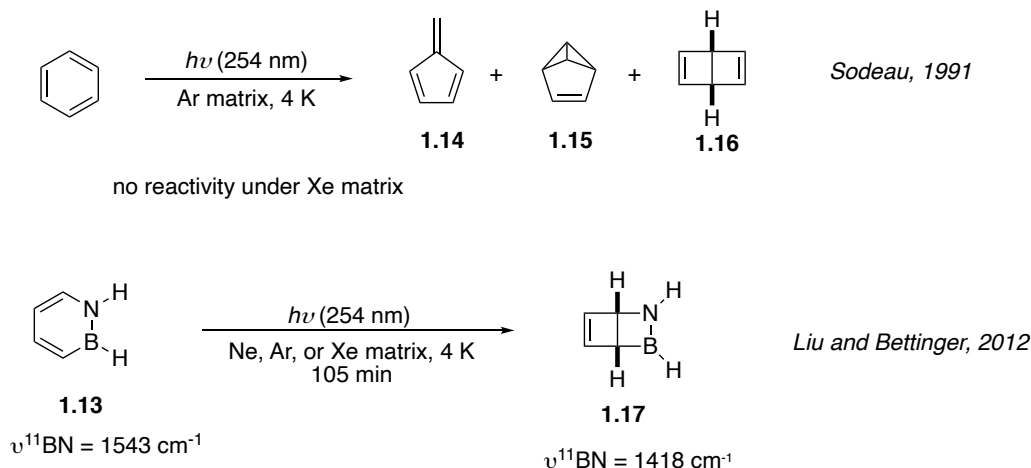
Scheme 1.5. Product distribution of benzene photoisomerization under different conditions

To complement the above gas- and liquid-phase experiments, Sodeau later studied benzene photoisomerization in noble gas matrices.³² Irradiation of benzene condensed in argon at 4 K with 254 nm light yields three valence isomers **1.14**, **1.15**, and **1.16** as primary products (Scheme 1.6). Like benzene, parent 1,2-azaborine **1.13** absorbs light in the UVC region ($\lambda_{\text{max}} = 269 \text{ nm}$, $\epsilon = 15632 \text{ M}^{-1}\text{-cm}^{-1}$),¹⁰ thus it is intriguing to explore if **1.13** exhibits photoreactivity similar to that of the all-carbon system. Sodeau's work served as the model for initial investigation of photoisomerization of **1.13** attempted collaboratively by the Liu and Bettinger groups in 2012. A sample of **1.13** condensed in a noble gas matrix was

³¹ Ward, H. R.; Wishnok, J. S. *J. Am. Chem. Soc.* **1968**, *90*, 1085–1086.

³² Johnstone, D. E.; Sodeau, J. R. *J. Phys. Chem.* **1991**, *95*, 165–169.

irradiated with 254 nm light while reaction progress was monitored by IR spectroscopy (Scheme 1.6).³³ After 105 min, starting material peaks were completely replaced by a new set of signals, and no further changes were observed even after another 20 h of irradiation. The measured product spectrum correlated well to that calculated for 2-aza-3-borabicyclo[2.2.0]hex-5-ene **1.17** (Dewar azaborine), the anticipated BN-isostere of **1.16**. Notably, photoisomerization of **1.13** affords **1.17** exclusively under matrix isolation conditions rather than a mixture of valence isomers observed in benzene photoisomerization. Moreover, in xenon matrix (xenon strongly promotes singlet to triplet inter-system crossing through the heavy atom effect),³² there is no photoreactivity of benzene observed, thus the possible involvement of triplet states is ruled out. The fact that **1.17** was found to also form in a xenon matrix indicates that photoisomerization of **1.13** may occur along a pathway different from that of benzene (involved in triplet states is also possible).



Scheme 1.6. Comparison of photoisomerization of benzene and **1.13** in noble gas matrices

³³ Brough, S. A.; Lamm, A. N.; Liu, S.-Y.; Bettinger, H. F. *Angew. Chem. Int. Ed.* **2012**, *51*, 10880–10883.

The mechanism of photoisomerization of **1.13** has been studied computationally. The calculation results from Kim and Lim predict the involvement of intermediates on the S_1 excited- and S_0 ground-state surfaces, making **1.17** the final product of a series of both photochemical and thermal elementary steps.³⁴ The dark portion of this model notably aligns with that computed earlier by Bettinger for the thermal reverse reaction of **1.17**→**1.13**.³⁵ As shown in Figure 1.3, this transformation was calculated to proceed stepwise, rather than concertedly, through two transition states (**1.18**[‡] and **1.19**[‡]) with an overall barrier of 22.2 kcal/mol. This sizable barrier supported the feasibility of isolating **1.17** under ambient conditions. Additional calculations from Bettinger,³⁵ however, indicated that the relatively unhindered aminoborane unit in **1.17** would be prone to dimerization, a process with a predicted barrier of only 3.4 kcal/mol.

³⁴ Kim, J.; Moon, J.; Lim, J. S. *ChemPhysChem* **2015**, *16*, 1670–1675

³⁵ Bettinger, H. F.; Hauler, O. Beilstein *J. Org. Chem.* **2013**, *9*, 761–766.

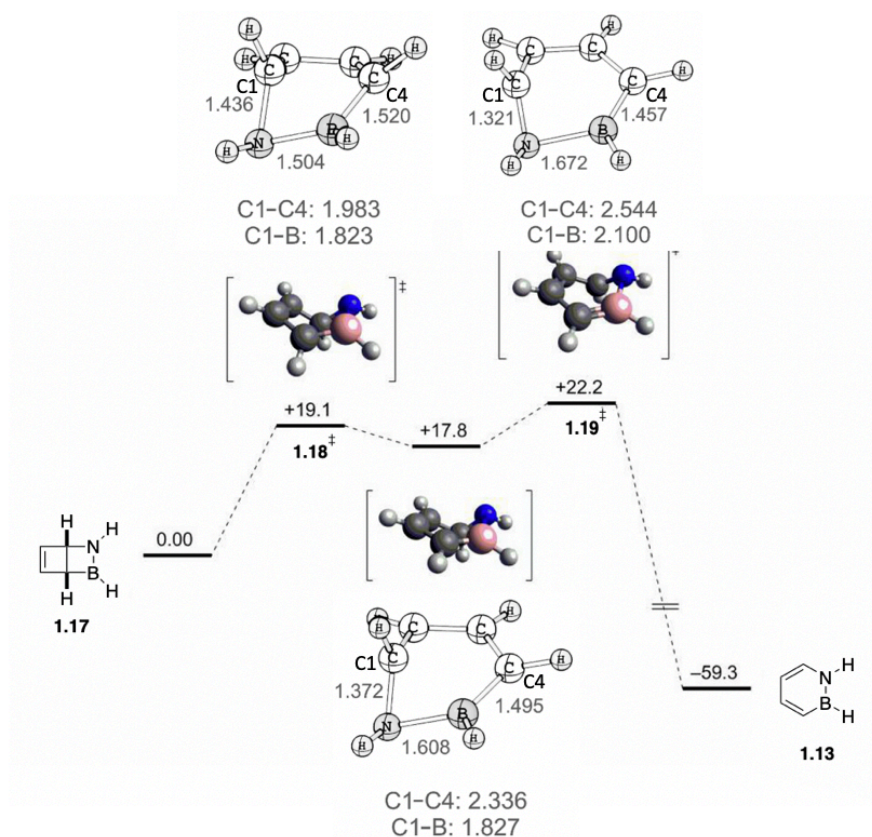
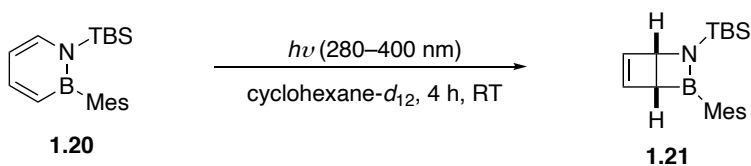


Figure 1.3. Potential energy surface for thermally-driven reversion of **1.17** to **1.13**. ΔE values (kcal/mol) were calculated using CCSD(T)/cc-pVQZ//CCSD(T)/TZVP, with zero-point vibrational energies obtained at the CCSD(T)/DZVP level of theory. C1–N, N–B, C4–B, C1–C4, and C1–B distances are given in angstroms (Å).

Encouraged by the finding of a sizable barrier for thermal ring opening of **1.17**, we investigated the photochemistry of 1,2-azaborine in solution.³⁶ We reasoned that dimerization of the aminoborane moiety could be suppressed by kinetic stabilization by bulky substituents at B and N. Particularly, the more sterically encumbered N-silylated, B-mesitylated 1,2-azaborine **1.20** was irradiated under UV (280–400 nm) in cyclohexane-

³⁶ Edel, K.; Yang, X.; Ishibashi, J. S. A.; Lamm, A. N.; Maichle-Mössner, C.; Giustra, Z. X.; Liu, S.-Y.; Bettinger, H. F. *Angew. Chem. Int. Ed.* **2018**, *57*, 5296–5300.

d_{12} solution at room temperature (Scheme 1.7). Gratifyingly, **1.20** exclusively converted to Dewar isomer **1.21** within 4 hours on the basis of ^1H NMR analysis (Figure 1.4). More importantly, **1.21** itself proved exceptionally stable at room temperature, reverting back to **1.20** only with application of a moderate degree of heat ($t_{1/2} = 25$ min at $100\text{ }^\circ\text{C}$). The Dewar isomer **1.21** could be isolated after the photoreaction as a colorless oil.



Scheme 1.7. Photoisomerization of **1.20** to **1.21** under ambient conditions

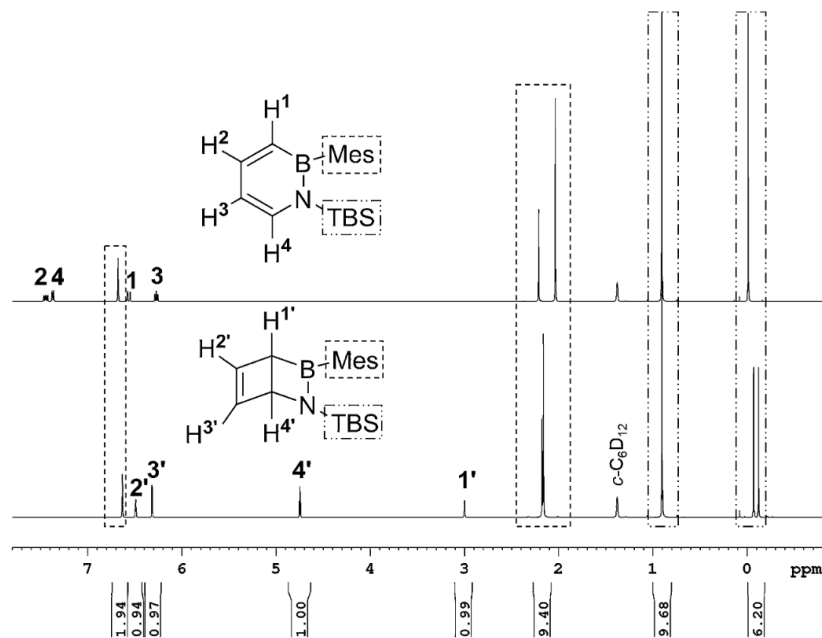


Figure 1.4. ^1H NMR spectra of **1.20** (top) and **1.21** (bottom, after photo-irradiation)

in $c\text{-C}_6\text{D}_{12}$

The kinetics of ring-opening from **1.21** to **1.20** were studied by NMR spectroscopy in *d*₂-tetrachloroethane over a rather narrow temperature range (358–373K).³⁶ Arrhenius treatment of the first-order reaction data gave an activation energy (E_a) of (27.0 ± 1.2) kcal/mol, significantly higher than the barrier previously calculated for the ring-opening of **1.17**.³⁵ Our collaborator from Bettinger group re-modeled the reaction pathway using **1.21** and **1.20** explicitly. When they investigated the ring opening of **1.21** at B3LYP/6–311+G** level, they claim that in the presence of the bulky substituents, the thermal ring-opening reaction is no longer stepwise, but rather concerted with a strongly distorted transition state (**1.22[‡]**).³⁶ The lowest energy barrier of 26.1 kcal/mol obtained is in very good agreement with the experimental data, which indicates that the bulky substituents not only stabilize the Dewar isomer with respect to dimerization, but also retard ring opening probably due to the increased steric repulsion of the adjacent bulky groups in the planar geometrical arrangement in **1.20**.³⁶

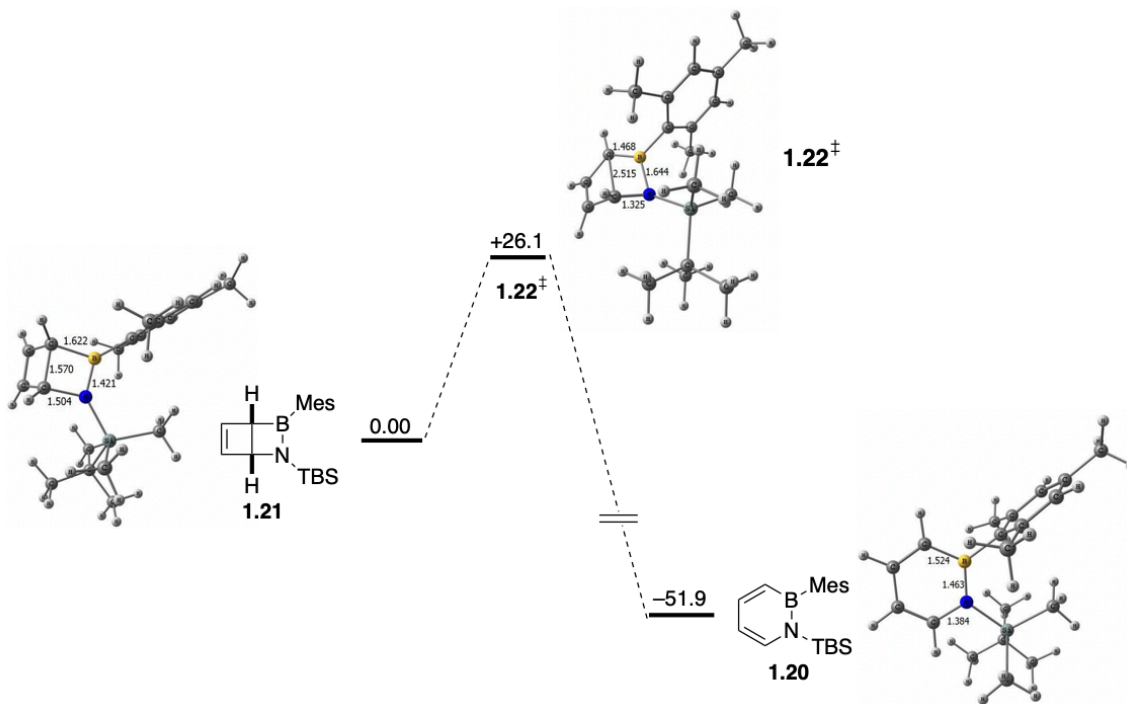
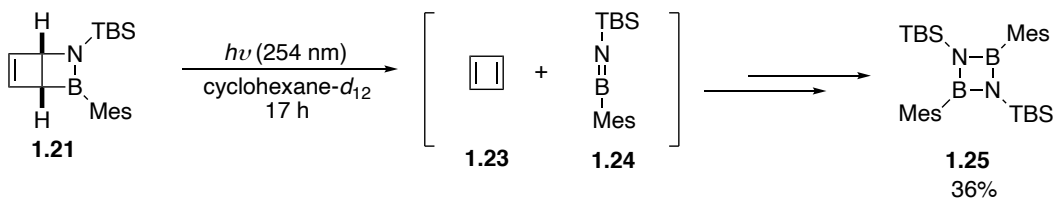


Figure 1.5. Potential energy surface for thermally-driven ring-opening of **1.21** to **1.20**

ΔE values (kcal/mol) were calculated at the B3LYP/6-31G* level of theory

The photochemistry of **1.20** under shorter UV wavelength (254 nm) in solution was also explored. Although irradiation of **1.20** with 254 nm light also quickly resulted in photoisomerization to **1.21**, upon extended photolysis at 254 nm, the Dewar isomer slowly underwent cycloreversion to the corresponding cyclobutadiene **1.23** and iminoborane **1.24**. The latter could dimerize in situ to form the isolable 1,3,2,4-diazadiboretidine **1.25** (Scheme 1.8).



Scheme 1.8. Photodecomposition of Dewar 1,2-azaborine **1.21** under 254 nm light

1.1.3 Valence Isomer Pairs as Potential Molecular Solar Thermal Systems (MOST)

Another inspiration from calculation model (perhaps from chemistry instinct as well) is that 1,2-azaborine **1.20** is substantially lower in energy as to its Dewar isomer **1.21**, yet **1.21** is exceptionally stable at room temperature. Given the relatively high quantum yield of ($46 \pm 8\%$) and high selectivity of our photoisomerization,³⁶ we were wondering if the 1,2-azaborine valence isomer pair could serve as a candidate for the storage of solar energy. A promising technology is molecular solar thermal systems (MOST),³⁷ in which photons induce photoisomerization to a high-energy species that has a sufficiently high activation barrier for the reversible reaction and releases thermal energy only on demand (e.g., in the presence of a catalyst). Beside *E/Z* isomerization of CC or NN double bonds³⁸ and photo-dimerization of anthracene,³⁹ several valence isomer pairs, such as norbornadiene/quadracyclane,⁴⁰ the fulvalene diruthenium system,⁴¹

³⁷ For representative research in the field of MOST, see: a) Lennartson, A.; Moth-Poulsen, K. *Molecular Devices for Solar Energy Conversion and Storage*, Springer, Singapore, **2018**, pp.327–352. b) Lennartson, A.; Roffey, A.; Moth-Poulsen, K. *Tetrahedron Lett.* **2015**, *56*, 1457–1465. c) Kucharski, T. J.; Tian.; Akbulatov, S.; Boulatov, R. *Energy Environ. Sci.* **2011**, *4*, 4449–4472. d) Jorner, K.; Dreos, A.; Emanuelsson, R.; El Bakouri, O.; Galvan, I. F.; Börjesson, K.; Feixas, F.; Lindh, R.; Zietz, B.; Moth-Poulsen, K.; Ottosson, H. *J. Mater. Chem. A* **2017**, *5*, 12369–12378. e) Dreos, A.; Börjesson, K.; Wang, Z.; Roffey, A.; Norwood, Z.; Moth-Poulsen, K. *Energy Environ. Sci.* **2017**, *10*, 728–734. f) Börjesson, K.; Lennartson, A.; Moth-Poulsen, K. *ACS Sustainable Chem. Eng.* **2013**, 585–590. g) Dubonosov, D. A.; Bren, A. V.; Chernov, V. A. *Russ. Chem. Rev.* **2002**, *71*, 917–927.

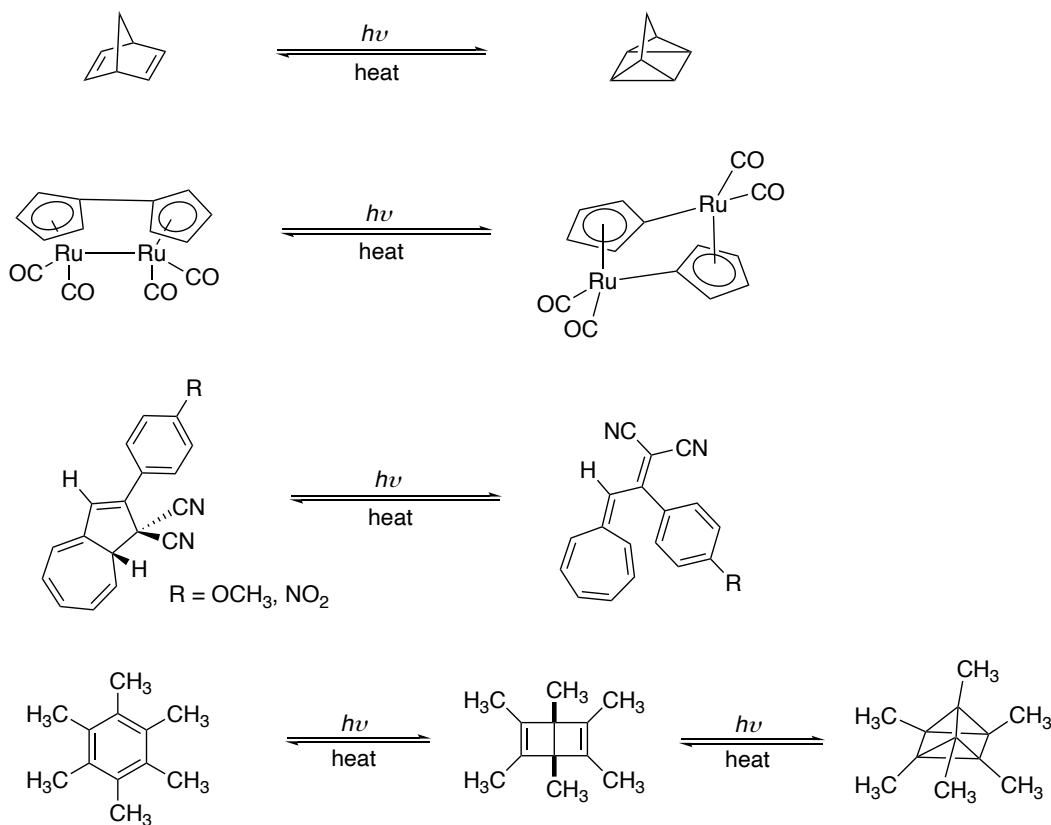
³⁸ a) Caia, V.; Cum, G.; Gallo, R.; Mancini, V.; Pitoni, E.; *Tetrahedron Lett.* **1983**, *24*, 3903–3904. b) Bastianelli, C.; Caia, V.; Cum, G.; Gallo, R.; Mancini, V. *J. Chem. Soc. Perkin Trans.* **1991**, *2*, 679–683. c) Kolpak, A. M.; Grossman, J. C. *Nano Lett.* **2011**, *11*, 3156–3162. d) Feng, Y.; Liu, H.; Luo, W.; Liu, E.; Zhao, N.; Yoshino, K.; Feng, W. *Sci. Rep.* **2013**, *3*, 3260 e) Kucharski, T. J.; Ferralis, N.; Kolpak, A.M.; Zheng, J. O.; Nocera, D.G.; Grossman, J. C. *Nat. Chem.* **2014**, *6*, 441–447.

³⁹ Stein, G. *Irs. J. Chem.* **1975**, *14*, 213–225.

⁴⁰ a) Gray, V.; Lennartson, A.; Ratanalert, P.; Börjesson, K.; Moth-Poulsen, K. *Chem. Commun.* **2014**, *50*, 5330–5332. b) Yoshida, Z.-I. *J. Photochem.* **1985**, *29*, 27–40.

⁴¹ a) Moth-Poulsen, K.; Coso, D.; Börjesson, K.; Vinokurov, N.; Meier, S.; Majumdar, K.; Vollhardt, K. P. C.; Segalman, R. A. *Energy Environ. Sci.* **2012**, *5*, 8534–8537. b) Lennartson, A.; Moth-Poulsen, K. *J. Fluorine Chem.* **2014**, *161*, 24–28. c) Börjesson, K.; Dzebo, D.; Albinsson, B.; Moth-Poulsen, K. *J. Mater. Chem. A* **2013**, *1*, 8521–8524. d) Kanai, Y.; Srinivasan, V.; Meier, S. K.; Vollhardt, K. P. C.; Grossman, J. C. *Angew. Chem. Int. Ed.* **2010**, *49*, 8926–8929. e) Harpham, M. R.; Nguyen, S. C.; Hou, J.; Z. C. Grossman, C.; Harris, B.; Mara, M.W.; Stickrath, A. B.; Kanai, Y. A.; Kolpak, M.; Lee, D.; Liu, D.-J.; Lomont, J. P.; Moth-Poulsen K.; Vinokurov, L.; Chen, N. X.; Vollhardt, K. P. C. *Angew. Chem. Int. Ed.* **2012**, *51*, 7692–7696.

dihydroazulene/vinylheptafulvene,⁴² and hexamethyl-benzene (HMB), which undergoes photoisomerization to hexamethyl Dewar benzene (HMDB) and hexamethyl prismane,⁴³ are considered as potential MOST systems (Scheme 1.9).



Scheme 1.9. Valence isomer pairs studied in the context of energy storage

Of particular interest in this regard, we turned our attention to transitional metal catalyst that could promote the retro-isomerization efficiently at room temperature, thereby providing a proof-of-concept of the potential utility of 1,2-azaborine valence isomer pair

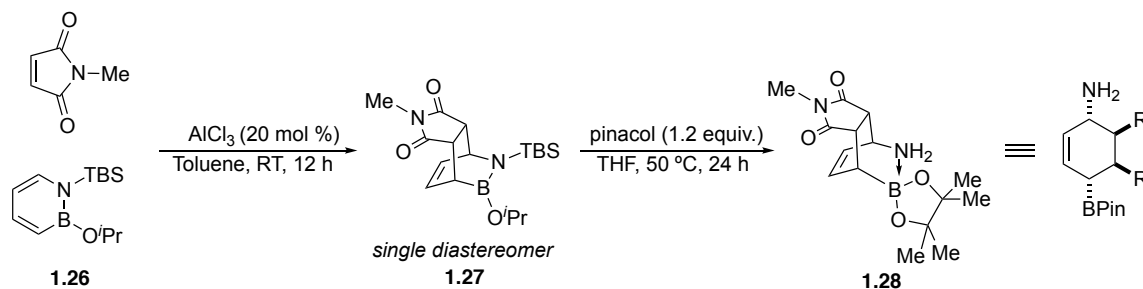
⁴² a) Daub, J.; Knöchel, T.; Mannschreck, A. *Angew. Chem. Int. Ed.* **1984**, *23*, 960–961. b) Abedi, M.; Pápai, M.; Mikkelsen, K. V.; Henriksen, N. E.; Møller, K. B. *J. Phys. Chem. Lett.* **2019**, *10*, 3944–3949.

⁴³ a) Schaefer, W.; Hellmann, H. *Angew. Chem. Int. Ed. Engl.* **1967**, *6*, 518–525. b) Hogeveen, H.; Volger, H. C. *Chem. Commun.* **1967**, 1133–1134. c) Adam, W.; Chang, J. C. *Int. J. Chem. Kinet.* **1969**, *1*, 487–492.

in molecular solar thermal system applications. Detailed results will be discussed in section 1.2.

1.1.4 1,2-Azaborines as 4C+1B+1N Synthons

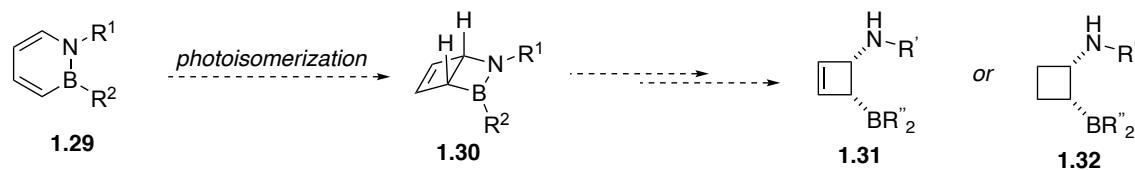
With solution-phase photoisomerization of 1,2-azaborines established, we aimed to further explore the synthetic utility of the Dewar photoisomer. In 2015, the Liu group reported the first example of [4+2] cycloaddition of 1,2-azaborines.²⁵ Specifically, *N*-TBS-*B*-*O*^{*i*}Pr-1,2-azaborine **1.26** undergoes irreversible Diels–Alder reaction with electron-deficient dienophiles such as *N*-methylmaleimide to afford the Diels–Alder adduct **1.27** as a single diastereomer, further B–N bond alcoholysis of **1.27** yields formally 1,4-aminoborylated cyclohexene derivative **1.28** (Scheme 1.10). This report is arguably the first investigation of 1,2-azaborines as 4C+1N+1B synthons in organic synthesis.



Scheme 1.10. 1,2-Azaborine as a 4C+1N+1B synthon: Diels–Alder reaction

We envisioned that 1,2-azaborines could serve as synthons to access four-member ring motifs based on the framework of 1,2-azaborines photoisomerization. Specifically, given the relative lability of the B–N bond, the Dewar isomer **1.30** would lead to a vicinal aminoborylated cyclobutene **1.31** or cyclobutane **1.32** (Scheme 1.11). Considering the

limited methods to access functionalized cyclobutene or cyclobutane core in general,^{44,45} the achievement this hypothesis would likely prove a valuable addition to the toolkits of construction four-membered carbocycles.



Scheme 1.11. Proposed access to 1,2-aminoborylated four-membered ring motif

1.1.5 Stereoselective Synthesis of Cyclobutanes

Cyclobutanes are prevalent structural motifs found in many natural products.⁴⁶ Moreover, cyclobutane motifs are gaining more interests in medicinal chemistry due to their structural rigidity.⁴⁷ In contrast, the occurrence of cyclobutanes in marketed drugs is rare compared to the high prevalence of cyclohexane, cyclopentane, and cyclopropane motifs.^{45c,48} One major reason is arguably due to the synthetic challenge of constructing

⁴⁴ for select reviews of substituted cyclobutene synthesis, see: a) Gauvry, N.; Lescop, C.; Huet, F. *Eur. J. Org. Chem.* **2006**, 5207–5218. b) Luparia, M.; Audisio, D.; Maulide, N. *Synlett* **2011**, 735–740. c) Misale, A.; Niyomchon, S.; Maulide, N. *Acc. Chem. Res.* **2016**, *49*, 2444–2458.

⁴⁵ for select reviews of substituted cyclobutane synthesis, see: a) Alcaide, B.; Almendros, P.; Aragoncillo, C. *Chem. Soc. Rev.* **2010**, *39*, 783–816. b) Hong, Y. J.; Tantillo, D. J. *Chem. Soc. Rev.* **2014**, *43*, 5042–5050. c) Gutekunst, W. R.; Baran, P. S. *J. Org. Chem.* **2014**, *79*, 2430–2452 d) Xu, Y.; Conner, M. L.; Brown, M. K. *Angew. Chem., Int. Ed.* **2015**, *54*, 11918–11928. e) Poplata, S.; Troster, A.; Zou, Y. Q.; Bach, T. *Chem. Rev.* **2016**, *116*, 9748–9815. f) Wang, M.; Lu, P. *Org. Chem. Front.*, **2018**, *5*, 254–259. g) Wen, K. G.; Peng, Y. Y.; Zeng, X. P. *Org. Chem. Front.* **2020**, *7*, 2576–2597.

⁴⁶ a) Dembitsky, V. M. *J. Nat. Med.* **2008**, *62*, 1–33. b) Beniddir, M. A.; Evanno, L.; Joseph, D.; Skiredj, A.; Poupon, E. *Nat. Prod. Rep.* **2016**, *33*, 820–842. c) Fan, Y. Y.; Gao, X. H.; Yue, J. M. *Sci China Chem*, **2016**, *59*, 1126–1141. d) Hancock, E. N.; Brown, M. K. *Chem. - Eur. J.* **2021**, *27*, 565–576.

⁴⁷ The introduction of a cyclobutane fragment is often used to achieve a conformational restriction. Meanwhile, unlike a double bond or a cyclopropane unit, the cyclobutane ring does not disturb the electronic properties. For selective examples, see: a) Radchenko, D. S.; Pavlenko, S. O.; Grygorenko, O. O.; Volochnyuk, D. M.; Shishkina, S. V.; Shishkin, O. V.; Komarov, I. V. *J. Org. Chem.* **2010**, *75*, 5941–5952. b) Feskov, I. O.; Chernykh, A. V.; Kondratov, I. S.; Klyachina, M.; Daniliuc, C. G.; Haufe, G. *J. Org. Chem.* **2017**, *82*, 12863–12868.

⁴⁸ McGrath, N. A.; Brichacek, M.; Njardarson, J. T. *J. Chem. Ed.* **2010**, *87*, 1348–1349.

cyclobutane scaffolds especially in a regio- and stereo-selective manner.^{45c,49} To address this challenge, [2+2] cycloaddition between alkenes is considered as the most direct approach.^{45e} Many recent advances in [2+2] cycloaddition have been focused on visible light photocatalysis as showcased by the two representative examples in Scheme 1.12a.⁵⁰ In particular, Yoon's group using chiral Lewis acid catalyst and photo-sensitizer to achieve enantioselective [2+2] cycloadditions between two olefins.^{50a} Despite the impressive progress, typical challenges for [2+2] photo-cycloaddition approach still remain, such as the selection between homo- and hetero-dimerization, the orientation of olefin during cyclization, and stereo-control could be even more challenging with potential *E/Z* olefin isomerization (Scheme 1.12b).^{45e} Besides [2+2] cycloaddition (Scheme 1.13, approach a), various other approaches have been developed to access cyclobutane derivatives stereoselectively (Scheme 1.13), such as ionic cyclization (approach b),⁵¹ ring contraction reaction from pyrrolidines (approach c),⁵² and Wagner-Meerwein shifts of cyclopropanols (approach d).⁵³ An alternative logic that has been flourishing recently is to construct a highly versatile cyclobutane core which could be further functionalized to access structurally diverse cyclobutanes (approach e).⁵⁴

⁴⁹ Scholz, S. O.; Kidd, J. B.; Capaldo, L.; Flikweert, N. E.; Littlefield, R. W.; Yoon, T. P. *Org. Lett.* **2021**, *23*, 3496–3501.

⁵⁰ For selected reviews, see: reference 42d, 42e. For selected examples, see: a) Blum, T. R.; Miller, Z. D.; Bates, D. M.; Guzei, I. A.; Yoon, T. P. *Science*. **2016**, *354*, 1391–1395. b) Zhao, J.; Brosmer, J. L.; Tang, Q.; Yang, Z.; Houk, K. N.; Diaconescu, P. L.; Kwon, O. *J. Am. Chem. Soc.* **2017**, *139*, 9807–9810.

⁵¹ For selected examples, see: a) Panish, R.; Chintala, S. R.; Boruta, D. T.; Fang, Y.; Taylor, M. T.; Fox, J. M. *J. Am. Chem. Soc.* **2013**, *135*, 9283–9286. b) Wang, Y.-M.; Bruno, N. C.; Placeres, A. L.; Zhu, S.; Buchwald, S. L. *J. Am. Chem. Soc.* **2015**, *137*, 10524–10527. c) Zhao, N.; Yin, S. Q.; Xie, S. L.; Yan, H.; Ren, P.; Chen, G.; Chen, F.; Xu, J. *Angew. Chem., Int. Ed.* **2018**, *57*, 3386–3390. d) Shu, C.; Noble, A.; Aggarwal, V. K. *Angew. Chem., Int. Ed.* **2019**, *58*, 3870–3874.

⁵² Hui, C.; Brieger, L.; Strohmam, C.; Antonchick, A. P. *J. Am. Chem. Soc.* **2021**, *143*, 18864–18870.

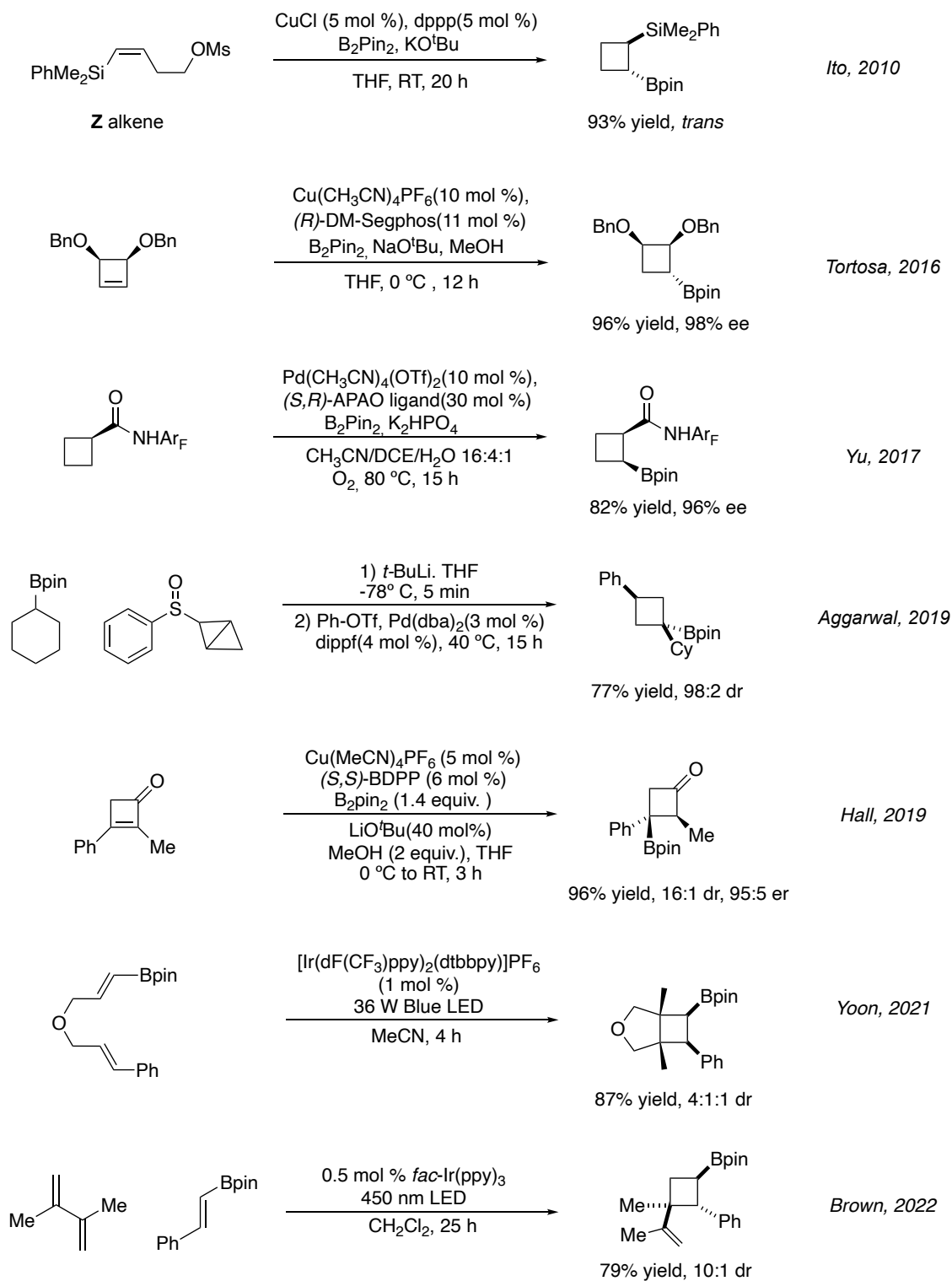
⁵³ Kleinbeck, F.; Toste, F. D. *J. Am. Chem. Soc.* **2009**, *131*, 9178–9179.

⁵⁴ Martín-Heras, V.; Parra, A.; Tortosa, M. *Synthesis*. **2018**, *50*, 470–484.

Within the context of constructing a highly versatile cyclobutane core (approach e), stereo-defined cyclobutylboronic esters are of particular interest since they present high configurational stability at the C–B bonds and provide a powerful synthetic handle for further transformations that are stereospecific or stereoselective.⁵⁵ The representative state of the art in stereoselective synthesis of cyclobutylboronic esters are shown in Scheme 1.14,^{49,56} including: ring-closure approach from the Ito group; desymmetrization approach from the Tortosa group; directed C–H activation strategy from the Yu group; bicyclobutanes strain release strategy from the Aggarwal group; conjugate borylation from the Hall group as well as photosensitized [2+2] cycloaddition from the Yoon group and the Brown group. Despite the recent progress, the development of novel and versatile routes to access cyclobutane scaffolds remain to be significant. To this end, we found our proposed approach (Scheme 1.11, see page 20) quite appealing as it features a stereospecific photoisomerization hypothetically leading to aminoborylated cyclobutanes bearing the *cis* configuration, which is not easily accessible by any other methods. Detailed discussion will be disclosed in section 1.3.

⁵⁵ Sandford, C.; Aggarwal, V. K. *Chem. Commun.* **2017**, *53*, 548–5494.

⁵⁶ a) Ito, H.; Toyoda, T.; Sawamura, M. *J. Am. Chem. Soc.* **2010**, *132*, 5990–5992. b) Guisán-Ceinos, M.; Parra, A.; Martín-Hetas, V.; Tortosa, M. *Angew. Chem. Int. Ed.* **2016**, *55*, 6969–6972; c) He, J.; Shao, Q.; Wu, Q.; Yu, J.-Q. *J. Am. Chem. Soc.* **2017**, *139*, 3344–3347. d) Fawcett, A.; Biberger, T.; Aggarwal, V. K. *Nat. Chem.* **2019**, *11*, 117–122. e) Clement, H. A.; Boghi, M.; McDonald, R. M.; Bernier, L.; Coe, J. W.; Farrell, W.; Helal, C. J.; Reese, M. R.; Sach, N. W.; Lee, J. C.; Hall, D. G. *Angew. Chem. Int. Ed.* **2019**, *58*, 18405–18409. f) Liu, Y.; Ni, D.; Stevenson, B. G.; Tripathy, V.; Braley, S. E.; Raghavachari, K.; Swiek, J. R.; Brown, M. K. *Angew. Chem. Int. Ed.* **2022**, *61*, e202200725 (early view).



Scheme 1.14 Stereoselective synthesis of cyclobutylboronic esters

1.2 Rhodium-catalyzed Ring-opening Reaction of the Dewar Photoisomer to Form 1,2-Azaborines

1.2.1 Potential Utility of 1,2-Azaborine Valence Isomer Pairs in Solar Energy Storage

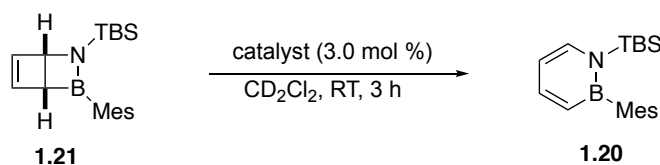
(Portions of this sub-chapter have appeared in the following publication: Edel, K.; Yang, X.; Ishibashi, J. S. A.; Lamm, A. N.; Maichle-Mössmer, C.; Giustra, Z. X.; Liu, S.-Y.; Bettinger, H. F. "The Dewar Isomer of 1,2-dihydro-1,2-azaborinines: Isolation, Fragmentation, and Energy Storage" *Angew. Chem. Int. Ed.* **2018**, *57*, 5296–5300.)

1.2.1.1 Catalysts Survey for Ring-opening Retro-isomerization Reaction

We hypothesized that the double bond of our Dewar azaborine could bind to a metal complex thereby interfering with the uncatalyzed pathway of ring-opening reaction to form the azaborine. If such binding could lower the activation barrier of rate-determining step, it could potentially promote the retro-isomerization without heating. We began our investigation by treating the Dewar substrate **1.21** with various transition metal catalysts⁵⁷ and Lewis acid catalysts⁵⁸ in solution, which are known to form π -complex with alkenes. As shown in Table 1.2, Wilkinson's catalyst was found to be uniquely effective, furnishing **1.20** from **1.21** cleanly within 1 hour at room temperature with 3.0 mol% of catalytic loading (entry 7). Compared to Rh-based Wilkinson's catalyst, other metal catalysts were either not effective (less than 15% conversion after 3 hours) or not active at all.

⁵⁷ a) Crabtree, R. H. *The Organometallic Chemistry of The Transition Metals*, 7th Edition, WILEY Publishing, **2019**, pp.121–145. b) Premkumar, J. R.; Vijay, D. V.; Sastry, G. N. *Dalton Trans*, **2012**, *41*, 4965–4975.

⁵⁸ a) Song, Y.-S.; Yoo, B. R.; Lee, G.-H.; Jung, N. I. *Organometallics*, **1999**, *18*, 3109–3115. b) Penafiel, J.; Maron, L.; Harder S. *Angew. Chem. Int. Ed.* **2015**, *54*, 201–206.



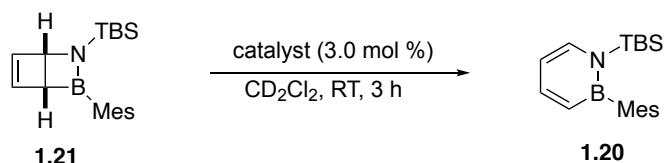
entry	catalyst	conversion (%) ^a
1	(Cy ₃ P) ₂ (PhCH)RuCl ₂	15%
2	[Ir(cod)Cl] ₂	12%
3	Ni(CO) ₂ (PPh ₃) ₂	0%
4	IPrAuCl	0%
5	Pt(PPh ₃) ₄	5%
6	Pd(PPh ₃) ₄	0%
7	RhCl(PPh₃)₃	100%^b
8	AgOTf	2%
9	ZnCl ₂	0%
10	Sc(OTf) ₃	0%
11	no catalyst	0%

^aDetermined by ¹H NMR integration based on 1,3,5-trimethoxybenzene as internal standard.

^bFull conversion to azaborine was observed within 1h.

Table 1.2. Initial survey of various transition metal catalysts and Lewis acid catalysts

More detailed screening of rhodium-based catalysts was therefore carried out. As revealed in Table 1.3, [Rh(C₂H₄)₂Cl]₂ served as an equally effective catalyst (entry 2), whereas more hindered cyclooctadiene- or norbornadiene-containing analogues proved to be not effective (entry 3-4). Moreover, cationic Rh(I) species (entry 5-6) as well as Rh(III) complex (entry 7) were not suitable for ring-opening retro-isomerization.



entry	catalyst	conversion (%) ^a
1	RhCl(PPh₃)₃	100%^b
2	[Rh(C₂H₄)₂Cl]₂	100%^b
3	[Rh(nbd)Cl] ₂	2%
4	[Rh(cod)Cl] ₂	3%
5	(nbd) ₂ RhBF ₄	0%
6	[Rh(cod)(PPh ₃) ₂]PF ₆	2%
7	[Rh(Cp [*])Cl] ₂	0%
8	Rh(nbd)(PPh ₃)Cl Polymer	1%

^aDetermined by ¹H NMR integration based on 1,3,5-trimethoxybenzene as internal standard.

^bFull conversion to azaborine was observed within 1h.

Table 1.3. Screening of various Rh-based catalysts

1.2.1.2 Reaction Calorimetry Study

With the optimal catalytic system established, we aimed to determine the energy stored in the strained Dewar photoisomer **1.21**. The heat of the ring-opening reaction was measured in a reaction calorimeter. The integration of the heat-flow curve of the ring-opening reaction catalyzed by the Wilkinson catalyst (3.0 mol %) gave consistently ΔH of -47.6 ± 1.0 kcal/mol (Figure 1.6). This value agrees with our DFT computations³⁴ and compares favorably to those of other known molecular solar thermal (MOST) systems: the measured reaction enthalpy for the norbornadiene/quadracyclane system (Scheme 1.9 top, see page 18) is $\Delta H = -21$ kcal/mol;⁵⁹ $\Delta H = -20$ kcal/mol for the fulvalene diruthenium system (Scheme 1.9 bottom, see page 18).^{41d} Combined with the discovery that irradiation of 1,2-azaborine in cyclohexane solution leads to full conversion and exclusive formation

⁵⁹ An, X.-W.; Xie Y.-D. *Thermochim. Acta* **1993**, *220*, 17–25.

of Dewar valence isomer with high quantum yield ((46±8) % with 284 nm light source),³⁶ this calorimetry study provides a proof of concept of the potential utility of 1,2-azaborine valence isomer pair in molecular solar thermal system applications. Future efforts would be directed toward tuning the absorption profile of our system to the visible light range and investigating immobilized catalysts for practical applications.

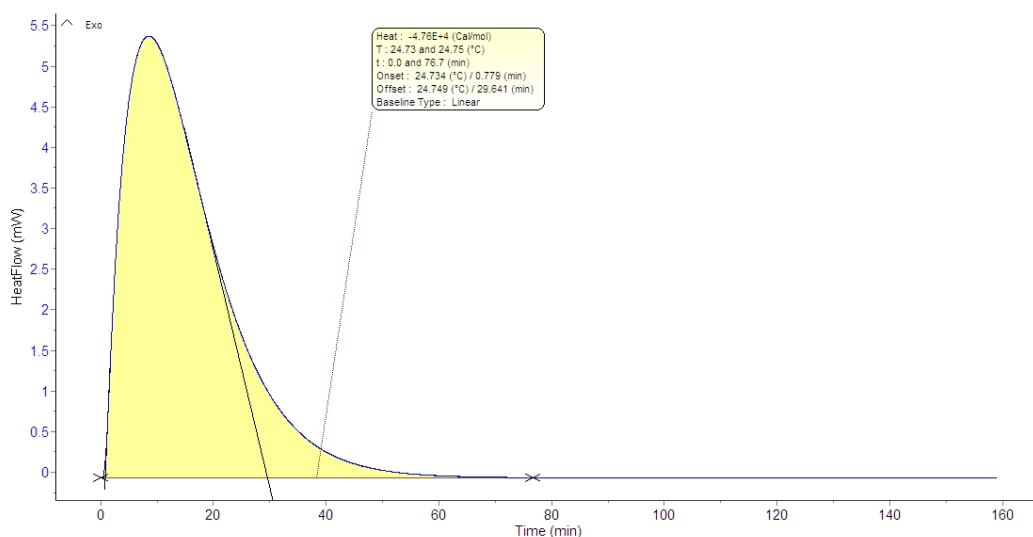


Figure 1.6. A representative heat-flow trace (after integration, the average value of ΔH is -47.6 kcal/mol, with a standard deviation of ± 0.968 kcal/mol)

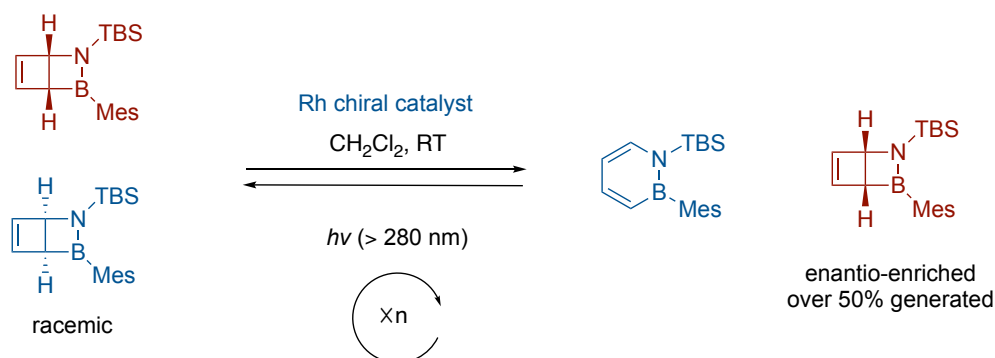
1.2.2 Accessing Enantioenriched Dewar Photoisomers via Kinetic Resolution⁶⁰

1.2.2.1 Proposed Mechanisms and Discussion

Inspired by the discovery that certain Rh-based catalysts could efficiently catalyze the retro-isomerization of the Dewar isomer, we envisioned that we could potentially use chiral Rh-based catalysts to kinetically resolve the two Dewar enantiomers, leaving one isomer enantio-enriched. Considering that the resulting azaborines could again be photo-

⁶⁰ The contents of this section are unpublished work.

isomerized to generate the racemic Dewar isomers, we could in theory apply such kinetic resolution strategy continuously in the presence of light and chiral catalysts, which could overcome the limitation of maximum 50% yield in a typical kinetic resolution reaction (Scheme 1.15).⁶¹



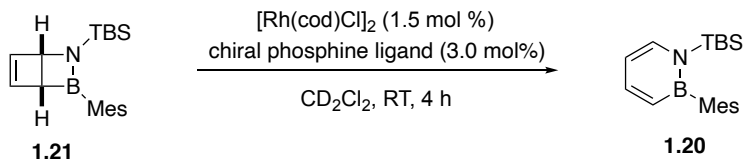
Scheme 1.15. Proposed strategy: novel continuous kinetic resolution strategy affording the enantio-enriched Dewar isomer

Our initial efforts began with the catalyst screening of different types of privileged chiral ligands,⁶² aiming to find the most selective chiral ligand in a typical kinetic resolution scenario without applying the light. The selective factor could be calculated via Kagan's equation ($s = \frac{k_R}{k_S} = \frac{\log [(1-c)(1-ee)]}{\log [(1-c)(1+ee)]}$) suitable for first order kinetics. After a survey of ligands, we typically found that bidentate phosphine based chiral ligands offered varied reactivity and selectivity (for some representative examples, see Table 1.4). So far, the most effective ligand is chiral DIOP ligand with moderate selectivity factor around 3.

⁶¹ a) Keith, J. M.; Larrow, J. F.; Jacobsen, E. N. *Adv. Synth. Catal.* **2001**, *343*, 5–26. b) Vedejs, E; Jure. M. *Angew. Chem. Int. Ed.* **2005**, *44*, 3974–4001.

⁶² a) Yoon, T. P.; Jacobsen, E. N. *Science*, **2003**, *299*, 1691–1693. b) Brown, J G. *Organometallics* **2014**, *33*, 5912–5923. c) Müller, D. J.; Schlepphorst C.; Glorius, F. *Chem. Soc. Rev.*, **2017**, *46*, 4845–4854.

Table 1.4. Initial investigation of bidentate chiral phosphine ligands



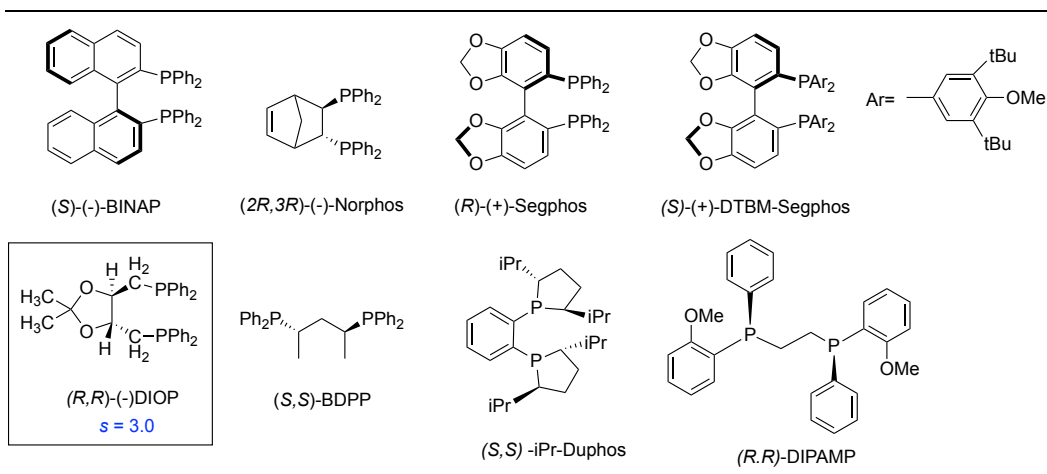
entry	chiral ligand	conversion (%) ^a	ee ^b	S ^c
1	(S)-(-)-BINAP	15%	3%	1.5
2	(2 <i>R</i> ,3 <i>R</i>)-(-)-Norphos	7%	1%	1.3
3	(<i>R</i>)-(+)-Segphos	23%	11%	2.7
4	(<i>S</i>)-(+)-DTBM-Segphos	13%	6%	2.4
5	(<i>R</i> , <i>R</i>)-(-)-DIOP ^d	48%	37%	3.0
6	(<i>S</i> , <i>S</i>)-BDPP ^d	95%	9%	1.1
7	(<i>S</i> , <i>S</i>)-iPr-Duphos	61%	36%	2.3
8	(<i>R</i> , <i>R</i>)-(-)-DIPAMP ^d	98%	16%	1.1

^aDetermined by ¹H NMR integration.

^bMeasured by HPLC (OD-H column, 0.1% / 99.9% isopropanol/hexanes).

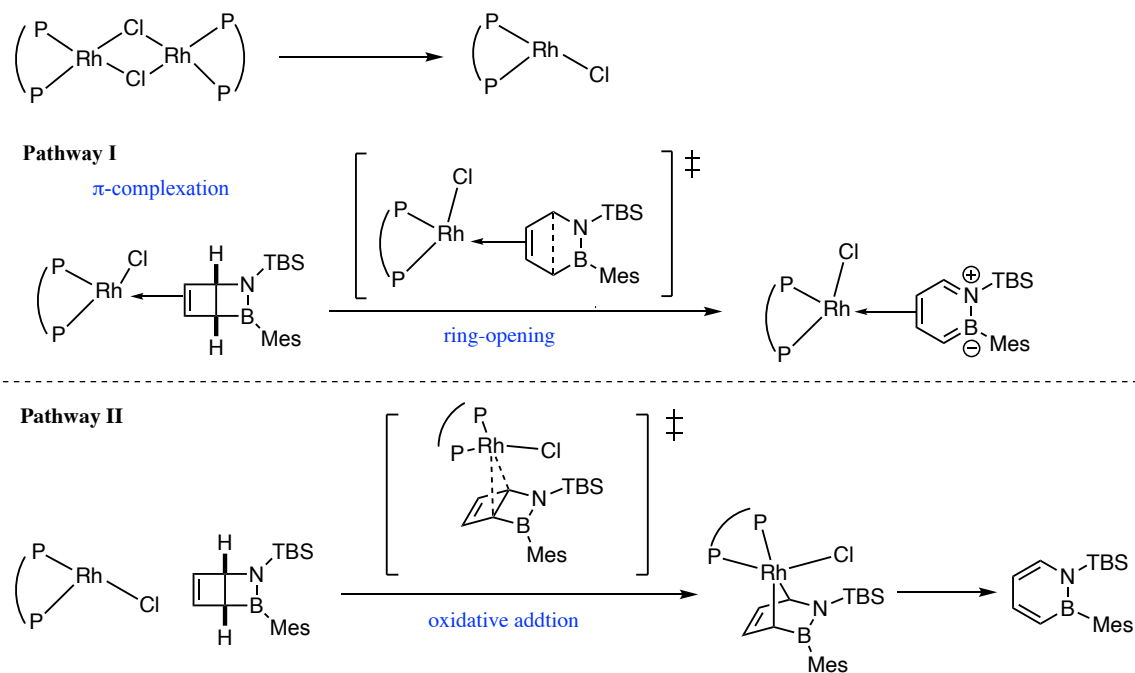
^cCalculated via Kagan's equation.

^dReaction stopped at 1.5 hours.



Meanwhile, we believe that a better understanding of the reaction mechanism would be helpful to chiral ligand design, therefore we carried out computational studies and some kinetic experiments to elucidate the mechanism. We proposed two possible pathways (Scheme 1.16): in the first pathway, the Rh-monomer is proposed to facilitate ring-opening via formation of π -complex with the substrate in the resting state and the

transition state; the second pathway involves oxidative insertion into the bridge-head C–C bond. Our collaborators carried out DFT calculations which showed that the ring-opening pathway I is favored.⁶³ In addition, kinetic experiments reveal a 1st order dependence on the Dewar substrate and half order of the Rh catalyst, indicating that the Rh dimer is likely to be the resting state. At this moment, continued effort toward DFT calculations are underway to corroborate experimental kinetic data and to try using DIOP ligand to build the stereo-chemical model in the diastereomeric transition state, which hopefully could help us to design more selective DIOP derivatives or other types of chiral ligands.



Scheme 1.16. Two proposed pathways for Rh-catalyzed retro-isomerization

⁶³ DFT calculations: calculated by Walid Lamine from University of Pau and Pays de l'Adour (E2S-UPPA) using SMD(CH₂Cl₂)-B3LYP-GD3BJ//B3LYP/SDD+f(Rh)-6-31G**

1.3 Accessing *cis*-Aminoborylated Cyclobutanes and Further Derivatizations

(Portions of this chapter have appeared in the following publication: Giustra, Z. X.*; Yang, X.*; Chen, M.; Bettinger, H. F.; Liu, S.-Y. "Accessing 1,2-Substituted Cyclobutanes through 1,2-Azaborine Photoisomerization" *Angew. Chem. Int. Ed.* **2019**, *58*, 18918–18922.)

1.3.1 Modifications of 1,2-Azaborines and Photoisomerization in Flow

In addition to the discovery of retro-isomerization reaction, we also endeavored to develop a way to furnish aminoborylated cyclobutanes based on the framework of 1,2-azaborine photoisomerization, especially considering the lack of general methods to access such motif with effective stereo-control.

The original solution-phase 1,2-azaborine photoisomerization experiments were conducted in standard J. Young NMR tubes under irradiation from a high-pressure mercury lamp.⁶⁴ Although this particular setup was suitable for milligram-scale reaction, it was deemed ill-suited for carrying out synthesis of the photoisomer in the substantially greater quantities needed to facilitate the further derivatization study. Simple adjustment by increasing the size of the reaction vessel was anticipated to lead to decreased reaction efficiency as a consequence of diminished relative depth of light penetration into the reaction medium.⁶⁴ For the desired scale-up of the photoisomerization reaction, we thus considered it would be more advantageous to optimize the conditions for a continuous-flow reactor configuration instead.⁶⁵ An apparatus suitable for this purpose was assembled

⁶⁴ Gauvry, N.; Huet, F. *J. Org. Chem.* **2001**, *66*, 583–588.

⁶⁵ For representative reviews of flow photochemistry, see: a) Knowles, J. P.; Elliott, L. D.; Booker-Milburn, K. I. *Beilstein J. Org. Chem.* **2012**, *8*, 2025–2052. b) Su, Y.; Straathof, N. J. W.; Hessel, V.; Noël, T. *Chem.*

in accordance with Berry and Booker-Milburn's general design.^{66,67} Practically, we have our UV-transmissive tubing circled around the quartz glass cylinder with cooling water pass through to maintain the temperature. The compound is continuously injected by a syringe pump into the tube which is irradiated by a medium-pressure mercury lamp, locating in the middle of the quartz cylinder. The reaction outflow was continuously collected into a vial with N₂ protection. (see Experiment Section for full details)

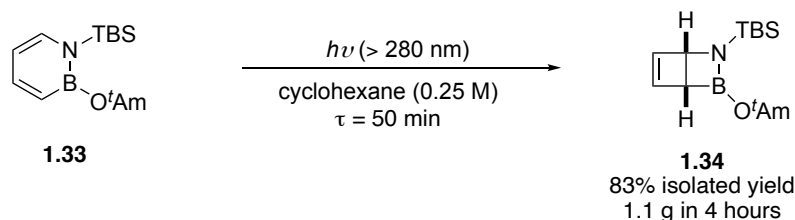
Along with the above change in photoreactor type, we also chose to modify the 1,2-azaborine substrate from those studied previously³⁶ to better align with our main objective of developing a post-isomerization cyclobutane derivatization sequence. Specifically, *tert*-amyloxy-substituted **1.33** was selected to maintain strong steric shielding of the corresponding photoisomer while still allowing subsequent ligand exchange at the boron center that would lead to a boronic ester. Solutions of **1.33** in cyclohexane were thus injected into the flow photoreactor to determine a combination of concentration and reactor residence time (τ) that would afford complete conversion comparable to that of the original NMR experiments. Since the two variables share an inverse relationship in this regard, i.e., higher concentrations require longer residence times and vice versa, we compromised between maximizing concentration and minimizing residence time and settled on $\tau = 50$

Eur. J. **2014**, *20*, 10562–10589. c) Cambié, D.; Bottecchia, C.; Straathof, N. J. W.; Hessel, V.; Noël, T. *Chem. Rev.* **2016**, *116*, 10276–10341.

⁶⁶ The apparatus set-up largely contributed by Dr. Zachary Xavier Giustra. For reference of original set-up from Barry and Booker-Milburn, see: Hook, B. D. A.; Dohle, W.; Hirst, P. R.; Pickworth, M.; Berry, M. B.; Booker-Milburn, K. I. *J. Org. Chem.* **2005**, *70*, 7558–7564.

⁶⁷ For recent applications using similar set-up, see: a) Gutierrez, A. C.; Jamison, T. F. *J. Flow Chem.* **2011**, *1*, 24–27. b) Maskill, K. G.; Knowles, J. P.; Elliott, L. D.; Alder, R. W.; Booker-Milburn, K. I. *Angew. Chem. Int. Ed.* **2013**, *52*, 1499–1502. c) Wojcik, F.; Lei, S.; O'Brien, A. G.; Seeberger, P. H.; Hartmann, L. *Beilstein J. Org. Chem.* **2013**, *9*, 2395–2403. d) Wojcik, F.; O'Brien, A. G.; Götze, S.; Seeberger, P. H.; Hartmann, L. *Chem. Eur. J.* **2013**, *19*, 3090–3098. e) Willumstad, T. P.; Haze, O.; Mak, X. Y.; Lam, T. Y.; Wang, Y.-P.; Danheiser, R. L. *J. Org. Chem.* **2013**, *78*, 11450–11469.

min for substrate solutions of 0.25 M. Following this protocol, the 5 mL test reactor enabled the formation of ~1.2 mmol of photoisomer **1.34** per hour cleanly (1.1 g in 4 hours) with a typical isolated yield of 83% (Scheme 1.17).



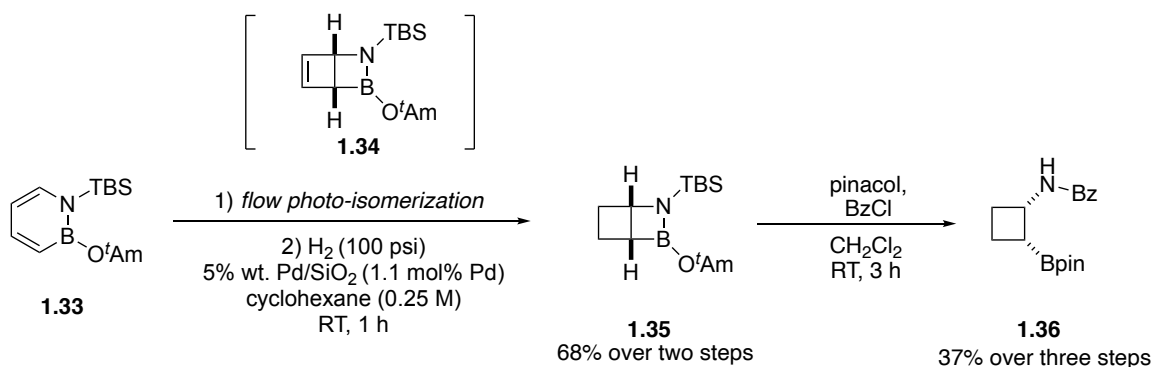
Scheme 1.17. Photoisomerization of 1,2-azaborine **1.33** in flow.

1.3.2 Diastereoselective Synthesis of Highly Substituted Aminoborylated Cyclobutanes

With sizeable quantities of **1.34** in hand, we subjected the photoisomer to catalytic hydrogenation to reduce the all-carbon ring of the bicycle to a cyclobutane. Since this reaction proceeded equally well using the crude cyclohexane solution of **1.34** obtained directly from the photoreactor, the two processes were generally telescoped to prepare azaborabicyclohexane **1.35** in 68% yield over two steps. Simultaneous addition of pinacol and benzoyl chloride led to the desired B–N bond dissociation with concomitant exchange of the nitrogen protecting group,⁶⁸ furnishing the more robust benzamidocyclobutyl boronic ester **1.36** (Scheme 1.18).⁶⁹

⁶⁸ Koch, C.; Kahnes, M.; Schülz, M.; Görls, H.; Westerhausen, M. *Eur. J. Inorg. Chem.* **2008**, 1067–1077.

⁶⁹ This sequence was pioneered by Zachary Xavier Giustra.



Scheme 1.18. Synthesis of 1,2-aminoborylated cyclobutane **1.36**

Single crystal X-ray diffraction analysis of **1.36** confirmed the molecule had retained the *cis* relative stereochemistry of the nitrogen and boron groups originally defined by the stereospecific photoisomerization of **1.33** (Figure 1.7).⁷⁰

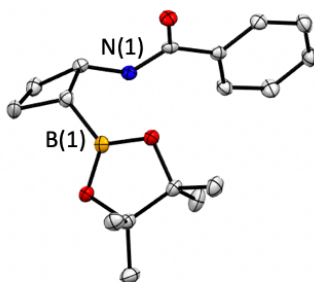
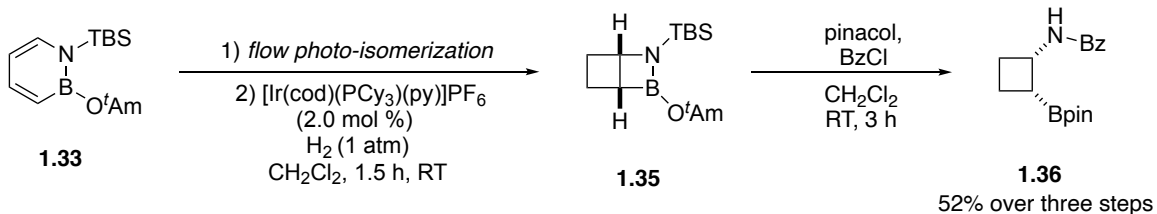


Figure 1.7. ORTEP drawing of **1.36** generated with the program Mercury using single-crystal X-ray diffraction data (hydrogens were omitted for clarity)

Later on, a practically more favorable hydrogenation condition was developed using homogenous Crabtree's catalyst under atmospheric H₂ pressure. Without the need of high-pressure hydrogenation in a Parr-Bomb reactor, the three-step sequence could be

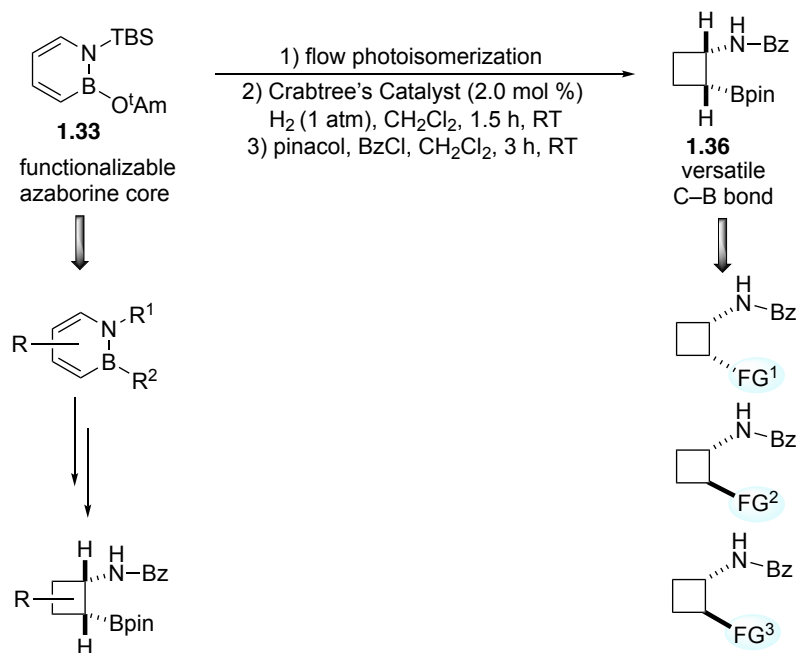
⁷⁰ According to Woodward-Hoffmann rules, 4 π -e⁻ electrocyclic ring closure is allowed to be disrotatory under photochemical conditions.

carried out in one-pot fashion to streamline the cyclobutane synthesis with improved efficiency (Scheme 1.19).



Scheme 1.19. Streamlined synthesis of **1.36** in one pot

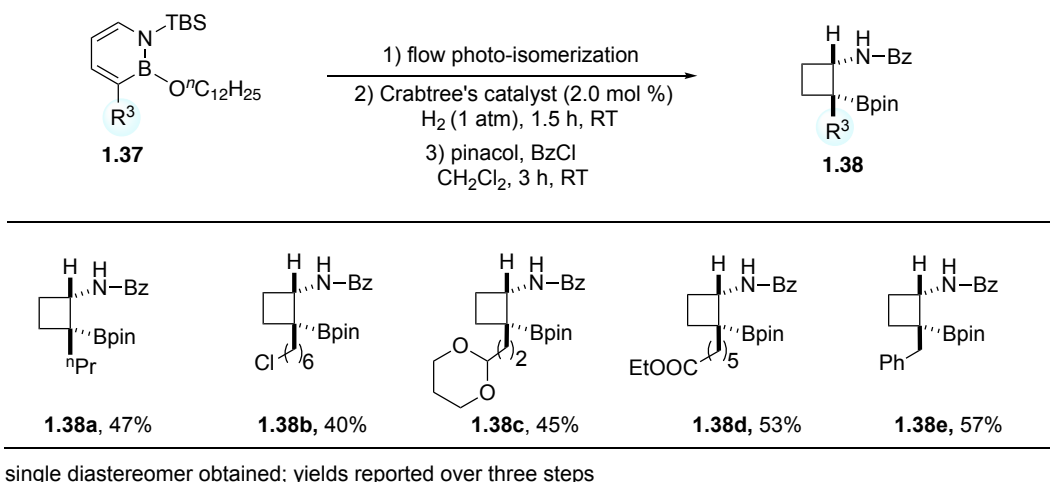
With the optimized protocols established, we aimed to further demonstrate the versatility of our approach. We envisioned that we could functionalize the azaborine core at “early stage”, and the introduced functionalities could potentially be translated to the cyclobutane ring. Furthermore, the C–B bond in the cyclobutane product could serve as a powerful functional handle at “late stage”, which should allow us to access diverse array of cyclobutane derivatives (Scheme 1.20).



Scheme 1.20. Proposed strategy to furnish diverse cyclobutane derivatives

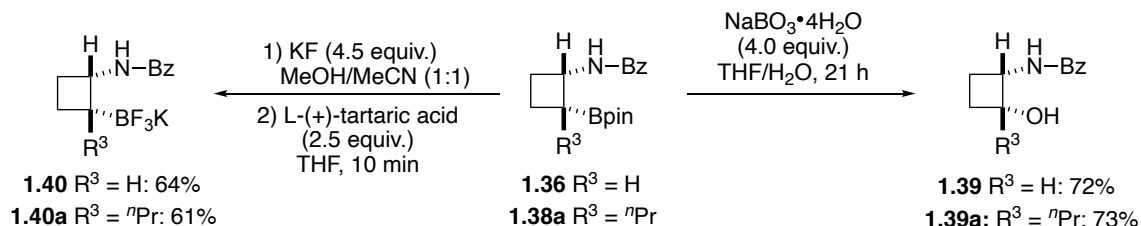
With those ideas in mind, we first tried to functionalize the B–Cl azaborine core **1.8** using recently developed methods from our group. Specifically, bromide was installed onto C3 position selectively via electrophilic aromatic substitution and various substituents were introduced via Negishi cross-coupling.⁷¹ Gratifyingly, C3-substituted 1,2-azaborines **1.37** are also suitable substrates for the photoisomerization, producing highly substituted aminoborylated cyclobutanes **1.38** in a diastereo-selective fashion. As shown in Scheme 1.21, a variety of azaborines **1.37** were applied to the optimized conditions to access aminoborylated cyclobutanes bearing tertiary boronic esters **1.38** (**1.38a–1.38e**). Alkyl chloride (**1.38b**), acetal (**1.38c**), carboxylic acid ester (**1.38d**), and benzyl (**1.38e**) groups are all tolerated, with the corresponding products obtained in moderate yields from the three-step sequence.

⁷¹ Brown, A. N.; Li, B.; Liu, S.-Y. *J. Am. Chem. Soc.* **2015**, *137*, 8932–8935.



Scheme 1.21. Diastereoselective synthesis of aminoborylated cyclobutanes bearing tertiary boronic esters

To further demonstrate the utility of the aminoborylated cyclobutane product, we then explored the transformations of C–B bond for diversity-oriented synthesis at late stage. For instance, mild oxidation^{56b} of **1.36** and **1.38a** can be achieved with complete retention of the *cis* stereochemistry, yielding the *N*-protected cyclobutyl β -amino alcohols **1.39** and **1.39a** (Scheme 1.22). Boronic esters **1.36** and **1.38a** can also be readily converted into potassium trifluoroborate salts **1.40** and **1.40a** using the KF/tartaric acid procedure developed by Lennox and Lloyd-Jones (Scheme 1.22).⁷²



Scheme 1.22. Functionalizations of aminoborylated cyclobutanes

⁷² Lennox, A. J. J.; Lloyd-Jones, G. C. *Angew. Chem. Int. Ed.* **2012**, *51*, 9385–9388.

Additional C–B bond functionalizations can be performed with the secondary aminoborylated cyclobutane **1.36**. For example, silver-catalyzed radical fluorination with Selectfluor generated *trans* amino fluorinated cyclobutanes **1.41** stereoselectively (Scheme 1.23a).⁷³ Compound **1.36** can also undergo Giese type of reaction with methyl vinyl ketone in the presence of Lewis base and iridium dual catalyst under photoredox conditions to produce **1.42** (Scheme 1.23b).⁷⁴ Finally, although Suzuki–Miyaura cross-coupling for arylation of **1.36** directly was unsuccessful, dual iridium photoredox/nickel catalysis⁷⁵ proved effective for the (hetero)arylation of the borate salt **1.40** after some modest modifications of the reported conditions.⁷⁶ As shown in Scheme 1.23c, both phenyl and pyridyl bromides coupled with **1.40** to afford 2-(hetero)arylated amido-cyclobutanes **1.43** in moderate to good yields, with the *trans* diastereomer formed as the major product (see X-ray crystallographic data in experimental section).⁷⁷

⁷³ Li, Z.; Wang, Z.; Zhu, L.; Tan, X.; Li, C. *J. Am. Chem. Soc.* **2014**, *136*, 16439–16443.

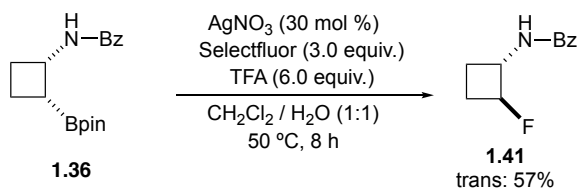
⁷⁴ Lima, F.; Sharma, U. K.; Grunenber, L.; Saha, D.; Johannsen, S.; Sedelmeier, J.; Van der Eycken, E. V.; Ley, S. V. *Angew. Chem. Int. Ed.* **2017**, *56*, 15136–15140.

⁷⁵ For representative review, see: Tellis, J. C.; Kelly, C. B.; Primer, D. N.; Jouffroy, M.; Patel, N. R.; Molander, G. A. *Acc. Chem. Res.* **2016**, *49*, 1429–1439.

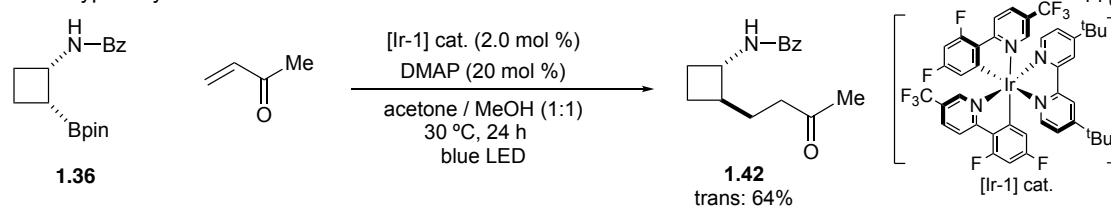
⁷⁶ This chemistry was explored by Zachary Xavier Giustra. For reference, see: Primer, D. N.; Karakaya, I.; Tellis, J. C.; Molander, G. A. *J. Am. Chem. Soc.* **2015**, *137*, 2195–2198.

⁷⁷ For a possible rationale of the stereoselectivity, see: Gutierrez, O.; Tellis, J. C.; Primer, D. N.; Molander, G. A.; Kozłowski, M. C. *J. Am. Chem. Soc.* **2015**, *137*, 4896–4899.

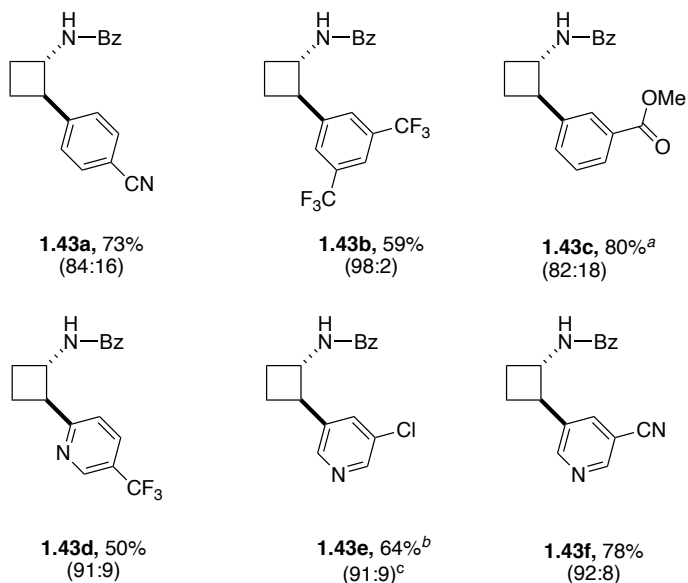
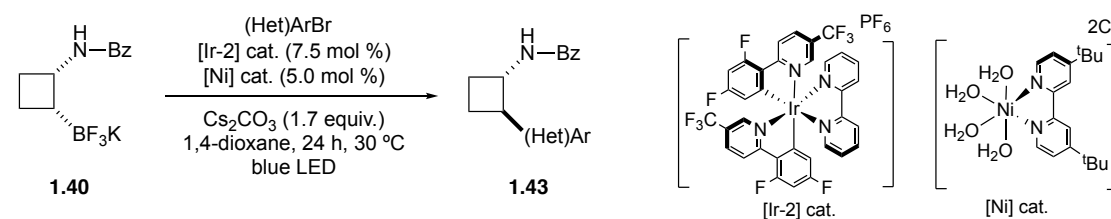
a. Radical fluorination



b. Giese-type alkylation



c. Ir/Ni catalyzed cross-coupling and substrate scope



Values in parentheses are the trans/cis diastereomeric ratios of isolated material.

^aUsing aryl iodide.

^bYield of the isolated trans diastereomer only.

^cFrom ¹H NMR analysis of the crude mixture.

Scheme 1.23. Additional functionalizations of cyclobutyl boronic ester/borate salt

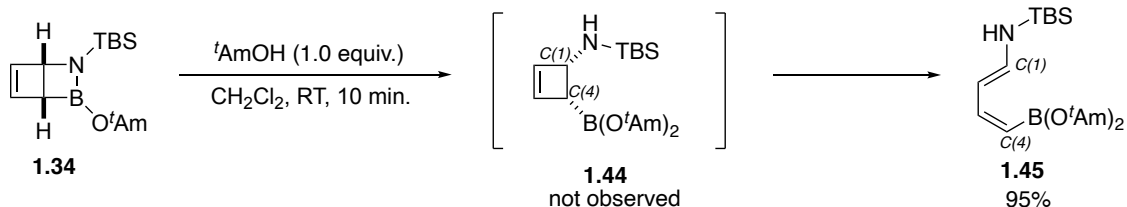
1.3.3 Summary

In summary, we have provided the seminal demonstration of the synthetic utility of the 1,2-azaborine reagent in the preparation of functionalized cyclobutane derivatives. We developed a practically scalable and efficient flow conditions for the regio- and diastereoselective photoisomerization of 1,2-azaborines. This advance supported new exploration of a synthetic route converting the Dewar photoisomer ultimately to a *cis*-1,2-aminoborylated cyclobutane **1.36** and analogues **1.39** bearing quaternary carbon centers. Furthermore, the boron atom in the aminoborylated cyclobutanes serves as a versatile functionalization handle for diversity-oriented synthesis at late stage to access a variety of amino-cyclobutane derivatives.

1.4 Stereospecific Ring-opening of the Dewar Photoisomer to Afford Dienes and Tandem Diels-Alder Reactions

Along with the cyclobutane synthesis, we also attempted to access cyclobutene motif via direct B–N bond cleavage. After treating **1.34** with ^tAmOH (Scheme 1.24), we did not observe the desired formation of cyclobutene **1.44**. Nevertheless, the ¹H NMR spectrum of the crude reaction was fairly clean with multiple peaks in the vinyl region. We reasoned that upon B–N bond cleavage, the cyclobutene ring could undergo ring-opening to afford the diene **1.45**.⁷⁸ The reaction turns out to be quite fast under room temperature, suggesting that the ring opening process is highly favorable from the strained bicyclic Dewar ring to generate a conjugated diene.

⁷⁸ The Woodward–Hoffmann rules allow the conrotatory ring opening of cyclobutenes: a) Woodward, R. B.; Hoffmann, R. *Angew. Chem. Int. Ed. Engl.* **1969**, *8*, 781–853. For comprehensive archive of cyclobutene ring opening reactions, see: b) Murakami, M.; Matsuda, T. Cyclobutene Ring Opening Reactions. Knöchel, P. *Comprehensive Organic Synthesis, 2nd Edition*, Elsevier, **2014**, 732–782.



Scheme 1.24. Facile ring-openings of Dewar **1.34** to form dienamine **1.45**

More intriguingly, we observed only one diastereomer based on the ^1H NMR spectrum, and additional 2D gCOSY and NOESY NMR analysis were conducted to confirm the *E,Z*-stereochemistry of **1.45**. The specific *E,Z*-stereochemistry echoes with Houk's model of torquoselectivity on the top of conrotatory thermal ring-opening of cyclobutenes.⁷⁹ According to Houk's model, the term torquoselectivity was coined to describe the rotational preferences of cyclobutene substituents. The so-called donor substituents, such as nitrogen,⁸⁰ preferentially rotate outward so as to favorably align a filled p or π orbital with the σ^* orbital of the cleaving cyclobutene C(3)–C(4) σ bond in the transition state; likewise, acceptor substituents, such as boron,⁸¹ rotate inward to maximize the overlap of an empty orbital with the C(3)–C(4) σ orbital. Cyclobutene **1.44** is thus in a sense doubly primed to undergo spontaneous ring-opening to afford single *E,Z*-diastereomer under standard conditions.

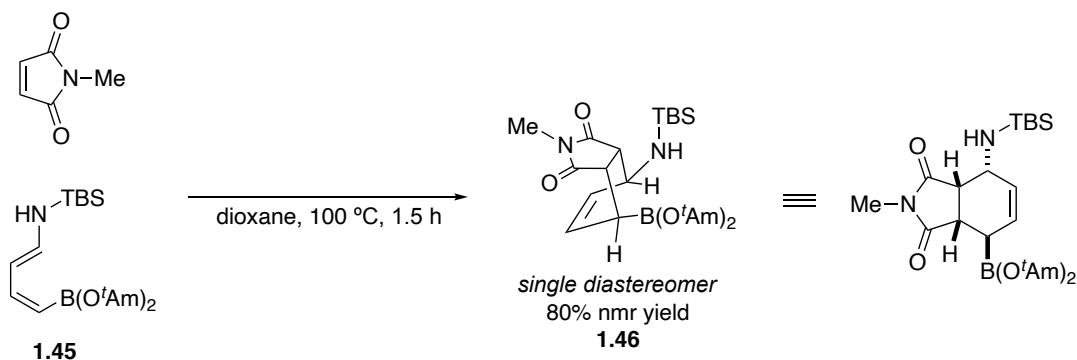
In 2015, our group demonstrated that 1,2-azaborines can engage in Lewis acid catalyzed [4+2] thermo cycloaddition reactions with electron-deficient dienophiles.²⁵ Particularly, 1,2-azaborines **1.26** reacted with *N*-methylmaleimide to afford the Diels-Alder adduct **1.27** as a single diastereomer (Scheme 1.10, see page 19), and further B–N

⁷⁹ Dolbier, W. R. Jr.; Koroniak, H.; Houk, K. N.; Sheu, C. *Acc. Chem. Res.* **1996**, *29*, 471–477.

⁸⁰ De Nanteuil, F.; De Simone, F.; Frei, R.; Benfatti, F.; Serrano, E.; Waser, J. *Chem. Commun.* **2014**, *50*, 10912–10928.

⁸¹ Murakami, M.; Usui, I.; Hasegawa, M.; Matsuda, T. *J. Am. Chem. Soc.* **2005**, *127*, 1366–1367.

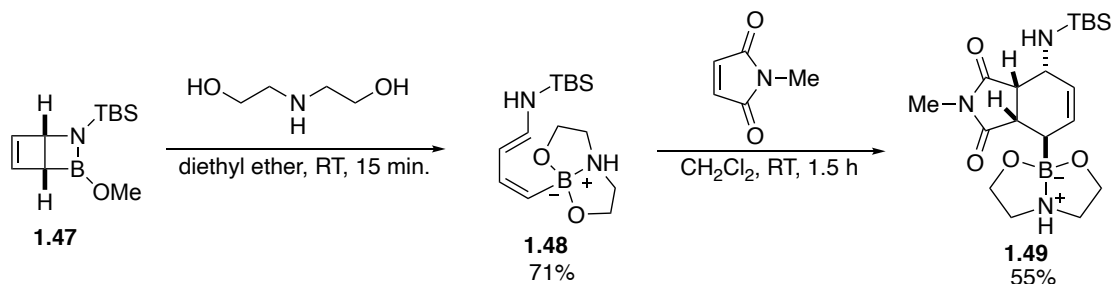
bond alcoholysis gave the 1,4-aminoborylated cyclohexane derivative **1.28**. One can treat 1,2-azaborine **1.26** as a *Z,Z*-diene which will lead to the cyclohexene with amino and boronic ester *cis* to each other. With the recognition of *E,Z*-stereochemistry of diene **1.45**, we were driven to investigate its reactivity in the Diels-Alder reaction since it would potentially produce the *trans* cyclohexene analogues. The formation of the DA adduct **1.46** between **1.45** and *N*-methylmaleimide proceeded under elevated temperature without the need of Lewis acid catalyst (Scheme 1.25). 2D NMR analysis suggested that only the *endo* product **1.46** was generated with amino and boronic ester *trans* to each other.



Scheme 1.25. Diels-Alder reaction of diene **1.45** with *N*-methylmaleimide

We then reasoned that diene **1.45** is not electron-rich in a sense that it has a push-pull character with electron-donor amine and electron-acceptor boron. This might explain why relatively high temperature was required for the Diels-Alder reaction to occur even with such electron-deficient dienophile. To mitigate the push-pull effect, we figured that we could treat Dewar **1.47** with diethanolamine (DEA), which would lead to a tetra-coordinated boronate diene **1.48** after ring-opening and concomitant boron ligand exchange (Scheme 1.26). Notably, the subsequent Diels-Alder reaction between diene **1.48**

and *N*-methylmaleimide proceeded smoothly at room temperature with formation of single diastereomer **1.49**. (Scheme 1.26)



Scheme 1.26. Ring-opening with DEA and tandem DA reaction of **1.48**

1.5 Conclusions and Future Outlook

In summary, we have demonstrated the isolation of the Dewar valence isomer from photoisomerization of 1,2-azaborines in solution and developed a photo-flow system to generate the Dewar isomer in large quantities. The fundamental discovery and technical implementation supported our explorations of the synthetic utility of the Dewar isomer in three veins. First, we have provided a seminal route to access *cis* aminoborylated cyclobutanes with demonstrations of further derivatizations of the boron unit. This work serves as another example of the utility of 1,2-azaborine motif as a 4C+1N+1B synthon in organic synthesis. Secondly, we have discovered a rhodium-catalyzed ring-opening reaction of Dewar to form 1,2-azaborines. Follow-up research is focusing on exploring selective chiral Rh-based catalysts to kinetically resolve the two Dewar enantiomers. In the third vein, we have found that Dewar 1,2-azaborines could undergo rapid ring-opening to afford *E,Z*-dienes suitable for a tandem Diels-Alder reaction. Future efforts will be directed toward expanding the dienophile substrate scope of this transformation.

1.6 Experimental Section

1.6.1 General Considerations

All materials synthesis was performed in oven-dried glassware under a nitrogen atmosphere using standard syringe techniques. Unless otherwise noted, all reagents were obtained from commercial sources and used as received. Bulk volumes of acetonitrile, dichloromethane, pentane, and tetrahydrofuran were passed through an alumina column and dispensed from a solvent purification system under argon.

The following compounds were purified prior to use: *tert*-Amyl alcohol and CD₂Cl₂ were dried over CaH₂, distilled, subjected to three freeze-pump-thaw cycles, and stored in a Schlenk flask in a nitrogen glovebox. 5% wt. Pd/silica was purchased from Strem and dried at 140 °C under vacuum overnight. Pinacol was purchased from Acros and recrystallized from cold diethyl ether. 1-Bromo-4-fluorobenzene and 3,5-bis(trifluoromethyl)bromobenzene were degassed by three freeze-pump-thaw cycles and stored in a nitrogen glovebox. Pd(*t*-Bu₃P)₂ catalyst was purchased from Strem. Organozinc zinc bromide reagents were purchased from Alfa Aesar in a form of 0.5M solution in THF. Crabtree's catalyst was purchased from TCI.

The following compounds were prepared according to previously reported procedures: **1.8**,⁸² [Ni(dtbbpy)(H₂O)₄]Cl₂,⁸³ [Ir(dFCF₃ppy)₂(bpy)]PF₆.⁸⁴

⁸² A. J. V. Marwitz, M. H. Matus, L. N. Zakharov, D. A. Dixon, S.-Y. Liu, *Angew. Chem. Int. Ed.* **2009**, *48*, 973–977.

⁸³ Á. Gutiérrez-Bonet, J. C. Tellis, J. K. Matsui, B. A. Vara, G. A. Molander, *ACS Catal.* **2016**, *6*, 8004–8008.

⁸⁴ T. M. Monos, A. C. Sun, R. C. McAtee, J. J. Devery III, C. R. J. Stephenson, *J. Org. Chem.* **2016**, *81*, 6988–6994.

[Ir(dFCF₃ppy)₂(dtbbpy)]PF₆ synthesized by the same method as [Ir(dFCF₃ppy)₂(bpy)]PF₆; spectral analysis of the material obtained accorded with that in the literature.⁸⁵

¹H, ¹³C, ¹¹B, and ¹⁹F NMR spectra were measured on either a Varian Unity Inova 500 MHz or Varian Unity Inova 600 MHz spectrometer. All NMR chemical shifts are reported in ppm; coupling constants are reported in Hz. ¹H and ¹³C spectra were internally referenced to residual solvent peaks; ¹¹B spectra were externally referenced to a standard of BF₃•Et₂O (δ = 0.0 ppm), and ¹⁹F spectra were likewise referenced to a standard of α,α,α-trifluorotoluene (δ = -63.7 ppm). In ¹³C NMR analysis, peaks for carbon atoms adjacent to a boron center were generally not observed owing to quadrupolar broadening.

All IR spectra were measured on a Bruker Alpha-P FT-IR equipped with a single crystal diamond ATR module, and values are reported in cm⁻¹.

High-resolution mass spectrometry (HRMS) data were generated in Boston College facilities using direct analysis in real-time (DART) on a JEOL AccuTOF DART spectrometer or electrospray ionization (ESI) on an Advion Expression CMS.

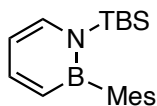
Single-crystal X-ray diffraction data were generated in Boston College facilities from measurements with a Bruker Kappa Apex Duo fully automated diffractometer.

1.6.2 Experimental Procedures of Chapter 1.2

1.6.2.1 Experimental Procedure

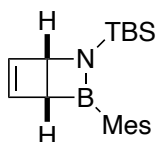
Synthesis and Characterization of Compound 1.20 and 1.21

⁸⁵ G. J. Choi, Q. Zhu, D. C. Miller, C. J. Gu, R. R. Knowles, *Nature* **2016**, 539, 268–271.



1-(*tert*-butyldimethylsilyl)-2-mesityl-1,2-dihydro-1,2-azaborine (1.20)

To a 20 ml vial with a magnetic stir bar was charged with B-Cl precursor **1.8** (1 equiv, 311.5mg, 1.000 mmol) in 5 ml of diethyl ether. The mixture was cooled to -20 °C and 1.5 equiv. of Mes-Li was added portionally. Let the reaction gradually warm up to room temperature and react for 3 hours. The mixture was filtered through Acrodisc and the solvent was pumped off under vacuo. The crude residue was purified by flash column chromatograph (SiO₂; 100% hexane) to give the desired product as a white solid. The procedure was repeated for two time to give 87% average yield. **¹H NMR** (CDCl₃, 500 MHz) δ 7.57 (dd, 1H, *J* = 11.0, 6.3 Hz), 7.45 (d, 1H, *J* = 6.9 Hz), 6.80 (s, 2H), 6.65 (d, 1H, *J* = 10.9 Hz), 6.39 (t, 1H, *J* = 6.3 Hz), 2.30 (s, 3H), 2.10 (s, 6H), 0.93 (s, 9H), 0.02 (s, 6H); **¹³C NMR** (CDCl₃, 126 MHz) δ 142.6, 138.8, 138.2, 136.4, 126.8, 111.4, 27.4, 23.4, 21.2, 19.2, -3.3; **¹¹B NMR** (CDCl₃, 160 MHz) δ 39.9; **IR** 3067, 2959, 2859, 1610, 1523, 1391, 1322, 1264, 1228, 1196, 1110, 1030, 976, 821, 766 cm⁻¹; **HRMS** (DART) calcd. for C₁₉H₃₁BNSi [M+H⁺]: 312.22405, found 312.22428.



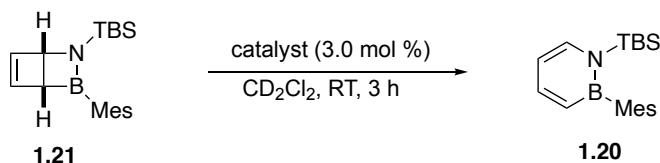
2-(*tert*-butyldimethylsilyl)-3-mesityl-2-aza-3-borabicyclo[2.2.0]hex-5-ene(1.21)

A solution of **1.20** (0.623 g, 2.00 mmol) in anhydrous cyclohexane (8.0 mL) was injected at 0.1 mL·min⁻¹ via syringe pump into the flow photoreactor. An additional 6.0 mL of pure cyclohexane was then injected at the same rate to clear the tubing of remaining

material. The total outflow collected in the receiving vials was concentrated *in vacuo* under N₂ to afford the product as a pale yellow liquid (0.579 g, 93%). ¹H NMR (CDCl₃, 500 MHz) δ 6.75 (s, 1H), 6.56 (td, 1H, *J* = 2.3, 1.1 Hz), 6.37 (t, 1H, *J* = 2.2 Hz), 4.79 (t, 1H, *J* = 2.2 Hz), 3.04 (dd, 1H, *J* = 2.1, 1.1 Hz), 2.25 (s, 3H), 2.21 (d, 6H, *J* = 2.1 Hz), 0.91 (s, 9H), -0.04 (s, 3H), 0.10 (s, 3H); ¹³C NMR (CDCl₃, 126 MHz) δ 143.5, 139.1, 138.1, 136.9, 126.8, 63.2, 26.9, 26.3, 22.2, 21.2, 18.2, -5.6, -5.9; ¹¹B NMR (CDCl₃, 160 MHz) δ 52.6; IR 2954, 2929, 2857, 1620, 1575, 1440, 1360, 1255, 1200, 1097, 1004, 940, 830, 790 cm⁻¹; HRMS (DART) calcd. for C₁₉H₃₁BNSi [M+H⁺]: 312.22405, found 312.22437.

General Procedure for Catalyst Screening of Retro-isomerization Reaction:

A 0.064 M CD₂Cl₂ stock solution of Dewar substrate (**1.21**) and internal standard (1,3,5-trimethoxybenzene) was prepared by dissolving 0.10 g **1.21** and 0.054 g 1,3,5-trimethoxybenzene in a 5.0 mL volumetric flask. Another stock solution consisting of 0.010 g of catalyst in 1.0 mL CD₂Cl₂ was prepared separately. A volume of catalyst solution corresponding to 3 mol % catalyst loading was added via microliter syringe to 0.50 mL (0.032 mmol **1.21**) of the substrate/internal standard solution. (For dimeric catalyst precursors, a volume corresponding to 1.5 mol % precursor was added.) After allowing the reaction mixture to stir at room temperature for 3 h, the conversion was determined by ¹H NMR (Table 11).



entry	catalyst	conversion (%) ^a
1	RhCl(PPh₃)₃	100%^b
2	[Rh(C₂H₄)₂Cl]₂	100%^b
3	[Rh(nbd)Cl] ₂	2%
4	[Rh(cod)Cl] ₂	3%
5	(nbd) ₂ RhBF ₄	0%
6	[Rh(cod)(PPh ₃) ₂]PF ₆	2%
7	[Rh(Cp ⁺)Cl ₂] ₂	0%
8	Rh(nbd)(PPh ₃)Cl Polymer	1%
9	(Cy ₃ P) ₂ (PhCH)RuCl ₂	15%
10	[Ir(cod)Cl] ₂	12%
11	Ni(CO) ₂ (PPh ₃) ₂	0%
12	IPrAuCl	0%
13	Pt(PPh ₃) ₄	5%
14	Pd(PPh ₃) ₄	0%
15	AgOTf	2%
16	ZnCl ₂	0%
17	Sc(OTf) ₃	0%
18	no catalyst	0%

^aDetermined by ¹H NMR integration based on 1,3,5-trimethoxybenzene as internal standard;

^bFull conversion to azaborine **1.20** was observed within 1h.

Table 1.5. Survey of catalysts for the retro-isomerization reaction to **1.20**

Procedure for Calorimetric Experiment:

A 0.064 M CD₂Cl₂ stock solution of Dewar substrate (**1.21**) was prepared by dissolving 0.10 g **1.21** in a 5.0 mL volumetric flask. Another 0.011 M CD₂Cl₂ stock solution of Wilkinson's catalyst was also prepared by dissolving 0.020 g RhCl(PPh₃)₃ in a 2.0 mL volumetric flask. In a glovebox, 0.50 mL of substrate solution (0.032 mmol **1.21**) were added to the bottom of a Setaram-C80 calorimeter Hastelloy sample cell; the bottom half of the cell was sealed with a puncturable aluminum foil before 89 μL of catalyst

solution (3 mol % catalyst) and an additional 0.30 mL CD₂Cl₂ solvent were added on top of the foil via microliter syringe. An empty reference cell was likewise prepared under N₂. Both cells were loaded into the Setaram-C80 calorimeter and were allowed to equilibrate at 25 °C until zero heat flow was achieved (which took approximately 3 hours). Data collection was initiated just prior to puncturing the aluminum foil and was continued until the observed heat flow had returned to zero, indicating completion of the reaction. (Complete conversion of starting material **1.21** to 1,2-azaborine **1.20** was subsequently confirmed by ¹¹B NMR and ¹H NMR). The measured heat flow trace was integrated using the Setaram software SetSoft 2000 to determine the ΔH_{rxn} of the retro-isomerization reaction. The calorimetric measurements were repeated five times and the corresponding average value of ΔH_{rxn} with standard deviation is reported. (Table 1.6) The average value of ΔH is -47.6 kcal/mol, with a standard deviation of ± 0.968 kcal/mol.⁸⁶

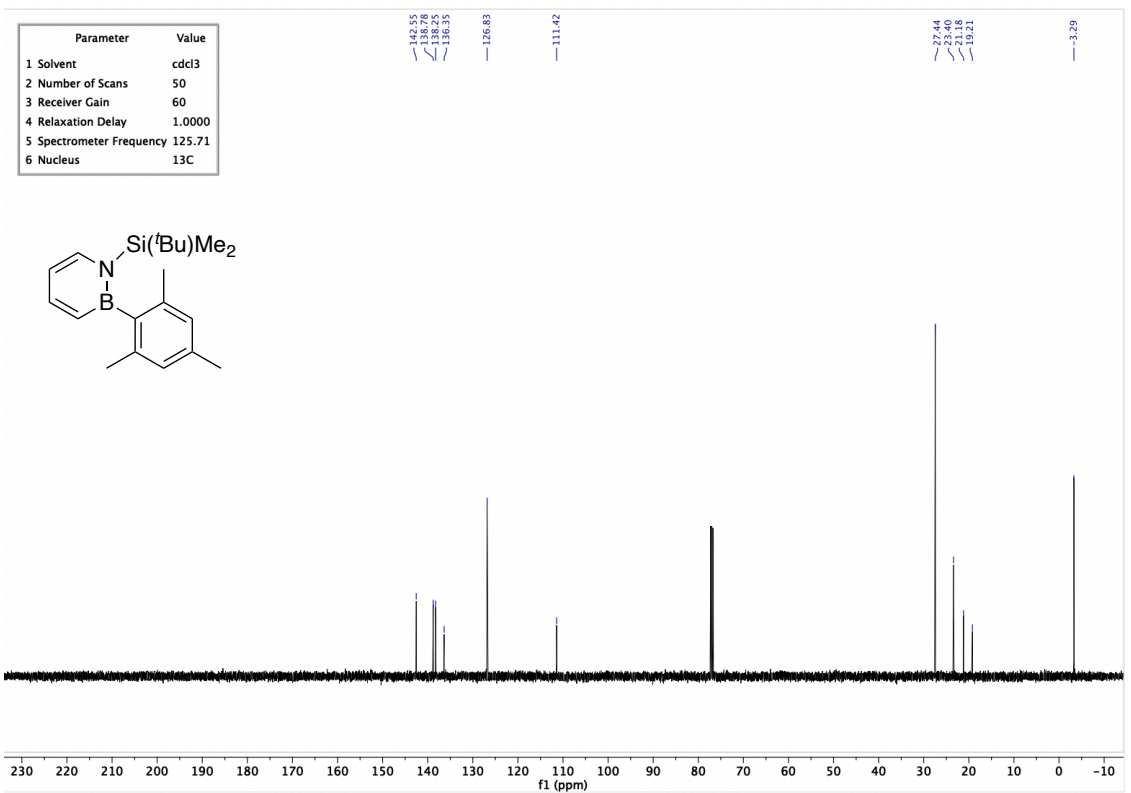
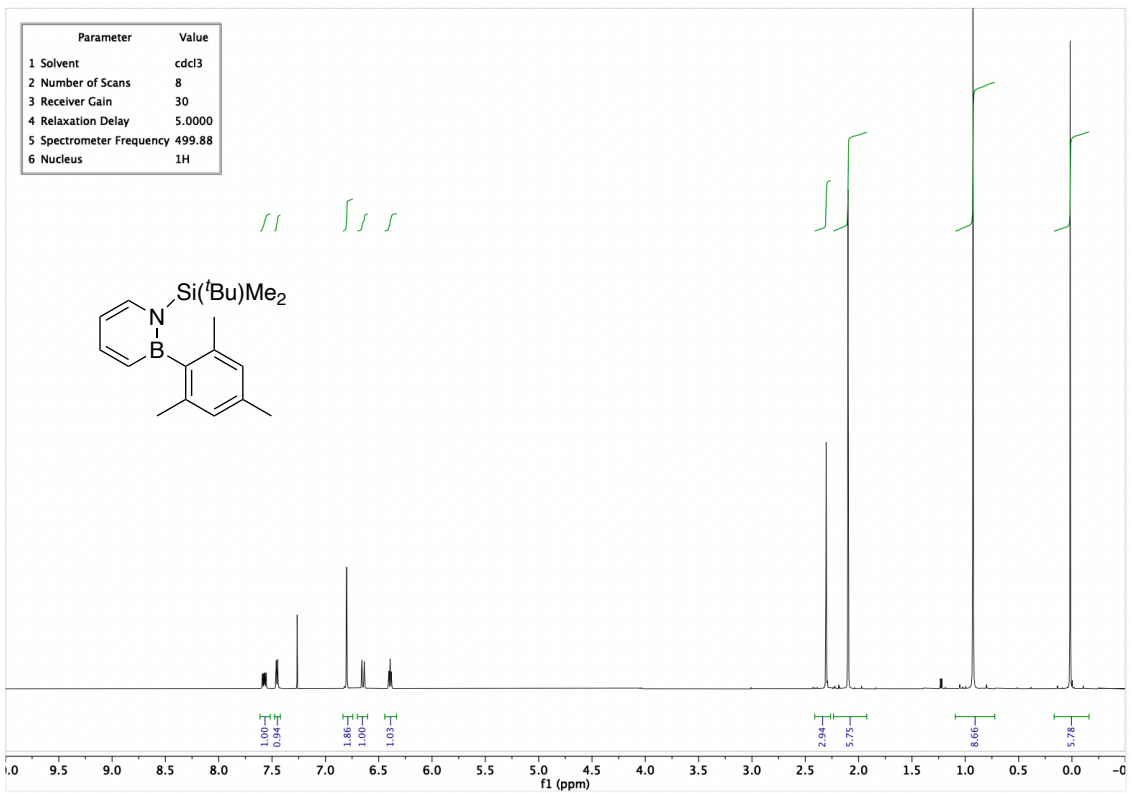
Trial	ΔH kcal/mol
1	-48.4
2	-48.8
3	-47.0
4	-47.6
5	-46.1

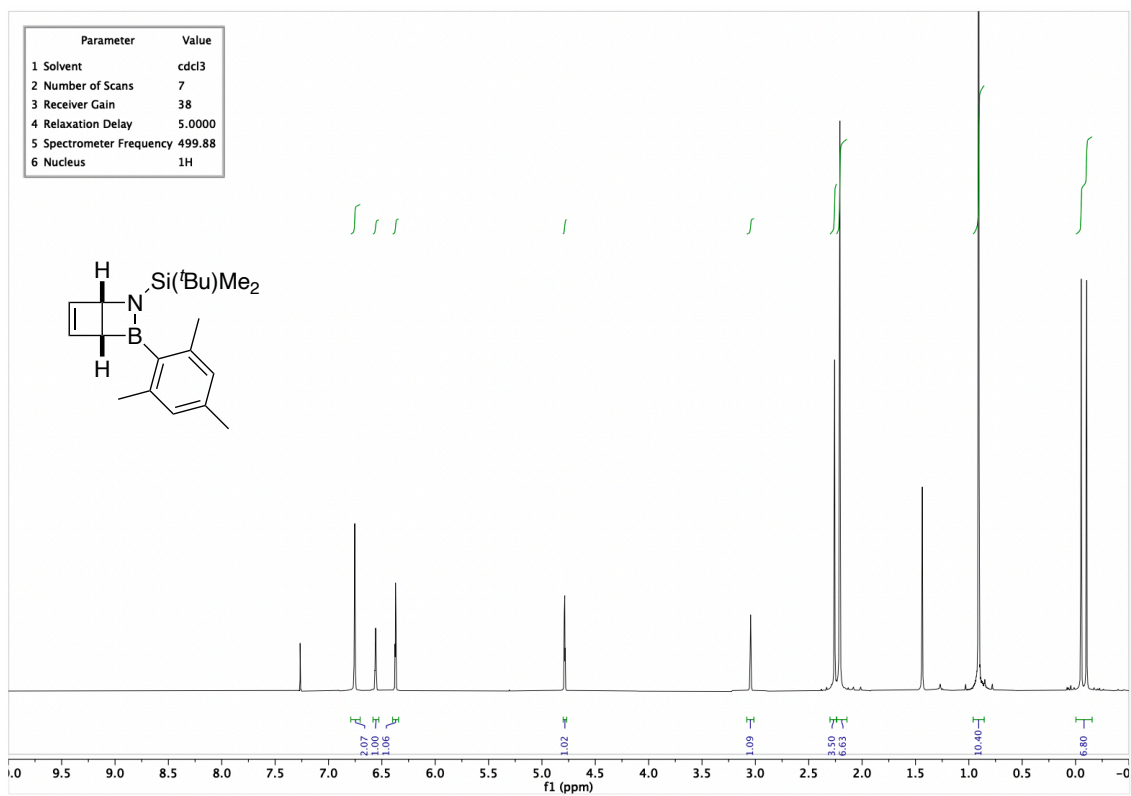
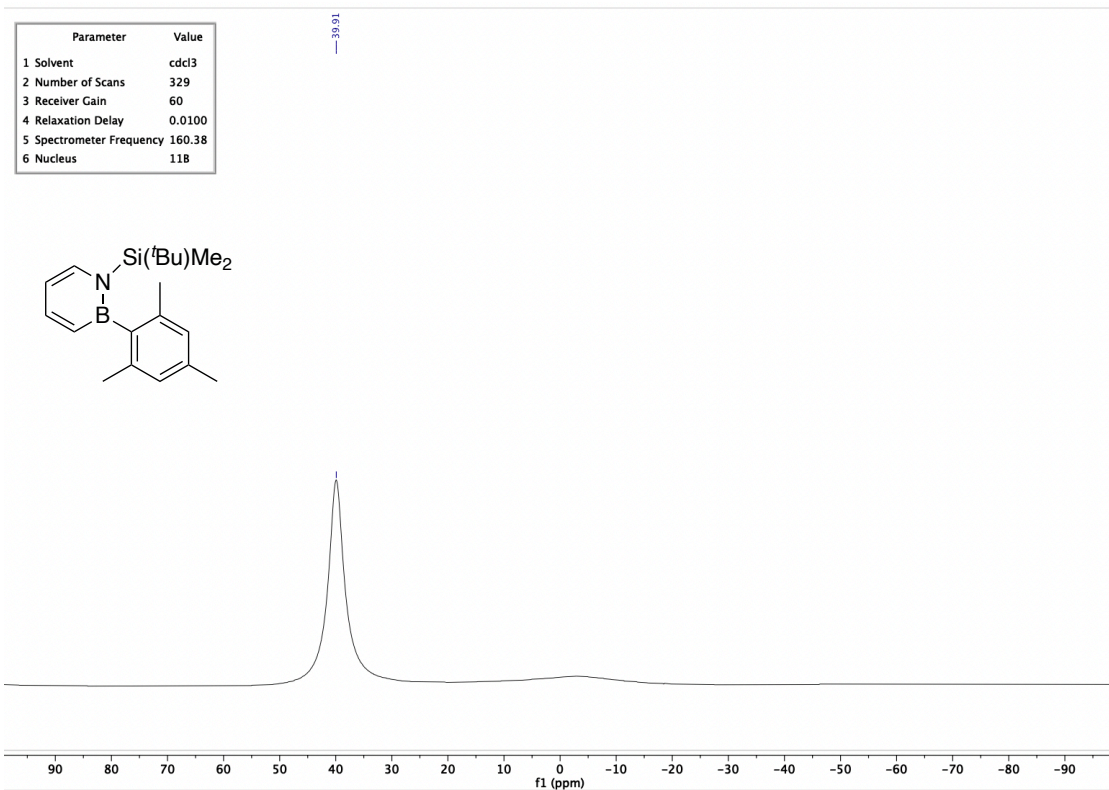
Table 1.6. Heat measured from calorimetric experiments

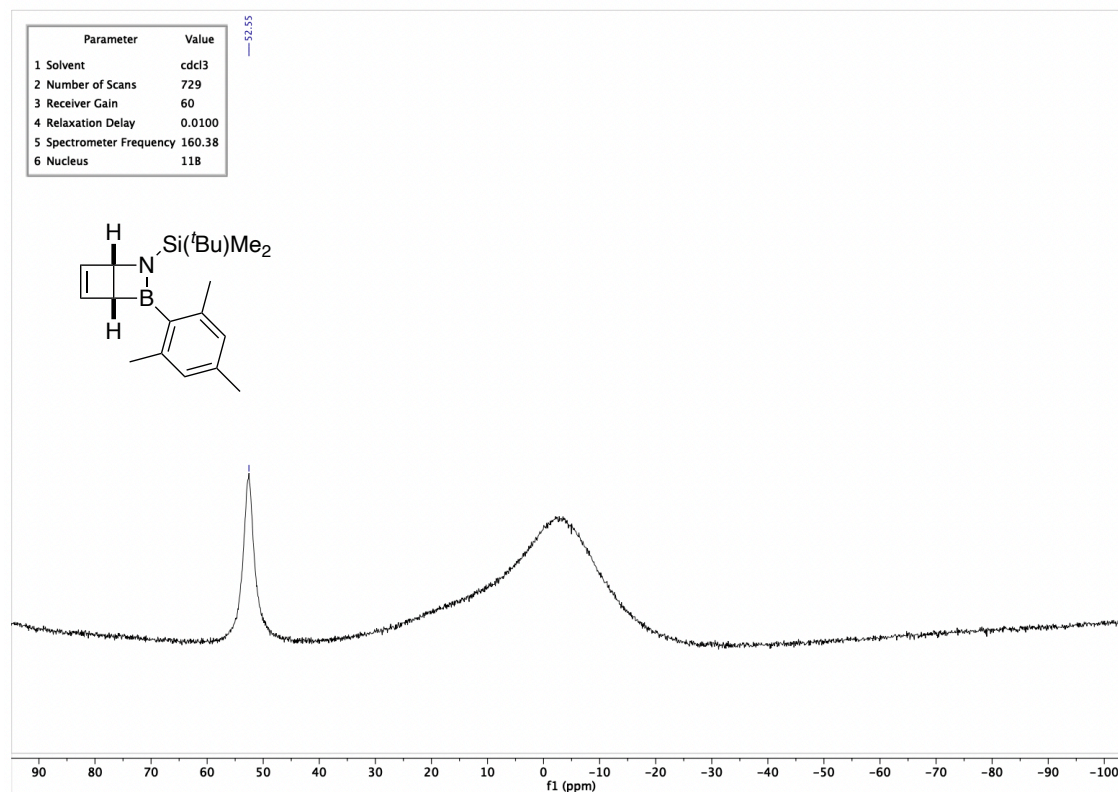
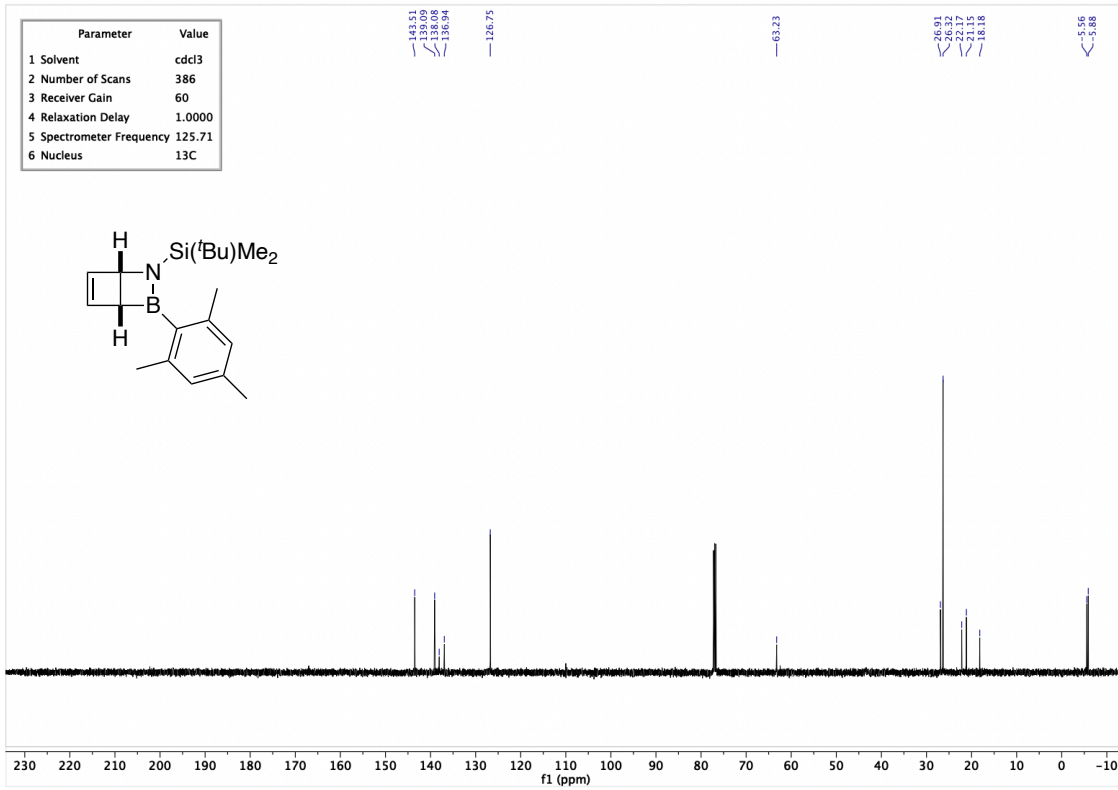
1.6.2.2 Analytical Data

NMR Spectra

⁸⁶ For a representative heat-flow trace integration, please see **Figure 1.6** in Chapter 1.2.1.2.





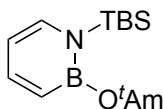


1.6.3 Experimental Procedures of Chapter 1.3

1.6.3.1 Details of Photoreactor Assembly

The flow photoreactor setup used in this work was assembled in accordance with prior system designs by Berry and Booker-Milburn and Seeberger and Hartmann.^{66,87} Approximately 1.1 m of 1/16" OD x 0.030" ID FEP tubing (IDEX), for a total reactor volume of 5.0 mL, was coiled in a single layer around the outside of a quartz immersion well housing a 450 W quartz, medium-pressure mercury vapor arc lamp (Hanovia, PC 451050) surrounded by a cylindrical Pyrex filter. The tubing inlet was connected directly to a plastic syringe fitted with a 21G x 1 1/2 needle, while the outlet was inserted through a septum screw cap on a 20 mL scintillation vial. This vial was also connected through the septum cap to a nitrogen line featuring a drying tube filled with Drierite. The immersion well was enclosed in a cardboard box lined with aluminum foil, while the syringe and collection vial were situated outside the box. A sufficient flow of cold (12 °C) water was provided to the well to prevent the temperature of its outer surface from significantly rising above ambient. Prior to each use of the reactor, 6 mL of anhydrous cyclohexane were flushed through the tubing into a vial sealed under N₂ in a glovebox.

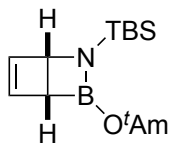
1.6.3.2 Synthetic Procedures and Characterizations of New Compounds



1-(*tert*-butyldimethylsilyl)-2-(*tert*-amyloxy)-1,2-dihydro-1,2-azaborine (1.33)

⁸⁷ F. Wojcik, A. G. O'Brien, S. Götze, P. H. Seeberger, L. Hartmann *Chem. Eur. J.* **2013**, *19*, 3090–3098.

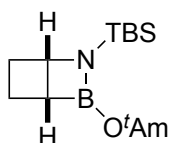
To a solution of **1.8** (3.82 g, 16.8 mmol) in CH₂Cl₂ (44.0 mL) was added anhydrous Et₃N (2.35 mL, 16.9 mmol), followed by *tert*-amyl alcohol (1.85 mL, 17.0 mmol). The solution was allowed to stir at 22 °C for 15 h. Volatiles were completely removed *in vacuo* under N₂. Pentane was added to the residue and the resulting suspension was filtered through a pad of silica gel, which was subsequently flushed with additional pentane. The combined filtrates were concentrated *in vacuo* under N₂ to afford the product as a clear, colorless oil (3.39 g, 72%). ¹H NMR (CD₂Cl₂, 600 MHz) δ 7.38 (dd, 1H, *J* = 11.9, 6.1 Hz), 7.05 (d, 1H, *J* = 6.7 Hz), 6.23 (d, 1H, *J* = 11.8 Hz), 5.83 (t, 1H, *J* = 6.4 Hz), 1.79 (q, 2H, *J* = 7.5 Hz), 1.35 (s, 6H), 0.92 (s, 9H), 0.88 (t, 3H, *J* = 7.4 Hz), 0.39 (s, 6H); ¹³C NMR (CD₂Cl₂, 151 MHz) δ 145.2, 139.5, 106.7, 76.2, 35.2, 28.2, 27.2, 19.4, 9.3, -2.2; ¹¹B NMR (CD₂Cl₂, 160 MHz) δ 29.4; IR 2968, 2929, 2883, 2857, 1609, 1511, 1457, 1399, 1286, 1261, 1249, 1177, 1154, 1112, 991 cm⁻¹; HRMS (DART) calcd. for C₁₅H₃₁BNOSi [M+H⁺]: 280.2268, found 280.2279.



2-(*tert*-butyldimethylsilyl)-3-(*tert*-amyloxy)-2-aza-3-borabicyclo[2.2.0]hex-5-ene (1.34).

A solution of **1.33** (0.840 g, 3.01 mmol) in anhydrous cyclohexane (12.0 mL) was injected at 0.1 mL·min⁻¹ via syringe pump into the flow photoreactor described above. An additional 6.0 mL of pure cyclohexane was then injected at the same rate to clear the tubing of remaining material. The total outflow collected in the receiving vials was concentrated *in vacuo* under N₂ to afford the product as a pale yellow liquid (0.697 g, 83%). ¹H NMR

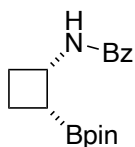
(CD₂Cl₂, 500 MHz) δ 6.49 (td, 1H, J = 2.4, 1.0 Hz), 6.26 (d, 1H, J = 2.3 Hz), 4.24 (t, 1H, J = 2.5 Hz), 2.90 (dd, 1H, J = 2.4, 1.0 Hz), 1.55 (q, 2H, J = 7.5 Hz), 1.26 (s, 6H), 0.91–0.84 (m, 12H), 0.03 (s, 3H), 0.02 (s, 3H); ¹³C NMR (CD₂Cl₂, 126 MHz) δ 142.7, 142.0, 76.6, 58.1, 36.9, 29.2, 29.0, 26.5, 18.5, 8.8, –5.1, –5.3; ¹¹B NMR (CD₂Cl₂, 192 MHz) δ 32.4; IR 2954, 2929, 2857, 1620, 1575, 1440, 1332, 1200, 1004, 940, 830, 790, 713, 671 cm⁻¹; HRMS (DART) calcd. for C₁₅H₃₀BNO₂Si [M+H₃O⁺]: 280.2268, found 280.2279.



1-(*tert*-butyldimethylsilyl)-2-(*tert*-amyloxy)-2-aza-3-borabicyclo[2.2.0]hexane (1.35)

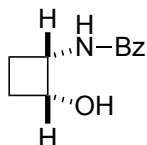
A solution of **1.34** (1.26 g, 4.50 mmol) in cyclohexane (18.0 mL) was injected at 0.1 mL·min⁻¹ via syringe pump into the flow photoreactor described above. An additional 5.0 mL of pure cyclohexane was then injected at the same rate to clear the tubing of remaining material. The total outflow collected in the receiving vials was transferred to a 100 mL round-bottom flask, and 5% wt. Pd/silica (94.0 mg, 0.0442 mmol, 1.0 mol% Pd) was added. The flask was sealed in a Parr bomb, which was subsequently pressurized with H₂ (100 psi). The reaction mixture was allowed to stir under pressure at 22 °C for 1 h. After this time, the system was depressurized, and Pd/silica was removed under N₂ by filtration of the suspension through an acrodisc. The filtrate was concentrated *in vacuo* to afford the product as a yellow-orange liquid (0.861 g, 68%). ¹H NMR (CD₂Cl₂, 600 MHz) δ 3.87–3.82 (m, 1H), 2.37 (tt, 1H, J = 11.9, 6.0 Hz), 2.28 (dt, 1H, J = 10.6, 4.2 Hz), 2.12 (qd, 1H, J = 11.1, 5.3 Hz), 1.93–1.85 (m, 1H), 1.80–1.73 (m 1H), 1.52 (q, 2H, J = 7.5 Hz), 1.22 (s, 6H), 0.93–0.85 (m, 12H), 0.06 (s, 3H), 0.00 (s, 3H); ¹³C NMR (CD₂Cl₂, 126 MHz) δ 75.9,

55.3, 36.9, 30.8, 29.0, 28.8, 26.7, 18.5, 17.3, 8.9, -4.4, -4.9; ^{11}B NMR (CD_2Cl_2 , 192 MHz) δ 32.1; IR 2970, 2929, 2856, 1625, 1462, 1408, 1365, 1302, 1256, 1237, 1202, 1177, 1145, 1116 cm^{-1} ; HRMS (DART) calcd. for $\text{C}_{15}\text{H}_{33}\text{BNOSi}$ [$\text{M}+\text{H}^+$]: 282.2436, found 282.2424.



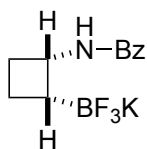
1-benzamido-2-(4,4,5,5-tetramethyl-1,3,2-dioxaborolan-2-yl)cyclobutane (1.36)

To a solution of **1.35** (0.688 g, 2.45 mmol) in CH_2Cl_2 (7.0 mL) was added pinacol (296 mg, 2.50 mmol, 1.02 equiv.), followed by benzoyl chloride (0.285 mL, 2.45 mmol, 1.00 equiv.). The solution was allowed to stir at 22 °C for 3 h. After this time, the reaction mixture was concentrated *in vacuo*, and the product was isolated from the resulting residue by silica gel chromatography (5% to 25% EtOAc in hexanes) as a white solid (0.397 g, 54%). Crystals suitable for single-crystal X-ray diffraction analysis were obtained by slow evaporation of a diethyl ether solution. ^1H NMR (CD_2Cl_2 , 600 MHz) δ 7.78 (d, 2H, $J = 6.9$ Hz), 7.60 (br s, 1H), 7.52–7.47 (m, 1H), 7.44 (t, 1H, $J = 7.5$ Hz), 4.72 (p, 1H, $J = 8.5$ Hz), 2.44–2.37 (m, 1H), 2.29–2.21 (m, 1H), 2.06–1.94 (m, 2H), 1.76–1.70 (m, 1H), 1.29 (d, 12H, $J = 1.8$ Hz); ^{13}C NMR (CD_2Cl_2 , 151 MHz) δ 165.8, 135.6, 131.6, 128.9, 127.3, 84.1, 45.8, 32.4, 25.24, 25.21, 17.6; ^{11}B NMR (CD_2Cl_2 , 160 MHz) δ 33.6; IR 3373, 3057, 2982, 2869, 1637, 1578, 1522, 1486, 1415, 1380, 1334, 1310, 1276, 1235, 1211, 1164, 1137, 1088, 1074, 1016, 999, 960 cm^{-1} ; HRMS (DART) calcd. for $\text{C}_{17}\text{H}_{25}\text{BNO}_3$ [$\text{M}+\text{H}^+$]: 302.1927, found 302.1928.



***cis*-2-benzamidocyclobutanol (1.39)**

In accordance with a previously reported protocol,⁵⁶ **1.36** (52.6 mg, 0.175 mmol) and NaBO₃•4H₂O (109 mg, 0.708 mmol, 4.0 equiv.) were suspended in a mixture of THF (0.80 mL) and water (0.80 mL). The reaction mixture was allowed to stir at 22 °C for 21 h. After this time, the reaction mixture was diluted with additional water and EtOAc. The layers were separated, and the aqueous phase was extracted 3x with EtOAc; the combined organic extracts were dried over Na₂SO₄, vacuum-filtered through a Büchner funnel, and concentrated *in vacuo*. The product was isolated from the resulting residue by silica gel chromatography (40% EtOAc in hexanes) as a white solid (24.0 mg, 72%). ¹H NMR (acetone-*d*₆, 500 MHz) δ 7.88 (d, 2H, *J* = 8.8 Hz), 7.62–7.48 (m, 2H), 7.48–7.40 (m, 2H), 4.56–4.45 (m, 2H), 4.38 (d, 1H, *J* = 4.4 Hz), 2.21–2.07 (m, 3H), 1.94–1.84 (m, 1H); ¹³C NMR (acetone-*d*₆, 151 MHz) δ 167.1, 136.2, 132.0, 129.3, 128.1, 70.2, 50.6, 28.5, 25.9; IR 3256 (br), 2922, 1632, 1577, 1530, 1491, 1355, 1290, 1180, 1164, 1125, 1112, 1080, 1005 cm⁻¹; HRMS (DART) calcd. for C₁₁H₁₄NO₂ [M+H⁺] 192.1019, found 192.1013.



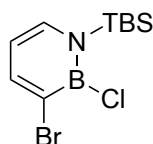
potassium (2-benzamidocyclobutyl)trifluoroborate (1.40)

In accordance with a previously reported protocol,⁷² to a solution of **1.36** (1.65 g, 5.48 mmol) in MeOH (11 mL) and acetonitrile (11.0 mL) was added a solution of KF (1.45

g, 25.0 mmol, 4.55 equiv.) in water (2.6 mL). A solution of L-(+)-tartaric acid (2.06 g, 13.7 mmol, 2.50 equiv.) in THF (11.0 mL) was then added in portions over the course of 6 min, with the reaction mixture vigorously stirred (1000 rpm) by the action of a magnetic stir bar. Upon completion of the addition, the reaction mixture was allowed to continue stirring for 2 min before a portion of acetonitrile (18.0 mL) was added. The reaction mixture was again allowed to stir for 2 min before a second portion of acetonitrile (6.0 mL) was added. The reaction mixture was vacuum-filtered through a glass-fritted funnel, and the solids were washed 3x with 30 mL acetonitrile. The filtrate was concentrated *in vacuo* and further dried under high vacuum. The resulting solid residue was redissolved in a minimal amount of acetone; CH₂Cl₂ was carefully added to the solution to induce precipitation of the product. The resulting suspension was sonicated for ~10 min before the insoluble material was collected by vacuum-filtration to afford the product as a white solid (0.991 g, 64%). ¹H NMR (acetone-*d*₆, 500 MHz) δ 7.79 (appd, 3H, *J* = 6.6 Hz), 7.48–7.36 (m, 3H), 4.54–4.42 (m, 1H), 2.26–2.17 (m, 1H), 2.04–1.95 (m, 1H, partial overlap with solvent peak), 1.72–1.54 (m, 3H); ¹³C NMR (acetone-*d*₆, 151 MHz) δ 166.5, 137.2, 131.4, 129.1, 127.6, 47.5, 32.0, 18.4; ¹¹B NMR (acetone-*d*₆, 160 MHz) δ 5.7 (q, *J* = 63.7); ¹⁹F NMR (acetone-*d*₆, 470 MHz) δ –140.0 to –140.7 (m, 3F); IR 3332, 2937, 2864, 1617, 1576, 1527, 1488, 1441, 1374, 1320, 1283, 1108, 1097, 1029, 948 cm⁻¹; HRMS (DART) calcd. for C₁₁H₁₂BNOF₃ [M–K⁺]: 242.0964, found 242.0976.

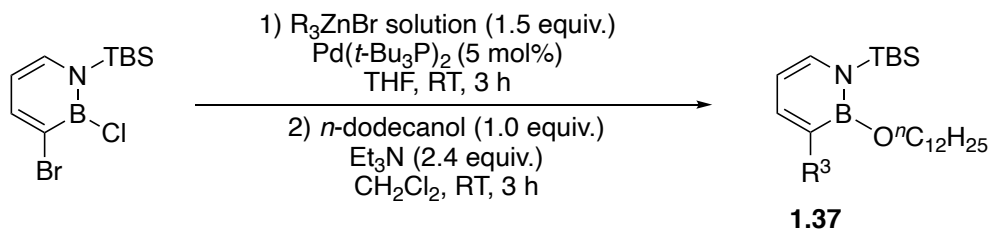
Synthesis and Characterization of C3-substituted 1,2-azaborines 1.37

In adaptation of a previously reported Negishi Cross-coupling method,⁷¹ C3 position of B-Cl azaborine **1.8** was functionalized with diverse groups. Few different procedures were followed depending on different substitutes on boron.



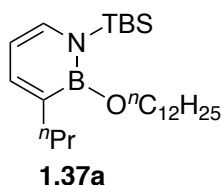
First, C3-bromo substituted B-Cl-azaborine **1.8** was synthesized based on reported method,⁷¹ a 100 mL round bottom flask was charged with 1 equiv. of B-Cl azaborine (3.000 g, 13.02 mmol) together with a magnetic stir bar in 30 mL of CH₂Cl₂. The mixture was cooled to 0 °C in an ice/water bath. In a separate vessel, 1.00 equiv. of Br₂ (2.018 g, 13.02 mmol) was diluted in 5 mL CH₂Cl₂ then was added dropwise to the azaborine solution over course of 10 minutes. The reaction was stirred for 15 minutes at 0 °C and was allowed to warm to room temperature and continued until ¹H NMR analysis indicated completion (around 1h). Solvent was removed under reduced pressure. Vacuum distillation (62–65 °C, 120 mT) provided product as a clear, colorless liquid (2.98 g, 74%).

Procedure for the Synthesis of Compound **1.37a-1.37e** and Characterization

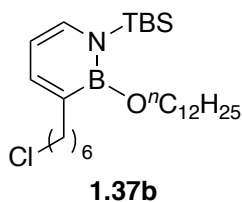


In N₂ glovebox, to a 20 ml vial with a magnetic stir bar was charged with C3-bromo B-Cl precursor (1 equiv., 306.5mg, 1.000 mmol) and Pd(*t*-Bu₃P)₂ catalyst (5 mol %, 25.5 mg, 0.0500mmol), 2.0 mL of THF was added. The mixture was stirred for 5 minutes before adding 3.0 mL of organo-zinc bromide (0.5 M in THF) solution. The reaction was allowed to stirred for 3 hours. At this point, 1.0 mL CH₂Cl₂ was added to quench the reaction. The solvent was pumped off and reconstitute in pentane. The solids were filtered off and the

filtrate was concentrated in *vacuo*. The crude residue was purified by flash column chromatograph (SiO₂; x: y pentane: diethyl ether) to give the desired product as a colorless oil (most time colorless, sometimes get a pale yellow oil for **1.37b**). The procedure to synthesize each compound was carried out at least 2 times. The average yield was reported.

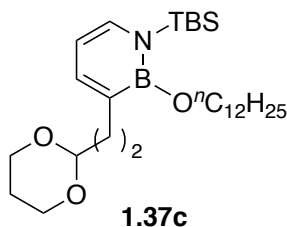


The desired product was obtained by flash column chromatography (100:0 pentane to diethyl ether) with average yield of 52%. **¹H NMR** (CD₂Cl₂, 500 MHz) δ 7.15 (d, *J* = 6.4 Hz, 1H), 6.92 (d, *J* = 6.7 Hz, 1H), 5.82 (t, *J* = 6.5 Hz, 1H), 4.12 (t, *J* = 7.2 Hz, 2H), 2.49 (dd, *J* = 9.2, 6.5 Hz, 2H), 1.74–1.71 (p, *J* = 7.2 Hz, 2H), 1.53–1.49 (h, *J* = 7.4 Hz, 2H), 1.43–1.24 (m, 18H), 0.98 (t, *J* = 7.3 Hz, 3H), 0.95 (t, 3H), 0.94 (s, 9H), 0.40 (s, 6H). **¹³C NMR** (CD₂Cl₂, 126 MHz) δ 144.5, 135.9, 106.0, 65.3, 38.2, 32.3, 31.9, 29.66, 29.65 (2C), 29.61, 29.5, 29.4, 26.6, 26.0, 25.8, 22.7, 18.6, 13.9, 13.8, –2.7; **¹¹B NMR** (CD₂Cl₂, 160 MHz) δ 30.2; **IR** 2926, 2855, 1609, 1527, 1369, 1285, 1080, 811cm⁻¹; **HRMS** (DART) calcd. for C₂₅H₅₁BNOSi [M+H⁺]: 420.38275, found 420.38381.

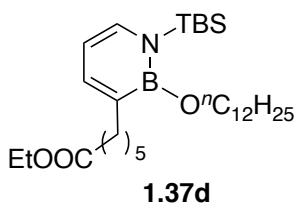


The desired product was obtained by flash column chromatography (98:2 pentane to diethyl ether) with average yield of 47%. **¹H NMR** (CD₂Cl₂, 400MHz) δ 7.13 (d, *J* = 6.5 Hz, 1H), 6.91 (d, *J* = 6.7 Hz, 1H), 5.80 (t, *J* = 6.6 Hz, 1H), 4.09 (t, *J* = 7.1 Hz, 2H), 3.54 (t,

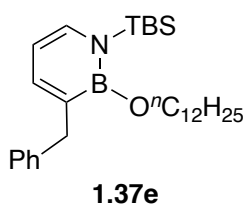
$J = 6.8$ Hz, 2H), 2.50 (t, $J = 7.7$ Hz, 2H), 1.79 (t, $J = 7.3$ Hz, 2H), 1.69 (t, $J = 7.1$ Hz, 2H), 1.54–1.38 (m, 6H), 1.42–1.28 (m, 18H), 0.90 (t, 3H), 0.91 (s, 9H), 0.39 (s, 6H). ^{13}C NMR (CD_2Cl_2 , 101 MHz) δ 144.4, 136.0, 106.0, 65.3, 45.2, 35.9, 32.7, 32.6, 32.3, 31.9, 29.66 (2C), 29.64, 29.61, 29.5, 29.4, 28.9, 26.9, 26.6, 26.0, 22.7, 18.6, 13.9, -2.7; ^{11}B NMR (CD_2Cl_2 , 160 MHz) δ 30.2; **IR** 2926, 2854, 1609, 1463, 1400, 1527, 1369, 1287, 1262, 1205, 1157, 1128, 1080, 1007, 841, 811, 784, 741 cm^{-1} ; **HRMS** (DART) calcd. for $\text{C}_{28}\text{H}_{56}\text{BNOSiCl}$ [$\text{M}+\text{H}^+$]: 496.39073, found 496.39160.



The desired product was obtained by flash column chromatography (90:10 pentane to diethyl ether) with average yield of 51%. ^1H NMR (CD_2Cl_2 , 500MHz) δ 7.15 (d, $J = 6.4$ Hz, 1H), 6.92 (d, $J = 6.7$ Hz, 1H), 5.80 (t, $J = 6.5$ Hz, 1H), 4.53 (t, $J = 5.1$ Hz, 1H), 4.12 (t, $J = 7.3$ Hz, 2H), 4.07 (dd, $J = 11.5, 4.9$ Hz, 2H), 3.75 (td, $J = 12.3, 2.5$ Hz, 2H), 2.56 (t, 2H), 2.13–1.95 (m, 1H), 1.79–1.64(m, 5H), 1.44–1.18 (m, 18H), 0.90 (t, 3H), 0.92 (s, 9H), 0.39 (s, 6H); ^{13}C NMR (CD_2Cl_2 , 126 MHz) δ 147.7, 136.2, 106.0, 101.9, 66.7, 65.4, 38.0, 32.3, 31.9, 29.8, 29.68, 29.67, 29.64, 29.61, 29.5, 29.3, 26.6, 26.0, 25.9, 22.7, 18.6, 13.9, -2.7; ^{11}B NMR (CD_2Cl_2 , 160 MHz) δ 29.9; **IR** 2954, 2926, 2864, 1609, 1527, 1467, 1401, 1371, 1286, 1260, 1206, 1146, 1135, 1080, 841, 823, 811, 764, 726 cm^{-1} ; **HRMS** (DART) calcd. for $\text{C}_{28}\text{H}_{55}\text{BNO}_3\text{Si}$ [$\text{M}+\text{H}^+$]: 492.40388, found 492.40370.



The desired product was obtained by flash column chromatography (95:5 pentane to diethyl ether) with average yield of 54%. **¹H NMR** (CD₂Cl₂, 500MHz) δ 7.13 (d, *J* = 6.5 Hz, 1H), 6.90 (d, *J* = 6.7 Hz, 1H), 5.79 (t, *J* = 6.5 Hz, 1H), 4.10 (dt, *J* = 11.3, 7.0 Hz, 4H), 2.49 (t, *J* = 7.8 Hz, 2H), 2.29 (t, *J* = 7.5 Hz, 2H), 1.66 (dt, *J* = 21.9, 7.4 Hz, 4H), 1.48 (p, *J* = 7.4 Hz, 2H), 1.41–1.26 (m, 20H), 1.24 (t, *J* = 7.1 Hz, 3H), 0.91 (s, 9H), 0.89 (t, 3H), 0.38 (s, 6H); **¹³C NMR** (CD₂Cl₂, 126 MHz) δ 173.4, 144.4, 136.0, 106.0, 65.4, 60.0, 35.8, 34.2, 32.4, 32.3, 31.9, 29.63, 29.62, 29.61, 29.58, 29.53, 29.3, 29.1, 26.6, 25.6, 24.9, 22.6, 18.6, 14.0, 13.8, -2.7; **¹¹B NMR** (CD₂Cl₂, 160 MHz) δ 30.0; **IR** 2926, 2855, 1738, 1609, 1527, 1464, 1401, 1399, 1370, 1288, 1261, 1206, 1136, 1104, 1080, 1034, 841, 823, 811, 784, 739 cm⁻¹; **HRMS** (DART) calcd. for C₃₀H₅₉BNO₃Si [M+H⁺]: 520.43518, found 520.43508.



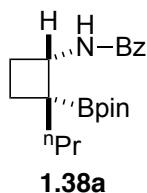
The desired product was obtained by flash column chromatography (100:0 pentane to diethyl ether) with average yield of 57%. **¹H NMR** (CD₂Cl₂, 500MHz) δ 7.30 (t, *J* = 7.5 Hz, 2H), 7.18 (dd, *J* = 19.2, 7.5 Hz, 3H), 7.12 (d, *J* = 6.4 Hz, 1H), 7.02 (d, 1H), 5.88 (t, *J* = 6.6 Hz, 1H), 4.03–3.93 (m, 4H), 1.56 (t, *J* = 7.1 Hz, 2H), 1.43–1.20 (m, 20H), 0.95 (s, 9H), 0.94 (t, 3H), 0.42 (s, 6H); **¹³C NMR** (CD₂Cl₂, 126 MHz) δ 146.6, 143.0, 136.8, 128.5,

128.1 , 125.5, 106.0, 65.4, 41.6, 32.2, 31.9, 29.67 (2C), 29.62, 29.60, 29.41, 29.37, 26.6, 25.8, 22.7, 18.7, 13.9, -2.7; ^{11}B NMR (CD_2Cl_2 , 160 MHz) δ 30.2; IR 2926, 2855, 1609, 1527, 1370, 1289, 1093, 811, 728 cm^{-1} ; HRMS (DART) calcd. for $\text{C}_{29}\text{H}_{51}\text{BNOSi}$ [$\text{M}+\text{H}^+$]: 468.38275, found 468.38058.

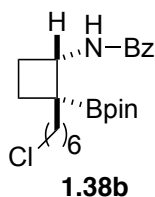
General procedure for Synthesis of Compound 1.38a–1.38e

A solution of 0.75 mmol **1.37** in anhydrous cyclohexane (5.0 mL) was injected at 0.1 $\text{mL}\cdot\text{min}^{-1}$ via syringe pump into the flow photoreactor described above. An additional 6.0 mL of pure cyclohexane was then injected at the same rate to push out the desired material which was collected in the receiving vial. The solvent was concentrated in vacuo under N_2 . Then 2 ml of CH_2Cl_2 was added into the vial together with a stir bar. Purge the vial with N_2 and vacuum it. Meanwhile, a balloon charged with H_2 was prepared. The hydrogen gas was injected and the solution was stirred vigorously for 2 minutes. 1ml CH_2Cl_2 stock solution of Crabtree's catalyst (2 mol %) was then injected via syringe. The reaction mixture was allowed to stir under 1 atm H_2 for 1.5 h. The solvent was pumped off and reconstitute in pentane to filter off the catalyst. Then filtrate was concentrated. The residue was reconstituted in CH_2Cl_2 and treated with benzoyl chloride and pinacol to give tertiary boronate esters bearing cyclobutane motifs within 3 h. The desired products **1.38a–1.38e** were purified by preparative thin layer chromatography as colorless oil.

Characterization of 1.38a–1.38e

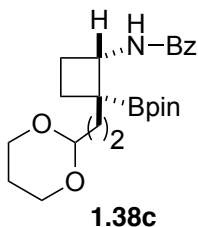


The desired product was purified by preparative thin layer chromatography (Silica plates; using 75:25 pentane to diethyl ether as eluent). From **1.36a** to **1.38a**, combined average yield is 47%. (first batch: 118.4 mg, 46%; second batch: 123.6 mg, 48%). $^1\text{H NMR}$ (CD_2Cl_2 , 500 MHz) δ 7.82–7.76 (m, 2H), 7.72 (d, $J = 8.9$ Hz, 1H), 7.56–7.47 (m, 1H), 7.45 (dd, $J = 8.2, 6.6$ Hz, 2H), 4.32 (q, $J = 8.8$ Hz, 1H), 2.29 (dtd, $J = 10.1, 8.1, 1.7$ Hz, 1H), 1.93–1.85 (m, 1H), 1.84–1.73 (m, 1H), 1.72–1.62 (m, 1H), 1.59–1.43 (m, 2H), 1.33 (d, $J = 7.6$ Hz, 12H), 1.21–1.12 (m, 2H), 0.87 (t, $J = 7.3$ Hz, 3H); $^{13}\text{C NMR}$ (CD_2Cl_2 , 126 MHz) δ 164.9, 135.2, 130.9, 128.3, 126.6, 83.5, 51.9, 41.8, 28.1, 24.9, 24.7, 24.4, 19.8, 14.5; $^{11}\text{B NMR}$ (CD_2Cl_2 , 160 MHz) δ 34.3; **IR** 3419, 2974, 2956, 2930, 2869, 1665, 1602, 1579, 1524, 1445, 1382, 1341, 1276, 1138, 847, 800 cm^{-1} ; **HRMS** (DART) calcd. for $\text{C}_{20}\text{H}_{31}\text{BNO}_3$ [$\text{M}+\text{H}^+$]: 344.2389, found 344.2402.

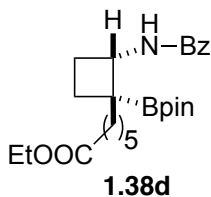


The desired product was purified by preparative thin layer chromatography (Silica plates; using 60:15:25 pentane to diethyl ether to dichloromethane as eluent). From **1.37b** to **1.38b**, combined average yield is 40%. (first batch: 119.7 mg, 38%; second batch: 132.3 mg, 42%). $^1\text{H NMR}$ (CD_2Cl_2 , 500 MHz) δ 7.8–7.75 (m, 2H), 7.69 (d, $J = 8.9$ Hz, 1H), 7.53–7.46 (m, 1H), 7.44 (t, $J = 7.5$ Hz, 2H), 4.30 (q, $J = 8.9$ Hz, 1H), 3.49 (t, $J = 6.8$ Hz, 2H), 2.3–2.22 (m, 1H), 1.88 (t, $J = 10.0$ Hz, 1H), 1.78 (p, $J = 10.1$ Hz, 1H), 1.69 (dt, $J = 12.2, 7.5$ Hz, 3H), 1.52–1.44 (m, 1H), 1.38–1.33 (m, 4H), 1.32 (d, $J = 9.3$ Hz, 12H), 1.15 (td, $J = 12.0, 5.5$ Hz, 2H); $^{13}\text{C NMR}$ (CD_2Cl_2 , 126 MHz) δ 167.8, 137.8, 133.6, 131.0, 129.3, 86.2, 54.5, 47.9, 41.8, 35.2, 32.0, 30.7, 29.3, 28.9, 27.5, 27.4, 27.1; $^{11}\text{B NMR}$

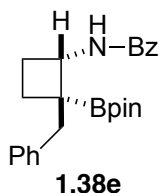
(CD₂Cl₂, 160 MHz) δ 34.4; **IR** 3414, 2928, 2855, 2182, 1661, 1526, 1488, 1383, 1313, 1139, 738 cm⁻¹; **HRMS** (DART) calcd. for C₂₃H₃₆BNO₃Cl [M+H⁺]: 420.24713, found 420.24813.



The desired product was purified by preparative thin layer chromatography (Silica plates; using 35:65 pentane to diethyl ether as eluent). From **1.37c** to **1.38c**, combined average yield is 45%. (first batch: 140.1 mg, 45%; second batch: 140.2 mg, 45%). **¹H NMR** (CD₂Cl₂, 500 MHz) δ 7.81–7.74 (m, 2H), 7.60 (d, J = 9.0 Hz, 1H), 7.54–7.47 (m, 1H), 7.44 (t, J = 7.5 Hz, 2H), 4.44 (t, J = 5.1 Hz, 1H), 4.30 (q, J = 8.8 Hz, 1H), 4.02 (dd, J = 10.5, 5.5 Hz, 2H), 3.71 (tdd, J = 11.5, 8.2, 2.6 Hz, 2H), 2.28 (q, J = 8.7 Hz, 1H), 2.06–1.93 (m, 1H), 1.90–1.77 (m, 2H), 1.72 (td, J = 12.9, 4.9 Hz, 1H), 1.67–1.53 (m, 3H), 1.51–1.44 (m, 1H), 1.41 (m, 1H), 1.32 (d, J = 6.7 Hz, 12H); **¹³C NMR** (CD₂Cl₂, 126 MHz) δ 167.6, 137.7, 133.6, 131.0, 129.3, 105.0, 86.3, 69.3, 54.4, 35.9, 34.7, 30.5, 28.5, 27.3, 27.2, 27.1; **¹¹B NMR** (CD₂Cl₂, 160 MHz) δ 34.1; **IR** 3419, 2973, 2930, 2850, 1665, 1525, 1382, 1314, 1276, 1140, 847, 800 cm⁻¹; **HRMS** (DART) calcd. for C₂₃H₃₅BNO₅ [M+H⁺]: 416.26028, found 416.26012.



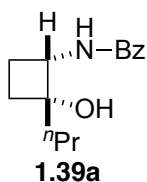
The desired product was purified by preparative thin layer chromatography (Silica plates; using 65:35 pentane to diethyl ether as eluent). From **1.37d** to **1.38d**, combined average yield is 53%. (first batch: 166.3 mg, 50%; second batch: 186.2 mg, 56%). **¹H NMR** (CD₂Cl₂, 500 MHz) δ 7.86–7.73 (m, 2H), 7.69 (d, *J* = 9.0 Hz, 1H), 7.55–7.48 (m, 1H), 7.45 (dd, *J* = 8.3, 6.6 Hz, 2H), 4.31 (q, *J* = 8.8 Hz, 1H), 4.06 (q, *J* = 7.1 Hz, 2H), 2.34–2.24 (m, 1H), 2.22 (t, *J* = 7.6 Hz, 2H), 1.89 (t, *J* = 10.0 Hz, 1H), 1.78 (p, *J* = 10.1 Hz, 1H), 1.68 (td, *J* = 12.2, 4.8 Hz, 1H), 1.60–1.43 (m, 4H), 1.33 (d, *J* = 7.5 Hz, 12H), 1.30–1.25 (m, 3H), 1.21 (t, *J* = 7.1 Hz, 3H), 1.19–1.11 (m, 1H); **¹³C NMR** (CD₂Cl₂, 126 MHz) δ 176.1, 167.6, 137.8, 133.6, 131.0, 129.3, 86.2, 62.6, 54.5, 41.7, 36.8, 32.2, 30.8, 28.7, 27.46, 27.37, 27.36, 27.1, 16.7; **¹¹B NMR** (CD₂Cl₂, 160 MHz) δ 34.4; **IR** 3420, 2977, 2933, 2856, 1733, 1663, 1524, 1487, 1382, 1373, 1313, 1270, 1168, 1140, 852, 736, 711, 696, 678 cm⁻¹; **HRMS** (DART) calcd. for C₂₅H₃₉BNO₅ [*M*+H⁺]: 444.29158, found 444.29144.



The desired product was purified by preparative thin layer chromatography (Silica plates; using 75:25 pentane to diethyl ether as eluent). From **1.37e** to **1.38e**, combined average yield is 57%. (first batch: 158.5 mg, 54%; second batch: 176.1 mg, 60%). **¹H NMR** (CD₂Cl₂, 500 MHz) δ 7.62 (d, *J* = 7.7 Hz, 2H), 7.53–7.44 (m, 2H), 7.44–7.36 (m, 2H), 7.24 (d, *J* = 8.3 Hz, 2H), 7.21–7.13 (m, 2H), 7.12–7.05 (m, 1H), 4.54 (q, *J* = 8.8 Hz, 1H), 2.97 (d, *J* = 13.4 Hz, 1H), 2.88 (d, *J* = 13.5 Hz, 1H), 2.29 (dt, *J* = 10.8, 8.1 Hz, 1H), 1.94 (t, *J* = 9.8 Hz, 1H), 1.79 (p, *J* = 10.1 Hz, 1H), 1.71–1.57 (m, 1H), 1.23 (d, *J* = 10.4 Hz, 12H); **¹³C NMR** (CD₂Cl₂, 126 MHz) δ 167.9, 142.2, 138.0, 133.5, 132.0, 130.9, 130.5, 129.2, 128.5,

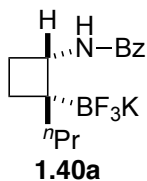
86.4, 54.2, 46.6, 31.0, 27.28, 27.24, 27.15; ^{11}B NMR (CD_2Cl_2 , 160 MHz) δ 34.1; **IR** 3417, 2976, 1653, 1522, 1488, 1381, 1316, 1141, 848, 704 cm^{-1} ; **HRMS** (DART) calcd. for $\text{C}_{24}\text{H}_{31}\text{BNO}_3$ [$\text{M}+\text{H}^+$]: 392.23915, found 392.23915.

Synthesis and Characterization of compound **1.39a**



In accordance with a previously reported protocol,⁵⁶ **1.38a** (85.8 mg, 0.250 mmol) and $\text{NaBO}_3 \cdot 4\text{H}_2\text{O}$ (154 mg, 1.00 mmol, 4.0 equiv.) were suspended in a mixture of THF (1.50 mL) and water (1.50 mL). The reaction mixture was allowed to stir at 22 °C for 21 h. After this time, the reaction mixture was diluted with additional water and EtOAc. The layers were separated, and the aqueous phase was extracted 3x with EtOAc; the combined organic extracts were dried over MgSO_4 , vacuum-filtered through a fritted funnel, and concentrated *in vacuo*. The product was isolated from the resulting residue by flash column chromatography (SiO_2 ; 70: 30 hexane to EtOAc) as a white solid. The procedure was repeated two times giving 73% average yield. (first batch: 42.6 mg, 73%; second batch: 43.0 mg, 74%). 2D ^1H NMR analysis confirmed the retention of the *cis* stereochemistry. ^1H NMR (CD_2Cl_2 , 600 MHz) δ 7.90–7.60 (m, 2H), 7.54–7.46 (m, 1H), 7.44 (dd, $J = 8.4$, 7.0 Hz, 2H), 6.82 (d, 1H), 4.34 (q, $J = 7.7$ Hz, 1H), 2.27 (dtd, $J = 12.3$, 8.2, 4.4 Hz, 1H), 2.04–1.97 (m, 1H), 1.96–1.83 (m, 2H), 1.68–1.56 (m, 2H), 1.46–1.34 (m, 2H), 0.94 (t, $J = 7.3$ Hz, 3H); ^{13}C NMR (CD_2Cl_2 , 151 MHz) δ 169.2, 137.3, 133.9, 131.1, 129.5, 81.9, 53.9, 45.5, 33.0, 27.4, 19.1, 16.8; **IR** 3291, 2916, 2849, 1979, 1634, 1541, 1265, 738 cm^{-1} ; **HRMS** (DART) calcd. for $\text{C}_{14}\text{H}_{20}\text{BNO}_2$ [$\text{M}+\text{H}^+$]: 234.14886, found 234.14819.

Synthesis and Characterization of compound **1.40a**



In accordance with a previously reported protocol,⁷² to a solution of **1.38a** (85.8 mg, 0.250 mmol) in MeOH (1.00 mL) and acetonitrile (1.00 mL) was added a solution of KF (65.1 mg, 1.12 mmol, 4.50 equiv.) in water (0.250 mL). A solution of L-(+)-tartaric acid (93.8 mg, 0.625 mmol, 2.50 equiv.) in THF (1.50 mL) was then added in portions over the course of 10 minutes (~0.150 mL per minute), with the reaction mixture vigorously stirred (1000 rpm) by the action of a magnetic stir bar. Upon completion of the addition, the reaction mixture was allowed to continue stirring for 3 minutes before a portion of acetonitrile (2.00 mL) was added. The reaction mixture was again allowed to stir for 2 minutes before a second portion of acetonitrile (1.00 mL) was added. The reaction mixture was vacuum-filtered through a glass-fritted funnel, and the solids were washed 3x with 2.00 mL acetonitrile. The filtrate was concentrated *in vacuo* and further dried under high vacuum. The resulting solid residue was redissolved in a minimal amount of acetone; CH₂Cl₂ was carefully added to the solution to induce precipitation of the product. The resulting suspension was sonicated for ~10 min before the insoluble material was collected by vacuum-filtration to afford the product as a white solid. Procedure was repeated second time to give 61% average yield. (first batch 48.4 mg, 60%; second batch 50.1mg, 61%). ¹H NMR (acetone-*d*₆, 500 MHz) δ 7.81–7.78 (m, 2H), 7.74–7.65 (m, 1H), 7.47–7.44 (m, 1H), 7.43–7.38 (m, 2H), 4.08 (q, *J* = 8.5 Hz, 1H), 2.15–2.09 (m, 1H), 1.97–1.78 (m, 2H), 1.48–1.27 (m, 4H), 1.19–1.10 (m, 1H), 0.81 (t, *J* = 7.1 Hz, 3H); ¹³C NMR (acetone-*d*₆, 126 MHz)

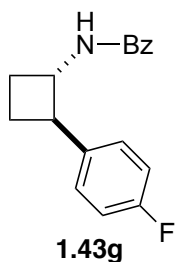
δ 164.7, 136.2, 130.4, 128.2, 126.7, 52.8, 43.4, 27.3, 24.9 (br), 24.4, 18.8, 15.0; ^{11}B NMR (acetone- d_6 , 160 MHz) δ 6.0; ^{19}F NMR (acetone- d_6 , 470 MHz) δ -143.04 to -143.27 (m, 3F); IR 3330, 2927, 2867, 1617, 1574, 1529, 1375, 1320, 1285, 1029, 850, 743 cm^{-1} ; HRMS (DART) calcd. for $\text{C}_{14}\text{H}_{18}\text{BNOF}_3[\text{M-K}^+]$: 284.14326, found 284.14384.

General Procedure for Arylation of **1.40**

In adaptation of a previously reported procedure,⁷⁶ to a 40 mL scintillation vial equipped with a magnetic stir bar was added, under air, (hetero)aryl bromide (0.35 mmol) (if solid), **1.40** (1.5 equiv.), $[\text{Ni}(\text{dtbbpy})(\text{H}_2\text{O})_4]\text{Cl}_2$ (5.0 mol%), $[\text{Ir}(\text{dFCF}_3\text{ppy})_2(\text{bpy})]\text{PF}_6$ (7.5 mol%). The vial was transferred to a glovebox, wherein Cs_2CO_3 (1.7 equiv.) and anhydrous 1,4-dioxane (14 mL) were added. (If liquid, the (hetero)aryl bromide was added to the reaction mixture at this point via microliter syringe.) The vial's cap was wrapped thoroughly with Teflon tape and then Parafilm, before the vial itself was placed 4.5 cm away from a single A160WE Kessil lamp (40 W); the center of the lamp's LED array was aligned halfway between the bottom of the vial and the solvent level. The reaction mixture was allowed to stir for 24 h under irradiation from the lamp set to maximum brightness. (The light color was left at the factory setting, i.e., midway between actinic (blue) and 10,000K (white).) An overhead fan provided cooling for the entire duration of the reaction (vial external surface temperature ~ 30 °C). After 24 h, the reaction mixture was vacuum-filtered through a pad of Celite, which was rinsed 4x with 20 mL of EtOAc. The combined filtrates were concentrated *in vacuo*, and the desired products were isolated from the resulting residue by automated silica gel flash chromatography.

Assignment of Relative Stereochemistry to Cyclobutanes **1.43g**

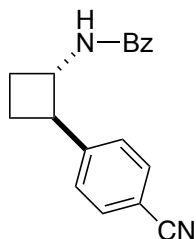
General procedure was followed using 38.5 μL of 1-bromo-4-fluorobenzene. After 24 h, ^{19}F NMR indicated the presence of both product (**1.43g**) and unconsumed starting material. The observed incomplete conversion presumably results from 1-bromo-4-fluorobenzene being a relatively more electron-rich substrate than those typically found effective with the conditions developed herein. Nevertheless, a sample of the major product diastereomer (14.1 mg, 15% unoptimized yield) was successfully isolated by column chromatography (10% to 20% EtOAc in hexanes). (^1H NMR peaks for the isolated material matched those of the major product species evident in the ^1H NMR spectrum of the crude reaction mixture.) Material suitable for single-crystal X-ray diffraction analysis was serendipitously obtained from this sample by evaporation of a CDCl_3 NMR solution in a capped 20 mL vial at 22 $^\circ\text{C}$. It was thus determined that the major diastereomer in this case possessed a *trans* configuration of the benzamido and 4-fluorophenyl substituents on the cyclobutane ring. On the basis of ^1H NMR chemical shifts and coupling constants highly similar to those in *trans*-**1.43g** for the α -amido CH (see below for full characterization data), *trans* relative stereochemistry was likewise assigned to all other major product diastereomers.



Characterization data for *trans*-**8g**: ^1H NMR (acetone- d_6 , 500 MHz) δ 8.09 (s, 1H), 7.89 (d, 2H, $J = 8.5$ Hz), 7.50 (t, 1H, $J = 7.2$ Hz), 7.43 (t, 2H, $J = 7.7$ Hz), 7.36 (dd, 2H, $J = 8.5, 5.6$ Hz), 7.04 (t, 2H, $J = 8.9$ Hz), 4.71 (p, 1H, $J = 8.8$ Hz), 3.64 (q, 1H, $J = 9.4$ Hz),

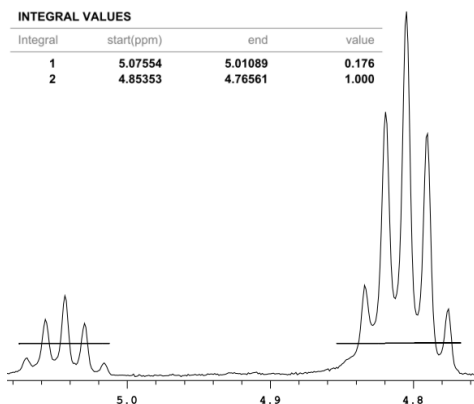
2.30 (q, 1H, $J = 8.3$ Hz), 2.20 (q, 1H, $J = 9.3$ Hz), 2.10 (p, 1H, $J = 9.9$ Hz, partial overlap with solvent peak), 1.79 (qd, 1H, $J = 10.4, 8.3$ Hz); ^{13}C NMR (acetone- d_6 , 151 MHz) δ 166.5, 162.4 (d, $J = 242.0$ Hz), 140.4, 136.0, 132.1, 129.3 (d, $J = 7.8$ Hz), 129.2, 128.2, 115.8 (d, $J = 21.0$ Hz), 52.0, 48.9, 27.9, 23.2; ^{19}F NMR (acetone- d_6 , 470 MHz) δ -117.8 to -118.0 (m, 1F); IR 3324, 3046, 2950, 2875, 1635, 1528, 1507, 1327, 1293, 1218, 1184, 1156 cm^{-1} ; HRMS (DART) calcd. for $\text{C}_{17}\text{H}_{17}\text{NOF}$ $[\text{M}+\text{H}^+]$ 270.1289, found: 270.1300.

Characterization of Cyclobutanes **1.43a–1.43f**



1-benzamido-2-(4-cyanophenyl)cyclobutane (**1.43a**)

General procedure was followed using 63.7 mg of 4-bromobenzonitrile to obtain cyclobutane **1.43a** by chromatography (15% to 25% EtOAc in hexanes) as an off-white solid (70.9 mg, 73%; 85:15 *trans:cis*⁸⁸). A second run of this experiment afforded **1.43a** (71.5 mg, 73%) in 82:18 dr. The average yield was thus reported as 73% and the average *trans:cis* ratio as 84:16. Repeated chromatographic treatments enabled separation of the *trans* and *cis* diastereomers for characterization purposes.

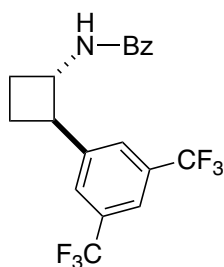


Characterization data for *trans*-**8a**: ¹H NMR (acetone-*d*₆, 600 MHz) δ 8.17 (d, 1H, *J* = 8.6 Hz), 7.90 (d, 2H, *J* = 6.8 Hz), 7.69 (d, 2H, *J* = 8.2 Hz), 7.55 (d, 2H, *J* = 8.0 Hz),

⁸⁸ Except where noted, the *trans:cis* ratio was determined by integration of the α -amido CH ¹H NMR peak, using specifically Agilent VNMRJ 4.2 software for the analysis.

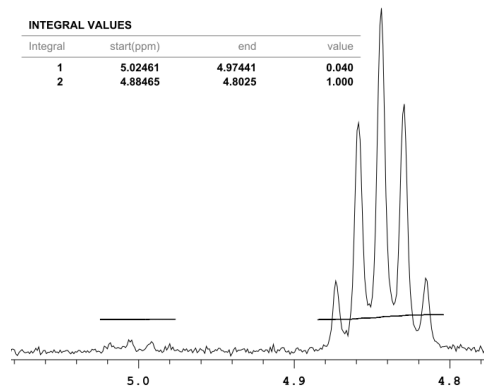
7.51 (t, 1H, $J = 7.3$ Hz), 7.44 (t, 2H, $J = 7.8$ Hz), 4.77 (p, 1H, $J = 8.7$ Hz), 3.76 (q, 1H, $J = 9.3$ Hz), 2.33 (q, 1H, $J = 9.3$ Hz), 2.25 (q, 1H, $J = 9.4$ Hz), 2.17 (p, 1H, $J = 9.6$ Hz), 1.91–1.81 (m, 1H); ^{13}C NMR (acetone- d_6 , 151 MHz) δ 166.6, 150.0, 135.8, 133.1, 132.2, 129.3, 128.7, 128.2, 119.7, 110.9, 108.2, 51.6, 49.7, 27.8, 22.8; IR 3284, 3058, 2955, 2856, 2227, 1727, 1632, 1605, 1525, 1332, 1292, 1106 cm^{-1} ; HRMS (DART) calcd. for $\text{C}_{18}\text{H}_{17}\text{N}_2\text{O}$ $[\text{M}+\text{H}^+]$ 277.1335, found 277.1337.

Characterization data for *cis*-**8a**: ^1H NMR (acetone- d_6 , 500 MHz) δ 7.64 (d, 2H, $J = 8.3$ Hz), 7.54–7.37 (m, 5H), 7.31 (t, 2H, $J = 7.7$ Hz), 5.00 (p, 1H, $J = 7.7$ Hz), 4.08–4.00 (m, 1H), 2.60–2.47 (m, 1H), 2.47–2.30 (m, 3H); ^{13}C NMR (acetone- d_6 , 126 MHz) δ 167.4, 147.2, 136.1, 132.7, 131.9, 130.3, 129.1, 128.0, 119.7, 110.7, 49.8, 47.0, 26.9, 21.6; IR 3272, 3064, 2951, 2872, 2223, 1726, 1624, 1532, 1505, 1332, 1291 cm^{-1} ; HRMS (DART) calcd. for $\text{C}_{18}\text{H}_{17}\text{N}_2\text{O}$ $[\text{M}+\text{H}^+]$ 277.1335, found 277.1341.

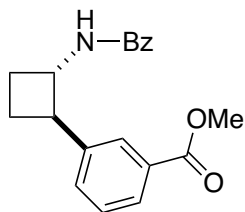


1-benzamido-2-(3,5-bis(trifluoromethyl)phenyl)cyclobutane (**1.43b**)

General procedure was followed using 60.5 μL of 3,5-bis(trifluoromethyl)-1-bromobenzene to obtain cyclobutane **1.43b** by chromatography (10% EtOAc in hexanes) as an off-white solid (84.9 mg, 62%; >98:2 *trans*:*cis*). A second run of this experiment afforded **1.43b** (75.4 mg, 56%) in 96:4 dr. The average yield was thus reported as 59% and the average *trans*:*cis* ratio as 98:2.

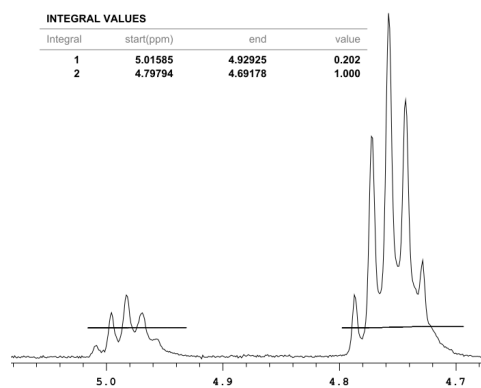


As the individual *trans* and *cis* diastereomers could not be separated by conventional chromatographic techniques, **1.43b** was characterized as a mixture: $^1\text{H NMR}$ (acetone- d_6 , 600 MHz) δ 8.18 (d, 1H, $J = 6.2$ Hz), 8.05 (s, 2H), 7.89 (d, 2H, $J = 7.0$ Hz), 7.86 (s, 1H), 7.77 (s, 0.11H), 7.67 (d, 0.14H, $J = 6.9$ Hz), 7.54 (d, 0.20H, $J = 7.8$ Hz), 7.51 (t, 1H, $J = 7.4$ Hz), 7.44 (t, 2H, $J = 7.7$ Hz), 7.40 (t, 0.13H, $J = 7.8$ Hz), 7.30 (t, 0.24H, $J = 7.6$ Hz), 5.01 (p, 0.16H, $J = 7.9$ Hz), 4.84 (p, 1H, $J = 8.6$ Hz), 4.20 (q, 0.15H, $J = 7.3$ Hz), 3.86 (q, 1H, $J = 9.3$ Hz), 2.63–2.52 (m, 0.32H), 2.50–2.42 (m, 0.21H), 2.42–2.31 (m, 2H), 2.25 (p, 1H, $J = 9.5$ Hz), 1.97 (qd, 1H, $J = 10.4, 8.6$ Hz); $^{13}\text{C NMR}$ (acetone- d_6 , 151 MHz) δ 166.8, 147.8, 135.8, 132.2, 132.1 (q, $J = 32.9$ Hz), 129.3, 128.6–128.4 (m), 128.2, 124.8 (q, $J = 271.8$ Hz), 120.9 (hept, $J = 3.7$ Hz), 51.6, 49.6, 27.5, 23.0; $^{19}\text{F NMR}$ (acetone- d_6 , 470 MHz) δ –62.3 (s, 6F); **IR** 3294, 1632, 1531, 1388, 1352, 1286, 1157, 1118 cm^{-1} ; **HRMS** (DART) calcd. for $\text{C}_{19}\text{H}_{16}\text{NOF}_6$ [$\text{M}+\text{H}^+$] 388.1131, found 388.1128.



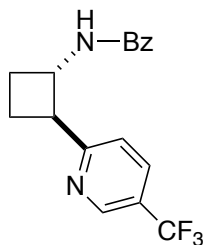
1-benzamido-2-(3-methoxycarbonylphenyl)cyclobutane (**1.43c**)

General procedure was followed using 91.6 mg of methyl 3-iodobenzoate to obtain cyclobutane **1.43c** by chromatography (15% to 25% EtOAc in hexanes) as a pale yellow solid (89.1 mg, 82%; 83:17 *trans:cis*). A second run of this experiment afforded **1.43c** (85.9 mg, 78%) in 82:18 dr. The average yield was thus reported as 80% and the average *trans:cis* ratio as 82:18.



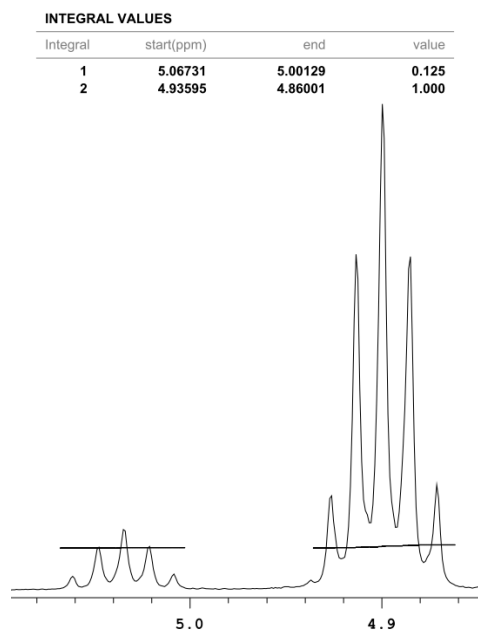
As the individual *trans* and *cis* diastereomers could not be separated by conventional chromatographic techniques, **1.43c** was characterized as a mixture: ¹H NMR (acetone-*d*₆, 600 MHz) δ 8.13 (d, 1H, *J* = 5.1 Hz), 7.94 (s, 1H), 7.89 (d, 2H, *J* = 8.3 Hz), 7.84 (d, 1H, *J* = 7.9 Hz), 7.78 (d, 0.26H, *J* = 7.1 Hz), 7.64 (d, 1H, *J* = 7.1 Hz), 7.53–7.47 (m, 2H), 7.47–7.33 (m, 3.47H), 7.28 (t, 0.49H, *J* = 7.6 Hz), 4.98 (p, 0.28H, *J* = 8.0 Hz), 4.76 (p, 1H, *J* = 8.8 Hz), 4.08–3.98 (m, 0.41H), 3.86 (s, 3H), 3.83 (s, 0.70H), 3.73 (q, 1H, *J* = 9.4 Hz), 2.56–2.49 (m, 0.3H), 2.46–2.30 (m, 1.70H), 2.24 (q, 1H, *J* = 9.8 Hz), 2.18–

2.08 (m, 1H), 1.91–1.82 (m, 1H); ^{13}C NMR (acetone- d_6 , 151 MHz) δ 167.5, 166.6, 144.9, 136.0, 134.2, 132.3, 132.1, 131.8 (minor), 131.3 (minor), 129.9, 129.6, 129.3, 129.2 (minor), 129.0 (minor), 128.6, 128.2, 128.1 (minor), 128.0 (minor), 52.44, 52.37 (minor), 52.0, 49.6 (minor), 49.3, 46.6 (minor), 28.1, 27.0 (minor), 23.0, 21.7 (minor); **IR** 3341, 3062, 2948, 1716, 1636, 1603, 1580, 1523, 1488, 1438, 1328, 1295, 1274, 1206, 1109, 1088 cm^{-1} ; **HRMS** (DART) calcd. for $\text{C}_{19}\text{H}_{20}\text{NO}_3$ $[\text{M}+\text{H}^+]$ 310.1438, found 310.1423.



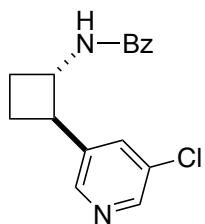
1-benzamido-2-(5-(trifluoromethyl)pyrid-2-yl)cyclobutane (**1.43d**)

General procedure was followed using 78.5 mg of 2-bromo-5-(trifluoromethyl)pyridine to obtain cyclobutane **1.43d** by chromatography (15% to 25% to 30% EtOAc in hexanes) as an off-white solid (52.3 mg, 47%; 89:11 *trans:cis*). A second run of this experiment afforded **1.43d** (59.0 mg, 52%) in 93:7 dr. The average yield was thus reported as 50% and the average *trans:cis* ratio as 91:9. Repeated chromatographic treatments enabled separation of the *trans* and *cis* diastereomers for characterization purposes.



Characterization data for *trans*-**1.43d**: $^1\text{H NMR}$ (acetone- d_6 , 500 MHz) δ 8.87 (s, 1H), 8.14 (d, 1H, $J = 8.8$ Hz), 8.01 (d, 1H, $J = 8.2$ Hz), 7.87 (d, 2H, $J = 7.1$ Hz), 7.57 (d, 1H, $J = 8.1$ Hz), 7.49 (t, 1H, $J = 7.4$ Hz), 7.42 (t, 2H, $J = 7.8$ Hz), 4.89 (p, 1H, $J = 8.4$ Hz), 3.87 (q, 1H, $J = 8.9$ Hz), 2.38–2.30 (m, 1H), 2.27–2.07 (m, 3H); $^{13}\text{C NMR}$ (acetone- d_6 , 151 MHz) δ 167.4, 166.6, 147.0 (q, $J = 4.2$ Hz), 135.9, 134.4 (q, $J = 3.6$ Hz), 132.1, 129.2, 128.2, 125.2 (q, $J = 271.2$ Hz), 124.8 (q, $J = 32.5$ Hz), 122.8, 51.6, 51.3, 27.6, 21.9; $^{19}\text{F NMR}$ (acetone- d_6 , 564 MHz) δ -61.8; **IR** 3300, 2988, 1635, 1605, 1533, 1394, 1329, 1207, 1166, 1117 cm^{-1} ; **HRMS** (DART) calcd. for $\text{C}_{17}\text{H}_{16}\text{N}_2\text{OF}_3$ $[\text{M}+\text{H}^+]$ 321.1209, found 321.1212.

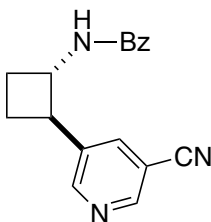
Characterization data for *cis*-**1.43d**: $^1\text{H NMR}$ (acetone- d_6 , 600 MHz) δ 8.94 (s, 1H), 7.96 (dd, 1H, $J = 8.3, 2.4$ Hz), 7.72 (br s, 1H), 7.55 (d, 2H, $J = 7.3$ Hz), 7.46–7.38 (m, 2H), 7.33 (t, 2H, $J = 7.6$ Hz), 5.03 (p, 1H, $J = 7.8$), 4.19–4.12 (m, 1H), 2.58–2.43 (m, 3H), 2.33–2.25 (m, 1H); $^{13}\text{C NMR}$ (acetone- d_6 , 151 MHz) δ 166.9, 166.3, 146.7 (q, $J = 4.2$), 135.9, 134.1 (q, $J = 3.3$ Hz), 132.0, 129.2, 127.9, 125.5, 125.2 (appd, $J = 270.8$ Hz), 124.7 (appd, $J = 32.3$ Hz), 49.1, 48.2, 28.0, 21.6; $^{19}\text{F NMR}$ (acetone- d_6 , 564 MHz) δ -61.9; **IR** 3267, 2960, 1627, 1604, 1530, 1326, 1258, 1126, 1079, 1013 cm^{-1} ; **HRMS** (DART) calcd. for $\text{C}_{17}\text{H}_{16}\text{N}_2\text{OF}_3$ $[\text{M}+\text{H}^+]$ 321.1209, found 321.1209.



1-benzamido-2-(5-chloropyrid-3-yl)cyclobutane (1.43e)

General procedure was followed using 67.7 mg of 3-bromo-5-chloropyridine to obtain cyclobutane *trans*-**1.43e** by chromatography (10% to 40% EtOAc in hexanes) as an off-white solid (65.4 mg, 65%); although *cis*-**1.43e** was also observed in the crude reaction mixture, it co-eluted with an unknown impurity and thus could not be isolated. A second run of this experiment afforded 64.1 mg (64%) of **1.43e**. The average yield was thus reported as 64%. A ratio of 91:9 *trans*:*cis* was estimated for an additional reaction conducted according to Procedure B (*vide infra*) with 3-bromo-5-chloropyridine in place of 4-bromobenzonitrile.

Characterization data for *trans*-**1.43e**: ¹H NMR (acetone-*d*₆, 600 MHz) δ 8.48 (s, 1H), 8.40 (d, 1H, *J* = 2.5 Hz), 8.15 (br s, 1H), 7.93–7.86 (m, 3H), 7.50 (t, 1H, *J* = 7.5 Hz), 7.43 (t, 2H, *J* = 7.8 Hz), 4.77 (p, 1H, *J* = 8.4 Hz), 3.69 (q, 1H, *J* = 9.2 Hz), 2.35 (q, 1H, *J* = 8.8 Hz), 2.31–2.17 (m, 3H), 1.97–1.87 (m, 1H); ¹³C NMR (acetone-*d*₆, 151 MHz) δ 166.7, 147.8, 147.2, 141.4, 135.8, 134.8, 132.4, 132.2, 129.3, 128.2, 51.6, 47.2, 27.8, 22.8; IR 3328, 2964, 1636, 1529, 1409, 1312, 1241, 1160, 1105, 1002 cm⁻¹; HRMS (DART) calcd. for C₁₆H₁₆N₂OCl [M+H⁺] 287.0946, found 287.0943.



1-benzamido-2-(5-cyanopyrid-3-yl)cyclobutane (**1.43f**)

General procedure was followed using 64.3 mg of 5-bromo-3-cyanopyridine to obtain cyclobutane **1.43f** by chromatography (15% to 50% EtOAc in hexanes) as a pale

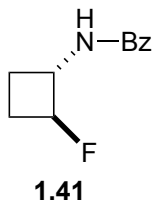
yellow solid (74.5 mg, 76%; 94:6 *trans:cis*⁸⁹). A second run of this experiment afforded **1.43f** (77.5 mg, 80%) in 90:10 dr. The average yield was thus reported as 78% and the average *trans:cis* ratio as 92:8. Chromatographic treatment enabled separation of the *trans* and *cis* diastereomers for characterization purposes.

Characterization data for *trans*-**1.43f**: **¹H NMR** (acetone-*d*₆, 500 MHz) δ 8.82 (s, 1H), 8.78 (s, 1H), 8.26 (s, 1H), 8.19 (br s, 1H), 7.89 (d, 2H, *J* = 7.0 Hz), 7.51 (t, 1H, *J* = 7.2 Hz), 7.43 (t, 2H, *J* = 7.6 Hz), 4.79 (p, 1H, *J* = 8.5 Hz), 3.75 (q, 1H, *J* = 9.0 Hz), 2.42–2.20 (m, 3H), 2.02–1.91 (m, 1H); **¹³C NMR** (acetone-*d*₆, 151 MHz) δ 166.8, 153.2, 151.1, 140.3, 138.5, 135.7, 132.2, 129.3, 128.3, 117.8, 110.5, 51.6, 47.3, 27.6, 22.7; **IR** 3285, 3052, 2981, 2947, 2866, 2331, 1639, 1538, 1491, 1426, 1343, 1306, 1295 cm⁻¹; **HRMS** (DART) calcd. for C₁₇H₁₆N₃O [M+H⁺] 278.1288, found 278.1294.

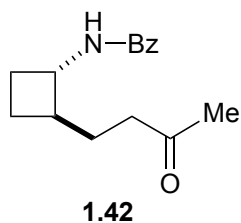
Characterization data for *cis*-**1.43f**: **¹H NMR** (acetone-*d*₆, 600 MHz) δ 8.69 (s, 2H), 8.13 (s, 1H), 7.66 (br s, 1H), 7.56 (d, 2H, *J* = 7.7 Hz), 7.43 (t, 1H, *J* = 7.4 Hz), 7.33 (t, 2H, *J* = 7.6 Hz), 5.01–4.92 (m, 1H), 4.13–4.06 (m, 1H), 2.63–2.52 (m, 1H), 2.52–2.38 (m, 3H); **¹³C NMR** (acetone-*d*₆, 151 MHz) δ 167.4, 154.8, 150.8, 139.5, 137.5, 135.7, 132.0, 129.2, 128.0, 117.8, 110.1, 49.9, 44.2, 26.4, 21.5; **IR** 3387, 3350, 2953, 2241, 2231, 1736, 1659, 1628, 1521, 1486, 1423, 1345, 1282, 1149, 1105 cm⁻¹; **HRMS** (DART) calcd. for C₁₇H₁₆N₃O [M+H⁺] 278.1288, found 278.1302.

Procedures and Characterizations of Additional C–B Bond Functionalization Products **1.41** and **1.42**

⁸⁹ Based on yields of separated isomers.



In adaptation of a previously reported procedure,⁷³ in a N₂-filled glovebox, **1.36** (45.2 mg, 0.150 mmol), AgNO₃ (7.6 mg, 0.045 mmol), Selectfluor (159 mg, 0.450 mmol) were added to a 20 mL vial containing a magnetic stir bar. Then, CH₂Cl₂ (0.70 mL), water (0.70 mL), and trifluoroacetic acid (69.0 μL, 0.900 mmol) were added successively at room temperature. The reaction mixture was allowed to stir at 50 °C for 24 hours under N₂ flow. At the conclusion of the reaction, the resulting mixture was extracted with EtOAc (10 mL × 3). The combined organic phases were dried over anhydrous MgSO₄. After removal of solvent under reduced pressure, the crude material was purified by silica gel chromatography with hexane/ethyl acetate 4:1 as the eluent to give the desired product with an average yield of 57% as a white solid. (first batch: 17.0 mg, 59%; second batch: 16.2 mg, 56%). 2D-NMR experiments are consistent with the trans-stereoisomer being formed as a single diastereomer. ¹H NMR (CD₂Cl₂, 500 MHz) δ 7.78 (d, *J* = 7.7 Hz, 2H), 7.59–7.52 (m, 1H), 7.47 (t, *J* = 7.9 Hz, 2H), 6.43 (br s, 1H), 4.91 (dq, *J* = 55.2, 7.6 Hz, 1H), 4.58 (m, 1H), 2.33–2.19 (m, 2H), 1.91 (dt, *J* = 19.3 Hz, 1H), 1.49 (p, *J* = 10.1 Hz, 1H). ¹³C NMR (CD₂Cl₂, 101 MHz) δ 166.6, 134.3, 131.5, 128.5, 126.8, 90.8 (d, ¹*J*_{CF} = 225.1 Hz), 52.4 (d, ²*J*_{CF} = 22.2 Hz), 23.7 (d, ³*J*_{CF} = 19.9 Hz), 18.3 (d, ²*J*_{CF} = 23.1 Hz); ¹⁹F NMR (CD₂Cl₂, 470 MHz): –165.0 (m); IR: 1637, 1579, 1536, 1491, 1340, 1294, 1265, 1056, 736, 702 cm⁻¹; HRMS (DART) calcd. for C₁₁H₁₃NOF [M+H⁺] 194.09757, found 194.09781.



In adaptation of a previously reported procedure,⁷⁴ to a 20 mL scintillation vial equipped with a magnetic stir bar was added, under N₂, **1.36** (60.2 mg, 0.200 mmol), the photoredox catalyst [Ir(dFCF₃ppy)₂(dtbbpy)]PF₆ (4.5 mg, 0.0040 mmol), and the Lewis base catalyst 4-dimethylaminopyridine (4.9 mg, 0.04 mmol). Then methyl vinyl ketone (65.5 μL, 0.800 mmol) was added followed by 2.0 mL of a degassed acetone/methanol (1:1) mixture to afford a clear yellow solution. The reaction mixture was allowed to stir while being irradiated with a commercial blue LED strip (16.0 W, 450 nm) for 24 hours. A fan provided cooling for the entire duration of the reaction (vial external surface temperature ~30 °C). After 24 h, the reaction mixture passed through a pad of Celite, with additional 3 x 10 mL of EtOAc as the eluent. The combined filtrates were concentrated in vacuo, and the desired product was isolated from the resulting crude residue by silica gel column chromatography to give to desired product with 64% average yield as a colorless oil (first batch: 31.0 mg, 63%; second batch: 33.1mg, 65%). 2D-NMR experiments are consistent with the *trans*-stereoisomer being formed as a single diastereomer. ¹H NMR (CD₂Cl₂, 500 MHz) δ 7.80–7.74 (m, 2H), 7.56–7.50 (m, 1H), 7.47 (td, *J* = 7.5 Hz, 2H), 6.39 (br s, 1H), 4.19 (p, *J* = 8.4 Hz, 1H), 2.58–2.39 (m, 2H), 2.34 (q, *J* = 8.9 Hz, 1H), 2.26–2.19 (m, 1H), 2.19 (s, 3H), 1.96–1.88 (m, 1H), 1.87–1.68(m, 3H), 1.41–1.35 (m, 1H); ¹³C NMR (CD₂Cl₂, 126 MHz) δ 208.7, 166.0, 134.8, 131.2, 128.4, 126.7, 50.2, 44.6, 40.7, 29.5, 28.7, 27.4, 21.3; IR: 2926, 2854, 1714, 1638, 1578, 1539, 1490, 1457, 1419, 1361, 1265,

953, 736,710 cm^{-1} ; **HRMS** (DART) calcd. for $\text{C}_{15}\text{H}_{20}\text{NO}_2$ $[\text{M}+\text{H}^+]$ 246.14886, found 246.14892.

1.6.3.3 X-ray Crystallographic Data

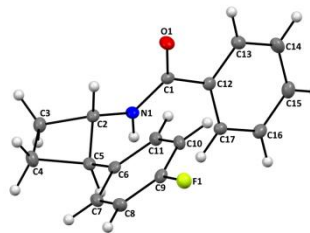
X-ray Crystallographic Data for 1.36 and *trans*-1.43g

Crystal data and structure refinement for **1.36**. (CCDC-1856962)

Identification code	C17H24BNO3	
Empirical formula	C17 H24 B N O3	
Formula weight	301.18	
Temperature	100(2) K	
Wavelength	1.54178 Å	
Crystal system	Monoclinic	
Space group	P2 ₁ /n	
Unit cell dimensions	a = 10.6189(3) Å α = 90° b = 14.2709(5) Å β = 99.5160(10)° c = 21.7864(7) Å γ = 90°	
Volume	3256.11(18) Å ³	
Z	8	
Density (calculated)	1.229 Mg/m ³	
Absorption coefficient	0.656 mm ⁻¹	
F(000)	1296	
Crystal size	0.420 x 0.220 x 0.180 mm ³	
Theta range for data collection	3.718 to 66.772°	
Index ranges	-12 ≤ h ≤ 12, -16 ≤ k ≤ 15, -24 ≤ l ≤ 25	
Reflections collected	20966	
Independent reflections	5722 [R(int) = 0.0258]	
Completeness to theta = 66.772°	99.1%	
Absorption correction	Semi-empirical from equivalents	
Max. and min. transmission	0.7528 and 0.6552	
Refinement method	Full-matrix least-squares on F ²	
Data / restraints / parameters	5722 / 0 / 413	
Goodness-of-fit on F ²	1.124	
Final R indices [I > 2σ(I)]	R1 = 0.0444, wR2 = 0.1123	
R indices (all data)	R1 = 0.0456, wR2 = 0.1133	
Extinction coefficient	n/a	
Largest diff. peak and hole	0.415 and -0.283 e.Å ⁻³	

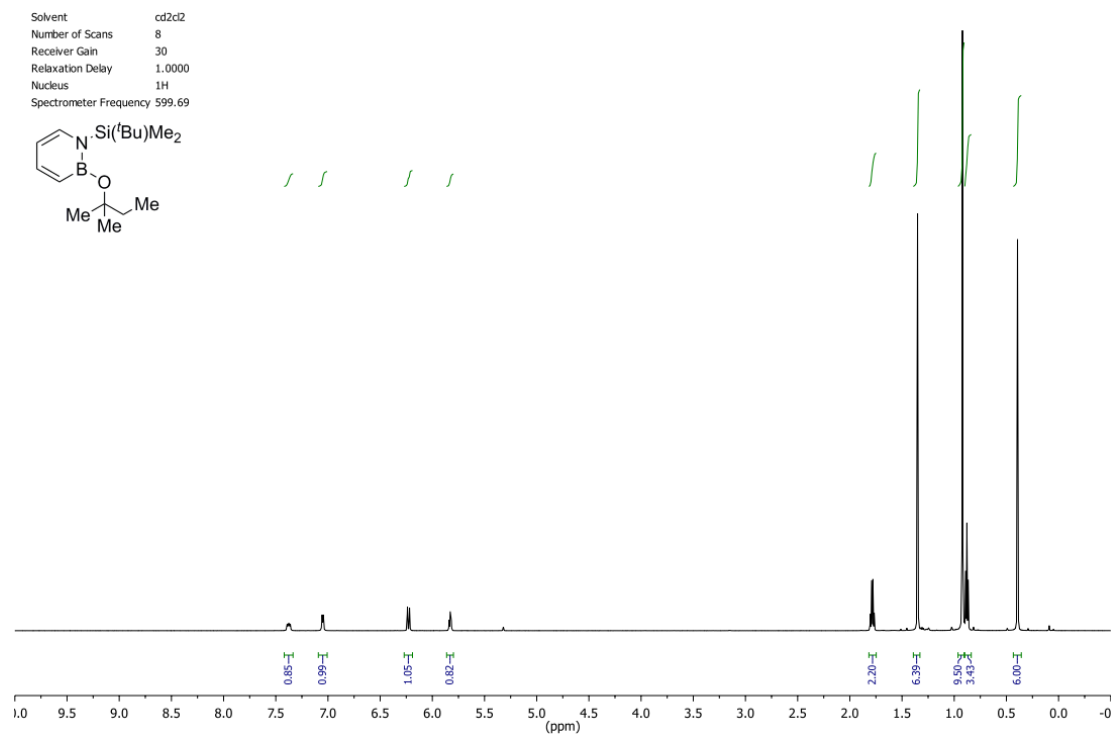
Crystal data and structure refinement for *trans*-**1.43g**. (CCDC-1856966)

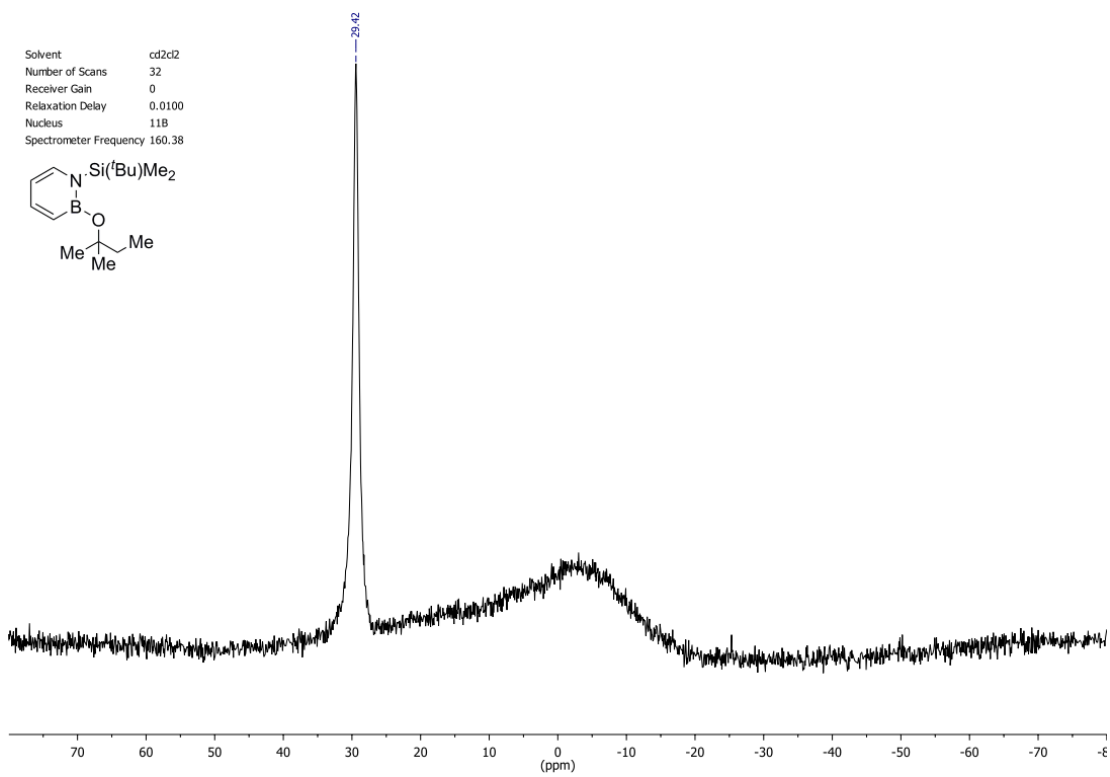
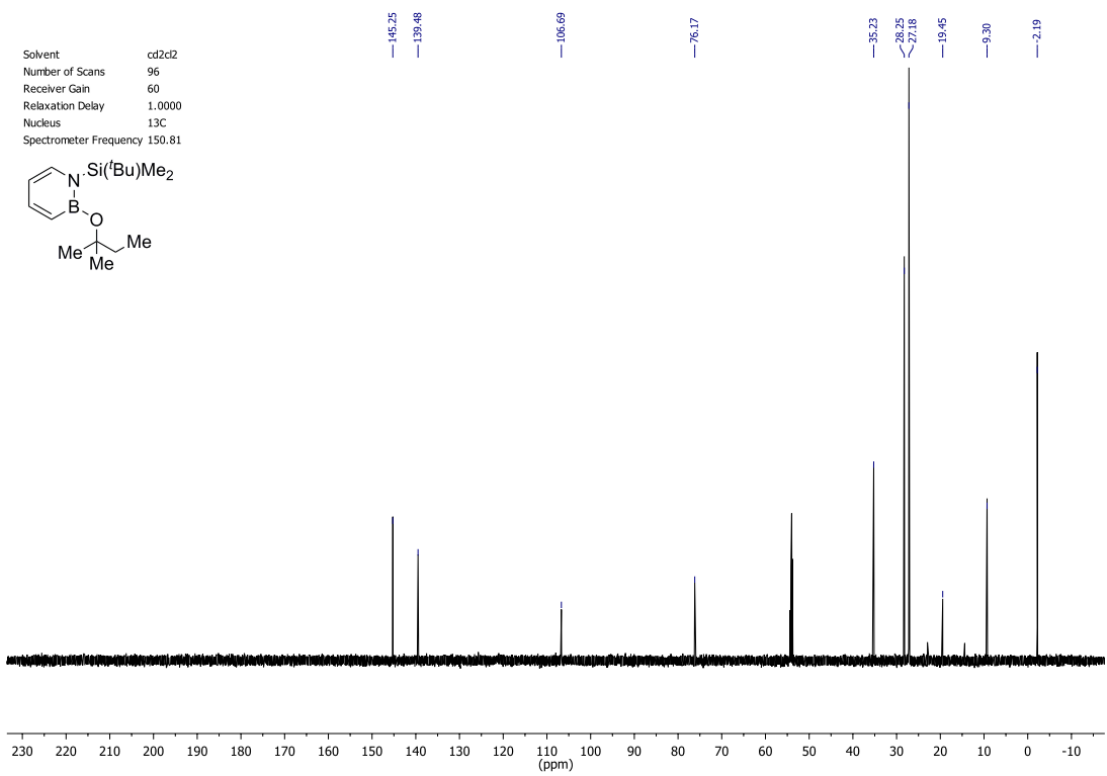
Identification code	C17H16FNO	
Empirical formula	C ₁₇ H ₁₆ F N O	
Formula weight	269.31	
Temperature	100(2) K	
Wavelength	1.54178 Å	
Crystal system	Monoclinic	
Space group	Cc	
Unit cell dimensions	a = 15.4079(6) Å	
	b = 11.0271(4) Å	β = 26.3440(10)°
	c = 10.0582(4) Å	γ = 90°
Volume	1376.50(9) Å ³	
Z	4	
Density (calculated)	1.300 Mg/m ³	
Absorption coefficient	0.730 mm ⁻¹	
F(000)	568	
Crystal size	0.480 x 0.390 x 0.220 mm ³	
Theta range for data collection	5.366 to 66.511°.	
Index ranges	-18 ≤ h ≤ 18, -11 ≤ k ≤ 13, -11 ≤ l ≤ 11	
Reflections collected	5216	
Independent reflections	2168 [R(int) = 0.0343]	
Completeness to theta = 66.511°	98.5%	
Absorption correction	Semi-empirical from equivalents	
Max. and min. transmission	0.7528 and 0.6303	
Refinement method	Full-matrix least-squares on F ²	
Data / restraints / parameters	2168 / 3 / 185	
Goodness-of-fit on F ²	1.083	
Final R indices [I > 2σ(I)]	R1 = 0.0291, wR2 = 0.0744	
R indices (all data)	R1 = 0.0291, wR2 = 0.0745	
Absolute structure parameter	0.01(5)	
Extinction coefficient	n/a	
Largest diff. peak and hole	0.193 and -0.182 e.Å ⁻³	



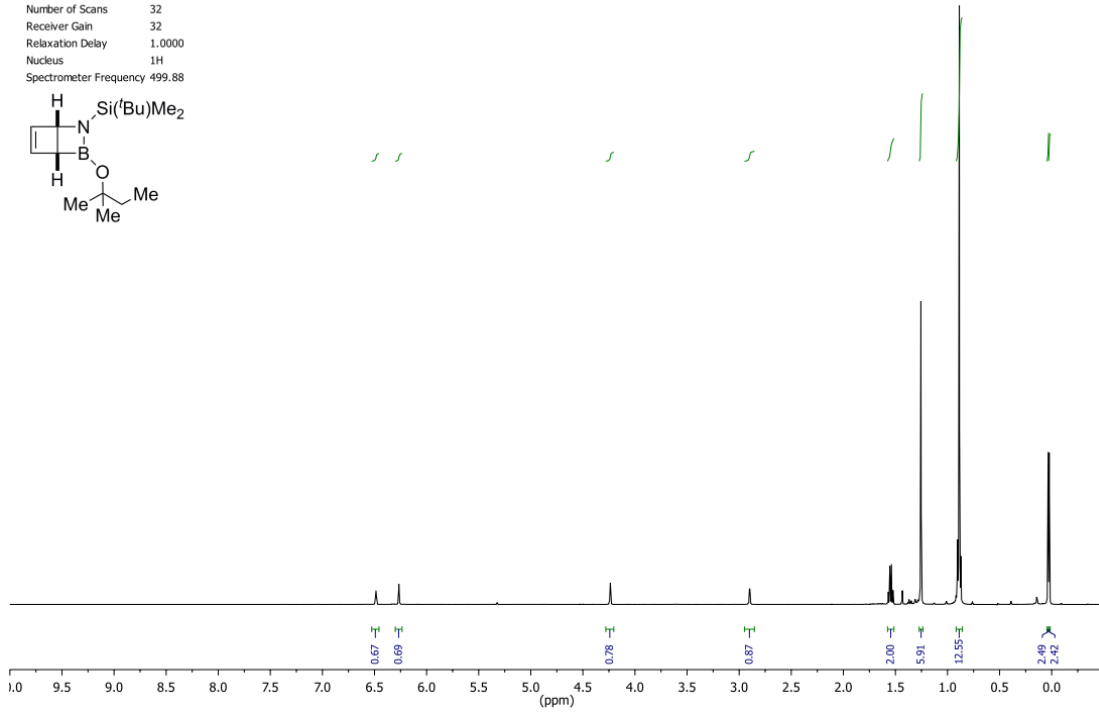
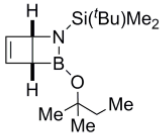
1.6.3.4 Analytical Data

NMR Spectra:

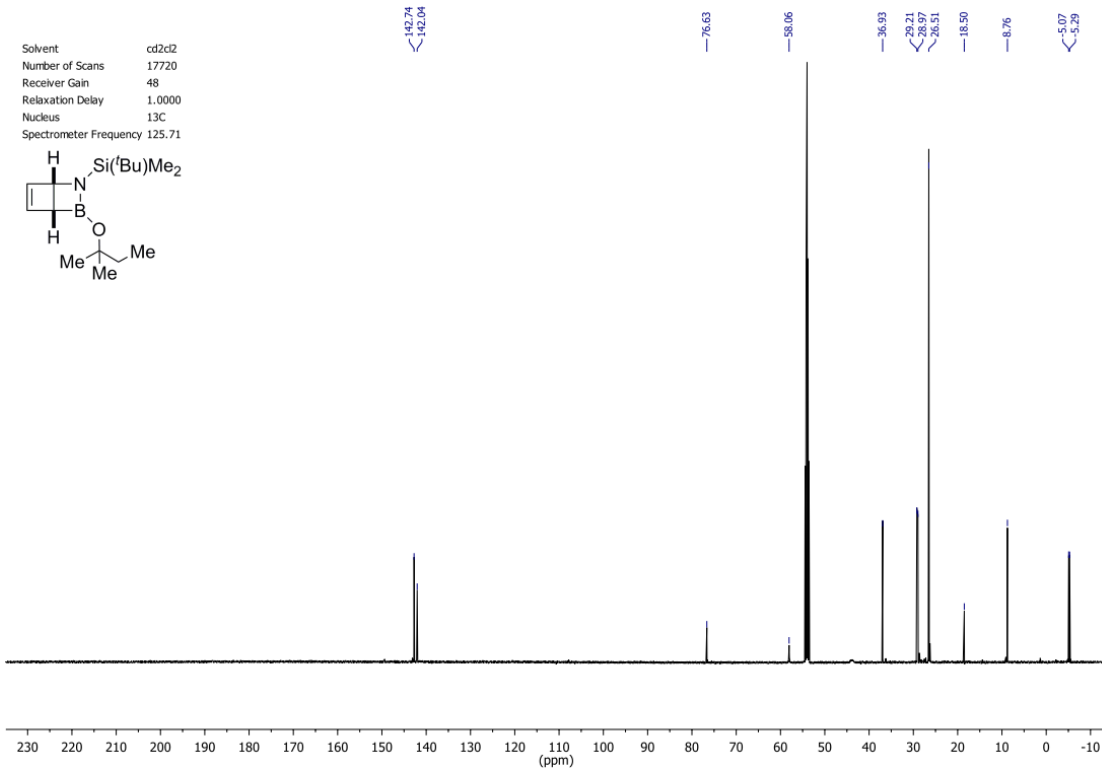
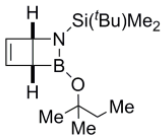


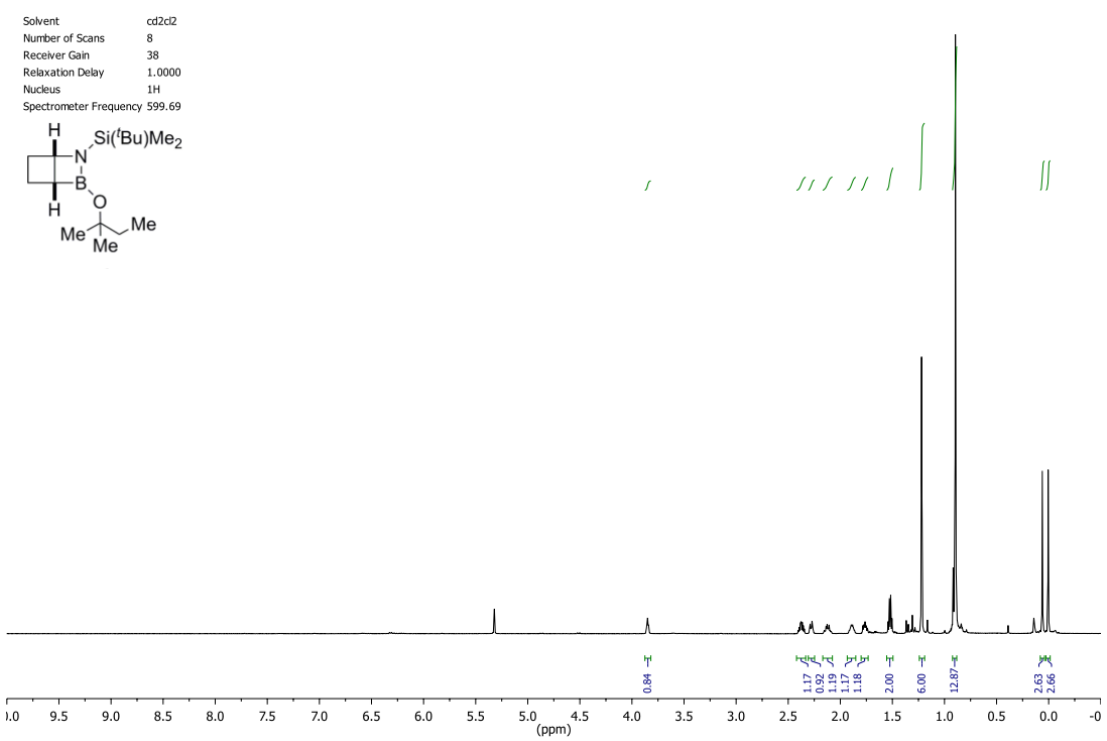
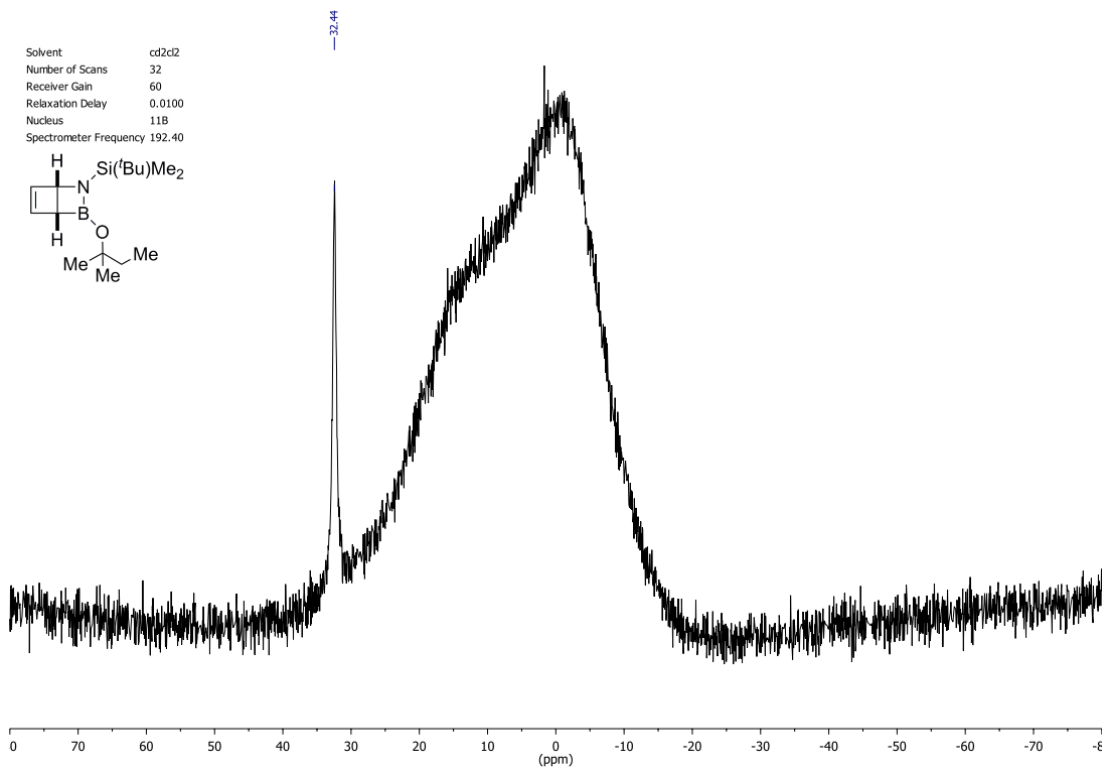


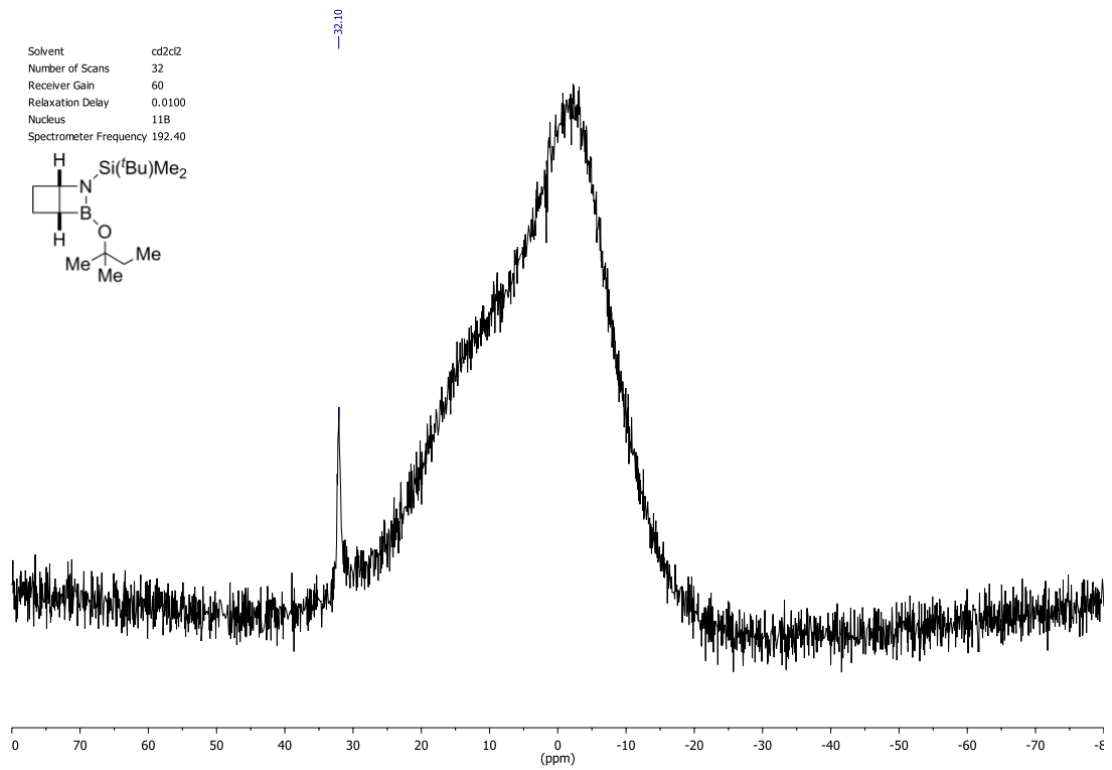
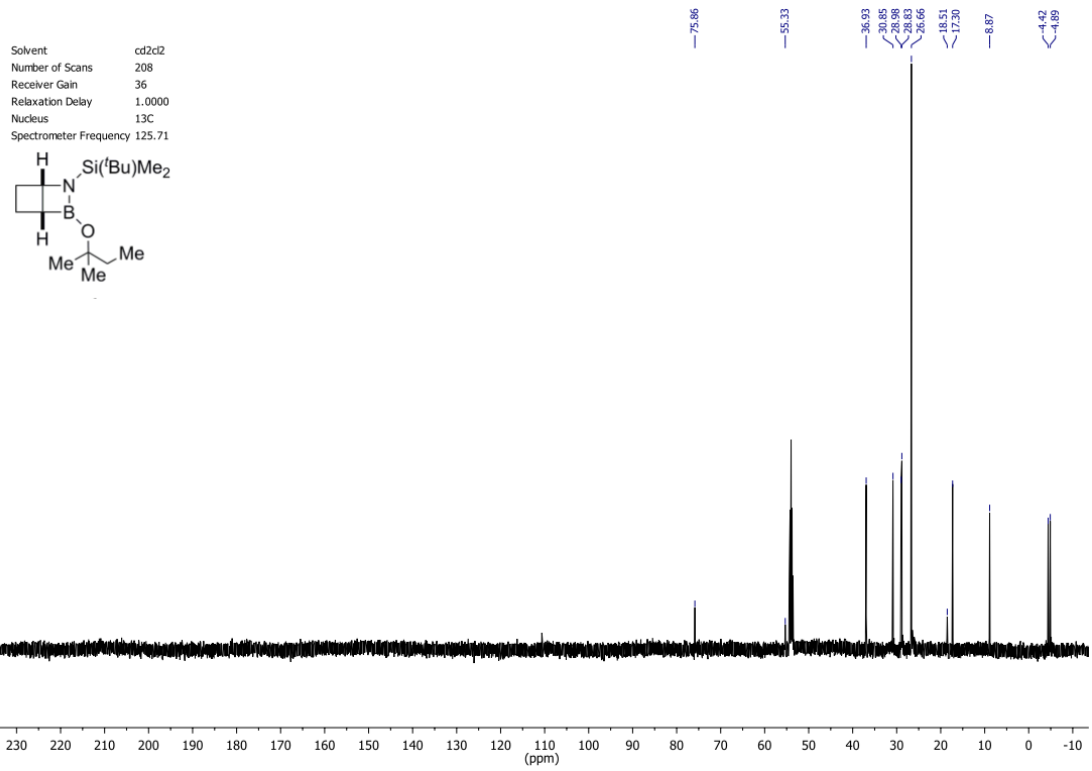
Solvent cd2cl2
 Number of Scans 32
 Receiver Gain 32
 Relaxation Delay 1.0000
 Nucleus 1H
 Spectrometer Frequency 499.88



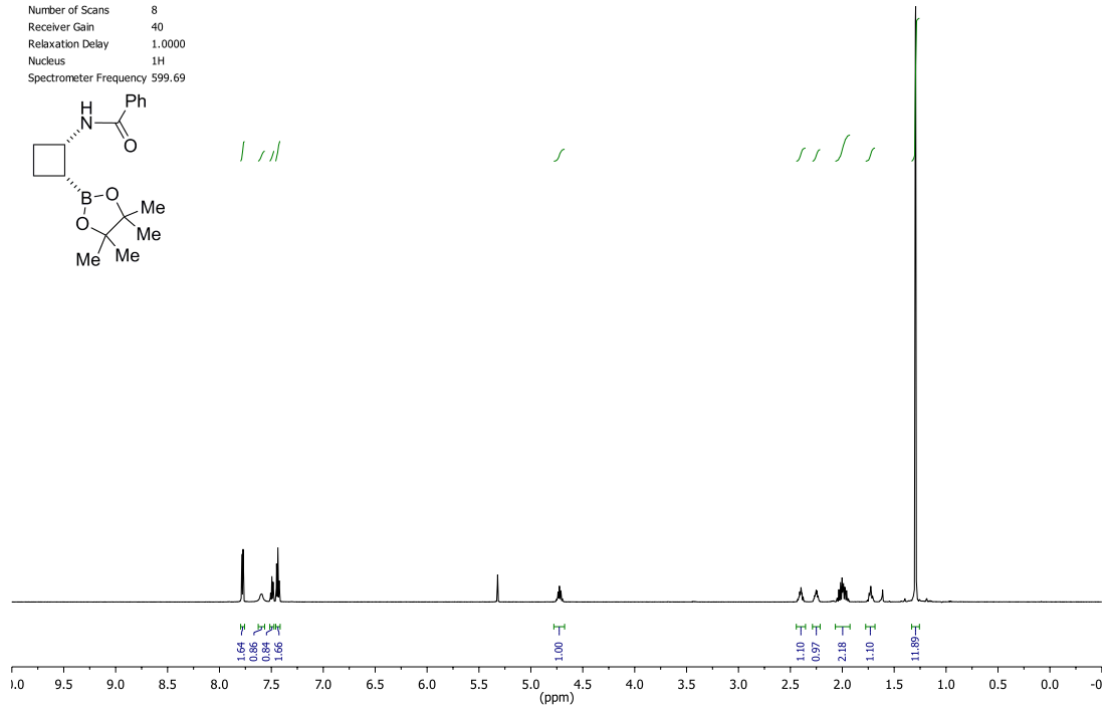
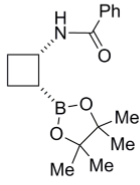
Solvent cd2cl2
 Number of Scans 17720
 Receiver Gain 48
 Relaxation Delay 1.0000
 Nucleus 13C
 Spectrometer Frequency 125.71



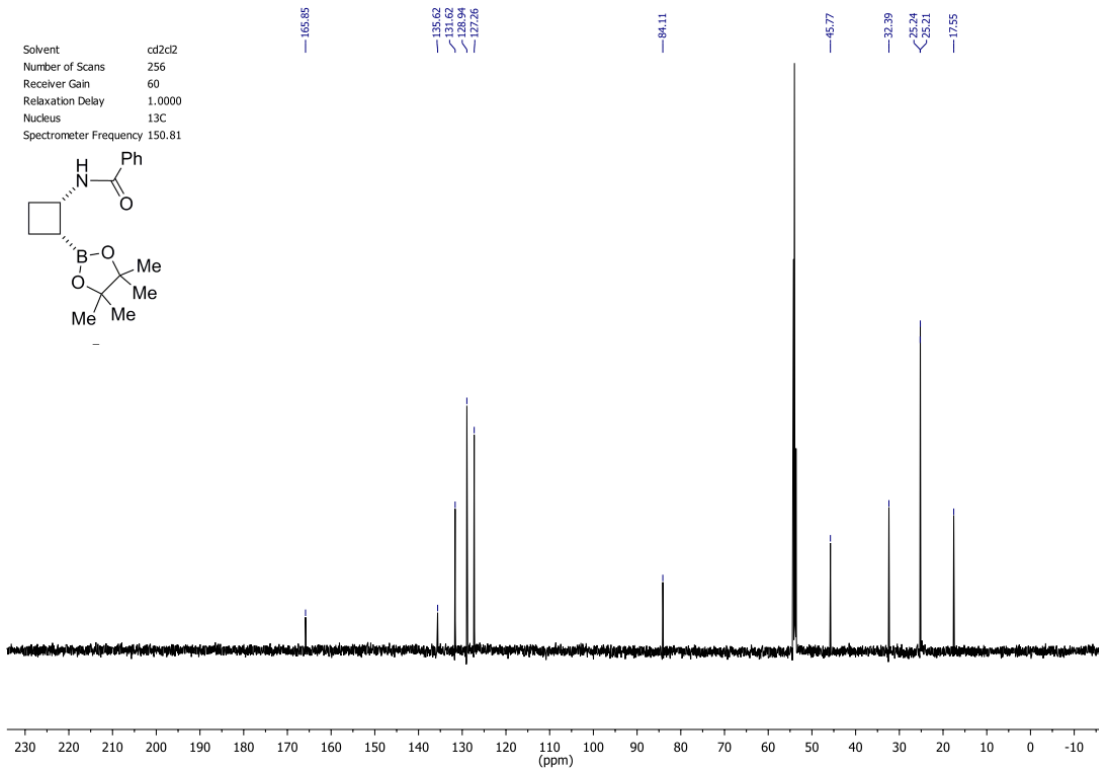
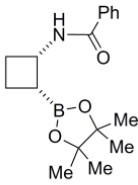


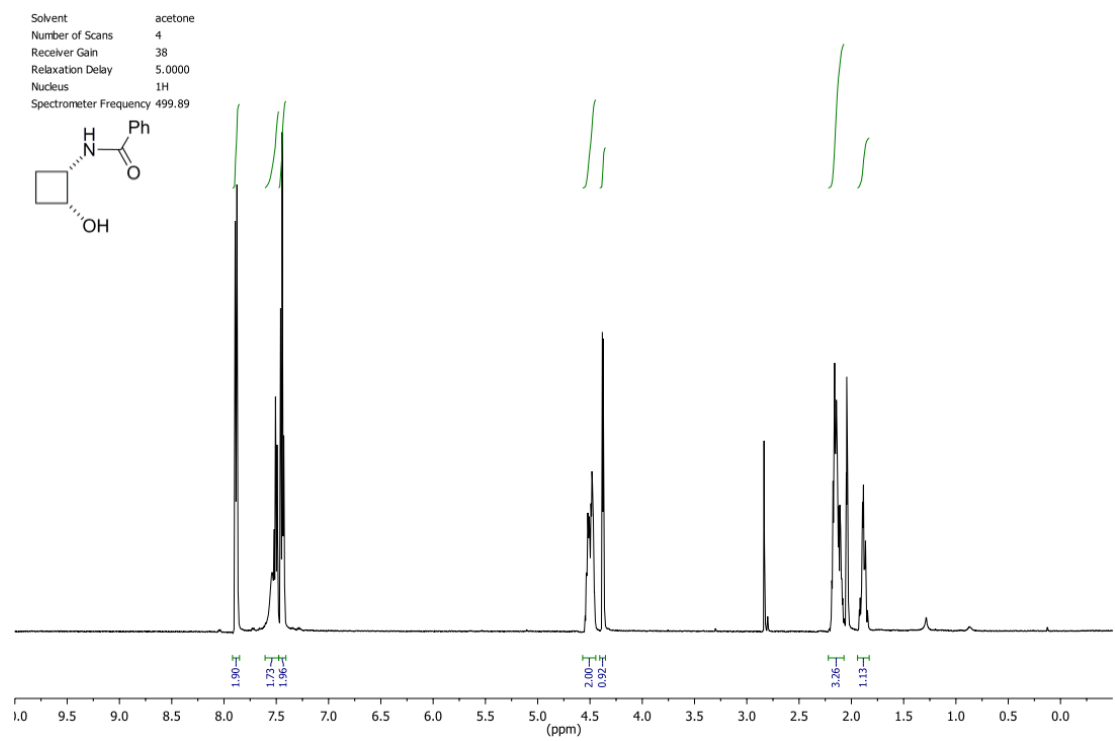
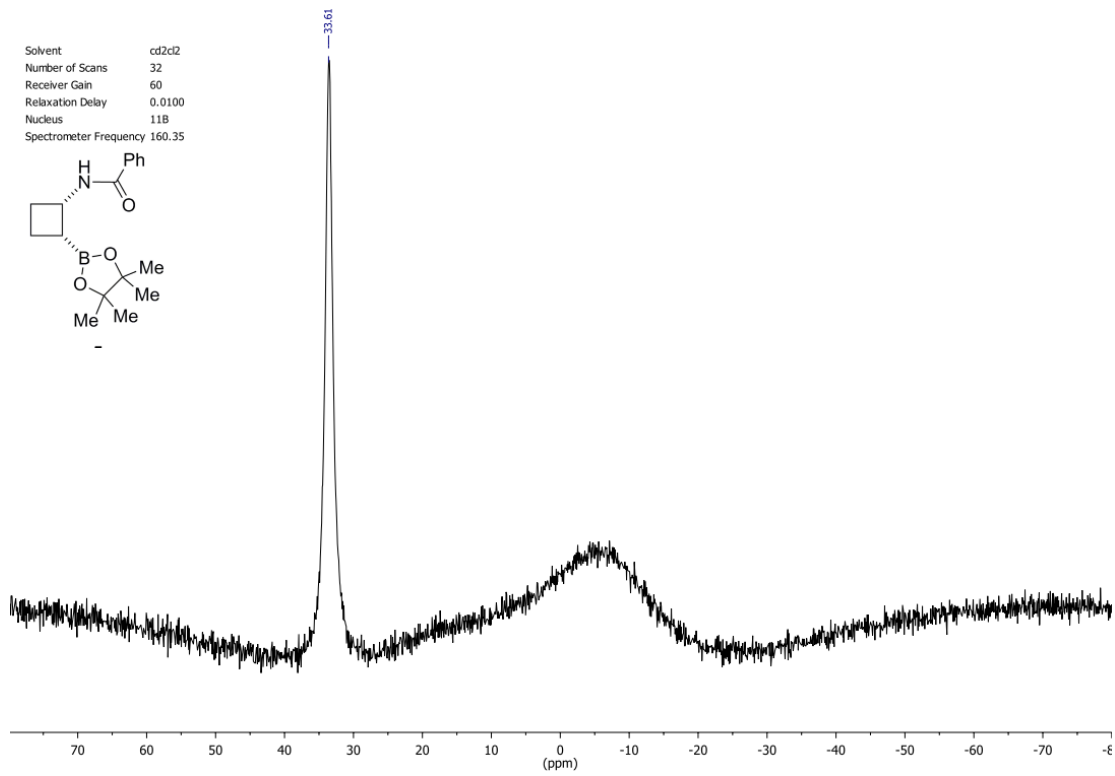


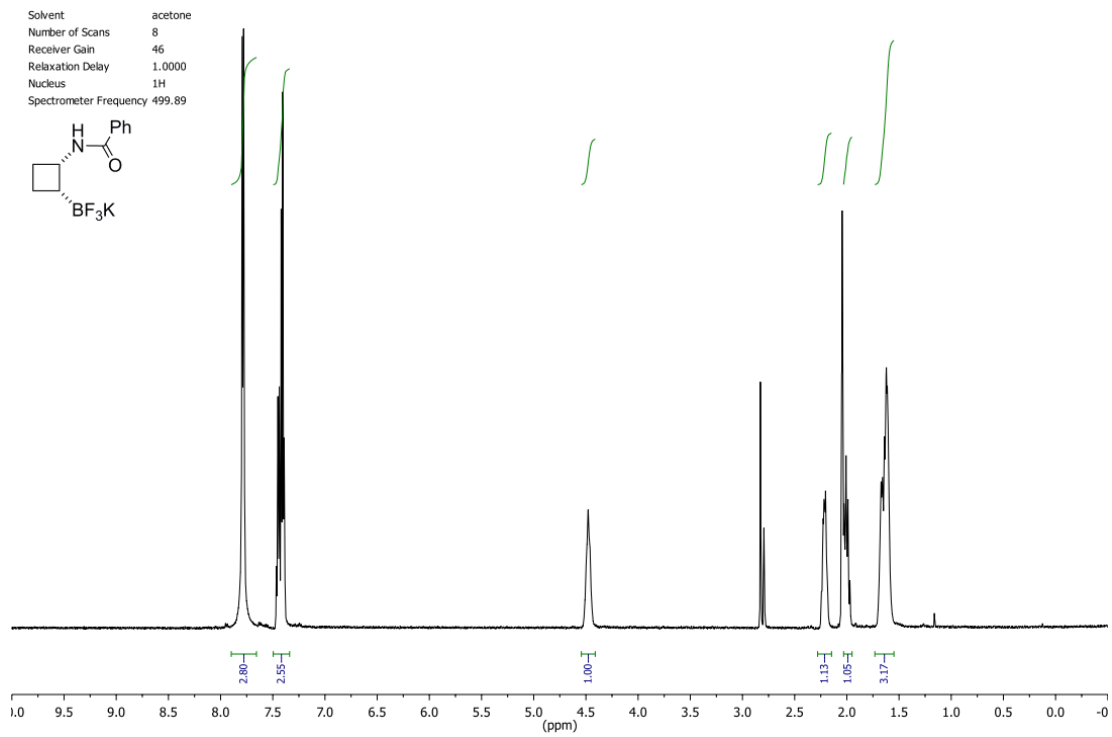
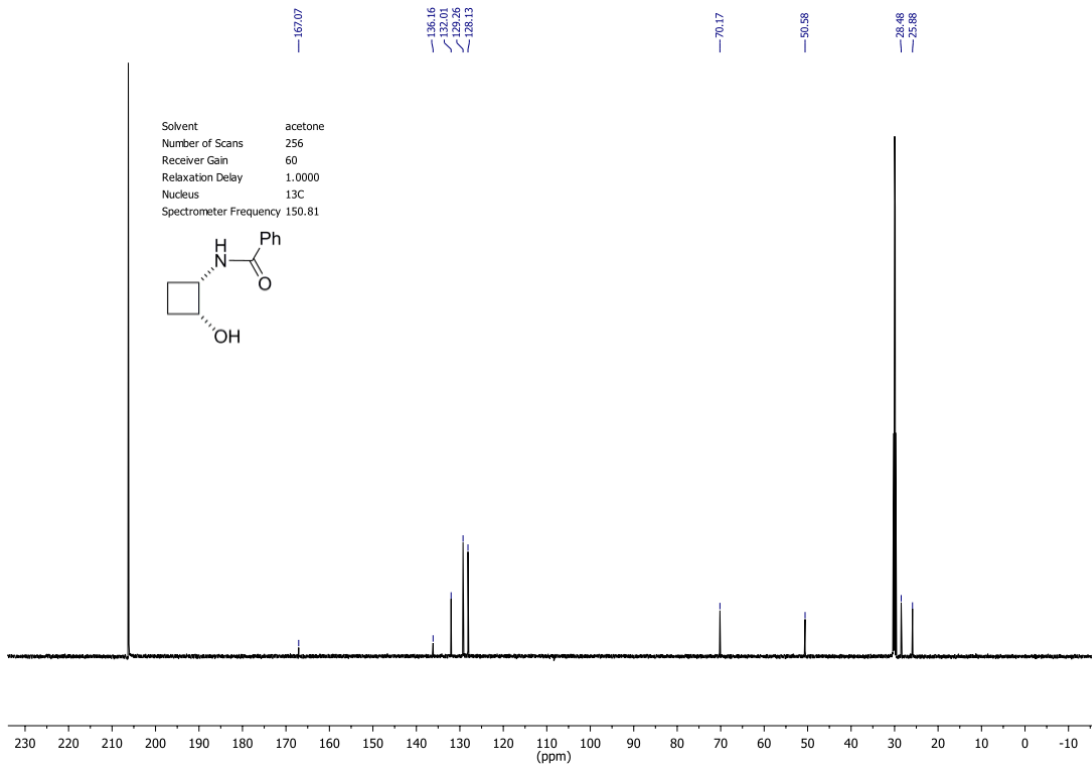
Solvent cd2c2
 Number of Scans 8
 Receiver Gain 40
 Relaxation Delay 1.0000
 Nucleus 1H
 Spectrometer Frequency 599.69

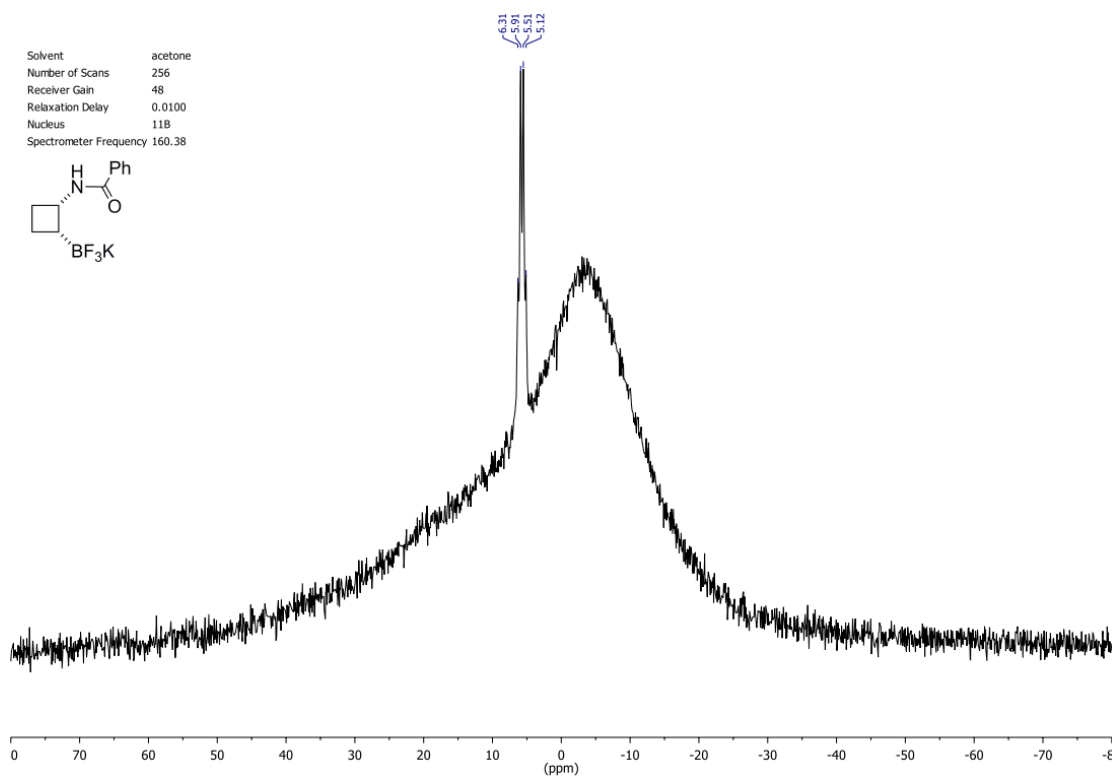
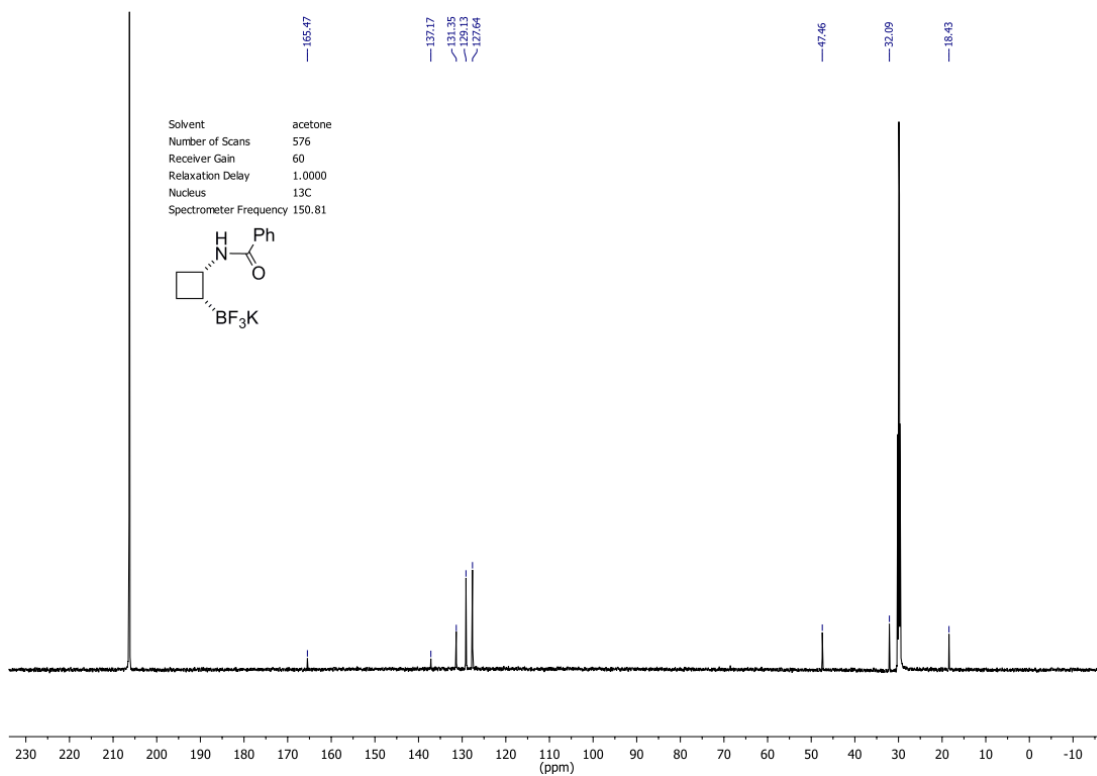


Solvent cd2c2
 Number of Scans 256
 Receiver Gain 60
 Relaxation Delay 1.0000
 Nucleus 13C
 Spectrometer Frequency 150.81

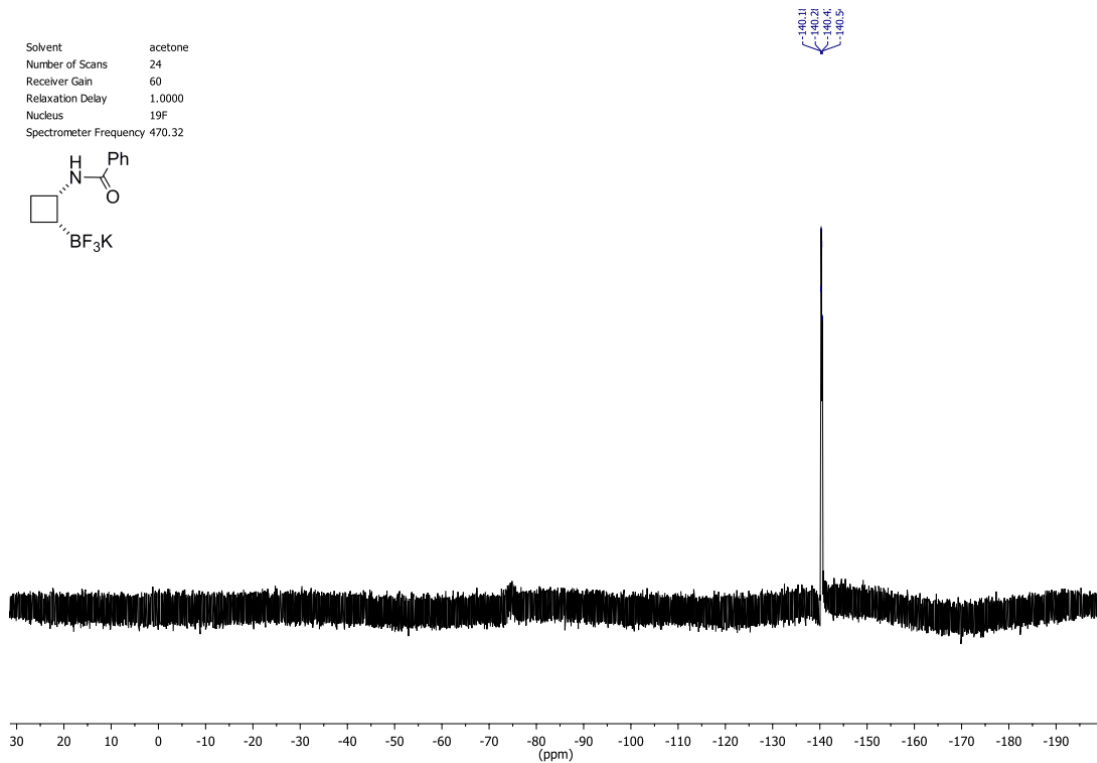
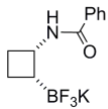




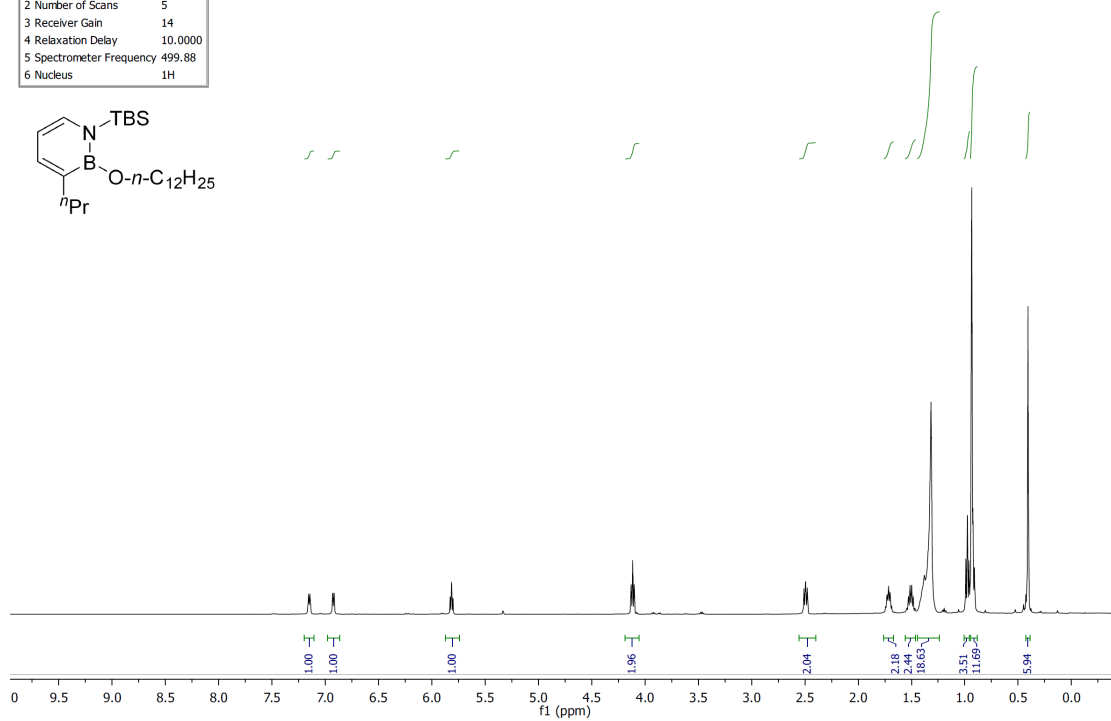
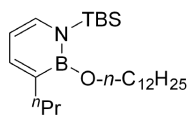




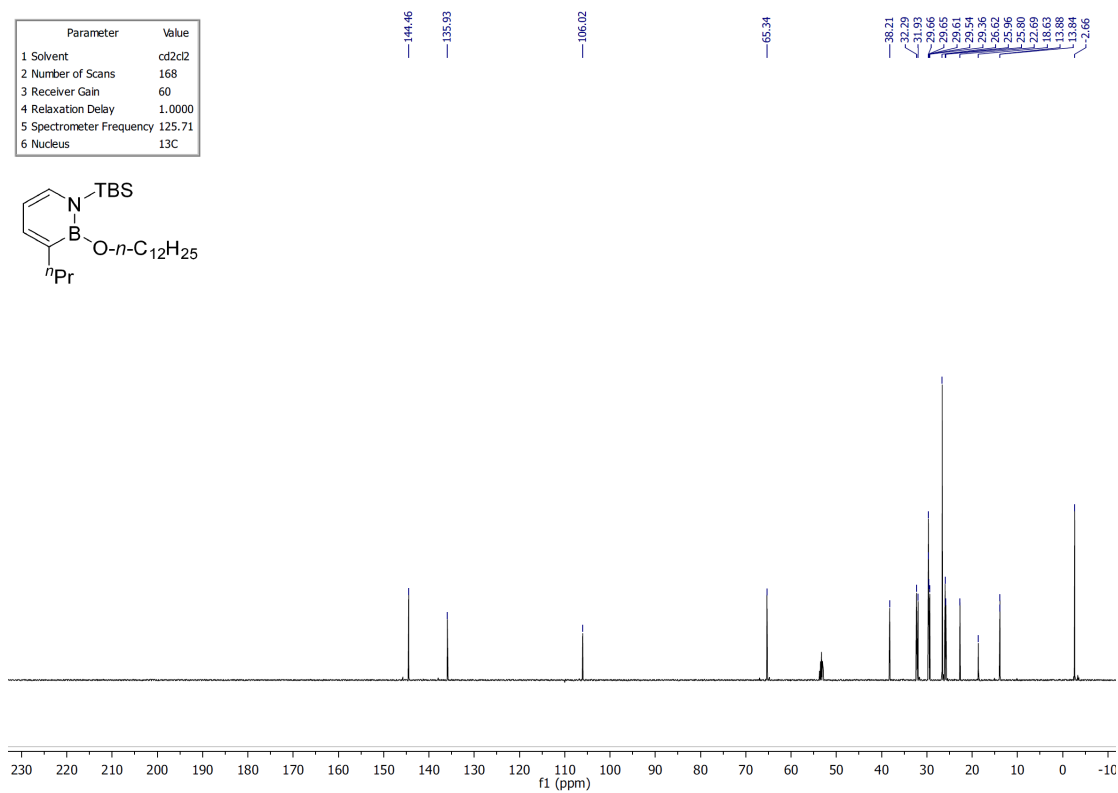
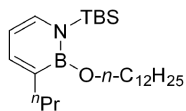
Solvent acetone
 Number of Scans 24
 Receiver Gain 60
 Relaxation Delay 1.0000
 Nucleus 19F
 Spectrometer Frequency 470.32



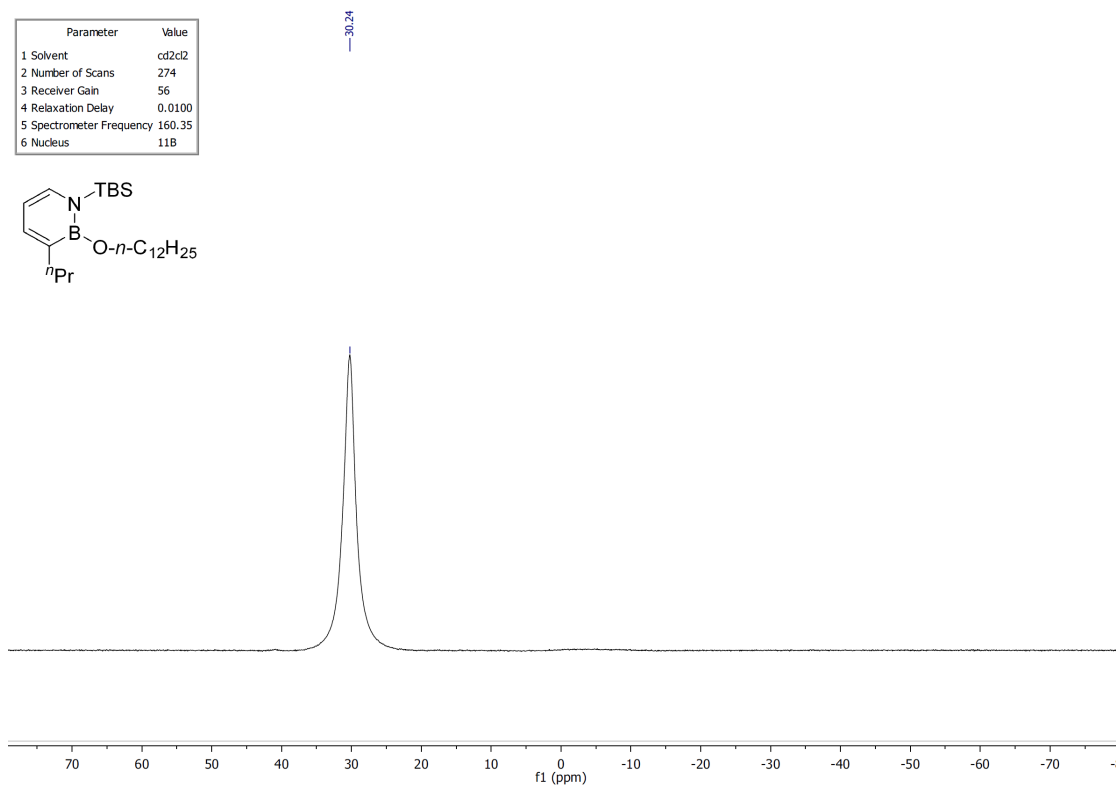
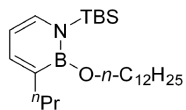
Parameter	Value
1 Solvent	cd2cl2
2 Number of Scans	5
3 Receiver Gain	14
4 Relaxation Delay	10.0000
5 Spectrometer Frequency	499.88
6 Nucleus	1H



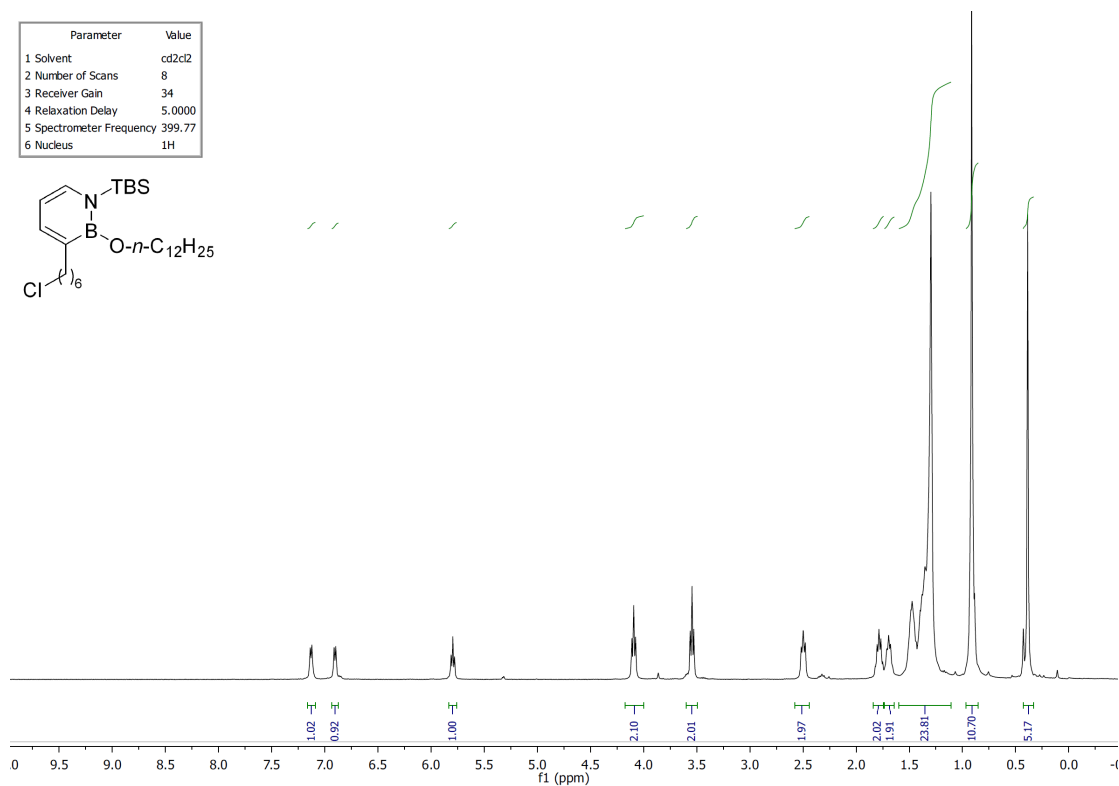
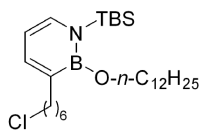
Parameter	Value
1 Solvent	cd2cl2
2 Number of Scans	168
3 Receiver Gain	60
4 Relaxation Delay	1.0000
5 Spectrometer Frequency	125.71
6 Nucleus	13C



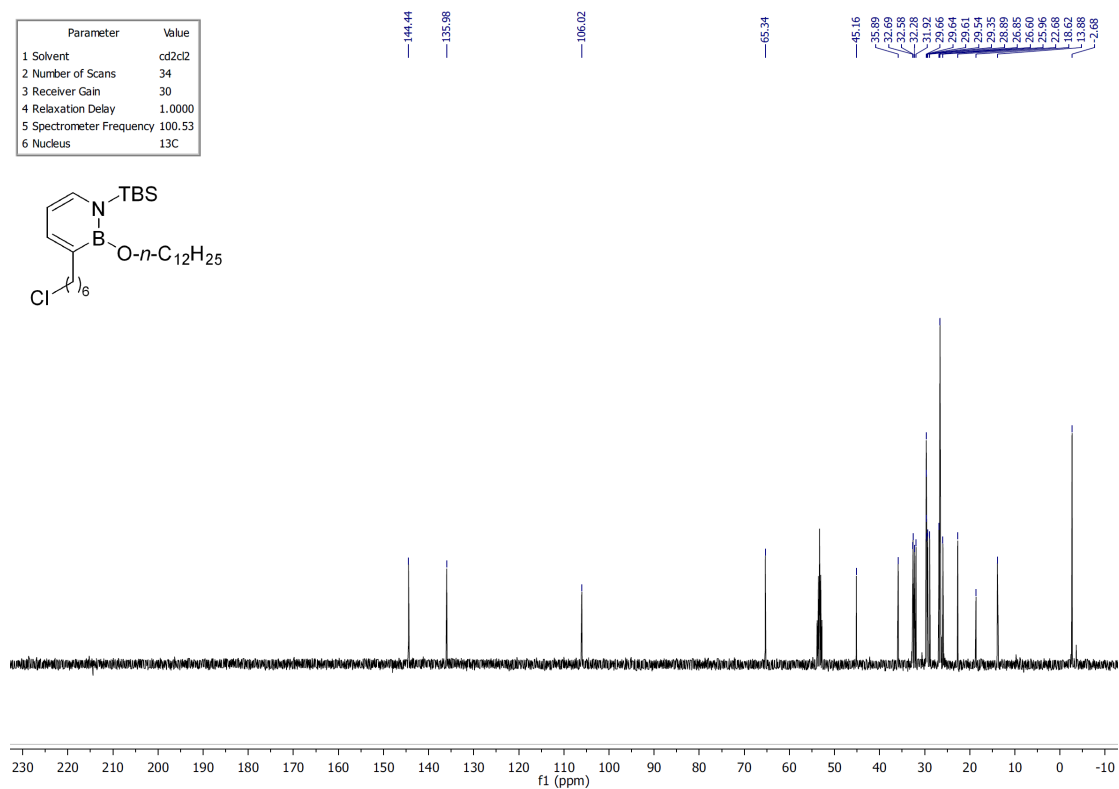
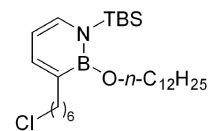
Parameter	Value
1 Solvent	cd2cl2
2 Number of Scans	274
3 Receiver Gain	56
4 Relaxation Delay	0.0100
5 Spectrometer Frequency	160.35
6 Nucleus	11B



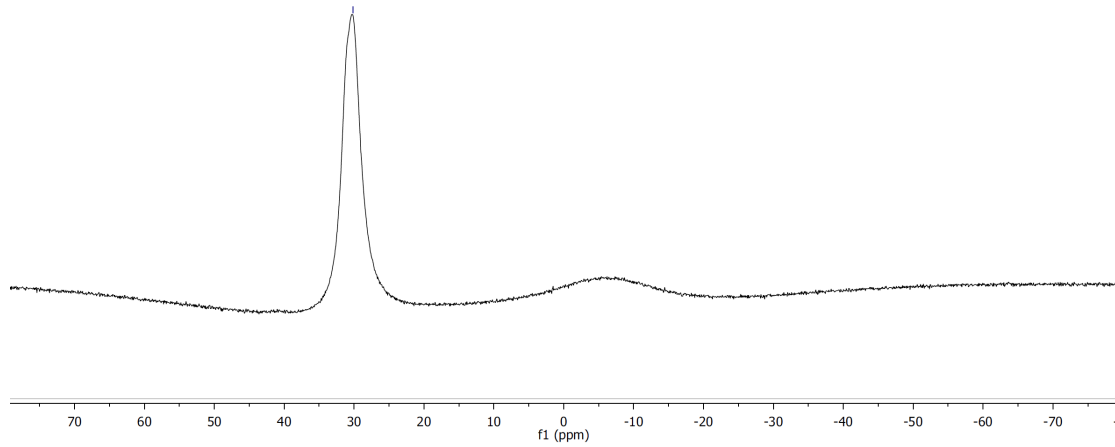
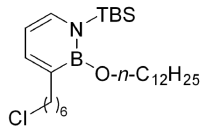
Parameter	Value
1 Solvent	cd2cl2
2 Number of Scans	8
3 Receiver Gain	34
4 Relaxation Delay	5.0000
5 Spectrometer Frequency	399.77
6 Nucleus	1H



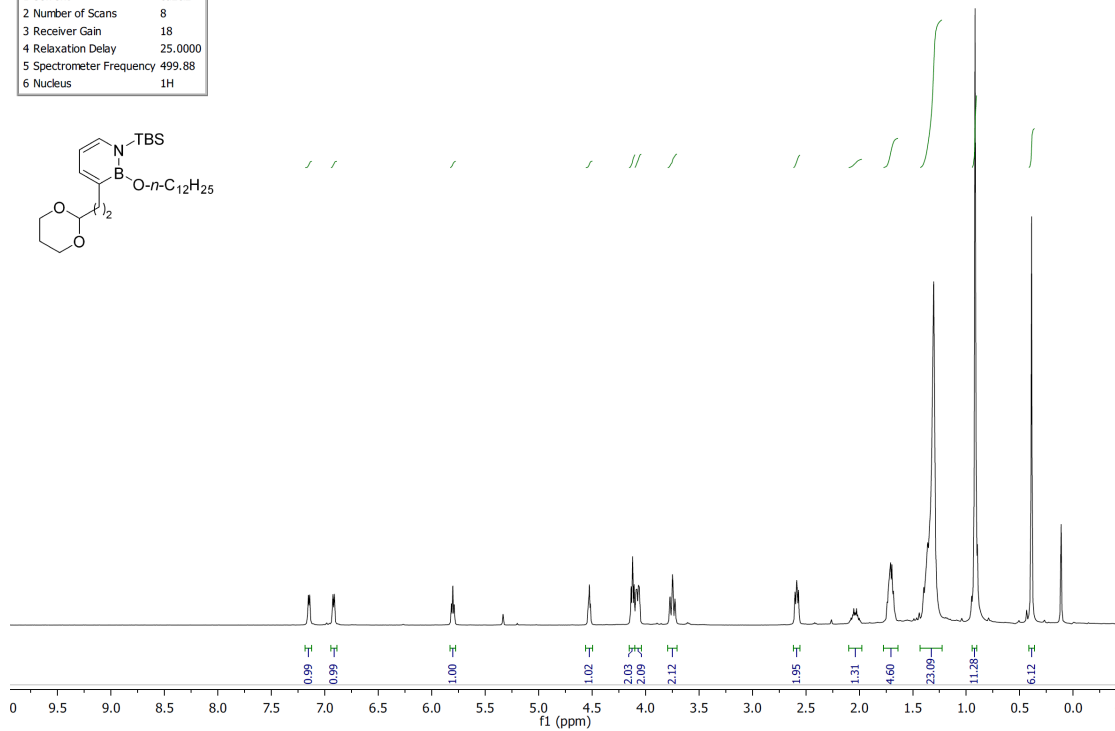
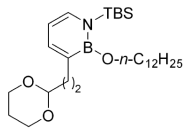
Parameter	Value
1 Solvent	cd2cl2
2 Number of Scans	34
3 Receiver Gain	30
4 Relaxation Delay	1.0000
5 Spectrometer Frequency	100.53
6 Nucleus	13C



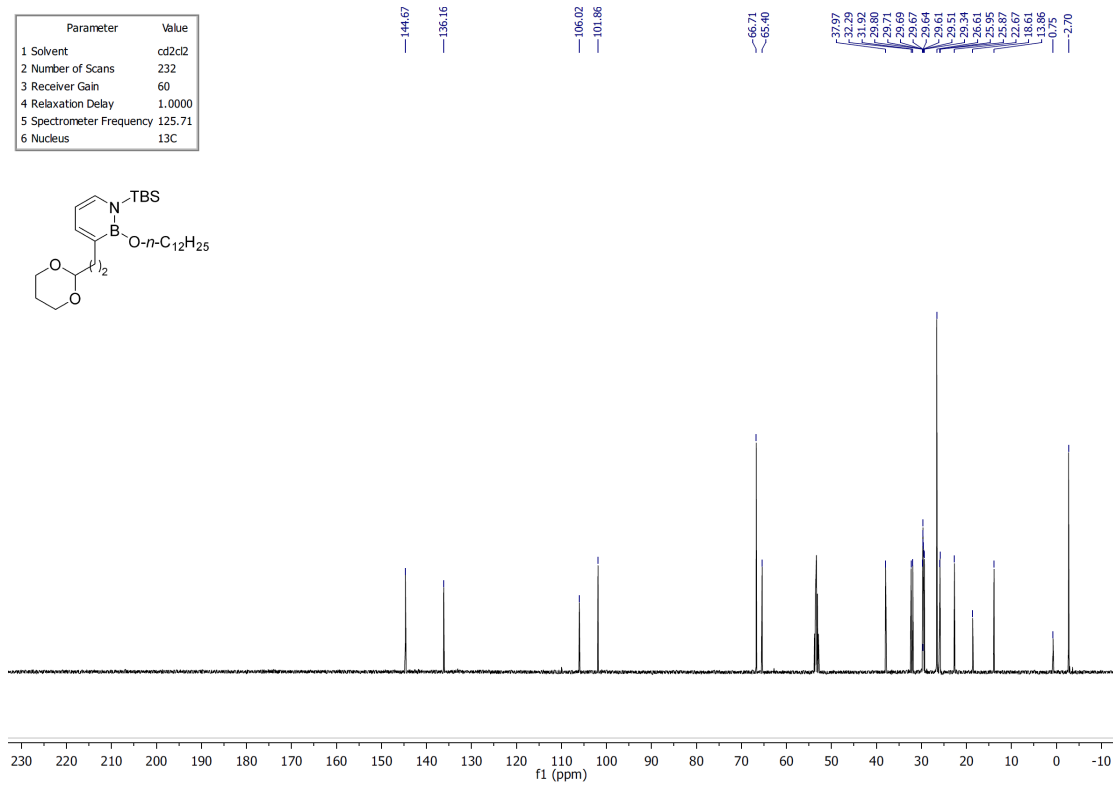
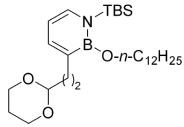
Parameter	Value
1 Solvent	cd2cl2
2 Number of Scans	159
3 Receiver Gain	56
4 Relaxation Delay	0.0100
5 Spectrometer Frequency	160.35
6 Nucleus	11B



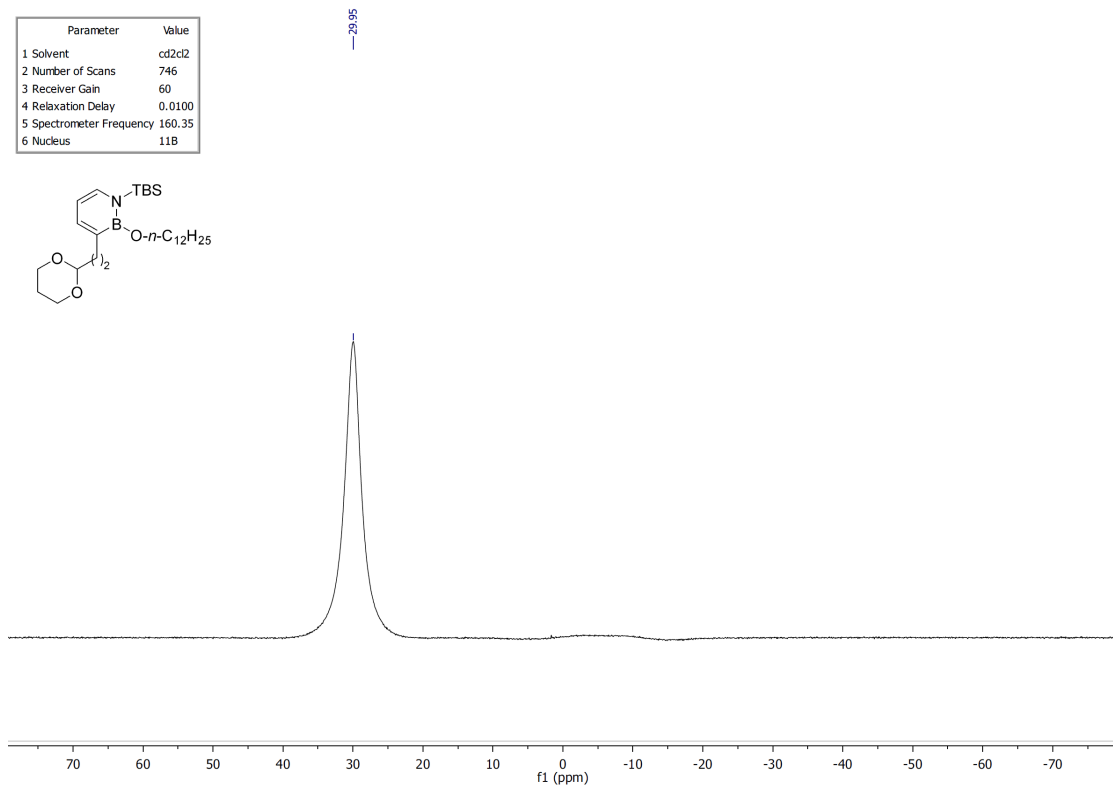
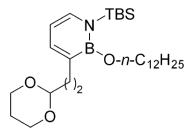
Parameter	Value
1 Solvent	cd2cl2
2 Number of Scans	8
3 Receiver Gain	18
4 Relaxation Delay	25.0000
5 Spectrometer Frequency	499.88
6 Nucleus	1H



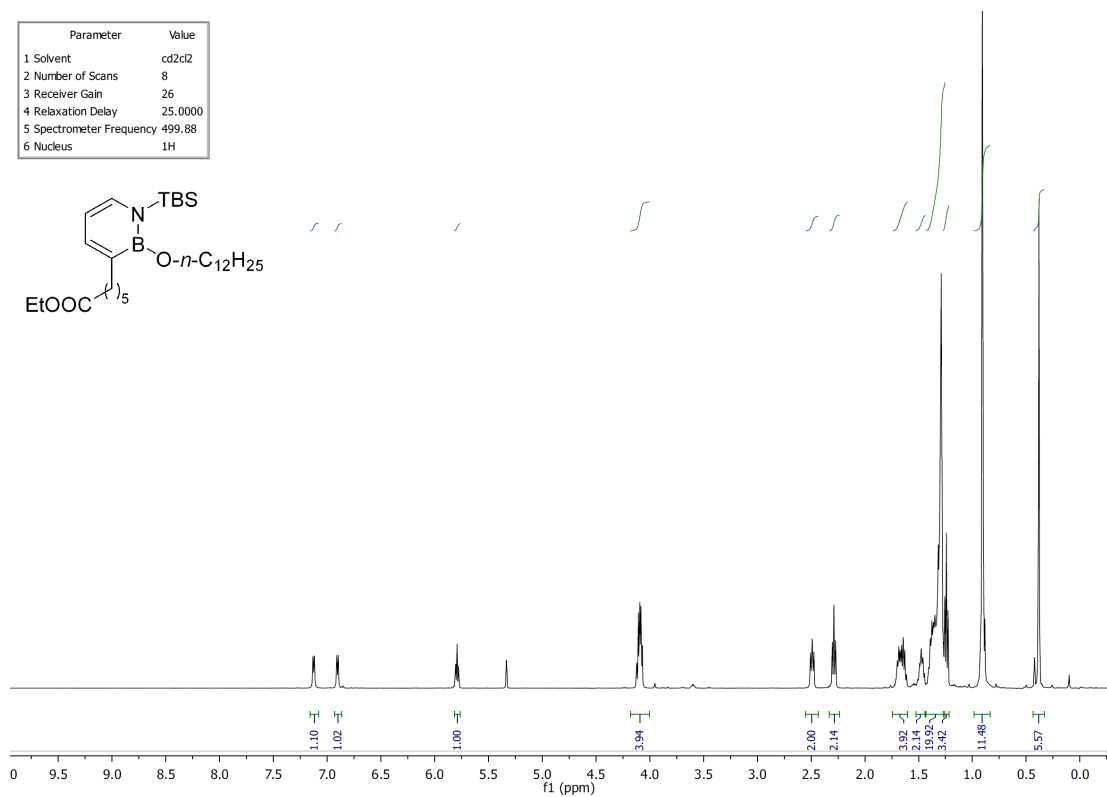
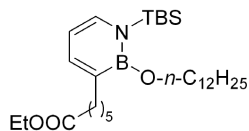
Parameter	Value
1 Solvent	cd2cl2
2 Number of Scans	232
3 Receiver Gain	60
4 Relaxation Delay	1.0000
5 Spectrometer Frequency	125.71
6 Nucleus	13C



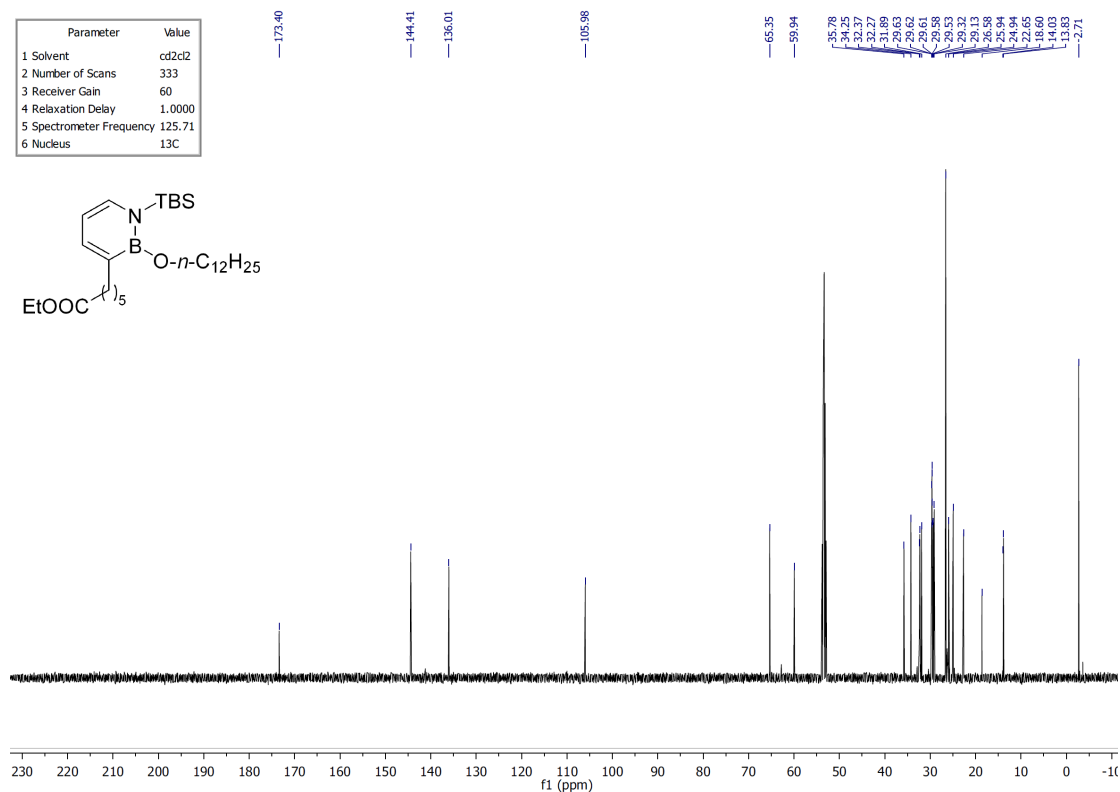
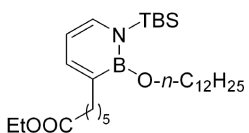
Parameter	Value
1 Solvent	cd2cl2
2 Number of Scans	746
3 Receiver Gain	60
4 Relaxation Delay	0.0100
5 Spectrometer Frequency	160.35
6 Nucleus	11B



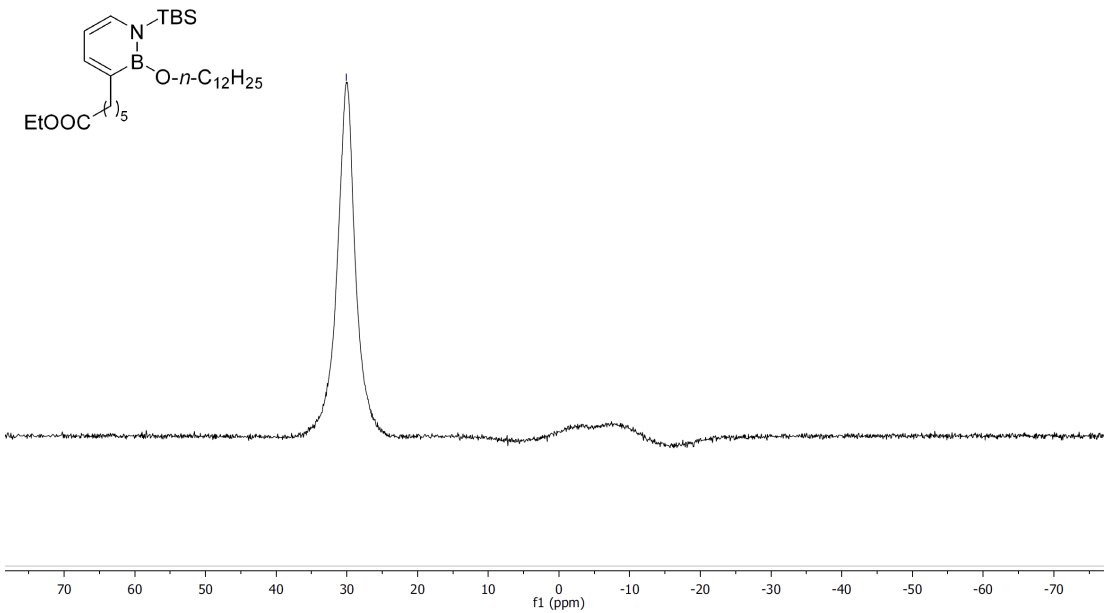
Parameter	Value
1 Solvent	cd2cl2
2 Number of Scans	8
3 Receiver Gain	26
4 Relaxation Delay	25.0000
5 Spectrometer Frequency	499.88
6 Nucleus	1H



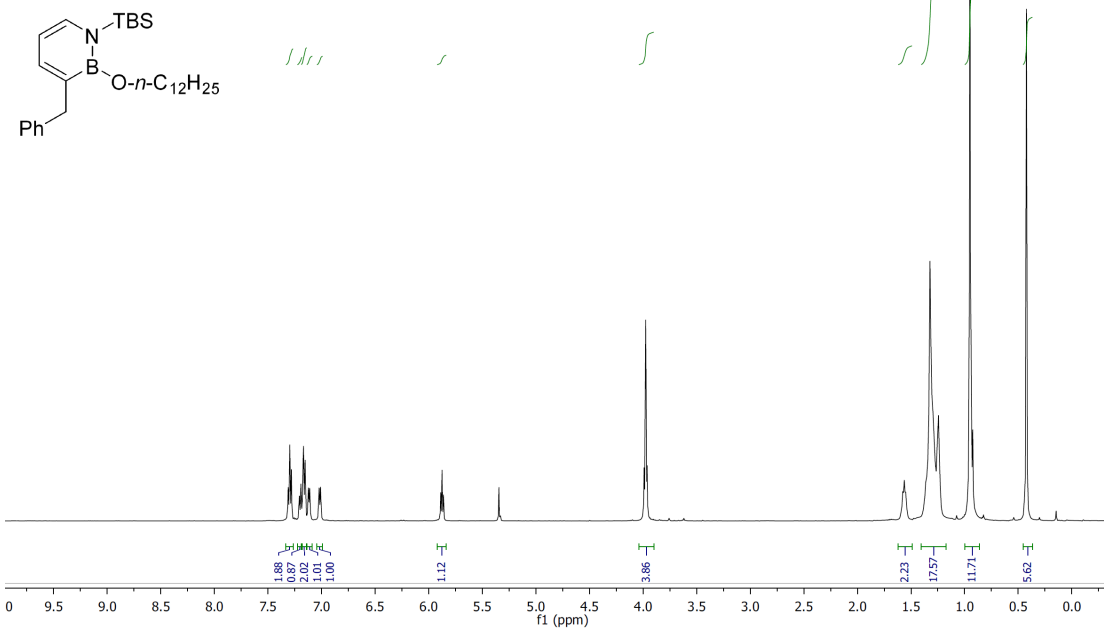
Parameter	Value
1 Solvent	cd2cl2
2 Number of Scans	333
3 Receiver Gain	60
4 Relaxation Delay	1.0000
5 Spectrometer Frequency	125.71
6 Nucleus	13C



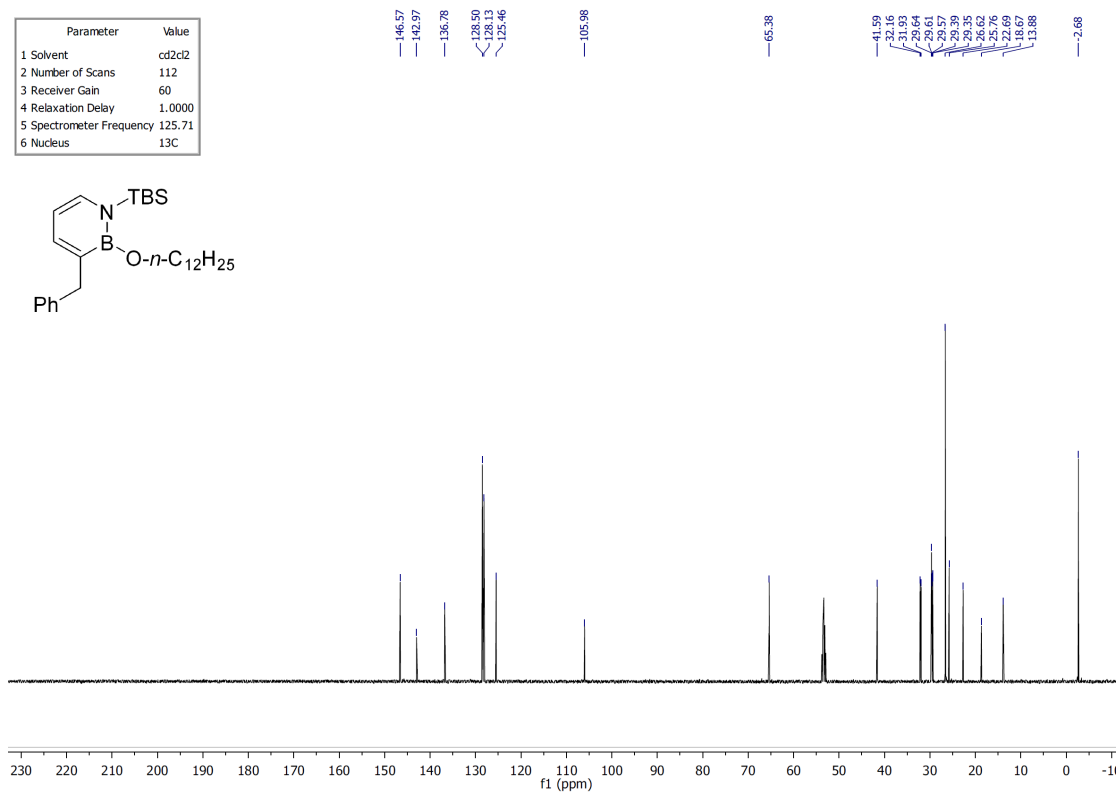
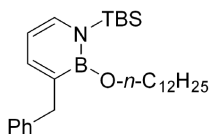
Parameter	Value
1 Solvent	cd2cl2
2 Number of Scans	851
3 Receiver Gain	56
4 Relaxation Delay	0.0100
5 Spectrometer Frequency	160.35
6 Nucleus	11B



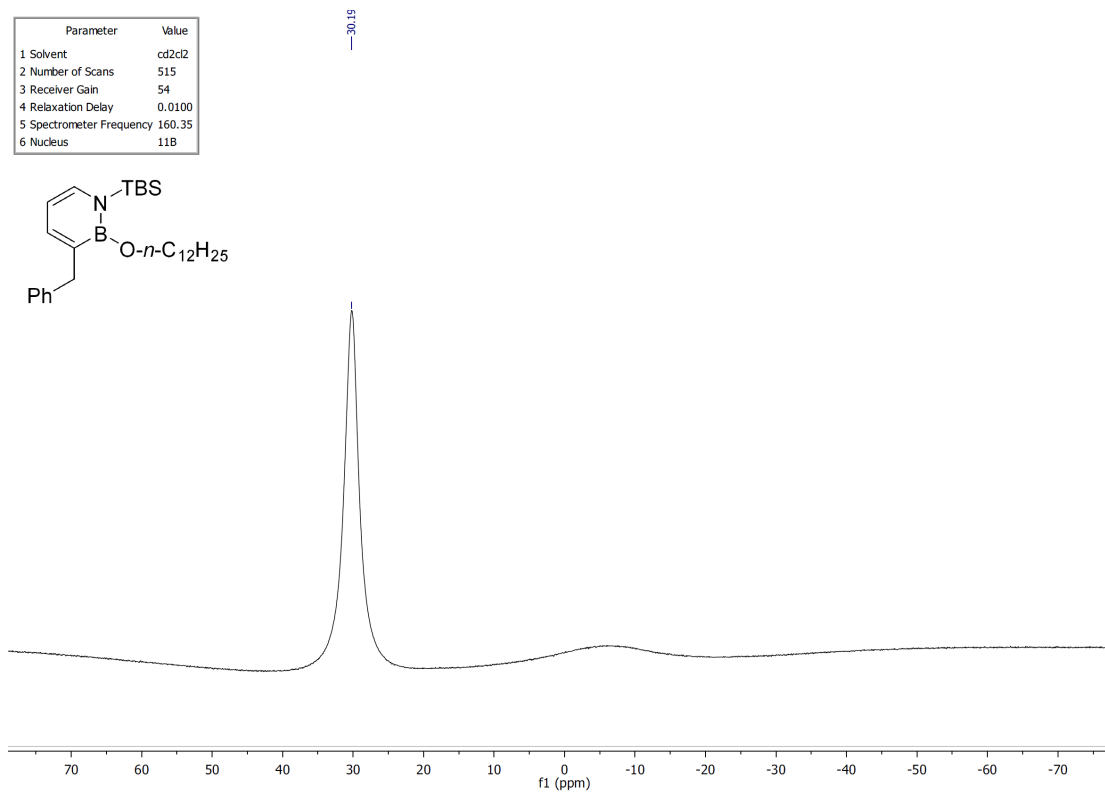
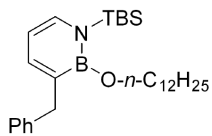
Parameter	Value
1 Solvent	cd2cl2
2 Number of Scans	16
3 Receiver Gain	14
4 Relaxation Delay	10.0000
5 Spectrometer Frequency	499.88
6 Nucleus	1H



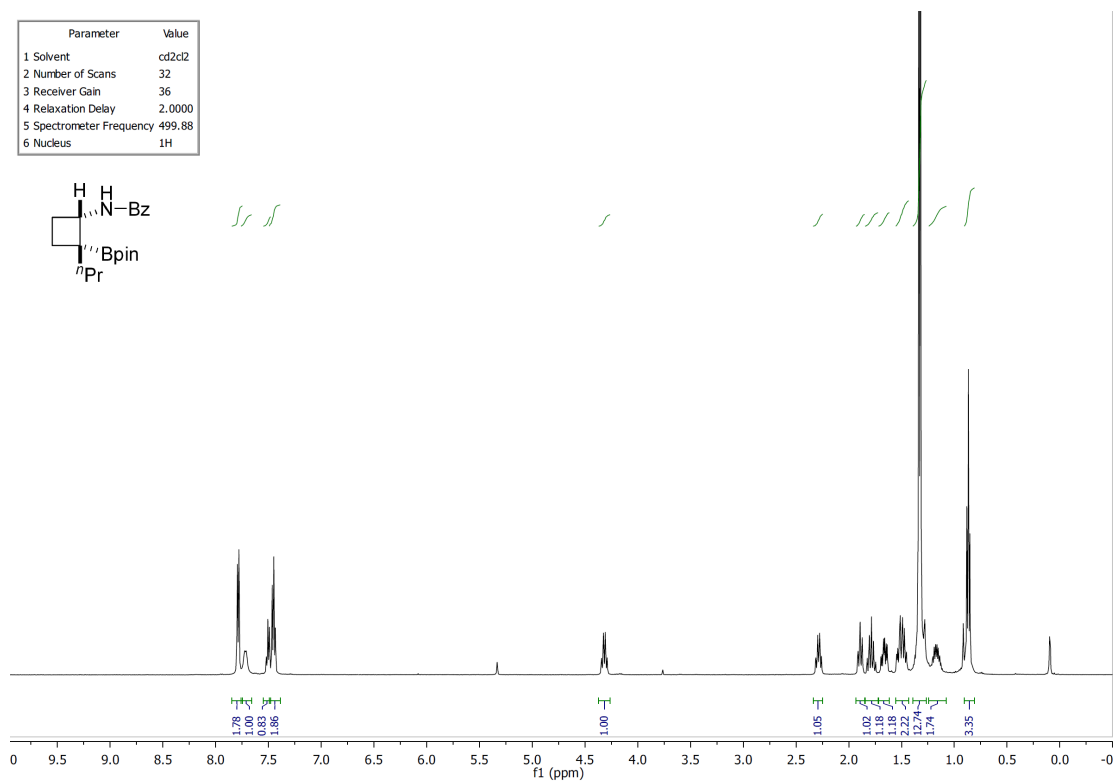
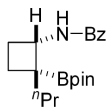
Parameter	Value
1 Solvent	cd2cl2
2 Number of Scans	112
3 Receiver Gain	60
4 Relaxation Delay	1.0000
5 Spectrometer Frequency	125.71
6 Nucleus	¹³ C



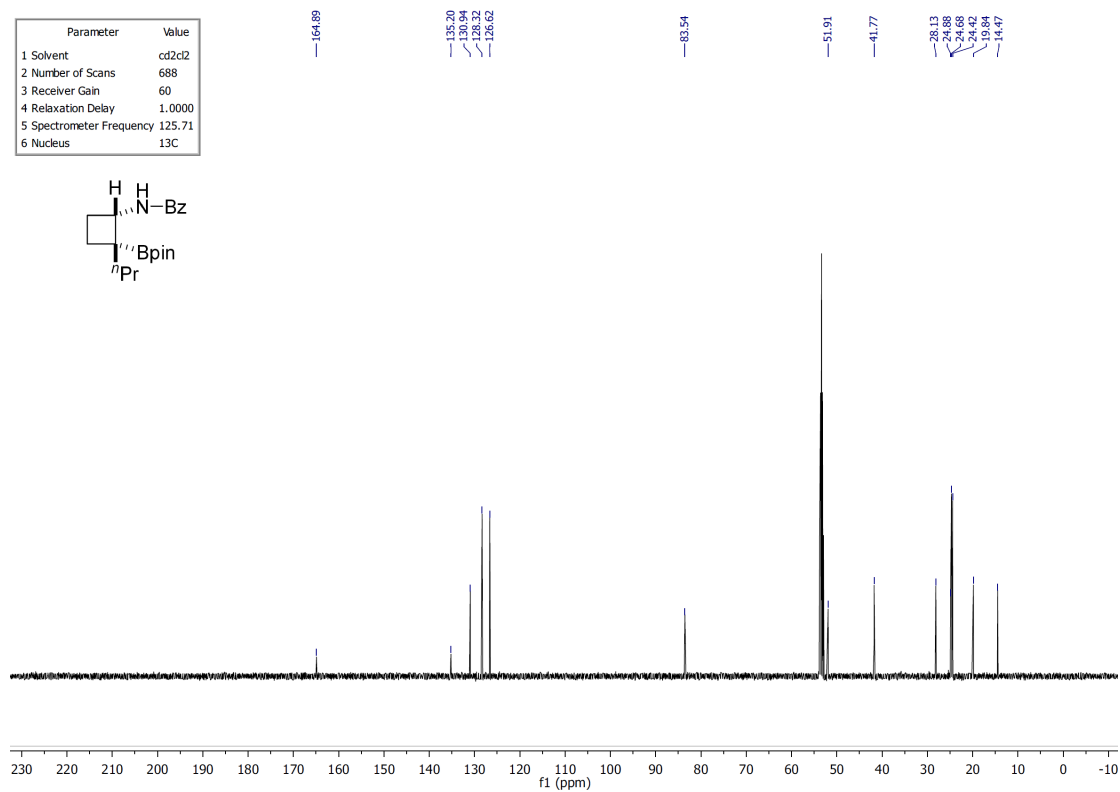
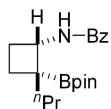
Parameter	Value
1 Solvent	cd2cl2
2 Number of Scans	515
3 Receiver Gain	54
4 Relaxation Delay	0.0100
5 Spectrometer Frequency	160.35
6 Nucleus	¹¹ B



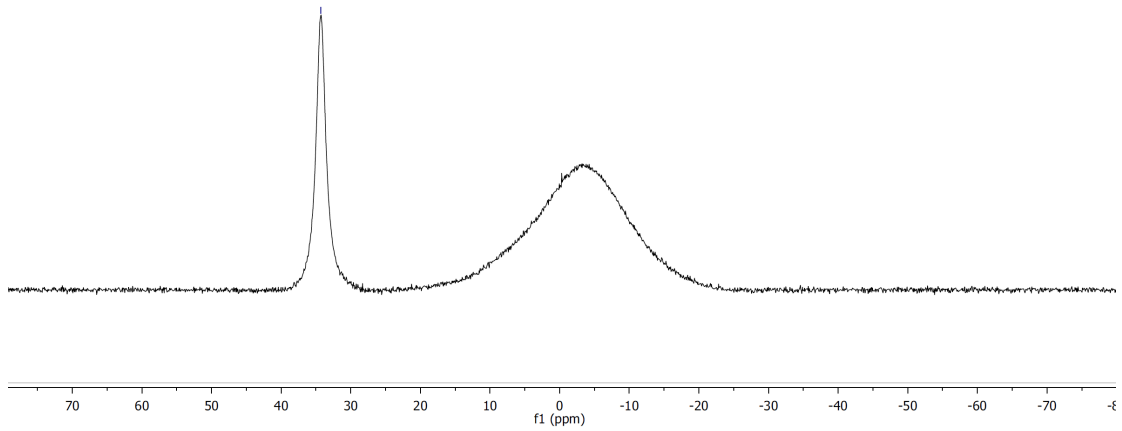
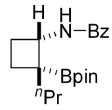
Parameter	Value
1 Solvent	cd2cl2
2 Number of Scans	32
3 Receiver Gain	36
4 Relaxation Delay	2.0000
5 Spectrometer Frequency	499.88
6 Nucleus	1H



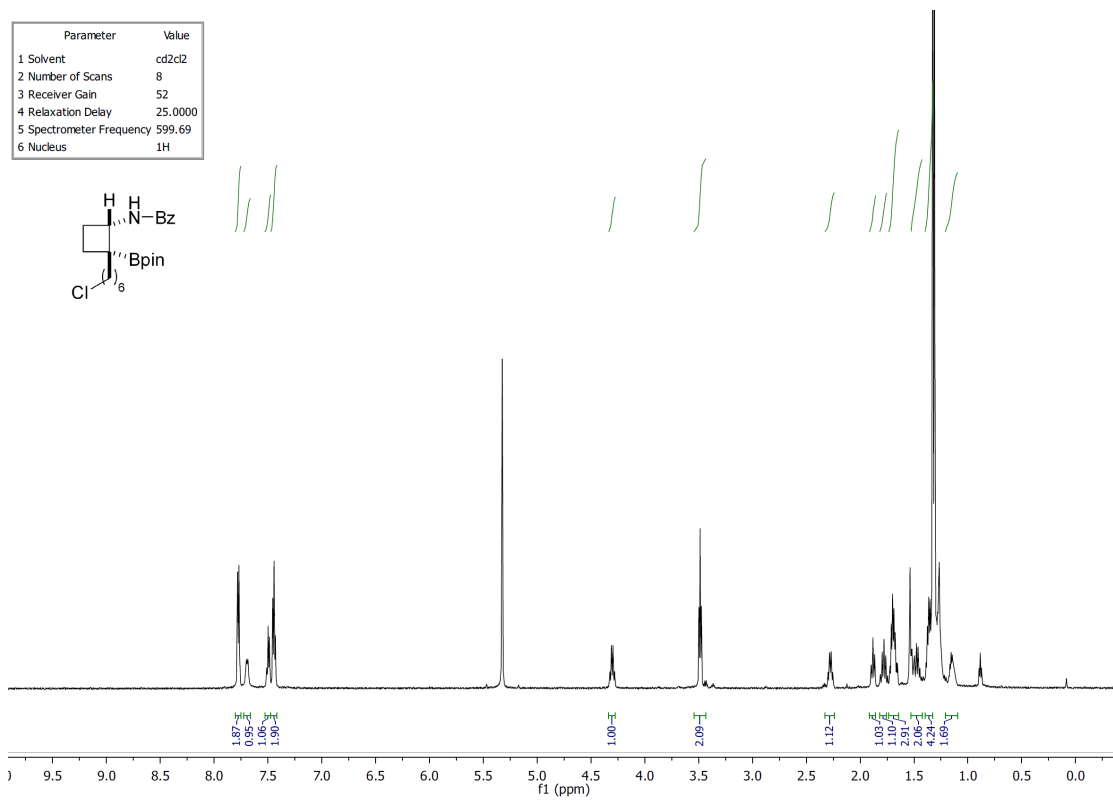
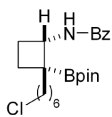
Parameter	Value
1 Solvent	cd2cl2
2 Number of Scans	688
3 Receiver Gain	60
4 Relaxation Delay	1.0000
5 Spectrometer Frequency	125.71
6 Nucleus	13C



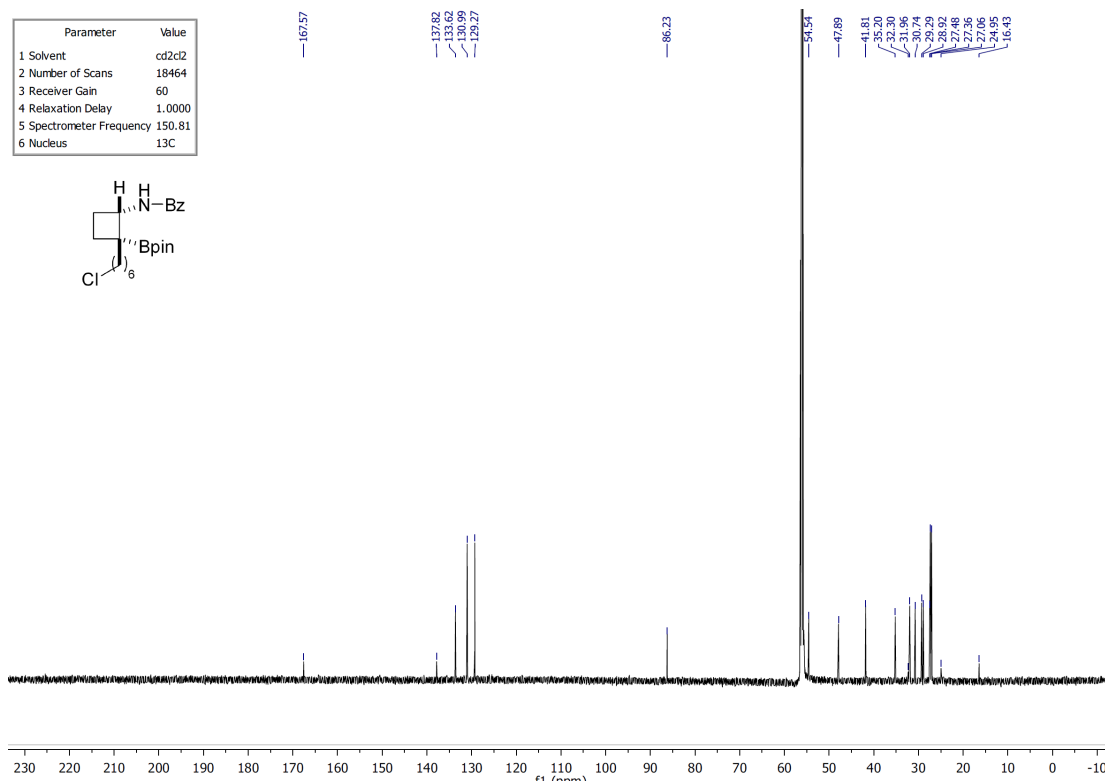
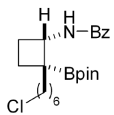
Parameter	Value
1 Solvent	cd2cl2
2 Number of Scans	1025
3 Receiver Gain	60
4 Relaxation Delay	0.0100
5 Spectrometer Frequency	160.38
6 Nucleus	11B



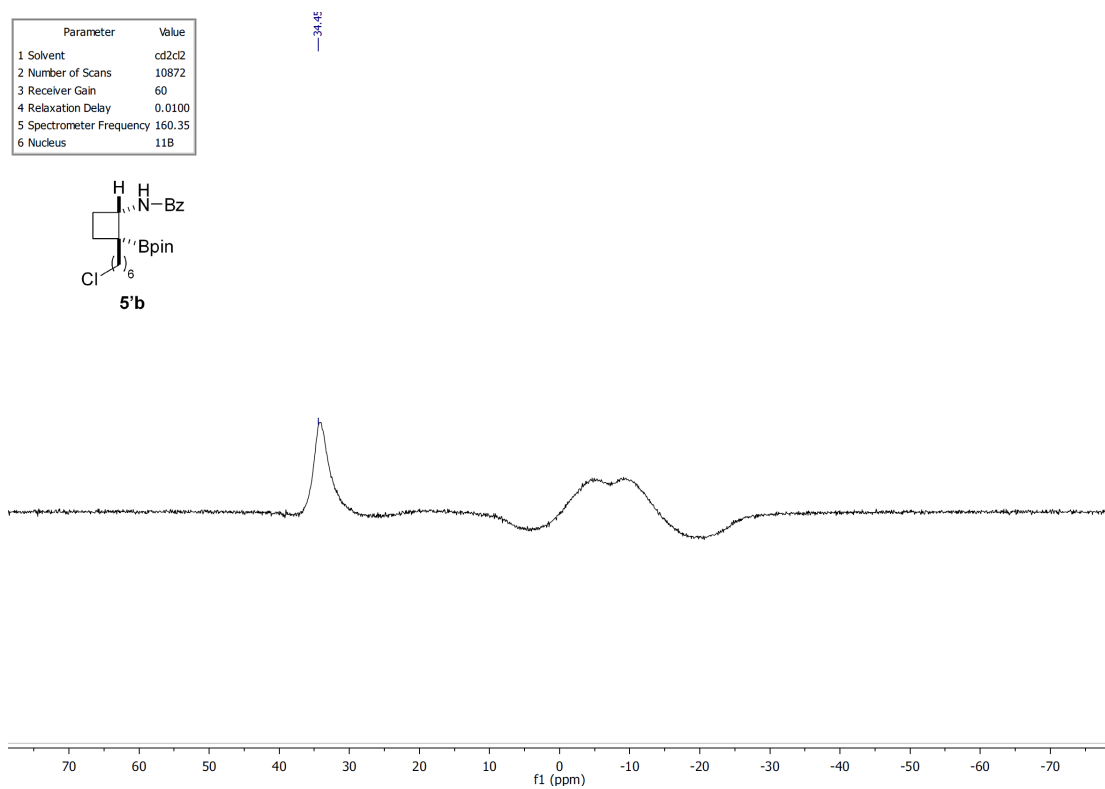
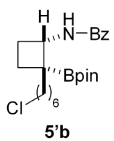
Parameter	Value
1 Solvent	cd2cl2
2 Number of Scans	8
3 Receiver Gain	52
4 Relaxation Delay	25.0000
5 Spectrometer Frequency	599.69
6 Nucleus	1H



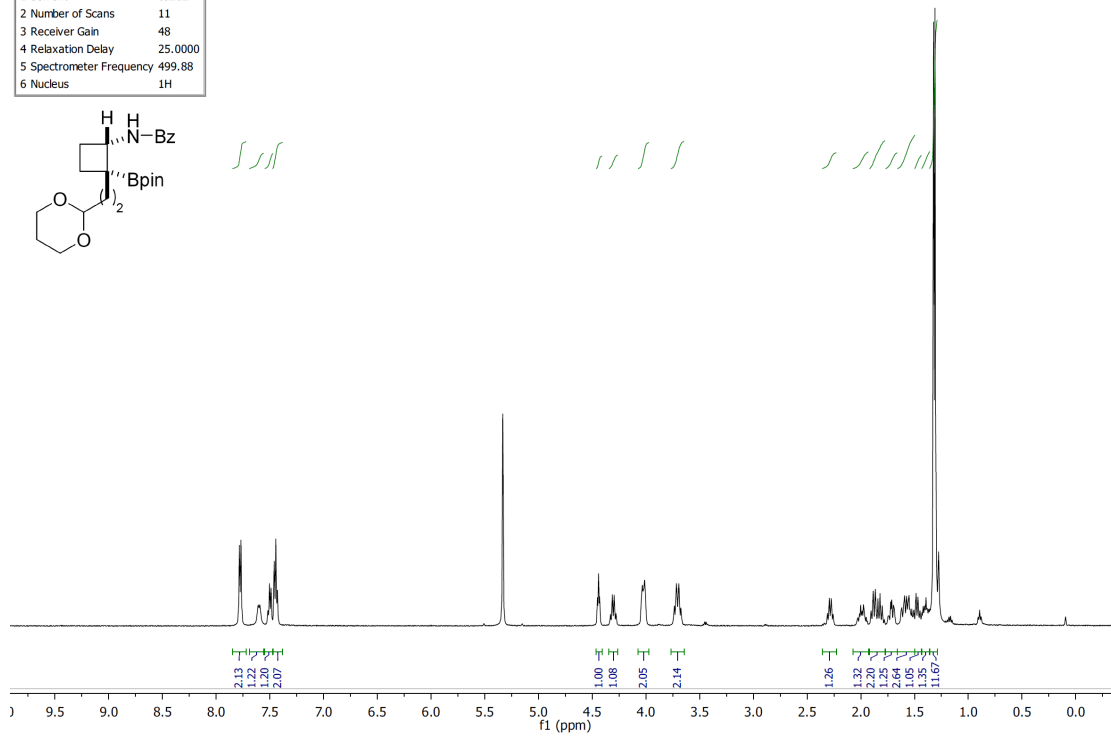
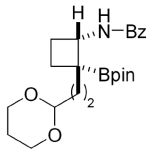
Parameter	Value
1 Solvent	cd2cl2
2 Number of Scans	18464
3 Receiver Gain	60
4 Relaxation Delay	1.0000
5 Spectrometer Frequency	150.81
6 Nucleus	13C



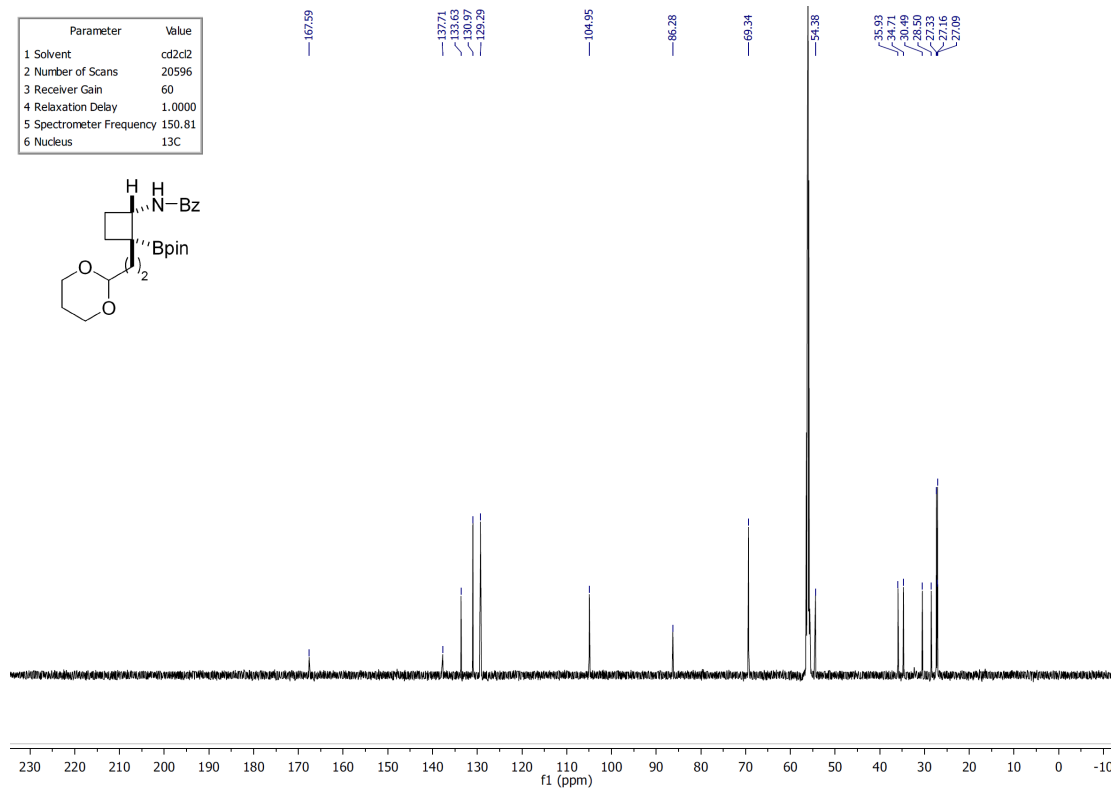
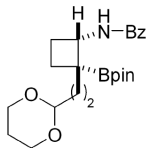
Parameter	Value
1 Solvent	cd2cl2
2 Number of Scans	10872
3 Receiver Gain	60
4 Relaxation Delay	0.0100
5 Spectrometer Frequency	160.35
6 Nucleus	11B



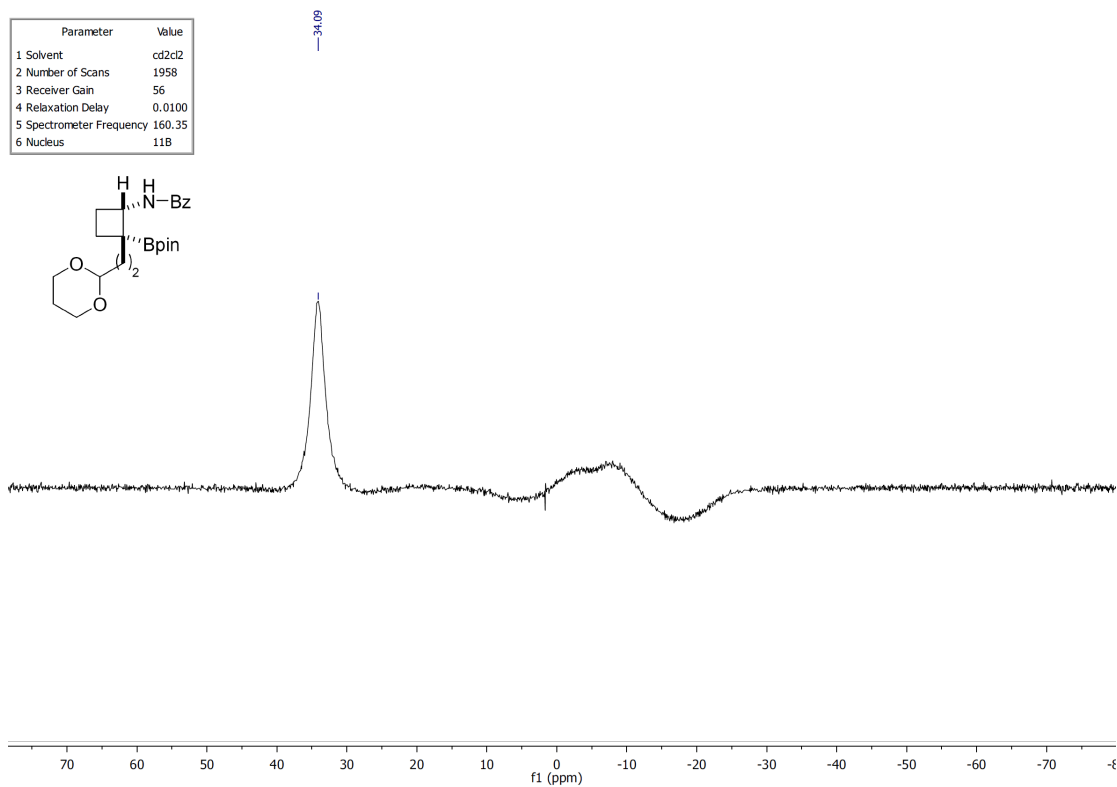
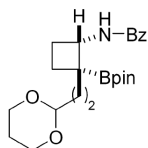
Parameter	Value
1 Solvent	cd2cl2
2 Number of Scans	11
3 Receiver Gain	48
4 Relaxation Delay	25.0000
5 Spectrometer Frequency	499.88
6 Nucleus	1H



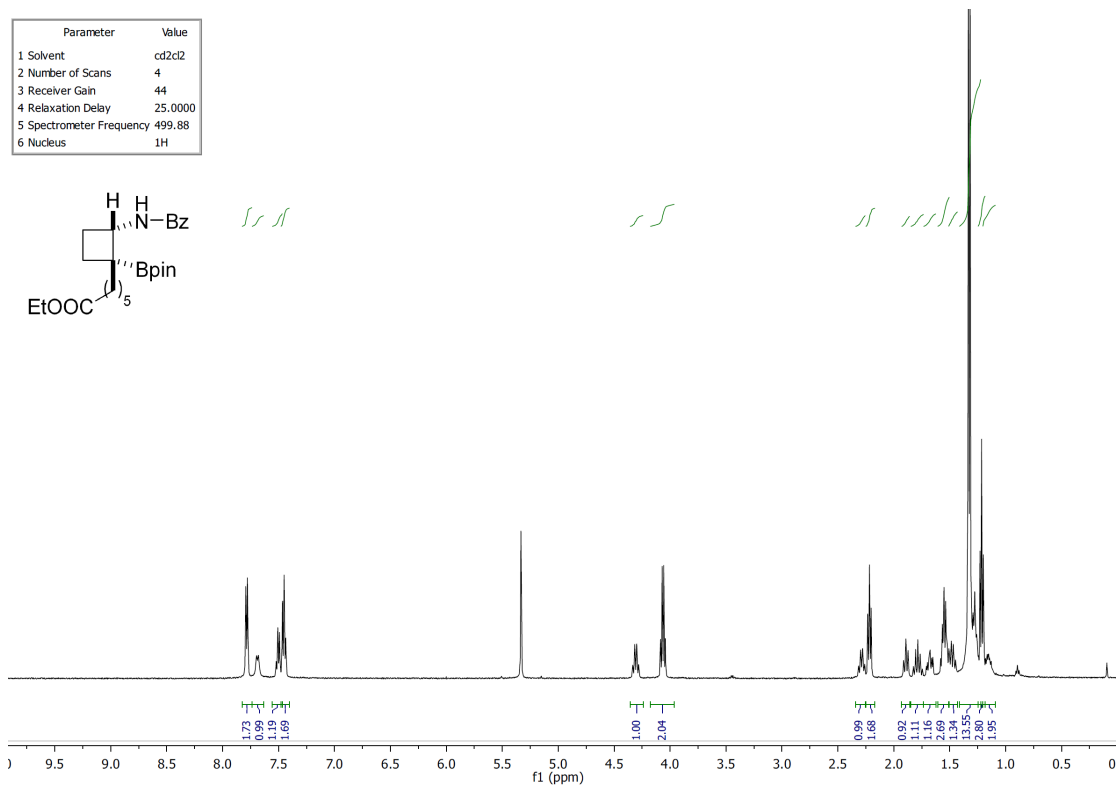
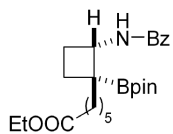
Parameter	Value
1 Solvent	cd2cl2
2 Number of Scans	20596
3 Receiver Gain	60
4 Relaxation Delay	1.0000
5 Spectrometer Frequency	150.81
6 Nucleus	13C



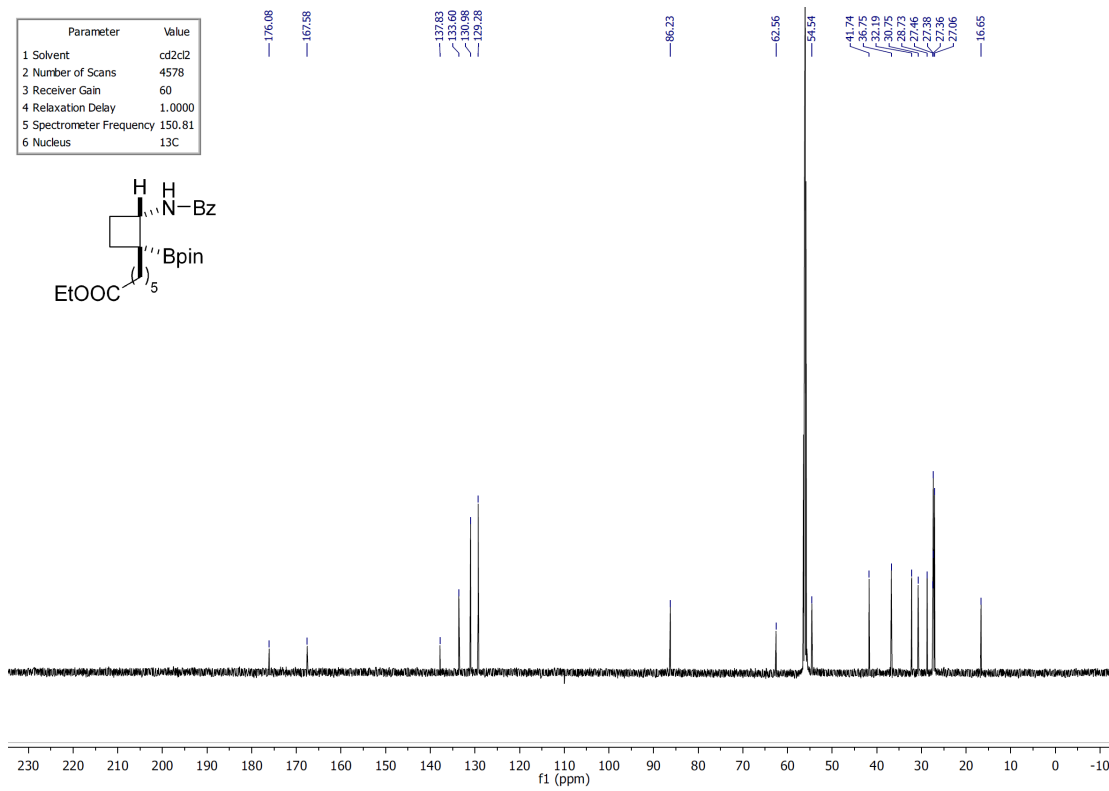
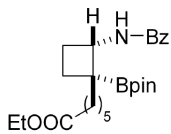
Parameter	Value
1 Solvent	cd2cl2
2 Number of Scans	1958
3 Receiver Gain	56
4 Relaxation Delay	0.0100
5 Spectrometer Frequency	160.35
6 Nucleus	11B



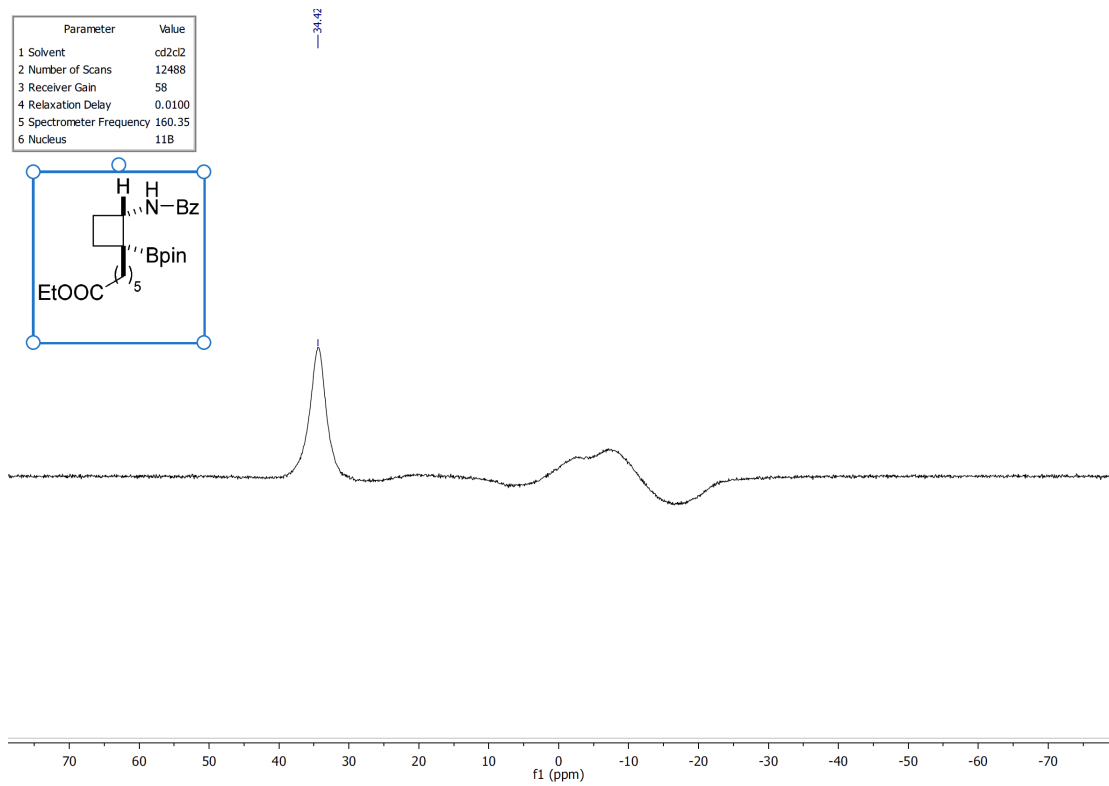
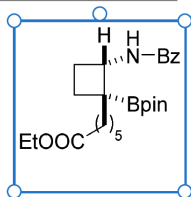
Parameter	Value
1 Solvent	cd2cl2
2 Number of Scans	4
3 Receiver Gain	44
4 Relaxation Delay	25.0000
5 Spectrometer Frequency	499.88
6 Nucleus	1H



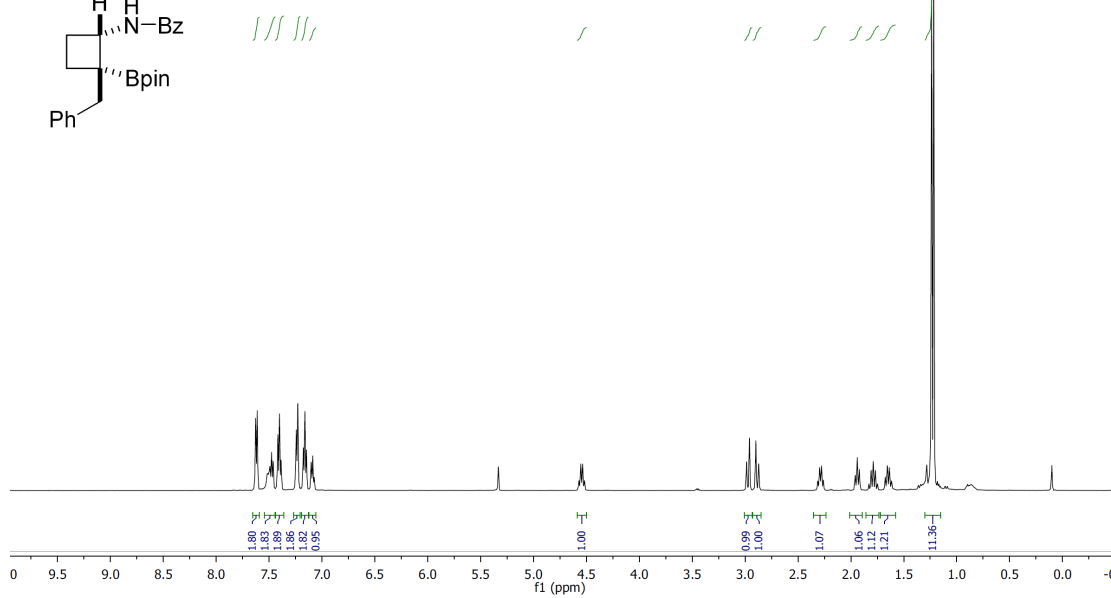
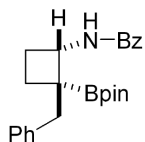
Parameter	Value
1 Solvent	cd2cl2
2 Number of Scans	4578
3 Receiver Gain	60
4 Relaxation Delay	1.0000
5 Spectrometer Frequency	150.81
6 Nucleus	13C



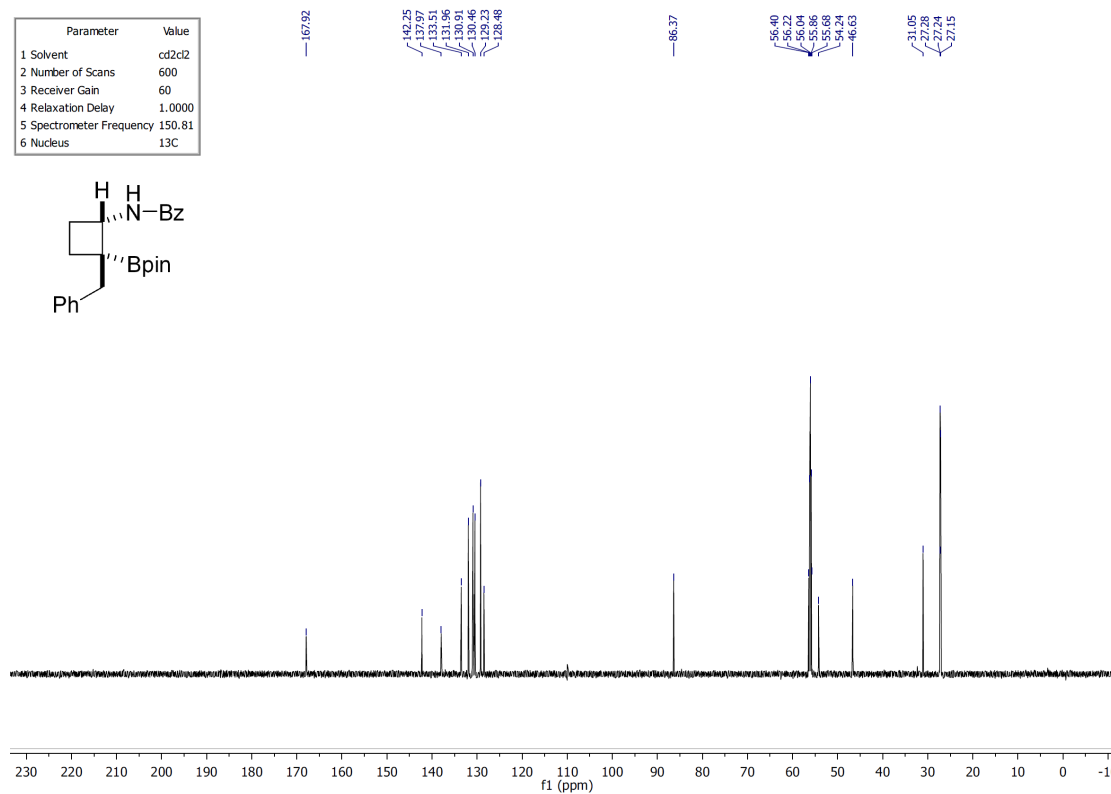
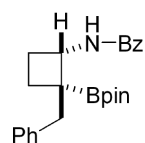
Parameter	Value
1 Solvent	cd2cl2
2 Number of Scans	12488
3 Receiver Gain	58
4 Relaxation Delay	0.0100
5 Spectrometer Frequency	160.35
6 Nucleus	11B



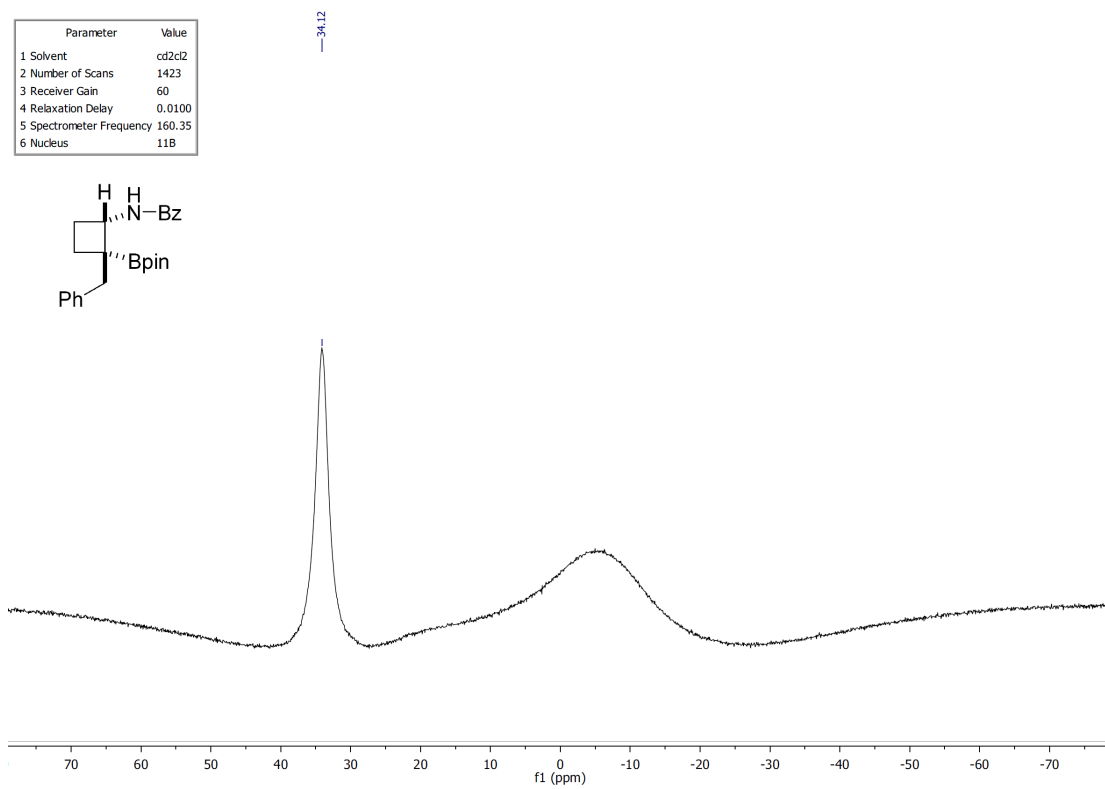
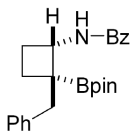
Parameter	Value
1 Solvent	cd2cl2
2 Number of Scans	8
3 Receiver Gain	34
4 Relaxation Delay	10.0000
5 Spectrometer Frequency	499.88
6 Nucleus	1H



Parameter	Value
1 Solvent	cd2cl2
2 Number of Scans	600
3 Receiver Gain	60
4 Relaxation Delay	1.0000
5 Spectrometer Frequency	150.81
6 Nucleus	13C

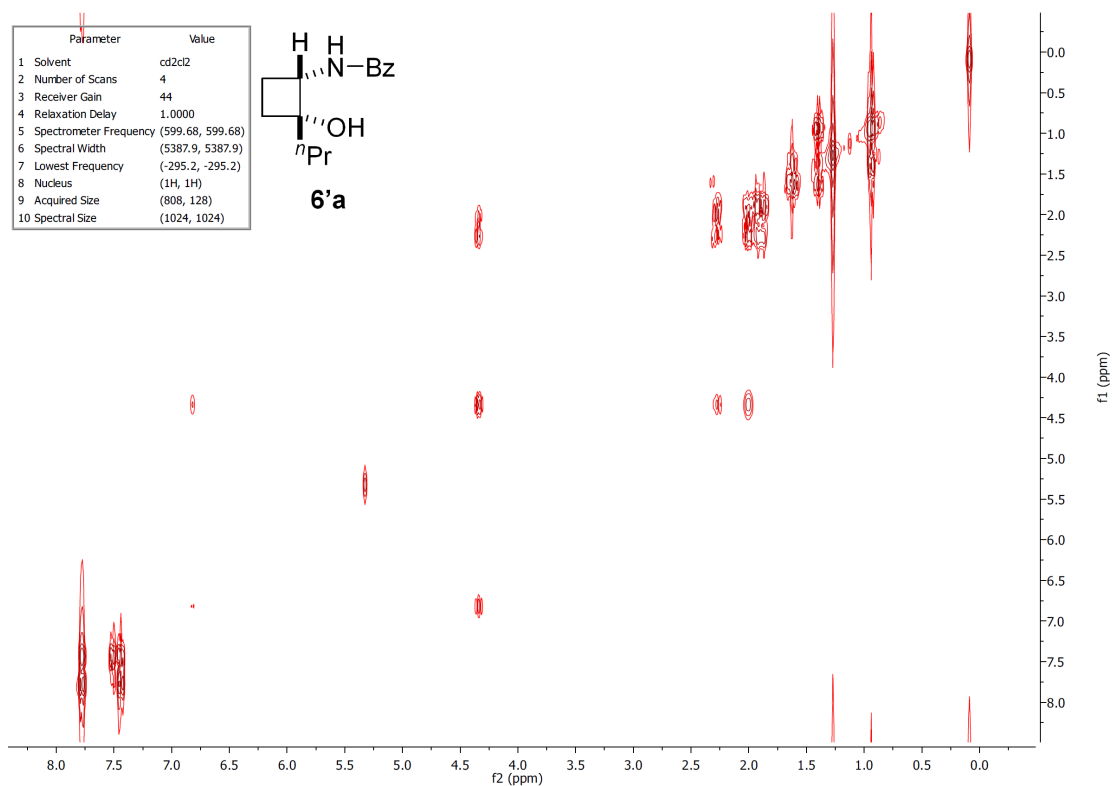
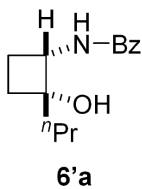


Parameter	Value
1 Solvent	cd2cl2
2 Number of Scans	1423
3 Receiver Gain	60
4 Relaxation Delay	0.0100
5 Spectrometer Frequency	160.35
6 Nucleus	11B

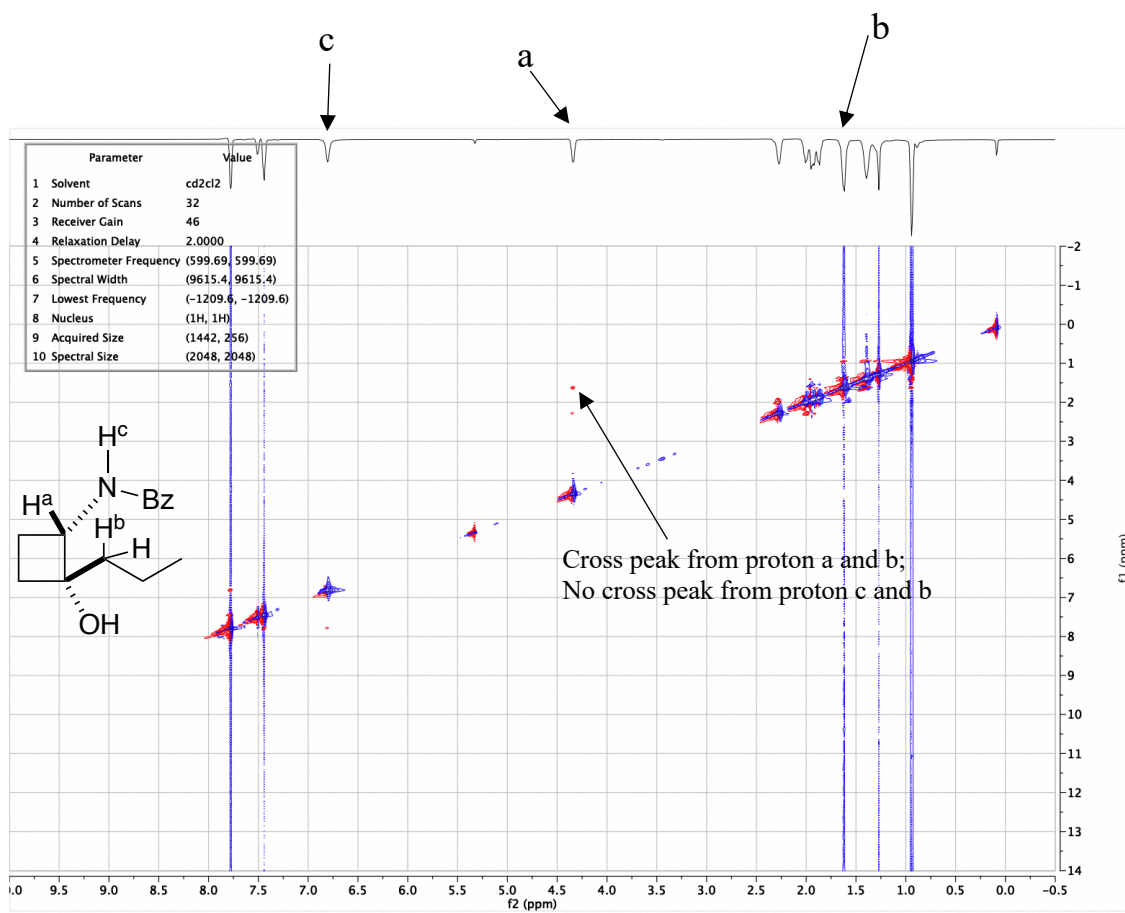


2D-gCOSY of Compound 1.39a

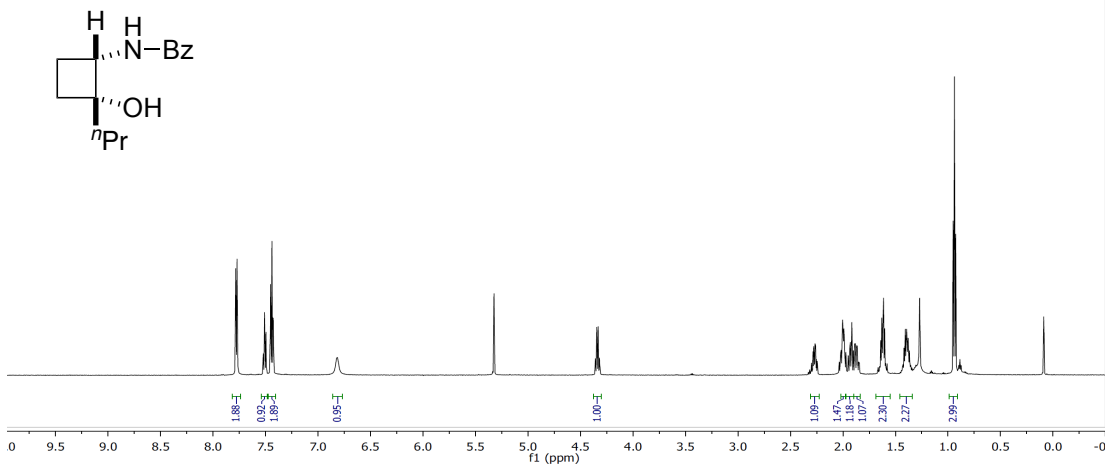
Parameter	Value
1 Solvent	cd2cl2
2 Number of Scans	4
3 Receiver Gain	44
4 Relaxation Delay	1.0000
5 Spectrometer Frequency	(599.68, 599.68)
6 Spectral Width	(5387.9, 5387.9)
7 Lowest Frequency	(-295.2, -295.2)
8 Nucleus	(1H, 1H)
9 Acquired Size	(808, 128)
10 Spectral Size	(1024, 1024)



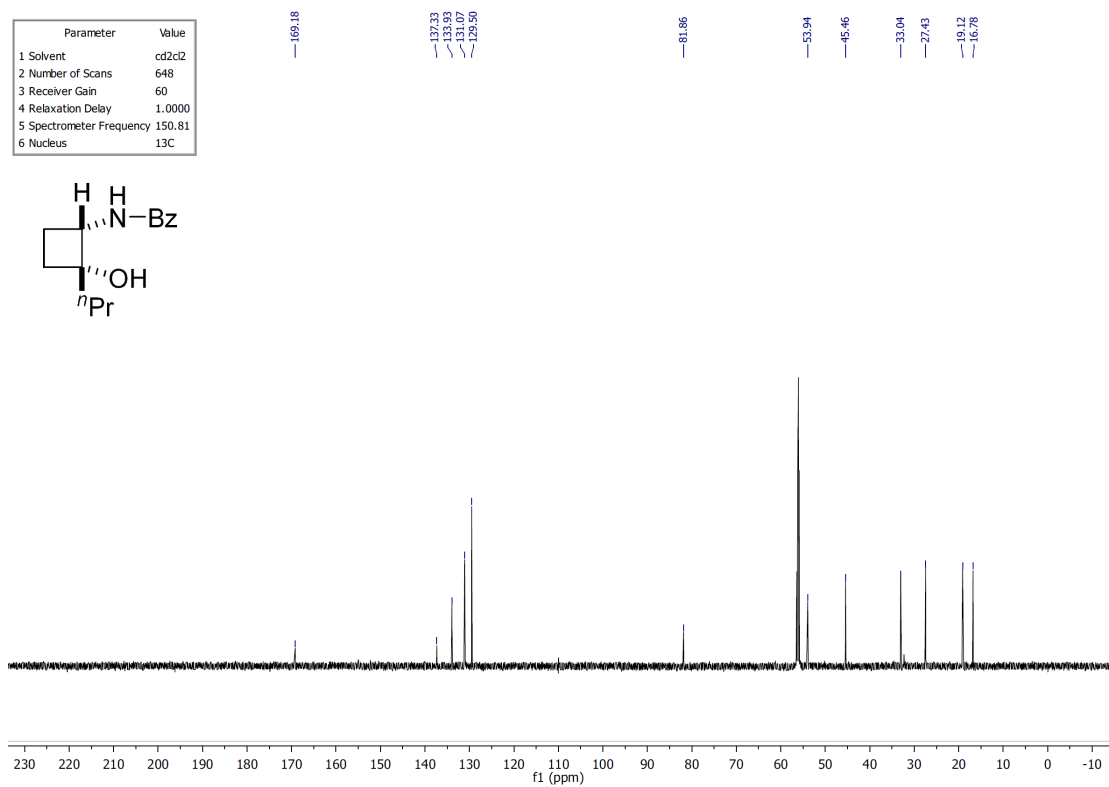
2D-NOESY of Compound 1.39a

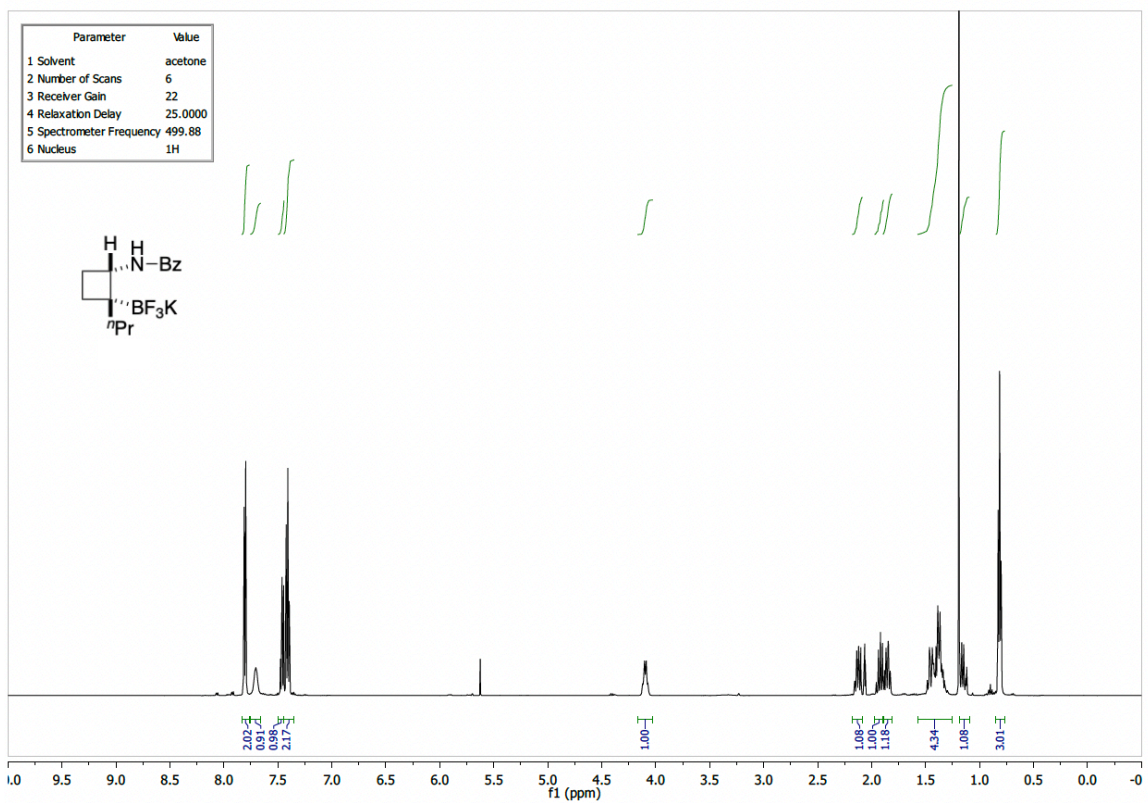


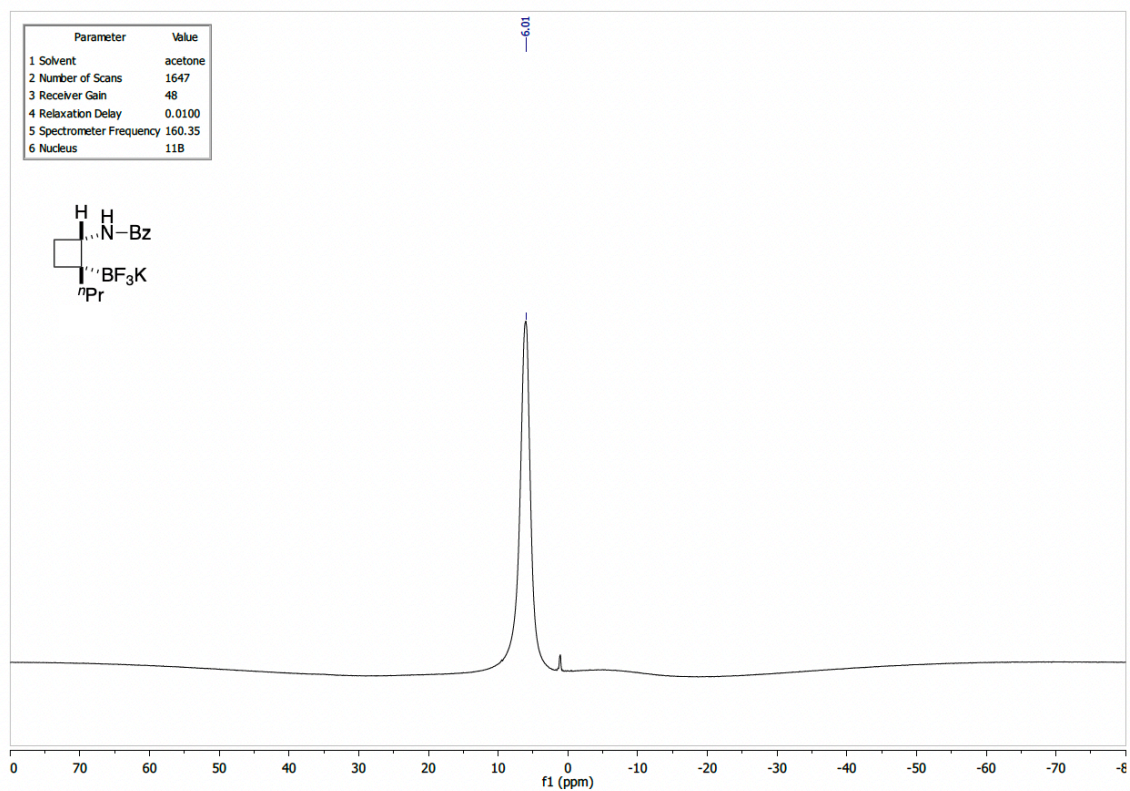
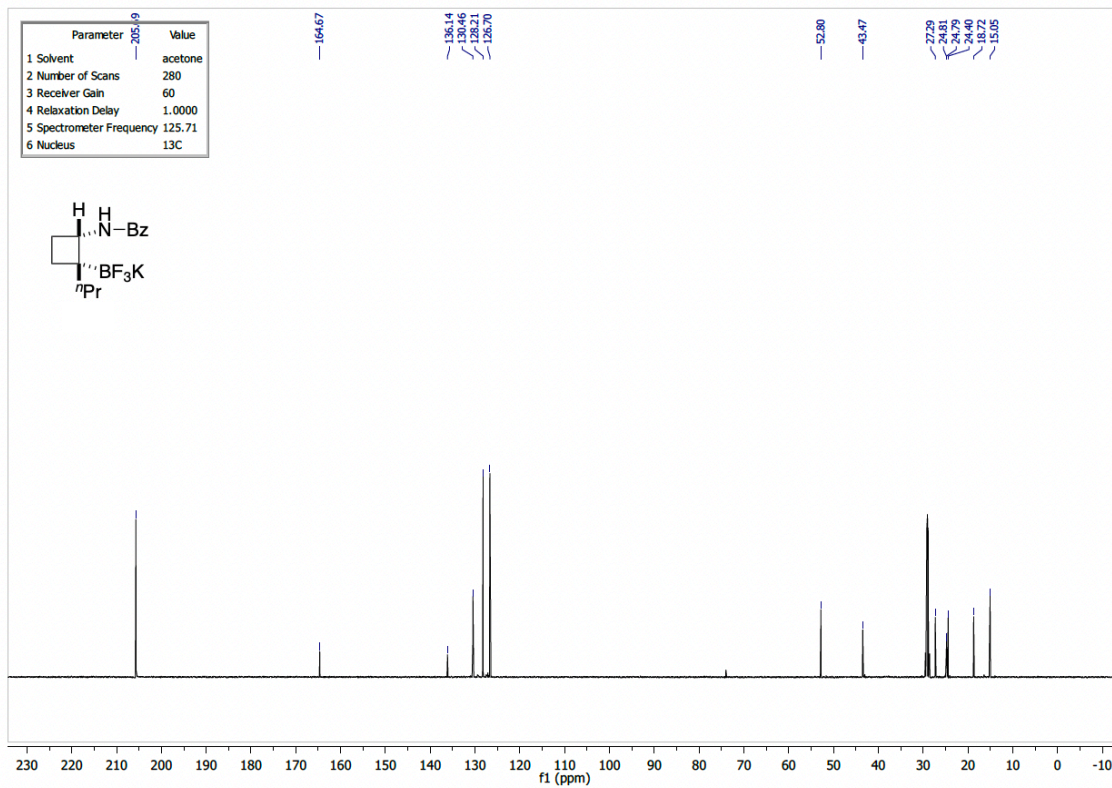
Parameter	Value
1 Solvent	cd2cl2
2 Number of Scans	8
3 Receiver Gain	44
4 Relaxation Delay	10.0000
5 Spectrometer Frequency	599.69
6 Nucleus	¹ H

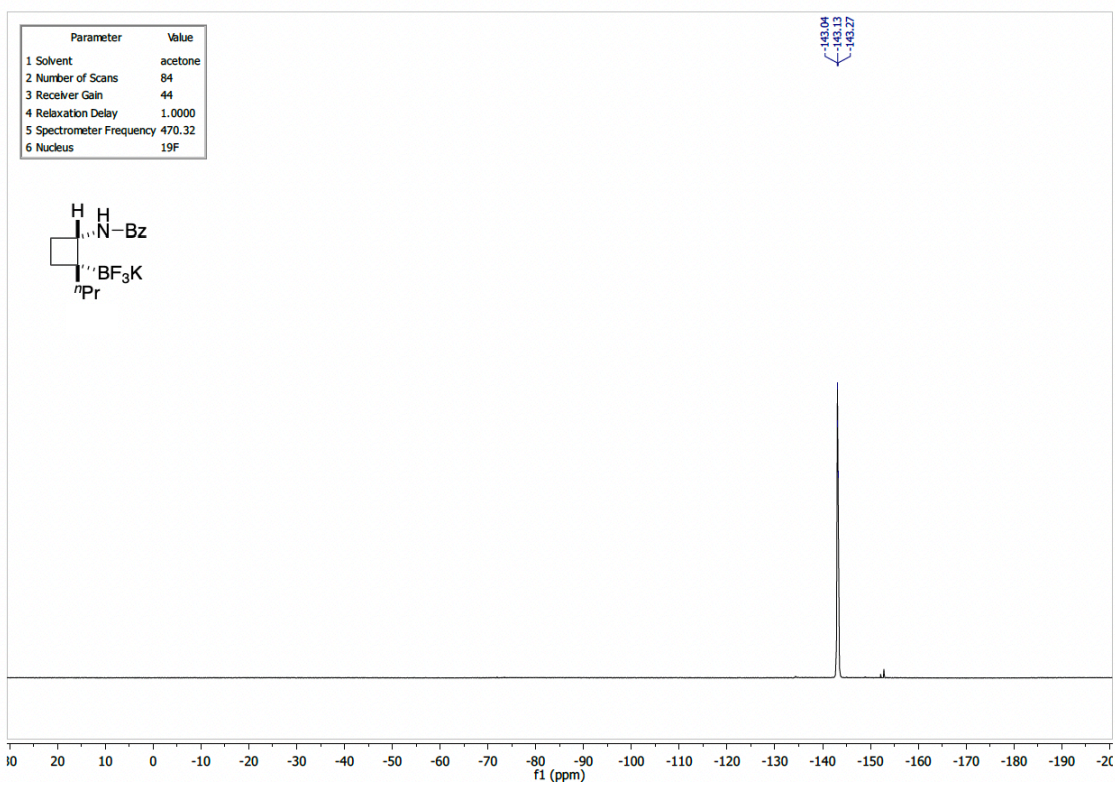


Parameter	Value
1 Solvent	cd2cl2
2 Number of Scans	648
3 Receiver Gain	60
4 Relaxation Delay	1.0000
5 Spectrometer Frequency	150.81
6 Nucleus	¹³ C

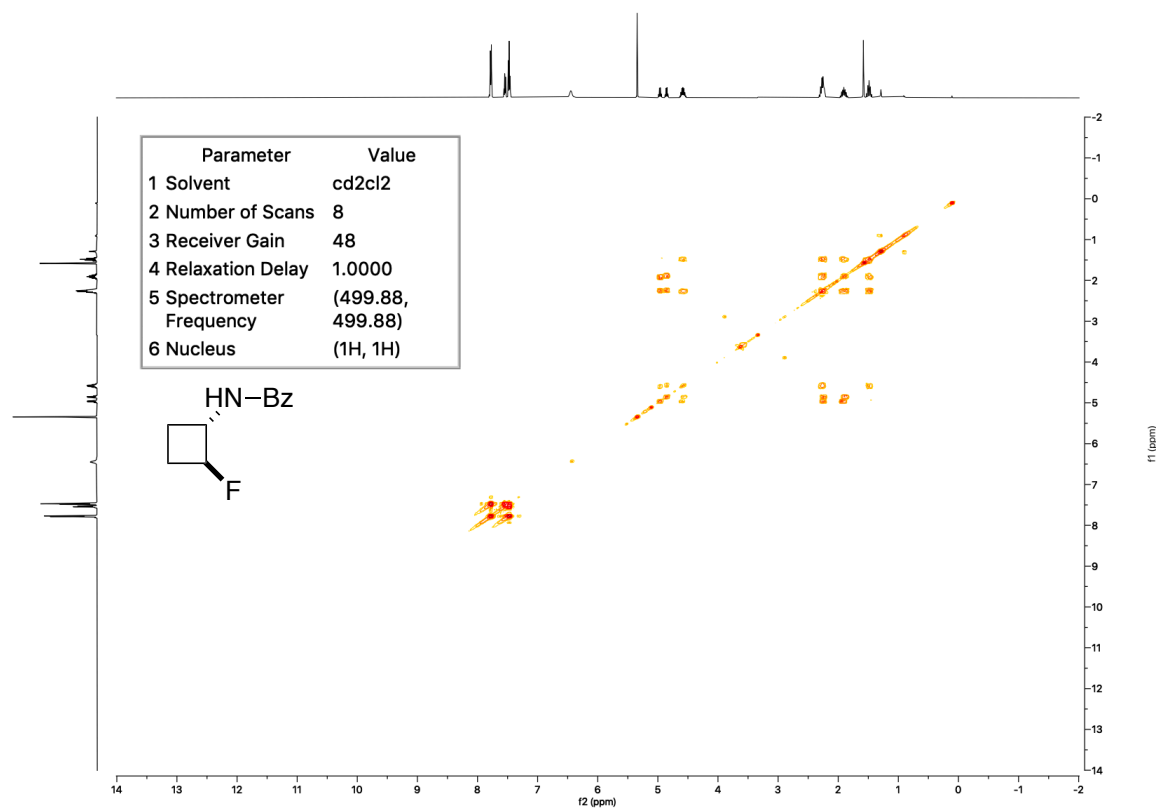




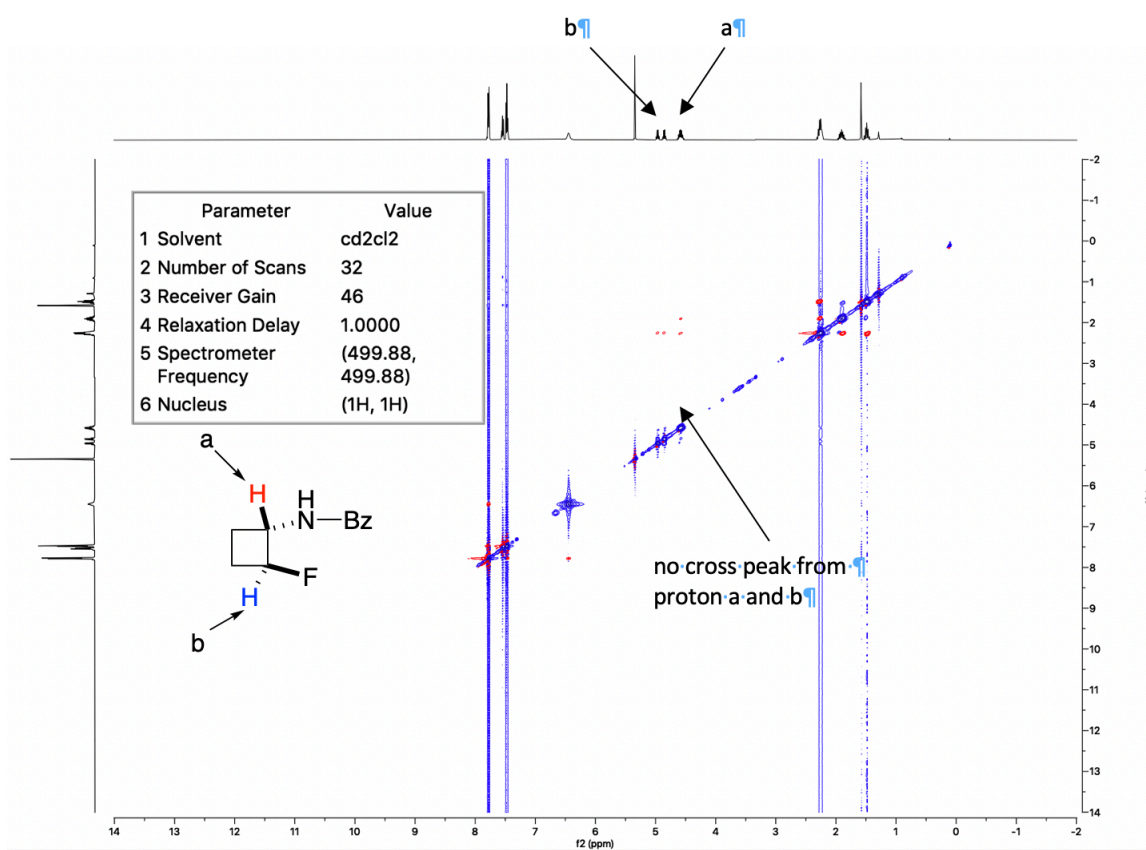


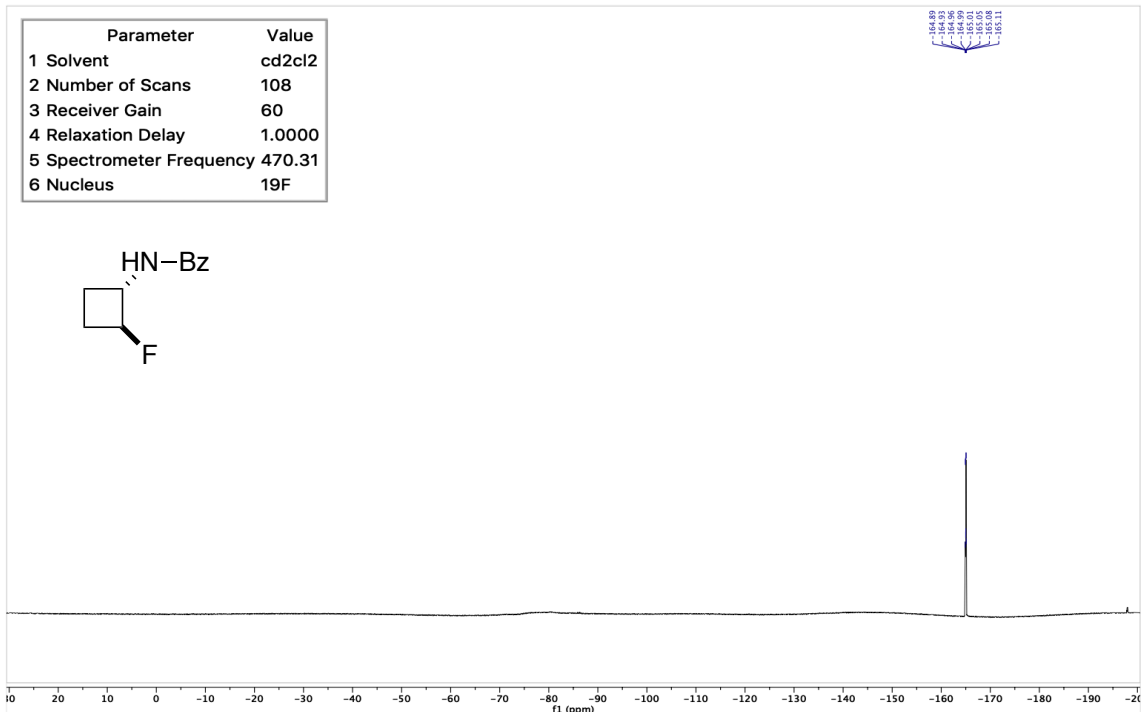
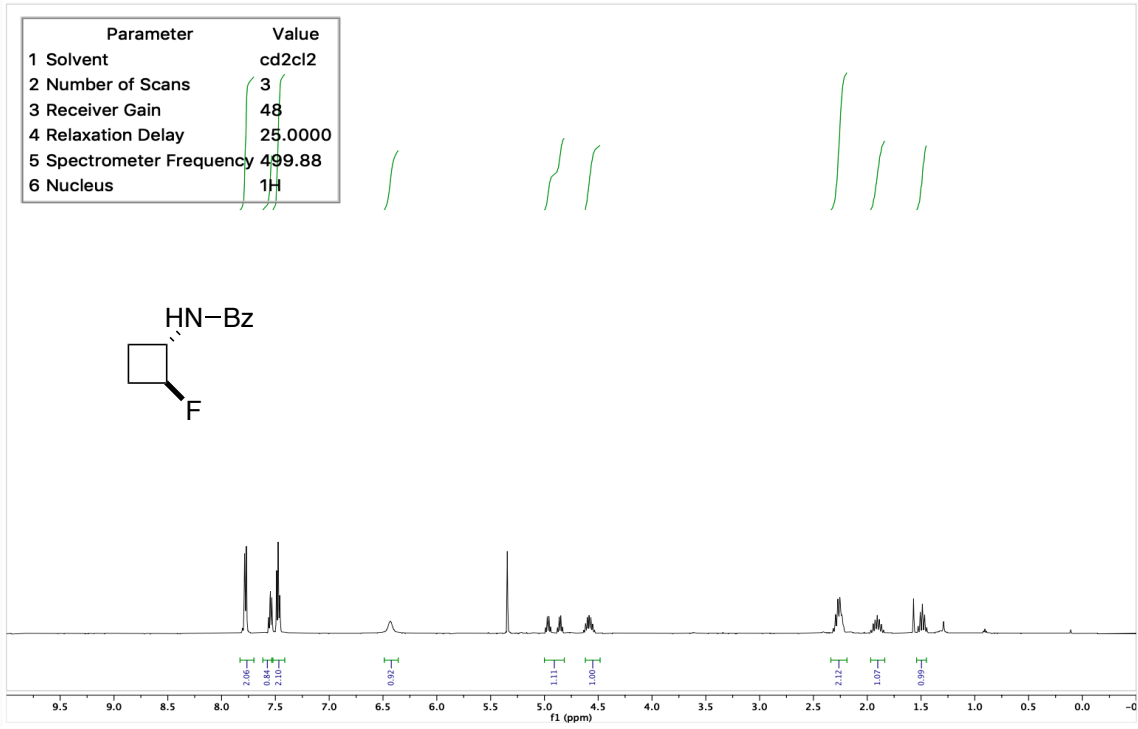


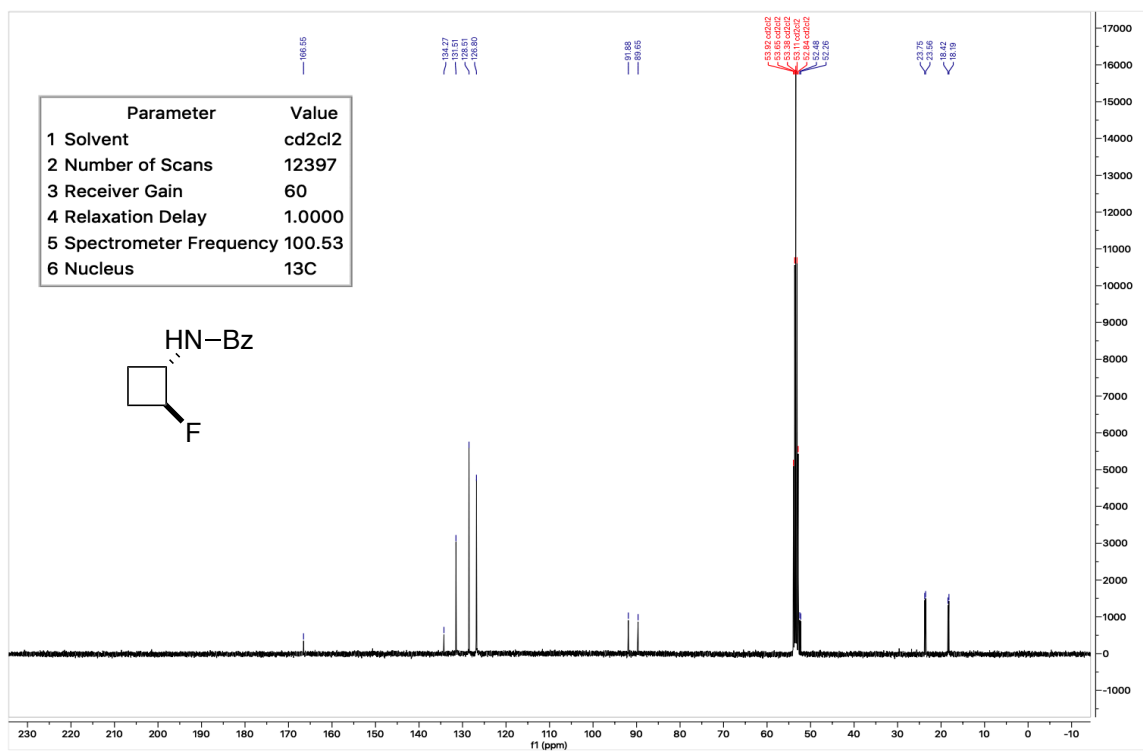
2D-Cosy of Compound **1.41**



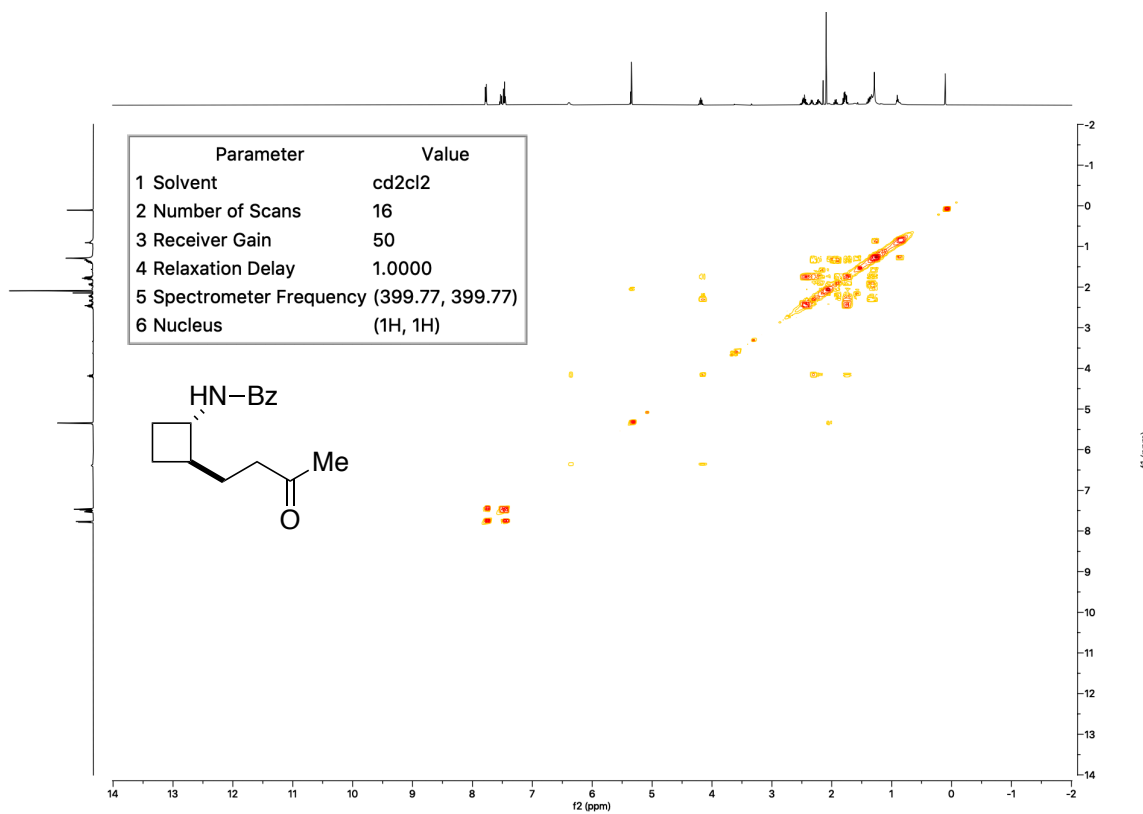
2D-NOESY of Compound 1.41



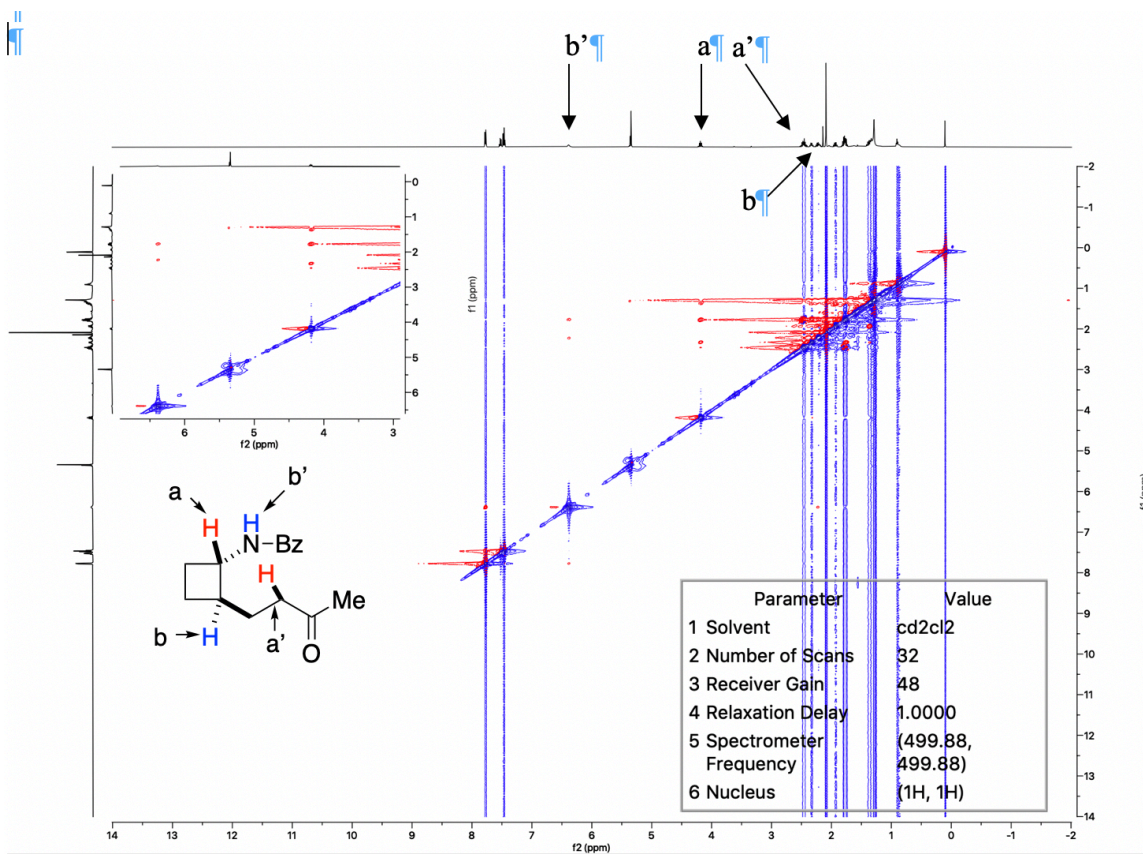


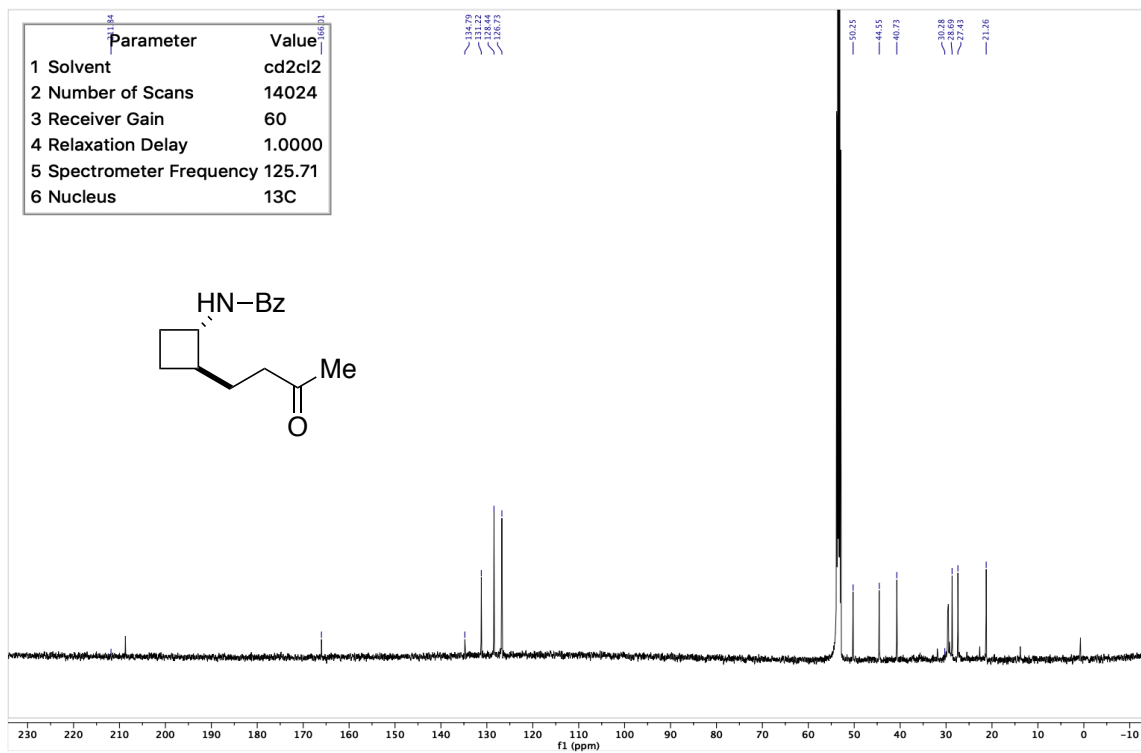
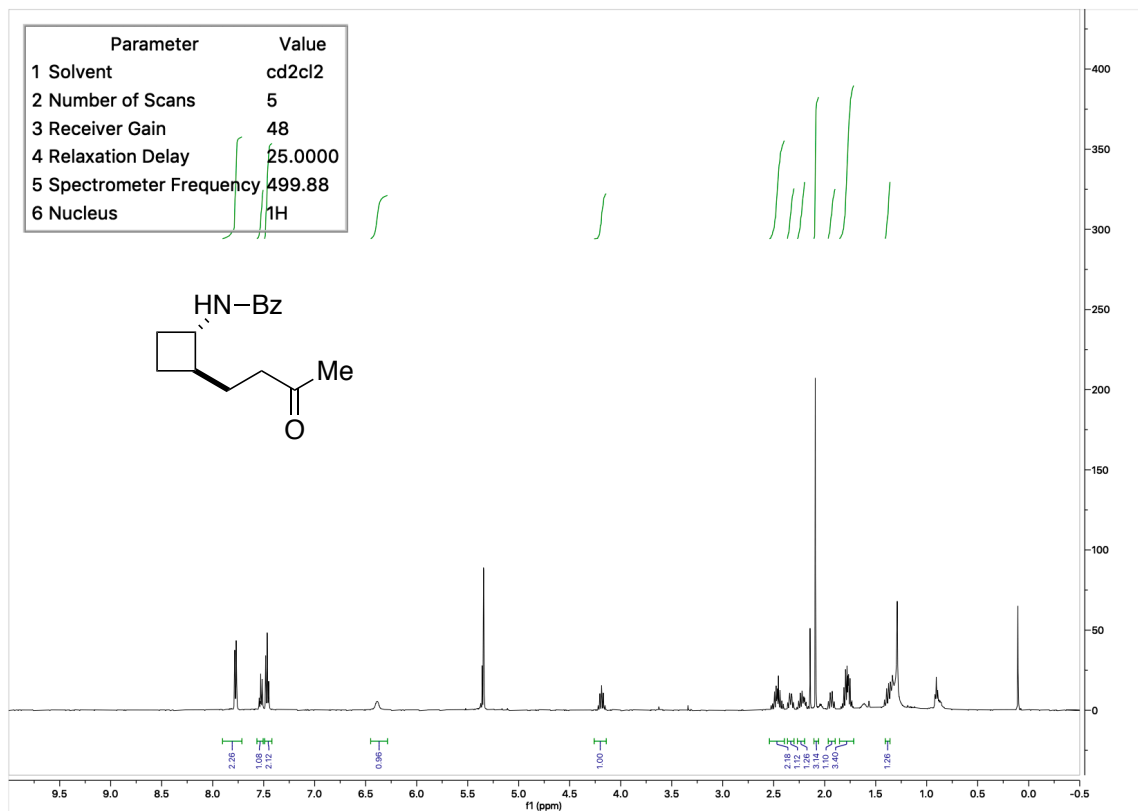


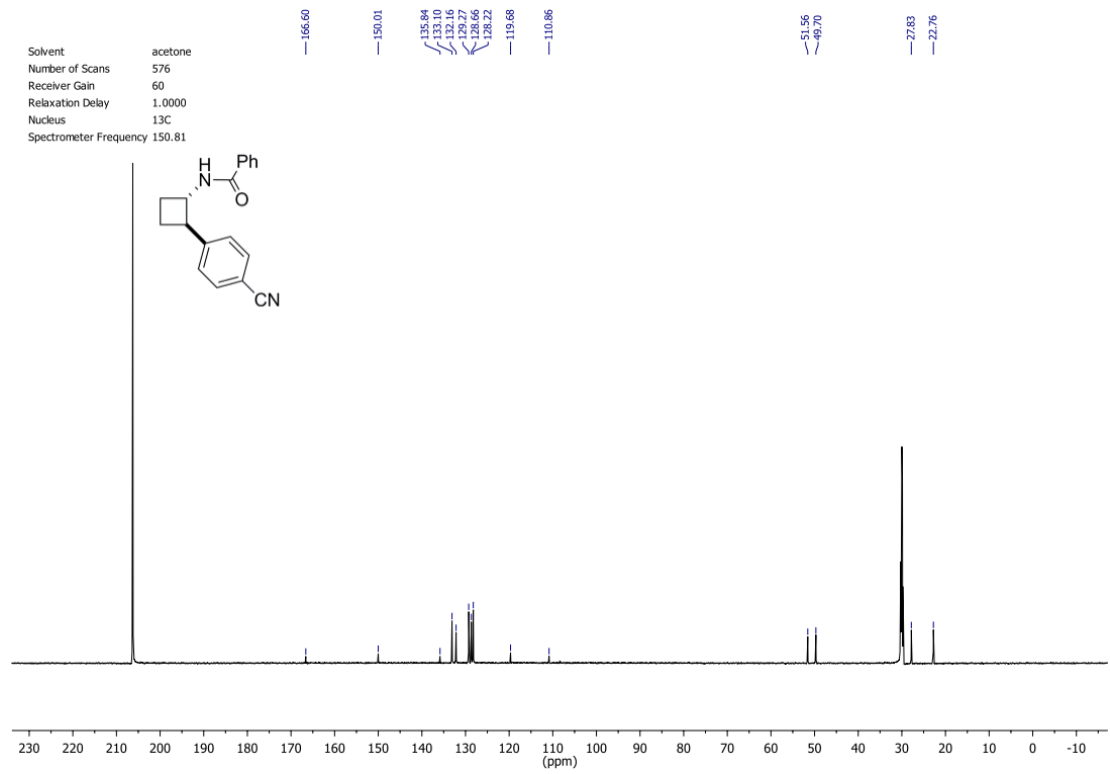
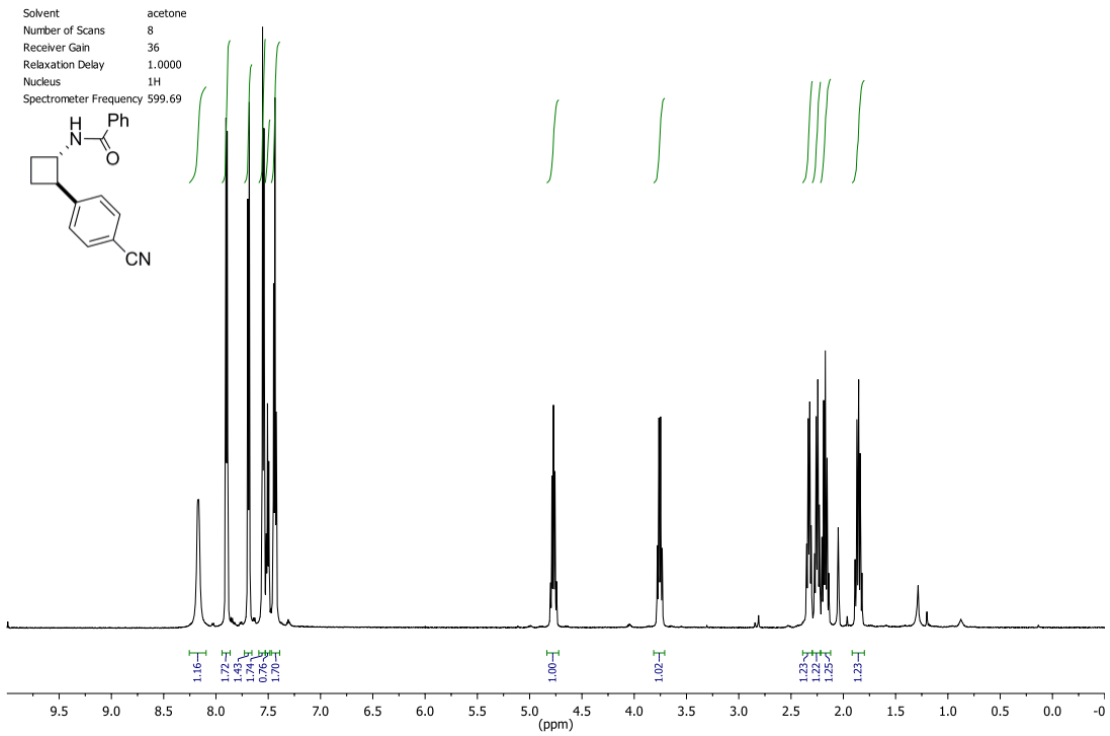
2D-Cosy of Compound 1.42

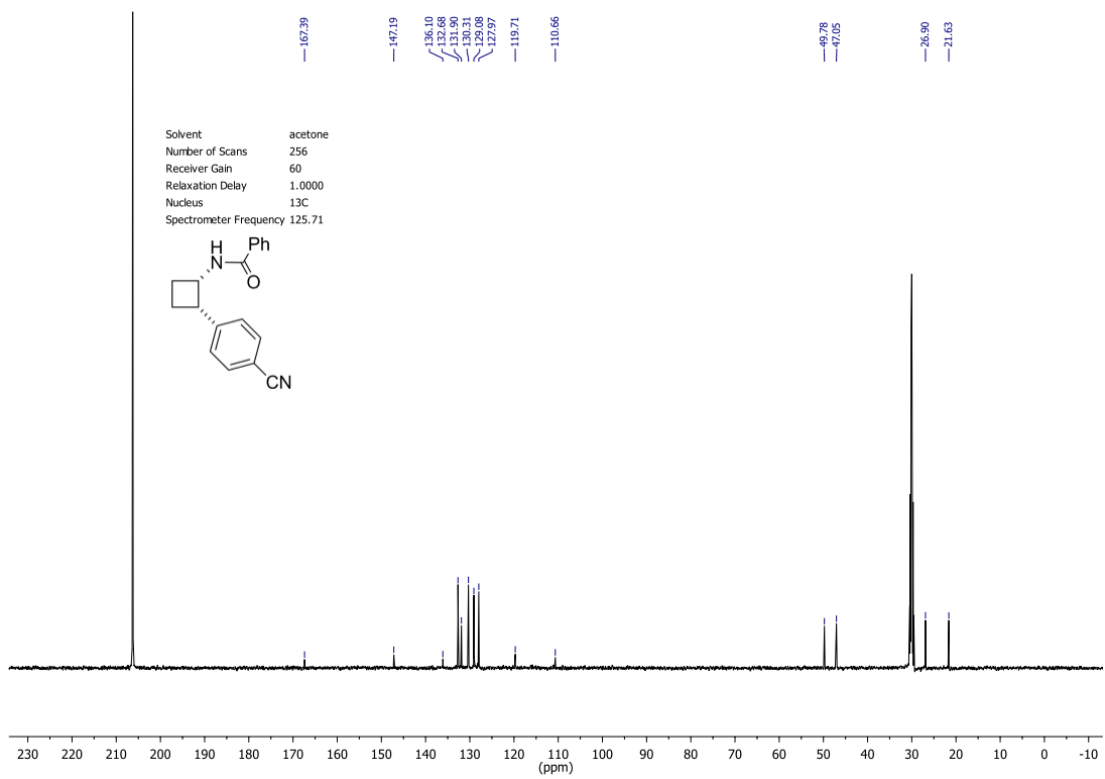
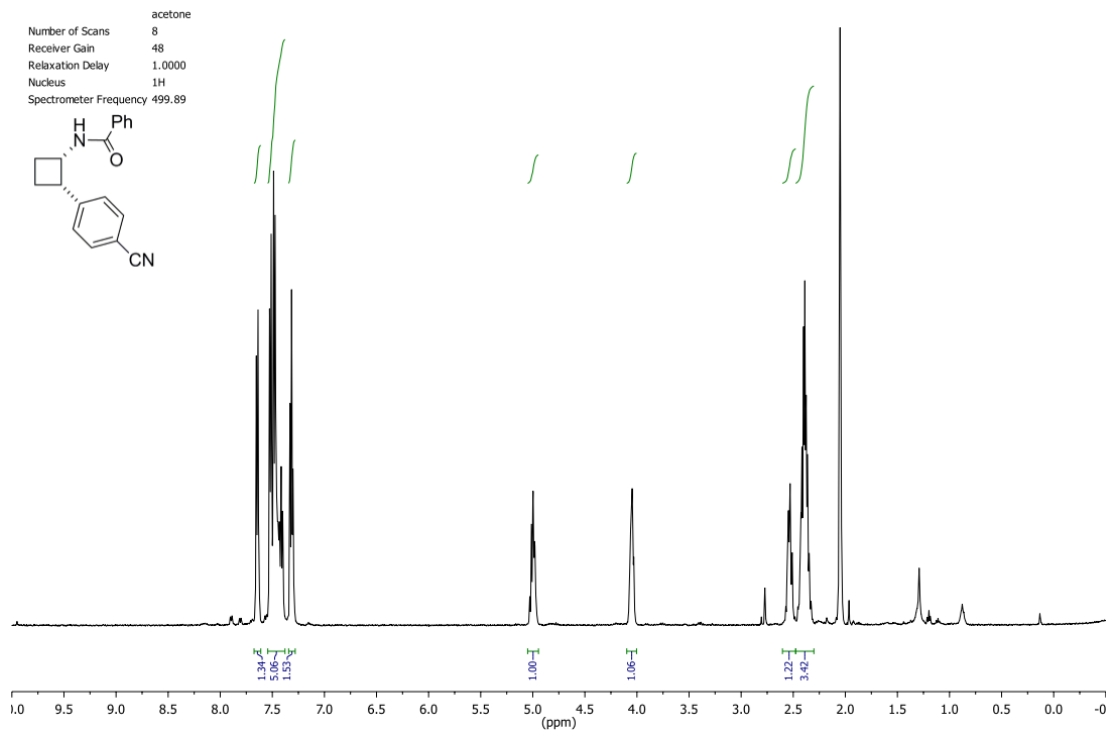


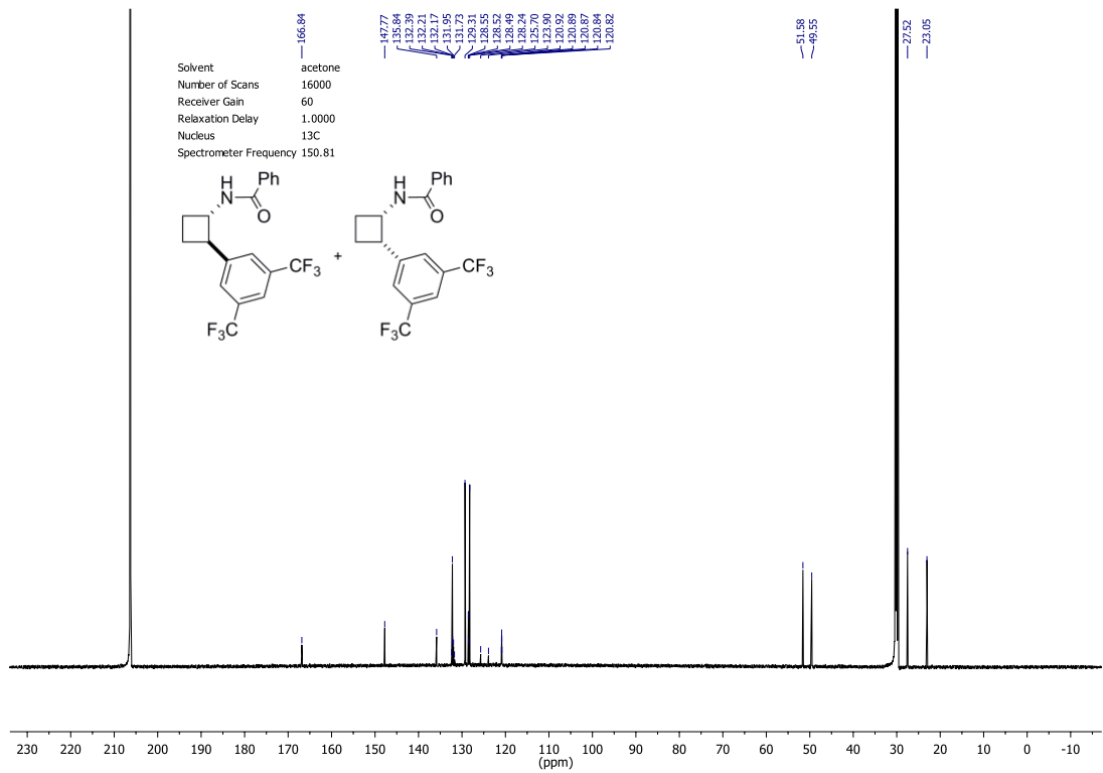
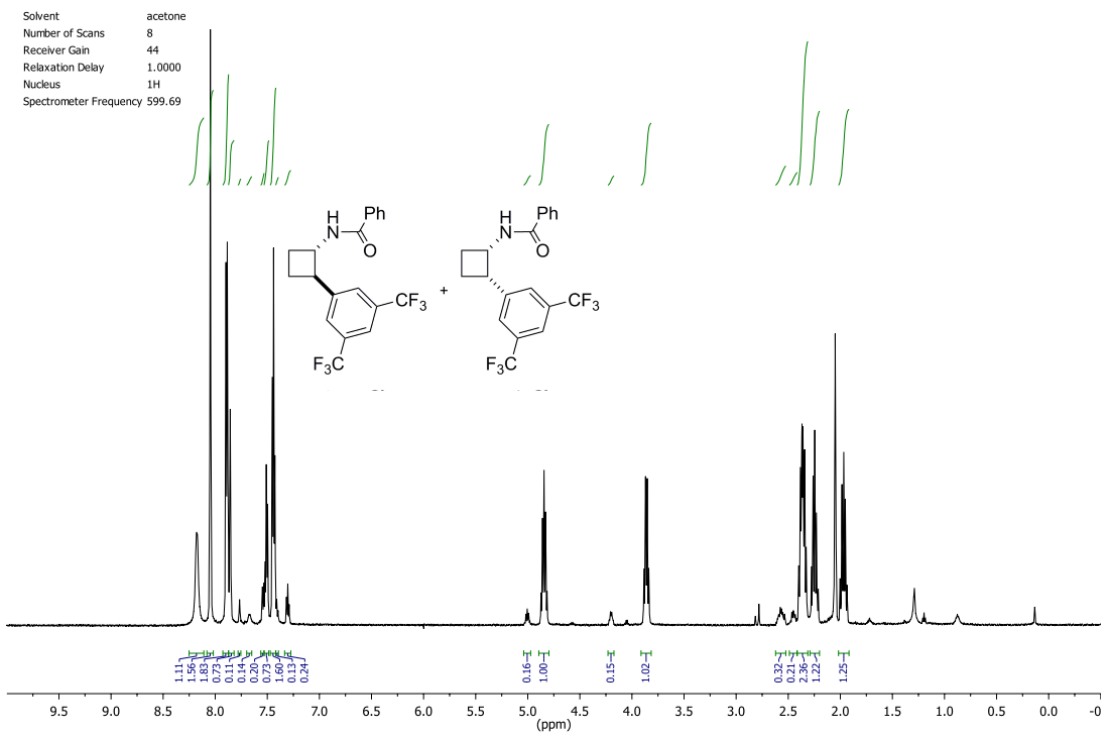
2D-NOESY of Compound 1.42

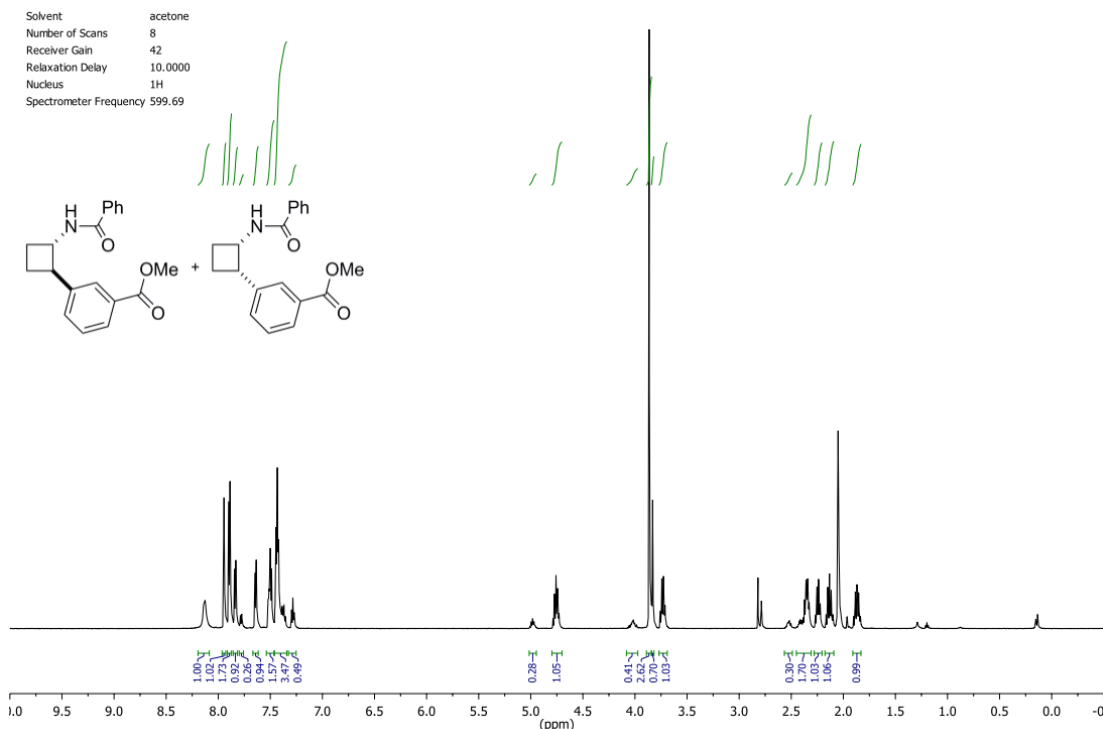
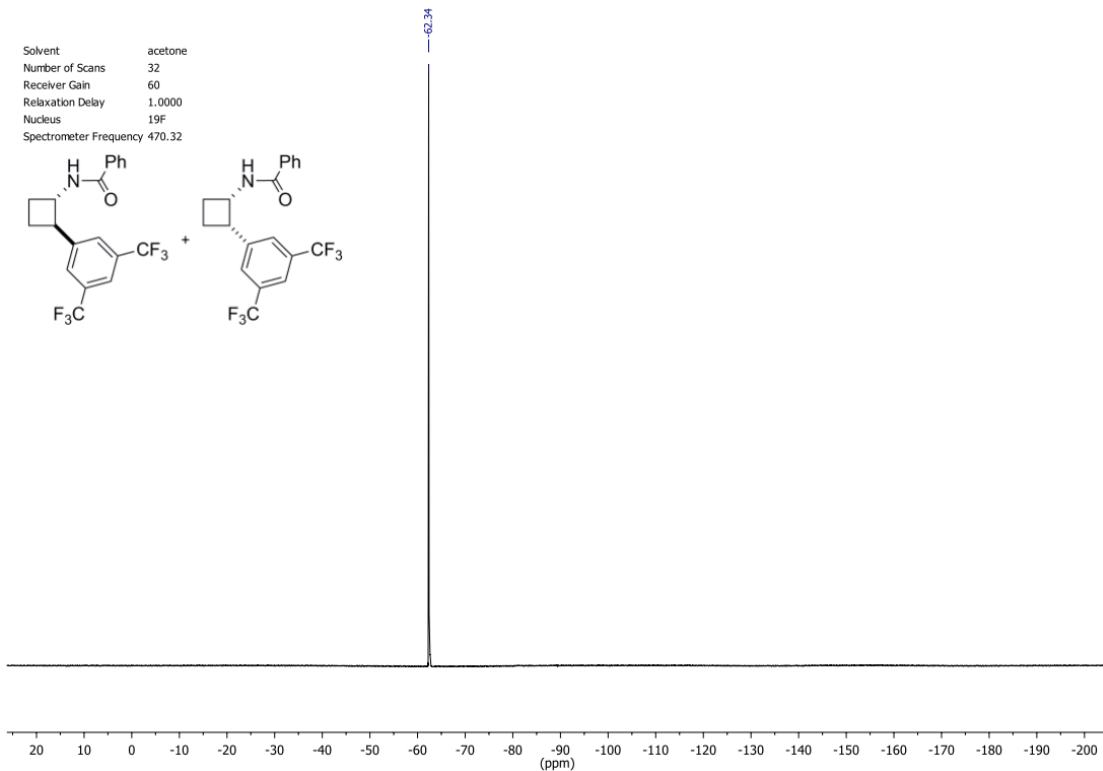


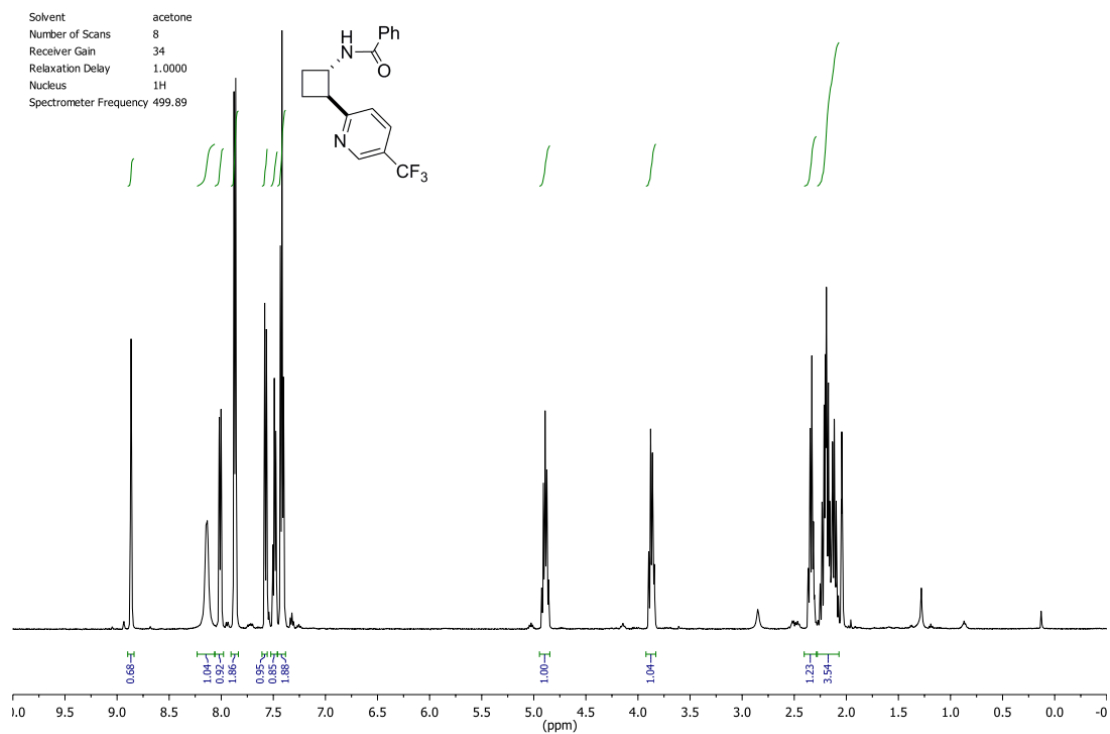
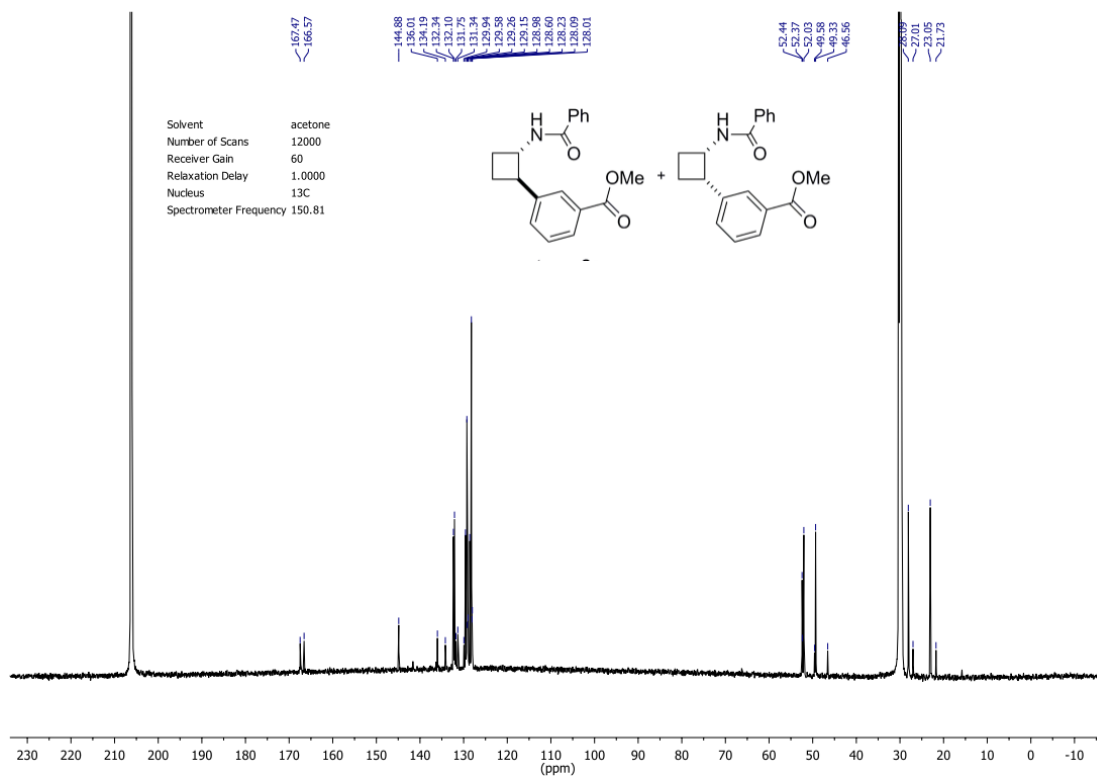


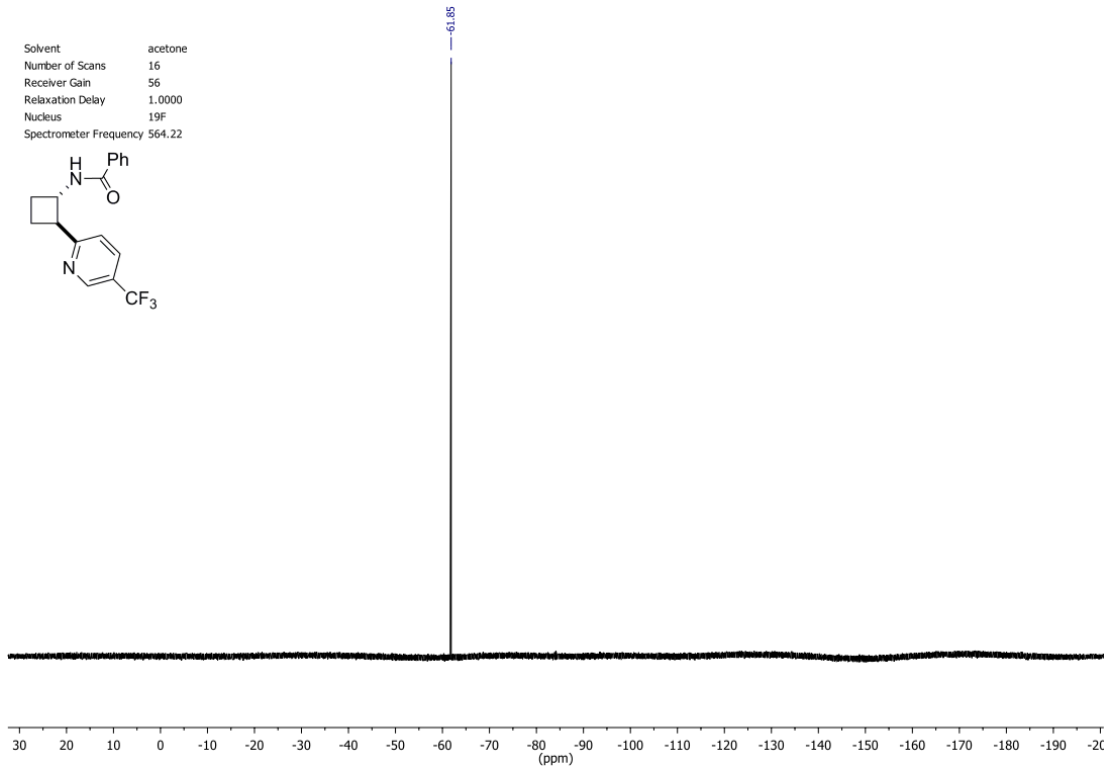
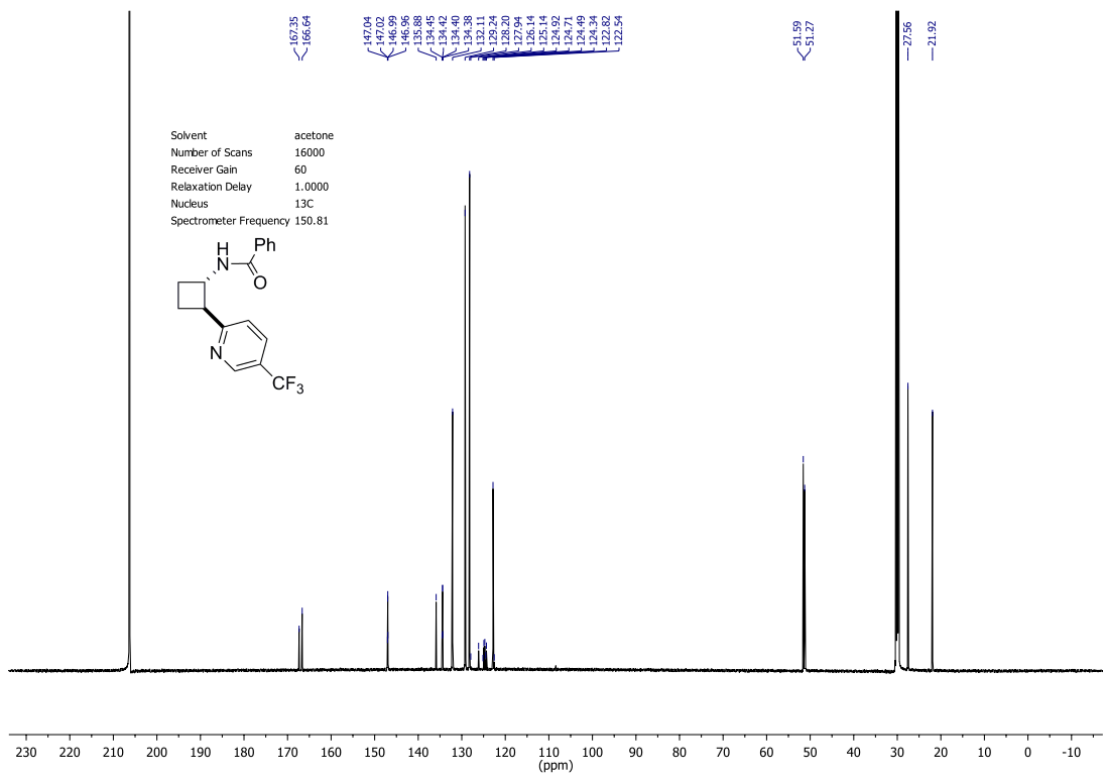


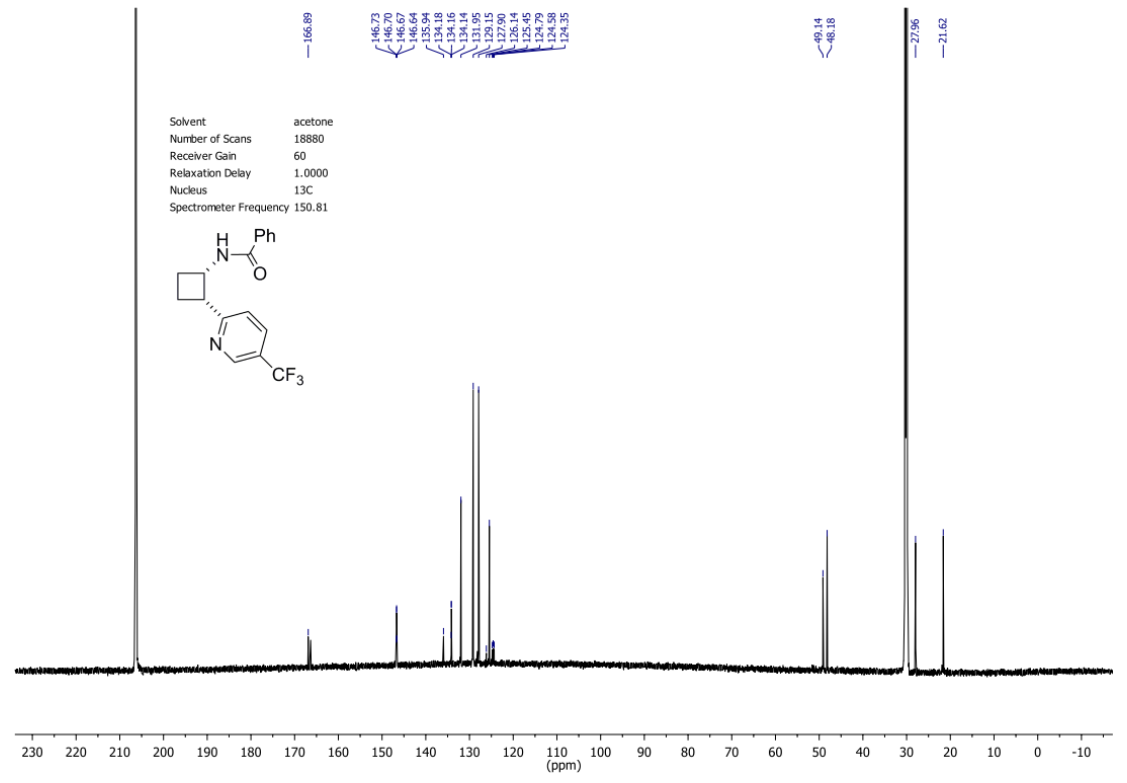
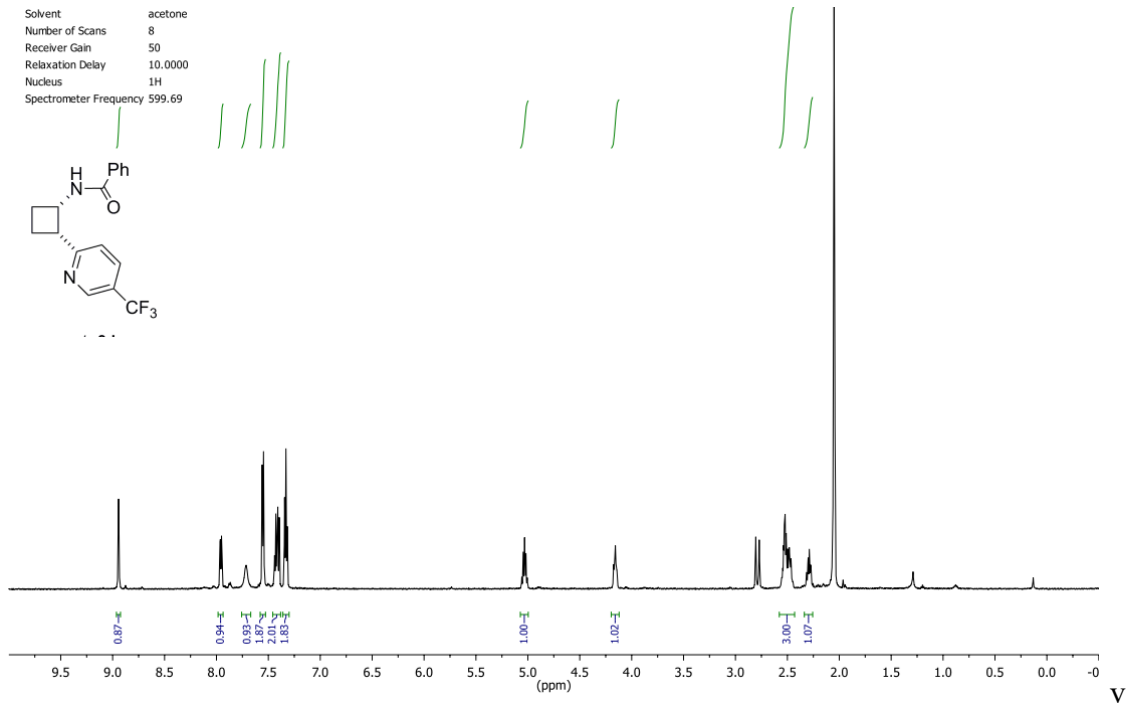




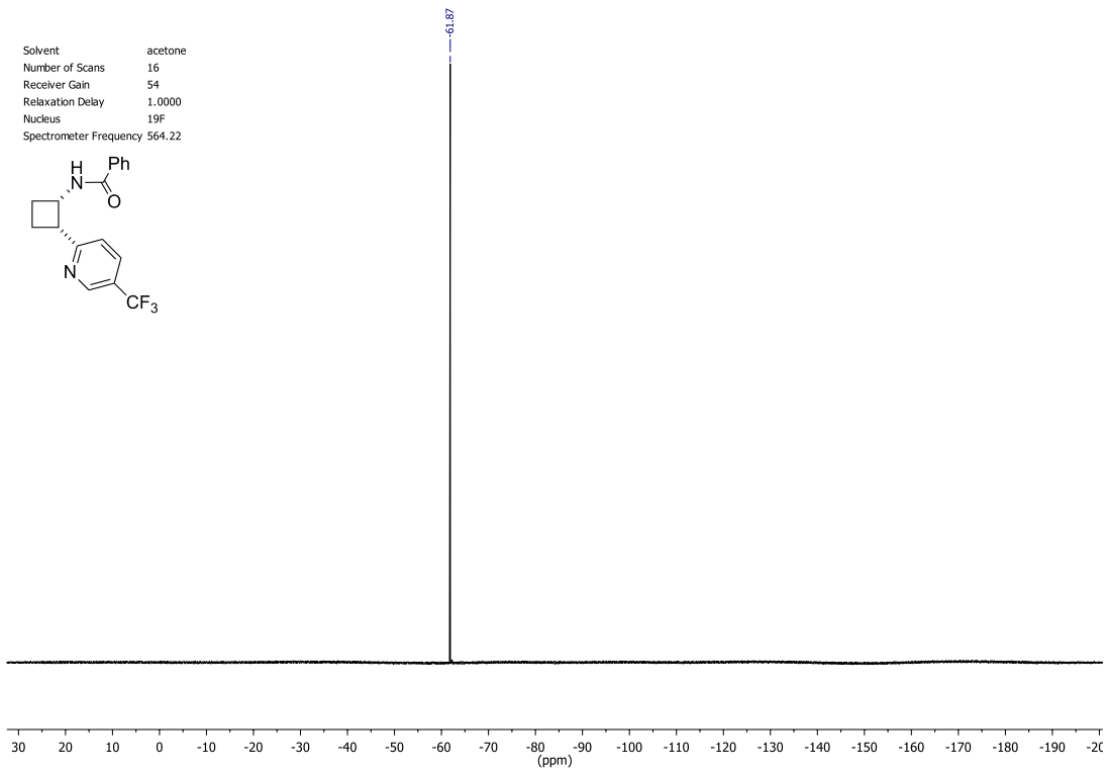
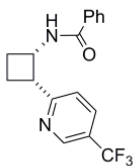




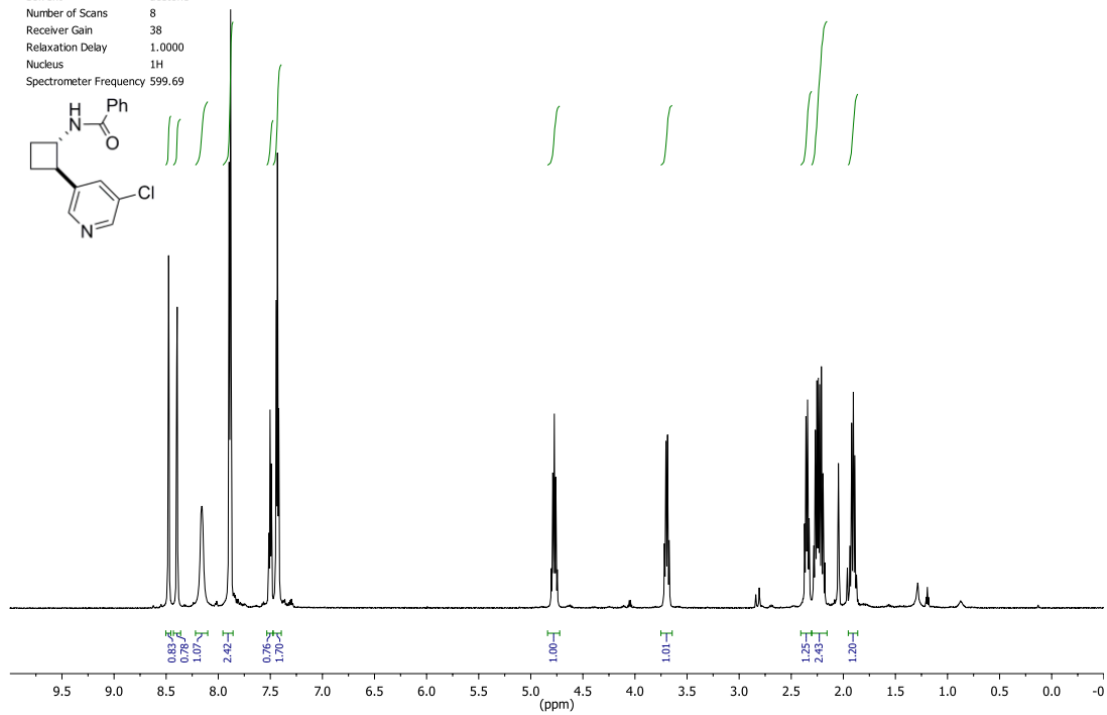
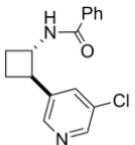


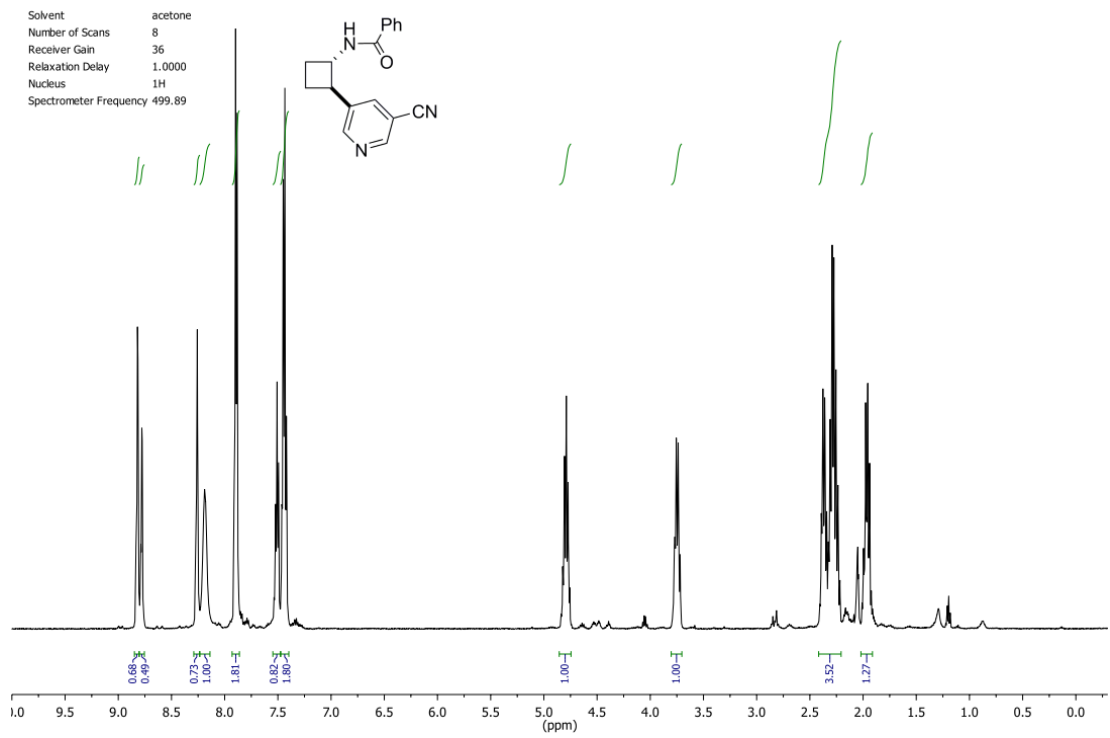
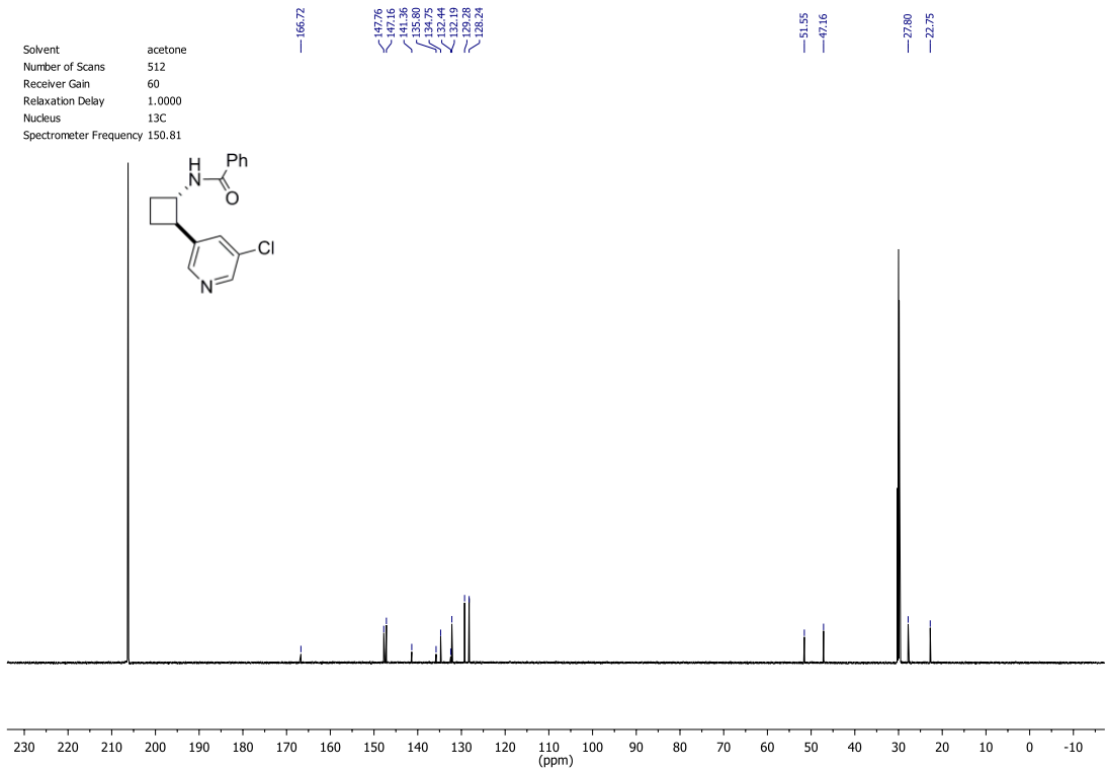


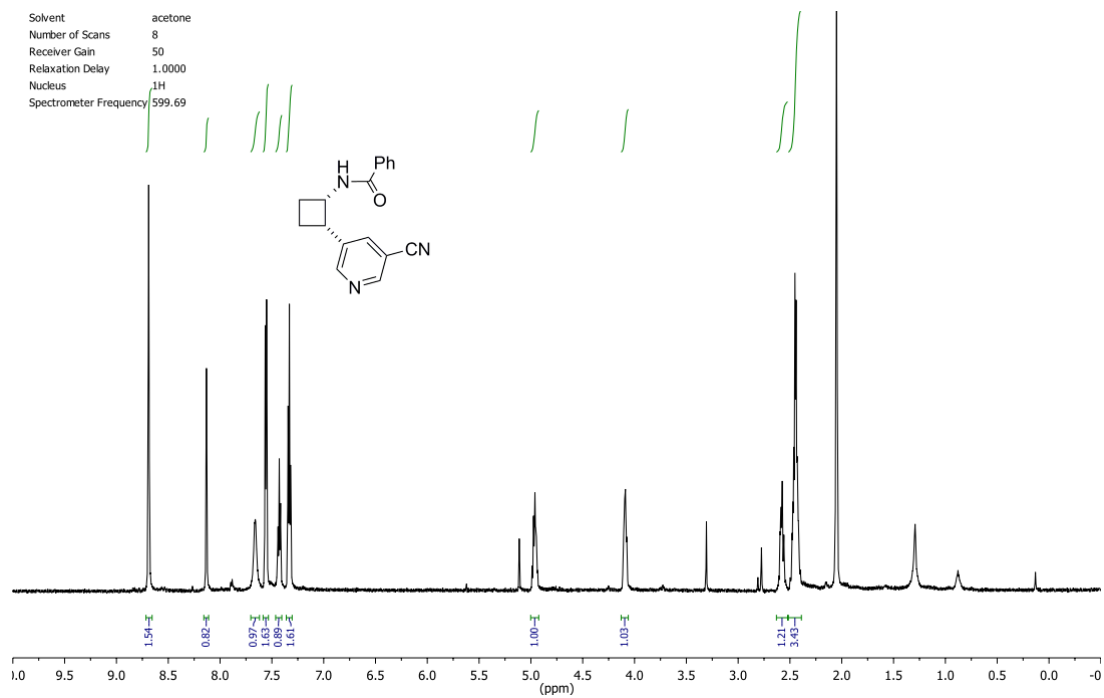
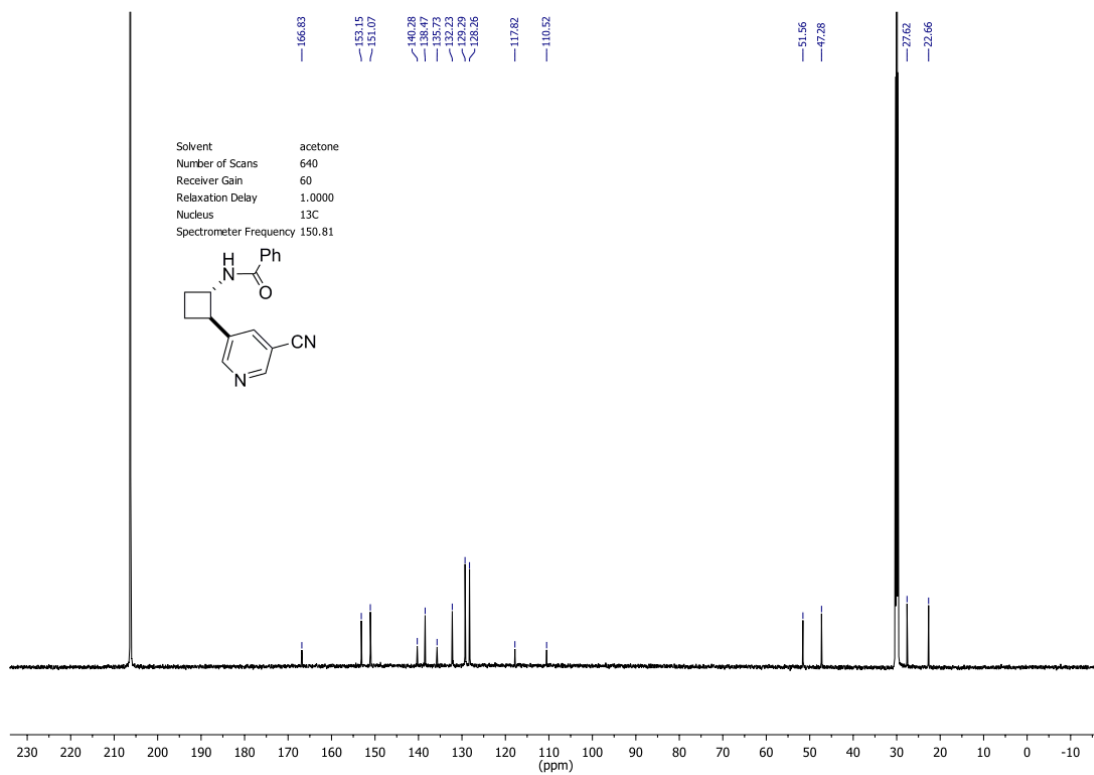
Solvent acetone
Number of Scans 16
Receiver Gain 54
Relaxation Delay 1.0000
Nucleus 19F
Spectrometer Frequency 564.22

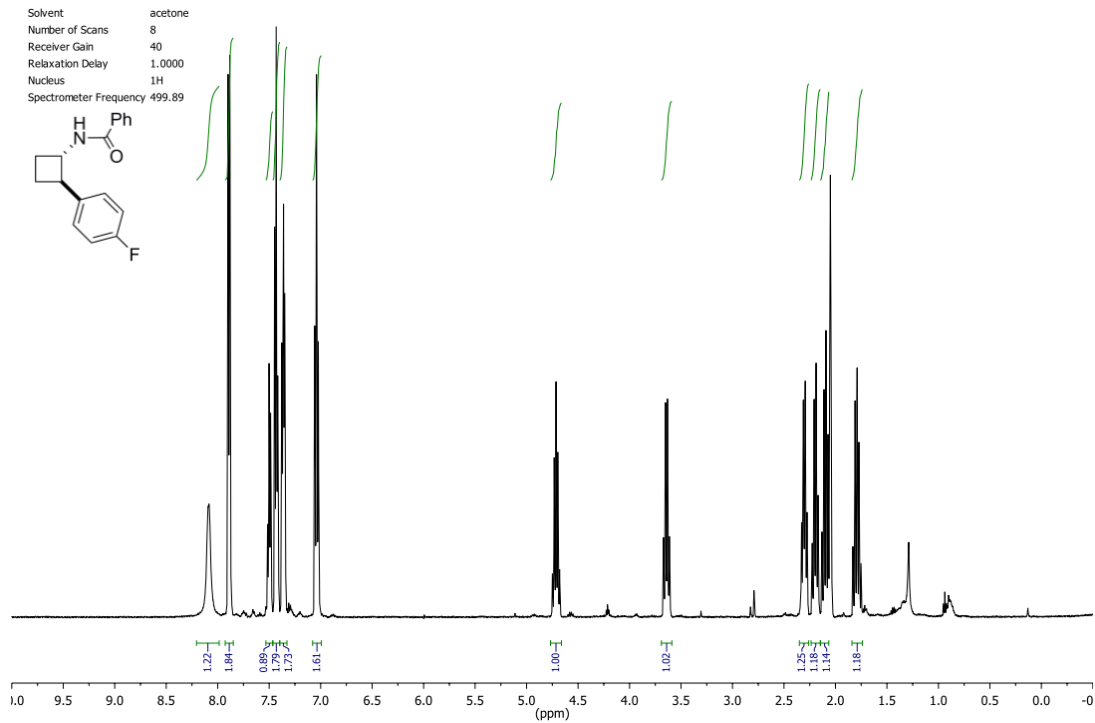
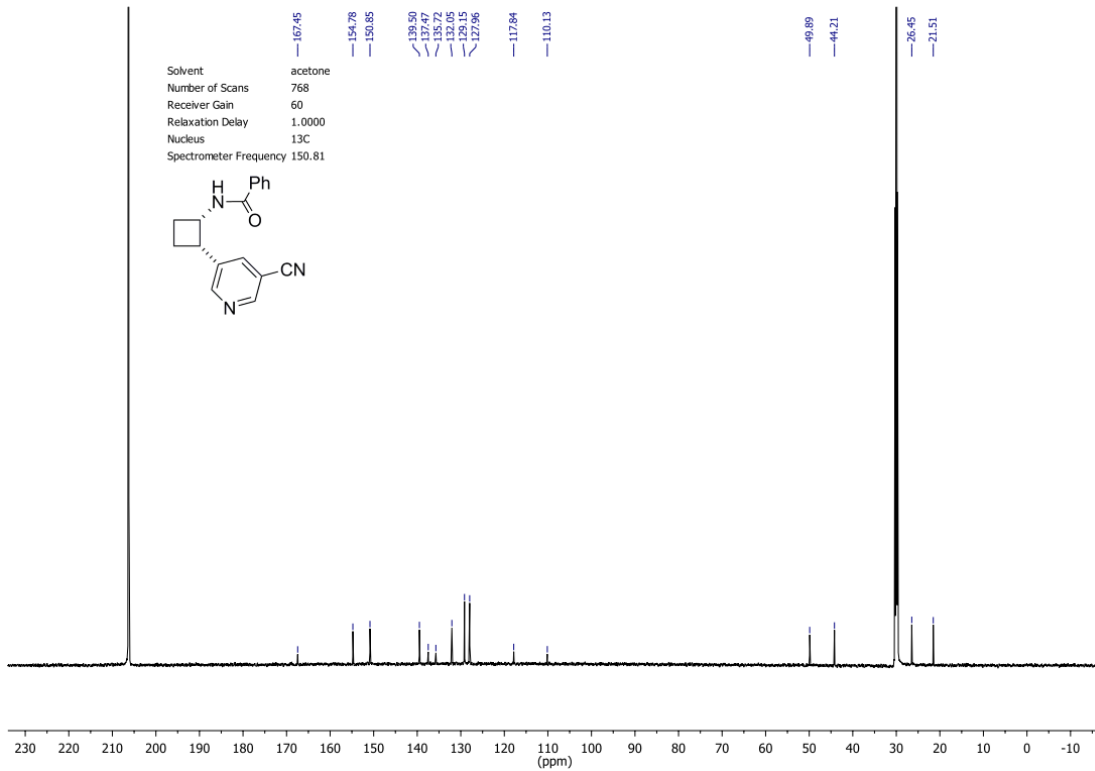


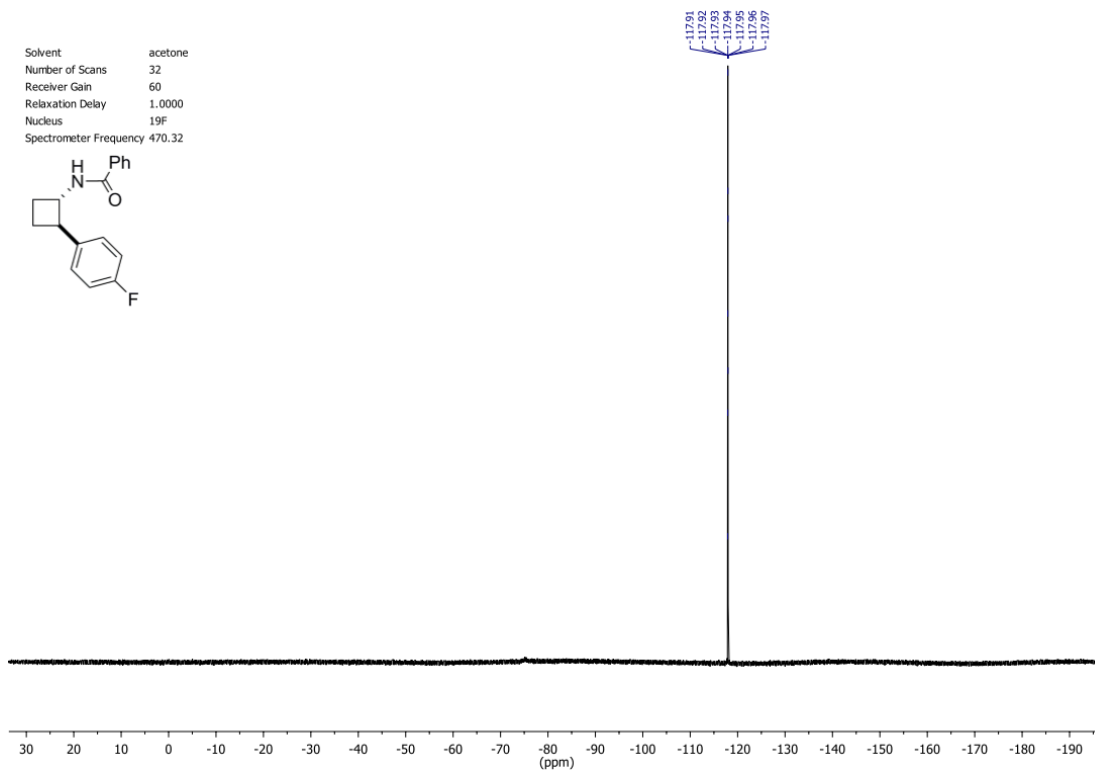
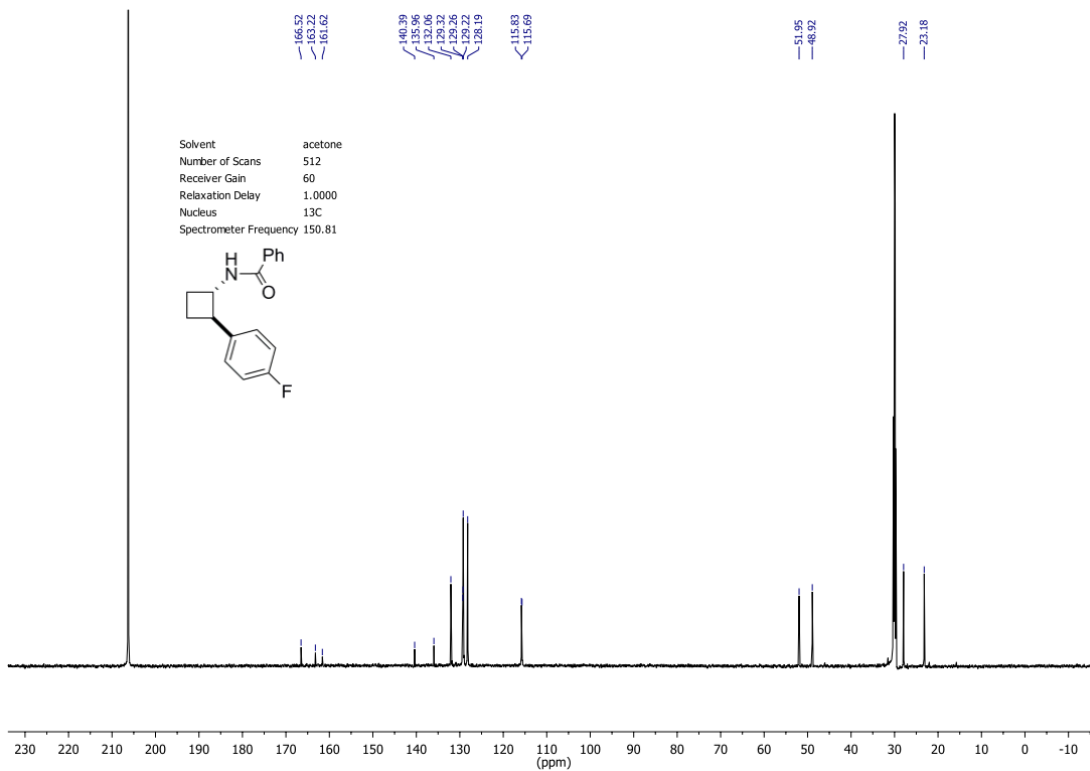
Solvent acetone
Number of Scans 8
Receiver Gain 38
Relaxation Delay 1.0000
Nucleus 1H
Spectrometer Frequency 599.69





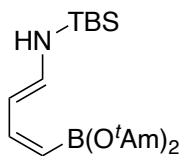






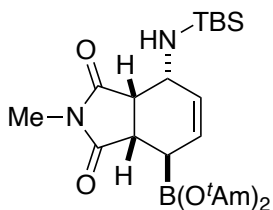
1.6.4 Experimental Procedures of Chapter 1.4

1.6.4.1 Procedure and Characterization for New Compounds



1.45

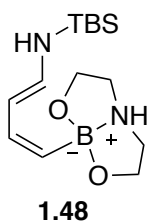
In N₂ glovebox, to a solution of Dewar 1,2-azaborine **1.34** (279.3 mg, 1.0 mmol) in CH₂Cl₂ (10.0 mL) was added *tert*-amyl alcohol (88.2 mg, 1.0 mmol). The solution was allowed to stir at 22 °C for 10 minutes. Volatiles were completely removed *in vacuo* under N₂ to afford the diene product **1.45** as a brown color oil (349.0 mg, 95%). Stereochemistry is confirmed by 2D Cosy and NOESY NMR collectively. ¹H NMR (CD₂Cl₂, 500 MHz) δ 6.52 (dd, 1H, *J* = 13.8, 10.9 Hz), 6.27 (t, 1H, *J* = 13.5 Hz), 6.18 (m, 1H), 4.86 (d, 1H, *J* = 13.8 Hz), 3.52 (d, 1H, *J* = 14.2 Hz), 1.65 (q, 4H, *J* = 7.5 Hz), 1.30 (s, 12H), 0.92–0.85 (m, 15H), 0.12 (s, 6H); ¹¹B NMR (CD₂Cl₂, 160 MHz) δ 25.1.



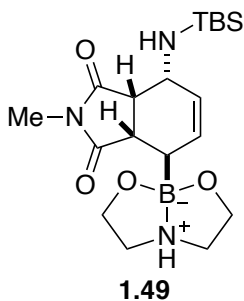
1.46

In N₂ glovebox, to a solution of diene **1.45** (73.5 mg, 0.20 mmol) in dioxane (2.0 mL) was added *N*-methylmaleimide (36.7 mg, 0.24 mmol). The solution was sealed in a 10 mL pressure vessel and allowed to stir at 100°C for 1.5 hours. After 1.5 hours, the reaction was cooled down to RT and the volatiles were completely removed *in vacuo*. Tetrachloroethane (8.5 μL, 0.08 mmol) was added as internal standard before NMR was

taken in CD₂Cl₂. (Based on the integration of ¹H NMR, the yield was calculated to be 80%)
Endo-product was exclusively formed based on 2D-NOESY NMR. ¹H NMR (CD₂Cl₂, 600 MHz) δ 5.74 (t, 1H, *J* = 10.3 Hz), 5.66 (dd, 1H, *J* = 9.7, 2.7 Hz), 3.88 (ddd, 1H, *J* = 12.7, 6.5, 3.1 Hz), 3.28 (dd, 1H, *J* = 7.8, 3.1 Hz), 3.13 (t, 1H, *J* = 7.7 Hz), 2.91 (s, 3H), 2.43 (d, 1H, *J* = 7.8 Hz), 2.13 (d, 1H, *J* = 12.7 Hz), 1.62 (q, 4H, *J* = 7.2, 5.0 Hz), 1.31 (s, 12H), 0.95–0.81 (m, 15H), 0.04 (s, 6H); ¹¹B NMR (CD₂Cl₂, 160 MHz) δ 29.4.

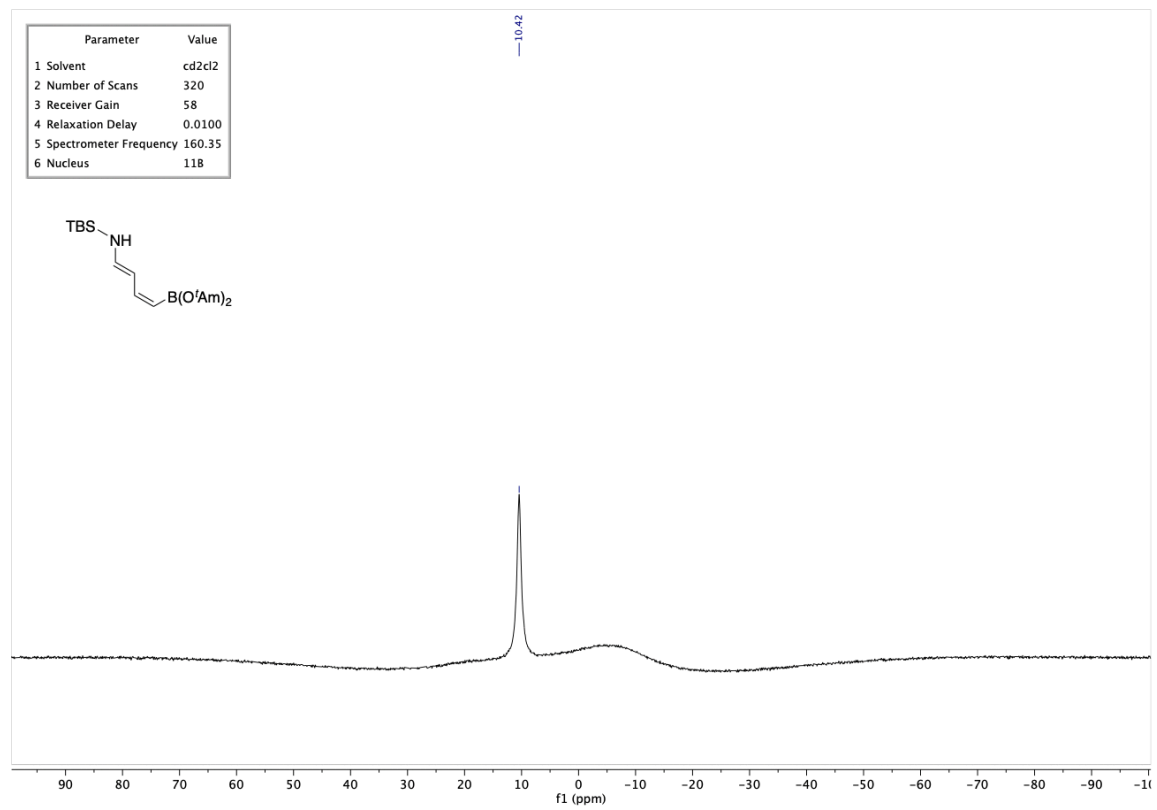
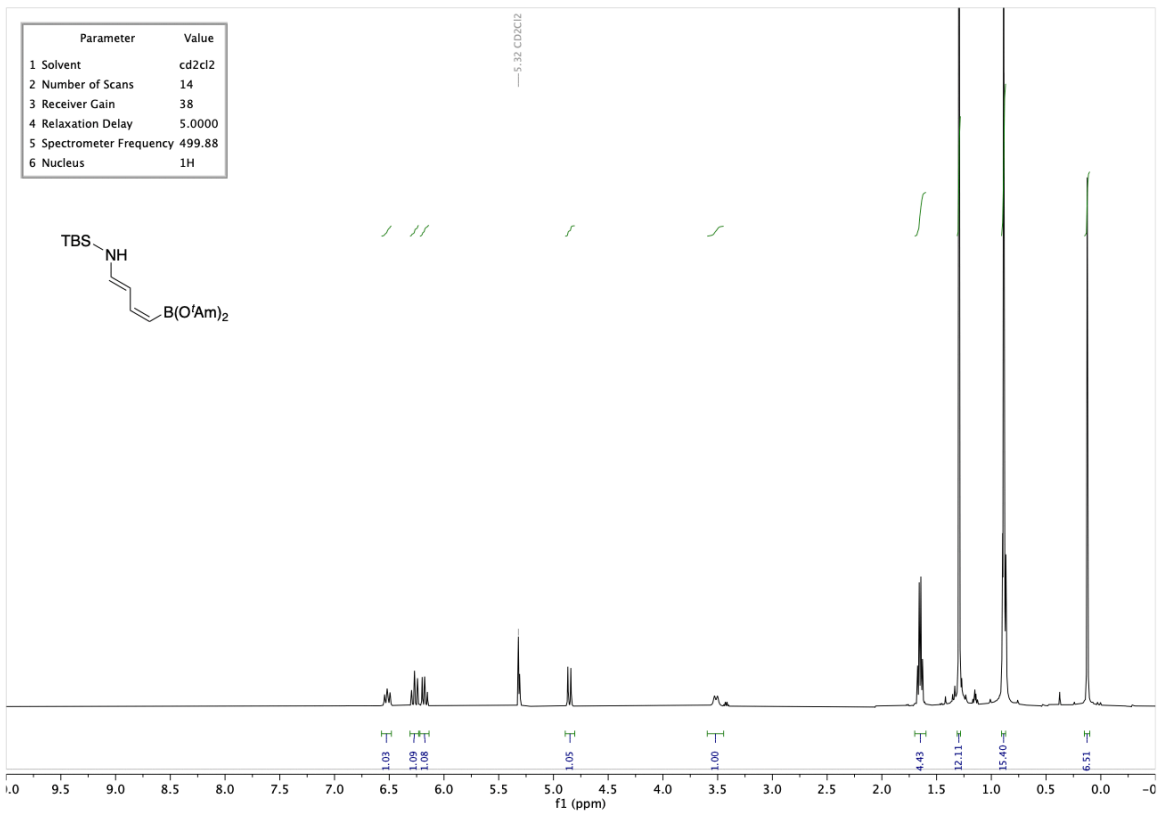


In N₂ glovebox, to a solution of Dewar 1,2-azaborine **1.47** (560.0 mg, 2.5 mmol) in diethyl ether (10.0 mL) was added diethanolamine (262.8 mg, 2.5 mmol). The solution was allowed to stir at 22 °C for 15 minutes. White solid was formed and crashed out of solution. The solid product **1.48** was isolated via filtration as a white powder (525.4 mg, 71%). ¹H NMR (CD₂Cl₂, 500 MHz) δ 6.34 (t, 1H, *J* = 12.4 Hz), 6.12 (t, 1H, *J* = 13.5 Hz), 5.93 (t, 1H, *J* = 12.9 Hz), 4.80 (d, 1H, *J* = 13.6 Hz), 4.14 (br s, 1H), 3.98–3.76 (br m, 4H), 3.42 (d, 1H), 3.36–2.61 (br m, 4H), 0.89(s, 9H), 0.10 (s, 6H); ¹³C NMR (CD₂Cl₂, 126 MHz) δ 139.4, 137.7, 106.6, 62.9, 51.5, 25.7, 17.9, 5.7; ¹¹B NMR (CD₂Cl₂, 160 MHz) δ 10.4.



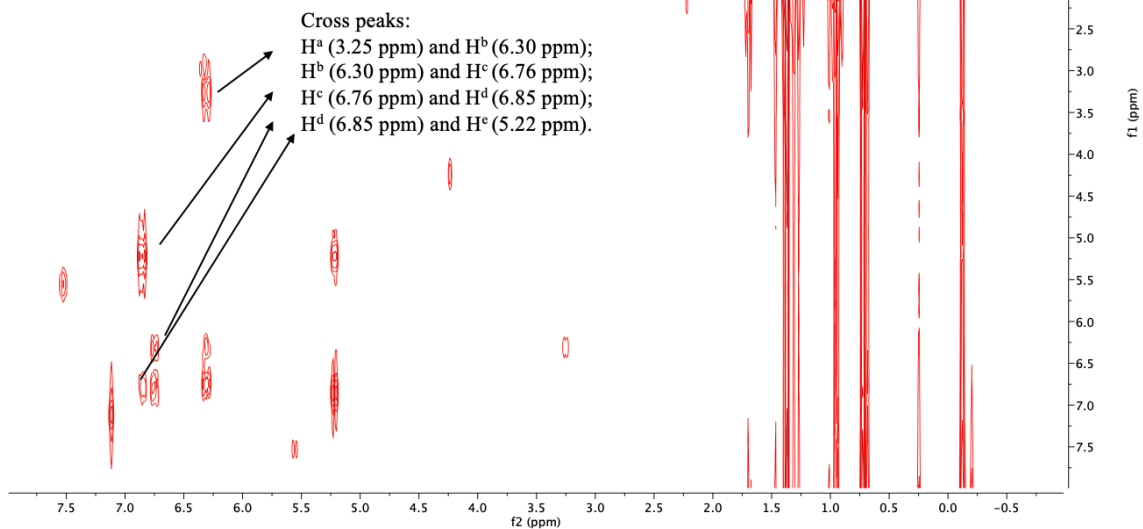
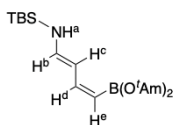
In N₂ glovebox, to a 20 mL vial was added diene **1.48** (148.2 mg, 0.50 mmol) and CH₂Cl₂ (5.0 mL). *N*-methylmaleimide (66.8 mg, 1.2 mmol) was added into the mixture. The solution was allowed to stir at RT for 1.5 hours. After 1.5 hours, the volatiles were completely removed *in vacuo*. The residue was triturated by diethyl ether and the solid product **1.49** was isolated via filtration as a white solid. (111.9 mg, 55%) ¹H NMR (CD₂Cl₂, 500 MHz) δ 6.83 (br s, 1H), 6.11 (ddd, 1H, *J* = 9.5, 6.2, 3.4 Hz), 5.90 (dd, 1H, *J* = 9.5, 2.8 Hz), 3.97 (m, 2H), 3.92–3.75 (m, 3H), 3.41 (m, 1H), 3.09 (m, 2H), 2.95 (m, 1H), 2.91 (s, 3H), 2.86 (m, 2H), 1.55 (d, 1H, *J* = 8.0 Hz), 0.81 (s, 9H), 0.63 (d, 1H, *J* = 12.2 Hz), 0.00 (s, 3H), -0.09 (s, 3H); ¹¹B NMR (CD₂Cl₂, 160 MHz) δ 11.6.

1.6.4.1 Analytic Data

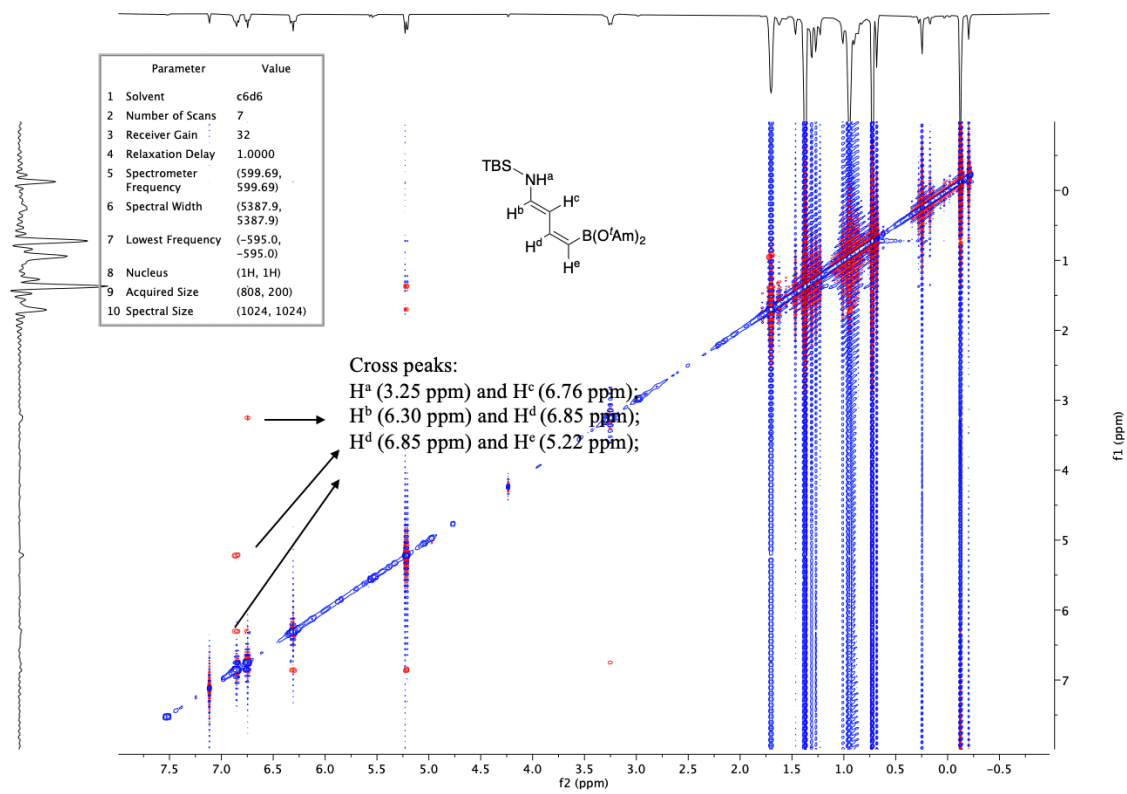


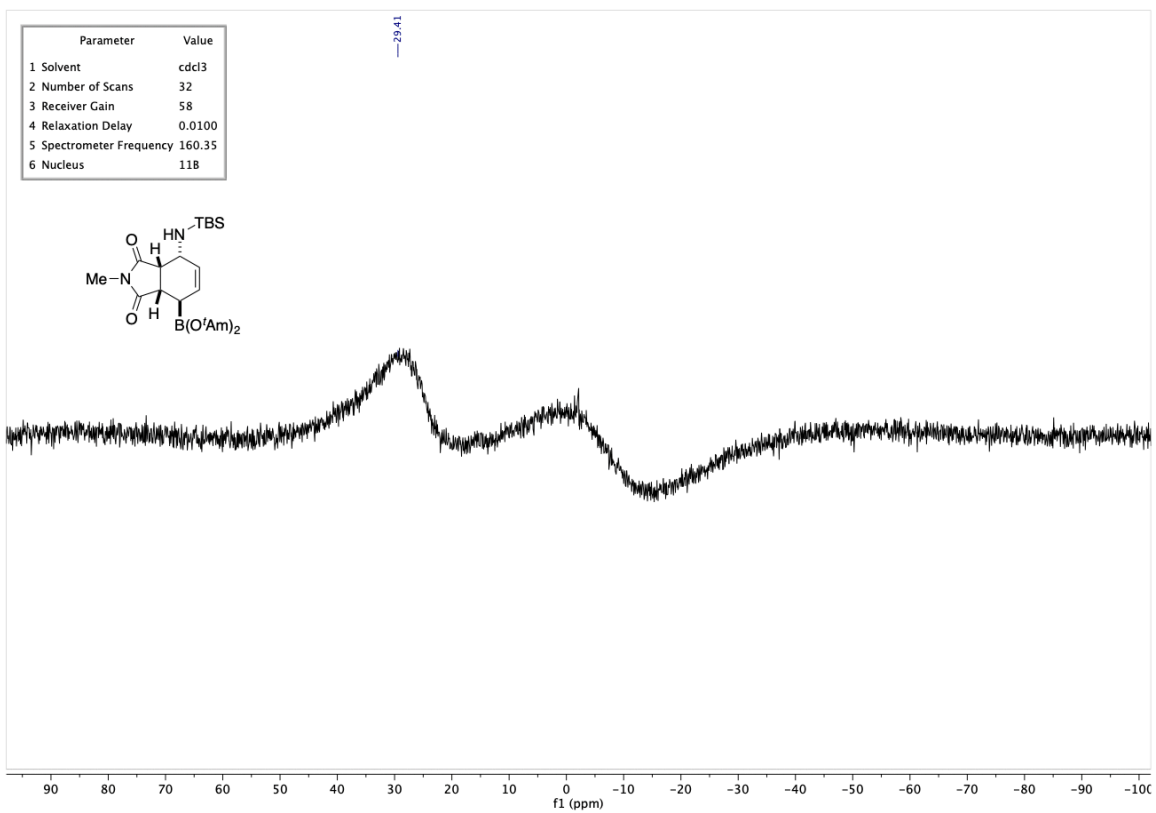
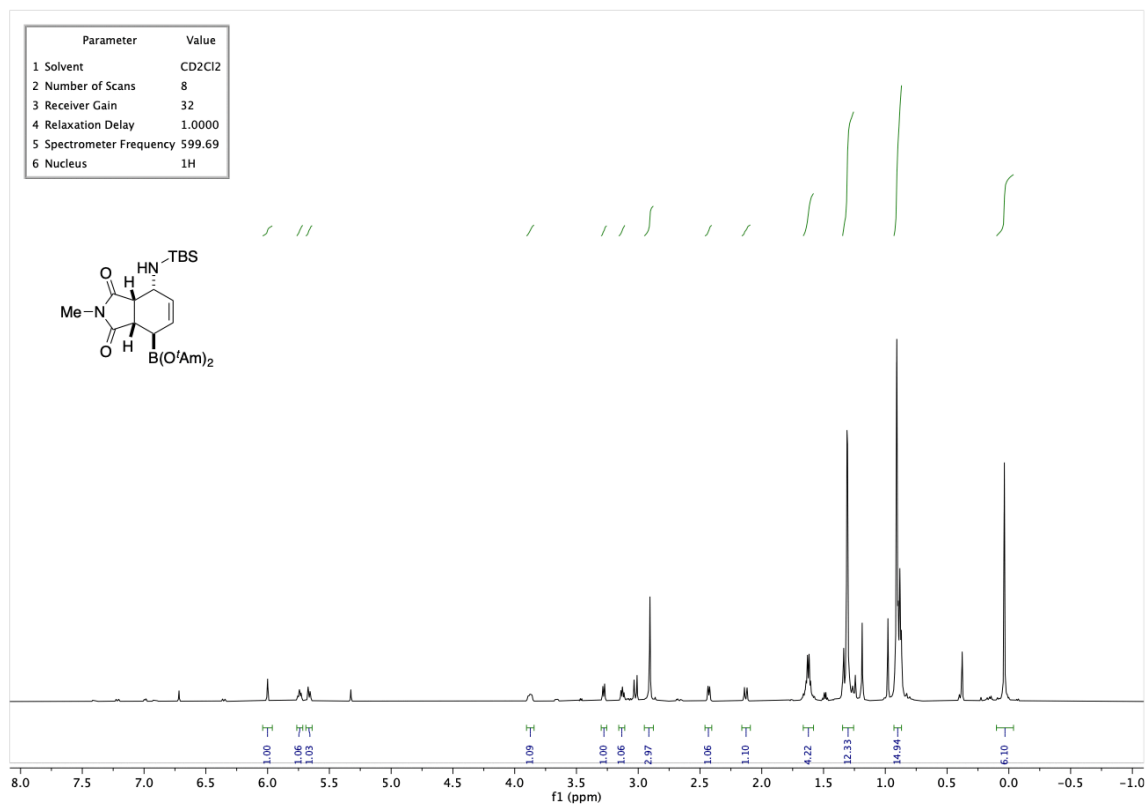
2D Cosy of Compound 1.45

Parameter	Value
1 Solvent	c6d6
2 Number of Scans	16
3 Receiver Gain	32
4 Relaxation Delay	1.0000
5 Spectrometer Frequency (599.69, 599.69)	
6 Spectral Width (5387.9, 5387.9)	
7 Lowest Frequency (-595.0, -595.0)	
8 Nucleus (1H, 1H)	
9 Acquired Size (808, 128)	
10 Spectral Size (1024, 1024)	

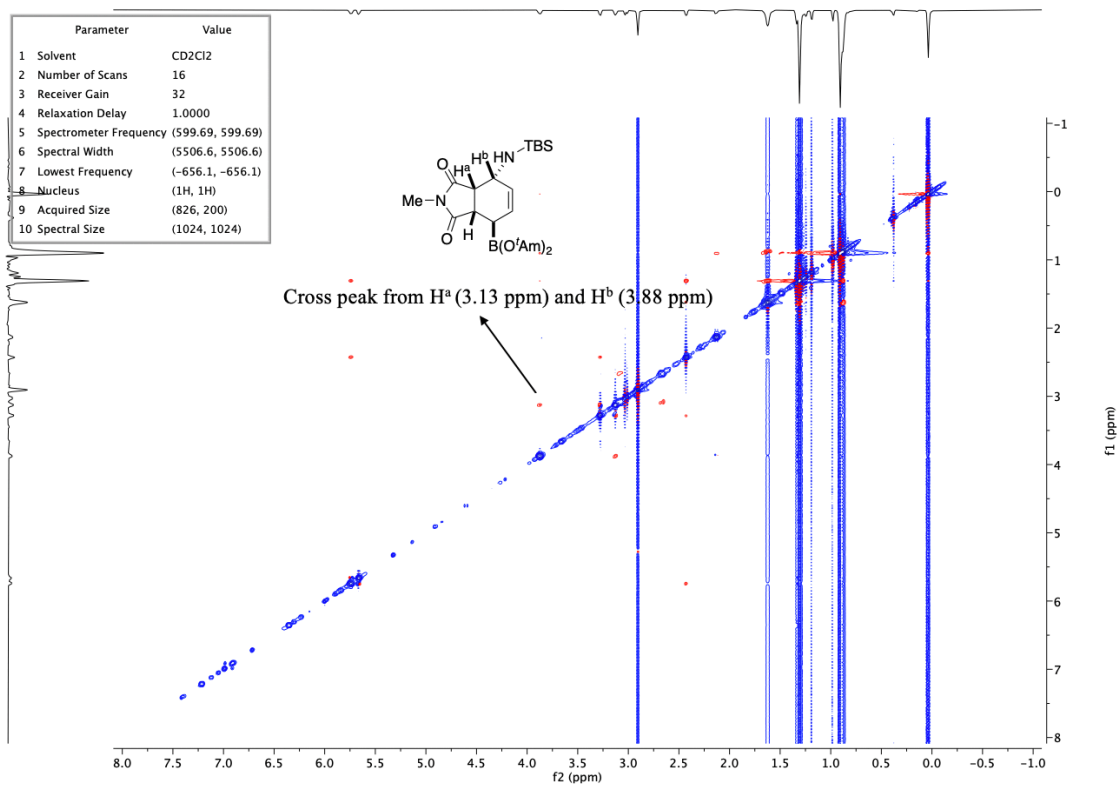


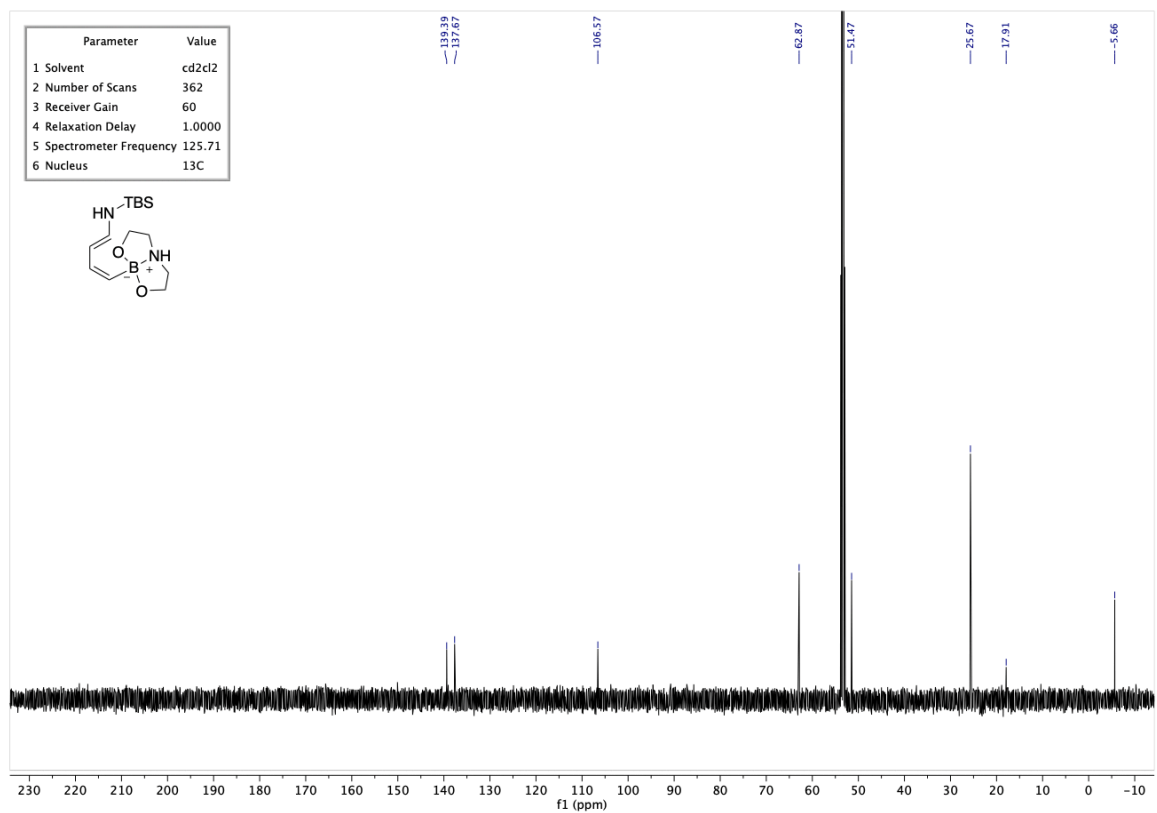
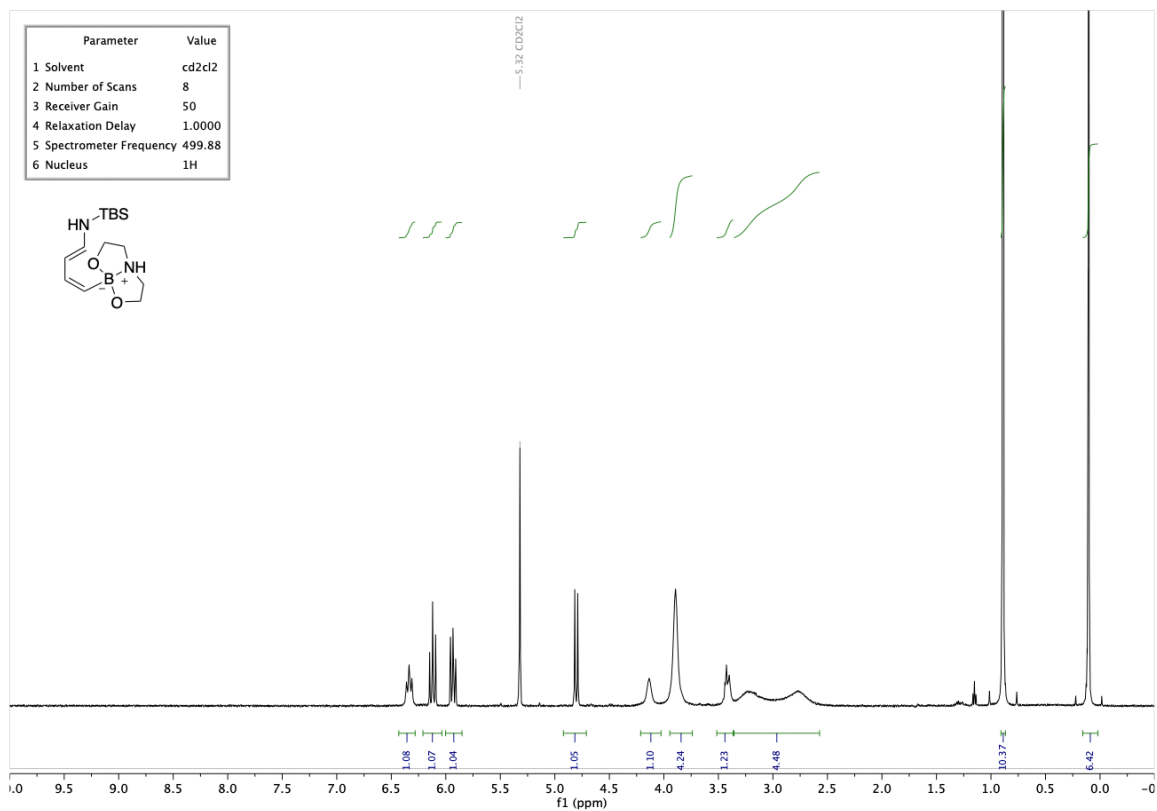
2D NOESY of Compound 1.45

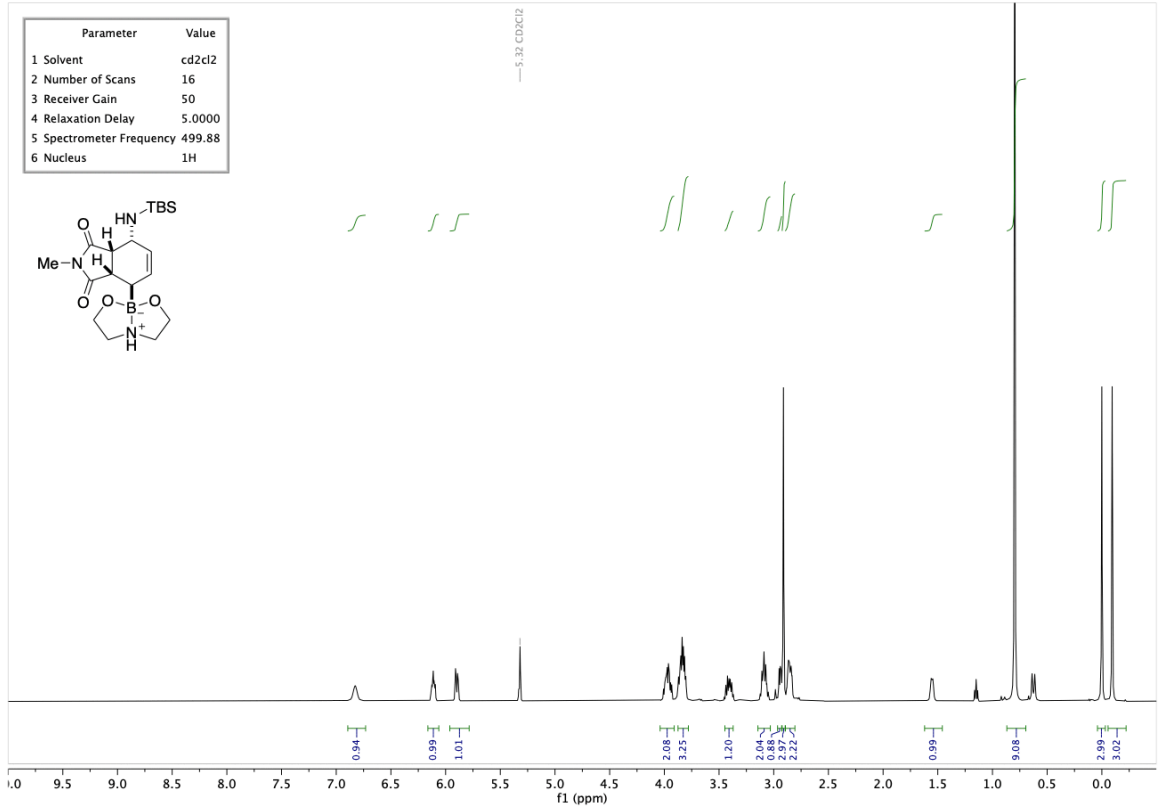
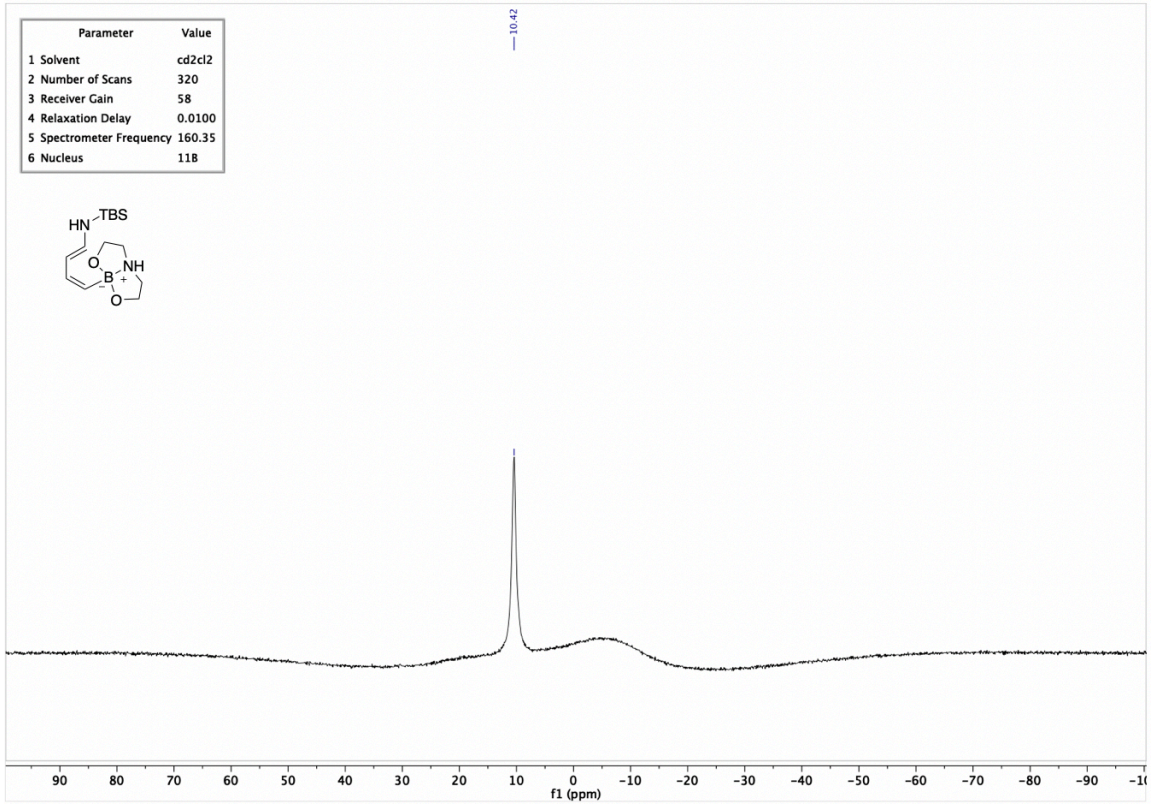


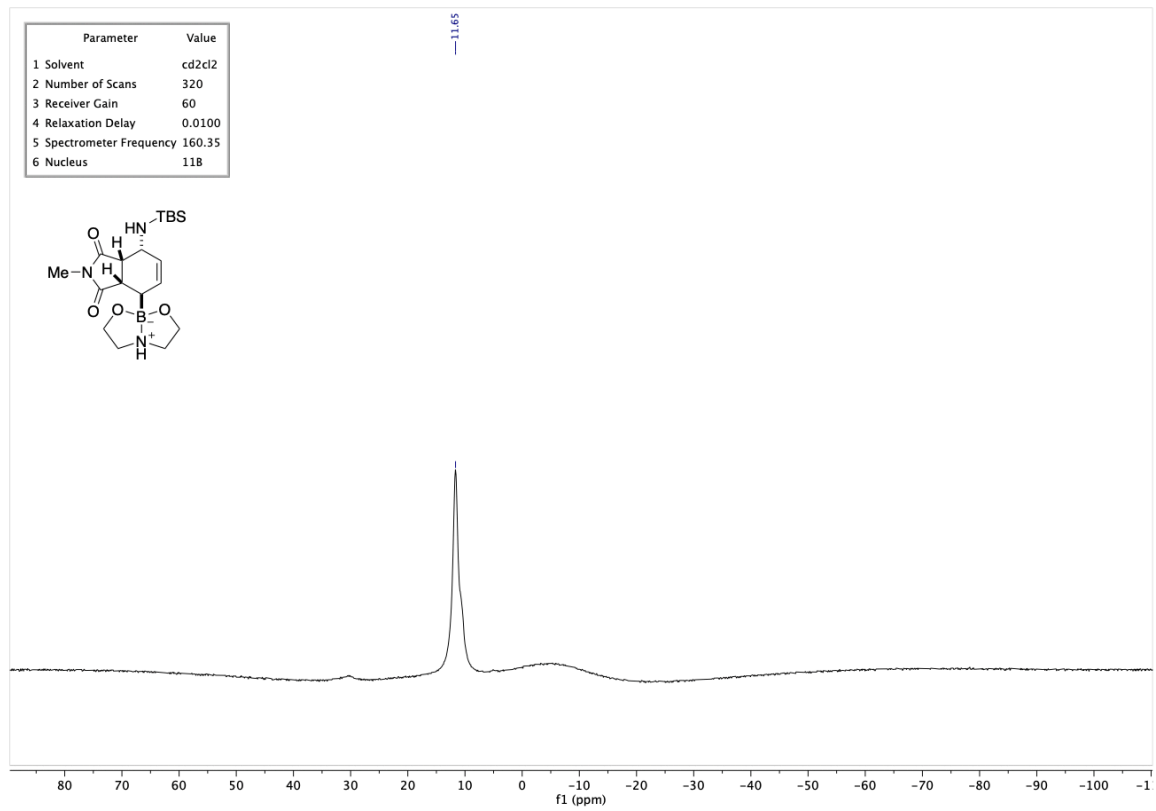


2D NOESY of Compound 1.46









Chapter 2

A Modular and Stereoselective Approach to Furnish β -Amino Cyclobutanols

2.1 Introduction

2.1.1 Chapter Overview

The main focus of this chapter is to introduce a modular and stereoselective approach to access β -amino cyclobutanols. Cyclic β -amino alcohols are important building blocks for the synthesis of biologically active molecules⁹⁰ and chiral catalysts,⁹¹ as showcased by those well-documented 5-membered and 6-membered homologues (Figure 2.1).⁹² Comparatively, 4-membered β -amino alcohols are less explored despite of their increasing interest in target synthesis and drug discovery (Figure 2.2).⁹³

⁹⁰ For representative book chapters and reviews, see: a) Senanayake, C. H.; Jacobsen, E. N. *Process Chemistry in the Pharmaceutical Industry*; Gadamasetti, K. G., Ed.; Marcel Dekker: New York, New York, 1999, Chapter 18, p327. b) Gallou, I.; Senanayake, C. H. *Chem. Rev.* **2006**, *106*, 2843–2874. c) Rouf, A.; Gupta, P.; Aga, M. A.; Kumar, B.; Parshad, R.; Taneja, S. C. *Tetrahedron: Asymmetry*. **2011**, *22*, 2134–2143. d) Chang, Y.; Zhang, J.; Yang, X.; Li, J.; Gao, L.; Huang S.; Guo, X.; Zhang, C.; Chang H.; Xu J. *Biotechnol. Lett.* **2020**, *42*, 1501–1511.

⁹¹ For representative reviews, see: a) Ager, D. J.; Prakash, I.; Schaad, D. R. *Chem. Rev.* **1996**, *96*, 835–875. b) Pu, L.; Yu, H.-B. *Chem. Rev.* **2001**, *101*, 757–824

⁹² For selected examples of bioactive molecules containing 5-membered and 6-membered chiral cyclic β -amino alcohols. see: a) Trivedi, B. K.; Padia, J. K.; Holmes, A.; Rose, S.; Wright, D. S.; Hinton, J.P.; Pritchard, M. C.; Eden, J. M.; Kneen, C.; Webdale, L.; Suman-Chauhan, N.; Boden, P.; Singh, L.; Field, M. J.; Hill, D. *J. Med. Chem.* **1998**, *41*, 38–45. b) Tsuji, Y.; Dobrev, D. *Vascular Health and Risk Management*. **2013**, *9*, 165–175. c) Dorsey, B. D.; McDonough, C.; McDaniel, S. L.; Levin, R. B.; Newton, C. L.; Hoffman, J. M.; Darke, P. L.; Zugay-Murphy, J. A.; Emini, E. A.; Schleif, W. A.; Olsen, D. B.; Stahlhut, M. W.; Rutkowski, C.A.; Kuo, L. C.; Lin, J.H.; Chen, I-W.; Michelson, S. R.; Holloway, M. K.; Huff, R.; Vacca, J. P. *J. Med. Chem.* **2000**, *43*, 3386–3399. d) Gross, M. F.; Beaudoin, S.; McNaughton-Smith, G.; Amato, G. S.; Castle, N. A.; Huan, C.; Zou, A.; Yu, W. *Bioorg. Med. Chem. Lett.* **2007**, *17*, 2849–2853. e) Liu, B.; Croy, C. H.; Hitchcock, S. A.; Allen, J. R.; Rao, Z.; Evans, D.; Bures, M. G.; Mckinzie, D. L.; Watt, M. L.; Gregory, G. S.; Hansen, M. M.; Hoogestraat, P. J.; Jamison, J. A.; Okha-Mokube, F. M.; Stratford, R. E.; Turner, W.; Bymaster, F.; Felder C. C. *Bioorg. Med. Chem. Lett.* **2015**, *25*, 4158–4163.

For selected examples of catalysts containing chiral cyclic β -amino alcohols. see: f) de Parrodi, C. A.; Juaristi, E. *Synlett.* **2006**, *17*, 2699–2715.

⁹³ a) Zhou, Q.; Snider, B. B. *Org. Lett.* **2011**, *13*, 526–529. b) Adlington, R. M.; Baldwin, J. E.; Jones, R. H.; Murphy J. A.; Parisi, M. F. *J. Chem. Soc. Chem. Commun.* **1983**, 1479–1481. c) Miller, D. D.; Hsu, F.-L.; Salman, K. N.; Patil, P. N. *J. Med. Chem.* **1976**, *19*, 180–184. d) Mohammad, T. S. H.; Reidl, C. T.; Zeller, M.; Becker, D. P. *Tetrahedron Lett.* **2020**, *61*, 151632.

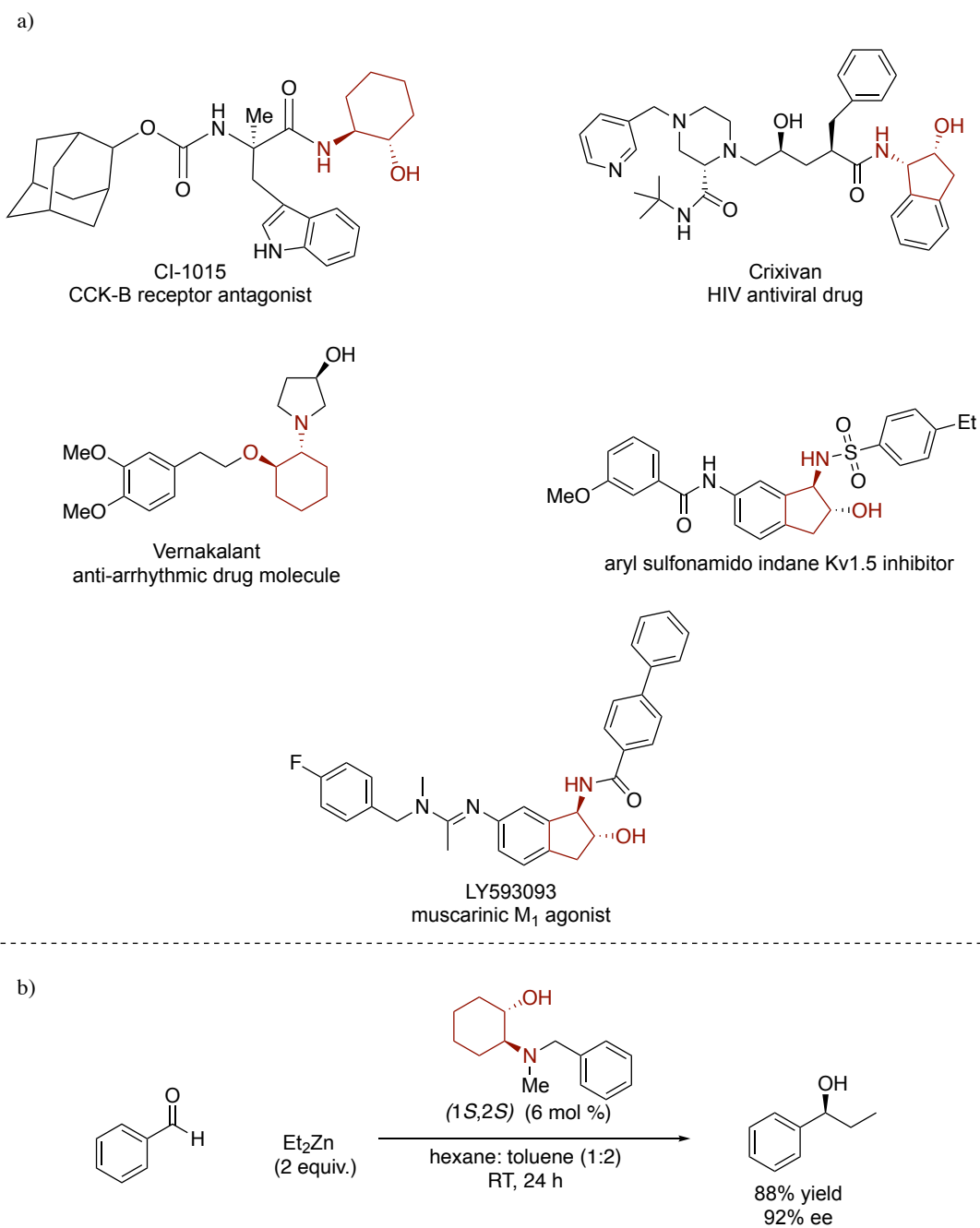


Figure 2.1. Well-documented examples of bioactive molecules (a) and chiral catalysts

(b) containing 5-membered and 6-membered cyclic β -amino alcohols

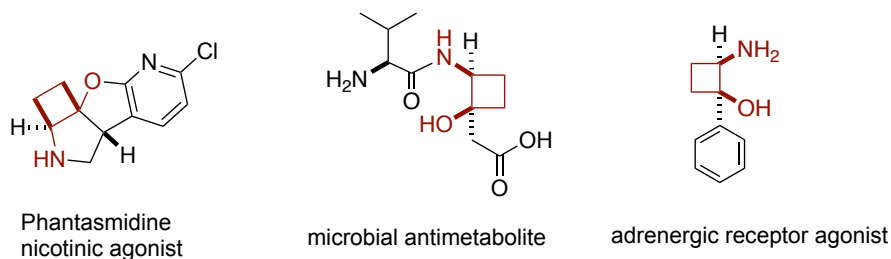


Figure 2.2. Examples of bioactive molecules containing 4-membered β -amino alcohols

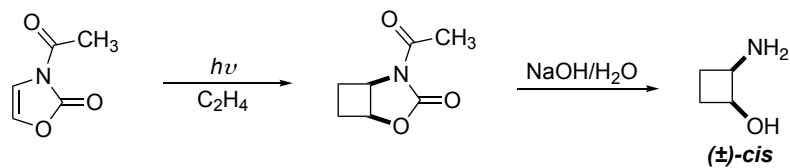
The development of cyclobutane β -amino alcohols in drug discovery and catalyst design is arguably limited by the lack of general and versatile preparative routes, especially those with effective stereocontrol. To make the parent *cis* cyclobutane β -amino alcohol, [2+2] photocycloaddition between 3-acetyloxazol-2(3*H*)-one and ethylene, reported by Hartmann and Heine in 1980, serves as an effective strategy (Scheme 2.1a).⁹⁴ Although straightforward, the scalability of such strategy could be doubtful. When Cannon and his team tried to apply this strategy to prepare sizeable quantities of *cis* cyclobutane β -amino alcohol as their target precursor, all of their attempts were unsuccessful.⁹⁵ Thus, an alternative strategy was pursued involving a multi-step sequence to produce the *cis* cyclobutane β -amino alcohol in adequate amount (Scheme 2.1b). In 1998, Bisel and Frahm reported the enantioselective synthesis of *cis* cyclobutane β -amino alcohol (Scheme 2.1c).⁹⁶ Their approach features an asymmetric reductive amination using (*R*)-(+)- and (*S*)-(-)-1-phenyl-ethylamine (PEA) as chiral auxiliaries (both enantiomers are available but only the sequence with the (*S*)-ligand is shown in Scheme 2.1c for simplicity).

⁹⁴ Hartmann, W.; Scholz, K.-H.; Heine, H. G. *Chem. Ber.* **1980**, *113*, 1884–1889.

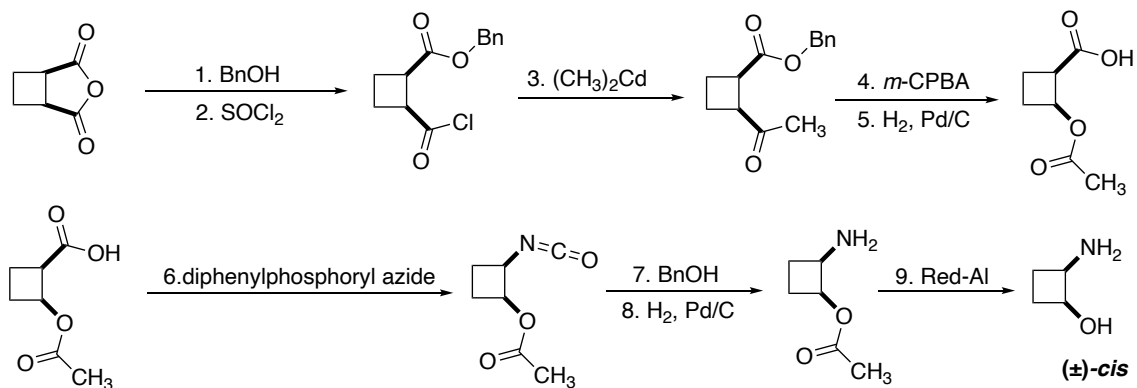
⁹⁵ Cannon, J. G.; Crockatt, D. M.; Long, J. P.; Maixner W. *J. Med. Chem.* **1982**, *25*, 1091–1094.

⁹⁶ Bisel, P.; Breitling, E.; Frahm, A. W. *Eur. J. Org. Chem.* **1998**, 729–733.

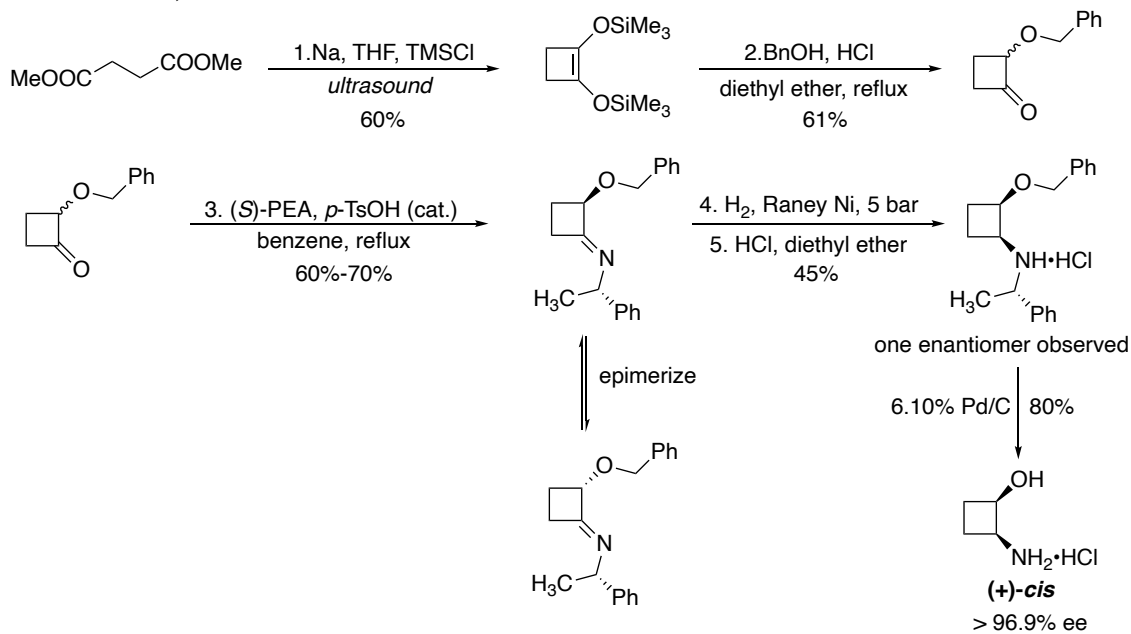
a. Hartmann and Heine, 1980



b. Cannon and Crockatt, 1982



c. Bisel and Frahm, 1998



Scheme 2.1. Reported strategies of stereoselective synthesis of *cis* cyclobutane β -amino alcohol

In summary, only limited methods are reported so far to access cyclobutane β -amino alcohols with *cis* stereoselectivity, which in a sense explains the relatively high price of parent *cis* cyclobutane β -amino alcohol from commercial sources.⁹⁷

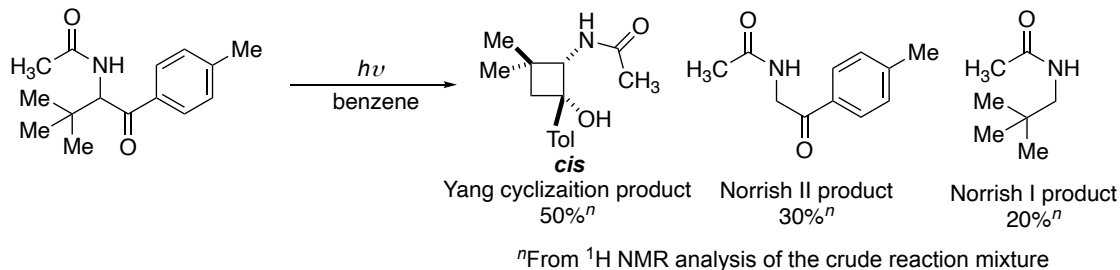
Beside the scarcity of methods to access the parent *cis* cyclobutane β -amino alcohol, there are also limited methods to generate poly-substituted analogues. In 2002, the Griesbeck group reported a photocyclization strategy from the α -amido alkyl-aryl ketones. Although the *cis* stereoselectivity could be achieved, the distribution of different Norrish/Yang type products as well as the reaction efficiency were at the mercy of different starting materials used (Scheme 2.2a).⁹⁸ More recently, Boddaert and Aitken applied [2+2] photo-cycloaddition/Hofmann rearrangement strategy to access 2-aminocyclobutane-1-carboxylic acid with all-*cis* geometry (Scheme 2.2b).⁹⁹ Notably, a bulky *tert*-butoxyl substituted olefin was required in order to achieve a moderate stereoselectivity. Furthermore, similar to other [2+2] photo-cycloadditions, specific substrates need to be employed, which would result in specific substituents and functionalities on the cyclobutane ring.

⁹⁷ Market price from the commercial vendor Enamine: 857 USD/g for parent amino alcohol and 831 USD/g for HCl salt. (Price can be varied over time)

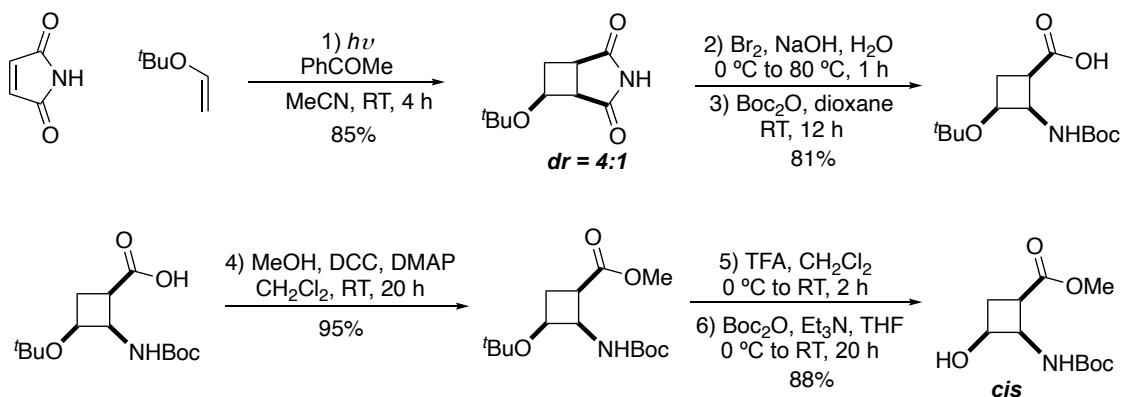
⁹⁸ Griesbeck, A. G.; Heckroth, H. *J. Am. Chem. Soc.* **2002**, *124*, 396–403.

⁹⁹ a) Chang, Z.; Boyaud, F.; Guillot, R.; Boddaert, T.; Aitken, D. J. *J. Org. Chem.* **2018**, *83*, 527–534. b) Chang, Z.; Guillot, R.; Boddaert, T.; Aitken, D. J. *J. Org. Chem.* **2019**, *84*, 10518–10525.

a. Photocyclization of α -amido alkylaryl ketones: *Griesbeck, 2002*



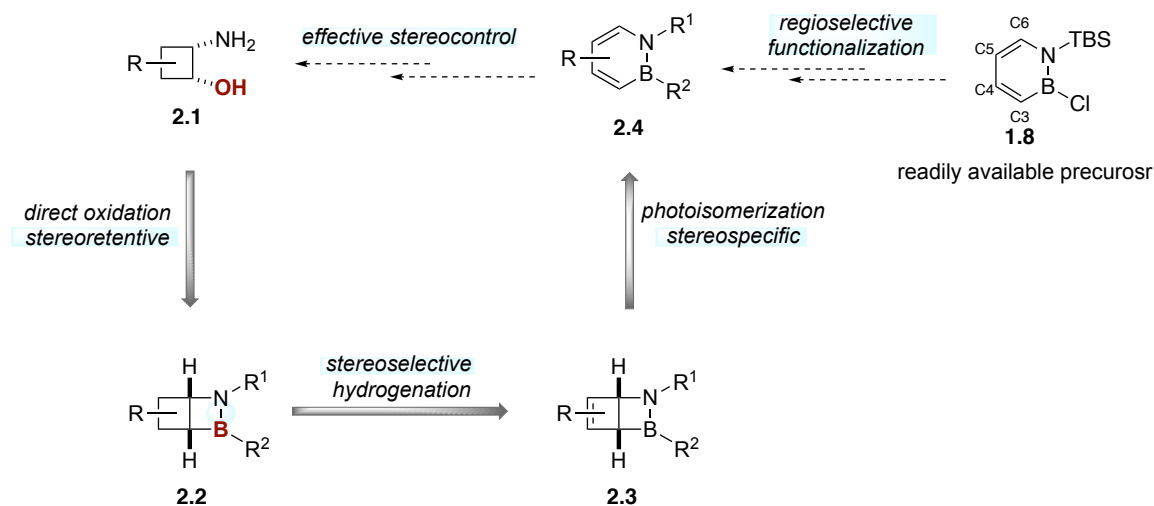
b. [2+2] Photo-cycloaddition approach: *Boddaert and Aitken, 2019*



Scheme 2.2. Stereoselective synthesis of poly-substituted *cis* cyclobutane β -amino alcohols

To enable new explorations of cyclobutane β -amino alcohols in drug discovery, we aimed to develop a more general and versatile approach to access diversified cyclobutane β -amino alcohols stereoselectively. As illustrated in Scheme 2.3, we hypothesized that the cyclobutane β -amino alcohol **2.1** could be furnished stereoretentively from the direct oxidation of the hydrogenated 1,2-azaborine-derived intermediates **2.2** bearing boron functionality. If hydrogenation of the 1,2-azaborine Dewar species **2.3** could also be achieved in a highly stereoselective fashion, then combined with the stereospecific photoisomerization of the 1,2-azaborine core **2.4**, we could establish a tandem sequence to access the cyclobutane β -amino alcohols with effective stereo-control.

More intriguingly, we envisioned that the 1,2-azaborine core could be functionalized regioselectively from the readily available precursor **1.8**, and if those functionalities could be translated onto the cyclobutane ring, that would allow us to selectively install various substituents on different positions over the ring, furnishing diverse poly-substituted cyclobutane β -amino alcohols that are not easily accessible by previously reported methods.



Scheme 2.3. Proposed access to cyclobutane β -amino alcohols via a modular and stereoselective approach

We reasoned that several key questions need to be addressed in order to achieve this modular and stereoselective approach: firstly, what substituents on boron and nitrogen should be installed for the regioselective functionalizations that are also suitable for the photoisomerization step; secondly, it was uncertain whether the functionalities we introduced on different positions of the azaborine core **2.4** could be translated onto Dewar **2.3** under photoisomerization conditions; thirdly, how do we achieve effective and stereoselective hydrogenations of Dewar alkenes (especially those sterically hindered ones); lastly, it was unclear whether the hydrogenation intermediate **2.2** could be oxidized

directly to furnish the final cyclobutane β -amino alcohols. The discussion in section 2.2 will be primarily focused on how we address those challenges in each individual step shown in Scheme 2.3.

2.1.2 Regioselective Functionalization of 1,2-Azaborines

The uniqueness of 1,2-azaborines lies in their stunning synthetic versatility as a result of the electronic desymmetrization of the heterocyclic ring, providing several modes of highly selective functionalization not accessible to their all-carbon homologues.¹⁰⁰ The alteration of the electron density throughout the aromatic π system was corroborated by computational studies,^{13a} as demonstrated by the electrostatic potential surface map of the parent 1,2-azaborine **1.13** (Figure 2.3). Capitalizing on their distinct electronic properties, our group recently developed diverse approaches to regioselectively functionalize 1,2-azaborines from the versatile 1,2-azaborine core **1.8** (Figure 2.3).¹⁰¹

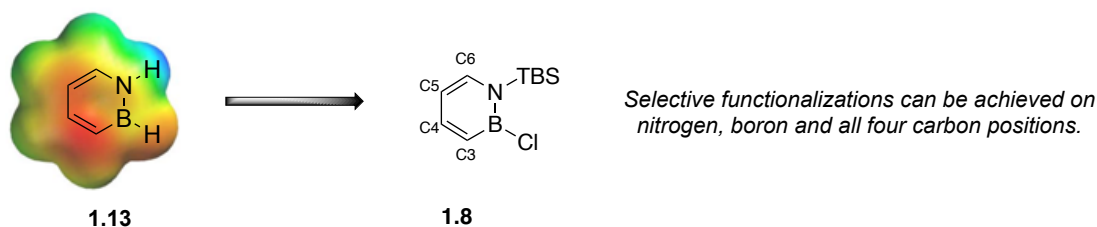


Figure 2.3. Electrostatic potential surface map of the parent 1,2-azaborine **1.13** and regioselective functionalization of **1.8**

N-TBS-*B*-Cl 1,2-azaborine **1.8** has emerged as a foundational building block for 1,2-azaborine derivatizations. One major advantage is that both chloride on boron and TBS

¹⁰⁰ Bhattacharjee, A.; Davies, G. H.; Saeednia, B.; Molander, G. A. *Adv. Synth. Catal.* **2020**, *363*, 1–19.

¹⁰¹ For a recent review, see: McConnell, C. R.; Liu, S.-Y. *Chem. Soc. Rev.* **2019**, *48*, 3436–3453.

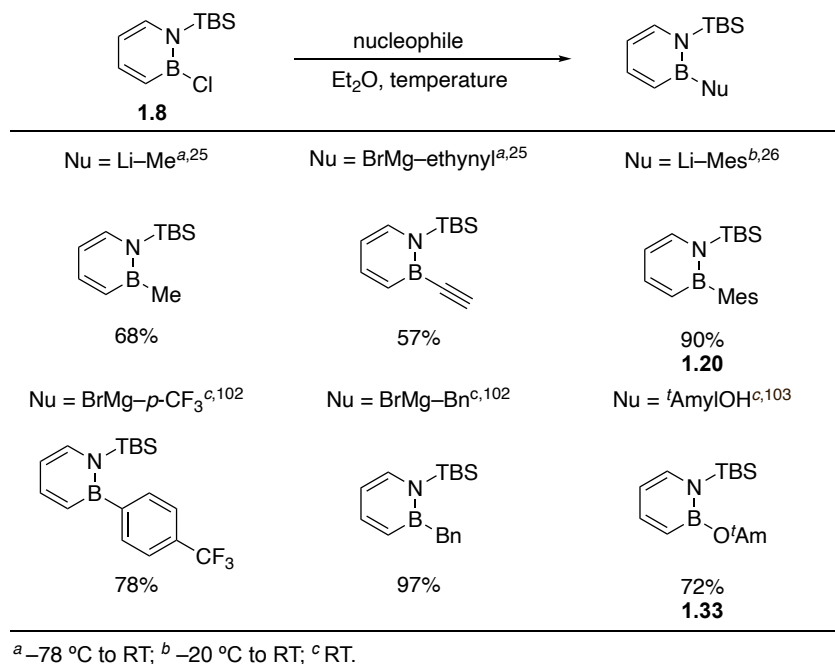
protecting group on nitrogen can serve as a flexible handle for substitution reaction. Moreover, their ease of substitution proves to be beneficial to selective functionalizations since certain substituents on nitrogen and boron can be pivotal to achieve the regioselectivity (*vide infra*).

Nucleophilic substitution is expected to be the most straightforward way to functionalize the B–Cl bond in compound **1.8**. The scope of nucleophiles includes alkyl,²⁵ aryl,^{25,26} alkynyl²⁵ and benzylic¹⁰² organometallic reagents; non-anionic nucleophiles such as alcohol^{25, 103} can also engage in the substitution reaction in the presence of exogenous base like triethyl amine (Scheme 2.4). The broad scope of substituents on boron have also opened up new chemical space of 1,2-azaborines as synthon in organic synthesis, as demonstrated in the Diels-Alder reaction²⁵ and photoisomerizations.^{36,103} In addition to nucleophilic substitution of B–Cl, our group also described a Rh-catalyzed arylation of B–Cl substituted azaborines with aryl stannanes (Scheme 2.5).¹⁰⁴

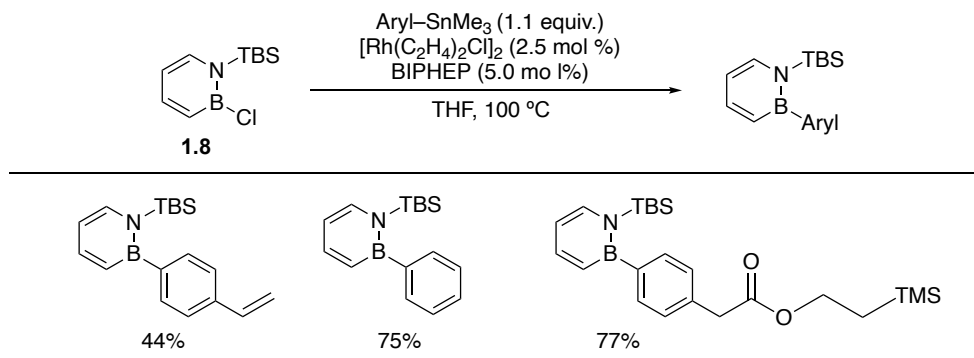
¹⁰² Baggett, A.; Liu, S.-Y. *J. Am. Chem. Soc.* **2017**, *139*, 15259–15264.

¹⁰³ Giustra, Z. X.*; Yang, X.*; Chen, M.; Bettinger, H. F.; Liu, S.-Y. *Angew. Chem. Int. Ed.* **2019**, *58*, 18918–18922.

¹⁰⁴ Rudebusch, G. E.; Zakharov, L. N.; Liu, S.-Y. *Angew. Chem. Int. Ed.* **2013**, *52*, 9316–9319.



Scheme 2.4. Nucleophilic substitution of *N*-TBS-*B*-Cl 1,2-azaborine **1.8**



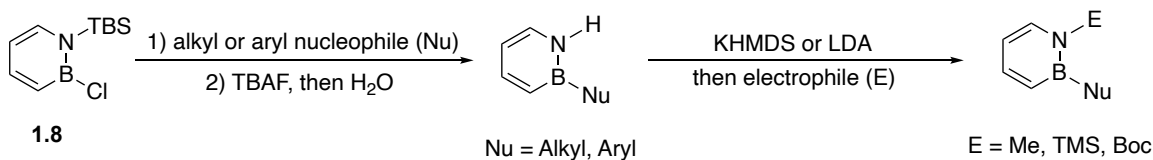
Scheme 2.5. Rh-catalyzed arylation of *B*-Cl 1,2-azaborines **1.8**

Manipulations of the substituents on nitrogen can be readily achieved after a compatible substituent on boron is introduced at first. For example, compound **1.8** could be difunctionalized in a tandem process (Scheme 2.6).^{25,26,105,106} After substitution with alkyl or aryl nucleophiles at the boron position, removal of TBS- group on nitrogen can be

¹⁰⁵ Pan, J.; Kampf, J. W.; Ashe, A. J. *Organometallics* **2004**, *23*, 5626–5629.

¹⁰⁶ Pan, J.; Kampf, J. W.; Ashe, A. J. *Organometallics* **2008**, *27*, 1345–1347.

achieved using tetrabutylammonium fluoride (TBAF). Quenching the intermediate with proton source like water affords the corresponding N–H 1,2-azaborines. The pK_a of the azaborine N–H bond has been determined to be approximately 26,¹⁰⁵ which can be deprotonated by amide bases such as LDA or KHMDS. Once deprotonated, various electrophiles such as MeI,¹⁰⁵ TMSCl,¹⁰⁶ or di-*tert*-butyldicarbonate²⁵ can be introduced to accomplish the nitrogen functionalization (Scheme 2.6).

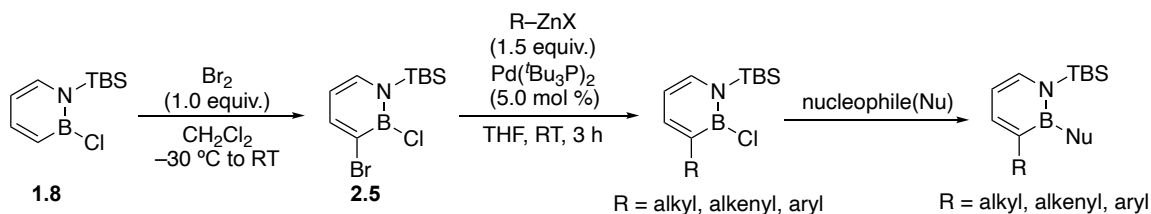


Scheme 2.6. Tandem process to achieve di-functionalization of *N*-TBS-*B*-Cl azaborine

1.8

N-TBS-*B*-Cl 1,2-azaborine **1.8** can also serve as a versatile precursor to access site-selective functionalizations of all the four carbon positions. For C3 functionalization, in 2007,¹⁰⁷ the Ashe group described the regioselective bromination of *N*-Et-*B*-Ph 1,2-azaborine at C3 position. This achievement paves the way for selective functionalization at C3 carbon via Negishi cross-coupling reported by our group (Scheme 2.7).⁷¹ Notably, the B–Cl bond in **2.5** is shown to be compatible with the Negishi cross-coupling conditions, allowing the introduction of alkyl, alkenyl and aryl substituents onto C3 position. In addition, the intact B–Cl bond is still available for subsequent nucleophilic substitutions on the boron position.

¹⁰⁷ Pan, J.; Kampf, J. W.; Ashe J. A. *Org. Lett.* **2007**, *9*, 679–681.



Scheme 2.7. Regio-selective functionalization at C3 position

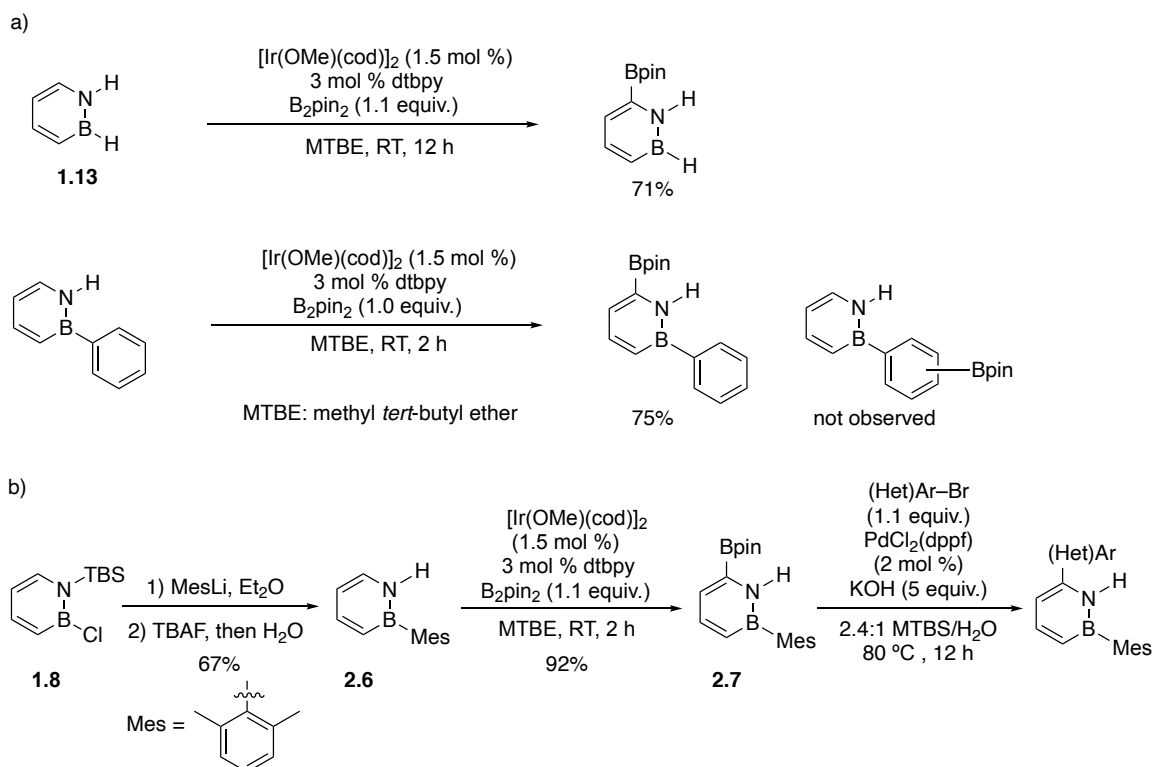
In addition to halide, boronic esters can provide another versatile handle for 1,2-azaborine derivatization at later stage.¹⁰⁸ In 2015, our group applied the iridium-catalyzed C-H borylation strategy¹⁰⁹ to 1,2-azaborines and discovered that borylation of parent 1,2-azaborine **1.13** resulted in selective formation the C6-borylated regioisomer (Scheme 2.8a).²⁶ Due to the absence of any steric influence in **1.13**, the regio-selectivity is dictated solely by electronic directing effects as such that the borylation typically occurs at the most acidic C–H bonds.¹¹⁰ Besides **1.13**, different substituents on boron are tolerated in the reaction, including aryl and alkoxide groups.²⁶ Moreover, the preference for borylating the 1,2-azaborine ring is maintained in the presence of a phenyl ring on the boron (Scheme 2.8a). Notably, from the versatile *N*-TBS-*B*-Cl 1,2-azaborine **1.8**, the precursor **2.6** could be readily prepared via the aforementioned tandem process (see Scheme 2.6, see page 157).

¹⁰⁸ Jonas Börgel and Tobias Ritter define late-stage functionalization (LSF) as follows: LSF is a desired chemoselective transformation on a complex molecule to provide at least one analog in sufficient quantity and purity for a given purpose without the necessity for installation of a functional group that exclusively serves the purpose to enable said transformation. Here to avoid misinterpretation: late-stage functionalizations of 1,2-azaborine does not belong to the category of LSF defined by Börgel and Ritter. For relevant reference, see: Börgel, J.; Ritter, T. *Chem.* **2020**, *6*, 1877–1887.

¹⁰⁹ For the reference of original catalytic conditions, see: a) Ishiyama, T.; Takagi, J.; Hartwig, J. F.; Miyaura, N. *Angew. Chem. Int. Ed.* **2002**, *41*, 3056–3058. For relevant reviews, see: b) Mkhalid, I. A.; Barnard, J. H.; Marder, T. B.; Murphy, J. M.; Hartwig, J. F. *Chem. Rev.* **2010**, *110*, 890–931. c) Hartwig, J. F. *Acc. Chem. Res.* **2012**, *45*, 864–873.

¹¹⁰ For representative examples, see: a) Vanchura, B. A.; Preshlock, S. M.; Roosen, P. C.; Kallepalli, V. A.; Staples, R. J.; Maleczka, R. E.; Singleton, D. A.; Smith, M. R., III. *Chem. Commun.* **2010**, *46*, 7724–7726. b) Tajuddin, H.; Harisson, P.; Bitterlich, B.; Collings, J. C.; Sim, N.; Batsanov, A. S.; Cheung, M. S.; Kawamorita, S.; Maxwell, A. C.; Shukla, L.; Morris, J.; Lin, Z.; Marder, T. B.; Steel, P. G. *Chem. Sci.* **2012**, *3*, 3505–3515.

With the suitable substituent on boron, the C6-borylated 1,2-azaborine **2.7** could then engage in Suzuki cross-coupling reactions with various aryl and hetero-aryl bromides (Scheme 2.8b).²⁶

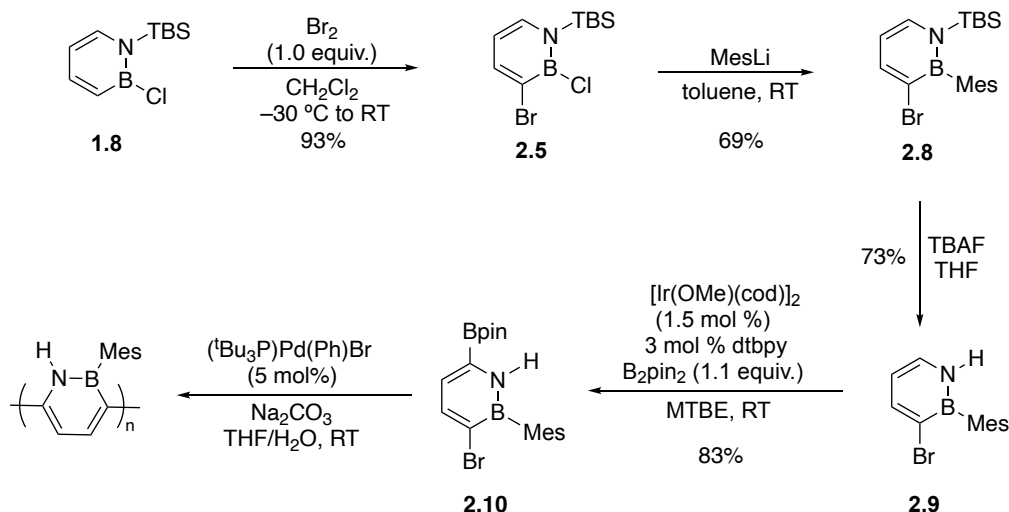


Scheme 2.8. C6 Borylation of 1,2-azaborines (a) and C6 late-stage functionalizations¹⁰⁸ from 1,2-azaborine **1.8** (b)

In 2015, our group synthesized C3–Br–C6–Bpin difunctionalized 1,2-azaborine **2.10** via a tandem C3 bromination, nucleophilic substitution, electrophilic substitution and C6 borylation sequence (Scheme 2.9).¹¹¹ Notably, the four sequential regioselective functionalization strategies (including two carbon positions, boron and nitrogen position)

¹¹¹ Baggett, A. W.; Guo, F.; Li, B.; Liu, S.-Y.; Jäkle, F. *Angew. Chem. Int. Ed.* **2015**, *54*, 11191–11195.

are found to be compatible, enabling the access to monomer building block **2.10** and subsequent Suzuki-Miyaura polycondensation reaction.



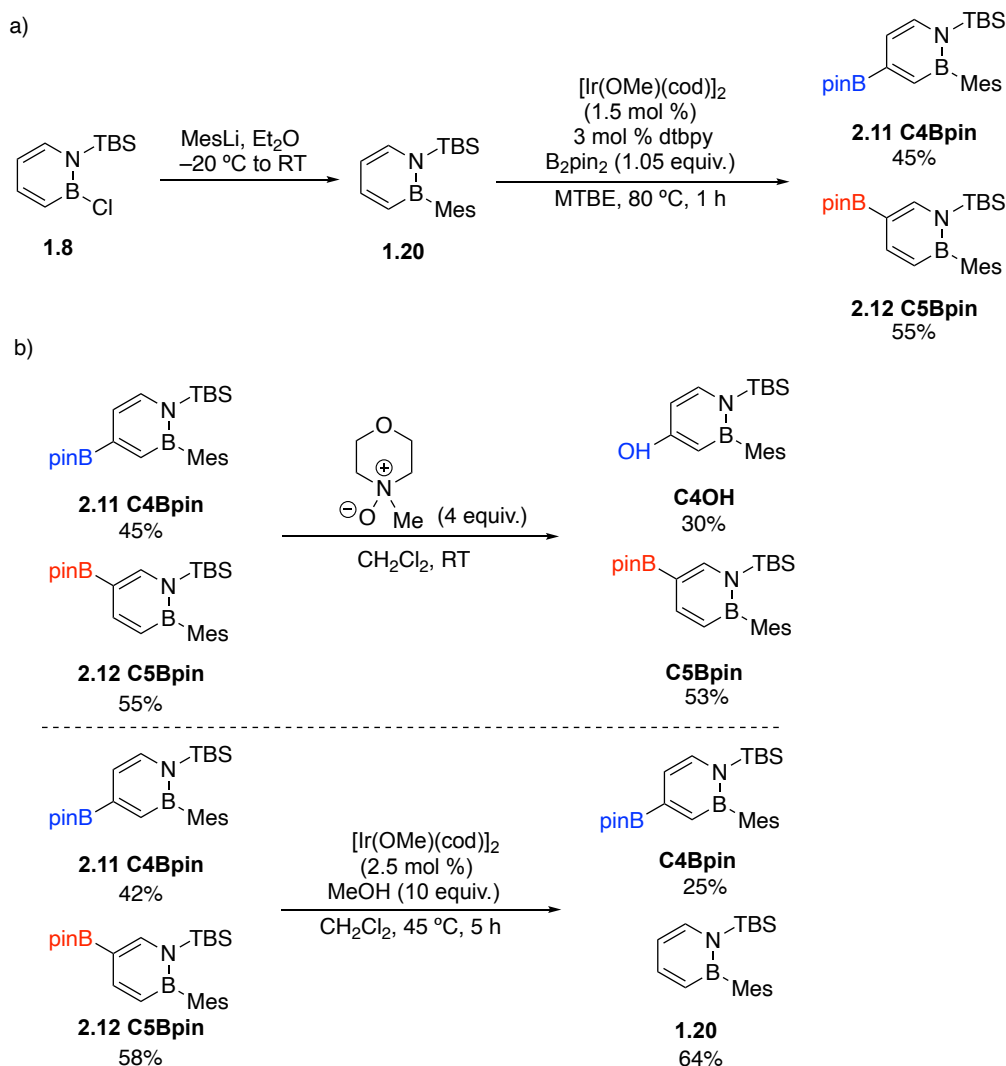
Scheme 2.9. Access to difunctionalized C3–Br–C6–Bpin 1,2-azaborine **2.10** monomer building block

As for functionalizations of 1,2 azaborines at C4 and C5 position, iridium catalyzed C–H borylation could also serve as an indirect strategy. In 2019, our group discovered that C–H borylation of *N*-TBS-*B*-Mes 1,2-azaborine **1.20** occurs in a non-regioselective fashion and only at elevated temperature (Scheme 2.10a),¹¹² affording a 1:1.2–1.4 mixture of C4- and C5-borylated regioisomers. It has been established that the regioselectivity of borylation for arenes is largely dictated by steric effects, not electronic factors.¹¹³ Therefore, it is not surprising that borylation of **1.20** occurs at both sterically accessible C4 and C5 positions non-selectively. Although physical methods to separate the two regioisomers

¹¹² McConnell, C. R.; Haeffner, F.; Baggett, A. W.; Liu, S.-Y. *J. Am. Chem. Soc.* **2019**, *141*, 9072–9078.

¹¹³ For mechanistic work of Ir-catalyzed borylation, see: a) Tamura, H.; Yamazaki, H.; Sato, H.; Sakaki, S. *J. Am. Chem. Soc.* **2003**, *125*, 16114–16126. b) Boller, T. M.; Murphy, J. M.; Hapke, M.; Ishiyama, T.; Miyaura, N.; Hartwig, J. F. *J. Am. Chem. Soc.* **2005**, *127*, 14263–14278.

were unsuccessful, reaction-based chemical methods could distinguish the two *mono*-borylated isomers as a consequence of 1,2-azaborine's distinct electronic structure. As shown in Scheme 2.10b, the distinct reactivity patterns of C4- and C5-borylated azaborine are demonstrated in both selective C4 oxidation with *N*-methylmorpholine *N*-oxide (NMO) and selective C5 proto-deborylation in the presence of iridium catalyst. In both cases, the unreacted or less reactive *mono*-borylated regioisomer could be recovered and isolated.

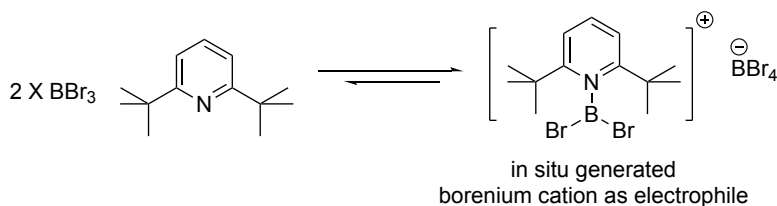
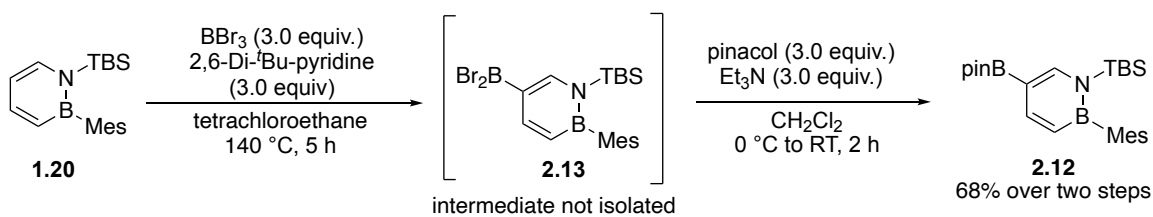


Scheme 2.10. Non-selective borylation of **1.20** at C4/C5 (a) and accessing *mono*-borylated regioisomer via resolution chemistry (b)

The study of iridium catalyzed C–H borylation of 1,2-azaborines **1.20** suggested when the most electronically activated C6 C–H was blocked by the bulky TBS group on the adjacent nitrogen, the C–H borylation regio-selectivity could be affected or completely overturned. The same rationale might also explain the C5 regio-selective electrophilic aromatic substitution of **1.20** with BBr₃ electrophile in the presence of a bulky base (Scheme 2.11).¹¹⁴ When combining BBr₃ with 2,6-*Di-tert*-butyl pyridine, the a based-stabilized borenium cation was proposed to be formed as the electrophile.¹¹⁵ The relatively bulky mesityl substituent on boron in **1.20** could effectively shield the another electron rich C3 position from this sizable electrophile and **1.20** underwent electrophilic aromatic substitution selectively at C5 position. The in situ-generated boron *di*-bromide intermediate **2.13** could be trapped by pinacol to afford **2.12** with more versatile boronic ester functionality. This electrophilic aromatic substitution strategy provides a direct way to selectively functionalize C5 position of 1,2-azaborine **1.20**.

¹¹⁴ The chemistry was explored primarily by my colleague Sierra Bentley.

¹¹⁵ For relevant references, see: a) Del Grosso, A.; Singleton, P. J.; Muryn, C. A.; Ingleson, M. J. *Angew. Chem. Int. Ed.* **2011**, *50*, 2102–2106. b) Iqbal, S. A.; Cid, J.; Procter, R. J.; Uzelac, M.; Yuan, K.; Ingleson, M. J. *Angew. Chem. Int. Ed.* **2019**, *131*, 15525–15529. For a review of borenium chemistry, see: c) De Vries, T. S.; Prokofjevs, A.; Vedejs, E. *Chem. Rev.* **2012**, *112*, 4246–4282.

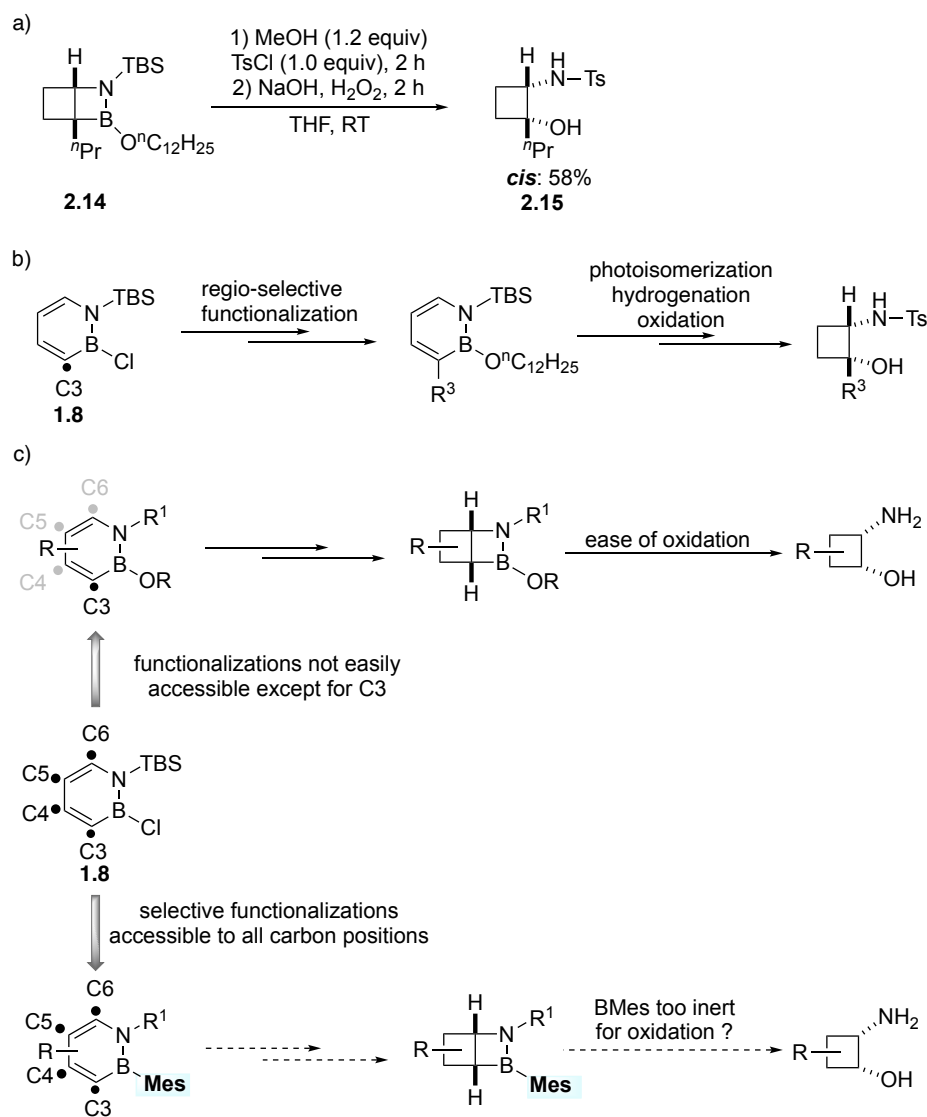


Scheme 2.11. Regio-selective direct borylation of **1.20** via electrophilic aromatic substitution

2.2 Strategic Choice of Substituent on Boron

In our previous work,¹⁰³ we demonstrated that the hydrogenated intermediate **2.14** with alkoxy substituent on boron is competent for stereospecific oxidation of C–B bond, affording the *cis*-cyclobutane β -amino alcohol **2.15** in a one-pot two-step sequence (Scheme 2.12a). It serves as a proof-of-concept that our telescoped photoisomerization-hydrogenation-oxidation sequence could translate the functionality from azaborines to cyclobutane β -amino alcohols (Scheme 2.12b). Practically, although the more amenable alkoxy substituent on boron could facilitate the late stage oxidation, only the C3 substituted B-alkoxy 1,2-azaborines **1.37** could be readily synthesized from the common precursor **1.8**, and C4-, C5- and C6-functionalized analogues were not easily accessible (Scheme 2.12c, see experimental section for detailed investigation). We envisioned that the key to achieve a modular approach lies in the strategic choice of substituent on boron that would allow us to functionalize all carbon positions of 1,2-azaborines regio-selectively.

Based on previous studies,^{26,103,112,114} functionalizations of 1,2-azaborines with the robust mesityl group on boron could be accomplished with no regio-ambiguity, and then it raises up the question whether the oxidation step could be achieved in the presence of the relatively inert mesityl group (Scheme 2.12c).

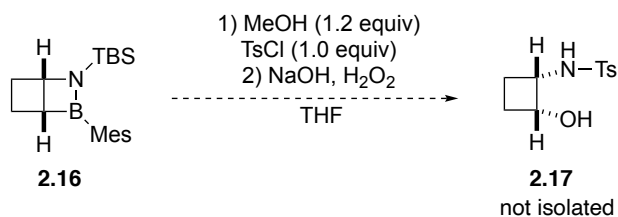


Scheme 2.12. Strategic choice of substituent on boron to achieve a modular approach

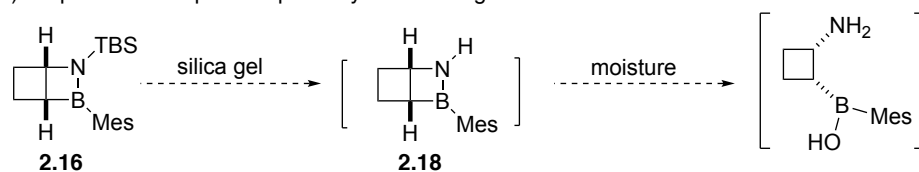
Not surprisingly, applying the oxidation conditions that was effective for **2.14** to B-Mes intermediate **2.16** afforded no desired oxidation product **2.17**, and **2.16** appeared to

be unreactive even at higher temperature with extended period of time (Scheme 2.13a). Interestingly, when we attempted to recover the unreacted **2.16** starting material from the crude reaction mixture over silica chromatography, we observed the partial decomposition of **2.16**. We hypothesized that the TBS- group might be removed over silica gel affording the free amine intermediate **2.18**, which was less robust toward the moisture and decomposed over time (Scheme 2.13b). Driven by this hypothesis, we envisioned that removing the bulky TBS- group on nitrogen first could facilitate the oxidation when the boron center was more accessible to the oxidizing reagents. Delightfully, after **2.16** was exposed to 2 equiv. of TBAF hydrate, a tetracoordinate borate species **2.19** (Scheme 2.13c, proposed structure) was observed by the ^{11}B NMR (9.1 ppm in THF) indicating that the boron was presumably attacked by the fluoride nucleophile. Sequential addition of tosyl chloride and triethylamine could re-protect the free amine, and subsequent oxidation could occur effectively in the same pot, producing the desired amino alcohol **2.17** in a stereoretentive fashion (Scheme 2.13c).

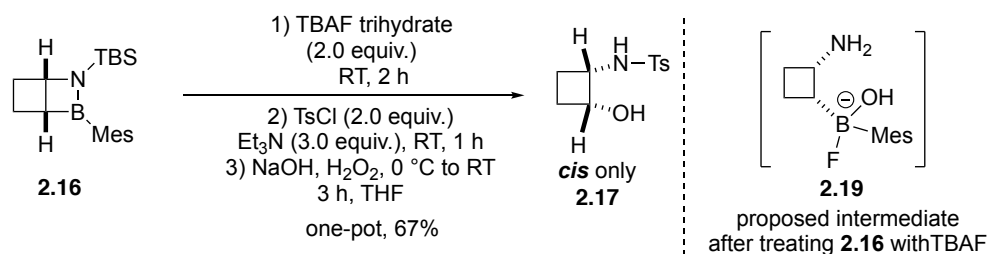
a) Unsuccessful oxidation of **2.16** using previously developed method



b) Proposed decomposition pathway over silica gel



c) Successful one-pot oxidation of **2.16** inspired by decomposition hypothesis



Scheme 2.13. Development of a one-pot strategy to oxidize B–Mes intermediate **2.16**

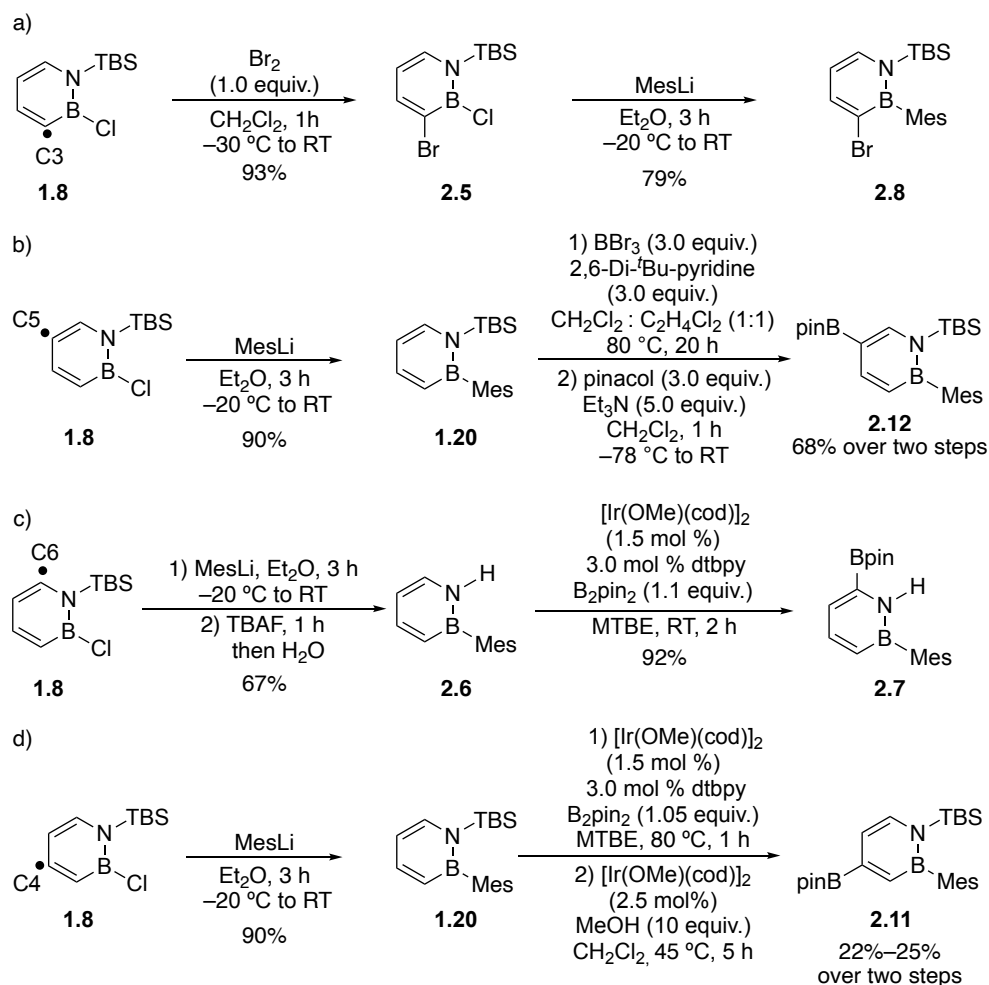
The development of an effective strategy to oxidize the B–Mes hydrogenation intermediate is a key breakthrough given that the robust mesityl group on boron is highly preferred for regio-selective functionalizations of 1,2-azaborines. The next goal is to prepare a diverse array of 1,2-azaborines and investigate the substrate scope of the photoisomerization that can translate those functionalities from 1,2-azaborines to the subsequent four-membered cycles.

2.3 Modular Synthesis of *Mono-* and *Di-*functionalized 1,2-Azaborines

As discussed above, to establish a modular approach to access cyclobutane β-amino alcohols, it is highly desirable to have a versatile 1,2-azaborine core that enables ready synthetic access to new substituted derivatives. To this end, the “building block”

functionalization strategy is particularly attractive,¹¹² since once the functional groups like Bpin and halide are introduced regio-selectively onto 1,2-azaborines, they can become powerful handles for broad diversification at specific ring positions.

Starting with our common 1,2-azaborine precursor **1.8**, either Bpin or bromide functional group could be readily installed at all the carbon positions within three steps. The mesityl group served as a universal substituent on boron that would allow us to access all the 1,2-azaborine building blocks regio-selectively. Electrophilic aromatic substitution of **1.8** with Br₂ occurred selectively at the C3 position,⁷¹ and treatment of **2.5** with MesLi in diethyl ether could produce C3Br B–Mes building block **2.8** (Scheme 2.14a). Notably, B–Cl nucleophilic substitution with MesLi occurred more rapidly than lithium-halogen exchange at the C3–Br position.¹¹¹ Alternatively, when the mesityl group was introduced first, electrophilic aromatic substitution of **1.20** with larger borenium cation electrophile took place at the C5 position selectively (Scheme 2.14b).¹¹⁴ The in situ-generated boron *di*-bromide intermediate was then treated with pinacol to afford the C5–Bpin B–Mes building block **2.12**. Iridium catalyzed C–H borylation of **2.6** occurred selectively at C6 position to furnish the C6-Bpin B–Mes building block **2.7** (Scheme 2.14c).²⁶ When the C6 position was shielded by the bulky TBS- group on the nitrogen, **1.20** underwent C–H borylation unselectively producing a mixture of C4/C5 *mono*-borylated regioisomers, and iridium catalyzed proto-deborylation was therefore applied to kinetically resolve two regioisomers, allowing for the isolation of C4–Bpin B–Mes building block **2.11** (Scheme 2.14d).¹¹²

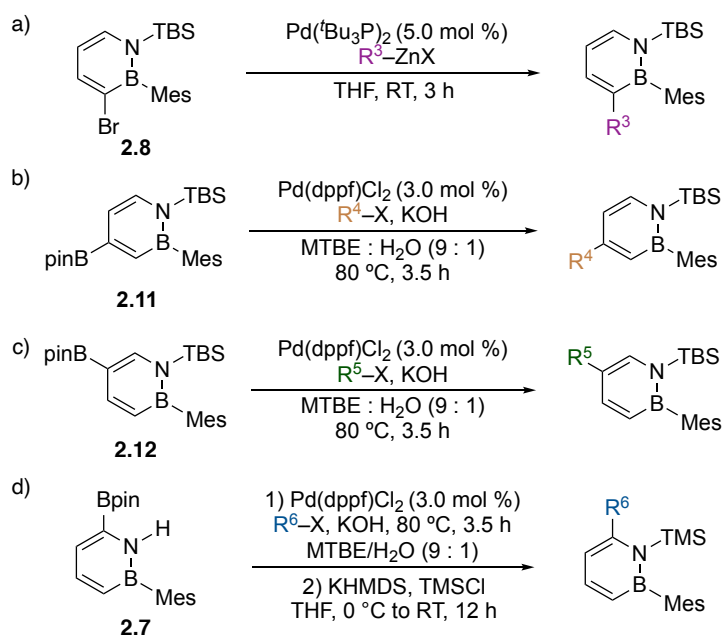


Scheme 2.14. Regio-selective preparation of 1,2-azaborine building blocks

The aforementioned building blocks with bromide or Bpin functionality could then engage in Negishi or Suzuki cross coupling reactions (Scheme 2.15).^{26,71,112} Notably, with the robust Mesityl substituent on the boron, reactive organozinc reagents as well as aqueous basic conditions could be well tolerated, allowing us to introduce diversified substituents onto the azaborine core in a modular fashion. As summarized in the Table 2.1,¹¹⁶ different sp^3 hybridized carbon substituents (**2.20–2.22**) could be installed at C3 position via Negishi cross-couplings. As for C4 to C6 position, Suzuki cross-coupling enabled the introduction

¹¹⁶ Substrate **2.22** and **2.35** is contributed by my colleague Tomoya Ozaki.

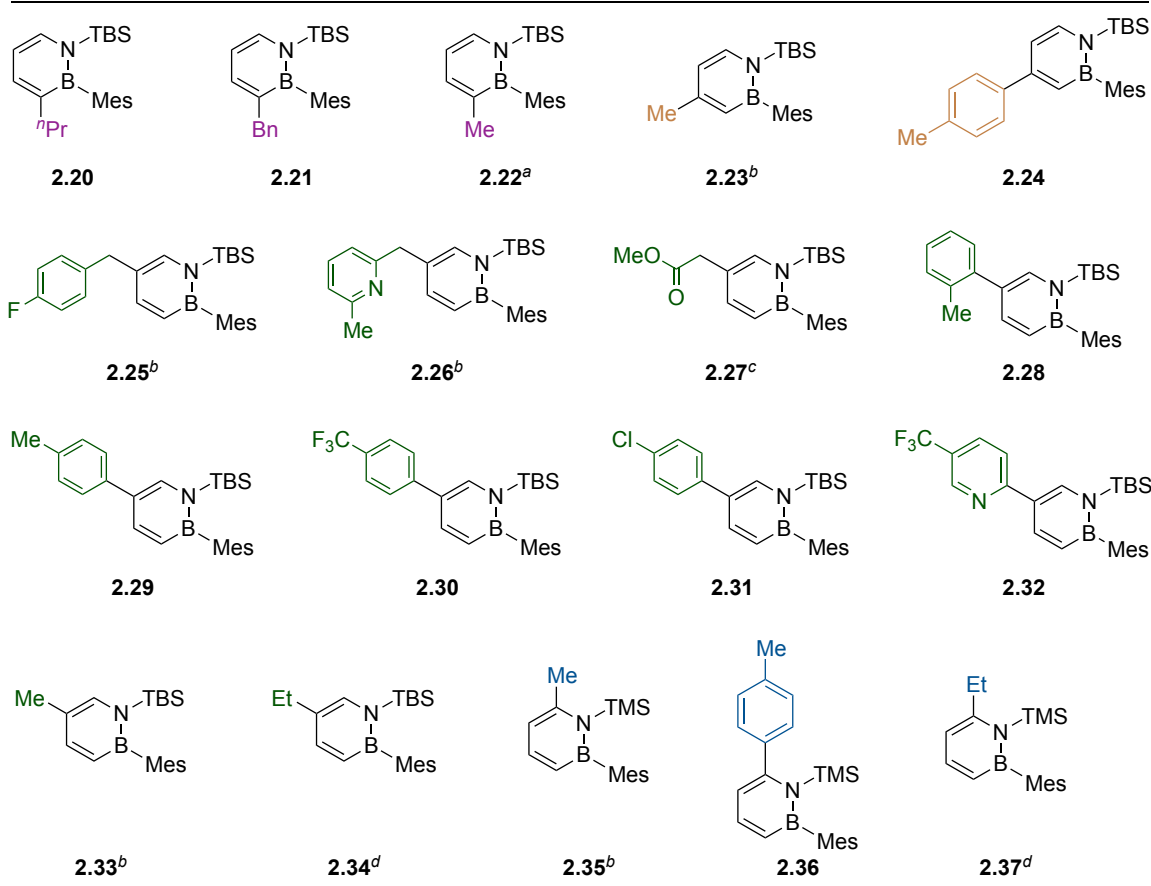
of various sp^2 or sp^3 hybridized carbon substituents under several different catalytic conditions. Specifically, all vinyl-(**2.34**, **2.37**)¹¹⁷ and aryl-(**2.24**, **2.28–2.32**, **2.36**) based electrophiles were tolerated under the same conditions shown in Scheme 2.15, while methyl-(**2.23**, **2.33**, **2.35**) and benzyl- (**2.25**) or benzyl-type (**2.26**) electrophiles were also suitable to conditions using same palladium catalyst with some variation of base and reaction time. C5-ester-substituted substrate **2.27** was synthesized using catalytic conditions developed by the Gooßen group via a palladium(0)-catalyzed cross-coupling of C5-Bpin-1,2-azaborine and α -bromoacetic acid derivatives.¹¹⁸



Scheme 2.15. Conditions for Negishi (a) and Suzuki (b,c,d) cross-couplings of 1,2-azaborine building blocks

¹¹⁷ For ethyl substituted substrate **2.34** and **2.37**, vinyl group was introduced first via Suzuki cross-coupling followed by hydrogenation.

¹¹⁸ Gooßen, L. J. *Chem. Commun.*, **2001**, 669–670.



^aDimethylzinc was used as the organozinc reagent in the Negishi cross-coupling.

^bPotassium phosphate tribasic monohydrate was used as base in the Suzuki cross-coupling; reactions were ran in 6 hours.

^cSuzuki cross-coupling conditions: methyl bromoacetate as the electrophile; Pd(OAc)₂ (3 mol %), P(*o*-tolyl)₃ (9 mol%), K₃PO₄·H₂O, THF : H₂O (9 : 1), 60 °C, 16 h.

^dVinyl bromide was used in the Suzuki cross-coupling first, followed by hydrogenation using Pd/C.

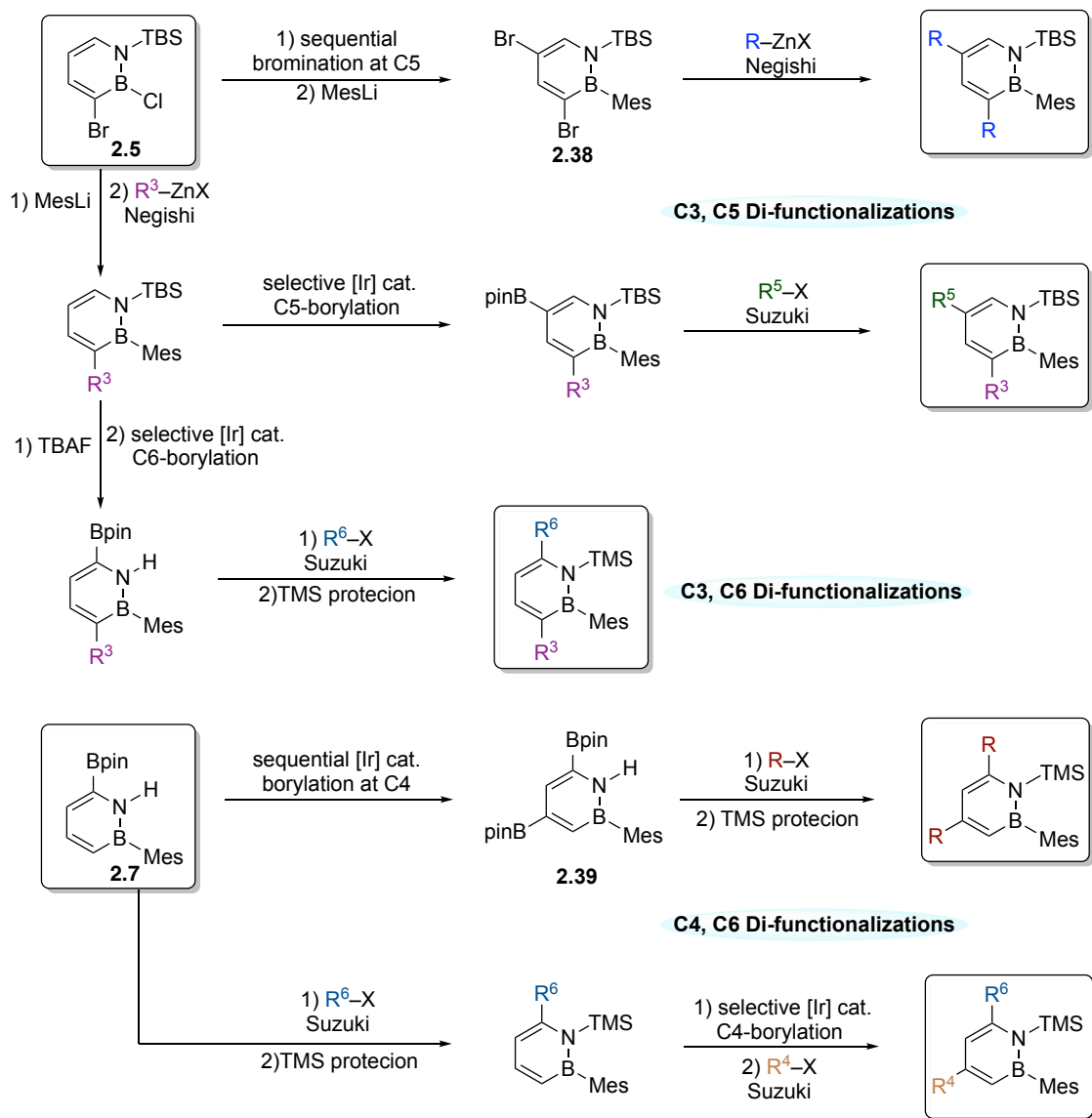
Table 2.1. Modular synthesis of *mono*-substituted¹¹⁹ 1,2-azaborine substrates

Along with *mono*-substituted 1,2-azaborine synthesis, we were also interested in *di*-functionalizations of 1,2-azaborines considering that the resulting substituted cyclobutane β -amino alcohols could be quite challenging to access using other reported methods. Intriguingly, we could utilize the *mono*-functionalized 1,2-azaborine as a synthon to establish protocols that allow us to either introduce the same substituent or different ones

¹¹⁹ Substituents on boron and nitrogen are not counted.

to two different carbon positions selectively (Scheme 2.16). For instance, from C3 *mono*-brominated 1,2-azaborine precursor **2.5**, a sequential bromination could be achieved to furnish the *di*-bromo 1,2-azaborine **2.38** as a building block to access *di*-functionalized 1,2-azaborines with same substituent at C3 and C5 position. Alternatively, we could install the first substituent at C3 position, and iridium catalyzed C–H borylation could introduce the Bpin group at C5 position selectively, which could serve as a handle for the second cross-coupling to afford C3,C5 *di*-functionalized 1,2-azaborines with different substituents. On the other hand, if the bulky TBS group on nitrogen was removed first, then the C6 position became the most activated and accessible position for borylation, resulting in the C3,C6 *di*-functionalized 1,2-azaborines. Similarly, taking advantage of the C6 *mono*-borylated building block **2.7**, we were also able to introduce the same or the different substituents at C4 and C6 positions, depending on the order of Suzuki cross-coupling and C4 selective borylation. Based on the modular protocols established, a variety of *di*-functionalized 1,2-azaborines featuring different substitutions patterns were prepared using the previously explored conditions (Table 2.2, see experimental section for detailed discussion and synthesis).^{26, 71,120}

¹²⁰ The preparation of the *di*-functionalized 1,2-azaborines typically takes several steps. The precursors and final substrates were prepared in a collective effort with my colleague Tomoya Ozaki. Substrates **2.42**, **2.45**, **2.48**, **2.49** were contributed by my colleague Tomoya Ozaki.



Scheme 2.16. Selective *di*-functionalizations of 1,2-azaborines

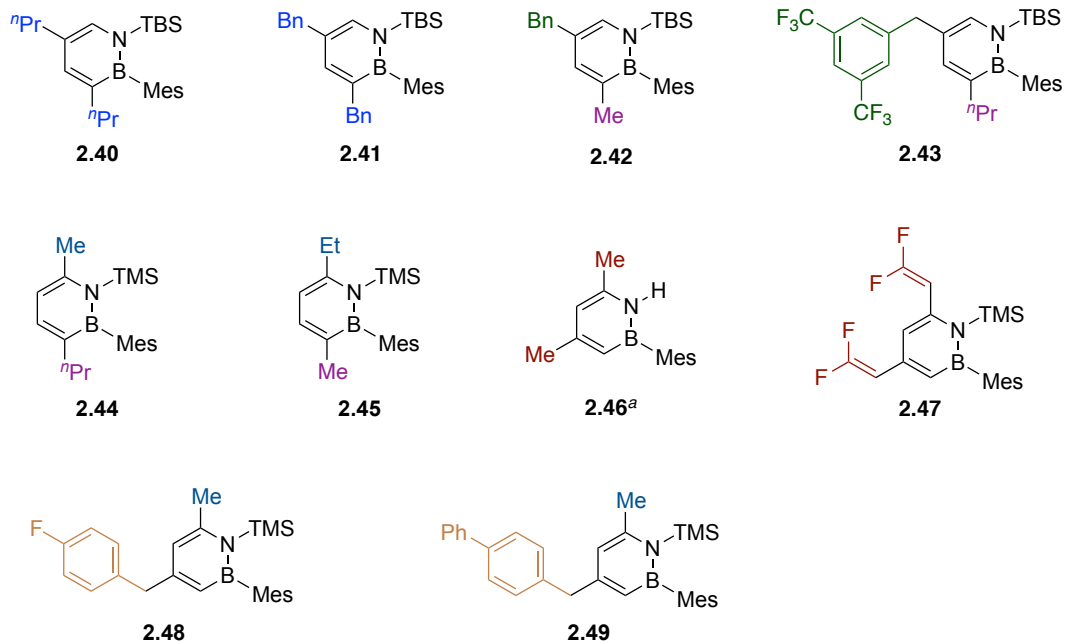
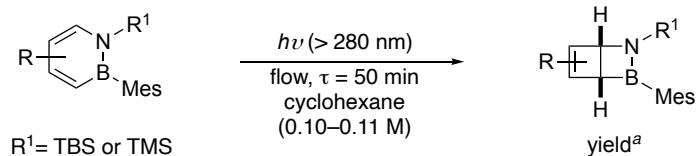


Table 2.2. Modular preparation of *di*-substituted 1,2-azaborine substrates

2.4 Investigations of the Substrate Scope of Photoisomerization

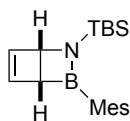
1,2-azaborines with different functional groups and substitution patterns were subjected to the photo-flow conditions to investigate the scope and versatility of photoisomerization.¹⁰³ As shown in Table 2.3, the photo-flow system was shown to tolerate various functional groups and different substitution patterns. Typically, 1,2-azaborines with sp^3 hybridized carbon substituents at all carbon positions could undergo photoisomerization effectively. *Di*-substituted 1,2-azaborines with different *di*-substitution patterns could also serve as suitable substrates as exemplified by Dewar **2.64–2.68**. Among these sp^3 hybridized carbon substituents, a variety of functionalities could be tolerated including alkyl groups (**2.50**, **2.53**, **2.60**, **2.63**, **2.66**, etc.), benzyl groups including fluorine and trifluoromethyl functionalities (**2.51**, **2.54**, **2.65**, **2.67**), carboxylic acid ester group (**2.56**), as well as pyridine fragment (**2.55**) and bi-aryl (**2.68**) fragment.



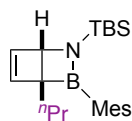
parent Dewar

R³ = alkyl

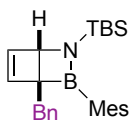
R⁴ = alkyl, Bpin



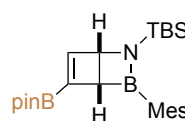
2.21, 91%



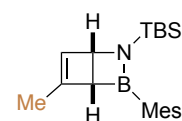
2.250, 91%



2.251, 92%

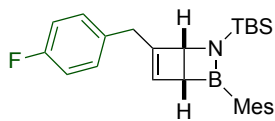


2.252, 93%

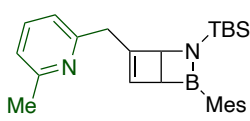


2.253, 93%

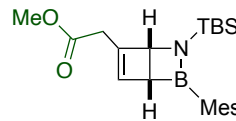
R⁵ = alkyl, aryl, Bpin



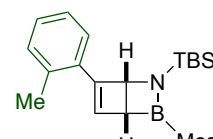
2.254, 95%



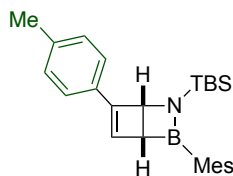
2.255, 90%



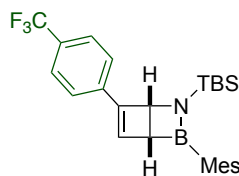
2.256, 95%



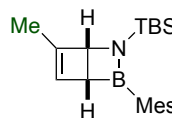
2.257, 91%



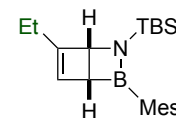
2.258, 94%



2.259, 94%



2.260, 94%

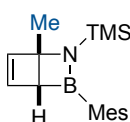


2.261, 93%

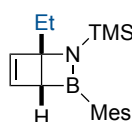
R⁶ = alkyl

R³, R⁵

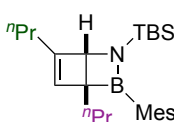
R³, R⁶



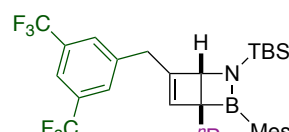
2.262, 92%



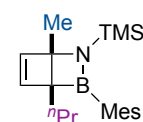
2.263, 93%



2.264, 92%

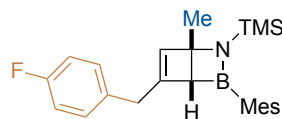


2.265, 93%

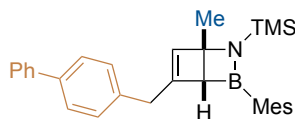


2.266, 91%

R⁴, R⁶



2.267, 93%



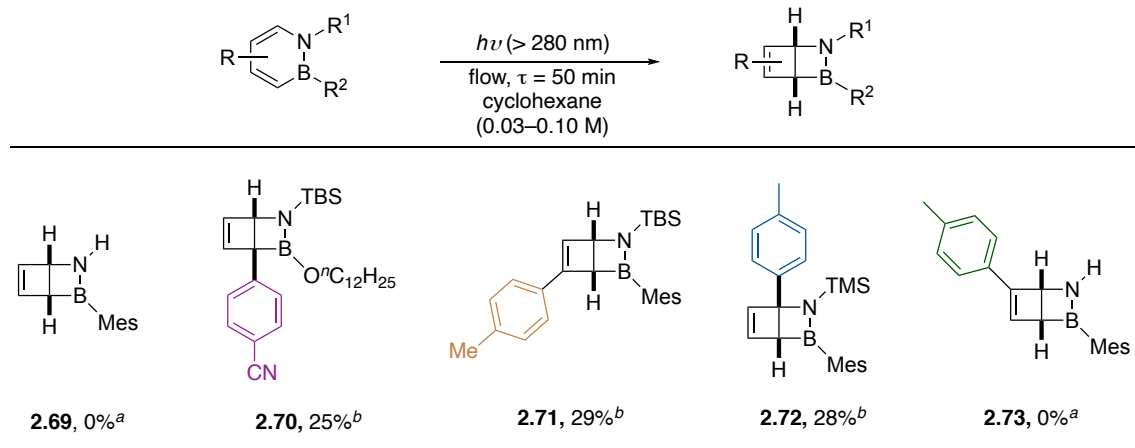
2.268, 91%

^aYield was calculated based on the mass recovered after removing the cyclohexane solvent.

Table 2.3. Substrate scope of 1,2-azaborines photoisomerization

Moreover, 1,2-azaborine building block with Bpin functionality (**2.52**) could be well-tolerated under photo-irradiation conditions allowing for derivatizations at post-photoisomerization stage.

Interestingly, the effectiveness of photoisomerization could vary significantly when 1,2-azaborines with aryl substituents at different positions were investigated. 1,2-azaborines with aryl groups at C5 position could undergo photoisomerization effectively with full consumption of the starting material (**2.57**, **2.58**, **2.59**). However, the photoisomerization of C3, C4 and C6 aryl-substituted analogues afforded only less than 30% conversion with majority of starting material remaining unreacted (Table 2.4, **2.70–2.72**). Adjustment of substrate concentration (more dilute) and injection rate (slower) did not help with improving the conversion significantly. Re-subjecting the collected materials to the photo-flow reactor again did not drive the reaction forward besides the observation of partial decomposition. The extinction coefficient of different aryl-substituted azaborine regioisomers was determined using Beer-Lambert law with the measurement of their UV-absorbance. C4 *p*-Tol 1,2-azaborine ($\epsilon = 13072 \text{ M}^{-1}\text{cm}^{-1}$) appeared to absorb the light more strongly than C5 *p*-Tol 1,2-azaborine ($\epsilon = 8485 \text{ M}^{-1}\text{cm}^{-1}$), suggesting that the less effective photoisomerization of C4 *p*-Tol 1,2-azaborine was not due to less efficient light absorbance. We speculate that there is a dynamic equilibrium established under the photo-irradiation for C3, C4 and C6 aryl-substituted 1,2-azaborines. And the reason was unclear so far why only C5 aryl-substituted 1,2-azaborines could generate the Dewar isomer with full conversion.

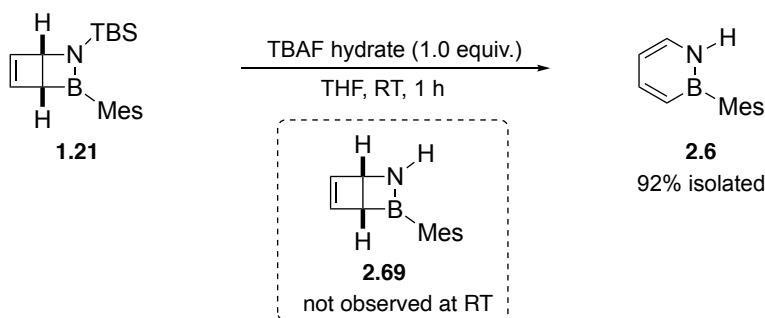


^aNo product was formed, and only 1,2-azaborine starting material remained.

^bThe percentage was calculated based on the crude nmr (the ratio between product and the sum of product plus remaining starting material).

Table 2.4. Challenging substrates for photoisomerization

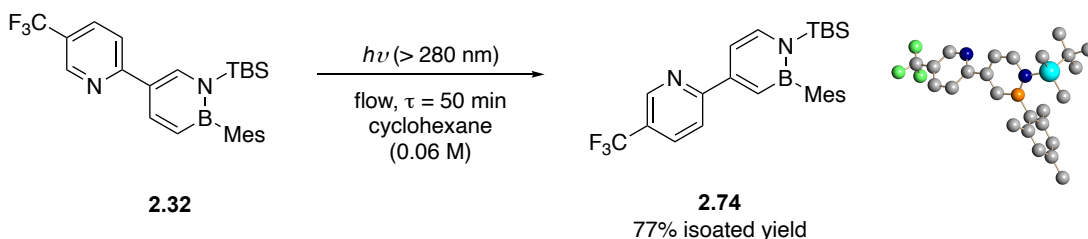
Notably, silyl protection group on nitrogen was found to be essential for the generation of Dewar product at room temperature, since the photoisomerization of N–H–B–Mes 1,2-azaborines afforded no Dewar product with only starting material retrieved (**2.69**, **2.73**). Further experimental elaborations shown in Scheme 2.17 suggested that N–H Dewar **2.69** would undergo facile retro-isomerization to produce N–H 1,2-azaborine **2.6** at room temperature even if **2.6** was an active substrate for photoisomerization.



Scheme 2.17. Experimental evidence of **2.69** being unstable at room temperature

Overall, after systematic investigation of the substrate scope in the photoisomerization step, we were delighted to discover that a broad range of substrates bearing diverse substitution patterns could exclusively produce the Dewar isomer in a clean and efficient fashion,¹²¹ thereby transferring the functionalities from the 1,2-azaborine core to subsequent four-membered cycles.

During our investigation of the photoisomerization substrate scope, we serendipitously discovered a novel photo-transposition reaction (Scheme 2.18). When C5-5-CF₃-pyridyl 1,2-azaborine **2.32** was subjected to more dilute photo-flow condition, a new azaborine species was observed and isolated. ¹H NMR analysis suggested a transposition from C5 to C4 substituted 1,2-azaborine **2.74**, which was then confirmed by X-ray crystallography (only the bond connectivity could be established due to poor crystal quality).



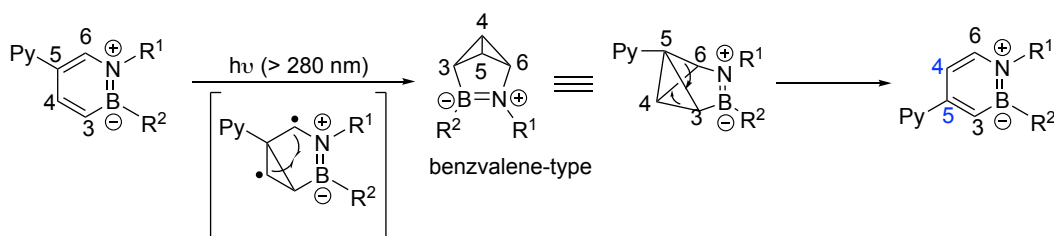
Scheme 2.18. Transposition of 1,2-azaborine **2.32** under photo-irradiation

Fundamental studies of photochemical transpositions of aromatic rings have been reported since 1960s in various systems including benzene derivatives,¹²² pyridine

¹²¹ Reaction was typically clean with no side product generated; therefore, no isolation was required for the photoisomerization step.

¹²² Bryce-Smith, D.; Gilbert, A. *Tetrahedron*. **1976**, 33, 1309–1326.

derivatives,¹²³ isoxazole derivatives,¹²⁴ thiophene derivatives,¹²⁵ and imidazole derivatives.¹²⁶ Those photo-transposition processes were proposed to undergo either a series of valence isomerizations in cases of benzene and pyridine,^{121,122} or a ring-contraction ring-expansion sequence like five-membered nitrogen heterocycles such as isoxazole and imidazole.^{124a,126} Our discovery shown in Scheme 2.18 represents the first example of the 1,2-azaborine photochemical transposition. Based on the literature review,¹²² we tentatively proposed a possible mechanism involving a benzvalene-type intermediate, followed by re-aromatization to accomplish the C4 and C5 rearrangement (Scheme 2.19).



Scheme 2.19. Proposed mechanism for 1,2-azaborine transposition

To test whether 1,2-azaborine photo-transposition is substrate specific, other C5-substituted 1,2-azaborine substrates were synthesized and subjected to the same photo-flow conditions. As shown in Scheme 2.20, photo-irradiation of C5-CF₃-aryl analogue **2.30** and non-conjugated analogue **2.26** containing C5-pyridine fragment generated Dewar isomers exclusively, suggesting that conjugated heteroaryl substituents might be required for the

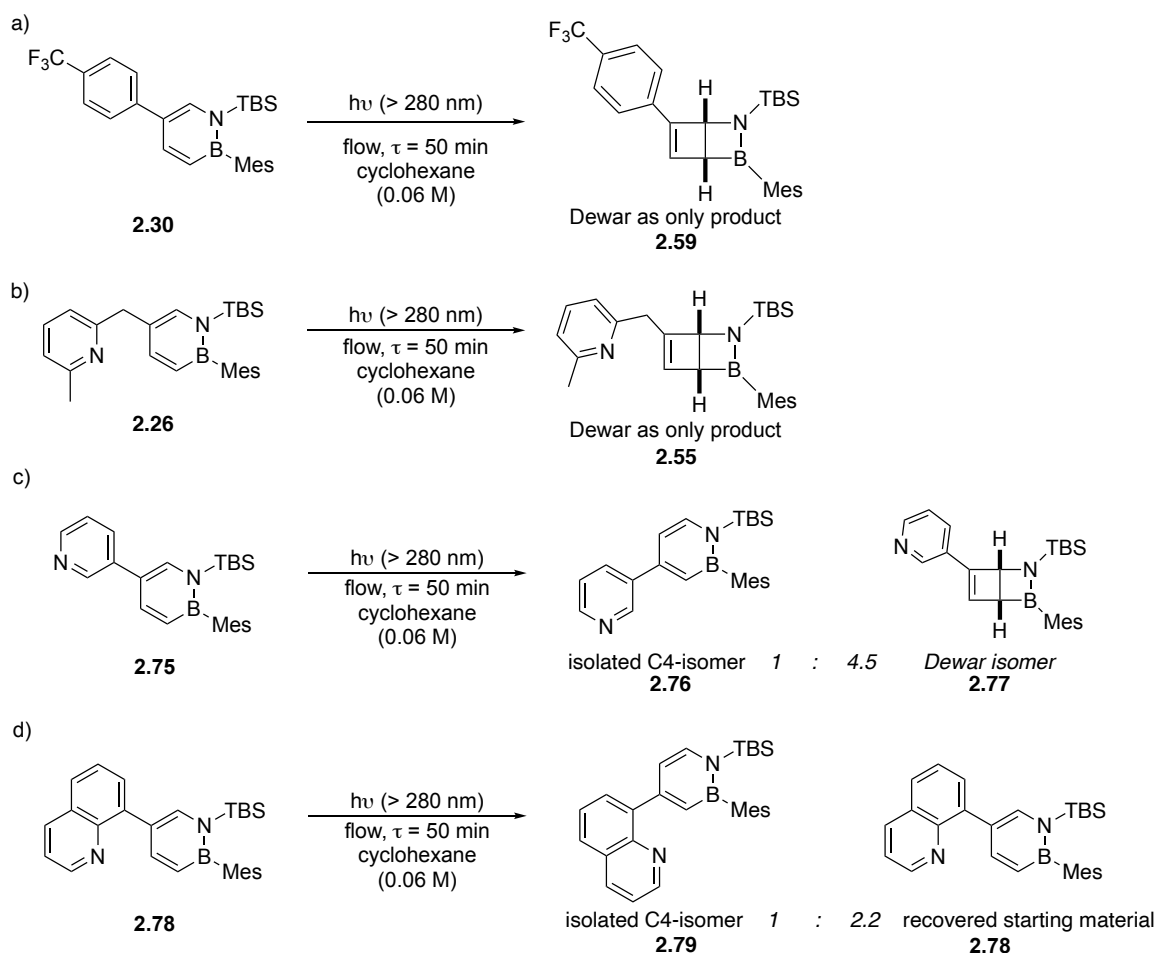
¹²³ a) Chambers, R. D.; Middleton, R.; Corbally, R. P. *J. Chem. Soc., Chem. Commun.*, **1975**, 731–732. b) Pavlik, J. W.; Kebede, N.; Thompson, M.; Day, A. C.; Barltrop, J. A. *J. Am. Chem. Soc.* **1999**, *121*, 5666–5673.

¹²⁴ a) Singh, B.; Ullman, E. F. *J. Am. Chem. Soc.* **1966**, *88*, 1844–1845. b) Singh, B.; Ullman, E. F. *J. Am. Chem. Soc.* **1967**, *89*, 6911–6916. c) Tanaka, H.; Osamura, Y.; Matsushita, T.; Nishimoto, K. *Bull. Chem. Soc. Jpn.* **1981**, *54*, 1293–1298.

¹²⁵ Wynberg, H.; van Driel, H. *J. Am. Chem. Soc.* **1965**, *87*, 3998–4000.

¹²⁶ Beak, P.; Messer, W. *Tetrahedron*, **1969**, *25*, 3287–3295.

transposition reaction. When C5-pyridyl 1,2-azaborine **2.75** was tested, the transposition C4-pyridyl isomer was indeed observed, together with Dewar isomer generated as the major product, indicating that the electronic property of pyridine substituent could affect the product distribution. Interestingly, C5-quinoline 1,2-azaborine **2.78** also underwent photo-transposition partially to afford the C4-quinoline isomer, in which case the Dewar isomer was not observed. Collectively, the early investigations suggested that 1) the transposition reaction was not limited to C5-5-CF₃-pyridyl 1,2-azaborine **2.32**, and 2) different pyridine derivatives at C5 position could lead to distinct product distribution among the transposition isomer, Dewar isomer, and starting material. Future efforts would be directed toward mechanism studies of 1,2-azaborine photochemical transposition as well as exploring the substrate scope of this transformation.

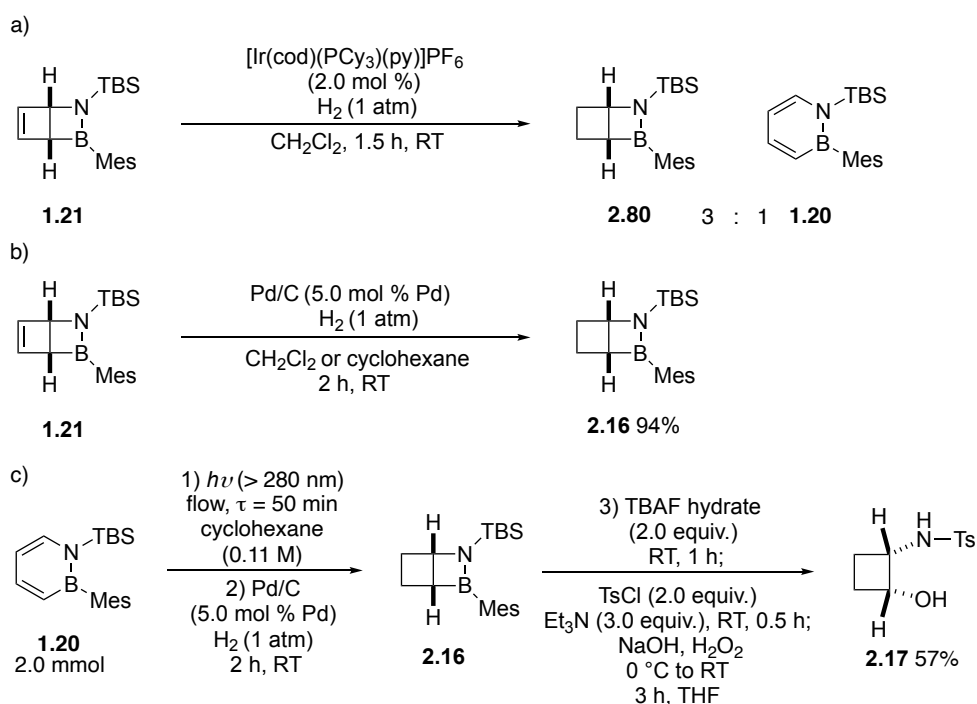


Scheme 2.20. Investigations of other C5-substituted analogues under photo-irradiation

2.5 Stereoselective Hydrogenation and Stereospecific Oxidation

Encouraged by a broad scope of photoisomerization, we sought to explore an effective hydrogenation condition to reduce Dewar double bond stereoselectively. We learned from the previous report that Crabtree's catalyst is effective for hydrogenation of C3-substituted Dewar intermediate.¹⁰³ However, one potential problem of using Crabtree's catalyst was the competitive retro-isomerization to form 1,2-azaborines (Scheme 2.21a). This is not desired as the hydrogenated intermediate is not suitable for chromatography (Scheme 2.13b, see page 166), and as a result, product purification could prove difficult.

Ideally, we would like to use a catalyst that could achieve the hydrogenation in a clean fashion while being easily removable so that we are able to telescope the subsequent oxidation step without the need of purification. Delightfully, we then discovered that heterogeneous palladium on carbon catalyst could serve our purpose to provide clean hydrogenation and ease of removal (Scheme 2.21b). Furthermore, the hydrogenation reaction could proceed efficiently in cyclohexane solution such that the photoisomerization-hydrogenation-oxidation could be telescoped without isolation of intermediates to prepare the parent cyclobutane β -amino alcohol with practical scalability (Scheme 2.21c).



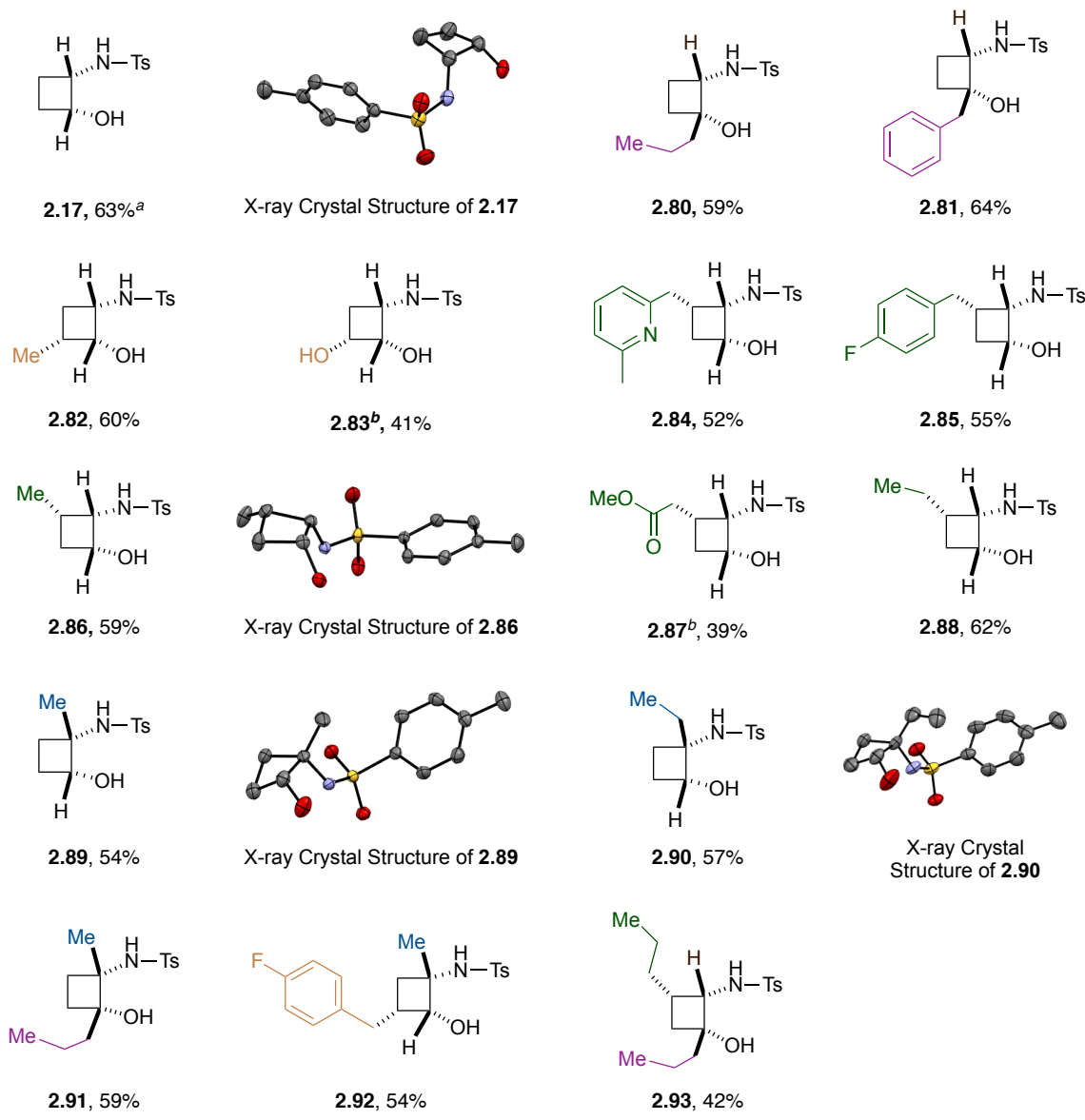
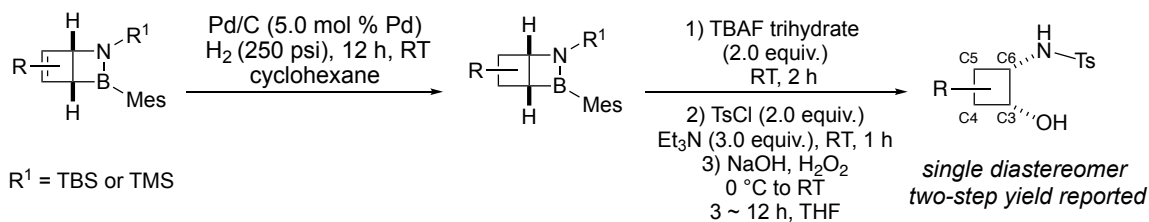
Scheme 2.21. Development of hydrogenation conditions and telescoped three-step sequence to access cyclobutane β -amino alcohol **2.17**

It was anticipated that C4 and C5 substituted Dewar compounds bearing hindered alkenes were challenging to be hydrogenated. To establish a general condition that could

hydrogenate most of the Dewar compounds, we then decided to carry out the hydrogenation in a pressure vessel. A standard hydrogenation condition was applied to all the Dewar substrates, and we typically observed one single diastereomer after hydrogenation suggesting our heterogeneous hydrogenation was highly stereoselective. Followed by the newly developed oxidation protocol, we were able to furnish a diverse array of poly-substituted cyclobutane β -amino alcohols in a stereospecific manner, producing one single diastereomer in all cases (Table 2.5). Relative stereochemistry at C3 and C6¹²⁷ are defined by the stereospecific photoisomerization with no epimerization during hydrogenation and oxidation steps, affording *cis* amino alcohols with C3 and C6 substituents *trans* to amino/alcohol group as showcased by the X-ray crystal structure of **2.89** and **2.90**. Stereochemistry at C4 and C5 were set up in the highly stereoselective hydrogenation step, and after stereo-retentive oxidation, C4 and C5 substituents were always *cis* to amino alcohol as confirmed by the X-ray crystal structure of **2.86**.

¹²⁷ Cyclobutane carbon atoms are numbered in the same way as 1,2-azaborine carbon atoms for the sake of consistency.

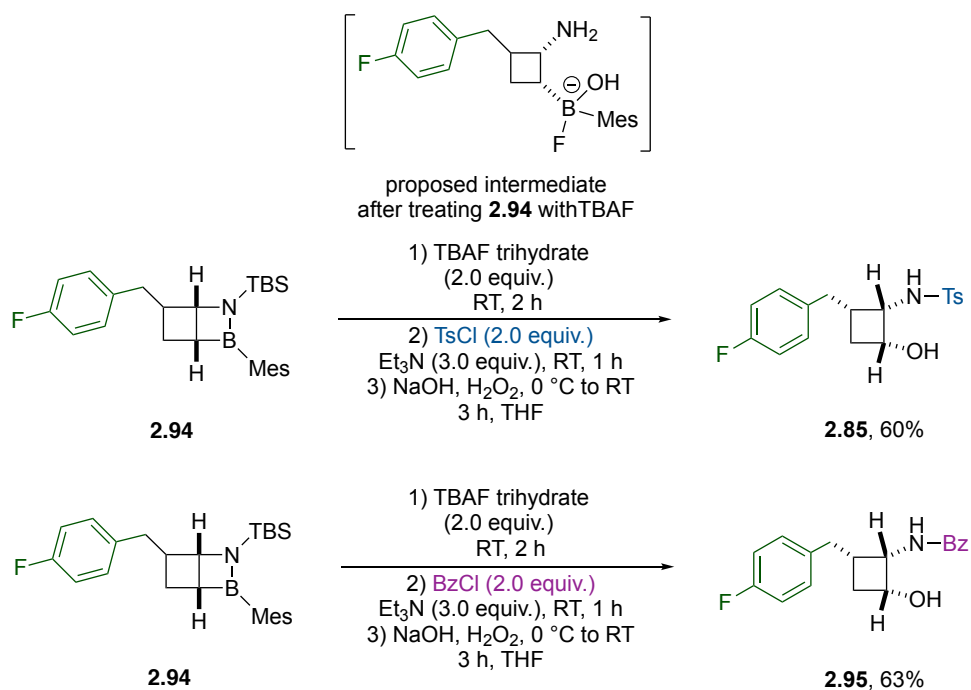
Table 2.5. Stereoselective hydrogenation and stereospecific oxidation to access poly-substituted cyclobutane β -amino alcohols



a. From 2.0 mmol scale

b. Instead of aqueous NaOH, PH = 7.0 buffer was used for those two entries.

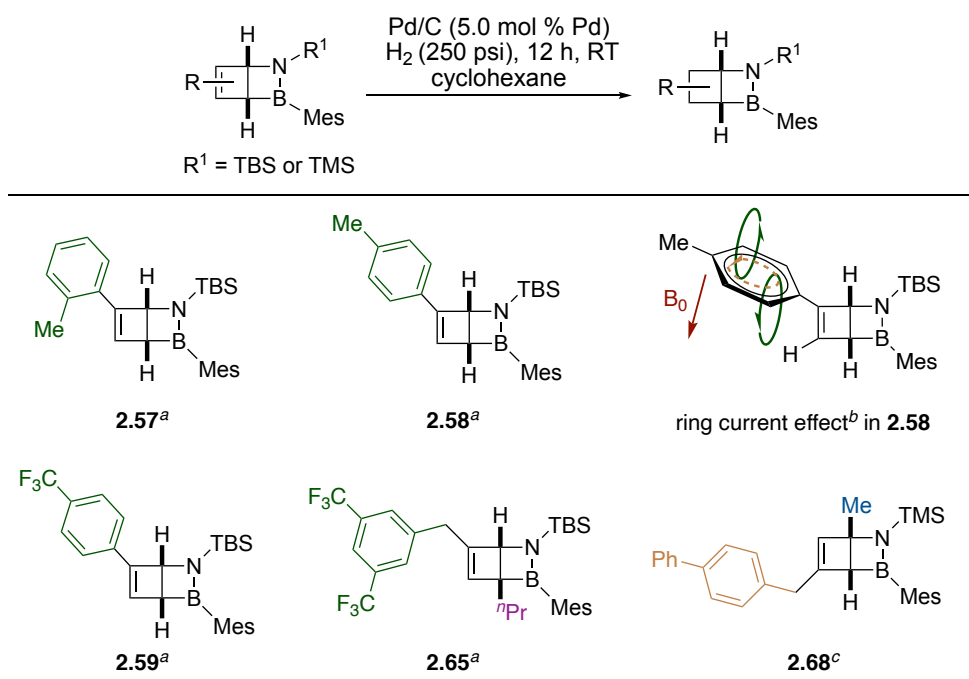
In the one-pot oxidation sequence, we discovered that after treating the hydrogenated intermediate with 2.0 equiv. of TBAF hydrate, the free amine intermediate could be protected with different electrophiles and the subsequent treatment of oxidizing reagents could afford the corresponding cyclobutane β -amino alcohols with similar efficiency (Scheme 2.22).



Scheme 2.22. Trapping with different amino protection groups during one-pot oxidation

Hydrogenation of several Dewar substrates under standard conditions were found to be unsuccessful primarily due to steric hindrance (Table 2.6). For instance, C5-aryl substituted Dewar compounds (**2.57**, **2.58**, **2.59**) could not be effectively hydrogenated even with mild heating at higher pressure. Presumably, the aryl group was locked perpendicular to the alkene double bond indicated by a shielded vinyl proton (proton

chemical shift is 1.82 ppm in CDCl₃) in ¹H NMR analysis (**2.58** in Table 2.6).¹²⁸ Such orientation could potentially prevent the alkene from approaching and binding to the catalyst metal surface,¹²⁹ resulting in unproductive hydrogenation. In addition, the hydrogenation was found to be quite sensitive to the sterics of both carbon substituents on the *di*-functionalized Dewar substrates as evidence by **2.65** and **2.68**.



^aNo product was formed under standard conditions; only starting material remained.

^bThe vinyl proton experiences shielding since the induced magnetic field goes in the opposite direction to the applied magnetic field. ¹H NMR chemical shift for the vinyl proton in **2.58** is 1.82 ppm.

^cNo product was formed under standard conditions; retro-isomerization to 1,2-azaborine was observed together with Dewar starting material.

Table 2.6. Challenging Dewar substrates for hydrogenation

¹²⁸ The ¹H NMR shift of **2.58** vinyl proton was found at around 1.8 ppm, presumably as a result of ring current effect.

¹²⁹ Mattson, B.; Foster, W.; Greimann, J.; Hoette, T.; Le, N.; Mirich, A.; Wankum, S.; Cabri, A.; Reichenbacher, C.; Schwanke, E. *J. Chem. Educ.* **2013**, *90*, 612–619.

2.6 Summary

In summary, we have provided a versatile synthetic toolkit toward cyclobutane β -amino alcohols synthesis. Capitalizing on the regio-selective *mono-/di-* functionalizations of 1,2-azaborines, we developed a tandem photoisomerization-hydrogenation-oxidation protocol to convert 1,2-azaborines to cyclobutane β -amino alcohols. With various functionalities translated from the 1,2-azaborine core to the cyclobutane ring, our protocol has demonstrated that a diverse array of cyclobutane β -amino alcohol derivatives could be forged with high level of modularity and stereoselectivity.

2.7 Experimental Section

2.7.1 General Considerations

All oxygen- and moisture-sensitive manipulations were performed in oven-dried glassware under a nitrogen atmosphere using either standard Schlenk techniques or a glove box. Cannula or gas tight syringes or were used to transfer liquid reagents and solvents in all the reactions. Unless otherwise noted, all reagents were obtained from commercial sources (TCI, Sigma-Aldrich, Strem, Acros, Oakwood, Fisher) and used as received. Bulk volumes of diethyl ether, dichloromethane, pentane, and tetrahydrofuran were passed through an alumina column and dispensed from a solvent purification system under argon.

The following compounds were purified prior to use: CDCl_3 was purchased from Cambridge Isotope Laboratories and was passed through K_2CO_3 plug and distilled over P_2O_5 under N_2 and stored in a Schlenk flask containing 4Å molecular sieves prior to use. 10% wt. Pd/silica was purchased from Strem and dried at 140 °C under vacuum overnight. Pinacol was purchased from Acros and recrystallized from cold diethyl ether. $\text{Pd}(\text{dppf})\text{Cl}_2$ was purchased from Sigma-Aldrich. $\text{Pd}(t\text{-Bu}_3\text{P})_2$ catalyst was purchased from Strem. Organozinc reagents were purchased from Alfa Aesar in a form of 0.5M solution in THF. Crabtree's catalyst was purchased from TCI. Extra dry cyclohexane was purchased from Thermo Fisher Scientific. Anhydrous tert-butyl methyl ether (MTBE) was purchased from Sigma Aldrich.

The following compounds were prepared according to previously reported procedures: **1.8**,¹⁰ **1.20**,²⁶ **2.5**,⁷¹ **2.6**,²⁶ **2.7**,²⁶ **2.11**¹¹² and the characterization data obtained were consistent with those reported in the literature.

^1H , ^{13}C , ^{11}B , and ^{19}F NMR spectra were measured on Varian Unity Inova 400, 500 or 600 MHz spectrometer at the Boston College nuclear magnetic resonance facility. All NMR chemical shifts are reported in ppm; coupling constants are reported in Hz. ^1H and ^{13}C spectra were internally referenced to residual solvent peaks (^1H CDCl_3 : $\delta = 7.26$ ppm, acetone- d_6 : $\delta = 2.05$ ppm; ^{13}C CDCl_3 : $\delta = 77.16$ ppm); ^{11}B spectra were externally referenced to a standard of $\text{BF}_3 \cdot \text{Et}_2\text{O}$ ($\delta = 0.0$ ppm), and ^{19}F spectra were likewise referenced to a standard of α,α,α -trifluorotoluene ($\delta = -63.7$ ppm). In ^{13}C NMR analysis, peaks for carbon atoms adjacent to a boron center were generally not observed owing to quadrupolar broadening.

The flow photoreactor was assembled according to previously reported set-up.¹⁰³

The hydrogenation was set-up in series 4760 mini non-stirred pressure vessel from the Parr Instrument Company.

All work-up and purification procedures were performed with reagent grade solvents (purchased from Fisher Scientific) in air unless otherwise noted.

All IR spectra were measured on a Bruker Alpha-P FT-IR equipped with a single crystal diamond ATR module, and values are reported in cm^{-1} .

High-resolution mass spectrometry (HRMS) data were generated in Boston College facilities using direct analysis in real-time (DART) on a JEOL AccuTOF DART spectrometer.

Single-crystal X-ray diffraction data were generated in Boston College facilities from measurements with a Bruker Kappa Apex Duo fully automated diffractometer.

2.7.2 Experimental Procedures for Synthesis of New Compounds

2.7.2.1 Experimental Procedures for Synthesis of *Mono-* and *Di-*Functionalized 1,2-Azaborines (Table 2.1 and Table 2.2)

Synthesis and Characterization of Compound 2.8



3-bromo-1-(*tert*-butyldimethylsilyl)-2-mesityl-1,2-dihydro-1,2-azaborine (2.8).

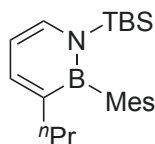
To a 50 ml round bottom flask with a magnetic stir bar was charged with C3-Br B-Cl precursor **2.5** (1.0 equiv., 750.5 mg, 2.45 mmol) in 10 mL of diethyl ether. The mixture was cooled to -20 °C and 1.5 equiv. of Mes-Li was added portionally. Let the reaction gradually warm up to room temperature and react for 3 hours. 10 mL of water was added into the mixture and the aqueous phase was extracted 3 x 10 mL with Hexane; the combined organic extracts were washed with brine and dried over MgSO₄, vacuum-filtered through a Büchner funnel, and concentrated *in vacuo*. The crude residue was purified by flash column chromatograph (silica gel; 100% hexane) to give the desired product as a white solid (679.0 mg, 71%). ¹H NMR (CDCl₃, 500 MHz) δ 7.95 (d, *J* = 7.1, 1H), 7.52 (d, *J* = 7.1, 1H), 6.87 (s, 2H), 6.34 (t, *J* = 6.9 Hz, 1H), 2.37 (s, 3H), 2.16 (s, 6H), 1.00 (s, 9H), 0.06 (s, 6H); ¹³C NMR (CDCl₃, 126 MHz) δ 144.3, 138.9, 137.9, 137.0, 127.0, 111.6, 27.6, 22.9, 21.5, 19.3, -3.0 (the signals for the two carbons adjacent to boron were not observed); ¹¹B NMR (CDCl₃, 160 MHz) δ 39.3; IR 3060, 2951, 2860, 1612, 1527, 1388, 1322, 1264, 1220, 1107, 1030, 970, 821, 765 cm⁻¹; HRMS (DART) calcd. for C₁₉H₃₀BBrNSi [M+H⁺]: 390.14185, found 390.14298.

Procedure for Synthesis of C3-Substituted Compounds 2.20, 2.21 via Negishi Cross-coupling



General Procedure A

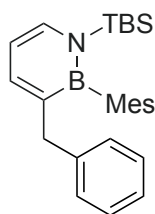
In adaptation of a previously reported Negishi Cross-coupling method:⁷¹ in N_2 glovebox, to a 20 ml vial with a magnetic stir bar was charged with C3-bromo B-Mes precursor **2.8** (1.0 equiv., 390.2 mg, 1.00 mmol) and $Pd(t-Bu_3P)_2$ catalyst (5.0 mol %, 25.6 mg, 0.0500 mmol), and 2.0 mL of THF was added. The mixture was stirred for 5 minutes before adding 3.0 mL of organo-zinc reagent (1.5 equiv., 1.50 mmol, 0.5 M in THF) solution. The reaction was allowed to be stirred at room temperature for 3 hours. At this point, 1.0 mL CH_2Cl_2 was added to quench the reaction. The solids were filtered off and the filtrate was concentrated in *vacuo*. The crude residue was purified by flash column chromatograph (silica gel; x% diethyl ether in hexane) to give the desired product. The procedure to synthesize each compound was carried out at least 2 times. The average yield was reported.



C3-propyl-1,2-azaborine (2.20).

The desired product was obtained by flash column chromatography (silica gel, 0 – 5% diethyl ether in hexane) as a colorless oil with an average yield of 76%. 1H NMR

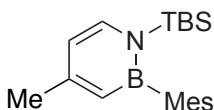
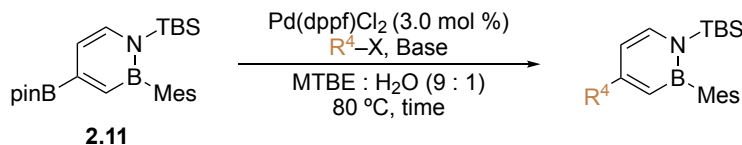
(CDCl₃, 500 MHz) δ 7.34 (dd, J = 6.6, 1.1 Hz, 1H), 7.31 (dd, J = 6.9, 1.2 Hz, 1H), 6.77 (m, 2H), 6.35 (t, J = 6.7 Hz, 1H), 2.30 (s, 3H), 2.11 – 2.06 (m, 2H), 2.05 (s, 6H), 1.37 – 1.25 (m, 2H), 0.93 (s, 9H), 0.77 (t, J = 7.3 Hz, 3H), -0.04 (s, 6H); ¹³C NMR (CDCl₃, 126 MHz) δ 139.5, 138.9, 136.2, 135.9, 126.9, 111.2, 36.9, 27.8, 23.3, 23.2, 21.4, 19.5, 14.3, -2.9 (the signals for the two carbons adjacent to boron were not observed); ¹¹B NMR (CDCl₃, 160 MHz) δ 40.2; IR 3067, 2959, 2930, 2859, 1610, 1523, 1472, 1391, 1322, 1264, 1228, 1196, 1165, 1110, 1030, 1008, 976, 892, 837, 821, 766, 739 cm⁻¹; HRMS (DART) calcd. for C₂₂H₃₇BNSi [M+H⁺]: 354.27828, found 354.27785.



C3-benzyl-1,2-azaborine (2.21).

The desired product was obtained by flash column chromatography (silica gel; 0 – 5% diethyl ether in hexane) as a colorless oil with an average yield of 80%. ¹H NMR (CDCl₃, 500 MHz) δ 7.32 (dd, J = 6.9, 1.2 Hz, 1H), 7.22 (dd, J = 6.5, 1.3 Hz, 1H), 7.17 – 7.06 (m, 3H), 6.88 – 6.81 (m, 2H), 6.75 (s, 2H), 6.33 (t, J = 6.7 Hz, 1H), 3.41 (s, 2H), 2.31 (s, 3H), 1.91 (s, 6H), 0.93 (s, 9H), -0.03 (s, 6H); ¹³C NMR (CDCl₃, 126 MHz) δ 142.3, 140.6, 139.0, 136.4, 136.4, 129.5, 127.9, 127.0, 125.3, 111.2, 41.4, 27.8, 23.0, 21.4, 19.5, -2.9 (the signals for the two carbons adjacent to boron were not observed); ¹¹B NMR (CDCl₃, 160 MHz) δ 40.7; IR 3061, 2985, 2926, 2859, 1610, 1527, 1472, 1371, 1289, 1228, 1196, 1165, 1093, 976, 811, 766, 728 cm⁻¹; HRMS (DART) calcd. for C₂₆H₃₇BNSi [M+H⁺]: 402.27828, found 402.27907.

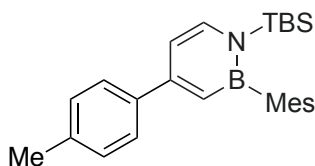
Synthesis of C4-Substituted Compounds **2.23**, **2.24** via Suzuki Cross-coupling



C4-methyl-1,2-azaborine (**2.23**).

Inside a drybox, a 10 mL pressure vessel was charged with a magnetic stir bar, **2.11** (1.0 equiv., 87.5 mg, 0.200 mmol), methyl iodide (6.0 equiv., 75.0 μ L, 1.20 mmol), Pd(dppf)Cl₂ (3.0 mol %, 4.9 mg, 6.00 μ mol). K₃PO₄ · H₂O (4.0 equiv., 184.2 mg, 0.800 mmol) was dissolved in 0.4 mL of H₂O (degassed by sparging with N₂ for 30 minutes before use) and was added into the pressure vessel with 3.6 mL of MTBE (total 4.0 mL of a 9 : 1 v : v mix of MTBE : H₂O was used as solvent). The reaction was sealed and heated at 80 °C for 6 hours. After cooling, 3 mL of water was added into the reaction mixture and the aqueous phase was extracted 3 x 3 mL with diethyl ether; the combined organic extracts were washed with brine and dried over MgSO₄, vacuum-filtered through a fritted funnel, and concentrated *in vacuo*. The crude residue was purified by flash column chromatography (silica gel; 100% hexane) to give the desired product as a colorless solid with an average yield of 77% (first batch: 50.5 mg, 78%; second batch: 49.7 mg, 76%). ¹H NMR (CDCl₃, 500 MHz) δ 7.36 (d, *J* = 6.9 Hz, 1H), 6.80 (s, 2H), 6.37 (dt, *J* = 2.0, 0.9 Hz, 1H), 6.24 (dd, *J* = 6.9, 2.2 Hz, 1H), 2.31 (s, 3H), 2.25 (s, *J* = 1.0 Hz, 3H), 2.11 (s, 6H), 0.94 (s, 9H), 0.01 (s, 6H); ¹³C NMR (CDCl₃, 126 MHz) δ 153.0, 138.9, 138.3, 136.3, 126.9, 114.0, 27.6, 24.5, 23.6, 21.3, 19.4, -3.2 (the signals for the two carbons adjacent to boron

were not observed); ^{11}B NMR (CDCl_3 , 160 MHz) δ 39.4; IR 2929, 2858, 1625, 1504, 1436, 1310, 1264, 1187, 1125, 840, 829, 801 cm^{-1} ; HRMS (DART) calcd. for $\text{C}_{20}\text{H}_{33}\text{BNSi}$ $[\text{M}+\text{H}^+]$: 326.24698, found 326.24679.

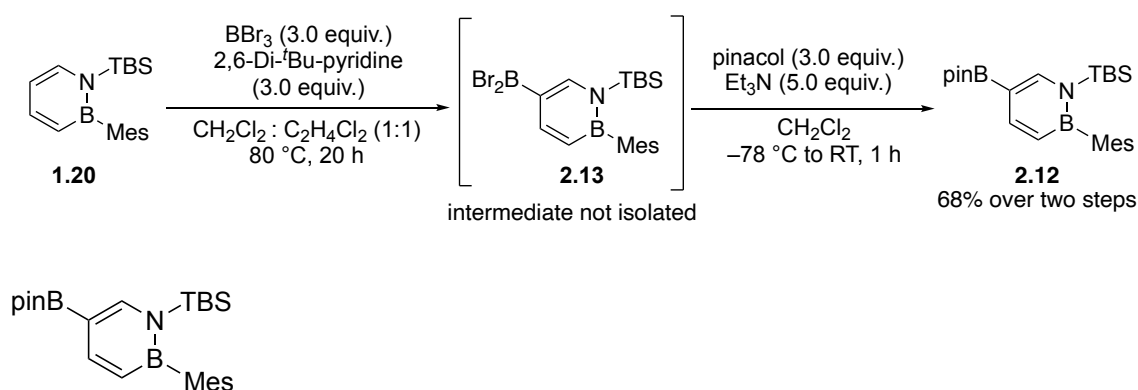


C4-*p*-Tolyl-1,2-azaborine (2.24).

In adaptation of a previously reported Suzuki Cross-coupling method:²⁶ inside a drybox, a 10 mL pressure vessel was charged with a magnetic stir bar, **2.11** (1.0 equiv., 150.0 mg, 0.343 mmol), 4-bromotoluene (1.0 equiv., 58.7 mg, 0.343 mmol), $\text{Pd}(\text{dppf})\text{Cl}_2$ (3.0 mol %, 8.4 mg, 10.3 μmol). KOH (4.0 equiv., 77.0 mg, 1.372 mmol) was dissolved in 0.4 mL of H_2O (degassed by sparging with N_2 for 30 minutes before use) and was added into the pressure vessel with 3.6 mL of MTBE (total 4.0 mL of a 9 : 1 v : v mix of MTBE : H_2O was used as solvent). The reaction was sealed and heated at 80 $^\circ\text{C}$ for 3.5 hours. After cooling, 3 mL of water was added into the reaction mixture and the aqueous phase was extracted 3 x 3 mL with diethyl ether; the combined organic extracts were washed with brine and dried over MgSO_4 vacuum-filtered through a fritted funnel, and concentrated *in vacuo*. The crude residue was purified by flash column chromatography (silica gel; 0 – 5% diethyl ether in hexane) to give the desired product as a colorless solid with an average yield of 90% (first batch: 120.0 mg, 87%; second batch: 129.4 mg, 94%). ^1H NMR (CDCl_3 , 500 MHz) δ 7.60 (d, J = 8.3 Hz, 2H), 7.55 (d, J = 7.2 Hz, 1H), 7.24 (d, J = 7.9 Hz, 2H), 6.89 (d, J = 2.4 Hz, 1H), 6.84 (s, 2H), 6.72 (dd, J = 7.1, 2.4, Hz, 1H), 2.40 (s, 3H), 2.34 (s, 3H), 2.16 (s, 6H), 0.98 (d, J = 1.1 Hz, 9H), 0.07 (d, J = 1.0 Hz, 6H); ^{13}C NMR (CDCl_3 ,

126 MHz) δ 153.2, 139.3, 139.1, 139.0, 138.0, 136.5, 129.4, 127.0, 126.8, 110.8, 27.6, 23.6, 21.4, 21.3, 19.4, -3.2 (the signals for the two carbons adjacent to boron were not observed); ^{11}B NMR (CDCl_3 , 160 MHz) δ 40.2; IR 2960, 2928, 2857, 1615, 1494, 1446, 1264, 1000, 840, 823, 804, 787, 734, 705 cm^{-1} ; HRMS (DART) calcd. for $\text{C}_{26}\text{H}_{37}\text{BNSi}$ $[\text{M}+\text{H}^+]$: 402.27828, found 402.27809.

Procedure for Selective C5-Borylation of *N*-TBS-*B*-Mes 1,2-azaobrine **1.20**



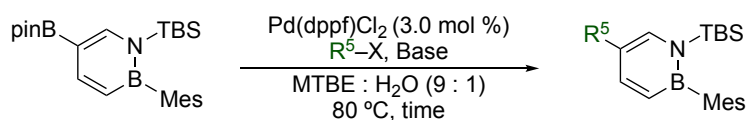
C5-Bpin-1,2-azaborine (**2.12**).

In a N_2 glovebox, a 100 mL pressure vessel was charged with a magnetic stir bar, **1.20** (1.0 equiv., 1.15 g, 3.69 mmol), BBr_3 (3.0 equiv., 11.1 mL 1.0 M BBr_3 in CH_2Cl_2 , 11.1 mmol), 2,6-Di-*t*-butylpyridine (3.0 equiv., 2.13 g, 11.1 mmol), and 11.1 mL 1,2-dichloroethane was added into the mixture. The reaction was sealed and heated at $80\text{ }^\circ\text{C}$ for 20 hours. After 20 hours, the reaction was cooled down to room temperature and the pressure vessel was transferred to N_2 glovebox. The supernatant was transferred to a 250 mL round bottom flask; the salts residue was washed three times using 10 mL CH_2Cl_2 each time and the supernatant was combined into the round bottom flask. The reaction was cooled down to $-78\text{ }^\circ\text{C}$ before a 7 mL CH_2Cl_2 solution of pinacol (3.0 equiv., 1.31 g, 11.1 mmol) and Et_3N (5.0 equiv., 2.58 mL, 18.5 mmol) was added drop-wise via syringe. Upon

the completion of addition, the reaction mixture was allowed to warm up to room temperature and stirred for 1 hour. Upon completion, sodium bicarbonate saturated aqueous solution was added slowly. The mixture was filtered through a fritted funnel. 30 mL of water was added into the reaction mixture and the aqueous phase was extracted 3 x 30 mL with CH₂Cl₂; the combined organic extracts were washed with brine and dried over MgSO₄, vacuum-filtered through a fritted funnel, and concentrated *in vacuo*. The crude residue was purified by flash column chromatography (silica gel; 0 – 10% diethyl ether in hexane) to give the desired product as a white solid (1.10 g, 68%). **¹H NMR** (CDCl₃, 500 MHz) δ 8.13 (s, 1H), 7.97 (d, *J* = 10.9 Hz, 1H), 6.86 (s, 2H), 6.70 (d, *J* = 10.8 Hz, 1H), 2.36 (s, 3H), 2.16 (s, 6H), 1.39 (s, 12H), 0.99 (s, 9H), 0.11 (s, 6H); **¹³C NMR** (CDCl₃, 126 MHz) δ 148.3, 146.8, 138.7, 136.5, 127.0, 83.3, 27.5, 25.0, 23.4, 21.3, 19.3, -3.1 (the signals for the three carbons adjacent to boron were not observed); **¹¹B NMR** (CDCl₃, 160 MHz) δ 41.0, 31.5; **IR** 2976, 2930, 2859, 2360, 1738, 1602, 1362, 1324, 1217, 1145, 810 cm⁻¹; **HRMS** (DART) calcd. for C₂₅H₄₂B₂NO₂Si [M+H⁺]: 438.31654, found 438.31624.

General Procedures for Synthesis of C5-Substituted Compounds 2.25–2.34 via Suzuki

Cross-coupling



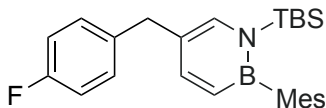
General Procedure B:

Inside a drybox, a 10 mL pressure vessel was charged with a magnetic stir bar, **2.12** (1.0 equiv., 150.0 mg, 0.343 mmol), alkyl halide (x equiv.), Pd(dppf)Cl₂ (3.0 mol %, 8.4 mg, 10.3 μmol). K₃PO₄·H₂O (4.0 equiv., 316.0 mg, 1.37 mmol) was dissolved in 0.5 mL

of H₂O (degassed by sparging with N₂ for 30 minutes before use) and was added into the pressure vessel with 4.5 mL of MTBE (total 5.0 mL of a 9 : 1 v : v mix of MTBE : H₂O was used as solvent). The reaction was sealed and heated at 80 °C for 6 hours. After cooling, 5 mL of water was added into the reaction mixture and the aqueous phase was extracted 3 x 5 mL with diethyl ether; the combined organic extracts were washed with brine and dried over MgSO₄, vacuum-filtered through a fritted funnel, and concentrated *in vacuo*. The crude residue was purified by flash column chromatography (silica gel) to give the desired product. The procedure to synthesize each compound was carried out at least 2 times. The average yield was reported.

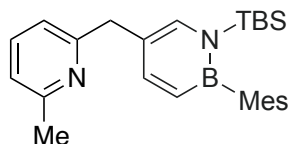
General Procedure C:

Inside a drybox, a 10 mL pressure vessel was charged with a magnetic stir bar, **2.12** (1.0 equiv., 150.0 mg, 0.343 mmol), aryl halide (1.0 equiv.), Pd(dppf)Cl₂ (3.0 mol %, 8.4 mg, 10.3 μmol). KOH (4.0 equiv., 76.9 mg, 1.37 mmol) was dissolved in 0.5 mL of H₂O (degassed by sparging with N₂ for 30 minutes before use) and was added into the pressure vessel with 4.5 mL of MTBE (total 5.0 mL of a 9 : 1 v : v mix of MTBE : H₂O was used as solvent). The reaction was sealed and heated at 80 °C for 3.5 hours. After cooling, 5 mL of water was added into the reaction mixture and the aqueous phase was extracted 3 x 5 mL with diethyl ether; the combined organic extracts were washed with brine and dried over MgSO₄, vacuum-filtered through a fritted funnel, and concentrated *in vacuo*. The crude residue was purified by flash column chromatography (silica gel) to give the desired product. The procedure to synthesize each compound was carried out at least 2 times. The average yield was reported.



C5-*p*-F-Bn-1,2-azaborine (2.25).

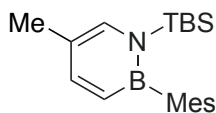
According to general procedure B (1.0 equiv. of *p*-F-Bn-Br was used), the product was purified by flash column chromatography (silica gel; 100% hexane) to give the desired product as a colorless solid with an average yield of 82% (first batch: 116.3 mg, 81%; second batch: 119.2 mg, 83%). **¹H NMR** (CDCl₃, 600 MHz) δ 7.44 (dd, *J* = 11.1, 1.8 Hz, 1H), 7.17 (dd, *J* = 8.4, 5.6 Hz, 2H), 7.12 (d, *J* = 1.7 Hz, 1H), 7.01 (t, *J* = 8.7 Hz, 2H), 6.79 (s, 2H), 6.62 (d, *J* = 11.1 Hz, 1H), 3.79 (s, 2H), 2.30 (s, 3H), 2.09 (s, 6H), 0.85 (s, 9H), -0.03 (s, 6H); **¹³C NMR** (CDCl₃, 151 MHz) δ 161.58 (d, ¹*J*_{CF} = 243.8 Hz), 145.0, 139.0, 136.98 (d, ⁴*J*_{CF} = 3.0 Hz), 136.9, 136.5, 130.43 (d, ³*J*_{CF} = 8.0 Hz), 127.0, 122.8, 115.3 (d, ²*J*_{CF} = 20.8 Hz), 39.1, 27.6, 23.6, 21.3, 19.2, -3.2 (the signals for the two carbons adjacent to boron were not observed); **¹¹B NMR** (CDCl₃, 160 MHz) δ 39.6; **¹⁹F NMR** (CDCl₃, 470 MHz) δ -117.5 (m); **IR** 2959, 2929, 2858, 1622, 1507, 1448, 1264, 1223, 1123, 849, 836, 805, 784 cm⁻¹; **HRMS** (DART) calcd. for C₂₆H₃₆BNFSi [M+H⁺]: 420.26886, found 420.26942.



C5-(6-methylpyridin-2-yl)methyl-1,2-azaborine (2.26).

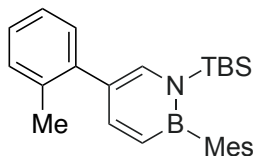
According to general procedure B (1.0 equiv. of 2-(bromomethyl)-6-Me-pyridine was used), the product was purified by flash column chromatography (silica gel; 20 – 33%

of diethyl ether in hexane) to give the desired product as a pale yellow solid with an average yield of 67% (first batch: 101.6 mg, 71%; second batch: 90.1 mg, 63%). **¹H NMR** (CDCl₃, 600 MHz) δ 7.55 – 7.46 (m, 2H), 7.22 (s, 1H), 7.00 (d, *J* = 7.6 Hz, 1H), 6.92 (d, *J* = 7.7 Hz, 1H), 6.78 (s, 2H), 6.62 (d, *J* = 11.1 Hz, 1H), 3.98 (s, 2H), 2.57 (s, 3H), 2.29 (s, 3H), 2.08 (s, 6H), 0.84 (s, 9H), -0.03 (s, 6H); **¹³C NMR** (CDCl₃, 126 MHz) δ 160.7, 157.9, 145.3, 139.0, 137.4, 137.0, 136.4, 126.9, 121.5, 120.8, 120.1, 42.4, 27.5, 24.5, 23.6, 21.3, 19.2, -3.2 (the signals for the two carbons adjacent to boron were not observed); **¹¹B NMR** (CDCl₃, 160 MHz) δ 39.5; **IR** 2961, 2927, 2857, 1621, 1577, 1501, 1452, 1378, 1265, 1186, 1123, 834, 787 cm⁻¹; **HRMS** (DART) calcd. for C₂₆H₃₈BN₂Si [M+H⁺]: 417.28918, found 417.29033.



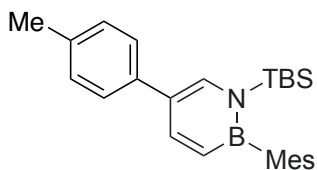
C5-methyl-1,2-azaborine (2.33).

According to general procedure B (5.0 equiv. of Me-I was used), the product was purified by flash column chromatography (silica gel; 0 – 2% of diethyl ether in hexane) to give the desired product as a colorless solid with an average yield of 90% (first batch: 101.0 mg, 90%; second batch: 109.7 mg, 90%). **¹H NMR** (CDCl₃, 600 MHz) δ 7.47 (d, *J* = 11.0 Hz, 1H), 7.22 (s, 1H), 6.79 (s, 2H), 6.59 (d, *J* = 11.1 Hz, 1H), 2.30 (s, 3H), 2.17 (d, *J* = 1.0 Hz, 3H), 2.09 (s, 6H), 0.92 (s, 9H), 0.00 (s, 6H); **¹³C NMR** (CDCl₃, 126 MHz) δ 145.8, 139.0, 136.4, 135.9, 127.0, 119.0, 27.6, 23.6, 21.3, 19.3, 19.2, -3.1 (the signals for the two carbons adjacent to boron were not observed); **¹¹B NMR** (CDCl₃, 160 MHz) δ 38.3; **IR** 2960, 2928, 2859, 1625, 1504, 1438, 1370, 1264, 1188, 1126, 829, 801, 783 cm⁻¹; **HRMS** (DART) calcd. for C₂₀H₃₃BNSi [M+H⁺]: 326.24698, found 326.24791.



C5-*o*-Tolyl-1,2-azaborine (2.28).

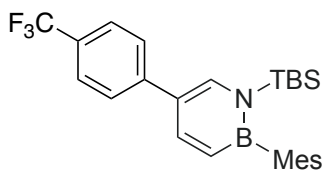
According to general procedure C, the product was purified by flash column chromatography (silica gel; 100% hexane) to give the desired product as a white solid with an average yield of 93% (first batch: 117.5 mg, 94%; second batch: 115.0 mg, 92%). ^1H NMR (CDCl_3 , 500 MHz) δ 7.59 (dd, $J = 11.0, 1.6$ Hz, 1H), 7.39 (d, $J = 1.6$ Hz, 1H), 7.29 (m, 4H), 6.84 (s, 2H), 6.70 (d, $J = 11.1$ Hz, 1H), 2.33 (s, 3H), 2.32 (s, 3H), 2.17 (s, 6H), 0.94 (d, $J = 1.0$ Hz, 9H), 0.04 (d, $J = 0.9$ Hz, 6H); ^{13}C NMR (CDCl_3 , 126 MHz) δ 145.2, 141.0, 139.0, 137.7, 136.6, 136.4, 130.4, 130.2, 127.0, 127.0, 125.9, 125.4, 27.7, 23.6, 21.4, 20.8, 19.3, -3.0 (the signals for the two carbons adjacent to boron were not observed); ^{11}B NMR (CDCl_3 , 160 MHz) δ 39.2; IR 2960, 2929, 2859, 1736, 1612, 1489, , 1359, 1264, 1125, 1001, 824, 787, 739 cm^{-1} ; HRMS (DART) calcd. for $\text{C}_{26}\text{H}_{37}\text{BNSi}$ [$\text{M}+\text{H}^+$]: 402.27828, found 402.27961.



C5-*p*-Tolyl-1,2-azaborine (2.29).

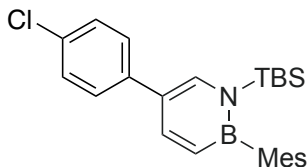
According to general procedure C, the product was purified by flash column chromatography (silica gel; 100% hexane) to give the desired product as a white solid with an average yield of 92% (first batch: 116.3 mg, 93%; second batch: 113.8 mg, 91%). ^1H NMR (CDCl_3 , 500 MHz) δ 7.94 (dd, $J = 11.2, 1.8$ Hz, 1H), 7.74 (d, $J = 1.8$ Hz, 1H), 7.46

(d, $J = 8.0$ Hz, 2H), 7.30 (d, $J = 7.8$ Hz, 2H), 6.89 (s, 2H), 6.82 (d, $J = 11.2$ Hz, 1H), 2.46 (s, 3H), 2.38 (s, 3H), 2.21 (s, 6H), 1.04 (s, 9H), 0.12 (s, 6H); ^{13}C NMR (CDCl₃, 126 MHz) δ 143.5, 139.0, 138.0, 136.8, 136.6, 135.9, 129.6, 127.0, 126.4, 125.0, 27.7, 23.6, 21.4, 21.3, 19.4, -3.0 (the signals for the two carbons adjacent to boron were not observed); ^{11}B NMR (CDCl₃, 160 MHz) δ 39.3; IR 2960, 2928, 2860, 1614, 1493, 1361, 1264, 1129, 1001, 825, 787, 740 cm⁻¹; HRMS (DART) calcd. for C₂₆H₃₇BNSi [M+H⁺]: 402.27828, found 402.27811.



C5-*p*-CF₃-phenyl-1,2-azaborine (2.30).

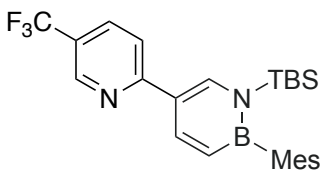
According to general procedure C, the product was purified by flash column chromatography (silica gel; 100% hexane) to give the desired product as a colorless oil with an average yield of 89% (first batch: 137.0 mg, 87%; second batch: 142.0 mg, 91%). ^1H NMR (CDCl₃, 600 MHz) δ 7.88 (dd, $J = 11.3, 1.8$ Hz, 1H), 7.74 (d, $J = 1.8$ Hz, 1H), 7.68 (d, $J = 8.1$ Hz, 2H), 7.60 (d, $J = 8.1$ Hz, 2H), 6.83 (s, 2H), 6.80 (d, $J = 11.2$ Hz, 1H), 2.32 (s, 3H), 2.13 (s, 6H), 0.98 (s, 9H), 0.08 (s, 6H); ^{13}C NMR (CDCl₃, 151 MHz) δ 144.5, 142.8, 139.0, 138.0, 136.9, 128.4 (q, $^2J_{\text{CF}} = 32.4$ Hz), 127.1, 126.6, 125.8 (q, $^3J_{\text{CF}} = 3.8$ Hz), 124.6 (q, $^1J_{\text{CF}} = 298.4$ Hz), 123.9, 27.6, 23.6, 21.4, 19.4, -3.0 (the signals for the two carbons adjacent to boron were not observed); ^{11}B NMR (CDCl₃, 160 MHz) δ 39.4; ^{19}F NMR (CDCl₃, 470 MHz) δ -63.0 (m); IR 2959, 2930, 2858, 1613, 1326, 1263, 1128, 1000, 843, 822, 741 cm⁻¹; HRMS (DART) calcd. for C₂₆H₃₄BNF₃Si [M+H⁺]: 456.25002, found 456.24968.



C5-*p*-Cl-phenyl-1,2-azaborine (2.31).

According to general procedure C, the product was purified by flash column chromatography (silica gel; 100% hexane) to give the desired product as a pale yellow solid with an average yield of 87% (first batch: 123.9 mg, 87%; second batch: 122.4 mg, 86%).

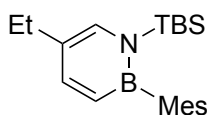
¹H NMR (CDCl₃, 600 MHz) δ 7.83 (dd, *J* = 11.2, 1.9 Hz, 1H), 7.65 (d, *J* = 1.8 Hz, 1H), 7.49 – 7.31 (m, 4H), 6.82 (s, 2H), 6.76 (d, *J* = 11.2 Hz, 1H), 2.31 (s, 3H), 2.12 (s, 6H), 0.97 (s, 9H), 0.06 (s, 6H); **¹³C NMR** (CDCl₃, 151 MHz) δ 143.04, 139.38, 138.97, 137.24, 136.76, 132.28, 129.05, 127.77, 127.09, 124.04, 27.66, 23.62, 21.35, 19.36, -3.04 (the signals for the two carbons adjacent to boron were not observed); **¹¹B NMR** (CDCl₃, 160 MHz) δ 40.1; **IR** 2960, 2928, 2857, 1613, 1492, 1446, 1263, 1094, 999, 822, 740 cm⁻¹; **HRMS** (DART) calcd. for C₂₆H₃₄BNSiCl [M+H⁺]: 422.22366, found 422.22320.



C5-(5-CF₃-pyridin-2-yl)-1,2-azaborine (2.32).

According to general procedure C, the product was purified by flash column chromatography (silica gel; 5% diethyl ether in hexane) to give the desired product as a light yellow solid with an average yield of 83% (first batch: 136.5 mg, 87%; second batch: 124.0 mg, 79%). **¹H NMR** (CDCl₃, 500 MHz) δ 8.87 (dt, *J* = 2.5, 0.9 Hz, 1H), 8.54

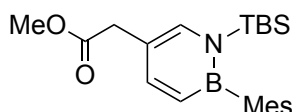
(d, $J = 1.8$ Hz, 1H), 8.20 (dd, $J = 11.4, 1.8$ Hz, 1H), 7.91 (ddd, $J = 8.4, 2.5, 0.8$ Hz, 1H), 7.68 (dt, $J = 8.5, 0.8$ Hz, 1H), 6.84 – 6.74 (m, 3H), 2.31 (s, 3H), 2.12 (s, 6H), 0.97 (s, 9H), 0.09 (s, 6H); $^{13}\text{C NMR}$ (CDCl_3 , 151 MHz) δ 160.7, 146.7 (q, $^3J_{\text{CF}} = 4.1$ Hz), 141.2, 138.9, 136.9, 133.8 (q, $^4J_{\text{CF}} = 3.5$ Hz), 127.1, 124.1 (q, $^1J_{\text{CF}} = 271.8$ Hz), 123.5 (q, $^2J_{\text{CF}} = 32.9$ Hz), 122.4, 118.0, 27.5, 23.5, 21.4, 19.2, -3.1 (the signals for the two carbons adjacent to boron were not observed); $^{11}\text{B NMR}$ (CDCl_3 , 160 MHz) δ 40.2; $^{19}\text{F NMR}$ (CDCl_3 , 470 MHz) δ -62.1 (m); **IR** 2959, 2930, 2861, 1738, 1505, 1328, 1305, 1266, 1131, 1084, 1005, 840, 822 cm^{-1} ; **HRMS** (DART) calcd. for $\text{C}_{25}\text{H}_{33}\text{BN}_2\text{F}_3\text{Si}$ [$\text{M}+\text{H}^+$]: 457.24527, found 457.24393.



C5-ethyl-1,2-azaborine (2.34).

Step 1: According to general procedure C (4.0 equiv. of vinyl-Br was used), the C5-vinyl precursor was purified by flash column chromatography (silica gel; 5% dichloromethane in hexane) to give a colorless oil. Step 2: To a 20 ml vial with a stir bar, C5 vinyl *N*-TBS-*B*-Mes azaborine precursor was added together with Pd/C (5 mol % Pd). The vial was vacuumed and recharged with H_2 balloon before 2.0 mL of dichloromethane was added as solvent. The mixture was allowed to be stirred at room temperature for 2 hours. The crude mixture was then filtered and concentrated *in vacuo*. The crude residue was purified by flash column chromatography (silica gel; 100% hexane) to afford the desired product as a white solid (average yield over two steps was 72%). $^1\text{H NMR}$ (CDCl_3 , 600 MHz) δ 7.51 (dd, $J = 11.0, 1.7$ Hz, 1H), 7.23 (d, $J = 1.8$ Hz, 1H), 6.80 (s, 2H), 6.61 (d, $J = 11.0$ Hz, 1H), 2.49 (q, $J = 7.5$ Hz, 2H), 2.30 (s, 3H), 2.10 (s, 6H), 1.22 (t, $J = 7.5$ Hz,

3H), 0.93 (s, 9H), 0.01 (s, 6H); ^{13}C NMR (CDCl_3 , 151 MHz) δ 144.9, 139.1, 136.4, 135.3, 127.0, 125.4, 27.7, 27.0, 23.6, 21.3, 19.4, 15.8, -3.1 (the signals for the two carbons adjacent to boron were not observed); ^{11}B NMR (CDCl_3 , 160 MHz) δ 39.4; IR 2961, 2930, 2853, 1622, 1609, 1502, 1472, 1362, 1264, 1008, 839, 825, 799 cm^{-1} ; HRMS (DART) calcd. for $\text{C}_{21}\text{H}_{35}\text{BNSi}$ [$\text{M}+\text{H}^+$]: 340.26263, found 340.26285.

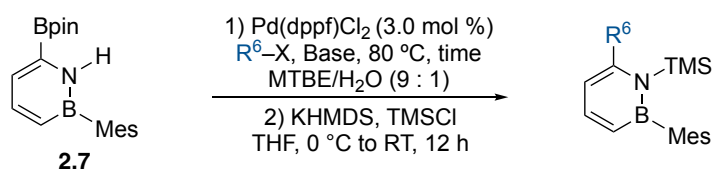


C5-ester-1,2-azaborine (2.27).

Slight modification of the procedure reported by Gooßen¹¹⁷: Inside a drybox, a 10 mL pressure vessel was charged with a magnetic stir bar, **2.12** (1.0 equiv., 150.0 mg, 0.343 mmol), methyl-2-bromoacetate (1.0 equiv., 52.5 mg, 0.343 mmol), $\text{Pd}(\text{OAc})_2$ (3.0 mol %, 2.3 mg, 10.3 μmol) and tri(*o*-tolyl)phosphine (9.0 mol%, 9.4 mg, 30.9 μmol). $\text{K}_3\text{PO}_4 \cdot \text{H}_2\text{O}$ (4.0 equiv., 316.0 mg, 1.37 mmol) was dissolved in 0.5 mL of H_2O (degassed by sparging with N_2 for 30 minutes before use) and was added into the pressure vessel with 3.0 mL of THF (total 3.5 mL of a 6 : 1 v : v mix of THF : H_2O was used as solvent). The reaction was sealed and heated at 60 °C for 16 hours. After cooling, 4 mL of water was added into the reaction mixture and the aqueous phase was extracted 3 x 4 mL with ethyl acetate; the combined organic extracts were washed with brine and dried over MgSO_4 , vacuum-filtered through a fritted funnel, and concentrated *in vacuo*. The crude residue was purified by flash column chromatography (silica gel; 5% diethyl ether in hexane) to give the desired product as a colorless oil with an average yield of 61%. (first batch: 85.5 mg, 65%; second batch: 75.0 mg, 57%). ^1H NMR (CDCl_3 , 500 MHz) δ 7.54 (d, $J = 11.1$ Hz, 1H), 7.38 (s, 1H), 6.81 (s, 2H), 6.66 (d, $J = 11.1$ Hz, 1H), 3.73 (s, 3H), 3.47 (s, 2H), 2.31 (s, 3H), 2.11 (s, 6H),

0.94 (s, 9H), 0.03 (s, 6H). ^{13}C NMR (CDCl_3 , 126 MHz) δ 172.7, 144.8, 139.0, 137.8, 136.6, 127.0, 116.5, 52.0, 39.2, 27.5, 23.5, 21.3, 19.2, -3.2 (the signals for the two carbons adjacent to boron were not observed); ^{11}B NMR (CDCl_3 , 160 MHz) δ 39.6; IR 2955, 2931, 2859, 1741, 1623, 1502, 1449, 1379, 1265, 1187, 1009, 934, 847, 836, 785 cm^{-1} ; HRMS (DART) calcd. for $\text{C}_{22}\text{H}_{35}\text{BNO}_2\text{Si}$ [$\text{M}+\text{H}^+$]: 384.25863, found 384.25856.

Synthesis of C6-Substituted Compounds **2.35**, **2.36**, **2.37** via Suzuki Cross-coupling

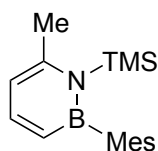


General Procedure D:

Step 1: Inside a drybox, a 10 mL pressure vessel was charged with a magnetic stir bar, **2.7** (1.0 equiv., 161.5 mg, 0.500 mmol), R^6 -halide (x equiv.), $\text{Pd}(\text{dppf})\text{Cl}_2$ (3.0 mol %, 12.2 mg, 15.0 μmol). Base (4.0 equiv.) was dissolved in 0.6 mL of H_2O (degassed by sparging with N_2 for 30 minutes before use) and was added into the pressure vessel with 5.4 mL of MTBE (total 6.0 mL of a 9 : 1 v : v mix of MTBE : H_2O was used as solvent). The reaction was sealed and heated at 80 °C for 3.5 to 6 hours. After cooling, 5 mL of water was added into the reaction mixture and the aqueous phase was extracted 3 x 5 mL with diethyl ether; the combined organic extracts were washed with brine and dried over MgSO_4 , vacuum-filtered through a fritted funnel, and concentrated *in vacuo*. The crude residue was purified by flash column chromatography (silica gel) to give the precursor.

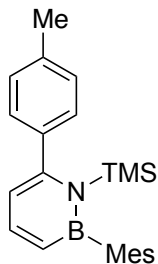
Step 2: A 20 mL scintillation vial was charged with the C6-substituted N-H precursor and 3.0 mL of THF. The solution was cooled down to 0 °C before 2.0 equiv. of KHMDS (0.5 M in toluene) was added via syringe dropwise with N_2 flow. The reaction mixture was

warmed up to room temperature and stirred for additional 30 minutes before 10.0 equiv. of TMSCl in THF solution was added in one portion. The reaction was allowed to be stirred at room temperature for 12 hours. Upon completion, the solvent was removed and the crude was purified by flash column chromatography (silica gel) to give the desired product. Procedure to synthesize each compound was carried out at least 2 times. The average yield over two-step sequence was reported.



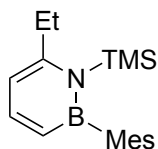
C6-methyl-1,2-azaborine (2.35).

According to general procedure D (For step 1: 4.5 equiv. of Me-I was used as electrophile; 4.0 equiv. of $K_3PO_4 \cdot H_2O$ was used as base; reaction took 6 hours), after TMS protection, the crude was purified by flash column chromatography (silica gel; 100% hexane) to give the desired product as a white solid with an average yield of 74% over two steps. 1H NMR ($CDCl_3$, 500 MHz) δ 7.45 (dd, $J = 10.9, 6.5$ Hz, 1H), 6.78 (s, 2H), 6.40 (d, $J = 10.9$ Hz, 1H), 6.26 (d, $J = 6.5$ Hz, 1H), 2.55 (s, 3H), 2.29 (s, 3H), 2.09 (s, 6H), 0.16 (s, 9H); ^{13}C NMR ($CDCl_3$, 126 MHz) δ 146.8, 143.4, 138.6, 136.3, 127.0, 114.8, 25.2, 23.5, 21.3, 4.8 (the signals for the two carbons adjacent to boron were not observed); ^{11}B NMR ($CDCl_3$, 160 MHz) δ 40.6; IR 2974, 2915, 2853, 1601, 1520, 1446, 1400, 1258, 1155, 1088, 845, 802, 764 cm^{-1} ; HRMS (DART) calcd. for $C_{17}H_{27}BNSi$ $[M+H^+]$: 284.20003, found 340.20003.



C6-*p*-tolyl-1,2-azaborine (2.36).

According to general procedure D (For step 1: 1.0 equiv. of TolyI–Br was used as electrophile; 4.0 equiv. of KOH was used as base; reaction took 3.5 hours), after TMS protection, the crude was purified by flash column chromatography (silica gel; 100% hexane) to give the desired product as a white solid with an average yield of 70% over two steps. $^1\text{H NMR}$ (CDCl_3 , 500 MHz *d*) δ 7.56 (dd, $J = 10.9, 6.5$ Hz, 1H), 7.32 (d, $J = 7.9$ Hz, 2H), 7.20 (d, $J = 7.8$ Hz, 2H), 6.85 (s, 2H), 6.63 (d, $J = 10.9$ Hz, 1H), 6.30 (d, $J = 6.5$ Hz, 1H), 2.41 (s, 3H), 2.31 (s, 3H), 2.26 (s, 6H), -0.15 (s, 9H); $^{13}\text{C NMR}$ (CDCl_3 , 126 MHz) δ 152.5, 142.8, 140.9, 139.7, 138.0, 137.0, 129.3, 128.7, 127.4, 116.1, 29.9, 24.0, 21.4, 4.6 (the signals for the two carbons adjacent to boron were not observed); $^{11}\text{B NMR}$ (CDCl_3 , 160 MHz) δ 42.0; **IR** 2960, 2930, 2859, 1731, 1613, 1445, 1392, 1264, 1155, 1018, 840, 808, 762 cm^{-1} ; **HRMS** (DART) calcd. for $\text{C}_{23}\text{H}_{31}\text{BNSi}$ $[\text{M}+\text{H}^+]$: 360.22773, found 360.22693.

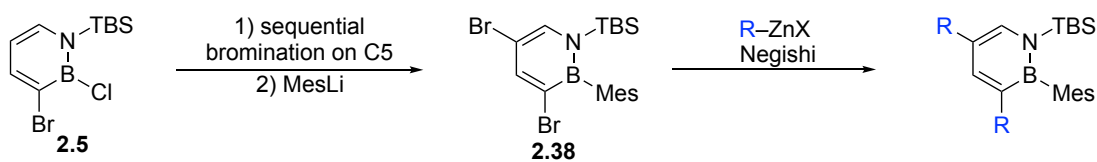


C6-ethyl-1,2-azaborine (2.37).

According to general procedure D (For Suzuki: 5.0 equiv. of vinyl–Br was used as electrophile; 4.0 equiv. of KOH was used as base; reaction took 3.5 hours), after hydrogenation followed by TMS protection, the crude was purified by flash column chromatography (silica gel; 100% hexane) to give the desired product as a white solid with an average yield of 68% over three steps. $^1\text{H NMR}$ (CDCl_3 , 500 MHz) δ 7.52 (dd, $J = 10.8$, 6.6 Hz, 1H), 6.80 (s, 2H), 6.42 (d, $J = 10.8$ Hz, 1H), 6.33 (d, $J = 6.7$ Hz, 1H), 2.87 (q, $J = 7.3$ Hz, 2H), 2.30 (s, 3H), 2.12 (s, 6H), 1.29 (t, $J = 7.8$ Hz, 3H), 0.15 (d, $J = 0.8$ Hz, 9H); $^{13}\text{C NMR}$ (CDCl_3 , 126 MHz) δ 153.5, 143.4, 138.7, 136.4, 127.1, 112.6, 30.0, 23.5, 21.3, 16.1, 4.7 (the signals for the two carbons adjacent to boron were not observed); $^{11}\text{B NMR}$ (CDCl_3 , 160 MHz) δ 40.5; **IR** 2959, 2923, 2851, 1603, 1520, 1455, 1402, 1371, 1258, 1092, 1048, 846, 801, 770 cm^{-1} ; **HRMS** (DART) calcd. for $\text{C}_{18}\text{H}_{29}\text{BNSi}$ [$\text{M}+\text{H}^+$]: 298.21568, found 298.21724.

Procedures for Synthesis of C3,C5-Di-Substituted Compounds 2.40–2.43

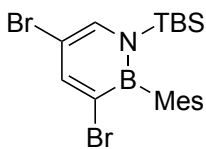
General Procedure E: Introduction of Same Substituent on C3 and C5 (substrates **2.40**, **2.41**)



Sequential bromination and MesLi substitution: In a glovebox, a 50 mL RBF was charged with a stir bar, C3-Br *N*-TBS-*B*-Cl 1,2-azaborine **2.5** (1.0 equiv. 350.0 mg, 1.14 mmol) and dichloromethane (6.0 mL). And the flask was transferred to fume hood and cooled down to -78 °C in dry ice/acetone bath. To a separate 20 mL vial charged with N_2 , elemental bromine (1.2 equiv., 219.0 mg, 70.0 μL , 1.71 mmol) was added into 4 mL dichloromethane. The bromine dichloromethane solution was then added dropwise by

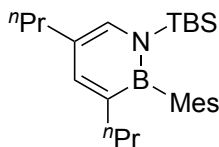
syringe into the stirring **2.5** solution at $-78\text{ }^{\circ}\text{C}$. Upon the completion of addition, the reaction mixture was allowed to warm up to room temperature while stirring for additional 2 hours. The mixture was then concentrated under reduced pressure. The RBF was brought into N₂ glove box and MesLi (3.5 equiv., 504.0 mg) and 10 mL Et₂O was added. The mixture was stirred at room temperature for 3 hours and then quenched with H₂O and extracted three times with Et₂O. The combined organic layer was washed with brine, and then dried over MgSO₄. The mixture was vacuum-filtered through a fritted funnel, and concentrated *in vacuo*. The crude residue was purified by flash column chromatography (silica gel; 0 – 1% diethyl ether in hexane) to obtain the desired product **2.38** as a brown oil (226.8 mg, 42%).

Negishi cross-coupling: in N₂ glovebox, to a 20 ml scintillation vial with a magnetic stir bar was charged with C3,C5-*di*-bromo precursor **2.38** (1.0 equiv., 150.0 mg, 0.320 mmol) and Pd(*t*-Bu₃P)₂ catalyst (5.0 mol %, 8.2 mg, 16.0 μmol), and 2.0 mL of THF was added. The mixture was stirred for 5 minutes before adding 2.0 mL of organo-zinc reagent R–ZnX (3.1 equiv., 1.00 mmol, 0.5 M in THF) solution. The reaction was allowed to be stirred at room temperature for 12 hours. At this point, 1.0 mL CH₂Cl₂ was added to quench the reaction. The solids were filtered off and the filtrate was concentrated *in vacuo*. The crude residue was purified by flash column chromatograph (silica gel) to give the desired product.



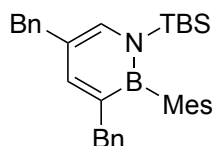
C3,C5-*di*-Br-1,2-azaborine (2.38).

According to general procedure E, the desired product **2.38** was obtained as a brown oil (226.8 mg, 42%). **¹H NMR** (CDCl₃, 500 MHz) δ 7.99 (s, 1H), 7.57 (s, 1H), 6.79 (s, 2H), 2.30 (s, 3H), 2.06 (s, 6H), 0.93 (s, 9H), -0.00 (s, 6H); **¹³C NMR** (CDCl₃, 126 MHz) δ 147.0, 139.0, 137.9, 137.5, 127.2, 104.6, 27.5, 22.9, 21.5, 19.4, -3.1 (the signals for the two carbons adjacent to boron were not observed); **¹¹B NMR** (CDCl₃, 160 MHz) δ 39.0; **IR** 2960, 2931, 2860, 1609, 1588, 1472, 1401, 1375, 1314, 1129, 1072, 1006, 975, 872, 839, 820, 790, 751 cm⁻¹; **HRMS** (DART) calcd. for C₁₉H₂₉BNSiBr₂ [M+H⁺]: 468.05236, found 468.05249.



C3,C5-di-*n*propyl-1,2-azaborine (2.40).

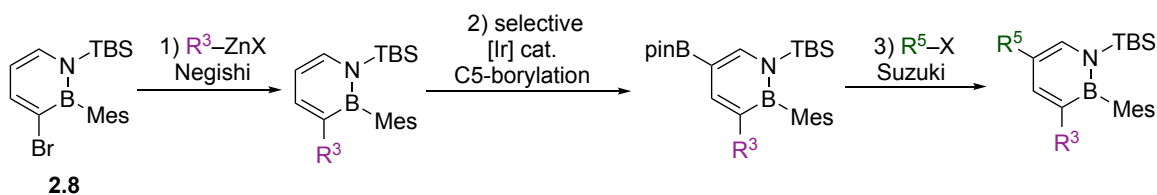
According to general procedure E (*n*Pr-ZnBr 0.5 M in THF was used as R-ZnX organozinc reagent), the crude was purified by flash column chromatography (silica gel; 100% hexane) to give the desired product as a colorless oil (98.0 mg, 77%) **¹H NMR** (CDCl₃, 500 MHz) δ 7.23 (s, 1H), 7.06 (s, 1H), 6.76 (s, 2H), 2.40 (t, 13.0 Hz, 2H), 2.29 (s, 3H), 2.08 (t, 14.7 Hz, 2H), 2.04 (s, 6H), 1.60 (m, 2H), 1.30 (m, 2H), 0.95 (t, *J* = 7.3 Hz, 3H), 0.92 (s, 9H), 0.77 (t, *J* = 7.3 Hz, 3H), -0.05 (s, 6H); **¹³C NMR** (CDCl₃, 126 MHz) δ 142.1, 139.0, 136.0, 133.4, 126.9, 123.3, 37.0, 36.3, 27.9, 24.4, 23.4, 23.3, 21.4, 19.4, 14.31, 14.0, -2.9 (the signals for the two carbons adjacent to boron were not observed); **¹¹B NMR** (CDCl₃, 160 MHz) δ 39.5; **IR** 2958, 2929, 2860, 1624, 1609, 1518, 1472, 1402, 1374, 1278, 1263, 1167, 1148, 848, 784 cm⁻¹; **HRMS** (DART) calcd. for C₂₅H₄₃BNSi [M+H⁺]: 396.32523, found 396.32536.

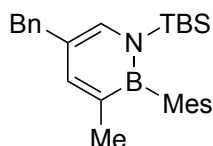


C3,C5-*di*-benzyl-1,2-azaborine (2.41).

According to general procedure E (Bn-ZnBr 0.5 M in THF was used as R-ZnX organozinc reagent), the crude was purified by flash column chromatography (silica gel; 100% hexane) to give the desired product as a white solid (106.0 mg, 69%) ^1H NMR (CDCl₃, 600 MHz) δ 7.32 – 7.29 (m, 2H), 7.23 – 7.16 (m, 4H), 7.10 – 7.06 (m, 3H), 6.94 (s, 1H), 6.79 – 6.74 (m, 2H), 6.71 (s, 2H), 3.78 (s, 2H), 3.38 (s, 2H), 2.29 (s, 3H), 1.85 (s, 6H), 0.80 (s, 9H), -0.12 (s, 6H); ^{13}C NMR (CDCl₃, 126 MHz) δ 143.3, 142.2, 141.3, 139.1, 136.3, 135.2, 129.4, 129.2, 128.5, 127.8, 127.0, 126.1, 125.2, 122.6, 41.6, 39.9, 27.7, 23.0, 21.4, 19.3, -2.9 (the signals for the two carbons adjacent to boron were not observed); ^{11}B NMR (CDCl₃, 160 MHz) δ 39.5; IR 2959, 2929, 2858, 1625, 1608, 1518, 1493, 1472, 1362, 1279, 1264, 1164, 1145, 830, 784, 719 cm⁻¹; HRMS (DART) calcd. for C₃₃H₄₃BNSi [M+H⁺]: 492.32523, found 492.32246.

Procedures for the Introduction of Different Substituents on C3 and C5 (substrates **2.42**, **2.43**)

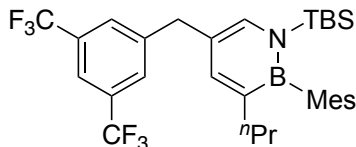




C3-methyl-C5-benzyl-1,2-azaborine (2.42).

Step-1(Introducing C3-substituent first via Negishi cross-coupling): relatively large scale reaction was carried out in adaption to general procedure A, to a 20 mL vial with magnetic stir bar was charged with precursor **2.8** (1.0 equiv., 337.6 mg, 0.865 mmol) and Pd(*t*-Bu₃P)₂ catalyst (5.0 mol %, 22.1 mg, 43.3 μmol), and 3 mL of THF was added. The mixture was stirred for 5 minutes before adding 1.0 mL of dimethyl zinc 1.2 M in toluene (1.5 equiv., 1.20 mmol) solution. The reaction was allowed to be stirred at room temperature for 3 hours. After work-up, the crude residue was purified by flash column chromatography (silica gel; 100% hexane) to give the C3-methyl-1,2-azaborine precursor as a colorless oil (239.0 mg, 86%). **Step-2** (Iridium catalyzed selective borylation at C5): in adaption to the reported procedure¹¹¹, a 10 mL pressure vessel was charged with C3-methyl-1,2-azaborine precursor from first step (1.0 equiv., 130.8 mg, 0.402 mmol), [Ir(OMe)(cod)]₂ (2.0 mol %, 5.3 mg, 8.0 μmol), 4,4'-di-*tert*-butyl-2,2'-bipyridine (dtbbpy) (4.0 mol %, 4.3 mg, 16.1 μmol), bis(pinacolato)diboron (B₂pin₂) (1.2 equiv., 122.5 mg, 0.482 mmol) and MTBE (2.0 mL). The reaction vessel was sealed and the reaction mixture was transferred to a fume hood before heated at 80 °C for 12 hours. After cooling, volatiles were removed under reduced pressure and the crude residue was purified by flash column chromatography (silica gel; 0 –10 % dichloromethane in hexane) to give the desired C3-methyl-C5-Bpin product as a colorless solid (135.8 mg, 75%). **Step-3** (Introducing C5-substituent via Suzuki cross-coupling): in adaption of general procedure B, a 10 mL

pressure vessel was charged with a magnetic stir bar, C3-methyl-C5-Bpin-1,2-azaborine precursor (1.0 equiv., 200.0 mg, 0.417 mmol), benzyl-bromide (1.0 equiv., 75.8 mg, 0.443 mmol), Pd(dppf)Cl₂ (3.0 mol %, 10.9 mg, 13.3 μmol). K₃PO₄·H₂O (4.0 equiv., 408.0 mg, 1.77 mmol) was dissolved in 0.6 mL of H₂O (degassed by sparging with N₂ for 30 minutes before use) and was added into the pressure vessel with 5.4 mL of MTBE (total 6.0 mL of a 9 : 1 v : v mix of MTBE : H₂O was used as solvent). The reaction was sealed and heated at 80 °C for 6 hours. After work-up, the crude residue was purified by flash column chromatography (silica gel; 0 – 2% diethyl ether in hexane) to give the desired product **2.42** as a colorless solid (101.3 mg, 55%). ¹H NMR (CDCl₃, 500 MHz) δ 7.34 – 7.26 (m, 2H), 7.24 – 7.19 (m, 4H), 6.96 (s, 1H), 6.76 (s, 2H), 3.78 (s, 2H), 2.28 (s, 3H), 2.03 (s, 6H), 1.75 (s, 3H), 0.84 (s, 9H), -0.09 (s, 6H); ¹³C NMR (CDCl₃, 126 MHz) δ 142.8, 141.5, 138.7, 136.2, 134.4, 129.2, 128.5, 127.0, 126.1, 122.6, 40.0, 27.7, 22.9, 21.7, 21.4, 19.3, -3.0 (the signals for the two carbons adjacent to boron were not observed); ¹¹B NMR CDCl₃, 160 MHz) δ 39.5; IR 2958, 2930, 2857, 1625, 1541, 1473, 1455, 1281, 1263, 1164, 1110, 828, 784 cm⁻¹; HRMS (DART) calcd. for C₂₇H₃₉BNSi [M+H⁺]: 416.29393, found 416.29405.



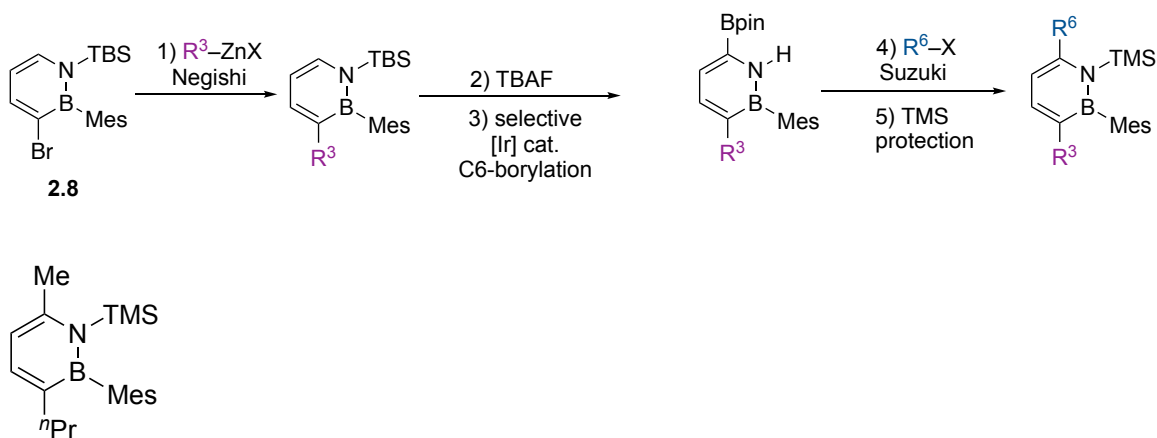
C3-propyl-C5-(3,5-bis-CF₃-benzyl)-1,2-azaborine (**2.43**).

Step-1(Introducing C3-substituent first via Negishi cross-coupling): relatively large scale reaction was carried out in adaption to general procedure A, to a 100 mL RBF with magnetic stir bar was charged with precursor **2.8** (1.0 equiv., 940.0 mg, 2.41 mmol) and Pd(*t*-Bu₃P)₂ catalyst (5.0 mol %, 61.5 mg, 0.120 mmol), and 7.8 mL of THF was added.

The mixture was stirred for 5 minutes before adding 7.2 mL of ⁿPr–ZnBr 0.5 M in THF (1.5 equiv., 3.60 mmol) solution. The reaction was allowed to be stirred at room temperature for 3 hours. After work-up, the crude residue was purified by flash column chromatograph (silica gel; 100% hexane) to give the C3-propyl-1,2-azaborine product **2.20** as a colorless oil (627.0 mg, 73%). **Step-2** (Iridium catalyzed selective borylation at C5): in adaption to the reported procedure¹¹¹, a 100 mL pressure vessel was charged with **2.20** from first step (1.0 equiv., 367.0 mg, 1.04 mmol), [Ir(OMe)(cod)]₂ (2.0 mol %, 13.8 mg, 0.034 mmol), 4,4'-di-tert-butyl-2,2'-bipyridine (dtbbpy) (4.0 mol %, 11.2 mg, 0.068 mmol), bis(pinacolato)diboron (B₂pin₂) (2.0 equiv., 527.4 g, 2.08 mmol) and MTBE (25.0 mL). The reaction vessel was sealed and the reaction mixture was transferred to a fume hood before heated at 80 °C for 12 hours. After cooling, volatiles were removed under reduced pressure and the crude residue was purified by flash column chromatography (silica gel; 3% diethyl ether in hexane) to give the desired C5-borylated product as a white solid (430.0 mg, 86%). **Step-3** (Introducing C5-substituent via Suzuki cross-coupling): in adaption of general procedure B, a 10 mL pressure vessel was charged with a magnetic stir bar, C3-propyl-C5-Bpin-1,2-azaborine precursor (1.0 equiv., 200.0 mg, 0.417 mmol), 3,5-bis(trifluoromethyl)benzyl-bromide (1.0 equiv., 128.1 mg, 0.417 mmol), Pd(dppf)Cl₂ (3.0 mol %, 10.2 mg, 12.5 μmol). K₃PO₄·H₂O (4.0 equiv., 384.0 mg, 1.67 mmol) was dissolved in 0.6 mL of H₂O (degassed by sparging with N₂ for 30 minutes before use) and was added into the pressure vessel with 5.4 mL of MTBE (total 6.0 mL of a 9 : 1 v : v mix of MTBE : H₂O was used as solvent). The reaction was sealed and heated at 80 °C for 6 hours. After work-up, the crude residue was purified by flash column chromatography (silica gel; 5 – 7% dichloromethane in hexane) to give the desired product **2.43** as a colorless solid (160.0

mg, 66%). **¹H NMR** (CDCl₃, 600 MHz) δ 7.76 (s, 1H), 7.68 (s, 2H), 7.20 (s, 1H), 6.97 (s, 1H), 6.77 (s, 2H), 3.95 (s, 2H), 2.31 (s, 3H), 2.12 – 2.03 (m, 8H), 1.37 – 1.24 (m, 2H), 0.83 (s, 9H), 0.76 (t, *J* = 7.3 Hz, 3H), -0.07 (s, 6H); **¹³C NMR** (CDCl₃, 151 MHz) δ 146.7, 144.0, 141.4, 138.9, 137.4, 134.3 (q, ²*J*_{CF} = 33.2 Hz), 131.66 (⁴*J*_{CF} = 3.7 Hz), 129.5, 125.9 (q, ¹*J*_{CF} = 272.4 Hz), 123.3, 122.74, 122.73 (q, ³*J*_{CF} = 7.7 Hz), 42.1, 39.4, 30.1, 25.7, 23.9, 21.7, 16.7, -0.6 (the signals for the two carbons adjacent to boron were not observed); **¹¹B NMR** (CDCl₃, 160 MHz) δ 40.1; **¹⁹F NMR** (CDCl₃, 470 MHz) δ -63.0 (m); **IR** 2959, 2931, 2861, 1624, 1374, 1277, 1172, 1136, 839, 825, 786 cm⁻¹; **HRMS** (DART) calcd. for C₃₁H₄₁BNF₆Si [M+H⁺]: 580.30016, found 580.29958.

Procedures for Synthesis of C3, C6-Di-Substituted 1,2-Azaborines 2.44, 2.45

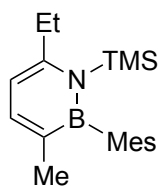


C3-propyl-C6-methyl-1,2-azaborine (2.44).

Step-1 (in adaption to general procedure A to introduce C3-propyl substituent Negishi cross-coupling): to a 100 mL RBF with magnetic stir bar was charged with precursor **2.8** (1.0 equiv., 940.0 mg, 2.41 mmol) and Pd(*t*-Bu₃P)₂ catalyst (5.0 mol %, 61.5 mg, 0.120 mmol), and 7.8 mL of THF was added. The mixture was stirred for 5 minutes before adding 7.2 mL of ⁿPr-ZnBr 0.5 M in THF (1.5 equiv., 3.60 mmol) solution. The

reaction was allowed to be stirred at room temperature for 3 hours. After work-up, the crude residue was purified by flash column chromatograph (silica gel; 100% hexane) to give the C3-propyl-1,2-azaborine product **2.20** as a colorless oil (627.0 mg, 73%). **Step-2** (TBAF deprotection): to a 50 mL RBF with magnetic stir bar was charged with precursor **2.20** (1.0 equiv., 488.0 mg, 1.38 mmol) and 8 mL THF. TBAF trihydrate (1.2 equiv., 522.8 mg, 1.66 mmol) was added and the reaction mixture was stirred at room temperature for 2.5 hours. Upon completion, the crude mixture was concentrated and the residue was purified by flash column chromatography (silica gel; 0 – 7% diethyl ether in hexane) to give the desired C3-propyl-*N*-*H*-*B*-Mes-1,2-azaborine product as a pale yellow oil (309.1 mg, 94%). **Step-3** (Iridium catalyzed selective C6 borylation): in adaption to the reported procedure²⁶, in a N₂ glovebox, a 50 mL round bottom flask containing a magnetic stir bar was charged with *N*-*H* precursor from step-2 (1.0 equiv., 309.1 mg, 1.29 mmol), [Ir(OMe)(cod)]₂ (2.0 mol %, 17.1 mg, 0.026 mmol), 4,4'-di-*tert*-butyl-2,2'-bipyridine (dtbbpy) (4.0 mol %, 13.9 mg, 0.052 mmol), bis(pinacolato)diboron (B₂pin₂) (1.1 equiv., 361.0 g, 1.42 mmol) and MTBE (10.0 mL). The reaction was stirred at room temperature for 2 hours. Upon completion, the volatiles were removed under reduced pressure and the crude residue was purified by flash column chromatography (silica gel; 5 – 10% diethyl ether in hexane) to give the C3-propyl-C6-borylated *N*-*H*-*B*-Mes-1,2-azaborine product as a white solid (281.2 mg, 60%). **Step-4** (Introducing C6-substituent via Suzuki cross-coupling): in adaption of general procedure B, a 10 mL pressure vessel was charged with a magnetic stir bar, C3-propyl-C6-Bpin *N*-*H* precursor from step 3 (1.0 equiv., 281.2 mg, 0.770 mmol), Methyl iodide (4.5 equiv., 216.0 μL, 3.47 mmol), Pd(dppf)Cl₂ (3.0 mol %, 18.9 mg, 23.1 μmol). K₃PO₄•H₂O (4.0 equiv., 709.3 mg, 2.31 mmol) was dissolved in 0.6

mL of H₂O (degassed by sparging with N₂ for 30 minutes before use) and was added into the pressure vessel with 5.4 mL of MTBE (total 6.0 mL of a 9 : 1 v : v mix of MTBE : H₂O was used as solvent). The reaction was sealed and heated at 80 °C for 6 hours. After work-up, the crude residue was purified by flash column chromatography (silica gel; 0 – 2% diethyl ether in hexane) to give the desired product C3-propyl-C6-methyl-*N*-*H*-*B*-Mes-1,2-azaborine as a white solid (168.6 mg, 86%). **Step-5** (TMS protection): to a 20 mL with a magnetic stir bar, C3-propyl-C6-methyl-*N*-*H*-*B*-Mes-1,2-azaborine (1.0 equiv., 105.3 mg, 0.416 mmol) was dissolved in 1.0 mL of THF. The solution was cooled down to 0°C before 1.7 mL of KHMDS 0.5M toluene solution (2.0 equiv., 0.832 mmol) was added dropwise via syringe over 5 minutes. The reaction mixture was gradually warmed up to room temperature while being stirred for addition 1 hour. Then, TMSCl (5.0 equiv., 264.0 μL, 2.08 mmol) was added in one portion and the reaction was allowed to stir at room temperature for three hours. The solvent was removed *in vacuo* and the crude residue was purified by flash column chromatography (silica gel; 100% hexane) to give the desired product **2.44** as a colorless oil (85.8 mg, 63%). **¹H NMR** (CDCl₃, 500 MHz) δ 7.22 (d, *J* = 6.8 Hz, 1H), 6.74 (s, 2H), 6.21 (d, *J* = 6.8 Hz, 1H), 2.52 (s, 3H), 2.29 (s, 3H), 2.03 (s, 6H), 1.99 – 1.92 (t, *J* = 6.7 Hz, 2H), 1.29 – 1.15 (m, 2H), 0.72 (t, *J* = 7.3 Hz, 3H), 0.13 (s, 9H); **¹³C NMR** (CDCl₃, 126 MHz) δ 143.8, 140.6, 138.6, 136.1, 126.9, 114.5, 36.5, 25.0, 23.4, 23.2, 21.4, 14.3, 5.0 (the signals for the two carbons adjacent to boron were not observed); **¹¹B NMR** (CDCl₃, 160 MHz) δ 40.7; **IR** 2956, 2924, 2869, 1606, 1538, 1453, 1372, 1357, 1257, 1159, 1068, 1024, 843, 809, 767 cm⁻¹; **HRMS** (DART) calcd. for C₂₀H₃₃BNSi [M+H⁺]: 326.24698, found 326.24624.



C3-methyl-C6-ethyl-1,2-azaborine (2.45).

Step-1 (in adaption to general procedure A to introduce C3-methyl substituent Negishi cross-coupling): to a 200 mL RBF with magnetic stir bar was charged with precursor **2.8** (1.0 equiv., 2.99 g, 7.66 mmol) and Pd(*t*-Bu₃P)₂ catalyst (5.0 mol %, 195.8 mg, 0.383 mmol), and 25 mL of THF was added. The mixture was stirred for 5 minutes before adding 9.6 mL of dimethyl-Zn 1.2 M in toluene (1.5 equiv., 11.5 mmol) solution. The reaction was allowed to be stirred at room temperature for 3 hours. After work-up, the crude residue was purified by flash column chromatograph (silica gel; 0 – 5% dichloromethane in hexane) to give the C3-methyl-*N*-TBS-1,2-azaborine product as a colorless oil (2.11 g, 85%). **Step-2** (TBAF deprotection): to a 50 mL RBF with magnetic stir bar was charged with C3-methyl-*N*-TBS-1,2-azaborine precursor (1.0 equiv., 764.0 mg, 2.35 mmol) and 10.0 mL THF. TBAF trihydrate (1.2 equiv., 889.0 mg, 2.82 mmol) was added and the reaction mixture was stirred at room temperature for 3 hours. Upon completion, the crude mixture was concentrated and the residue was purified by flash column chromatography (silica gel; 5% dichloromethane in hexane) to give the desired C3-ethyl-*N*-H-*B*-Mes-1,2-azaborine product as a pale yellow oil (408.9 mg, 83%). **Step-3** (Iridium catalyzed selective C6 borylation): in adaption to the reported procedure²⁶, in a N₂ glovebox, a 50 mL round bottom flask containing a magnetic stir bar was charged with *N*-H precursor from step-2 (1.0 equiv., 408.9 mg, 1.94 mmol), [Ir(OMe)(cod)]₂ (2.0 mol %, 25.7 mg, 0.039 mmol), 4,4'-di-*tert*-butyl-2,2'-bipyridine (dtbbpy) (4.0 mol %, 20.8 mg,

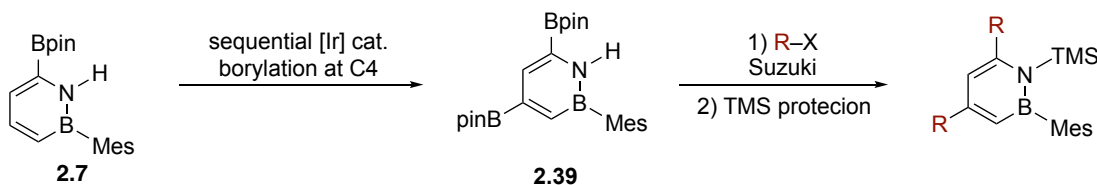
0.078 mmol), bis(pinacolato)diboron (B₂pin₂) (1.2 equiv., 591.2 g, 2.33 mmol) and MTBE (8.0 mL). The reaction was stirred at room temperature for 2 hours. Upon completion, the volatiles were removed under reduced pressure and the crude residue was purified by flash column chromatography (silica gel; 5 – 10% diethyl ether in hexane) to give the C3-methyl-C6-broylated *N*-H-*B*-Mes-1,2-azaborine product as a white solid (625.7 mg, 96%).

Step-4 and 5 (Introducing C6-substituent via Suzuki cross-coupling and hydrogenation): in adaption of general procedure B, a 15 mL pressure vessel was charged with a magnetic stir bar, C3-methyl-C6-Bpin *N*-H precursor from step 3 (1.0 equiv., 333.6 mg, 0.990 mmol), vinyl bromide (2.0 equiv., 198.0 μ L, 1.98 mmol), Pd(dppf)Cl₂ (3.0 mol %, 24.2 mg, 29.5 μ mol). K₃PO₄ · H₂O (4.0 equiv., 911.6 mg, 3.96 mmol) was dissolved in 0.5 mL of H₂O (degassed by sparging with N₂ for 30 minutes before use) and was added into the pressure vessel with 4.5 mL of MTBE (total 5.0 mL of a 9 : 1 v : v mix of MTBE : H₂O was used as solvent). The reaction was sealed and heated at 80 °C for 3.5 hours. After work-up, the crude residue was purified by flash column chromatography (silica gel; 0 – 10% dichloromethane in hexane) to give the desired product C3-methyl-C6-vinyl-*N*-H-*B*-Mes-1,2-azaborine as a colorless oil. The vinyl precursor was added to a 20 mL vial together with 10% wt. Pd/C (5 mol % Pd). The vial was vacuumed and recharged with H₂ balloon before 3.0 mL of dichloromethane was added as solvent. The mixture was allowed to be stirred at room temperature for 2 hours. The crude mixture was then filtered and concentrated *in vacuo*. The crude residue was purified by flash column chromatography (silica gel; 100% hexane) to afford the C3-methyl-C6-ethyl-*N*-H precursor as a colorless oil (140.5 mg, yield over two steps was 60%). **Step-6** (TMS protection): to a 20 mL with a magnetic stir bar, C3-methyl-C6-ethyl-*N*-H-*B*-Mes-1,2-azaborine (1.0 equiv., 140.5 mg,

0.587 mmol) was dissolved in 2.0 mL of THF. The solution was cooled down to 0°C before 1.2 mL of KHMDS 1.0M toluene solution (2.0 equiv., 1.17 mmol) was added dropwise via syringe over 5 minutes. The reaction mixture was gradually warmed up to room temperature while being stirred for addition 1 hour. Then, TMSCl (3.0 equiv., 223.0 μ L, 1.76 mmol) was added in one portion and the reaction was allowed to stir at room temperature for three hours. The solvent was removed *in vacuo* and the crude residue was purified by flash column chromatography (silica gel; 100% hexane) to give the desired product **2.44** as a colorless oil (90.3 mg, 49%). **¹H NMR** (CDCl₃, 500 MHz) δ 7.31 (d, *J* = 6.9 Hz, 1H), 6.79 (s, 2H), 6.27 (d, *J* = 6.9 Hz, 1H), 2.86 (q, *J* = 7.4 Hz, 2H), 2.31 (s, 3H), 2.06 (d, 6H), 1.72 (s, 3H), 1.29 (t, *J* = 7.4 Hz, 3H), 0.15 (s, 9H). **¹³C NMR** (CDCl₃, 126 MHz) δ 150.4, 141.5, 138.4, 136.1, 127.0, 112.1, 29.4, 22.9, 21.4, 21.2, 16.0, 4.9 (the signals for the two carbons adjacent to boron were not observed); **¹¹B NMR** (CDCl₃, 160 MHz) δ 40.8; **IR** 2968, 2932, 2911, 1609, 1540, 1455, 1373, 1357, 1258, 1160, 1056, 847, 772 cm⁻¹; **HRMS** (DART) calcd. for C₁₉H₃₁BNSi [M+H⁺]: 312.23133, found 312.23189.

Procedures for Synthesis of C4,C6-Di-Substituted Compounds 2.46–2.49

General Procedure F: Introduction of Same Substituent on C4 and C6

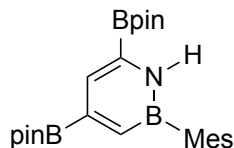


General Procedure F: Introduction of Same Substituent on C4 and C6 (substrates **2.46**, **2.47**)

Sequential borylation at C4: Inside a N₂ glovebox, to a 100 ml pressure vessel containing a magnetic stir bar was charged with [Ir(OMe)(cod)]₂ (4.0 mol %, 65.7 mg, 99.1

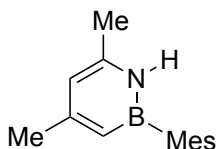
μmol), 4,4'-*di-tert-butyl-2,2'*-bipyridine (dtbbpy) (8.0 mol %, 53.2 mg, 0.198 mmol), bis(pinacolato)diboron (B_2pin_2) (2.0 equiv., 1.26 g, 4.95 mmol) and 10.0 mL MTBE. The catalyst mixture was aged for 15 minutes during which it turned color from light yellow to dark brown. Then C6-*mono*-Bpin 1,2-azaborine **2.7** (1.0 equiv., 800.0 mg, 2.48 mmol) was dissolved in 15.0 mL MTBE and was added to the reaction flask (total volume of 25.0 mL MTBE as solvent). The reaction was stirred at 80°C for 12 hours. When the reaction was judged to be complete by crude ^1H and ^{11}B NMR, the solution was concentrated under reduced pressure to yield a brown oil. Crude material was purified by flash column chromatography (silica gel, 10% of ethyl acetate in hexane) to give the desired *bis*-Bpin product **2.39** as a white solid. (1.03g, 93%).

C4 and C6 substituents was then introduced by treating **2.39** with Suzuki cross-coupling conditions described in general procedure D: Inside a drybox, a 10 mL pressure vessel was charged with a magnetic stir bar, **2.39** (1.0 equiv., 200.0 mg, 0.445 mmol), electrophile (R-halide, x equiv.), $\text{Pd}(\text{dppf})\text{Cl}_2$ (3.0 mol %, 10.9 mg, 13.4 μmol). Base (4.0 equiv.) was dissolved in 0.5 mL of H_2O (degassed by sparging with N_2 for 30 minutes before use) and was added into the pressure vessel with 4.5 mL of MTBE (total 5.0 mL of a 9 : 1 v : v mix of MTBE : H_2O was used as solvent). The reaction was sealed and heated at 80 °C for 3.5 to 6 hours. After cooling, 5 mL of water was added into the reaction mixture and the aqueous phase was extracted 3 x 5 mL with diethyl ether; the combined organic extracts were washed with brine and dried over MgSO_4 , vacuum-filtered through a fritted funnel, and concentrated *in vacuo*. The crude residue was purified by flash column chromatography (silica gel) to give the C4,C6-*di*-substituted *N*-Hprecursor.



C4,C6-di-Bpin-N-H-B-Mes-1,2-azaborine (2.39).

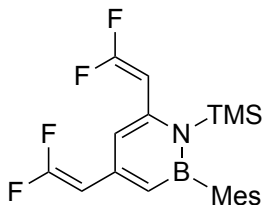
$^1\text{H NMR}$ (CDCl_3 , 500 MHz) δ 8.46-8.41 (br s, 1H), 7.68 (s, 1H), 7.33 (s, 1H), 6.84 (s, 2H), 2.30 (s, 3H), 2.14 (s, 6H), 1.32 (d, $J = 8.7$ Hz, 24H); $^{13}\text{C NMR}$ (CDCl_3 , 151 MHz) δ 140.3, 137.0, 127.1, 123.4, 84.7, 84.0, 25.0, 25.0, 23.33, 23.32 (the signals for the four carbons adjacent to boron were not observed); $^{11}\text{B NMR}$ (CDCl_3 , 160 MHz) δ 35.6, 30.3; **IR** 3391, 2978, 2930, 1610, 1409, 1372, 1318, 1165, 1140, 965, 879, 846, 733 cm^{-1} ; **HRMS** (DART) calcd. for $\text{C}_{25}\text{H}_{39}\text{B}_3\text{NO}_4$ [$\text{M}+\text{H}^+$]: 450.31528, found 450.31766.



C4,C6-di-methyl-N-H-B-Mes-1,2-azaborine (2.46).

For Suzuki cross-coupling: 10.0 equiv. of methyl-I was used as electrophile; 4.0 equiv. of $\text{K}_3\text{PO}_4 \cdot \text{H}_2\text{O}$ was used as base; reaction took 6 hours. After 6 hours, a mixture of C6-mono-methyl and C4,C6-di-methyl product was isolated and re-subjected to the Suzuki cross-coupling conditions for another 6 hours. The crude was purified by flash column chromatography (silica gel; 0 – 7% of dichloromethane in hexane) to give the desired product as a colorless solid (43.0 mg, 42%). $^1\text{H NMR}$ (CDCl_3 , 500 MHz) δ 7.55 – 7.35 (br s, 1H), 6.92 (s, 2H), 6.44 (s, 1H), 6.07 (s, 1H), 2.36 (s, 3H), 2.35 – 2.32 (m, 6H), 2.24 (s, 6H); $^{13}\text{C NMR}$ (CDCl_3 , 126 MHz) δ 154.9, 142.6, 140.3, 137.1, 127.2, 111.6, 25.3, 23.3, 22.0, 21.2 (the signals for the two carbons adjacent to boron were not observed); $^{11}\text{B NMR}$

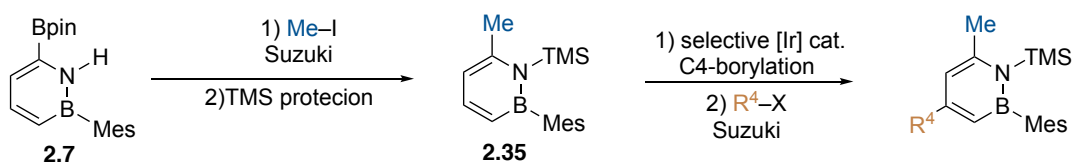
(CDCl₃, 160 MHz) δ 35.6; **IR** 3392, 2971, 2932, 2865, 1621, 1519, 1458, 1261, 1160, 1094, 826 cm⁻¹; **HRMS** (DART) calcd. for C₁₅H₂₁BN [M+H⁺]: 226.27113, found 226.27149.



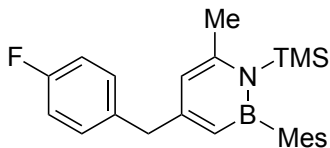
C4,C6-bis(2,2-*di*-fluorovinyl) N-TMS-B-Mes 1,2-azaborine (2.47).

For Suzuki cross-coupling: 6.0 equiv. of difluoro-vinyl-Br was used as electrophile; 4.0 equiv. of KOH was used as base; reaction took 3.5 hours. Both C4 and C6 Bpin were coupled, and no mono-coupling was observed. After TMS protection, the crude was purified by flash column chromatography (silica gel; 0–3% diethyl ether in hexane) to give the desired product as a pale yellow oil (52.0 mg, 30% yield over two steps). **¹H NMR** (CDCl₃, 500 MHz) δ 6.79 (s, 2H), 6.51 (d, *J* = 1.5 Hz, 1H), 6.44 (d, *J* = 2.0 Hz, 1H), 5.53 (dd, *J* = 21.5, 3.1 Hz, 1H), 5.12 (dd, *J* = 26.2, 4.0 Hz, 1H), 2.29 (s, 3H), 2.09 (s, 6H), 0.14 (s, 9H); **¹¹B NMR** (CDCl₃, 160 MHz) δ 40.8; **¹⁹F NMR** (CDCl₃, 470 MHz) δ -78.4 (m), -81.1(m), -82.7(m), -83.0(m); **IR** 3392, 2971, 2932, 2865, 1621, 1519, 1458, 1261, 1160, 1094, 826 cm⁻¹; **HRMS** (DART) calcd. for C₁₅H₂₁BN [M+H⁺]: 226.27113, found 226.27149.

Procedures for the Introduction of Different Substituents on C4 and C6 (substrates **2.48**, **2.49**)

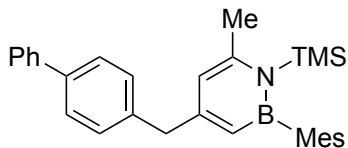


Step 1 and 2: In adaption to general procedure D, **2.35** was prepared by first Suzuki cross-coupling between C6-Bpin precursor **2.7** and methyl iodide, followed by TMS protection. **Step 3** (selective C4-borylation): Inside a N₂ glovebox, to a 15 mL pressure vessel containing a magnetic stir bar was charged with [Ir(OMe)(cod)]₂ (4.0 mol %, 14.4 mg, 21.4 μmol), 4,4'-*di*-tert-butyl-2,2'-bipyridine (dtbbpy) (8.0 mol %, 11.0 mg, 43.5 μmol), bis(pinacolato)diboron (B₂pin₂) (2.0 equiv., 291.8 mg, 1.09 mmol) and 2.0 mL MTBE. The catalyst mixture was aged for 15 minutes during which it turned color from light yellow to dark brown. Then C6-methyl 1,2-azaborine **2.35** (1.0 equiv., 154.0 mg, 0.544 mmol) was dissolved in 2.0 mL MTBE and was added to the reaction flask (total volume of 4.0 mL MTBE as solvent). The reaction was stirred at 80°C for 12 hours. Upon completion, the solution was concentrated under reduced pressure and the crude residue was purified by flash column chromatography (silica gel, 0 – 10% of diethyl ether in hexane) to give the desired C4-Bpin-C6-methyl-1,2-azaborine precursor as a pale yellow oil (185.8 mg, 84%). **Step 4** (second Suzuki to introduce C4 substituent): general procedure B was adopted.



C4-*p*-F-benzyl-C6-methyl-1,2-azaborine (2.48)

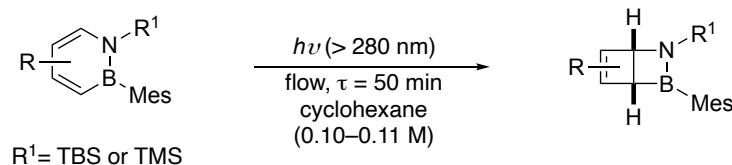
According to general procedure B, a 10 mL pressure vessel was charged with a magnetic stir bar, C4-Bpin-C6-Me-1,2-azaborine precursor from step 3 (1.0 equiv., 246.3 mg, 0.602 mmol), *p*-F-benzyl bromide (1.1 equiv., 125.1 mg, 0.662 mmol), Pd(dppf)Cl₂ (3.0 mol %, 14.74 mg, 18.0 μmol). K₃PO₄·H₂O (4.0 equiv., 553.0 mg, 1.81 mmol) was dissolved in 0.5 mL of H₂O (degassed by sparging with N₂ for 30 minutes before use) and was added into the pressure vessel with 4.5 mL of MTBE (total 5.0 mL of a 9 : 1 v : v mix of MTBE : H₂O was used as solvent). The reaction was sealed and heated at 80 °C for 6 hours. After work-up, the crude residue was purified by flash column chromatography (silica gel; 0 – 2% diethyl ether in hexane) to give the desired product **2.42** as a colorless solid (194.7 mg, 83%). ¹H NMR (CDCl₃, 500 MHz) δ 7.14 (dd, *J* = 8.5, 5.6 Hz, 2H), 6.95 (t, *J* = 8.7 Hz, 2H), 6.76 (s, 2H), 6.13 (d, *J* = 2.1 Hz, 1H), 6.04 (d, *J* = 2.1 Hz, 1H), 3.71 (s, 2H), 2.48 (s, 3H), 2.28 (s, 3H), 2.08 (s, 6H), 0.14 (s, 9H); ¹³C NMR (CDCl₃, 126 MHz) δ 161.5, ¹*J*_{CF} = 243.3 Hz, 155.9, 147.2, 138.5, 136.3, 136.1, 130.6, ³*J*_{CF} = 7.7 Hz, 127.0, 116.1, 115.18, ²*J*_{CF} = 21.1 Hz, 43.7, 25.2, 23.5, 21.3, 4.7 (the signals for the two carbons adjacent to boron were not observed); ¹¹B NMR (CDCl₃, 160 MHz) δ 40.3; ¹⁹F NMR (CDCl₃, 470 MHz) δ –117.7 (m); IR 2955, 2914, 2854, 1610, 1509, 1346, 1221, 1205, 1172, 1014, 845, 821 cm⁻¹; HRMS (DART) calcd. for C₂₄H₃₂BNFSi [M+H⁺]: 392.23756, found 392.23468.



C4-(1,1'-biphenyl-4-ylmethyl)-C6-methyl-1,2-azaborine (2.49)

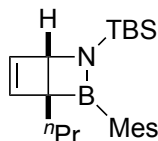
According to general procedure B, a 10 mL pressure vessel was charged with a magnetic stir bar, C4-Bpin-C6-Me-1,2-azaborine precursor from step 3 (1.0 equiv., 185.8 mg, 0.454 mmol), 1-bromomethyl-4-phenyl-benzene (1.0 equiv., 112.2 mg, 0.454 mmol), Pd(dppf)Cl₂ (3.0 mol %, 11.2 mg, 13.6 μmol). K₃PO₄ · H₂O (4.0 equiv., 417.0 mg, 1.36 mmol) was dissolved in 0.5 mL of H₂O (degassed by sparging with N₂ for 30 minutes before use) and was added into the pressure vessel with 4.5 mL of MTBE (total 5.0 mL of a 9 : 1 v : v mix of MTBE : H₂O was used as solvent). The reaction was sealed and heated at 80 °C for 6 hours. After work-up, the crude residue was purified by flash column chromatography (silica gel; 0 – 2% diethyl ether in hexane) to give the desired product **2.42** as a white solid (128.0 mg, 63%). ¹H NMR (CDCl₃, 500 MHz) δ 7.61 – 7.56 (m, 2H), 7.53 – 7.47 (m, 2H), 7.42 (t, *J* = 7.7 Hz, 2H), 7.35 – 7.29 (m, 1H), 7.29 – 7.26 (m, 2H), 6.77 (s, 2H), 6.21 (s, 1H), 6.12 (s, 1H), 3.79 (s, 2H), 2.50 (s, 3H), 2.28 (s, 3H), 2.10 (s, 6H), 0.15 (s, 9H); ¹³C NMR (CDCl₃, 126 MHz) δ 155.8, 147.0, 141.1, 139.5, 138.9, 138.5, 136.1, 129.5, 128.7, 127.1, 127.0, 127.0, 126.8, 116.2, 44.2, 25.1, 23.4, 21.2, 4.6 (the signals for the two carbons adjacent to boron were not observed); ¹¹B NMR (CDCl₃, 160 MHz) δ 40.8; IR 2959, 2928, 2857, 1623, 1601, 1520, 1491, 1442, 1363, 1280, 1264, 1164, 1029, 834, 784 cm⁻¹; HRMS (DART) calcd. for C₃₀H₃₇BNSi [M+H₃O⁺]: 450.27828, found 450.27791.

2.7.2.2 General Procedure for 1,2-Azaborine Photoisomerization (Dewar Substrates in Table 2.3)



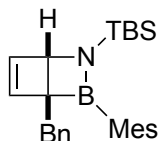
The flow photoreactor setup used in this work was assembled in accordance with prior system designs by Berry and Booker-Milburn and Seeberger and Hartmann.⁸⁷ For details of photoreactor assembly, see experimental procedures in part 1.5.3.1.¹⁰³ Prior to each use of the reactor, 6 mL of anhydrous cyclohexane were flushed through the tubing into a vial sealed under N₂ in a glovebox. The total volume of the reaction tube is 5.0 mL.

A solution of 1,2-azaborine (summarized in Table 2.1 and 2.2) in anhydrous cyclohexane (0.10–0.11 M) was injected at 0.1 mL·min⁻¹ via syringe pump into the flow photoreactor. An additional volume of pure cyclohexane was then injected at the same rate to clear the tubing of remaining material. The solution collected in the receiving vial was concentrated *in vacuo* under N₂ to afford the product. An efficient photoisomerization reaction typically generates the Dewar isomer as the only product with no 1,2-azaborine starting material left, in which case, purification is not required. All the NMR spectrum of Dewar compounds shown in this work are the “crude” NMR taken after the removal of cyclohexane solvent. Yield was calculated based on the product mass recovered after removing the cyclohexane solvent. The photoisomerization of each 1,2-azaborine compound was carried out at least 2 times. The average yield was reported.



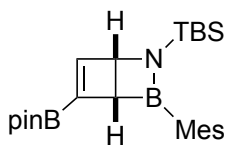
C3-*n*-propyl-Dewar (2.50)

The first syringe with anhydrous cyclohexane (1.0 mL) solution of **2.20** (38.0 mg, 0.108 mmol) was injected at 0.1 mL·min⁻¹ via syringe pump into the flow photoreactor. The second syringe with 5.5 mL of pure cyclohexane was then injected at the same rate. After 3.5 mL of cyclohexane in the second syringe was injected, change to the product collection vial before the last 2.0 mL of cyclohexane was injected to push out the Dewar product. The solution collected in the receiving vials was concentrated *in vacuo* under N₂ to afford the product as a pale yellow liquid with 91% average yield (Batch 1: 35.2 mg, 93%; Batch 2: 33.9 mg, 89%). ¹H NMR (CDCl₃, 600 MHz) δ 6.73 (d, *J* = 10.7 Hz, 2H), 6.60 (t, *J* = 2.4 Hz, 1H), 6.41 (d, *J* = 2.3 Hz, 1H), 4.42 (d, *J* = 2.5 Hz, 1H), 2.26 (d, *J* = 2.8 Hz, 6H), 2.15 (s, 3H), 1.75 (ddd, *J* = 13.6, 10.0, 6.0 Hz, 1H), 1.58 (ddd, *J* = 13.6, 9.9, 5.9 Hz, 1H), 1.28 (m, 2H), 0.90 (s, 9H), 0.83 (t, *J* = 7.4 Hz, 3H), -0.08 (s, 3H), -0.14 (s, 3H); ¹³C NMR (CDCl₃, 151 MHz) δ 147.2, 139.0, 137.8, 136.8, (126.93, 126.86 two diastereotopic 13C), 66.9, 32.4, 26.6, (22.77, 22.12 two diastereotopic 13C), 21.4, 21.0, 18.4 14.9, (-5.47, -5.51 two diastereotopic 13C), the signals for the two carbons adjacent to boron were not observed; ¹¹B NMR (CDCl₃, 160 MHz) δ 53.4; IR 2955, 2928, 2857, 1643, 1360, 1264, 992, 895, 833, 777, 732, 703 cm⁻¹; HRMS (DART) calcd. for C₃₀H₃₇BNSi [M+H₃O⁺]: 354.27828, found 354.27856.



C3-benzyl-Dewar (2.51)

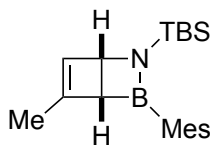
The first syringe with anhydrous cyclohexane (1.1 mL) solution of **2.21** (45.0 mg, 0.112 mmol) was injected at 0.1 mL·min⁻¹ via syringe pump into the flow photoreactor. The second syringe with 5.5 mL of pure cyclohexane was then injected at the same rate. After 3.4 mL of cyclohexane in the second syringe was injected, change to the product collection vial before the last 2.1 mL of cyclohexane was injected to push out the Dewar product. The solution collected in the receiving vials was concentrated *in vacuo* under N₂ to afford the product as a pale yellow oil with 92% average yield (Batch 1: 41.8 mg, 93%; Batch 2: 40.9 mg, 91%). ¹H NMR (CDCl₃, 500 MHz) δ 7.21 – 7.08 (m, 3H), 7.06 – 7.01 (m, 2H), 6.76 (d, *J* = 16.5 Hz, 2H), 6.45 (t, *J* = 2.4 Hz, 1H), 6.30 (d, *J* = 2.4 Hz, 1H), 4.47 (d, *J* = 2.5 Hz, 1H), 3.14 (d, *J* = 14.1 Hz, 1H), 2.90 (d, *J* = 14.0 Hz, 1H), 2.29 (d, *J* = 3.3 Hz, 6H), 2.12 (s, 3H), 0.91 (s, 9H), -0.06 (s, 3H), -0.10 (s, 3H); ¹¹B NMR (CDCl₃, 160 MHz) δ 52.8; IR 2968, 2920, 2858, 1743, 1488, 1363, 1208, 992, 895, 843, 795 cm⁻¹; HRMS (DART) calcd. for C₂₆H₃₇BNSi [M+H₃O⁺]: 402.27828, found 402.27791.



C4-Bpin-Dewar (2.52)

The first syringe with anhydrous cyclohexane (2.4 mL) solution of **2.11** (108.0 mg, 0.247 mmol) was injected at 0.1 mL·min⁻¹ via syringe pump into the flow photoreactor.

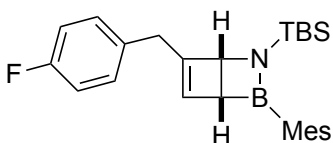
The second syringe with 5.5 mL of pure cyclohexane was then injected at the same rate. After 2.1 mL of cyclohexane in the second syringe was injected, change to the product collection vial before the last 3.4 mL of cyclohexane was injected to push out the Dewar product. The solution collected in the receiving vials was concentrated *in vacuo* under N₂ to afford the product as a pale yellow liquid with 93% average yield (Batch 1: 100.0 mg, 93%; Batch 2: 99.1 mg, 92%). ¹H NMR (CDCl₃, 600 MHz) δ 7.13 (s, 1H), 6.72 (s, 2H), 4.77 (d, *J* = 2.1 Hz, 1H), 3.14 (d, *J* = 2.1 Hz, 1H), 2.26 (s, 3H), 2.18 (br s, 6H), 1.25 (d, *J* = 6.0 Hz, 12H), 0.90 (s, 9H), -0.07 (s, 3H), -0.13 (s, 3H); ¹³C NMR (CDCl₃, 151 MHz) δ 153.8, 136.8, 126.7, 83.5, 63.5, 27.1, 26.5, 25.0, 24.7, 21.3, 18.3, (-5.47, -5.57 two diastereotopic ¹³C), the signals for the three carbons adjacent to boron were not observed; ¹¹B NMR (CDCl₃, 160 MHz) δ 49.2, 24.0; IR 2955, 2928, 2857, 1617, 1574, 1446, 1360, 1261, 1214, 1001, 895, 833, 785, 732 cm⁻¹; HRMS (DART) calcd. for C₂₅H₄₂B₂NO₂Si [M+H₃O⁺]: 438.31654, found 438.31749.



C4-methyl-Dewar (2.53)

The first syringe with anhydrous cyclohexane (1.3 mL) solution of **2.23** (42.4 mg, 0.130 mmol) was injected at 0.1 mL·min⁻¹ via syringe pump into the flow photoreactor. The second syringe with 5.5 mL of pure cyclohexane was then injected at the same rate. After 3.2 mL of cyclohexane in the second syringe was injected, change to the product collection vial before the last 2.3 mL of cyclohexane was injected to push out the Dewar product. The solution collected in the receiving vials was concentrated *in vacuo* under N₂

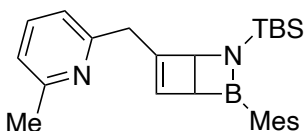
to afford the product as a pale yellow liquid with 93% average yield (Batch 1: 38.7 mg, 91%; Batch 2: 39.9 mg, 94%). $^1\text{H NMR}$ (CDCl_3 , 500 MHz) δ 6.79 (s, 2H), 6.07 (t, $J = 1.4$ Hz, 1H), 4.64 (d, $J = 2.3, 1$ H), 2.90 (d, $J = 2.3$, 1H), 2.29 (s, 3H), 2.23 (s, 6H), 1.86 – 1.77 (s, 3H), 0.92 (s, 9H), -0.06 (s, 3H), -0.10 (s, 3H); $^{13}\text{C NMR}$ (CDCl_3 , 126 MHz) δ 153.7, 138.0, 136.9, 131.6, 126.9, 59.1, 29.9, 26.5, 22.3, 21.3, 18.2, (-5.4, -5.8 two diastereotopic ^{13}C), the signals for the two carbons adjacent to boron were not observed; $^{11}\text{B NMR}$ (CDCl_3 , 160 MHz) δ 52.2; **IR** 2953, 2929, 2857, 1610, 1470, 1462, 1351, 1253, 1174, 994, 847, 818, 778, 740 cm^{-1} ; **HRMS** (DART) calcd. for $\text{C}_{20}\text{H}_{33}\text{BNSi}$ [$\text{M} + \text{H}_3\text{O}^+$]: 326.24698, found 326.24819.



C5-*p*-F-benzyl-Dewar (2.54)

The first syringe with anhydrous cyclohexane (3.0 mL) solution of **2.25** (130.0 mg, 0.310 mmol) was injected at 0.1 mL-min $^{-1}$ via syringe pump into the flow photoreactor. The second syringe with 5.5 mL of pure cyclohexane was then injected at the same rate. After 1.5 mL of cyclohexane in the second syringe was injected, change to the product collection vial before the last 4.0 mL of cyclohexane was injected to push out the Dewar product. The solution collected in the receiving vials was concentrated *in vacuo* under N_2 to afford the product as a pale yellow liquid with 95% average yield (Batch 1: 124.8 mg, 96%; Batch 2: 120.9 mg, 93%). $^1\text{H NMR}$ (CDCl_3 , 500 MHz) δ 7.20 (dd, $J = 8.5, 5.6$ Hz, 2H), 7.01 (t, $J = 8.7$ Hz, 2H), 6.78 (s, 2H), 6.04 (dt, $J = 2.1, 1.1$ Hz, 1H), 4.74 (t, $J = 2.4$ Hz, 1H), 3.56 (d, $J = 16.8$ Hz, 1H), 3.43 (d, $J = 16.9$, 1H), 2.90 (dt, $J = 2.5, 1.3$ Hz, 1H),

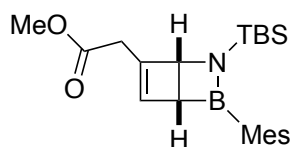
2.28 (s, 3H), 2.25 (br s, 6H), 0.91 (s, 9H), 0.17 (s, 3H), -0.14 (s, 3H); ^{13}C NMR (CDCl_3 , 126 MHz) δ 161.5 (d, $^1J_{\text{CF}} = 243.9$ Hz), 151.8, 138.1, 137.2, 135.8, 134.71 (d, $^4J_{\text{CF}} = 3.3$ Hz), 130.34 (d, $^3J_{\text{CF}} = 7.7$ Hz), 127.0, 115.24 (d, $^2J_{\text{CF}} = 21.3$ Hz), 63.3, 36.4, 26.6, 21.3, 18.3, (-3.1, -5.0 two diastereotopic ^{13}C), the signals for the two carbons adjacent to boron were not observed; ^{11}B NMR (CDCl_3 , 160 MHz) δ 52.6; ^{19}F NMR (CDCl_3 , 470 MHz) δ -117.4 (m); IR 3039, 2958, 2916, 2858, 1608, 1545, 1509, 1360, 1250, 1152, 1106, 932, 845, 797, 740 cm^{-1} ; HRMS (DART) calcd. for $\text{C}_{26}\text{H}_{36}\text{BNFSi}$ [$\text{M}+\text{H}^+$]: 420.26886, found 420.26916.



C5-(6-methyl-pyridin-2-yl)methyl-Dewar (2.55)

The first syringe with anhydrous cyclohexane (1.2 mL) solution of **2.26** (57.2 mg, 0.137 mmol) was injected at 0.1 $\text{mL}\cdot\text{min}^{-1}$ via syringe pump into the flow photoreactor. The second syringe with 5.5 mL of pure cyclohexane was then injected at the same rate. After 3.3 mL of cyclohexane in the second syringe was injected, change to the product collection vial before the last 2.2 mL of cyclohexane was injected to push out the Dewar product. The solution collected in the receiving vials was concentrated *in vacuo* under N_2 to afford the product as a pale yellow oil with 90% average yield (Batch 1: 50.6 mg, 89%; Batch 2: 52.0 mg, 92%). ^1H NMR (CDCl_3 , 400 MHz) δ 7.51 (t, $J = 7.6$ Hz, 1H), 7.03 (d, $J = 7.7$ Hz, 1H), 6.99 (d, $J = 7.6$ Hz, 1H), 6.75 (s 2H), 6.11 – 6.07 (m, 1H), 4.78 (t, $J = 2.4$ Hz, 1H), 3.76 – 3.57 (m, 2H), 2.91 – 2.88 (m, 1H), 2.55 (s, 3H), 2.26 (s, 3H), 2.22 (br s, 6H), 0.88 (s, 9H), 0.16 (s, 3H), -0.18 (s, 3H); ^{13}C NMR (CDCl_3 , 126 MHz) ^{13}C NMR (126

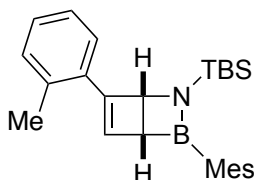
MHz, cdCl_3) δ 158.7, 158.0, 150.4, 138.1, 137.1, 136.6, 136.2, 126.9, 120.7, 112.0, 63.8, 39.8, 26.6, 26.0, 24.7, 21.3, 18.3, (-3.2, -5.1 two diastereotopic ^{13}C), the signals for the two carbons adjacent to boron were not observed; ^{11}B NMR (CDCl_3 , 160 MHz) δ 52.7; IR 2953, 2928, 2856, 1748, 1624, 1610, 1577, 1456, 1452, 1352, 1256, 1231, 986, 834, 804, 778, 756 cm^{-1} ; HRMS (DART) calcd. for $\text{C}_{26}\text{H}_{38}\text{BN}_2\text{Si}$ $[\text{M}+\text{H}^+]$: 417.28918, found 417.28986.



C5-ester-Dewar (2.56)

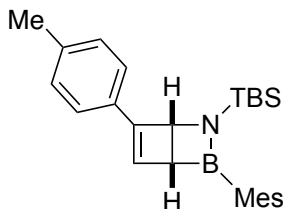
The first syringe with anhydrous cyclohexane (4.0 mL) solution of **2.27** (163.0 mg, 0.425 mmol) was injected at $0.1 \text{ mL}\cdot\text{min}^{-1}$ via syringe pump into the flow photoreactor. The second syringe with 5.5 mL of pure cyclohexane was then injected at the same rate. After 0.5 mL of cyclohexane in the second syringe was injected, change to the product collection vial before the last 5.0 mL of cyclohexane was injected to push out the Dewar product. The solution collected in the receiving vials was concentrated *in vacuo* under N_2 to afford the product as a pale yellow oil with 95% average yield (Batch 1: 156.5 mg, 96%; Batch 2: 155.3 mg, 95%). ^1H NMR (CDCl_3 , 500 MHz) δ 6.77 (s, 2H), 6.38 (dd, $J = 2.9, 1.9 \text{ Hz}$, 1H), 4.84 (t, $J = 2.4 \text{ Hz}$, 1H), 3.73 (s, 3H), 3.27 (dt, $J = 16.9, 1.1 \text{ Hz}$, 1H), 3.19 (dt, $J = 16.9, 2.2 \text{ Hz}$, 1H), 2.96 (dt, $J = 2.3, 1.2 \text{ Hz}$, 1H), 2.27 (s, 3H), 2.22 (br s, 6H), 0.92 (s, 9H), 0.12 (s, 3H), -0.18 (s, 3H); ^{13}C NMR (CDCl_3 , 126 MHz) δ 171.2, 144.1, 138.4, 138.1, 137.2, 126.9, 63.7, 51.9, 35.9, 26.6, 21.3, 18.3, (-3.4, -5.2 two diastereotopic ^{13}C), the signals for the two carbons adjacent to boron were not observed; ^{11}B NMR (CDCl_3 , 160

MHz) δ 52.7; **IR** 2957, 2930, 2858, 1741, 1620, 1542, 1449, 1370, 1260, 1185, 1006, 845, 833, 770 cm^{-1} ; **HRMS** (DART) calcd. for $\text{C}_{22}\text{H}_{35}\text{BNO}_2\text{Si}$ $[\text{M}+\text{H}^+]$: 384.25863, found 384.25906.



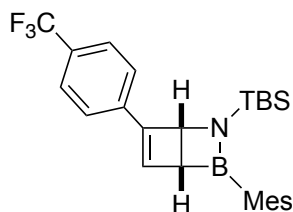
C5-*o*-tolyl-Dewar (2.57)

The first syringe with anhydrous cyclohexane (3.0 mL) solution of **2.28** (122.0 mg, 0.304 mmol) was injected at $0.1 \text{ mL}\cdot\text{min}^{-1}$ via syringe pump into the flow photoreactor. The second syringe with 5.5 mL of pure cyclohexane was then injected at the same rate. After 1.5 mL of cyclohexane in the second syringe was injected, change to the product collection vial before the last 4.0 mL of cyclohexane was injected to push out the Dewar product. The solution collected in the receiving vials was concentrated *in vacuo* under N_2 to afford the product as a pale yellow oil with 91% average yield (Batch 1: 109.8 mg, 90%; Batch 2: 112.2 mg, 92%). **^1H NMR** (CDCl_3 , 600 MHz) δ 7.26 – 7.13 (m, 4H), 6.82 (d, $J = 10.2 \text{ Hz}$, 2H), 3.81 (dd, $J = 6.0, 1.5 \text{ Hz}$, 1H), 3.70 (t, $J = 1.8 \text{ Hz}$, 1H), 2.47 (s, 3H), 2.31 (s, 3H), 2.28 (d, $J = 6.1 \text{ Hz}$, 6H), 1.67 (dd, $J = 6.0, 1.9 \text{ Hz}$, 1H), 0.95 (s, 9H), -0.02 (s, 3H), -0.17 (s, 3H); **^{13}C NMR** (CDCl_3 , 151 MHz) δ 138.7, 138.5, 138.2, 136.7, 134.5, 130.0, 128.7, 126.8, 126.8, 125.8, 57.9, 45.1, 36.4, 23.0, 22.8, (21.3, 20.9 two diastereotopic ^{13}C), 19.1, (-4.4, -4.9 two diastereotopic ^{13}C), the signals for the two carbons adjacent to boron were not observed; **^{11}B NMR** (CDCl_3 , 160 MHz) δ 52.2; **IR** 2956, 2928, 2857, 1612, 1558, 1472, 1462, 1361, 1341, 1258, 1236, 1010, 847, 834, 777 cm^{-1} ; **HRMS** (DART) calcd. for $\text{C}_{26}\text{H}_{37}\text{BNSi}$ $[\text{M}+\text{H}^+]$: 402.27828, found 402.27919.



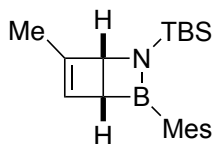
C5-*p*-tolyl-Dewar (2.58)

The first syringe with anhydrous cyclohexane (3.0 mL) solution of **2.29** (120.0 mg, 0.299 mmol) was injected at 0.1 mL·min⁻¹ via syringe pump into the flow photoreactor. The second syringe with 5.5 mL of pure cyclohexane was then injected at the same rate. After 1.5 mL of cyclohexane in the second syringe was injected, change to the product collection vial before the last 4.0 mL of cyclohexane was injected to push out the Dewar product. The solution collected in the receiving vials was concentrated *in vacuo* under N₂ to afford the product as a pale yellow oil with 94% average yield (Batch 1: 112.8 mg, 94%; Batch 2: 112.3 mg, 94%). ¹H NMR (CDCl₃, 500 MHz) δ 7.29 – 7.07 (m, 4H), 6.83 (d, *J* = 10.6 Hz, 2H), 3.95 (dd, *J* = 6.0, 1.6 Hz, 1H), 3.55 (t, *J* = 1.8 Hz, 1H), 2.39 (s, 3H), 2.33 (s, 3H), 2.26 (d, *J* = 25.6 Hz, 6H), 1.83 (dd, *J* = 6.0, 2.0 Hz, 1H), 0.98 (s, 9H), -0.09 (d, *J* = 2.7 Hz, 6H); ¹³C NMR (CDCl₃, 151 MHz) δ 138.3, 138.3, 136.7, 135.5, 133.9, 129.2, 129.2, 126.8, 126.6, 56.3, 46.0, 39.9, 22.8, 22.7, (21.33, 21.26 two diastereotopic ¹³C), 19.2 (-4.80, -4.83 two diastereotopic ¹³C), the signals for the two carbons adjacent to boron were not observed; ¹¹B NMR (CDCl₃, 160 MHz) δ 52.4; IR 2955, 2928, 2856, 1610, 1558, 1474, 1462, 1361, 1341, 1258, 1237, 1135, 1008, 847, 832, 778 cm⁻¹; HRMS (DART) calcd. for C₂₆H₃₇BNSi [M+H⁺]: 402.27828, found 402.27879.



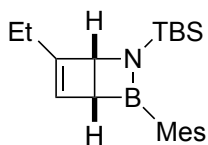
C5-*p*-CF₃-phenyl-Dewar (2.59)

The first syringe with anhydrous cyclohexane (1.2 mL) solution of **2.30** (55.0 mg, 0.121 mmol) was injected at 0.1 mL·min⁻¹ via syringe pump into the flow photoreactor. The second syringe with 5.5 mL of pure cyclohexane was then injected at the same rate. After 3.3 mL of cyclohexane in the second syringe was injected, change to the product collection vial before the last 2.2 mL of cyclohexane was injected to push out the Dewar product. The solution collected in the receiving vials was concentrated *in vacuo* under N₂ to afford the product as a yellow oil with 94% average yield (Batch 1: 52.2 mg, 95%; Batch 2: 51.7 mg, 94%). ¹H NMR (CDCl₃, 600 MHz) δ 7.55 (d, *J* = 8.0 Hz, 2H), 7.32 (d, *J* = 8.0 Hz, 2H), 6.79 (d, *J* = 12.0 Hz, 2H), 4.01 (dd, *J* = 6.1, 1.6 Hz, 1H), 3.61 (t, *J* = 1.9 Hz, 1H), 2.28 (s, 3H), 2.19 (d, *J* = 39.6 Hz, 6H), 1.92 (dd, *J* = 6.1, 2.1 Hz, 1H), 0.93 (s, 9H), -0.13 (d, *J* = 2.0 Hz, 6H); ¹¹B NMR (CDCl₃, 160 MHz) δ 51.0; ¹⁹F NMR (CDCl₃, 470 MHz) δ -62.3 (m); IR 2958, 2930, 2858, 1613, 1550, 1471, 1367, 1346, 1261, 1228, 1011, 843, 827, 770 cm⁻¹; HRMS (DART) calcd. for C₂₆H₃₄BNF₃Si [M+H⁺]: 456.25002, found 456.25118.



C5-methyl-Dewar (2.60)

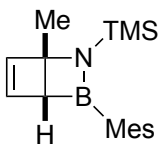
The first syringe with anhydrous cyclohexane (2.2 mL) solution of **2.33** (74.5 mg, 0.229 mmol) was injected at 0.1 mL·min⁻¹ via syringe pump into the flow photoreactor. The second syringe with 5.5 mL of pure cyclohexane was then injected at the same rate. After 2.3 mL of cyclohexane in the second syringe was injected, change to the product collection vial before the last 3.2 mL of cyclohexane was injected to push out the Dewar product. The solution collected in the receiving vials was concentrated *in vacuo* under N₂ to afford the product as a pale yellow liquid with 94% average yield (Batch 1: 70.3 mg, 94%; Batch 2: 71.0 mg, 95%). ¹H NMR (CDCl₃, 500 MHz) δ 7.00 – 6.50 (s, 2H), 6.16 (dt, *J* = 2.8, 1.4 Hz, 1H), 4.68 (t, *J* = 2.4 Hz, 1H), 2.86 (dt, 2.7, 1.4 Hz, 1H), 2.29 (s, 3H), 2.25 (br s, 6H), 1.87 (t, *J* = 1.9 Hz, 3H), 0.93 (s, 9H), 0.14 (s, 3H), -0.14 (s, 3H); ¹³C NMR (CDCl₃, 126 MHz) δ 148.9, 138.1, 137.0, 134.7, 126.9, 64.6, 26.6, 22.4, 21.3, 18.4, 16.0, (-3.3, -5.1 two diastereotopic ¹³C), the signals for the two carbons adjacent to boron were not observed; ¹¹B NMR (CDCl₃, 160 MHz) δ 52.6; IR 2953, 2929, 2857, 1610, 1462, 1351, 1253, 1174, 995, 847, 832, 804, 778 cm⁻¹; HRMS (DART) calcd. for C₂₀H₃₃BNSi [M+H⁺]: 326.24698, found 326.24926.



C5-ethyl-Dewar (**2.61**)

The first syringe with anhydrous cyclohexane (1.5 mL) solution of **2.34** (53.0 mg, 0.156 mmol) was injected at 0.1 mL·min⁻¹ via syringe pump into the flow photoreactor. The second syringe with 5.5 mL of pure cyclohexane was then injected at the same rate. After 3.0 mL of cyclohexane in the second syringe was injected, change to the product

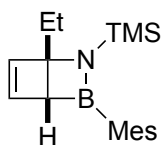
collection vial before the last 2.5 mL of cyclohexane was injected to push out the Dewar product. The solution collected in the receiving vials was concentrated *in vacuo* under N₂ to afford the product as a pale yellow liquid with 93% average yield (Batch 1: 50.1 mg, 94%; Batch 2: 49.3 mg, 93%). ¹H NMR (CDCl₃, 500 MHz) δ 6.75 (s, 2H), 6.15 – 6.11 (m, 1H), 4.69 (t, *J* = 2.4 Hz, 1H), 2.86 – 2.82 (m, 1H), 2.26 (s, 3H), 2.21 (br s, 6H), 2.20 – 2.08 (m, 2H), 1.09 (t, *J* = 7.4 Hz, 3H), 0.91 (s, 9H), 0.10 (s, 3H), -0.19 (s, 3H); ¹³C NMR (CDCl₃, 126 MHz) δ 155.4, 138.2, 137.0, 132.6, 126.9, 63.3, 29.9, 26.6, 23.5, 21.3, 18.4, 11.8, (-3.4, -5.1 two diastereotopic ¹³C), the signals for the two carbons adjacent to boron were not observed; ¹¹B NMR (CDCl₃, 160 MHz) δ 52.8; IR 2959, 2927, 2858, 1462, 1441, 1374, 1348, 1259, 1108, 1074, 1016, 850, 836, 825, 779 cm⁻¹; HRMS (DART) calcd. for C₂₁H₃₅BNSi [M+H⁺]: 340.26263, found 340.26301.



C6-methyl-Dewar (2.62)

The first syringe with anhydrous cyclohexane (3.0 mL) solution of **2.35** (84.5 mg, 0.298 mmol) was injected at 0.1 mL·min⁻¹ via syringe pump into the flow photoreactor. The second syringe with 5.5 mL of pure cyclohexane was then injected at the same rate. After 1.5 mL of cyclohexane in the second syringe was injected, change to the product collection vial before the last 4.0 mL of cyclohexane was injected to push out the Dewar product. The solution collected in the receiving vials was concentrated *in vacuo* under N₂ to afford the product as a pale yellow liquid with 92% average yield (Batch 1: 78.0 mg, 92%; Batch 2: 77.1 mg, 91%). ¹H NMR (CDCl₃, 500 MHz) δ 6.79 (s, 2H), 6.55 (dd, *J* = 2.4,

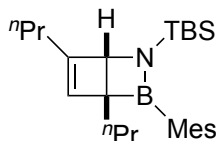
1.1 Hz, 1H), 6.41 (d, $J = 2.3$ Hz, 1H), 2.70 (d, $J = 1.1$ Hz, 1H), 2.30 (s, 3H), 2.25 (br s, 6H), 1.71 (s, 3H), 0.05 (s, 9H); $^{13}\text{C NMR}$ (CDCl_3 , 126 MHz) δ 141.7, 140.6, 137.1, 127.0, 72.2, 22.1, 21.8, 21.3, -0.2 (the signals for the two carbons adjacent to boron were not observed); $^{11}\text{B NMR}$ (CDCl_3 , 160 MHz) δ 51.3; **IR** 2955, 2918, 2858, 1739, 1609, 1520, 1443, 1358, 1252, 1155, 1029, 844, 803, 757 cm^{-1} ; **HRMS** (DART) calcd. for $\text{C}_{17}\text{H}_{27}\text{BNSi}$ [$\text{M}+\text{H}^+$]: 284.20003, found 284.20072.



C6-ethyl-Dewar (2.63)

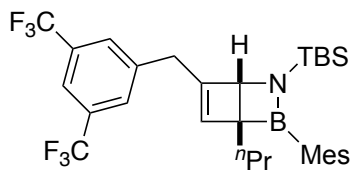
The first syringe with anhydrous cyclohexane (2.0 mL) solution of **2.37** (60.0 mg, 0.202 mmol) was injected at $0.1 \text{ mL}\cdot\text{min}^{-1}$ via syringe pump into the flow photoreactor. The second syringe with 5.5 mL of pure cyclohexane was then injected at the same rate. After 2.5 mL of cyclohexane in the second syringe was injected, change to the product collection vial before the last 3.0 mL of cyclohexane was injected to push out the Dewar product. The solution collected in the receiving vials was concentrated *in vacuo* under N_2 to afford the product as a pale yellow liquid with 92% average yield (Batch 1: 55.5 mg, 92%; Batch 2: 56.6 mg, 94%). $^1\text{H NMR}$ (CDCl_3 , 500 MHz) δ 6.76 (s, 2H), 6.52 (dd, $J = 2.4, 1.2$ Hz, 1H), 6.35 (d, $J = 2.4$ Hz, 1H), 2.71 (d, $J = 1.1$ Hz, 1H), 2.27 (s, 3H), 2.25 – 2.18 (br s, 6H), 2.06 – 2.00 (m, 1H), 1.96 – 1.92 (m, 1H), 0.99 (t, $J = 7.4$ Hz, 3H), 0.00 (s, 9H); $^{13}\text{C NMR}$ (CDCl_3 , 126 MHz) δ 141.0, 140.8, 137.2, 127.0, 76.8, 27.1, 27.1, 21.3, 10.1, -0.1 (the signals for the two carbons adjacent to boron were not observed); $^{11}\text{B NMR}$ (CDCl_3 , 160 MHz) δ 51.8; **IR** 2956, 2920, 2859, 1736, 1611, 1459, 1443, 1360, 1256, 1145, 1037,

847, 803, 781 cm^{-1} ; **HRMS** (DART) calcd. for $\text{C}_{18}\text{H}_{29}\text{BNSi}$ $[\text{M}+\text{H}^+]$: 298.21568, found 298.21661.



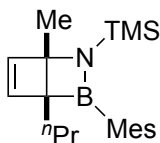
C3,C5-di-*n*propyl-Dewar (2.64)

The first syringe with anhydrous cyclohexane (1.0 mL) solution of **2.40** (42.0 mg, 0.106 mmol) was injected at 0.1 $\text{mL}\cdot\text{min}^{-1}$ via syringe pump into the flow photoreactor. The second syringe with 5.5 mL of pure cyclohexane was then injected at the same rate. After 3.5 mL of cyclohexane in the second syringe was injected, change to the product collection vial before the last 2.0 mL of cyclohexane was injected to push out the Dewar product. The solution collected in the receiving vials was concentrated *in vacuo* under N_2 to afford the product as a pale yellow oil with 92% average yield (Batch 1: 38.7 mg, 92%; Batch 2: 38.3 mg, 91%). **^1H NMR** (CDCl_3 , 600 MHz) δ 6.73 (d, $J = 5.6$ Hz, 2H), 6.24 – 6.10 (m, 1H), 4.28 (dd, $J = 2.8, 1.2$ Hz, 1H), 2.26 (d, $J = 6.2$ Hz, 6H), 2.15 (s, 3H), 2.13 – 2.09 (m, 1H), 1.81 – 1.75 (m, 1H), 1.62 – 1.46 (m, 3H), 1.28 (m, 3H), 0.98 (t, $J = 7.4$ Hz, 3H), 0.91 (s, 9H), 0.84 (t, $J = 7.4$ Hz, 3H), 0.08 (s, 3H), -0.24 (s, 3H); **^{13}C NMR** (CDCl_3 , 151 MHz) δ 152.2, (138.6, 137.8 two diastereotopic ^{13}C), 137.2, 136.6, (126.9, 126.8 two diastereotopic ^{13}C), 67.0, 33.0, 32.3, 26.8, (22.9, 22.1 two diastereotopic ^{13}C), 21.4, 20.9, 20.9, 18.4, 14.9, 14.2, (-3.0, -5.1 two diastereotopic ^{13}C), the signals for the two carbons adjacent to boron were not observed; **^{11}B NMR** (CDCl_3 , 160 MHz) δ 50.7; **IR** 2954, 2929, 2859, 1736, 1610, 1465, 1373, 1349, 1250, 1007, 992, 834, 809, 779, 743 cm^{-1} ; **HRMS** (DART) calcd. for $\text{C}_{25}\text{H}_{43}\text{BNSi}$ $[\text{M}+\text{H}^+]$: 396.32523, found 396.32490.



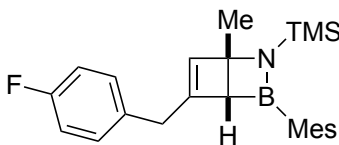
C3-*n*-propyl-C5-(3,5-*bis*-CF₃-benzyl)-Dewar (2.65)

The first syringe with anhydrous cyclohexane (1.1 mL) solution of **2.43** (65.0 mg, 0.112 mmol) was injected at 0.1 mL·min⁻¹ via syringe pump into the flow photoreactor. The second syringe with 5.5 mL of pure cyclohexane was then injected at the same rate. After 3.4 mL of cyclohexane in the second syringe was injected, change to the product collection vial before the last 2.1 mL of cyclohexane was injected to push out the Dewar product. The solution collected in the receiving vials was concentrated *in vacuo* under N₂ to afford the product as a pale yellow oil with 93% average yield (Batch 1: 60.0 mg, 93%; Batch 2: 55.6 mg, 93%). ¹H NMR (CDCl₃, 600 MHz) δ 7.77 (s, 1H), 7.70 (s, 2H), 6.75 (s, 2H), 6.14 – 6.08 (m, 1H), 4.35 (dd, *J* = 2.7, 1.2 Hz, 1H), 3.70 (d, *J* = 17.0 Hz, 1H), 3.56 (dt, *J* = 17.0, 1.6 Hz, 1H), 2.27 (d, *J* = 4.0 Hz, 6H), 2.17 (s, 3H), 1.85 – 1.74 (m, 1H), 1.62 – 1.53 (m, 1H), 1.32 – 1.23 (m, 2H), 0.90 (s, 9H), 0.84 (t, *J* = 7.4, 1.3 Hz, 3H), 0.14 (s, 3H), -0.20 (s, 3H); ¹³C NMR (CDCl₃, 151 MHz) δ 148.7, 141.8, 141.3, (138.4, 137.9 two diastereotopic ¹³C), 137.0, 131.8 (q, ²*J*_{CF} = 33.1 Hz), 129.26 (q, ⁴*J*_{CF} = 3.6 Hz), (127.07, 126.97 two diastereotopic ¹³C), 123.6 (q, ¹*J*_{CF} = 272.5 Hz), 120.33 (q, ³*J*_{CF} = 7.7 Hz), 66.8, 36.8, 32.6, 26.7, (22.9, 22.0 two diastereotopic ¹³C), 21.3, 20.8, 18.4, 14.8, (-2.6, -5.2 two diastereotopic ¹³C), the signals for the two carbons adjacent to boron were not observed; ¹¹B NMR (CDCl₃, 160 MHz) δ 50.6; ¹⁹F NMR (CDCl₃, 470 MHz) δ -62.7 (m); IR 2956, 2930, 2859, 1736, 1610, 1465, 1377, 1349, 1278, 1175, 1137, 995, 835, 821, 779 cm⁻¹; HRMS (DART) calcd. for C₃₁H₄₁BNF₆Si [M+H⁺]: 580.30016, found 580.29836.



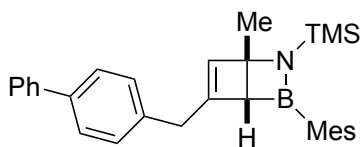
C3- η -propyl-C6-methyl-Dewar (2.66)

The first syringe with anhydrous cyclohexane (1.2 mL) solution of **2.44** (51.4 mg, 0.158 mmol) was injected at 0.1 mL \cdot min $^{-1}$ via syringe pump into the flow photoreactor. The second syringe with 5.5 mL of pure cyclohexane was then injected at the same rate. After 3.3 mL of cyclohexane in the second syringe was injected, change to the product collection vial before the last 2.2 mL of cyclohexane was injected to push out the Dewar product. The solution collected in the receiving vials was concentrated *in vacuo* under N₂ to afford the product as a pale yellow liquid with 91% average yield (Batch 1: 47.0 mg, 91%; Batch 2: 47.3 mg, 92%). **¹H NMR** (CDCl₃, 500 MHz) δ 6.79 – 6.62 (d, J =13.0 Hz, 2H), 6.57 (d, J = 2.4 Hz, 1H), 6.39 (d, J = 2.4 Hz, 1H), 2.27 (d, J = 2.6 Hz, 6H), 2.14 (s, 3H), 1.62 – 1.56 l(m, 1H), 1.54 (s, 3H), 1.46 – 1.40 (m, 1H), 1.36 – 1.30 (m, 1H), 1.26 – 1.20 (m, 1H), 0.81 (t, J = 7.3 Hz, 3H), -0.02 (s, 9H); **¹³C NMR** (CDCl₃, 126 MHz) δ 144.8, 141.0, 139.4, 138.0, 136.8, 126.9, 73.6, 30.6, 22.4, 22.0, 21.4, 20.7, 18.3, 15.1, -0.1 (the signals for the two carbons adjacent to boron were not observed); **¹¹B NMR** (CDCl₃, 160 MHz) δ 52.3; **IR** 2955, 2924, 2854, 1739, 1620, 1608, 1556, 1440, 1372, 1358, 1264, 850, 738 cm $^{-1}$; **HRMS** (DART) calcd. for C₂₀H₃₃BNSi [M+H⁺]: 326.24698, found 326.24776.



C4-*p*-F-benzyl-C6-methyl-Dewar (2.67)

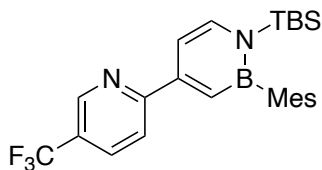
The first syringe with anhydrous cyclohexane (1.7 mL) solution of **2.48** (69.0 mg, 0.176 mmol) was injected at 0.1 mL·min⁻¹ via syringe pump into the flow photoreactor. The second syringe with 5.5 mL of pure cyclohexane was then injected at the same rate. After 2.8 mL of cyclohexane in the second syringe was injected, change to the product collection vial before the last 2.7 mL of cyclohexane was injected to push out the Dewar product. The solution collected in the receiving vials was concentrated *in vacuo* under N₂ to afford the product as a colorless solid with 93% average yield (Batch 1: 64.1 mg, 93%; Batch 2: 65.0 mg, 94%). ¹H NMR (CDCl₃, 600 MHz) δ 7.14 (dd, *J* = 8.5, 5.6 Hz, 2H), 6.98 (t, *J* = 8.7 Hz, 2 H), 6.80 (s, 2H), 5.93 (t, *J* = 1.7 Hz, 1H), 3.46 (d, *J* = 16.9 Hz, 1H), 3.34 (d, *J* = 17.0 Hz, 1H), 2.57 (d, *J* = 1.1 Hz, 1H), 2.30 (s, 3H), 2.25 (s, 6H), 1.65 (s, 3H), -0.01 (s, 9H); ¹³C NMR (CDCl₃, 151 MHz) δ 161.5 (d, ¹*J*_{CF} = 243.5 Hz), 152.6, 138.1, 137.0, 134.42, 134.40, 130.41 (d, ³*J*_{CF} = 8.0 Hz), 126.9, 115.15 (d, ²*J*_{CF} = 20.9 Hz), 67.5, 38.2, 22.3, 22.0, 21.3, -0.2 (the signals for the two carbons adjacent to boron were not observed); ¹¹B NMR (CDCl₃, 160 MHz) δ 48.3; ¹⁹F NMR (CDCl₃, 470 MHz) δ -117.6 (m); IR 3040, 2958, 2919, 2858, 1610, 1509, 1360, 1251, 1225, 1017, 970, 844, 797, 740 cm⁻¹; HRMS (DART) calcd. for C₂₄H₃₂BNFSi [M+H⁺]: 392.23756, found 392.23832.



C4-(1,1'-biphenyl-4-ylmethyl)-C6-methyl-Dewar (**2.68**)

The first syringe with anhydrous cyclohexane (1.2 mL) solution of **2.49** (56.3 mg, 0.125 mmol) was injected at 0.1 mL·min⁻¹ via syringe pump into the flow photoreactor. The second syringe with 5.5 mL of pure cyclohexane was then injected at the same rate.

After 3.3 mL of cyclohexane in the second syringe was injected, change to the product collection vial before the last 2.2 mL of cyclohexane was injected to push out the Dewar product. The solution collected in the receiving vials was concentrated *in vacuo* under N₂ to afford the product as a white solid with 91% average yield (Batch 1: 51.8 mg, 92%; Batch 2: 51.0 mg, 91%). ¹H NMR (CDCl₃, 500 MHz) δ 7.62 (d, *J* = 7.1 Hz, 2H), 7.54 (d, *J* = 8.0 Hz, 2H), 7.46 (t, *J* = 7.6 Hz, 2H), 7.36 (t, *J* = 7.3 Hz, 1H), 7.29 (d, *J* = 7.9 Hz, 2H), 6.82 (s, 2H), 6.02 (d, *J* = 1.6 Hz, 1H), 3.56 (d, *J* = 16.8 Hz, 1H), 3.43 (d, *J* = 16.8 Hz, 1H), 2.64 (d, *J* = 1.6 Hz, 1H), 2.29 (s, 3H), 2.26 (s, 6H), 1.67 (s, 3H), -0.00 (s, 9H); ¹³C NMR (CDCl₃, 126 MHz) δ 152.4, 141.1, 138.9, 138.0, 137.8, 136.8, 134.3, 129.4, 128.7, 127.1, 126.8, 67.4, 38.5, 22.2, 21.9, 21.2, -0.3 (the signals for the two carbons adjacent to boron were not observed); IR 2958, 2926, 2855, 1610, 1507, 1490, 1442, 1362, 1281, 1260, 1160, 1019, 835, 778 cm⁻¹; HRMS (DART) calcd. for C₃₀H₃₇BNSi [M+H₃O⁺]: 450.27828, found 450.27922.

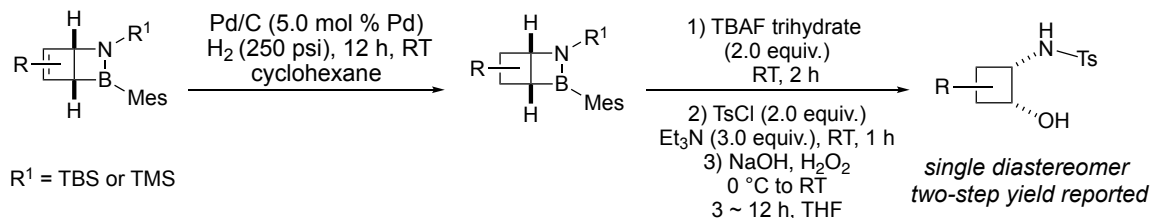


C4-(5-CF₃-pyridin-2-yl)-1,2-azaborine (2.74)

The first syringe with anhydrous cyclohexane (2.2 mL) solution of **2.32** (62.5 mg, 0.137 mmol) was injected at 0.1 mL·min⁻¹ via syringe pump into the flow photoreactor. The second syringe with 5.5 mL of pure cyclohexane was then injected at the same rate. After 2.3 mL of cyclohexane in the second syringe was injected, change to the product collection vial before the last 3.2 mL of cyclohexane was injected to push out the Dewar product. The solution collected in the receiving vials was concentrated *in vacuo* under N₂ to afford the

product as a pale yellow solid. ^1H and ^{11}B NMR analysis indicated a new 1,2-azaborine species was formed as the major product instead of anticipated Dewar product. The new species was isolated by flash column chromatograph (silical gel; 3 – 5% diethyl ether in hexane) as a pale yellow solid with 77% isolated yield (Batch 1: 30.8 mg/40.0 mg, 77%; 48.8 mg/62.5 mg, 78%). The structure was confirmed by X-ray crystallography. ^1H NMR (CDCl_3 , 500 MHz) δ 8.94 (dd, $J = 2.4, 1.1$ Hz, 1H), 7.95 (dd, $J = 8.4, 2.4$ Hz, 1H), 7.88 (d, $J = 8.3$ Hz, 1H), 7.63 (d, $J = 7.1$ Hz, 1H), 7.20 (ddd, $J = 7.1, 2.4, 1.0$ Hz, 1H), 7.17 (d, $J = 2.3$ Hz, 1H), 6.82 (s, 2H), 2.31 (s, 3H), 2.12 (s, 6H), 0.95 (s, 9H), 0.05 (s, 6H); ^{13}C NMR (CDCl_3 , 151 MHz) δ 161.6, 150.4, 146.34 (d, $J = 4.1$ Hz), 140.0, 139.0, 136.9, 133.95 (d, $J = 3.6$ Hz), 127.2, 125.5 (d, $J = 33.2$ Hz), 123.9 (d, $J = 272.2$ Hz), 120.9, 109.7, 27.6, 23.6, 21.4, 19.4, -3.2 (the signals for the two carbons adjacent to boron were not observed); ^{11}B NMR (CDCl_3 , 160 MHz) δ 40.3; ^{19}F NMR (CDCl_3 , 470 MHz) δ -62.3 (m); IR 2956, 2930, 2860, 1735, 1501, 1328, 1305, 1261, 1130, 1005, 841, 823 cm^{-1} ; HRMS (DART) calcd. for $\text{C}_{25}\text{H}_{33}\text{BN}_2\text{F}_3\text{Si}$ [$\text{M}+\text{H}^+$]: 457.24527, found 457.24402. Crystal of **2.17** was grown using slow evaporation method: 15.0 mg of **2.74** was dissolved in 0.4 mL of hexane : diethyl ether (1:1) in a 4 mL vial with septum screw cap. A 18G x 1 1/2 needle (1.2 mm x 40 mm) was fitted on the septum screw cap, and the vial was kept under 4°C in fridge. The crystal structure was confirmed by X-ray crystallography although the quality of data was rather low (unable to collect structure refinement data for publication purpose).

2.7.2.3 General Procedure for Sequential Hydrogenation and Oxidation towards the Cyclobutane β -amino alcohol in Table 2.5



General Procedure for Hydrogenation:

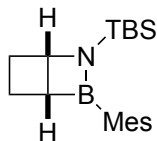
In a N_2 glovebox, to a 4 mL or 20 mL scintillation vial with a magnetic stir bar was charged with 10 wt. % Palladium on carbon (5.0 mol % of Pd) and cyclohexane solution of collected Dewar substrate (0.05–0.08 M). The vial was sealed with septum screw cap, and a 18G x 1 1/2 needle (1.2 mm x 40 mm) was fitted on the septum screw cap for atmosphere exchange. The vial was then placed in a Parr pressure vessel. The pressure vessel was sealed and transferred into a fume hood with the safety blast shield placed. The pressure vessel was pressurized, released and back-filled with hydrogen gas five times before charged with 250 psi hydrogen (caution: fix the hydrogen gas tank firmly during the whole process; apply hydrogen slowly through a pressure regulator; gently open the venting valve to release pressure). The pressure vessel was placed in the middle of stir plate and the reaction was allowed to be vigorously stirred for 12 hours. After 12 hours, the venting valve of pressure vessel was slowly opened to release H_2 carefully. The Parr pressure vessel was purged with N_2 for 5 minutes before brought into glovebox. The reaction mixture was filtered to remove the heterogenous catalyst and the filtrate was concentrated *in vacuo* under N_2 atmosphere. NMR was checked which shows only one diastereomer after hydrogenation. The hydrogenated intermediate was used directly for the

subsequent oxidation step without further purification. Hydrogenation of each Dewar compound was repeated at least twice.

General Procedure for Oxidation:

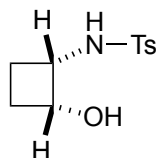
In a N₂ glovebox, to a 20 mL scintillation vial containing a magnetic stir bar was added hydrogenated intermediate (1.0 equiv.) and THF (concentration is around 0.1 M). TBAF trihydrate (2.0 equiv.) was added to the solution and the reaction mixture was allowed to stir for 2 hours at room temperature. At this point, an aliquot was checked by ¹¹B NMR which indicates the formation of tetra-coordinated borate species after ring-opening. Then, the ring-opened intermediate was trapped by 2.0 equiv. of Tos-Cl with additive of 3.0 equiv. of Et₃N. Precipitates were observed once the Et₃N was added. The reaction was left to be stirred for 1 hour. The crude mixture was filtered to remove the precipitates and the filtrate was combined in another 20 mL vial. The vial was cooled down to 0°C in an ice/water bath before saturated NaOH aqueous solution was added slowly (For base sensitive substrates, PH = 7.0 aqueous buffer was used instead). Then 25 equiv. of hydrogen peroxide (H₂O₂) 30% (w/w) in water solution was added via syringe dropwise under 0°C. The reaction was allowed to stir for 3 – 12 hours. Upon completion, the reaction was cooled down to 0°C and 25 equiv. of Na₂S₂O₃ saturated solution was added slowly. The aqueous layer was extracted with diethyl ether or ethyl acetate 5 times. The combined organic phase was washed with brine, dried over MgSO₄, vacuum-filtered through a fritted funnel, and concentrated *in vacuo*. The crude residue was purified by flash column chromatography (silica gel) or preparative thin layer chromatography (silica gel) to give the desired cyclobutane β-amino alcohol product. (Although the product was generally 254 nm UV-active, PMA (Phosphomolybdic Acid) or CAM (Cerium Ammonium Molybdate)

stain could be very helpful to clearly identify the product spot during TLC analysis). Yields were reported over two steps starting from the Dewar substrates.



2-(*tert*-butyldimethylsilyl)-3-mesityl-2-aza-3-borabicyclo[2.2.0]hexane (2.16)

The heterogenous catalyst was removed by filtration and the filtrate was concentrated *in vacuo* under N₂ atmosphere to give a pale yellow liquid. NMR was checked without further purification. ¹H NMR (CDCl₃, 500 MHz) δ 6.81 (s, 2H), 4.49 (td, *J* = 5.5, 3.9 Hz, 1H), 2.57 (tt, *J* = 10.9, 5.6 Hz, 1H), 2.49 (dt, *J* = 10.8, 3.8 Hz, 1H), 2.27 – 2.18 (m, 1H), 2.15 – 1.97 (m, 2H), 0.91 (s, 9H), 0.04 (s, 3H), -0.08 (s, 3H); ¹³C NMR (CDCl₃, 126 MHz) δ 137.0, 127.0, 61.6, 30.4, 26.5, 22.7, 21.3, 18.4, 16.8, (-5.0, -5.1 two diastereotopic ¹³C), the signals for the two carbons adjacent to boron were not observed; ¹¹B NMR (CDCl₃, 160 MHz) δ 53.9; IR 2950, 2929, 2856, 1610, 1470, 1437, 1352, 1268, 1252, 1107, 1025, 980, 932, 846, 832, 775 cm⁻¹; HRMS (DART) calcd. for C₁₉H₃₃BNSi [M+H₃O⁺]: 314.24698, found 314.24726.

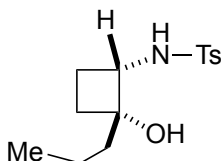


N-(2-hydroxycyclobutyl)-4-methylbenzenesulfonamide (2.17)

Parent Dewar **1.21** (622.6 mg, 2.0 mmol) was used for the telescoped hydrogenation and oxidation step. In adaption to the general procedure, the crude residue was purified by flash column chromatography (silica gel; 25 – 40% ethyl acetate in hexane)

to give the desired cyclobutane β -amino alcohol product as a white solid (304.0 mg, 63%). $^1\text{H NMR}$ (CDCl_3 , 600 MHz) δ 7.76 (d, $J = 7.9$ Hz, 2H), δ 7.29 (d, $J = 7.9$ Hz, 2H), 5.51 (d, $J = 8.2$ Hz, 1H), 4.29 (dd, $J = 5.3, 2.9$ Hz, 1H), 3.77 (dd, $J = 8.2, 5.2$ Hz, 1H), 2.58 (br s, 1H), 2.41(s, 3H) 2.12 – 1.90 (m, 3H), 1.78 (ddd, $J = 9.0, 5.5, 2.9$ Hz, 1H); $^{13}\text{C NMR}$ (CDCl_3 , 151 MHz) δ 143.7, 137.4, 129.84, 127.2, 70.2, 51.4, 26.6, 26.6, 21.7; **IR** 3492, 3275, 2955, 2930, 2872, 1598, 1495, 1337, 1307, 1152, 1087, 1018, 934, 812, 668, 551 cm^{-1} ; **HRMS** (DART) calcd. for $\text{C}_{11}\text{H}_{16}\text{NO}_3\text{S}$ [$\text{M}+\text{H}_3\text{O}^+$]: 242.08454, found 242.08533.

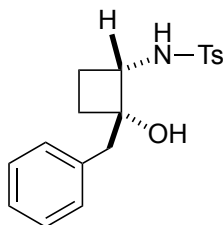
Crystal of **2.17** was grown using vapor diffusion method: 10.0 mg of **2.17** was dissolved in 0.3 mL of CDCl_3 in a 4 mL vial, and the uncapped 4 mL vial was placed inside a 20 mL vial with 3.5 mL of pentane. The 20 mL vial was capped and placed at ambient temperature.



***N*-(2-hydroxy-2-propylcyclobutyl)-4-methylbenzenesulfonamide (2.80)**

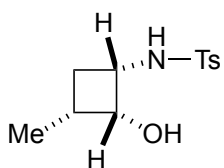
Dewar **2.50** (50.7 mg, 0.143 mmol) was used for the telescoped hydrogenation and oxidation step. Two batches were set up in parallel. In adaption to the general procedure, the crude residue was purified by flash column chromatography (silica gel; 25 – 40% ethyl acetate in hexane) to give the desired product as a white solid with 59% average yield (Batch 1: 24.3 mg, 60%; Batch 2: 23.9 mg, 59%). $^1\text{H NMR}$ (CDCl_3 , 600 MHz) δ 7.74 (d, $J = 8.2$ Hz, 2H), 7.28 (d, $J = 8.0$ Hz, 2H), 5.20 (d, $J = 9.0$ Hz, 1H), 3.54 (q, $J = 8.1$ Hz, 1H), 2.41 (s, 3H), 2.05 – 1.92 (m, 1H), 1.85 (s, 1H), 1.82 – 1.74 (m, 1H), 1.74 – 1.65 (m, 2H), 1.38 – 1.17 (m, 4H), 0.84 (t, $J = 7.1$ Hz, 3H); $^{13}\text{C NMR}$ (CDCl_3 , 151 MHz) δ 143.8, 138.2, 130.0, 127.5, 80.0, 54.1, 42.6, 29.6, 26.0, 21.9, 16.9, 14.6; **IR** 3485, 3274, 2956, 2930,

2871, 1599, 1495, 1334, 1304, 1158, 1093, 1019, 936, 815, 667, 550 cm^{-1} ; **HRMS** (DART) calcd. for $\text{C}_{14}\text{H}_{22}\text{NO}_3\text{S}$ [$\text{M}+\text{H}_3\text{O}^+$]: 284.13149, found 284.13209.



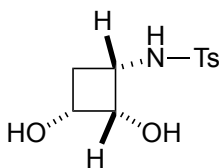
***N*-(2-benzyl-2-hydroxycyclobutyl)-4-methylbenzenesulfonamide (2.81)**

Dewar **2.51** (42.0 mg, 0.105 mmol) was used for the telescoped hydrogenation and oxidation step. Two batches were set up in parallel. In adaption to the general procedure, the crude residue was purified by preparative thin layer chromatography (silica gel; 40% ethyl acetate in hexane) to give the desired product as a white solid with 64% average yield (Batch 1: 23.4 mg, 66%; Batch 2: 21.2 mg, 62%). **^1H NMR** (CDCl_3 , 500 MHz) δ 7.77 (d, $J = 8.2$ Hz, 2H), 7.37 – 7.18 (m, 5H), 7.12 – 7.03 (m, 2H), 5.23 (d, $J = 9.3$ Hz, 1H), 3.72 (td, $J = 9.0, 7.2$ Hz, 1H), 2.72 (d, $J = 13.7$ Hz, 1H), 2.56 (d, $J = 13.7$ Hz, 1H), 2.43 (s, 3H), 2.07 – 1.95 (m, 1H), 1.90 – 1.79 (m, 3H), 1.70 – 1.58 (m, 1H); **^{13}C NMR** (CDCl_3 , 101 MHz) δ 143.6, 138.2, 136.1, 130.0, 129.8, 128.7, 127.3, 127.0, 79.4, 53.5, 45.9, 29.4, 26.2, 21.7; **IR** 3487, 3279, 2956, 2923, 2853, 1599, 1495, 1453, 1332, 1304, 1153, 1120, 1092, 1019, 937, 815, 703, 667, 572, 548 cm^{-1} ; **HRMS** (DART) calcd. for $\text{C}_{18}\text{H}_{22}\text{NO}_3\text{S}$ [$\text{M}+\text{H}_3\text{O}^+$]: 332.13149, found 332.13259.



***N*-(2-hydroxy-3-methylcyclobutyl)-4-methylbenzenesulfonamide (2.82)**

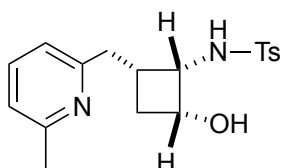
Dewar **2.53** (43.1 mg, 0.132 mmol) was used for the telescoped hydrogenation and oxidation step. Two batches were set up in parallel. In adaption to the general procedure, the crude residue was purified by flash column chromatography (silica gel; 25 – 40% ethyl acetate in hexane) to give the desired product as a white solid with 60% average yield (Batch 1: 20.3 mg, 60%; Batch 2: 20.7 mg, 61%). **¹H NMR** (CDCl₃, 400 MHz) δ 7.81 – 7.72 (d, 8.0 Hz, 2H), 7.30 (d, *J* = 8.0 Hz, 2H), 5.09 (d, *J* = 9.4 Hz, 1H), 4.15 (q, *J* = 4.9 Hz, 1H), 3.73 – 3.62 (m, 1H), 2.42 (s, 3H), 2.31 – 2.22 (m, 1H), 2.18 – 2.08 (m, 1H), 1.76 (br s, 1H), 1.60 (q, *J* = 10.1 Hz, 1H), 0.95 (d, *J* = 6.7 Hz, 3H); **¹³C NMR** (CDCl₃, 101MHz) δ 143.7, 137.6, 129.8, 127.3, 72.6, 48.1, 36.2, 29.8, 21.7, 13.0; **IR** 3497, 3287, 2966, 2930, 2870, 1599, 1495, 1332, 1306, 1158, 1091, 1025, 921, 815, 671, 580, 550 cm⁻¹; **HRMS** (DART) calcd. for C₁₂H₁₈NO₃S [M+H₃O⁺]: 256.10019, found 256.10075.



***N*-(2,3-dihydroxycyclobutyl)-4-methylbenzenesulfonamide (2.83)**

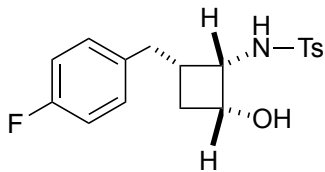
Dewar **2.52** (47.7 mg, 0.109 mmol) was used for the telescoped hydrogenation and oxidation step. Two batches were set up in parallel. In adaption to the general procedure (PH = 7.0 buffer was used in the oxidation step instead of aqueous NaOH solution), the crude residue was purified by preparative thin layer chromatography (silica gel; 72% ethyl acetate and 3% dichloromethane in hexane) to give the desired product as a white solid with 41% average yield (Batch 1: 11.5 mg, 42%; Batch 2: 11.0 mg, 41%). **¹H NMR** (CDCl₃, 600 MHz) δ 7.75 (d, *J* = 8.2 Hz, 2H), 7.30 (d, *J* = 8.0 Hz, 2H), 5.38 (d, *J* = 9.2 Hz, 1H), 4.24 (q, *J* = 4.5 Hz, 1H), 4.00 (d, *J* = 7.6 Hz, 1H), 3.53 – 3.48 (m, 1H), 3.03 (br s, 1H), 2.71

(br s, 1H), 2.57 – 2.50 (m, 1H), 2.43 (s, 3H), 1.85 (dt, $J = 12.5, 7.9$ Hz, 1H); ^{13}C NMR (CDCl₃, 126 MHz) δ 143.9, 137.2, 129.9, 127.3, 72.3, 63.6, 45.6, 38.7, 21.7; IR 3452, 3273, 2944, 1598, 1494, 1441, 1334, 1304, 1157, 1092, 1046, 916, 816, 667, 564, 548 cm⁻¹; HRMS (DART) calcd. for C₁₁H₁₆NO₄S [M+H₃O⁺]: 258.17019, found 258.17075.



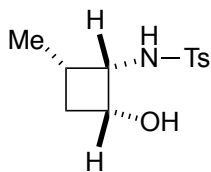
***N*-(2-hydroxy-4-((6-methylpyridin-2-yl)methyl)cyclobutyl)-4-methylbenzenesulfonamide (2.84)**

Dewar **2.55** (42.0 mg, 0.101 mmol) was used for the telescoped hydrogenation and oxidation step. Two batches were set up in parallel. In adaption to the general procedure, the crude residue was purified by preparative thin layer chromatography (silica gel; 50% ethyl acetate in hexane) to give the desired product as a pale yellow solid with 52% average yield (Batch 1: 18.6 mg, 54%; Batch 2: 16.9 mg, 49%). ^1H NMR (CDCl₃, 600 MHz) δ 9.38 (br s, 1H), 7.76 (d, $J = 7.9$ Hz, 2H), 7.59 (t, $J = 7.7$ Hz, 1H), 7.29 (d, $J = 8.0$ Hz, 2H), 7.07 (d, $J = 7.8$ Hz, 1H), 6.99 (d, $J = 7.6$ Hz, 1H), 4.30 – 4.26 (m, 1H), 3.69 (t, $J = 6.8$ Hz, 1H), 3.51 (dd, $J = 14.6, 10.5$ Hz, 1H), 2.89 (dd, $J = 14.5, 3.8$ Hz, 1H), 2.68 (br s, 1H) 2.64 (s, 3H), 2.40 (s, 3H), 2.36 – 2.22 (m, 1H), 1.67 (m, 1H), 0.90 – 0.80 (m, 1H); ^{13}C NMR (CDCl₃, 151 MHz) δ 159.1, 157.0, 143.3, 138.8, 137.3, 129.8, 127.2, 121.8, 121.4, 68.1, 52.8, 39.3, 37.0, 32.4, 23.6, 21.7; IR 3274, 3061, 2924, 2854, 1596, 1578, 1455, 1332, 1304, 1265, 1156, 1092, 814, 733, 666, 571, 548 cm⁻¹; HRMS (DART) calcd. for C₁₈H₂₃N₂O₃S [M+H₃O⁺]: 347.14239, found 347.14172.



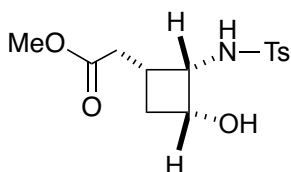
***N*-(2-(4-fluorobenzyl)-4-hydroxycyclobutyl)-4-methylbenzenesulfonamide (2.85)**

In the first batch, Dewar **2.54** (92.3 mg, 0.219 mmol) was used for the telescoped hydrogenation and oxidation step. In the second batch, Dewar **2.54** (44.2 mg, 0.105 mmol) was used for the telescoped hydrogenation and oxidation step. In adaption to the general procedure, the crude residue was purified by flash column chromatography (silica gel; 25 – 40% ethyl acetate in hexane) to give the desired product as a white solid with 54% average yield (Batch 1: 42.8 mg, 56%; Batch 2: 19.1 mg, 52%). **¹H NMR** (CDCl₃, 500 MHz) δ 7.75 (d, *J* = 8.3 Hz, 2H), 7.30 (d, *J* = 8.0 Hz, 2H), 7.00 (dd, *J* = 8.5, 5.6 Hz, 2H), 6.89 (t, *J* = 8.7 Hz, 2H), 5.43 (d, *J* = 8.6 Hz, 1H), 4.28 (q, *J* = 6.7 Hz, 1H), 4.00 – 3.94 (m, 1H), 2.82 – 2.61 (m, 2H), 2.52 – 2.44 (m, 1H), 2.43 (s, 3H) 2.25 – 2.14 (m, 1H), 2.11-2.04 (br s, 1H) 1.71 – 1.55 (m, 1H); **¹³C NMR** (CDCl₃, 126 MHz) δ 161.5 (d, ¹*J*_{CF} = 243.7 Hz), 143.8, 137.4, 135.50 (d, ⁴*J*_{CF} = 3.3 Hz), 129.99 (d, ²*J*_{CF} = 7.9 Hz), 129.9, 127.3, 115.2 (d, ³*J*_{CF} = 21.0 Hz), 66.8, 54.1, 36.5, 35.4, 34.0, 21.7; **¹⁹F NMR** (CDCl₃, 470 MHz) δ –117.5 (m); **IR** 3484, 3285, 2927, 1599, 1508, 1445, 1332, 1303, 1220, 1154, 1092, 872, 813, 669, 574, 547 cm⁻¹; **HRMS** (DART) calcd. for C₁₈H₂₁NO₃FS [M+H⁺]: 350.12207, found 350.12261.



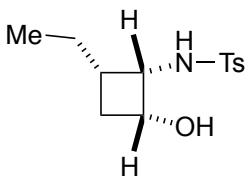
***N*-(2-hydroxy-4-methylcyclobutyl)-4-methylbenzenesulfonamide (2.86)**

Dewar **2.60** (30.6 mg, 0.095 mmol) was used for the telescoped hydrogenation and oxidation step. Two batches were set up in parallel. In adaption to the general procedure, the crude residue was purified by preparative thin layer chromatography (silica gel; 40% ethyl acetate in hexane) to give the desired product as a white solid with 59% average yield (Batch 1: 13.3 mg, 55%; Batch 2: 15.1 mg, 62%). **¹H NMR** (CDCl₃, 500 MHz) δ 7.77 (d, *J* = 8.9, 2H), 7.30 (d, *J* = 8.0 Hz, 2H), 5.18 (d, *J* = 8.9 Hz, 1H), 4.26 (q, *J* = 6.2, 5.8 Hz, 1H), 3.93 – 3.84 (m, 1H), 2.43 (s, 3H), 2.42 – 2.26 (m, 2H), 1.91 (s, 1H), 1.47 – 1.38 (m, 1H), 1.01 (d, *J* = 7.1 Hz, 3H); **¹³C NMR** (CDCl₃, 126 MHz) δ 143.7, 137.7, 129.8, 127.2, 68.0, 53.6, 35.4, 30.8, 21.7, 15.7; **IR** 3497, 3291, 2968, 2929, 2873, 1598, 1495, 1334, 1304, 1227, 1185, 1158, 1093, 922, 815, 670, 579, 549 cm⁻¹; **HRMS** (DART) calcd. for C₁₂H₁₈NO₃S [M+H⁺]: 256.10019, found 256.10075. Crystal of **2.86** was grown using vapor diffusion method: 13.3 mg of **2.86** was dissolved in 0.4 mL of CDCl₃ in a 4 mL vial, and the uncapped 4 mL vial was placed inside a 20 mL vial with 4.0 mL of pentane. The 20 mL vial was capped and placed at ambient temperature.



methyl 2-(3-hydroxy-2-((4-methylphenyl)sulfonamido)cyclobutyl)acetate (2.87)

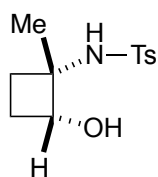
Dewar **2.56** (55.8 mg, 0.146 mmol) was used for the telescoped hydrogenation and oxidation step. Two batches were set up in parallel. In adaption to the general procedure (PH = 7.0 buffer was used in the oxidation step instead of aqueous NaOH solution), the crude residue was purified by flash column chromatography (silica gel; 40% ethyl acetate and 10% dichloromethane in hexane) to give the desired product as a white solid with 39% average yield (Batch 1: 17.8 mg, 40%; Batch 2: 17.2 mg, 38%). **¹H NMR** (CDCl₃, 600 MHz) δ 7.74 (d, *J* = 7.9 Hz, 2H), 7.31 (d, *J* = 7.9 Hz, 2H), 5.54 (d, *J* = 6.5 Hz, 1H), 4.28 (q, *J* = 6.1 Hz, 1H), 3.82 (q, *J* = 7.0, 6.5 Hz, 1H), 3.65 (s, 3H), 2.76 – 2.59 (m, 2H), 2.52 (dd, *J* = 16.2, 6.9 Hz, 1H), 2.42 (s, 3H), 2.41 – 2.36 (m, 2H), 1.70 – 1.61 (m, 1H); **¹³C NMR** (CDCl₃, 151 MHz) δ 173.8, 143.8, 136.8, 129.9, 127.3, 67.0, 53.5, 51.9, 35.2, 33.7, 32.0, 21.7; **IR** 3497, 3294, 2951, 2851, 1734, 1598, 1495, 1441, 1336, 1202, 1160, 1092, 1047, 816, 671, 550 cm⁻¹; **HRMS** (DART) calcd. for C₁₄H₂₀NO₅S [M+H⁺]: 314.10519, found 314.10477.



***N*-(2-ethyl-4-hydroxycyclobutyl)-4-methylbenzenesulfonamide (2.88)**

In the first batch, Dewar **2.61** (34.4 mg, 0.101 mmol) was used for the telescoped hydrogenation and oxidation step. In the second batch, Dewar **2.61** (41.7 mg, 0.122 mmol) was used for the telescoped hydrogenation and oxidation step. In adaption to the general procedure, the crude residue was purified by flash column chromatography (silica gel; 40% ethyl acetate in hexane) to give the desired product as a white solid with 62% average yield (Batch 1: 16.4 mg, 60%; Batch 2: 21.2 mg, 64%). **¹H NMR** (CDCl₃, 500 MHz) δ 7.76 (d,

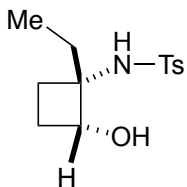
$J = 8.3$ Hz, 2H), 7.30 (d, $J = 8.1$ Hz, 2H), 5.24 (d, $J = 8.9$ Hz, 1H), 4.23 (q, $J = 6.9$, Hz, 1H), 3.96 – 3.84 (m, 1H), 2.42 (s, 3H), 2.32 – 2.25 (m, 1H), 2.15 – 2.07 (m, 1H), 2.01 – 1.84 (br s, 1H), 1.56 – 1.34 (m, 3H), 0.77 (t, $J = 7.3$ Hz, 3H); ^{13}C NMR (CDCl_3 , 126 MHz) δ 143.7, 137.5, 129.8, 127.3, 66.9, 54.0, 36.9, 34.1, 23.2, 21.7, 11.4; IR 3485, 3288, 2959, 2926, 2856, 1598, 1456, 1334, 1304, 1264, 1227, 1160, 1093, 814, 733, 703, 548 cm^{-1} ; HRMS (DART) calcd. for $\text{C}_{13}\text{H}_{20}\text{NO}_3\text{S}$ [$\text{M}+\text{H}^+$]: 270.11584, found 270.11594.



***N*-(2-hydroxy-1-methylcyclobutyl)-4-methylbenzenesulfonamide (2.89)**

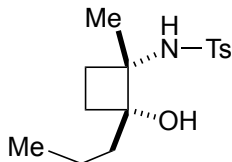
Dewar **2.62** (67.1 mg, 0.237 mmol) was used for the telescoped hydrogenation and oxidation step. Two batches were set up in parallel. In adaption to the general procedure, the crude residue was purified by flash column chromatography (silica gel; 25 – 40% ethyl acetate in hexane) to give the desired product as a white solid with 54% average yield (Batch 1: 33.1 mg, 55%; Batch 2: 31.7 mg, 52%). ^1H NMR (CDCl_3 , 500 MHz) δ 7.80 (d, $J = 8.0$ Hz, 2H), 7.29 (d, $J = 8.0$ Hz, 2H), 5.35 (s, 1H), 3.95 (t, $J = 5.9$ Hz, 1H), 2.75 (d, $J = 3.7$ Hz, 1H), 2.42 (s, 3H), 2.15 – 2.05 (m, 2H), 1.82 – 1.73 (m, 1H), 1.65 – 1.51 (m, 1H), 1.27 (s, 3H); ^{13}C NMR (CDCl_3 , 126 MHz) δ 143.3, 140.0, 129.7, 127.0, 74.1, 60.4, 29.2, 25.8, 25.1, 21.6; IR 3476, 3350, 2970, 2948, 1739, 1599, 1460, 1373, 1317, 1228, 1184, 1092, 948, 816, 737, 707, 666, 552 cm^{-1} ; HRMS (DART) calcd. for $\text{C}_{12}\text{H}_{18}\text{NO}_3\text{S}$ [$\text{M}+\text{H}^+$]: 256.10019, found 256.10150. Crystal of **2.89** was grown using vapor diffusion method: 15.1 mg of **2.89** was dissolved in 0.4 mL of CDCl_3 in a 4 mL vial, and the uncapped 4 mL

vial was placed inside a 20 mL vial with 4.0 mL of pentane. The 20 mL vial was capped and placed at ambient temperature.



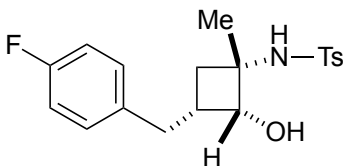
***N*-(1-ethyl-2-hydroxycyclobutyl)-4-methylbenzenesulfonamide (2.90)**

Dewar **2.63** (62.8 mg, 0.211 mmol) was used for the telescoped hydrogenation and oxidation step. Two batches were set up in parallel. In adaption to the general procedure, the crude residue was purified by flash column chromatography (silica gel; 25 – 40% ethyl acetate in hexane) to give the desired product as a white solid with 57% average yield (Batch 1: 31.2 mg, 55%; Batch 2: 33.5 mg, 59%). ¹H NMR (CDCl₃, 500 MHz) δ 7.81 (d, *J* = 8.0 Hz, 2H), 7.29 (d, *J* = 8.0 Hz, 2H), 5.26 (s, 1H), 4.00 (q, *J* = 6.1 Hz, 1H), 2.71 (d, *J* = 5.1 Hz, 1H), 2.42 (s, 3H), 2.13 – 2.04 (m, 2H), 1.89 – 1.65 (m, 2H), 1.63 – 1.40 (m, 2H), 0.68 (t, *J* = 7.4, 3H); ¹³C NMR (CDCl₃, 126 MHz) δ 143.2, 140.0, 129.7, 127.0, 72.0, 64.9, 30.9, 26.5, 26.1, 21.6, 7.7; IR 3460, 3300, 2969, 2947, 2879, 1741, 1599, 1458, 1379, 1319, 1286, 1231, 1183, 1092, 977, 816, 737, 707, 667, 551 cm⁻¹; HRMS (DART) calcd. for C₁₃H₂₀NO₃S [M+H⁺]: 270.11584, found 270.11659. Crystal of **2.90** was grown using vapor diffusion method: 12.7 mg of **2.90** was dissolved in 0.3 mL of CDCl₃ in a 4 mL vial, and the uncapped 4 mL vial was placed inside a 20 mL vial with 3.5 mL of pentane. The 20 mL vial was capped and placed at ambient temperature.



***N*-(2-hydroxy-1-methyl-2-propylcyclobutyl)-4-methylbenzenesulfonamide (2.91)**

Dewar **2.66** (43.0 mg, 0.133 mmol) was used for the telescoped hydrogenation and oxidation step. Two batches were set up in parallel. In adaption to the general procedure, the crude residue was purified by flash column chromatography (silica gel; 25 – 40% ethyl acetate in hexane) to give the desired product as a white solid with 59% average yield (Batch 1: 22.2 mg, 56%; Batch 2: 24.5 mg, 62%). **¹H NMR** (CDCl₃, 500 MHz) δ 7.78 (d, *J* = 8.3 Hz, 2H), 7.28 (d, *J* = 8.0 Hz, 2H), 5.45 (s, 1H), 2.42 (s, 3H), 2.13 – 2.04 (m, 2H), 1.83 – 1.67 (m, 2H), 1.67 – 1.60 (m, 1H), 1.52 – 1.29 (m, 4H), 1.26 (s, 3H) 0.91 (t, *J* = 7.1 Hz, 3H); **¹³C NMR** (CDCl₃, 126 MHz) δ 143.3, 139.9, 129.7, 127.3, 80.5, 61.1, 37.9, 31.6, 29.3, 21.7, 21.3, 16.4, 14.6; **IR** 3490, 3327, 2957, 2872, 1739, 1599, 1454, 1374, 1318, 1262, 1152, 1094, 942, 815, 737, 707, 587, 551 cm⁻¹; **HRMS** (DART) calcd. for C₁₅H₂₄NO₃S [M+H⁺]: 298.14714, found 298.14765.

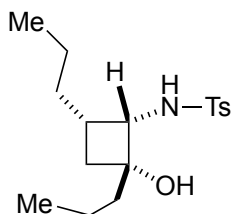


***N*-(3-(4-fluorobenzyl)-2-hydroxy-1-methylcyclobutyl)-4-methylbenzenesulfonamide (2.92)**

Dewar **2.67** (45.2 mg, 0.116 mmol) was used for the telescoped hydrogenation and oxidation step. Two batches were set up in parallel. In adaption to the general procedure,

the crude residue was purified by flash column chromatography (silica gel; 25 – 40% ethyl acetate in hexane) to give the desired product as a white solid with 54% average yield (Batch 1: 23.6 mg, 56%; Batch 2: 21.9 mg, 52%). $^1\text{H NMR}$ (CDCl_3 , 500 MHz) δ 7.80 (d, $J = 8.3$ Hz, 2H), 7.29 (d, $J = 8.0$ Hz, 2H), 7.10 (dd, $J = 8.5, 5.6$ Hz, 2H), 6.92 (t, $J = 8.7$ Hz, 2H), 5.29 (s, 1H), 4.02 (dd, $J = 5.9, 2.2$ Hz, 1H), 2.90 (dd, $J = 14.0, 8.2$ Hz, 1H), 2.83 – 2.74 (br s, 1H), 2.59 (dd, $J = 14.0, 7.4$ Hz, 1H), 2.46 – 2.37 (m, 4H), 1.92 (d, $J = 9.0$ Hz, 2H), 1.24 (s, 3H); $^{13}\text{C NMR}$ (CDCl_3 , 126 MHz) δ 161.4 (d, $^1J_{\text{CF}} = 243.5$ Hz), 143.6, 139.5, 136.38 (d, $^4J_{\text{CF}} = 3.0$ Hz), 130.04 (d, $^3J_{\text{CF}} = 7.7$ Hz), 129.7, 127.3, 115.2 (d, $^2J_{\text{CF}} = 21.0$ Hz), 75.8, 55.8, 39.6, 35.2, 33.8, 23.6, 21.7; $^{19}\text{F NMR}$ (CDCl_3 , 470 MHz) δ -117.6 (m); **IR** 3501, 3284, 3029, 2970, 1738, 1600, 1509, 1375, 1317, 1218, 1152, 1093, 955, 815, 737, 706, 574, 553 cm^{-1} ; **HRMS** (DART) calcd. for $\text{C}_{19}\text{H}_{23}\text{NO}_3\text{FS}$ $[\text{M}+\text{H}^+]$: 364.13772, found 364.13643.

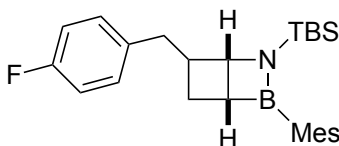
2D



***N*-(2-hydroxy-2,4-dipropylcyclobutyl)-4-methylbenzenesulfonamide (2.93)**

Dewar **2.64** (42.6 mg, 0.108 mmol) was used for the telescoped hydrogenation and oxidation step. Two batches were set up in parallel. In adaption to the general procedure, the crude residue was purified by preparative thin layer chromatography (silica gel; 40% ethyl acetate in hexane) to give the desired product as a white solid with 42% average yield (Batch 1: 14.7 mg, 42%; Batch 2: 15.1 mg, 43%). $^1\text{H NMR}$ (CDCl_3 , 500 MHz) δ 7.76 (d,

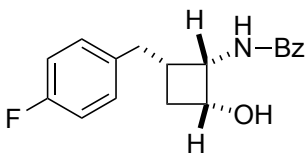
$J=8.0$ Hz 2H), 7.30 (d, $J = 8.0$ Hz, 2H), 5.17 (d, $J = 9.3$ Hz, 1H), 3.61 (t, $J = 8.8$ Hz, 1H), 2.42 (s, 3H), 2.21 – 2.14 (m, 1H), 2.03 – 1.97 (m, 1H), 1.65 (s, 1H), 1.47 (dd, $J = 12.5, 6.3$ Hz, 1H), 1.40 – 1.03 (m, 8H), 0.89 – 0.72 (m, 6H); ^{13}C NMR (CDCl_3 , 126 MHz) δ 143.6, 137.8, 129.7, 127.4, 76.4, 56.2, 42.8, 37.1, 33.6, 32.4, 21.6, 20.2, 16.5, 14.4, 14.2; IR 3483, 3303, 2958, 2869, 1739, 1598, 1455, 1366, 1304, 1264, 1228, 1159, 1093, 928, 813, 739, 706, 583, 549 cm^{-1} ; HRMS (DART) calcd. for $\text{C}_{17}\text{H}_{28}\text{NO}_3\text{S}$ $[\text{M}+\text{H}^+]$: 326.17844, found 326.17955.



2-(tert-butyl dimethylsilyl)-6-(4-fluorobenzyl)-3-mesityl-2-aza-3-borabicyclo[2.2.0]hexane (2.94)

The heterogenous catalyst was removed by filtration and the filtrate was concentrated *in vacuo* under N_2 atmosphere to give a pale yellow liquid. ^1H NMR (THF- d_8 , 500 MHz) δ 7.16 (dd, $J = 8.5, 5.5$ Hz, 2H), 6.96 (t, $J = 8.8$ Hz, 2H), 6.79 – 6.71 (br s, 2H), 4.70 (dd, $J = 5.9, 3.9$ Hz, 1H), 3.09 – 2.98 (m, 1H), 2.93 – 2.78 (m, 2H), 2.56 (br s, 3H), 2.40 – 2.34 (m, 2H), 2.21 (s, 6H), 2.04 (dt, $J = 12.0, 10.4$ Hz, 1H), 0.87 (s, 9H), 0.18 (s, 3H), -0.07 (s, 3H). ^{13}C NMR (THF- d_8 , 151 MHz) δ 162.5 (d, $^1J_{\text{CF}} = 242.4$ Hz), 138.1, 137.27 (d, $^4J_{\text{CF}} = 3.0$ Hz), 131.04 (d, $^3J_{\text{CF}} = 7.6$ Hz), 128.0, 115.81 (d, $^2J_{\text{CF}} = 21.3$ Hz), 65.4, 41.6, 38.5, 27.2, 23.5, 21.5, 19.5, (-3.3, -4.2 two diastereotopic ^{13}C), the signals for the two carbons adjacent to boron were not observed; ^{11}B NMR (THF- d_8 , 160 MHz) 54.0; ^{19}F NMR (THF- d_8 , 470 MHz) δ -119.1 (m); IR 2985, 2956, 2923, 2858, 1745, 1609, 1509,

1445, 1352, 1273, 1217, 1193, 979, 845 cm^{-1} ; **HRMS** (DART) calcd. for $\text{C}_{26}\text{H}_{37}\text{BNFSi}$ $[\text{M}+\text{H}^+]$: 422.13543, found 422.13619.



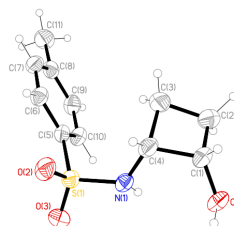
***N*-(2-(4-fluorobenzyl)-4-hydroxycyclobutyl)benzamide (2.95)**

General procedure for oxidation step was applied except for trapping with 2.0 equiv. of BzCl instead of TsCl. The yield was reported based on the one-pot oxidation step. The crude residue was purified by preparative thin layer chromatography (silica gel; 50% ethyl acetate in hexane) to give the desired product as a white solid with 63% yield. **^1H NMR** (CDCl_3 , 600 MHz) δ 7.80 (d, $J = 7.6$ Hz, 2H), 7.52 (t, $J = 7.4$ Hz, 1H), 7.45 (t, $J = 7.6$ Hz, 2H), 7.09 (dd, $J = 8.4, 5.6$ Hz, 2H), 6.98 (d, $J = 6.7$ Hz, 1H), 6.93 (t, $J = 8.7$ Hz, 2H), 4.72 (dt, $J = 7.5, 3.8$ Hz, 1H), 4.57 (q, $J = 6.5$ Hz, 1H), 2.95 (dd, $J = 11.5, 8.0$ Hz, 1H), 2.69 – 2.59 (m, 2H), 2.45 – 2.33 (m, 1H), 1.78 (dt, $J = 12.8, 6.4$ Hz, 1H), 1.66 – 1.55 (br s, 1H); **^{13}C NMR** (CDCl_3 , 151 MHz) δ 168.2, 161.5 (d, $^1J_{\text{CF}} = 243.5$ Hz), 135.67 (d, $^4J_{\text{CF}} = 3.2$ Hz), 134.5, 131.8, 130.02 (d, $^3J_{\text{CF}} = 8.0$ Hz), 128.8, 127.1, 115.28 (d, $^2J_{\text{CF}} = 21.2$ Hz), 65.8, 52.2, 35.9, 35.7, 35.1; **^{19}F NMR** (CDCl_3 , 470 MHz) δ -117.6 (m); **IR** 3391, 3353, 2963, 2929, 1789, 1735, 1637, 1603, 1509, 1278, 1157, 1088, 935, 815, 740, 575, 555 cm^{-1} ; **HRMS** (DART) calcd. for $\text{C}_{18}\text{H}_{19}\text{NO}_2\text{F}$ $[\text{M}+\text{H}^+]$: 300.13943, found 300.13929.

2.7.2.4 X-ray Crystallographic Data

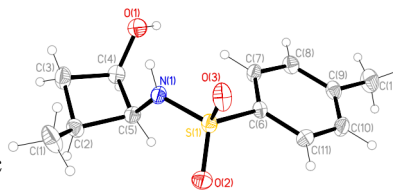
Crystal Data and Structure Refinement for **2.17**

Identification code	C11H15NO3S	
Empirical formula	C11 H15 N O3 S	
Formula weight	241.30	
Temperature	100(2) K	
Wavelength	0.71073 Å	
Crystal system	Monoclinic	
Space group	P2 ₁ /n	
Unit cell dimensions	a = 6.5365(8) Å	a = 90°
	b = 7.4158(11) Å	b = 94.914(4)°
	c = 24.246(4) Å	g = 90°
Volume	1171.0(3) Å ³	
Z	4	
Density (calculated)	1.369 Mg/m ³	
Absorption coefficient	0.268 mm ⁻¹	
F(000)	512	
Crystal size	0.360 x 0.220 x 0.160 mm ³	
Theta range for data collection	1.686 to 28.303°.	
Index ranges	-8<=h<=7, -9<=k<=9, -32<=l<=32	
Reflections collected	29045	
Independent reflections	2894 [R(int) = 0.0461]	
Completeness to theta = 25.242°	99.9 %	
Absorption correction	Semi-empirical from equivalents	
Max. and min. transmission	0.7457 and 0.7007	
Refinement method	Full-matrix least-squares on F ²	
Data / restraints / parameters	2894 / 2 / 154	
Goodness-of-fit on F	1.043	
Final R indices [I>2sigma(I)]	R1 = 0.0372, wR2 = 0.0925	
R indices (all data)	R1 = 0.0517, wR2 = 0.1031	
Extinction coefficient	n/a	
Largest diff. peak and hole	0.361 and -0.327 e. Å ⁻³	



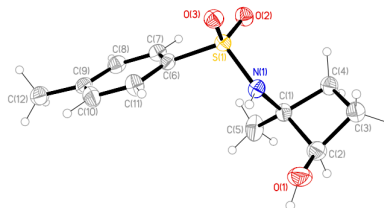
Crystal Data and Structure Refinement for **2.86**

Identification code	C12H17NO3S
Empirical formula	C ₁₂ H ₁₇ N O ₃ S
Formula weight	255.32
Temperature	173(2) K
Wavelength	0.71073°
Crystal system	Monoclinic
Space group	P2 ₁ /c
Unit cell dimensions	a = 6.4232(2) Å α = 90° b = 24.0930(7) Å β = 96.5920(10)° c = 8.1596(2) Å γ = 90°
Volume	1254.38(6) Å ³
Z	4
Density (calculated)	1.352 Mg/m ³
Absorption coefficient	0.254 mm ⁻¹
F(000)	544
Crystal size	0.320 x 0.220 x 0.130 mm ³
Theta range for data collection	2.651 to 28.298°.
Index ranges	-8 ≤ h ≤ 8, -31 ≤ k ≤ 32, -10 ≤ l ≤ 10
Reflections collected	14930
Independent reflections	3120 [R(int) = 0.0436]
Completeness to theta = 25.242°	100.0 %
Absorption correction	Semi-empirical from equivalents
Max. and min. transmission	0.7457 and 0.6973
Refinement method	Full-matrix least-squares on F ²
Data / restraints / parameters	3120 / 2 / 162
Goodness-of-fit on F ²	1.057
Final R indices [I > 2σ(I)]	R1 = 0.0393, wR2 = 0.0922
R indices (all data)	R1 = 0.0520, wR2 = 0.0998
Extinction coefficient	n/a
Largest diff. peak and hole	0.359 and -0.363 e. Å ⁻³

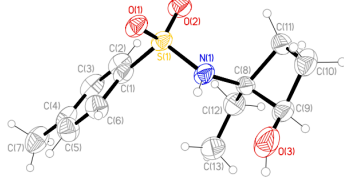


Crystal Data and Structure Refinement for **2.89**

Identification code	C12H17NO3S	
Empirical formula	C12 H17 N O3 S	
Formula weight	255.32	
Temperature	173(2) K	
Wavelength	1.54178 Å	
Crystal system	Monoclinic	
Space group	P2 ₁ /c	
Unit cell dimensions	a = 10.7828(7) Å	α = 90°
	b = 16.1968(11) Å	β = 102.058(2)°
	c = 7.2382(5) Å	γ = 90°
Volume	1236.24(14) Å ³	
Z	4	
Density (calculated)	1.372 Mg/m ³	
Absorption coefficient	2.312 mm ⁻¹	
F(000)	544	
Crystal size	0.360 x 0.220 x 0.100 mm ³	
Theta range for data collection	4.192 to 66.445°	
Index ranges	-12 ≤ h ≤ 12, -18 ≤ k ≤ 19, -8 ≤ l ≤ 8	
Reflections collected	18288	
Independent reflections	2166 [R(int) = 0.0268]	
Completeness to theta = 66.445°	99.4 %	
Absorption correction	Semi-empirical from equivalents	
Max. and min. transmission	0.7528 and 0.6080	
Refinement method	Full-matrix least-squares on F ²	
Data / restraints / parameters	2166 / 0 / 163	
Goodness-of-fit on F ²	1.101	
Final R indices [I > 2σ(I)]	R1 = 0.0432, wR2 = 0.1125	
R indices (all data)	R1 = 0.0434, wR2 = 0.1126	
Extinction coefficient	n/a	
Largest diff. peak and hole	0.754 and -0.313 e. Å ⁻³	

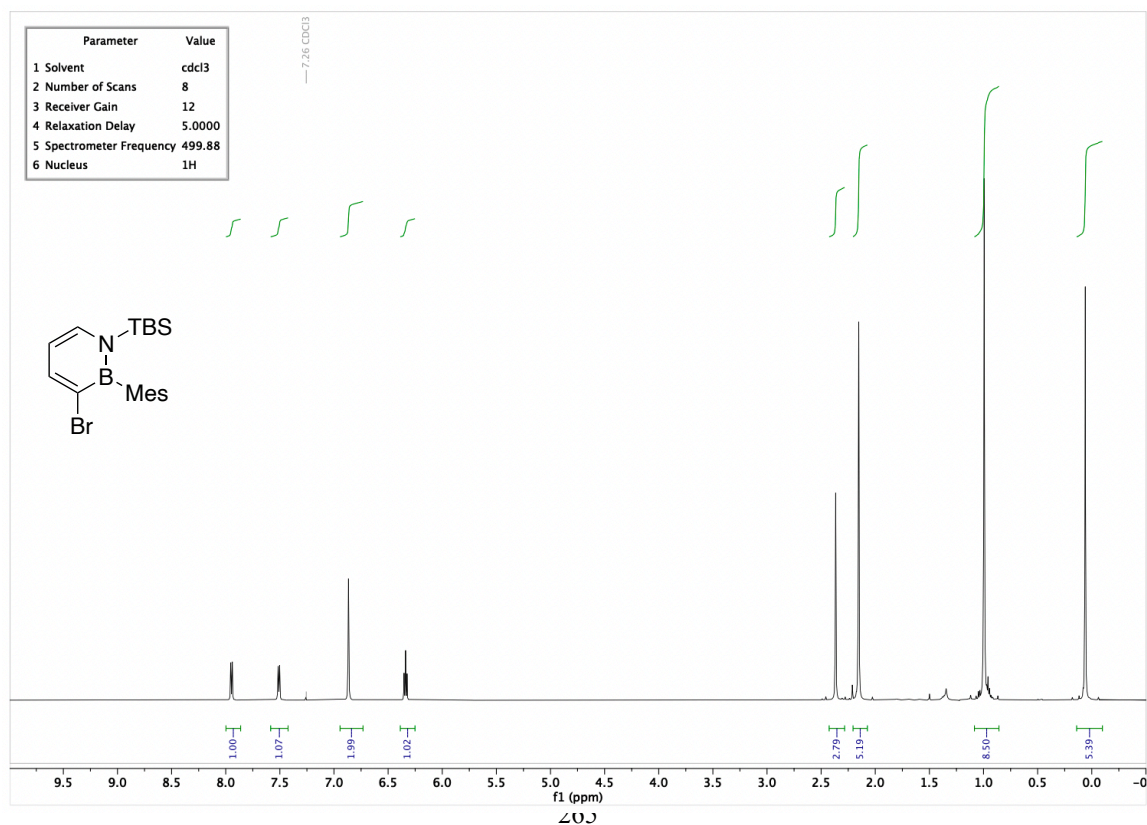
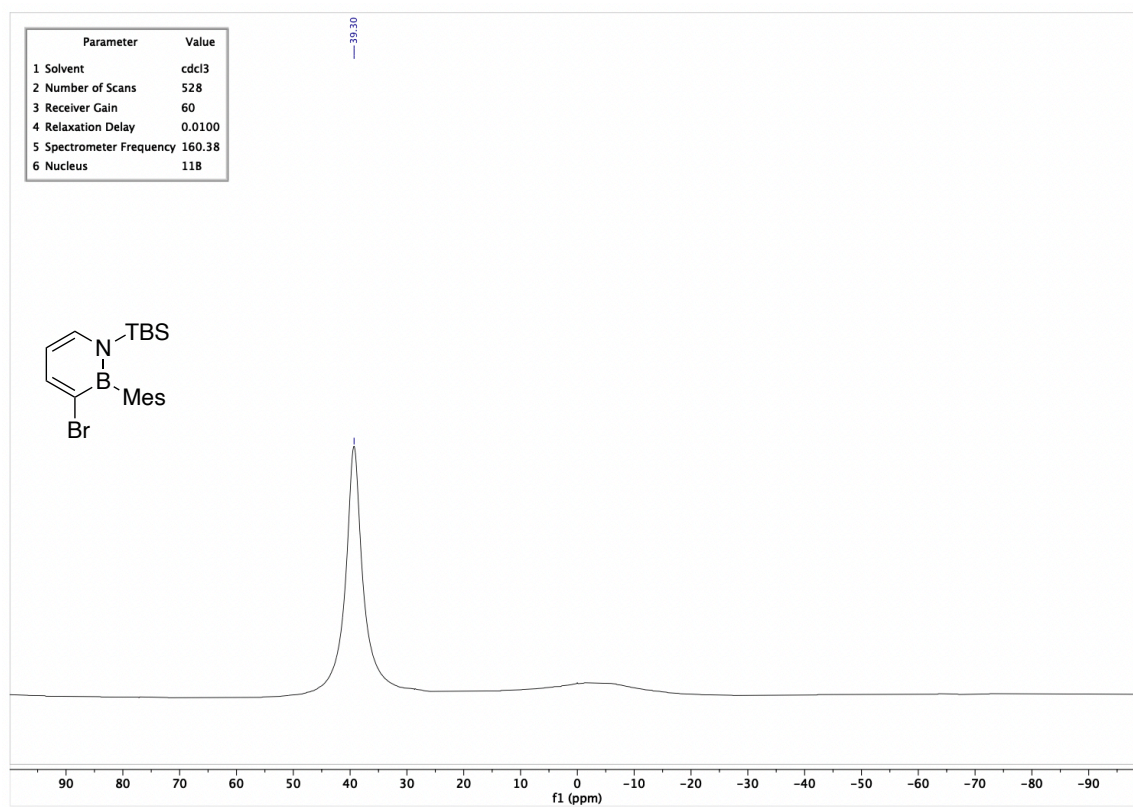


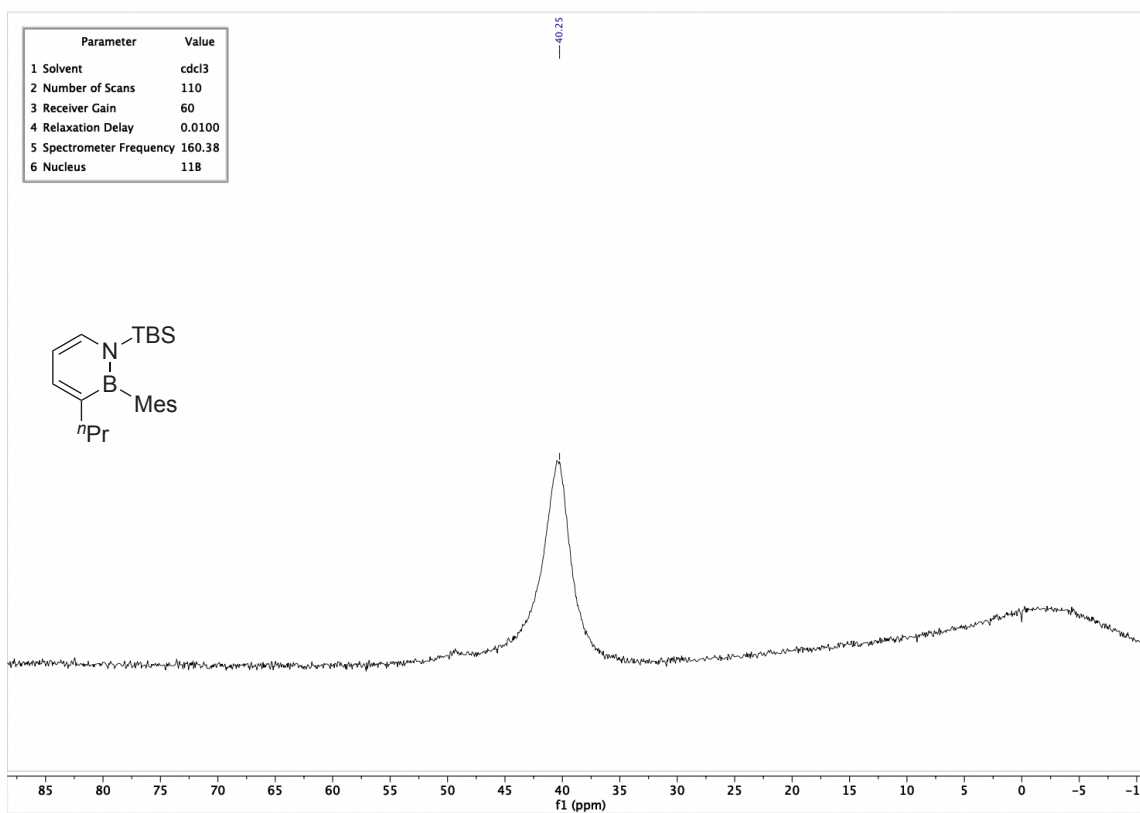
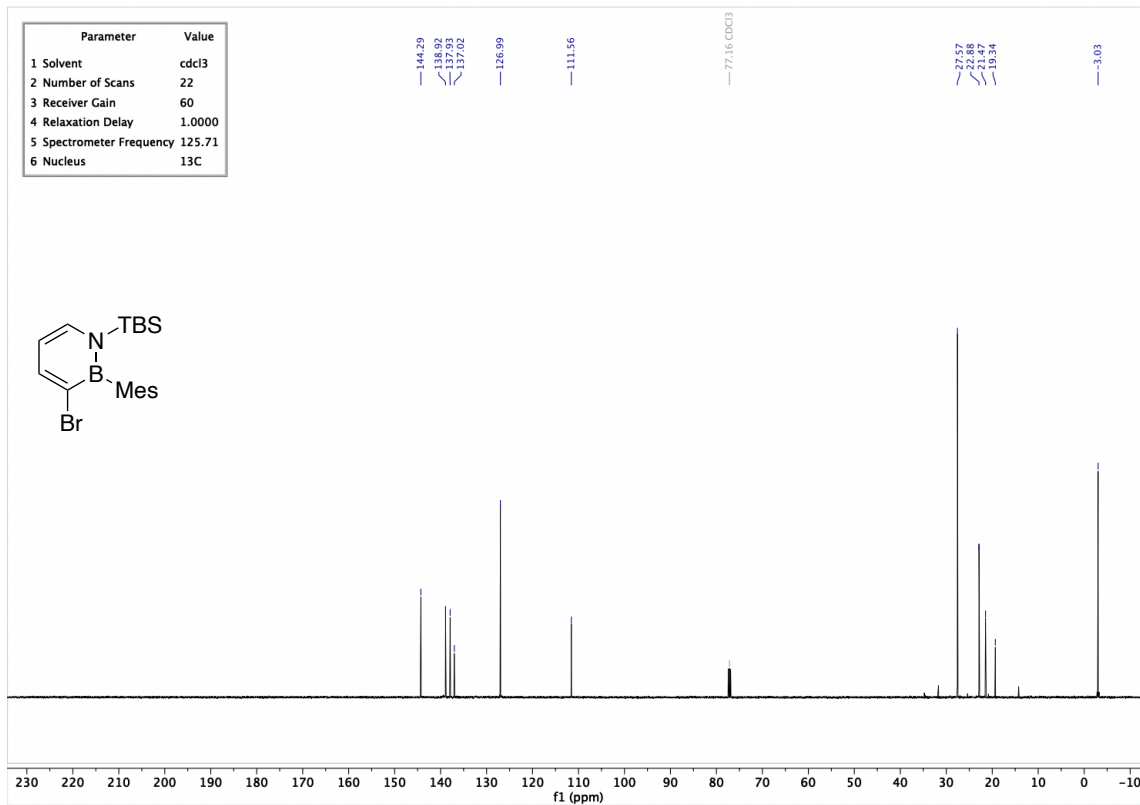
Crystal Data and Structure Refinement for **2.90**

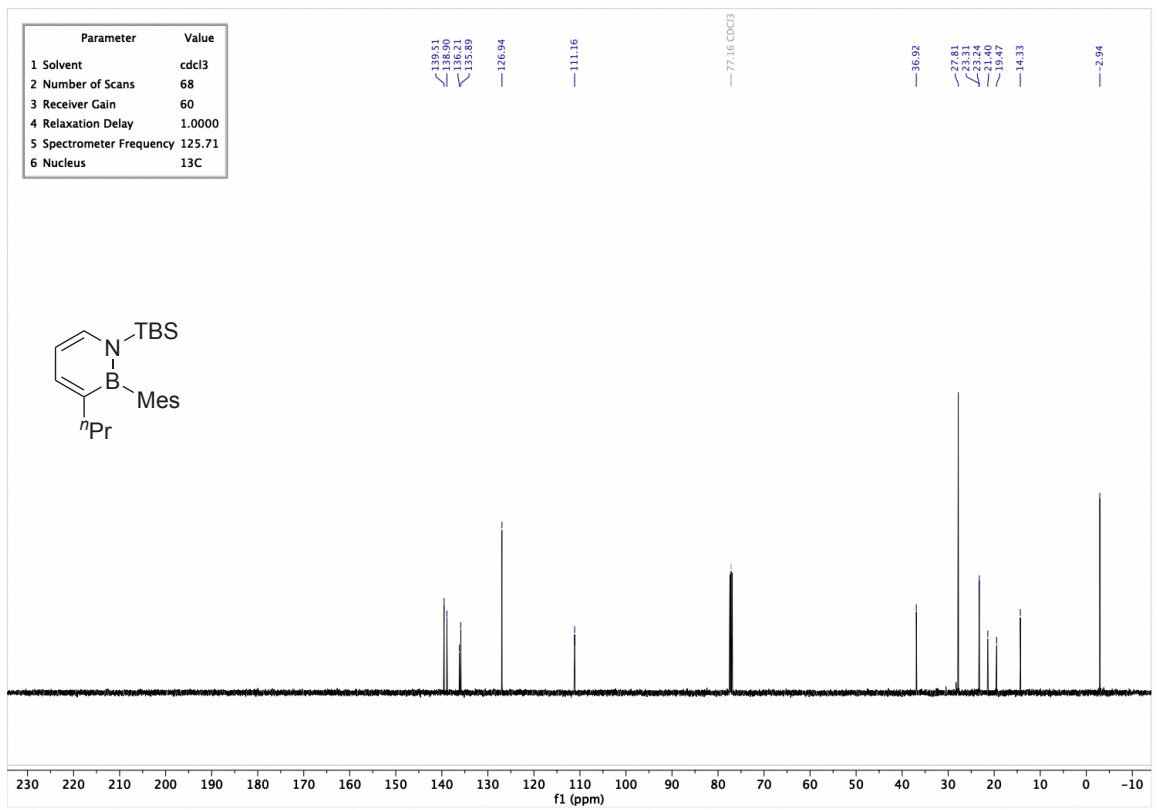
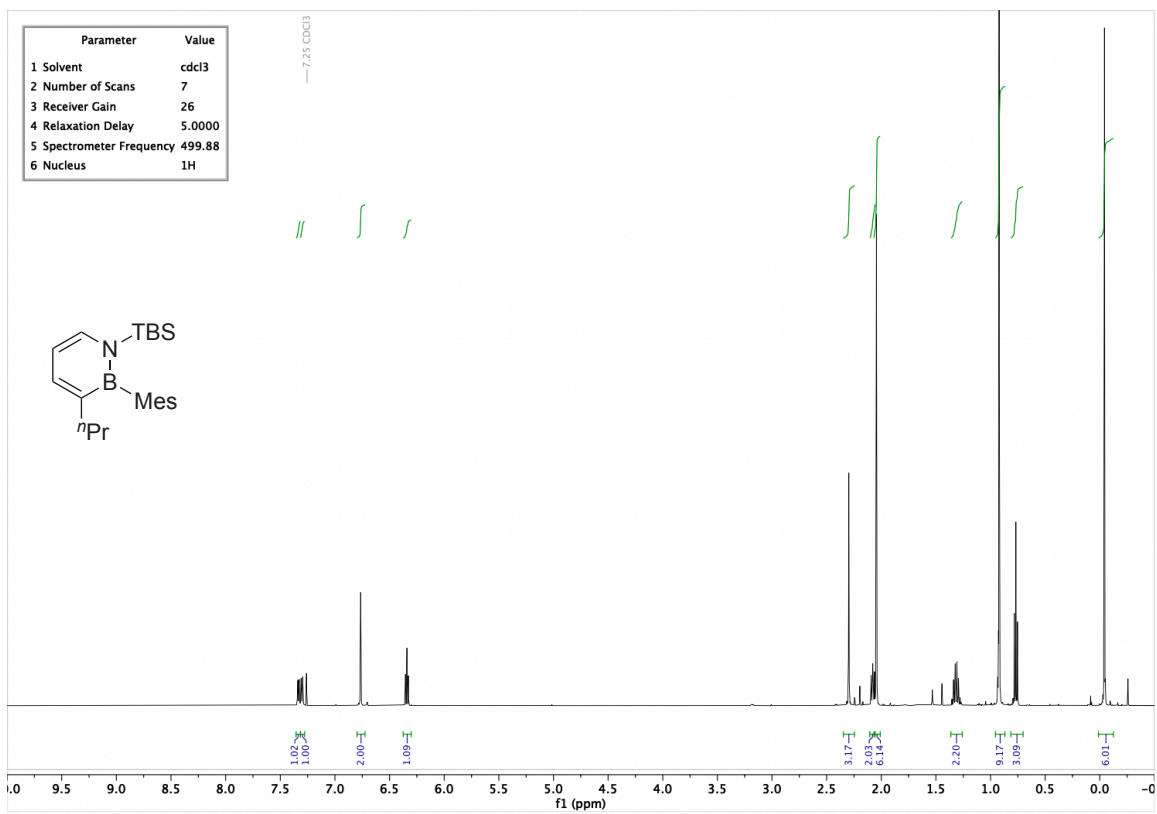
Identification code	C13H19NO3S	
Empirical formula	C13 H19 N O3 S	
Formula weight	269.35	
Temperature	100(2) K	
Wavelength	0.71073 Å	
Crystal system	Monoclinic	
Space group	P2 ₁ /c	
Unit cell dimensions	a = 11.1464(9) Å	α = 90°
	b = 16.7906(13) Å	β = 104.529(3)°
	c = 7.5194(6) Å	γ = 90°
Volume	1362.29(19) Å ³	
Z	4	
Density (calculated)	1.313 Mg/m ³	
Absorption coefficient	0.238 mm ⁻¹	
F(000)	576	
Crystal size	0.380 x 0.280 x 0.140 mm ³	
Theta range for data collection	1.887 to 28.386°	
Index ranges	-14 ≤ h ≤ 14, -22 ≤ k ≤ 22, -8 ≤ l ≤ 10	
Reflections collected	27554	
Independent reflections	3390 [R(int) = 0.0342]	
Completeness to theta = 25.242°	100.0 %	
Absorption correction	Semi-empirical from equivalents	
Max. and min. transmission	0.7457 and 0.6319	
Refinement method	Full-matrix least-squares on F ²	
Data / restraints / parameters	3390 / 498 / 237	
Goodness-of-fit on F ²	1.057	
Final R indices [I > 2σ(I)]	R1 = 0.0384, wR2 = 0.0931	
R indices (all data)	R1 = 0.0539, wR2 = 0.1032	
Extinction coefficient	n/a	
Largest diff. peak and hole	0.232 and -0.340 e. Å ⁻³	

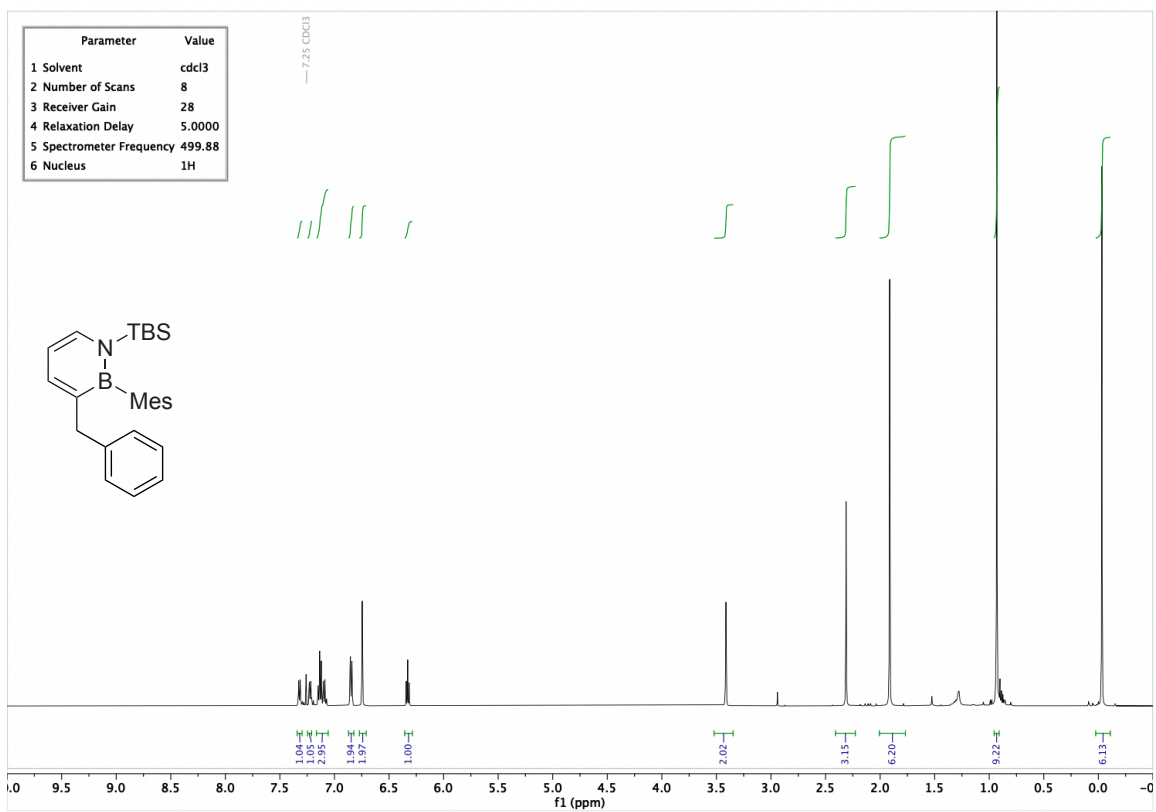
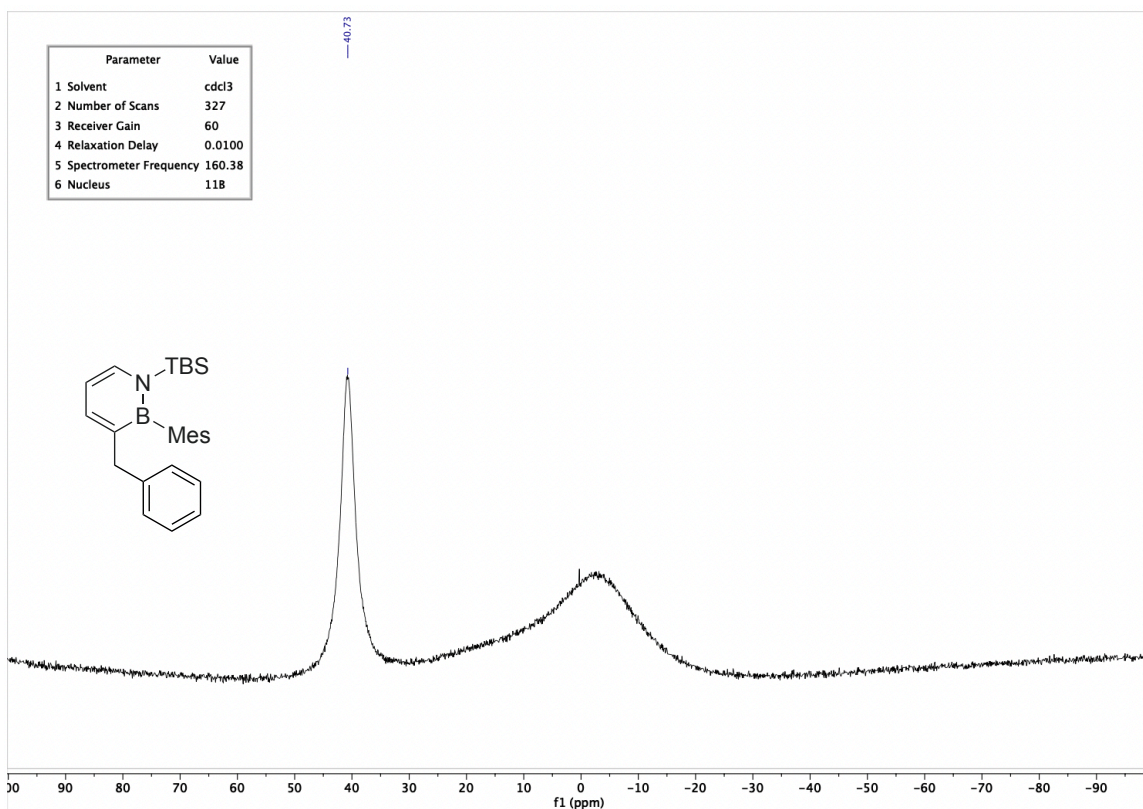
2.7.3 Analytical Data

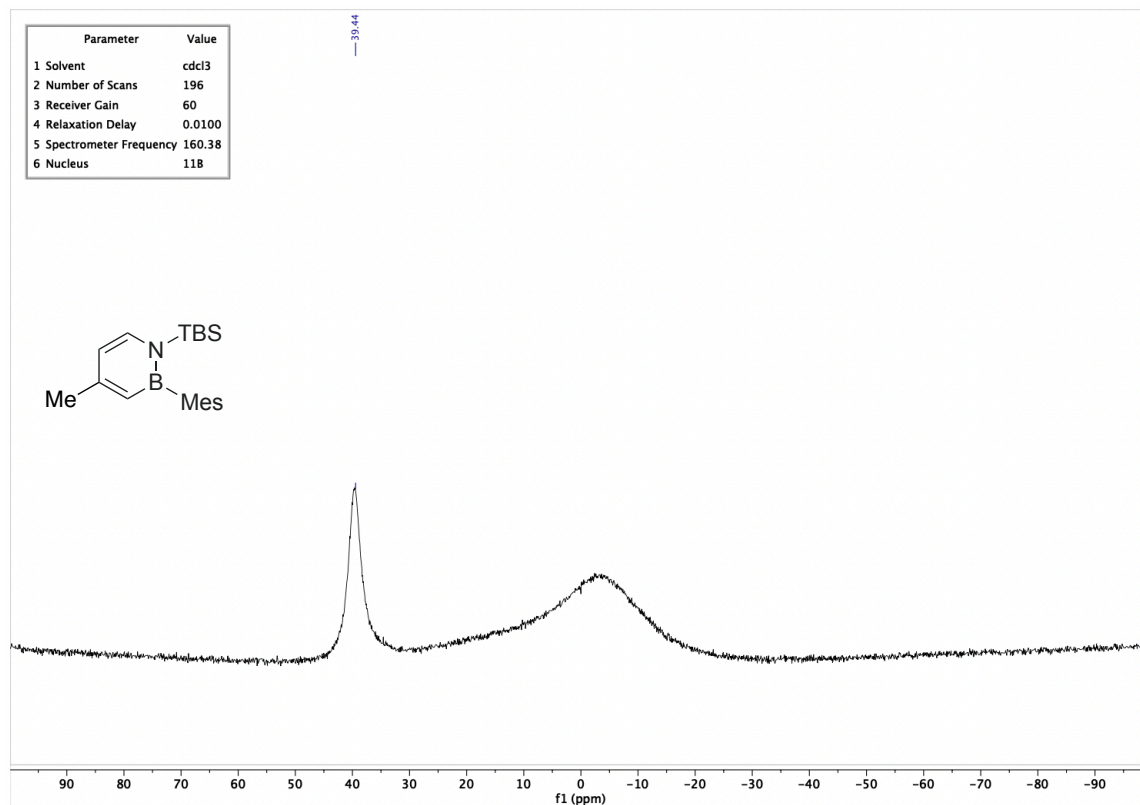
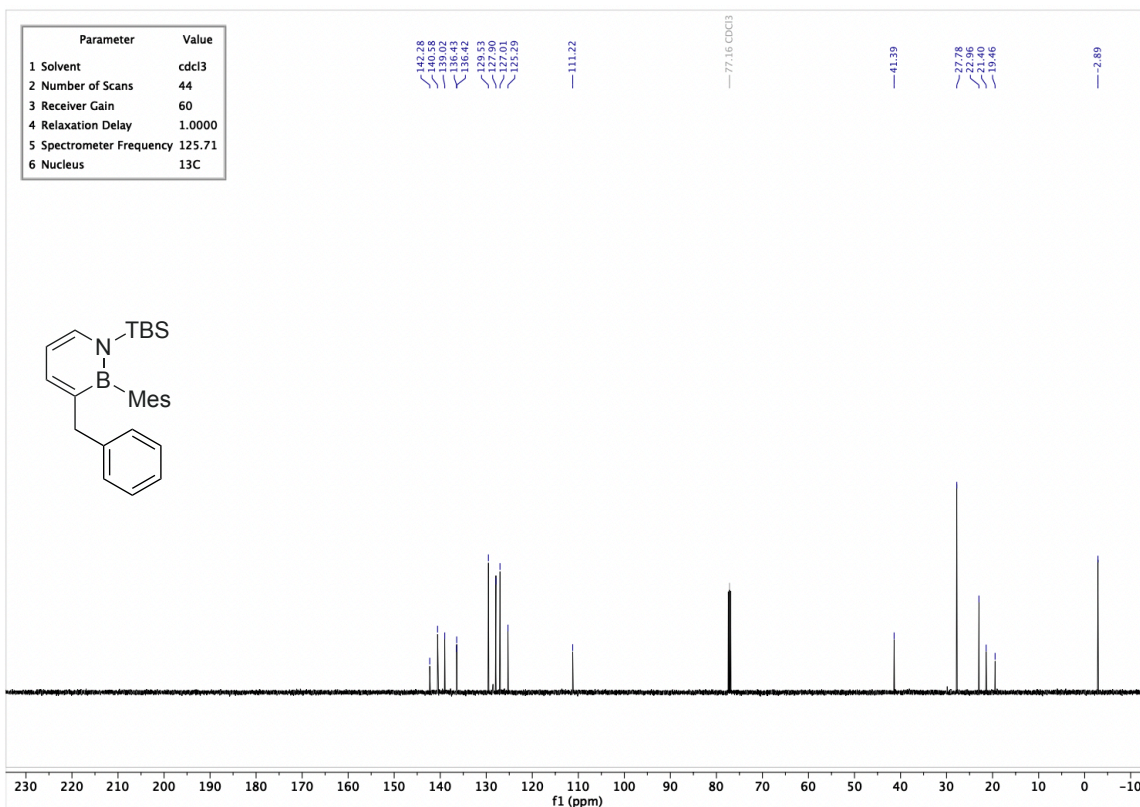
NMR spectra

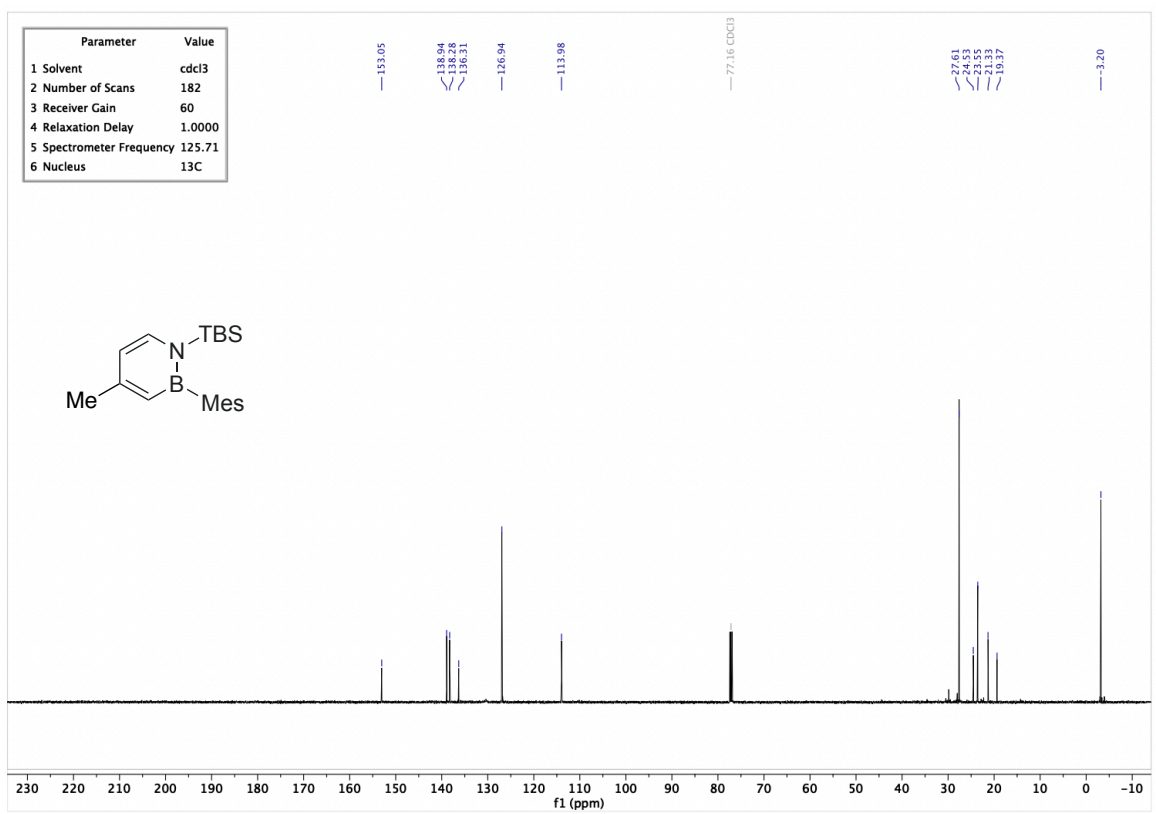
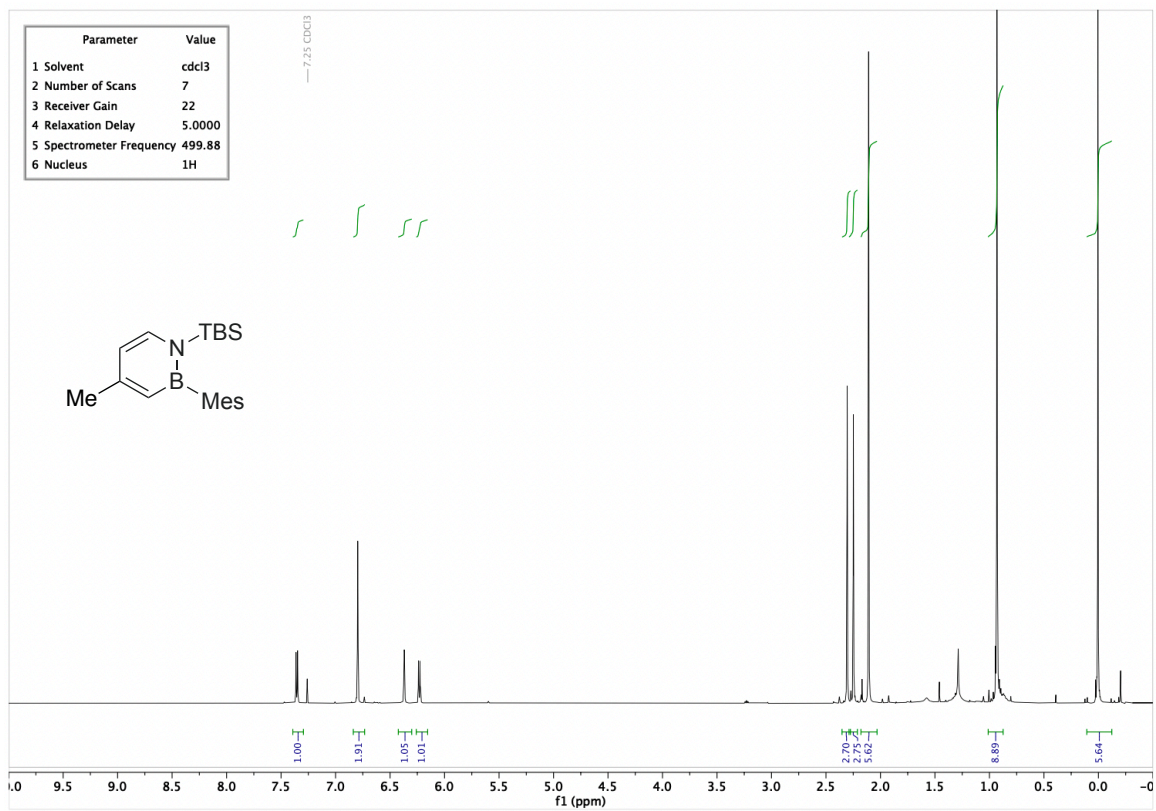


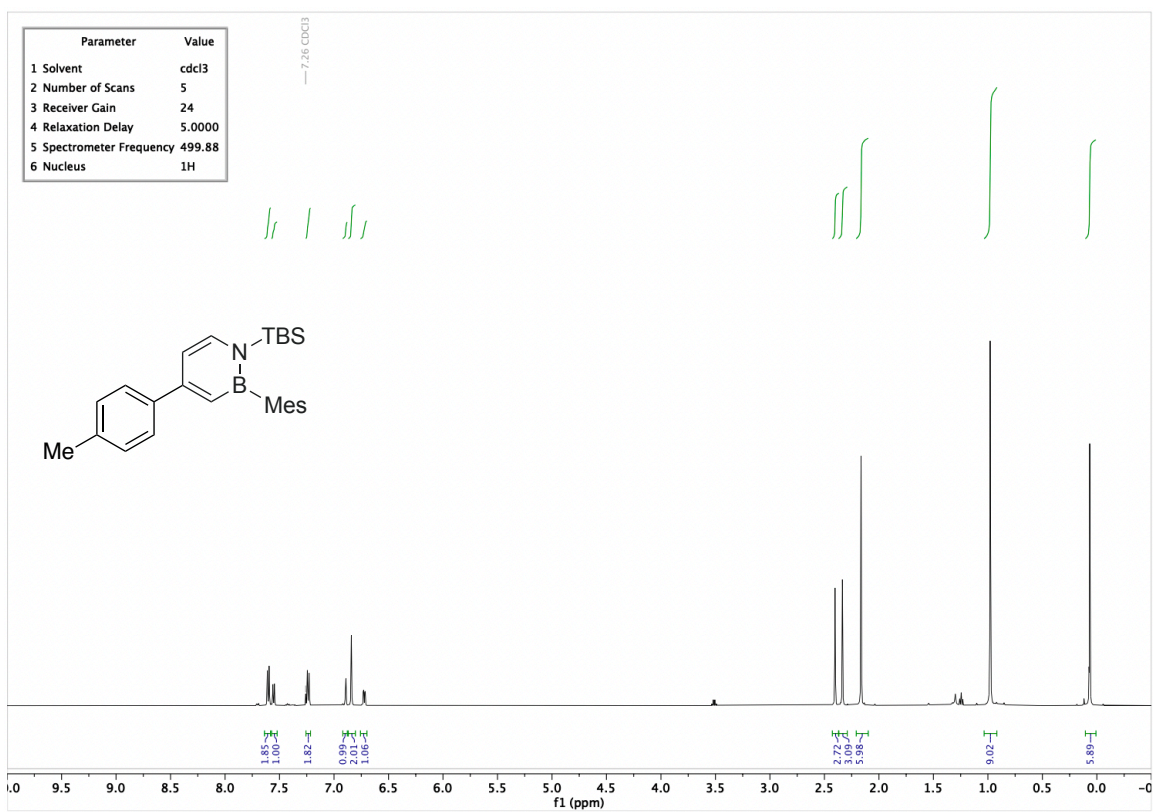
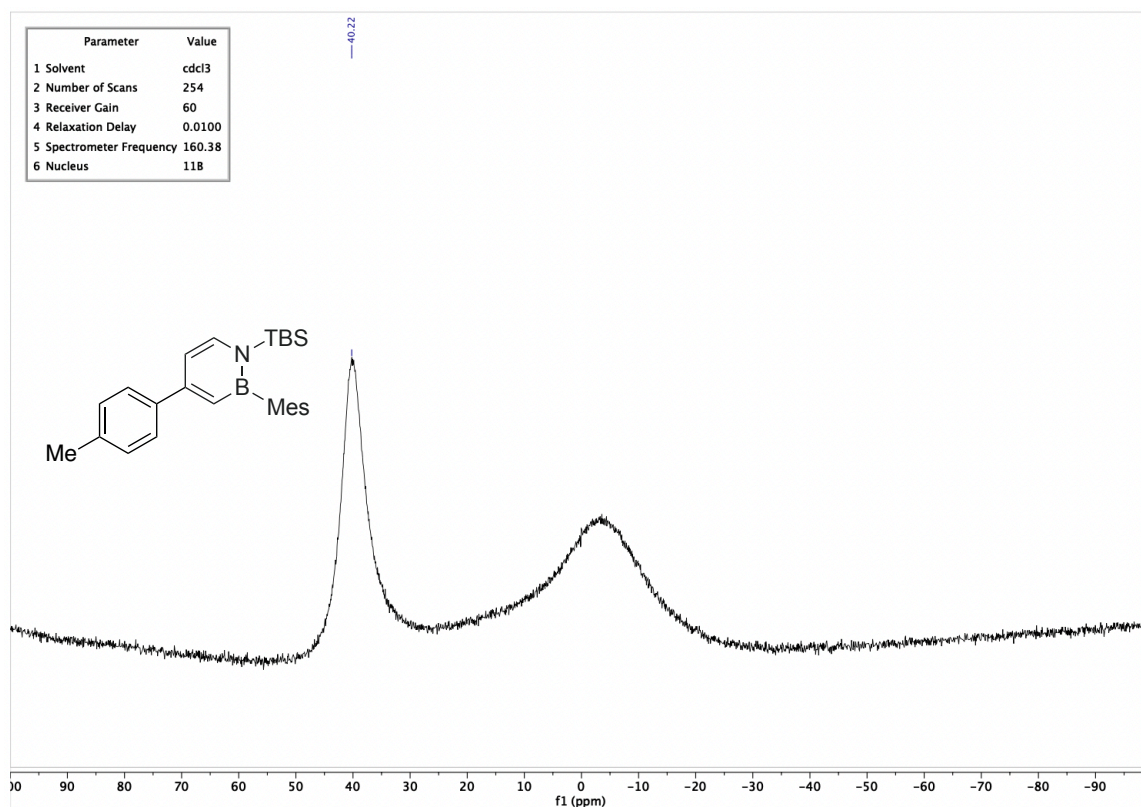


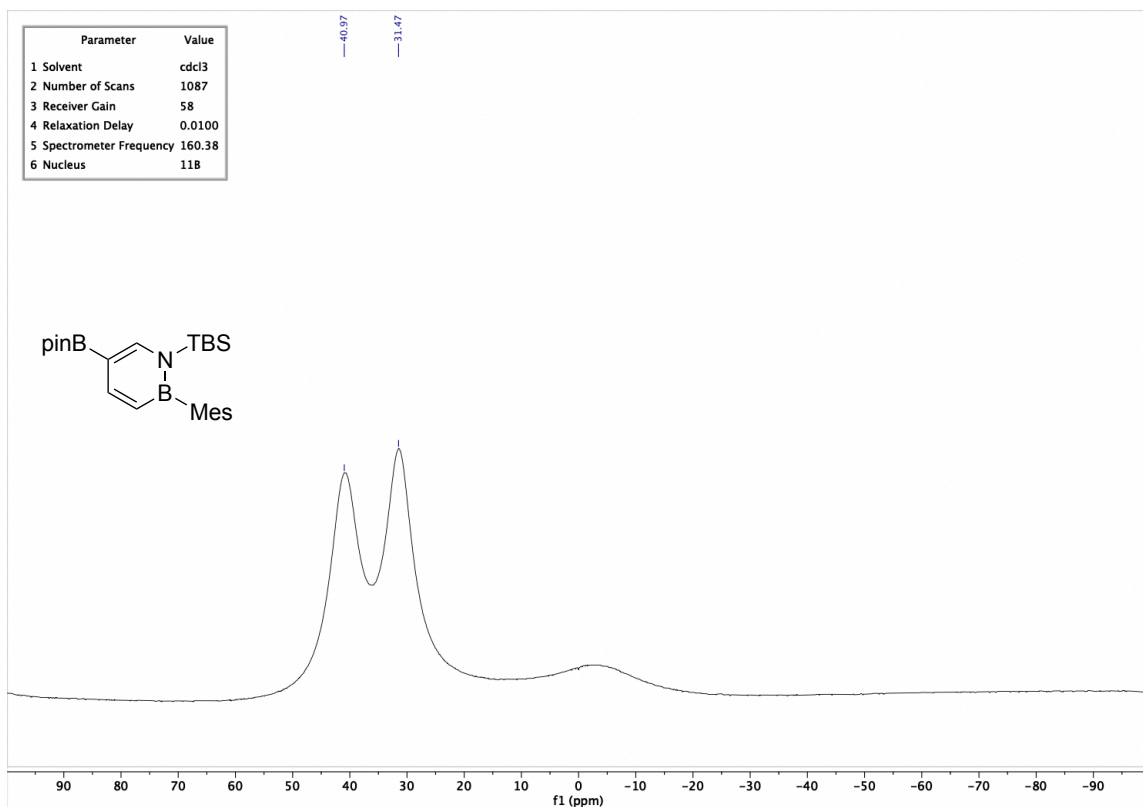
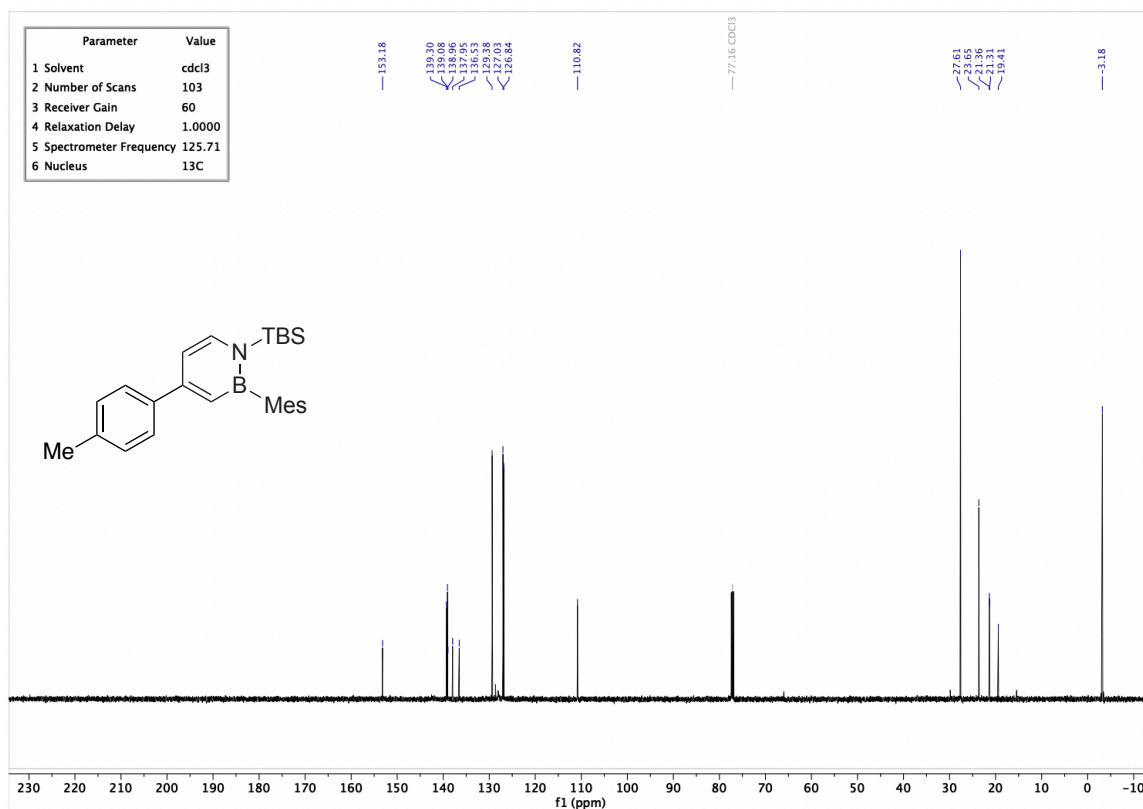


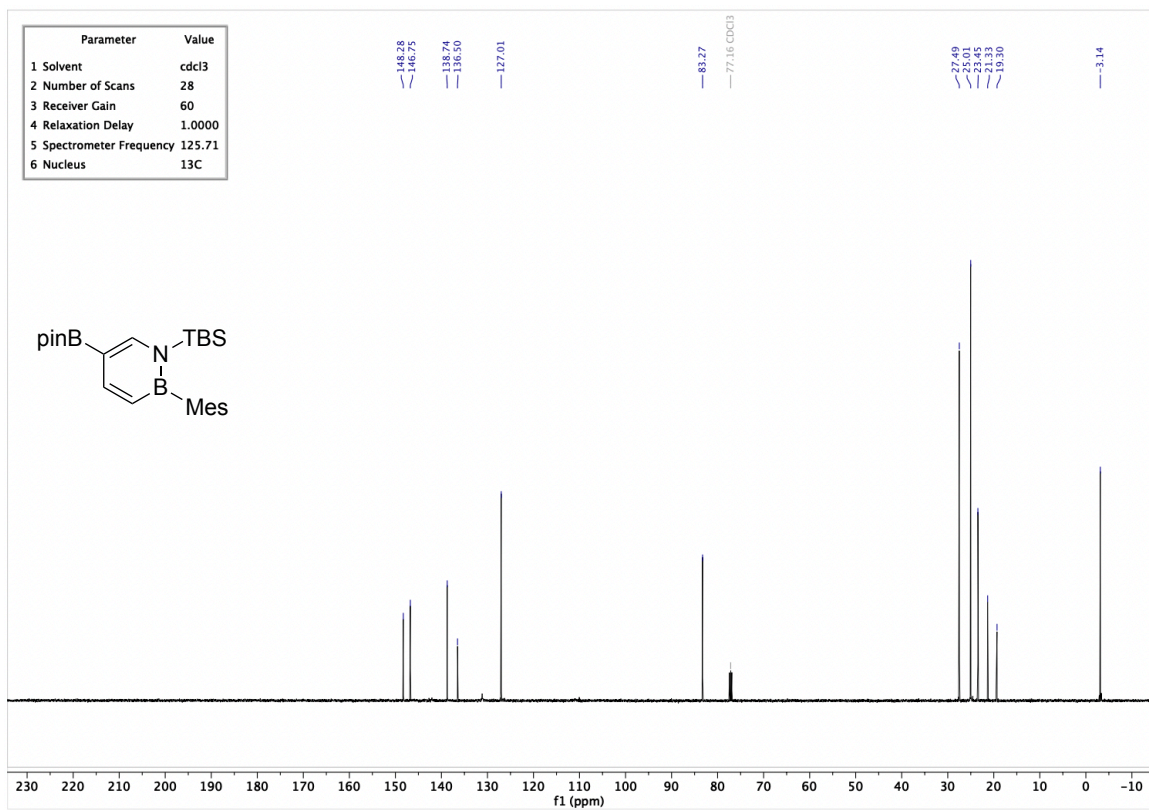
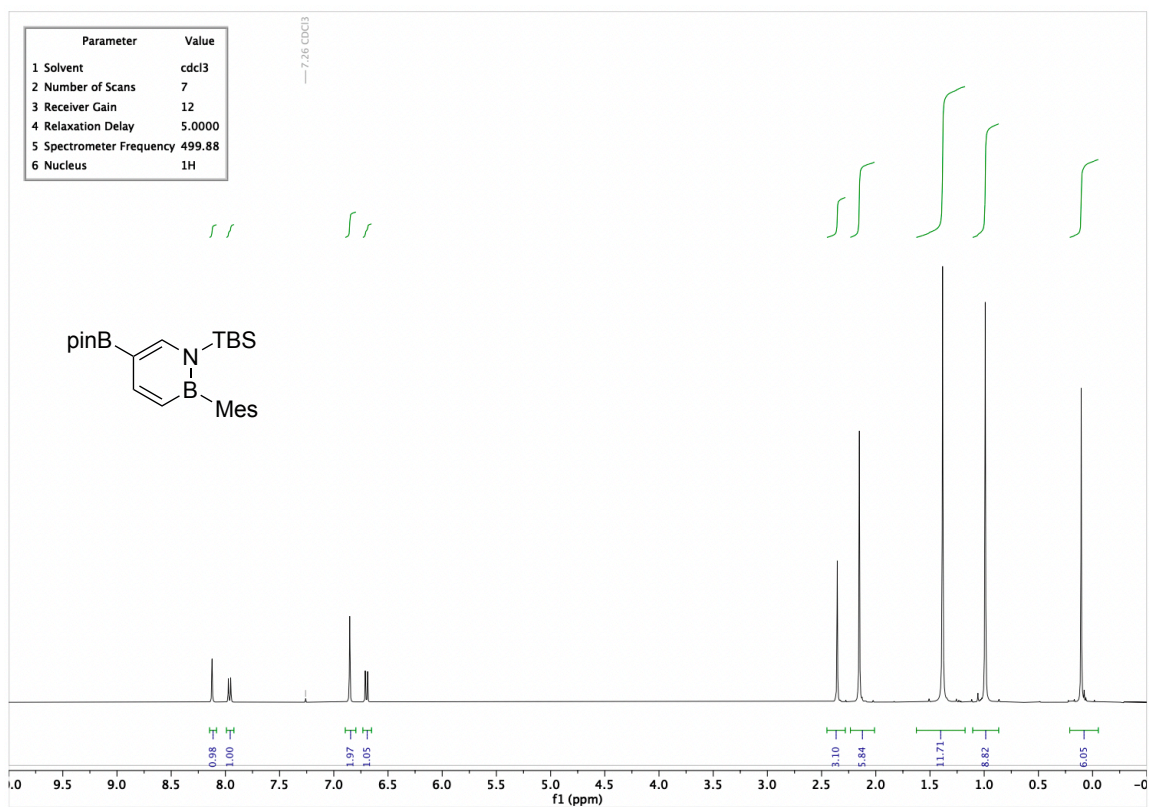


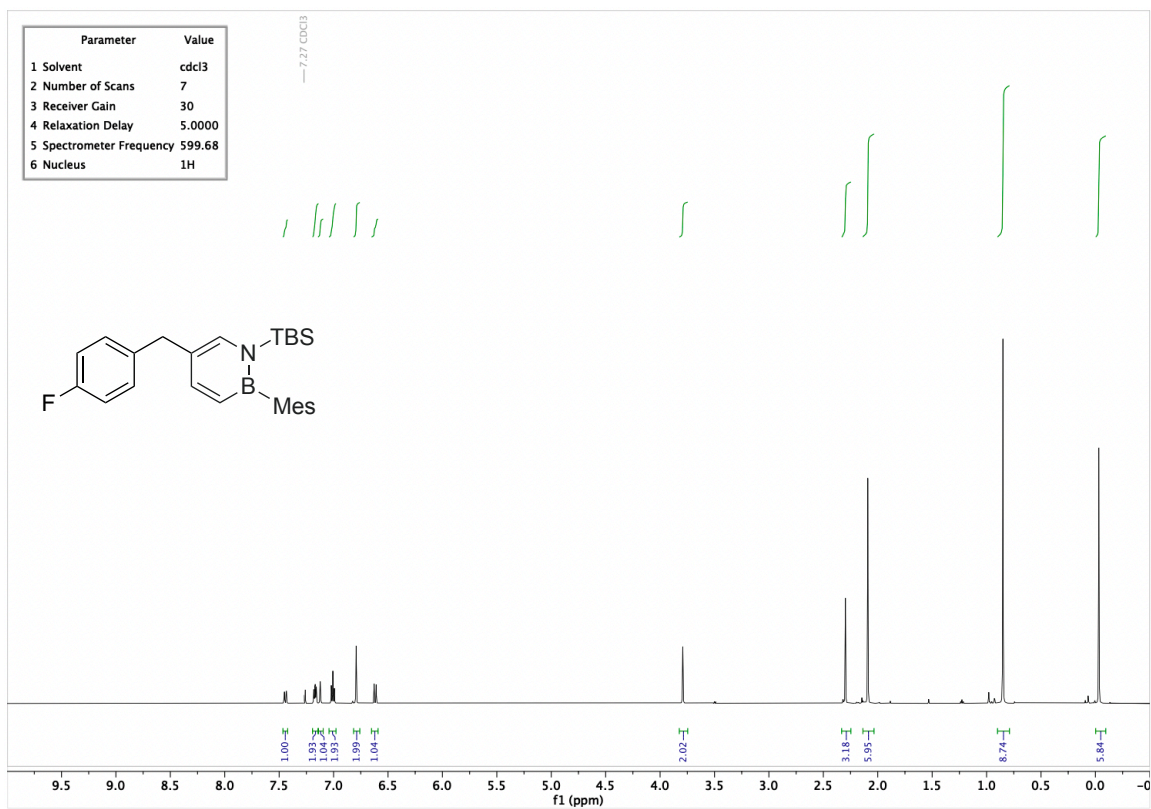
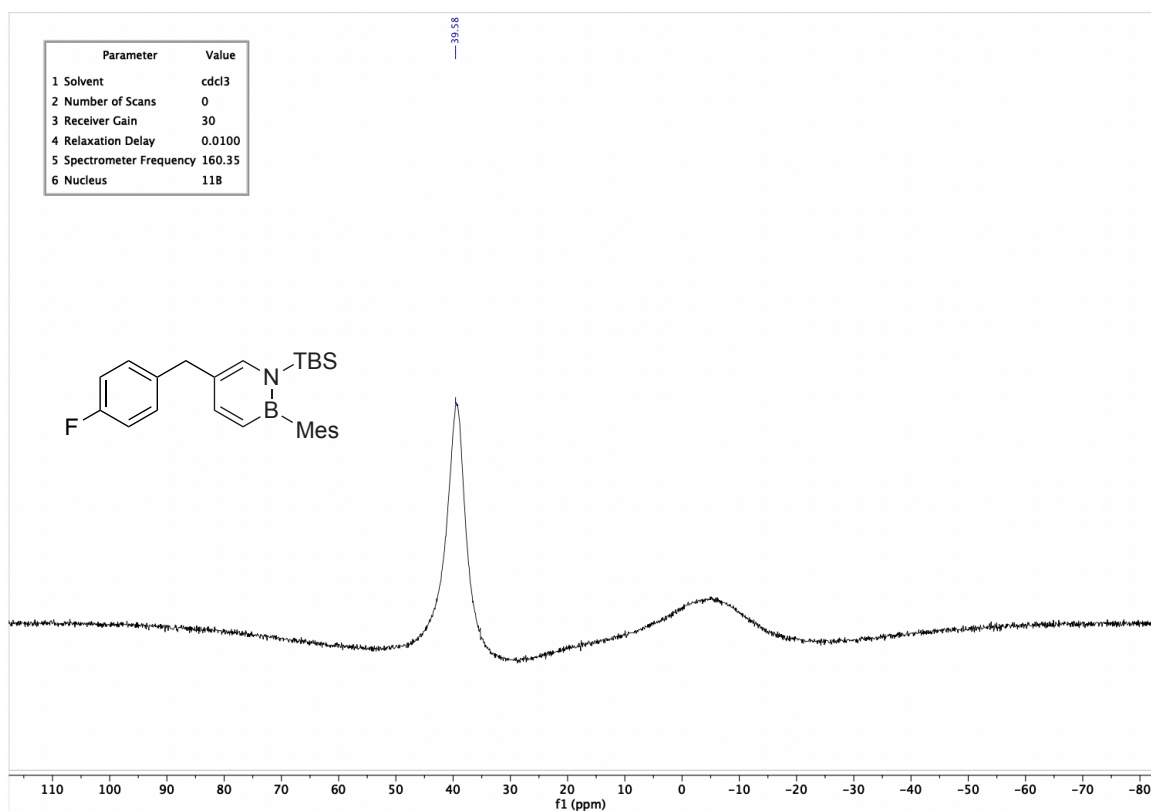


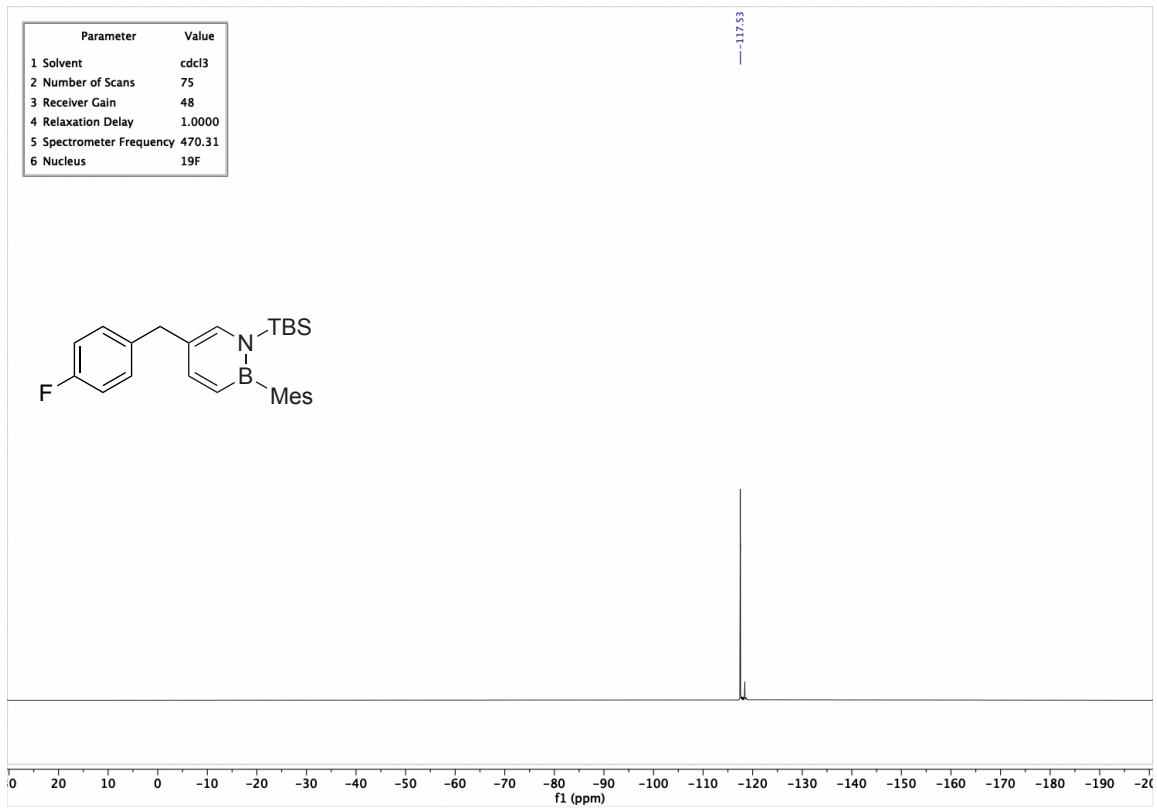
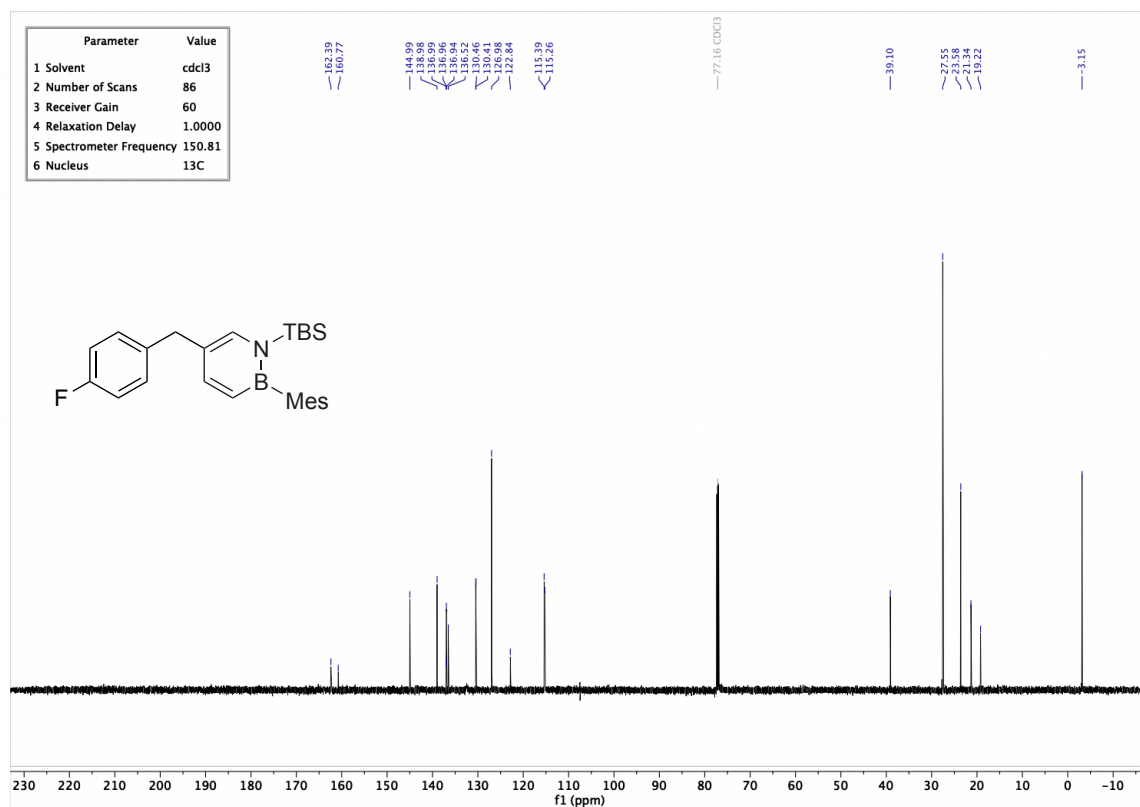


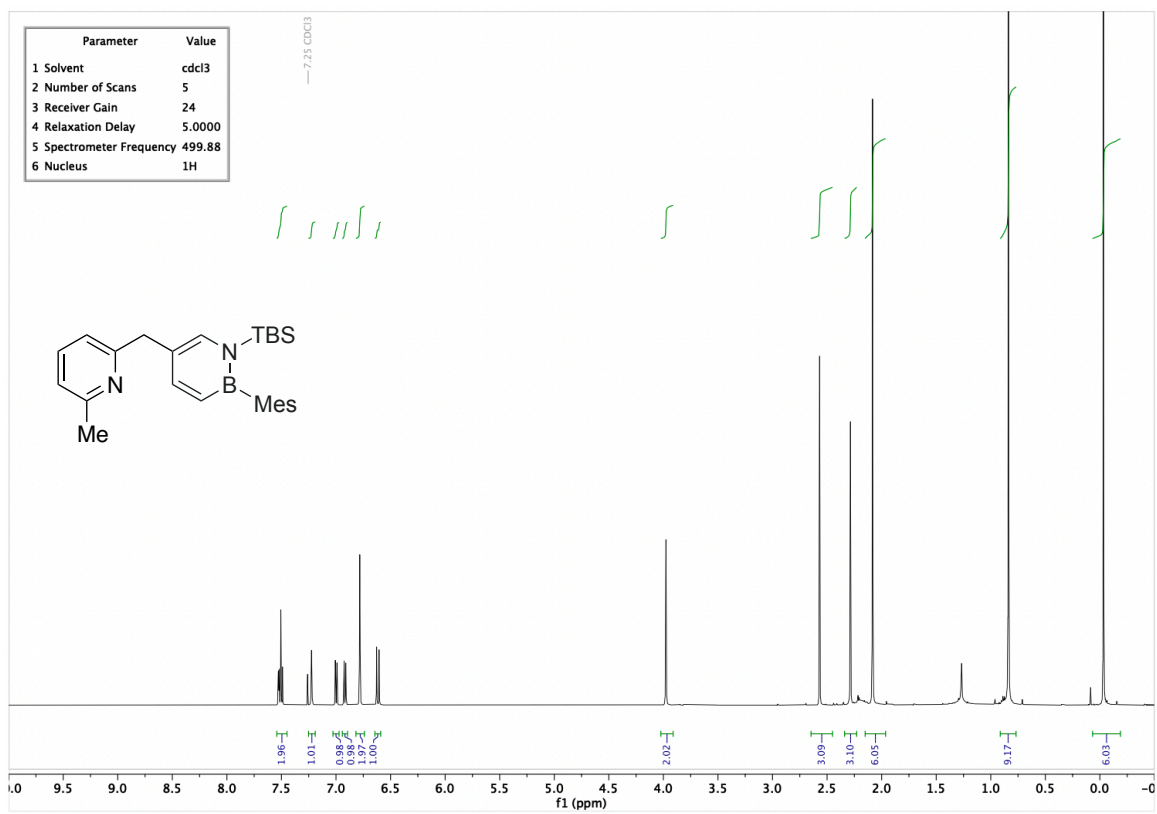
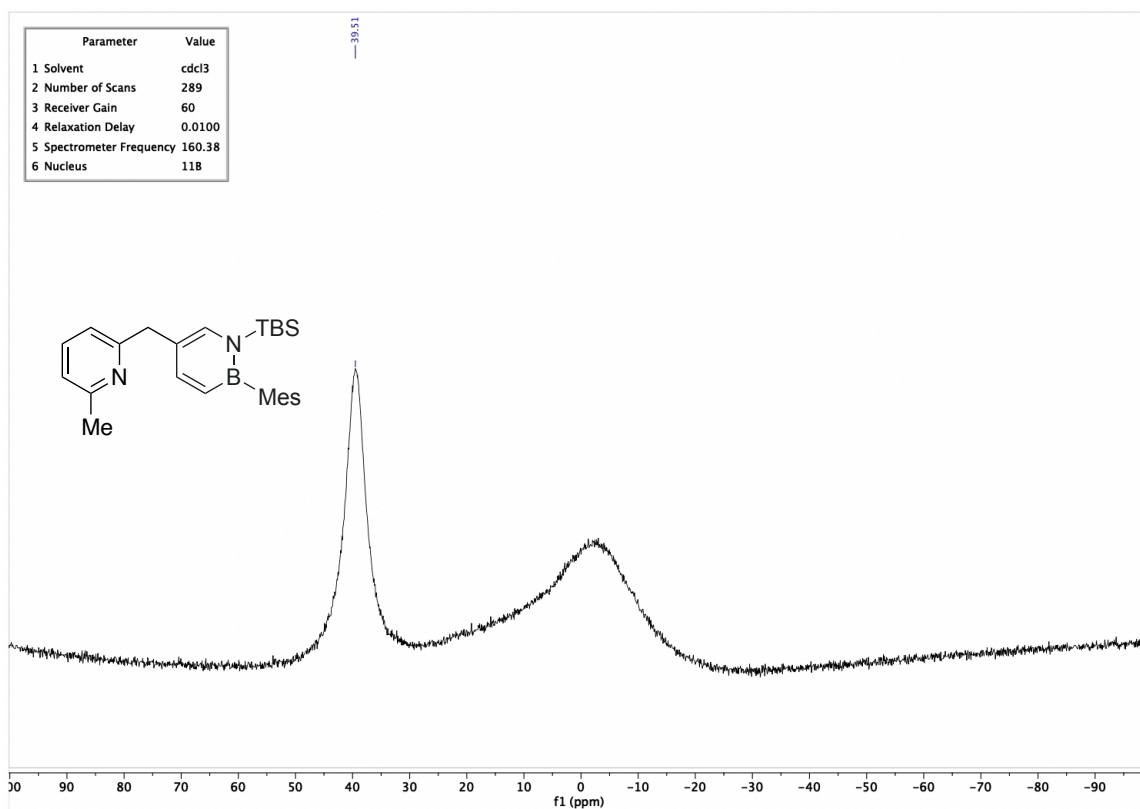


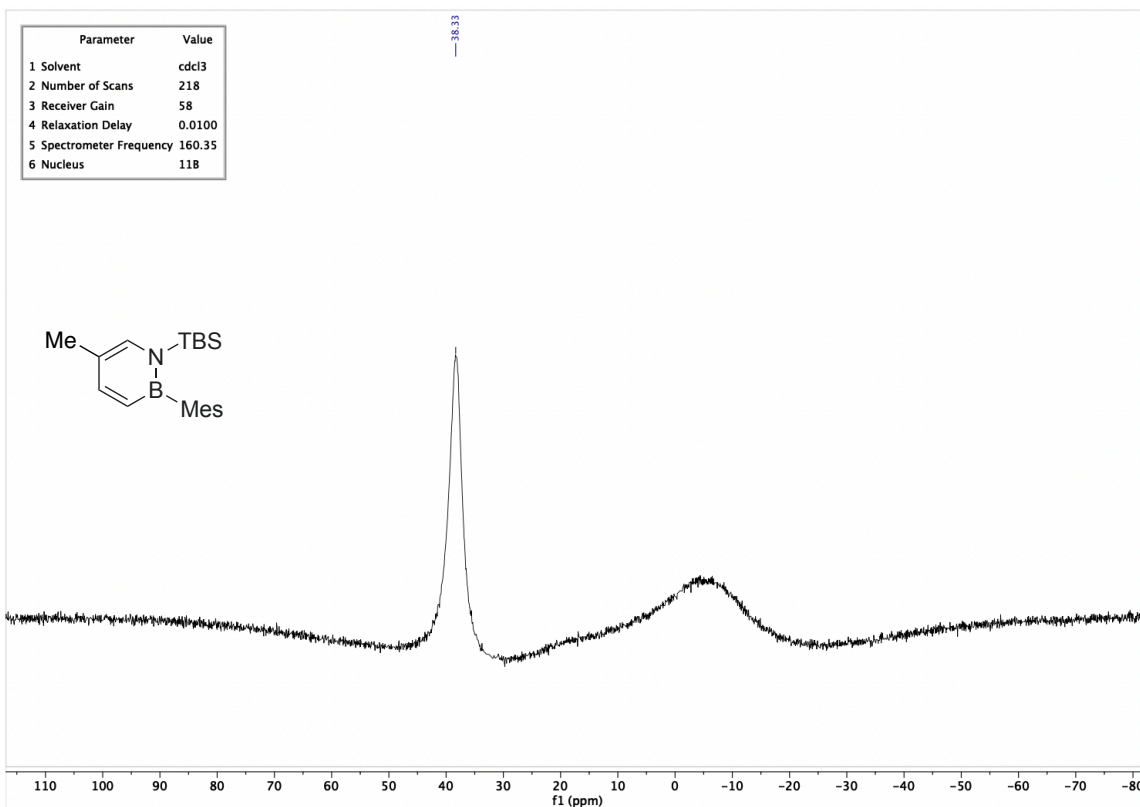
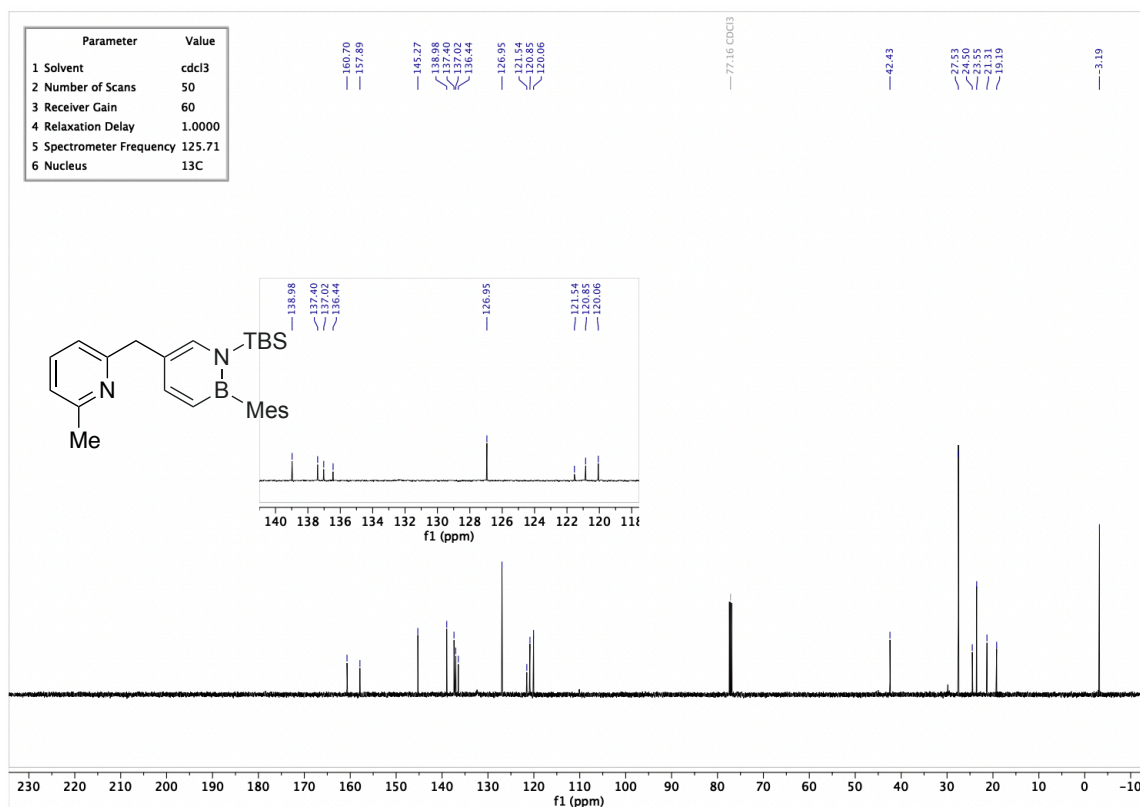


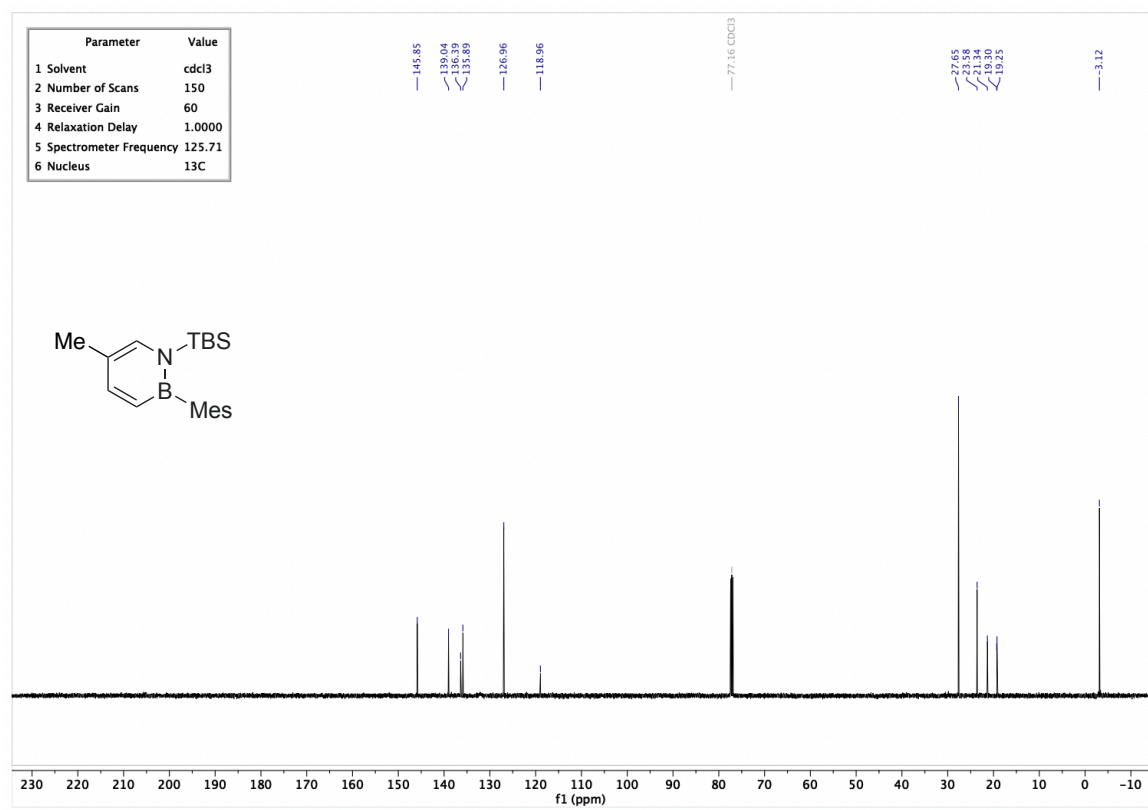
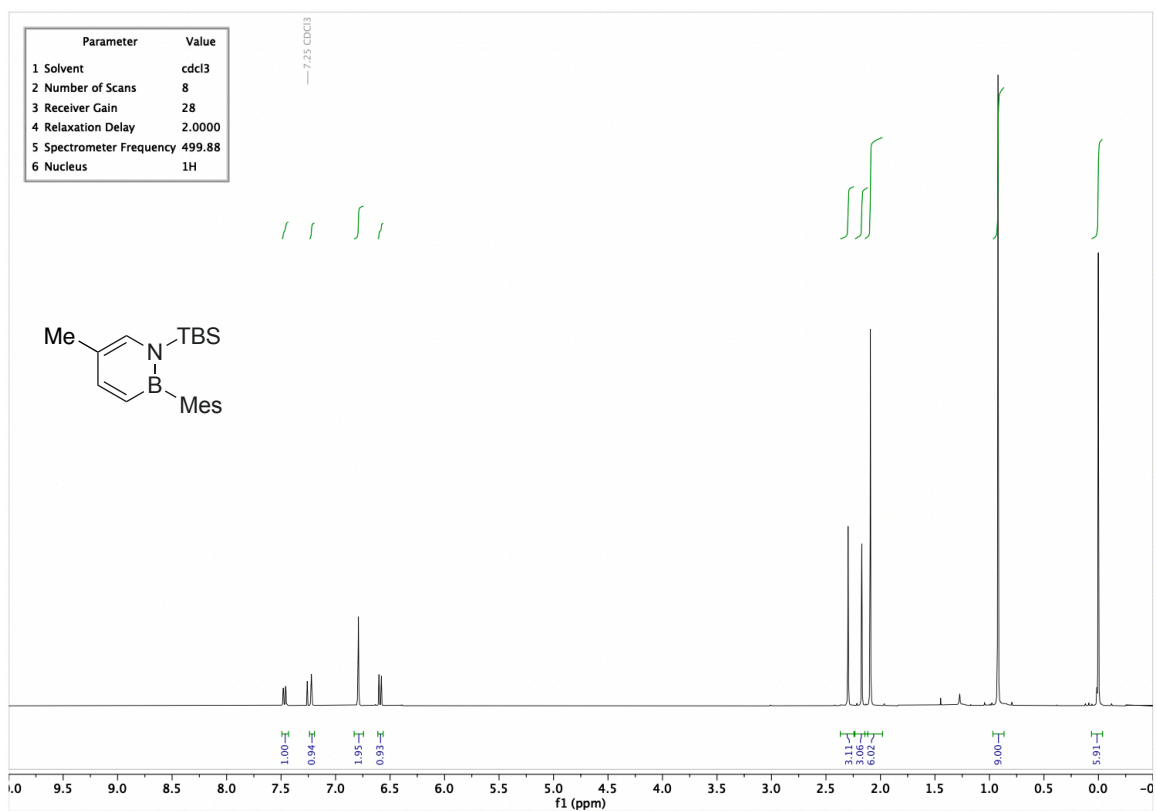


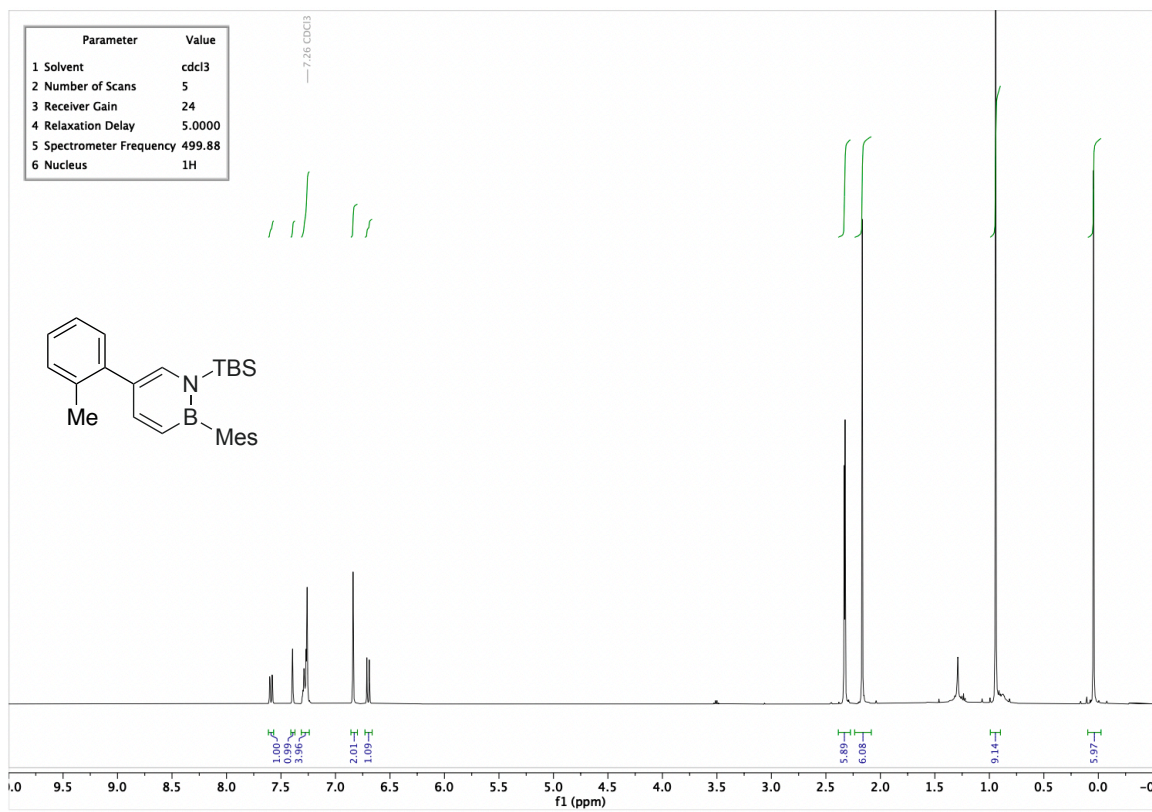
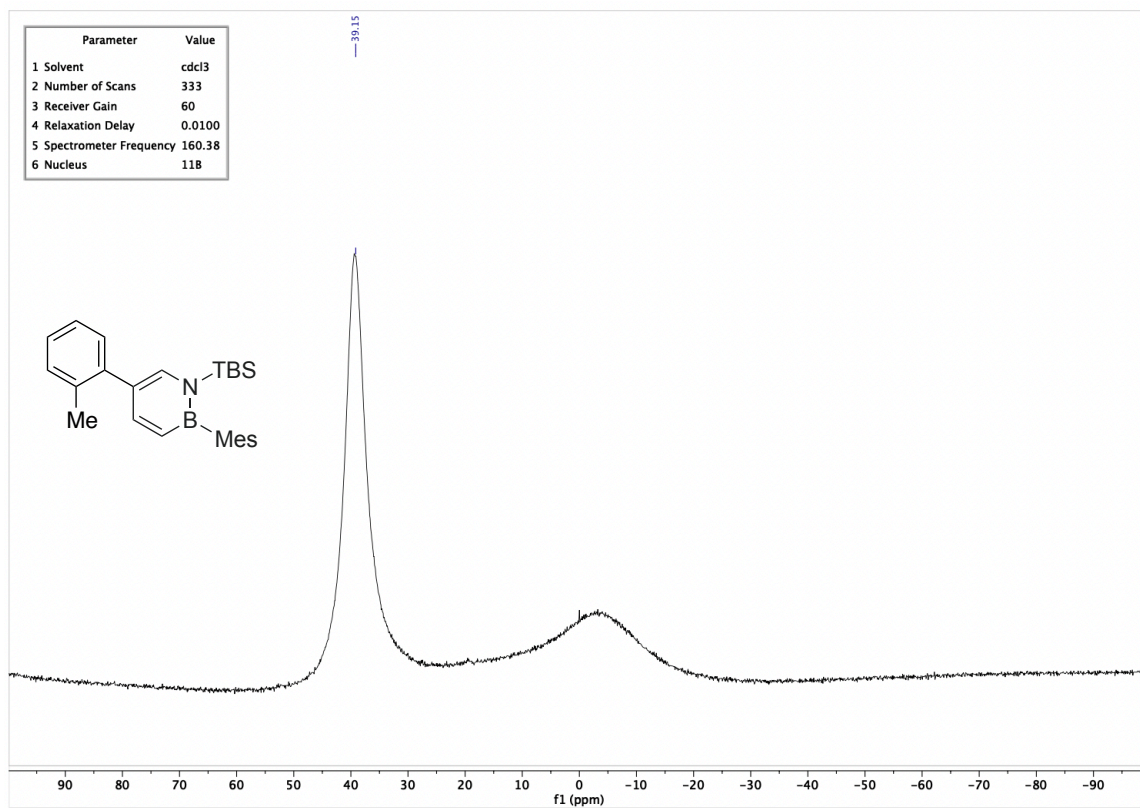


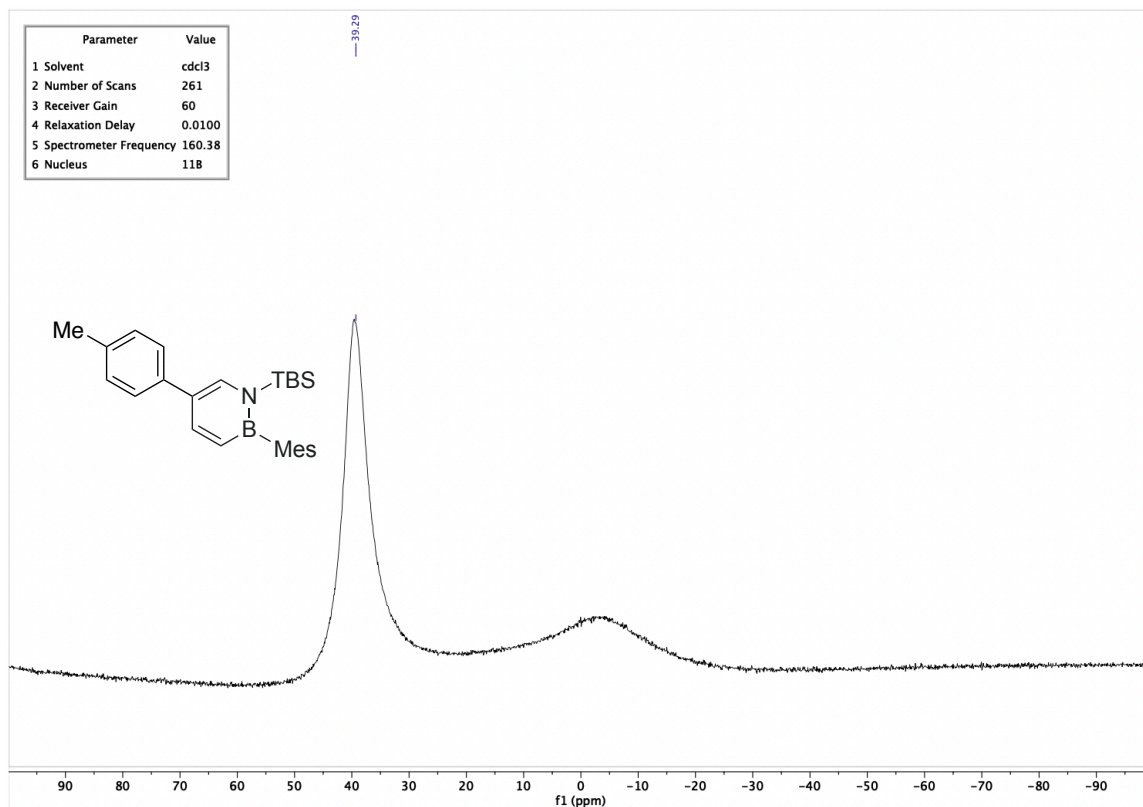
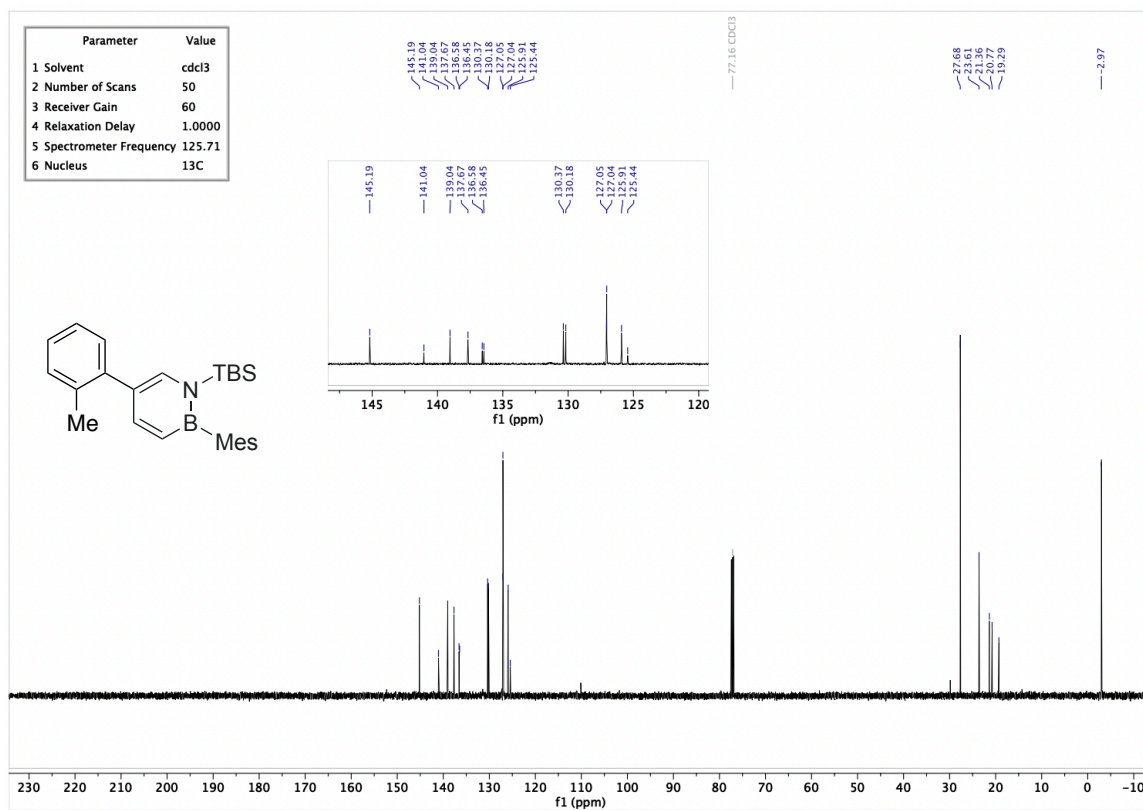


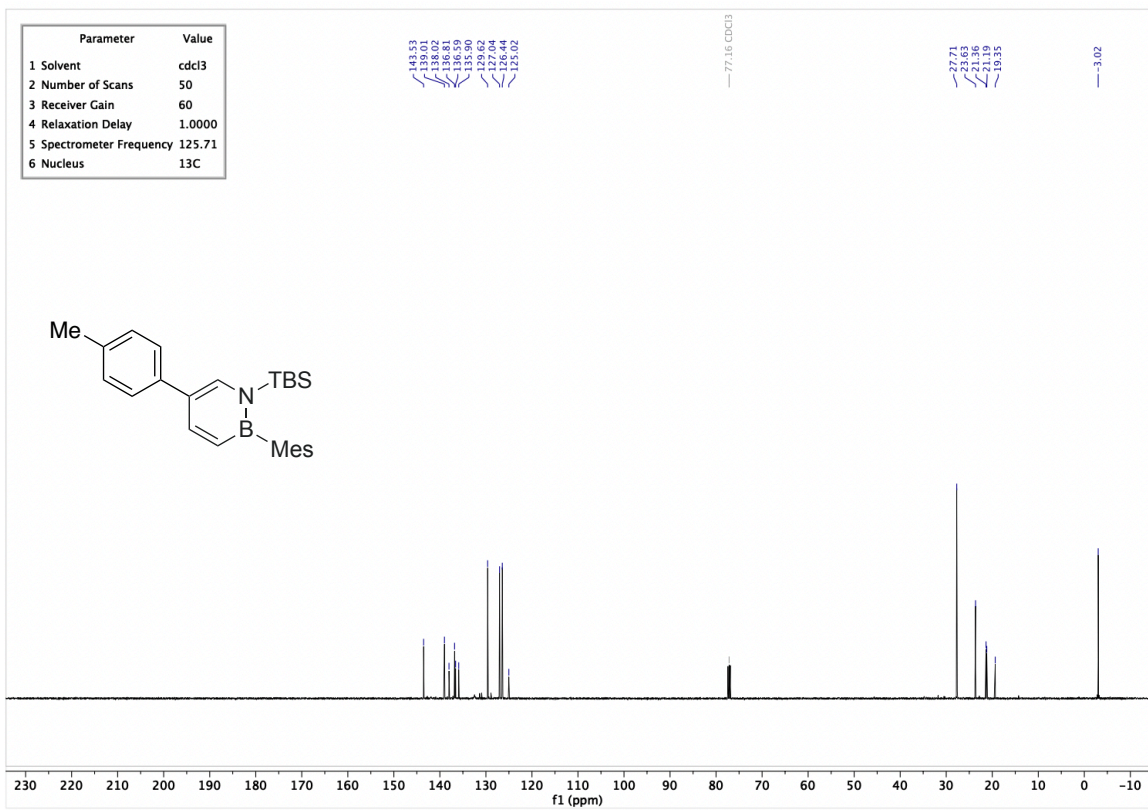
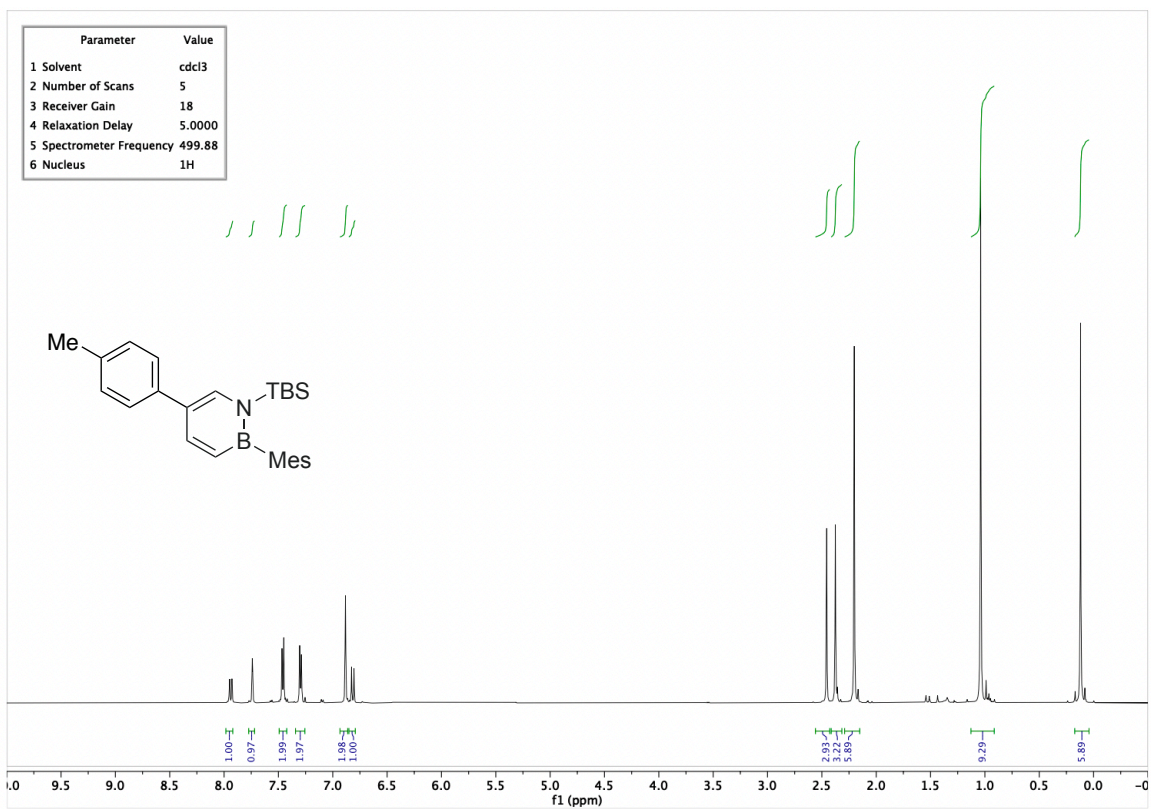


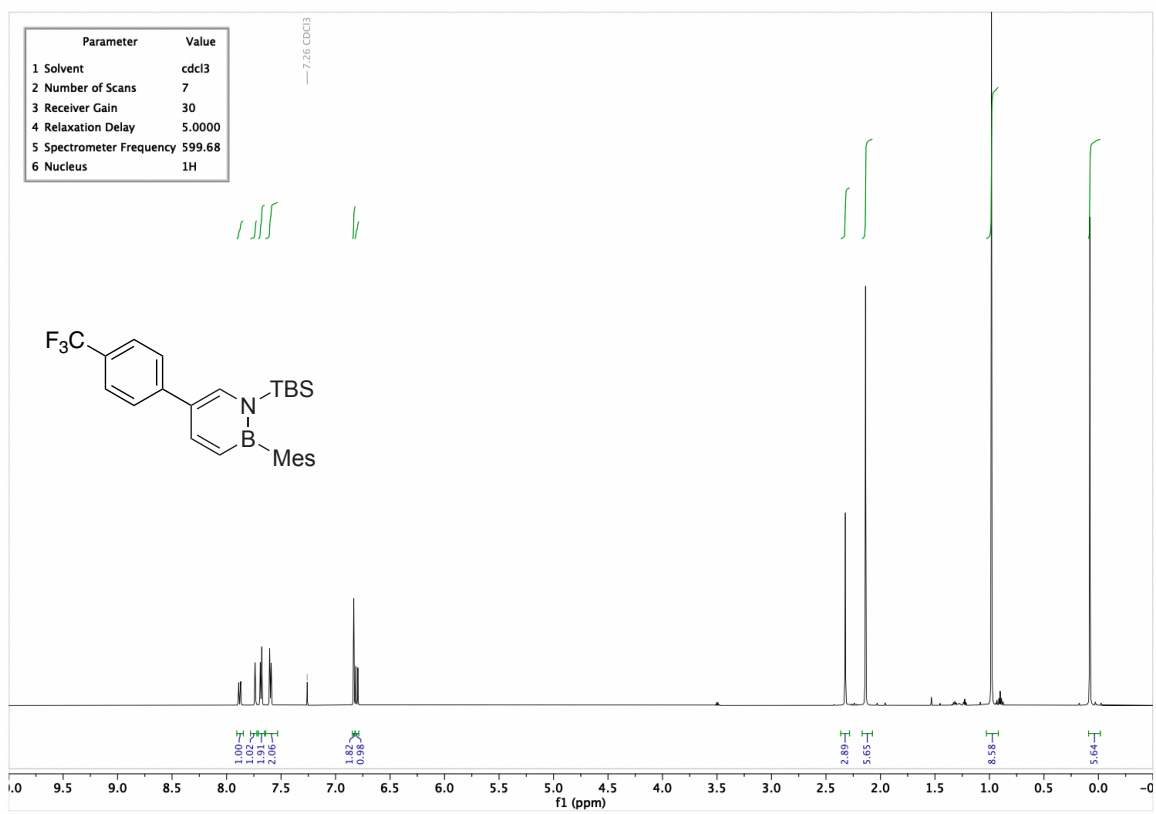
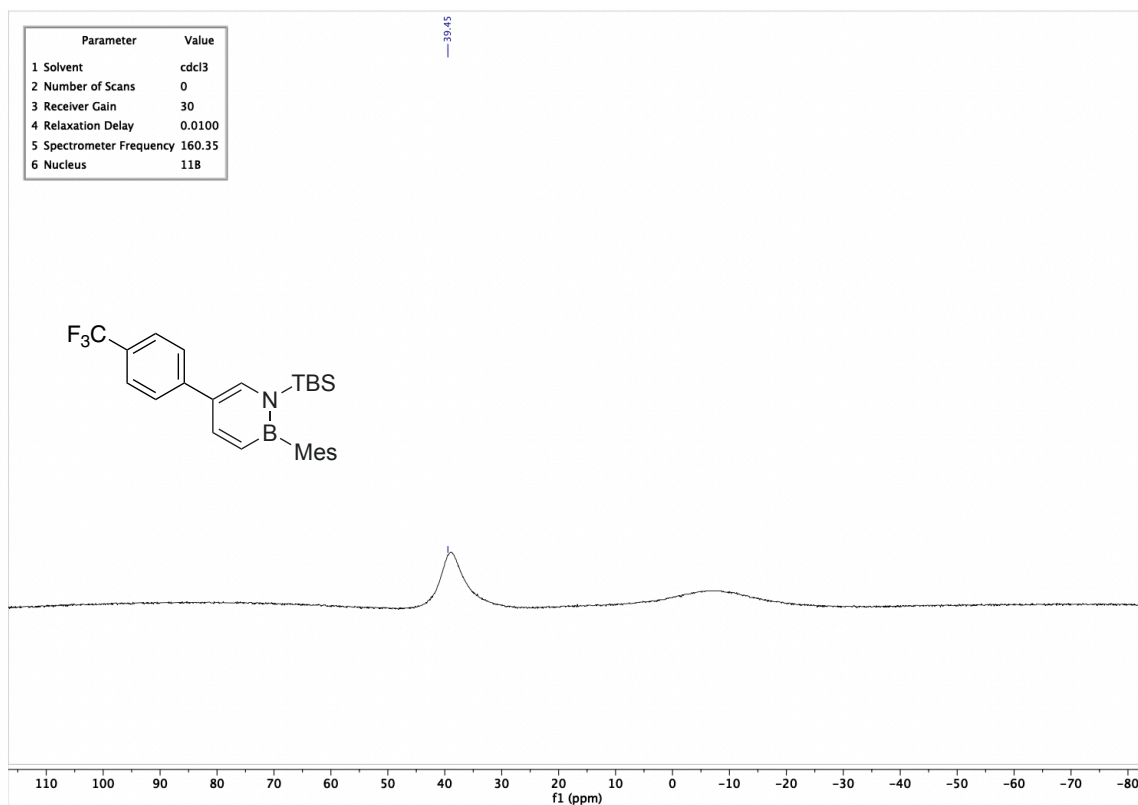


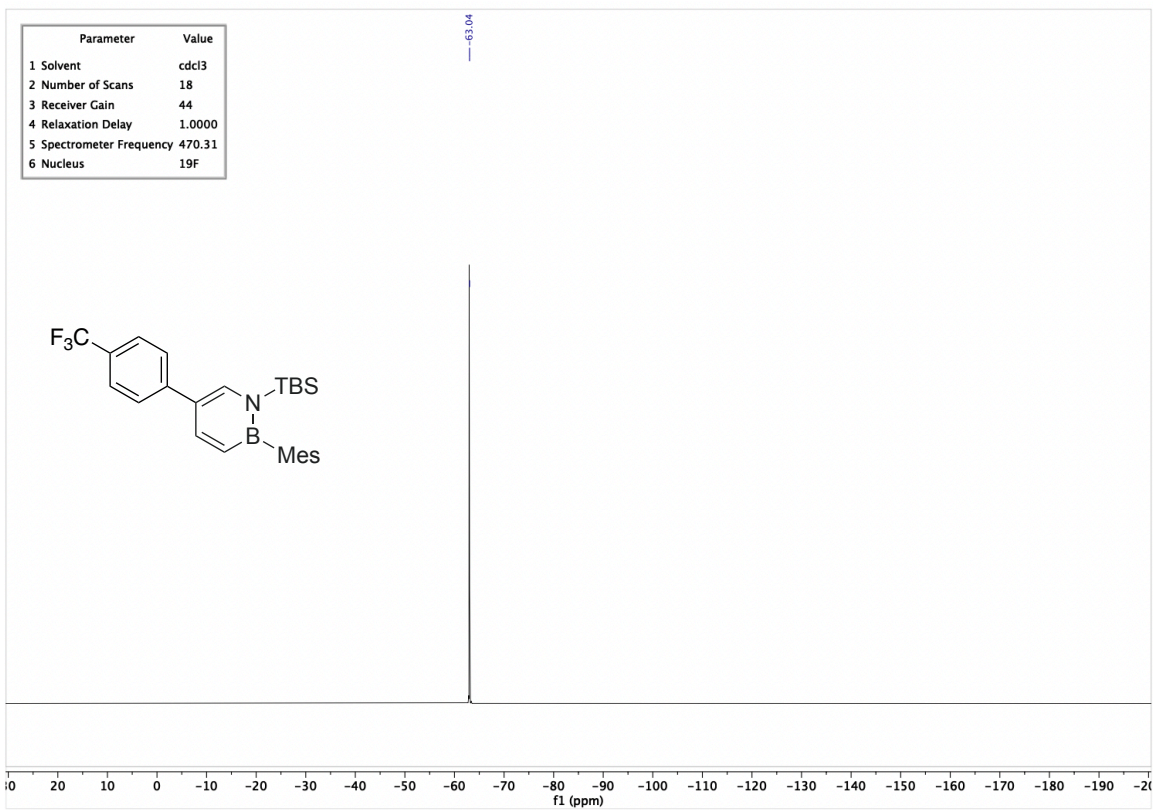
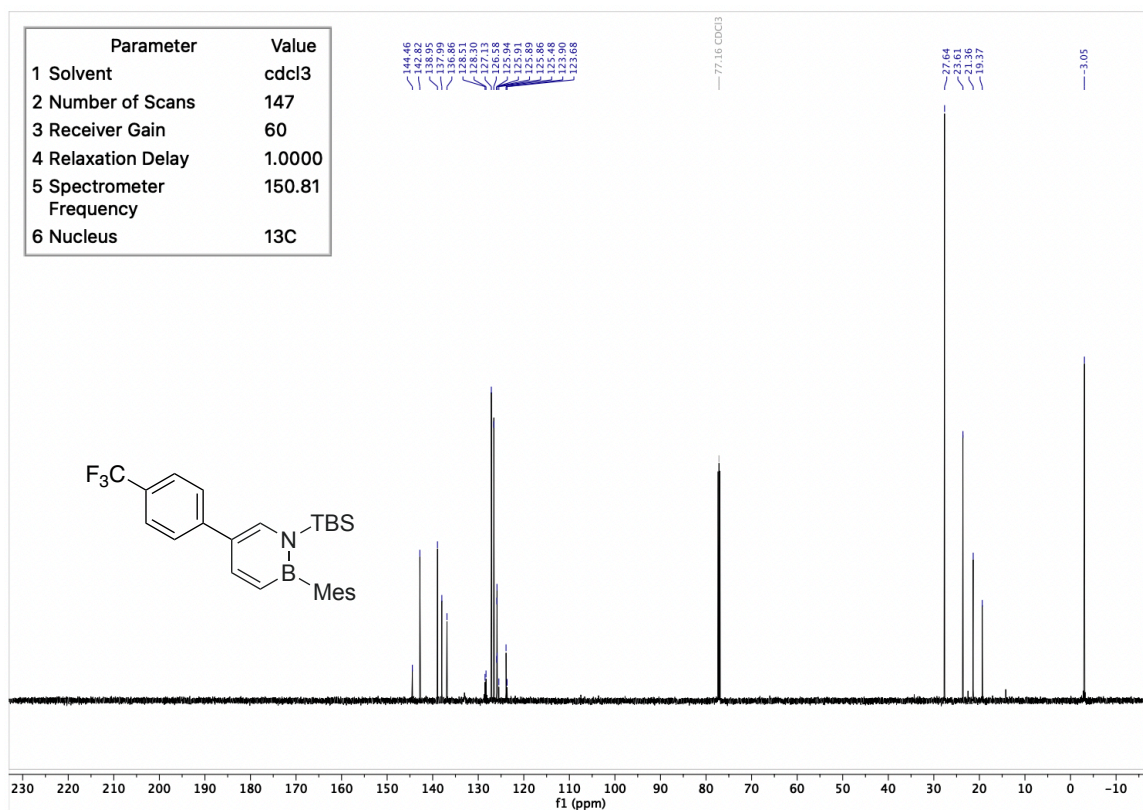


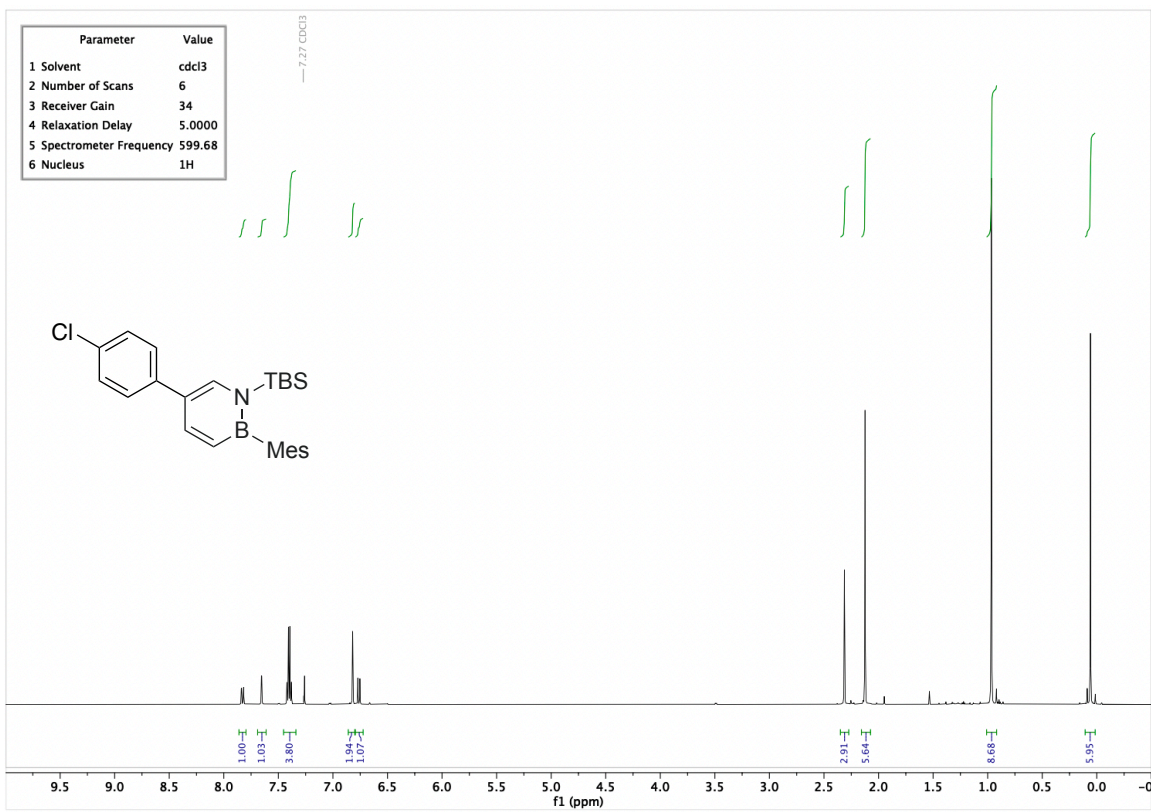
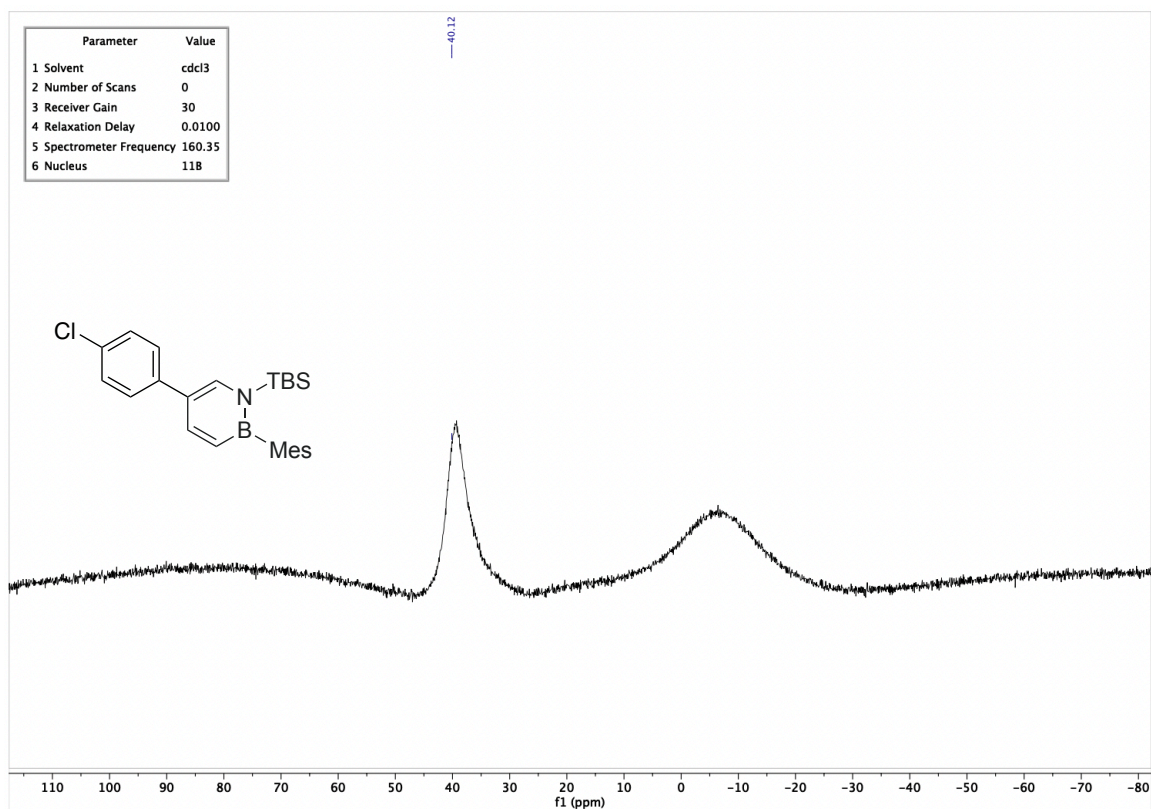


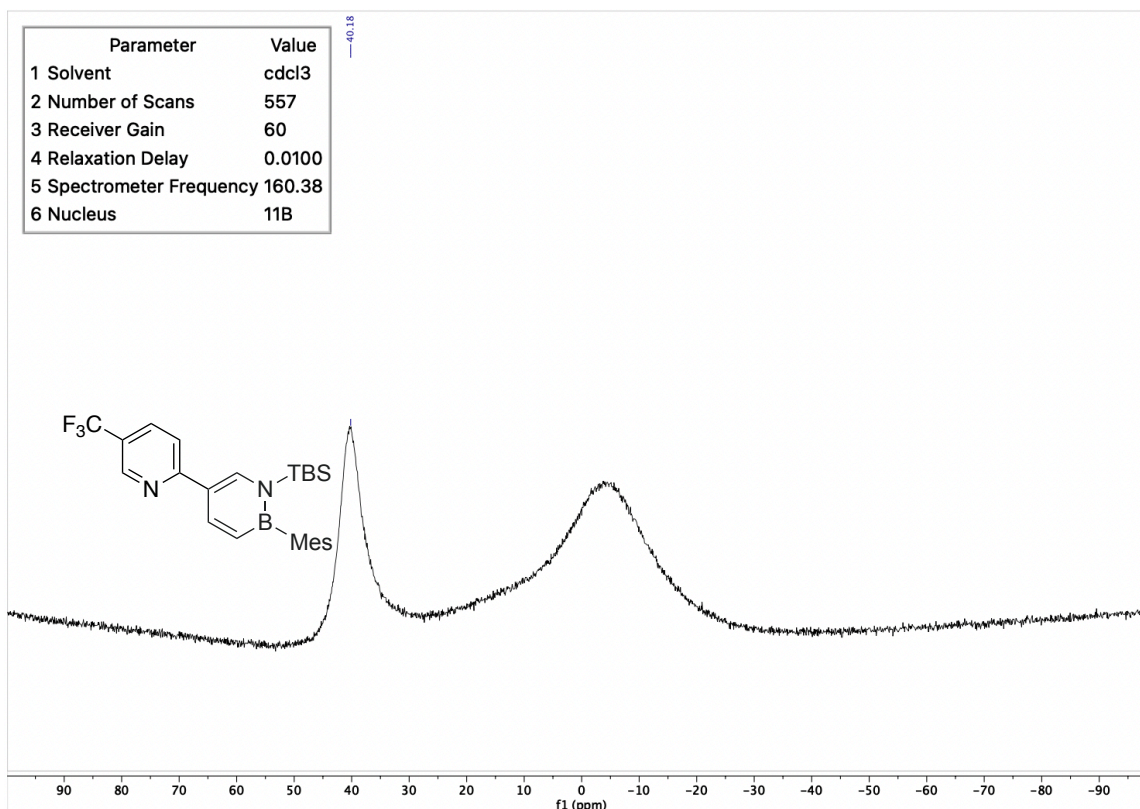
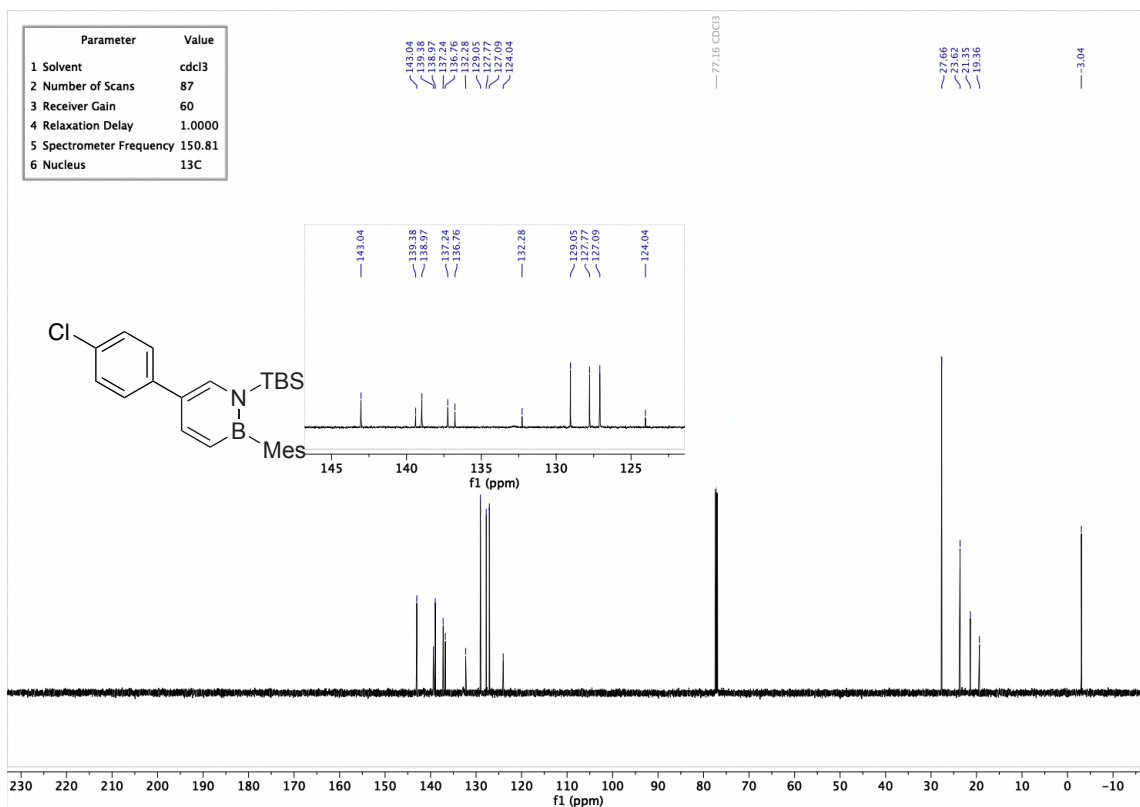


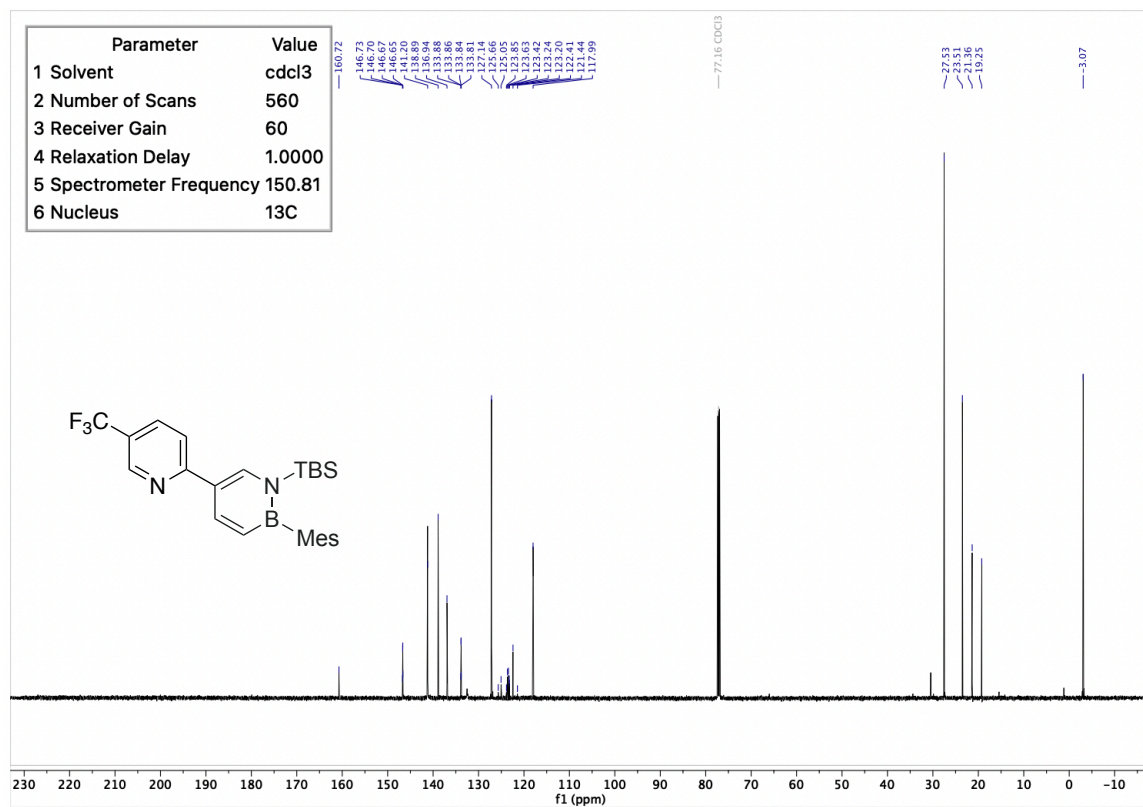
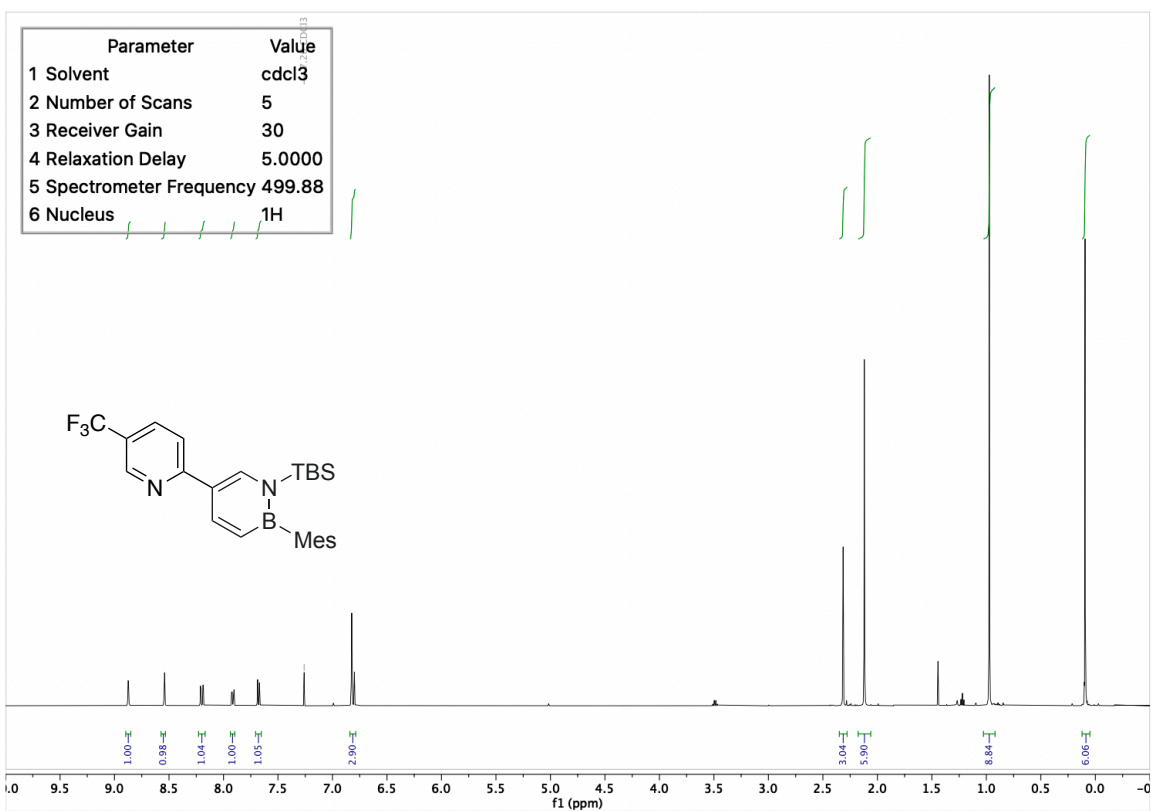


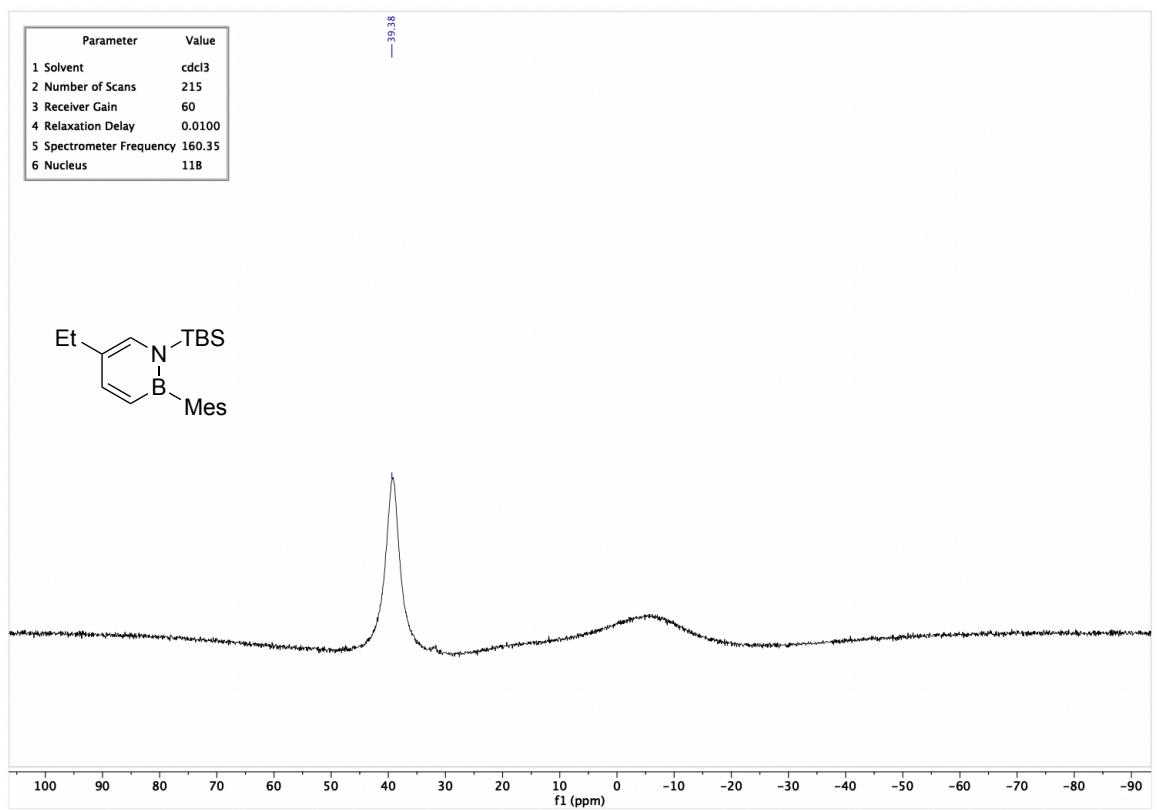
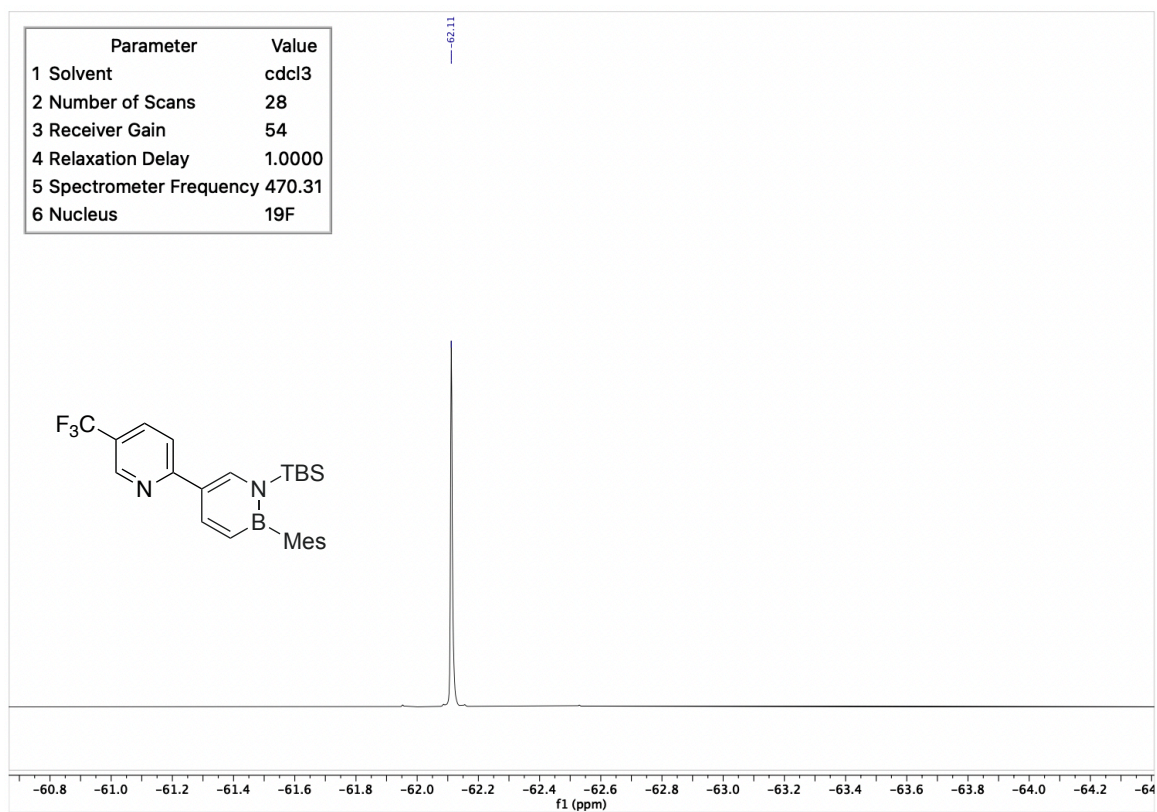


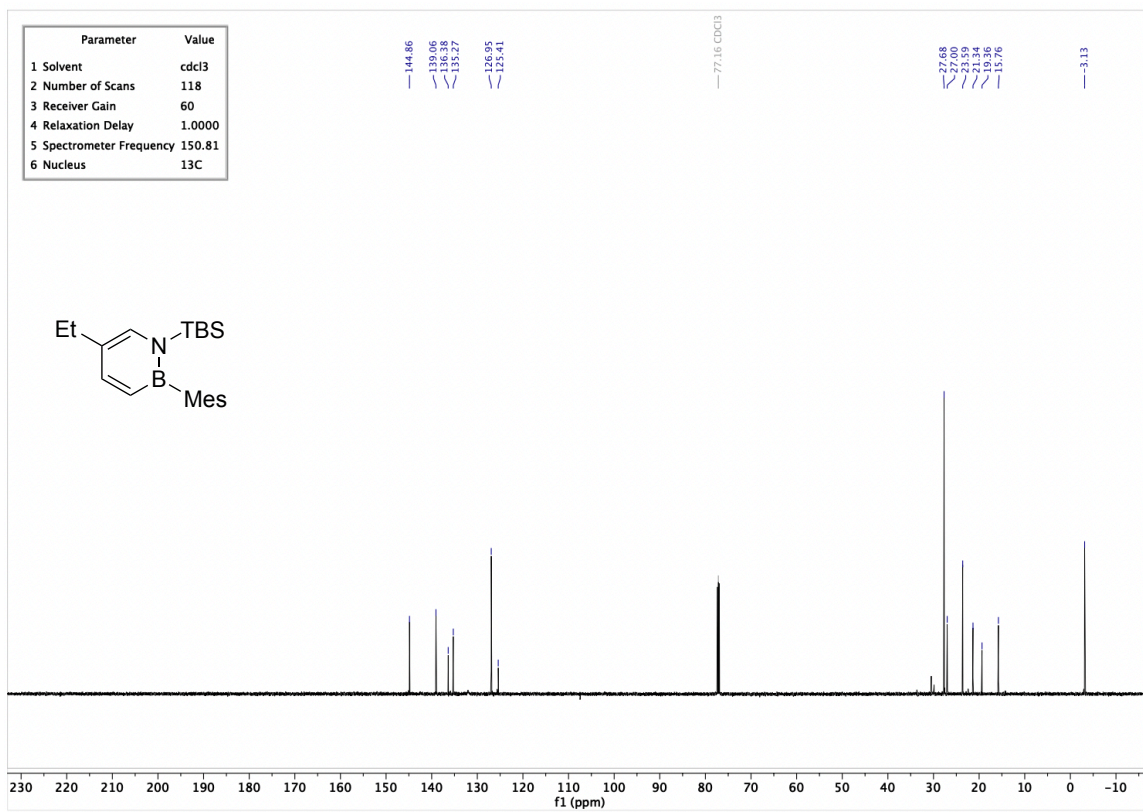
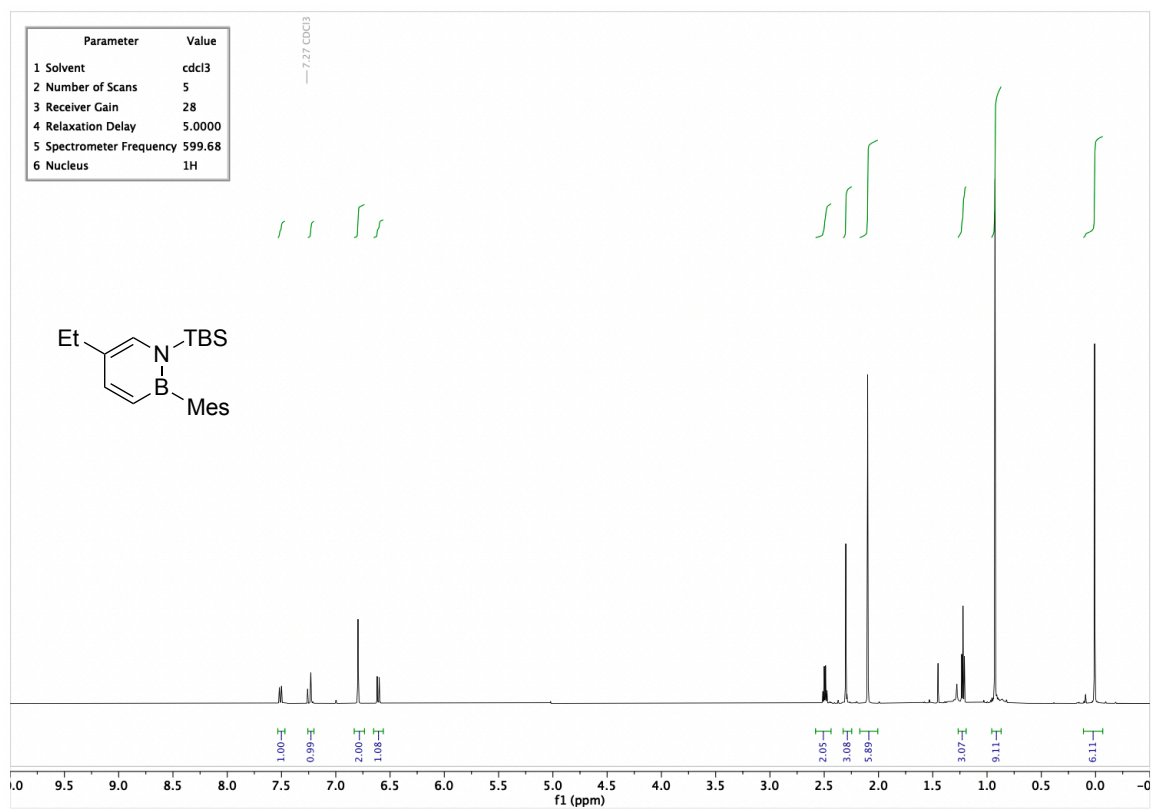


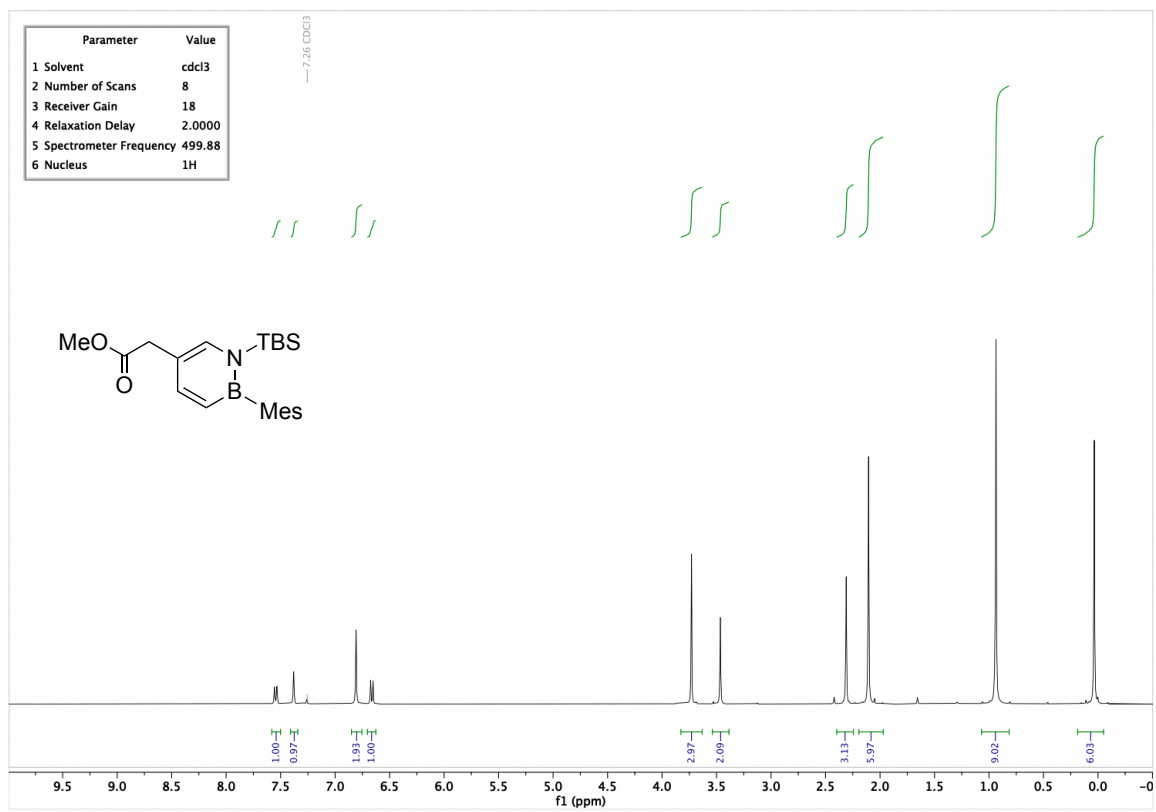
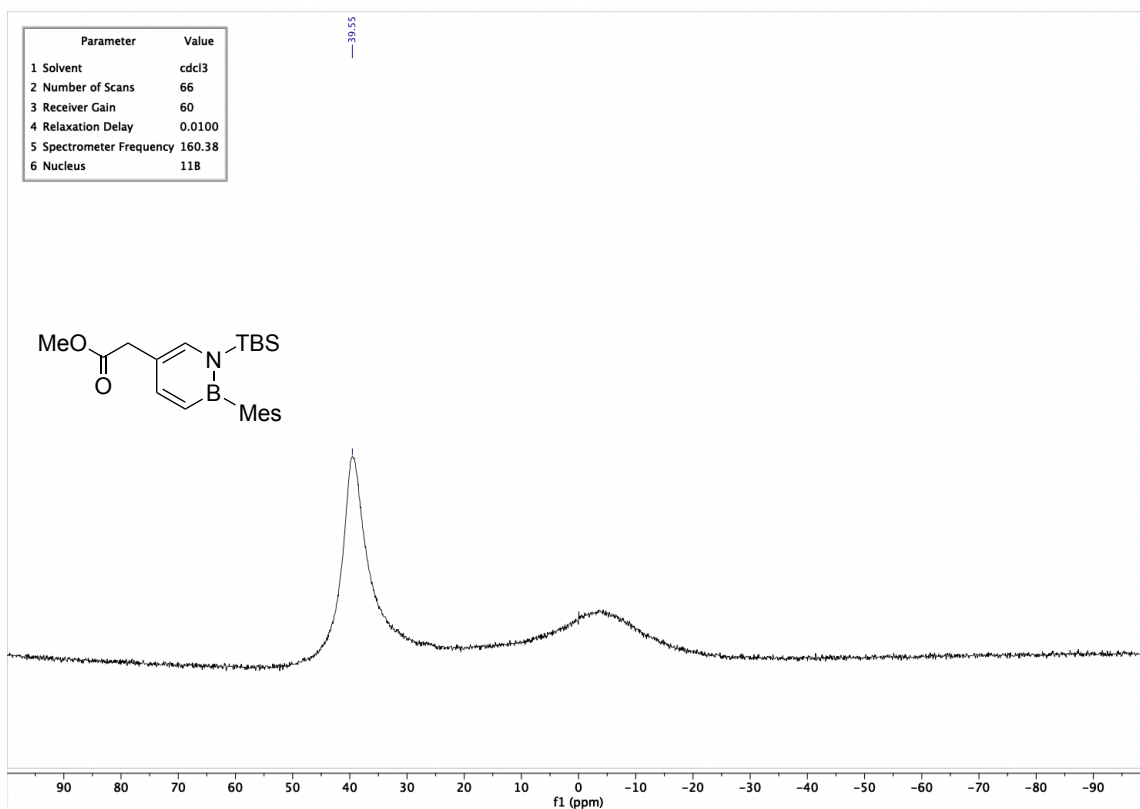


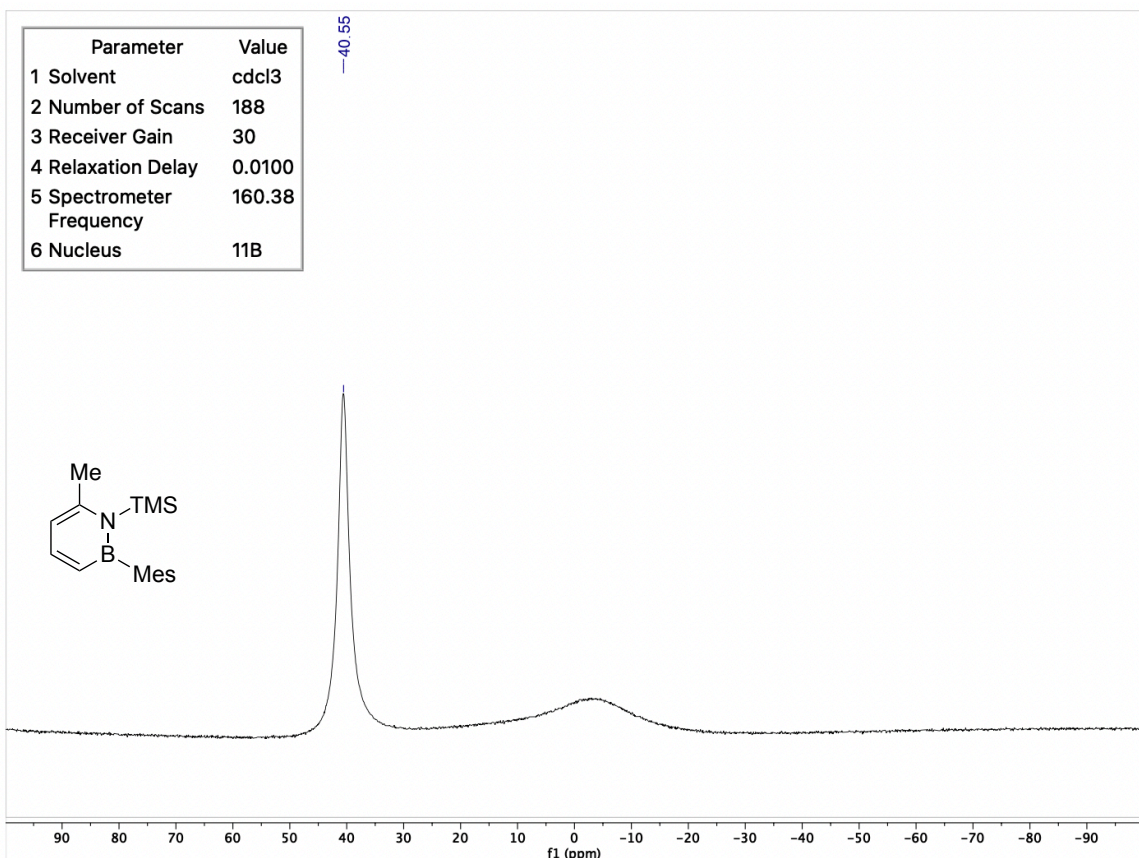
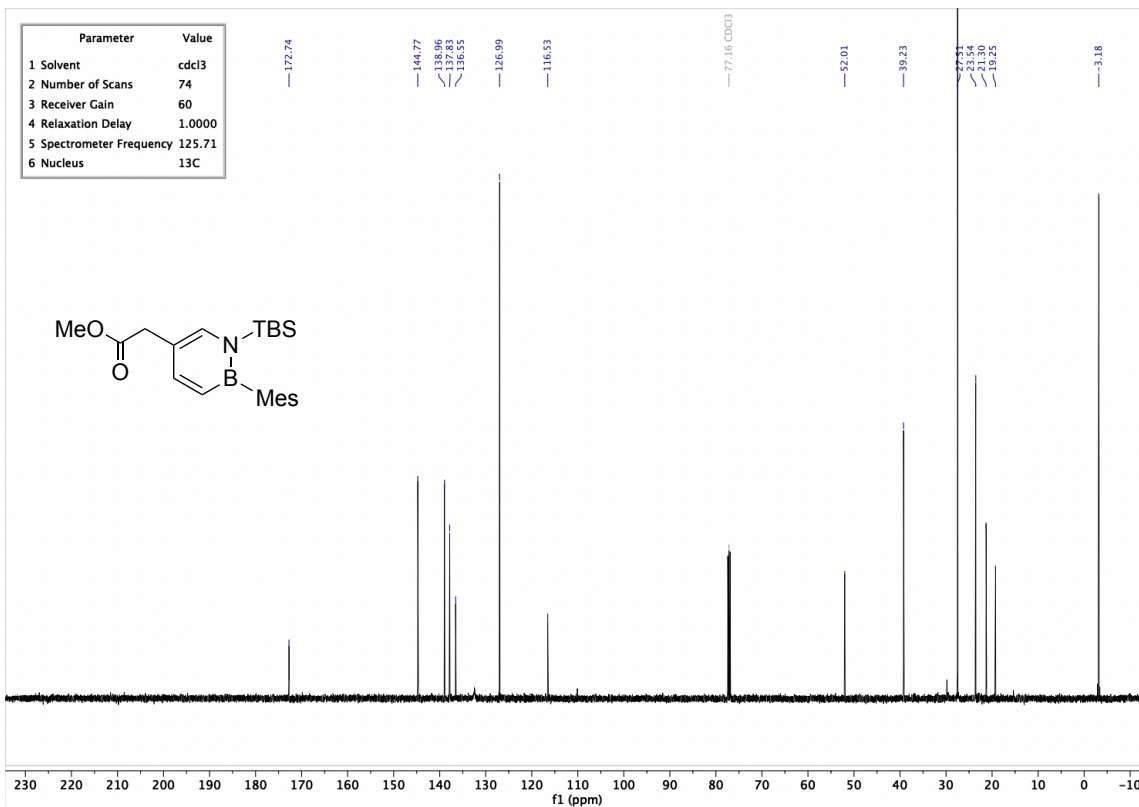


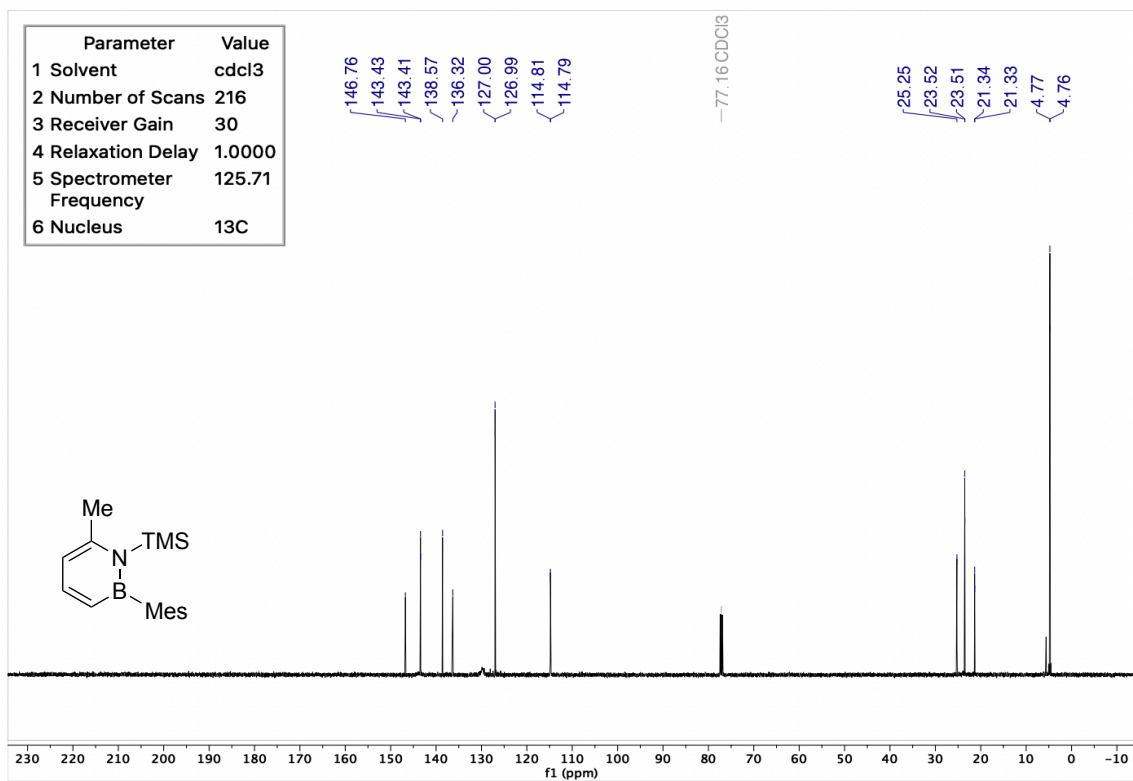
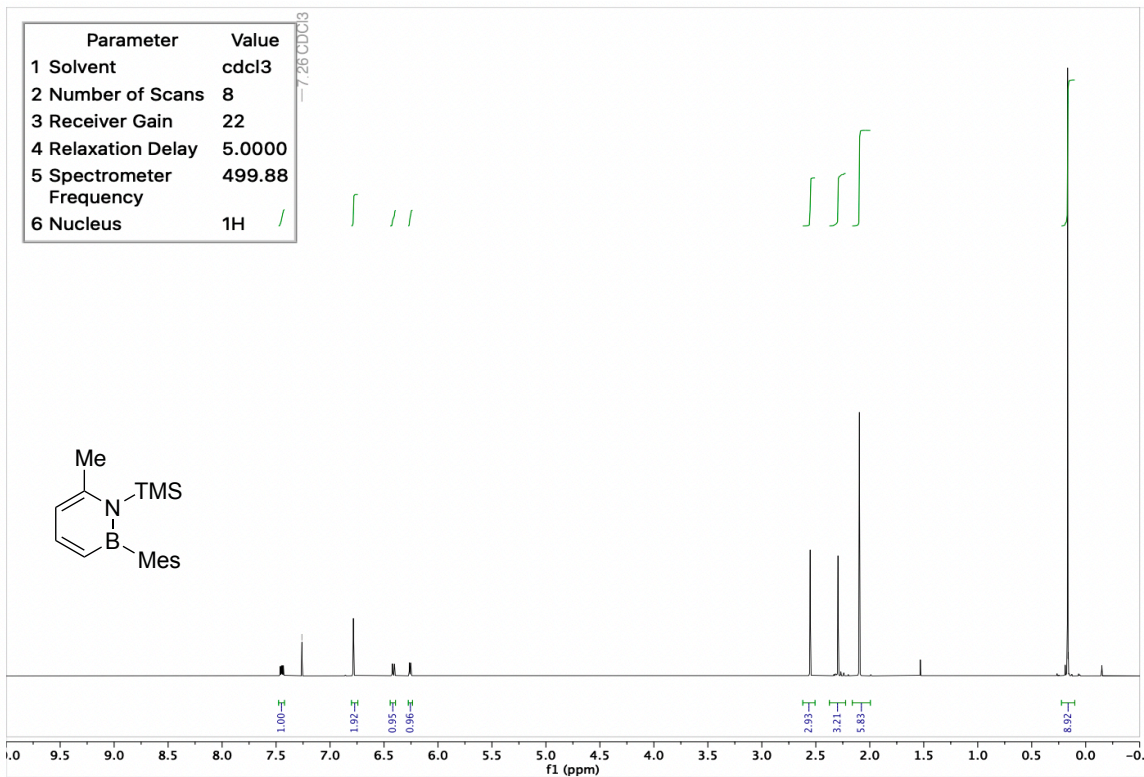


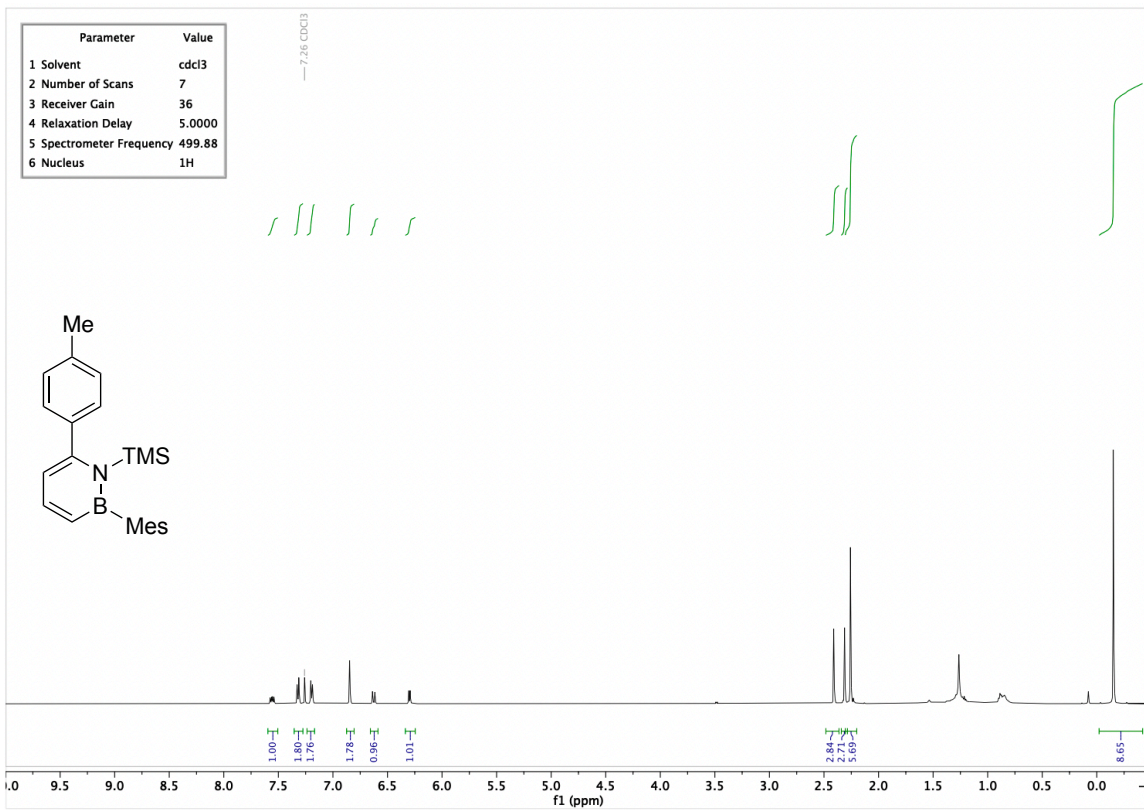
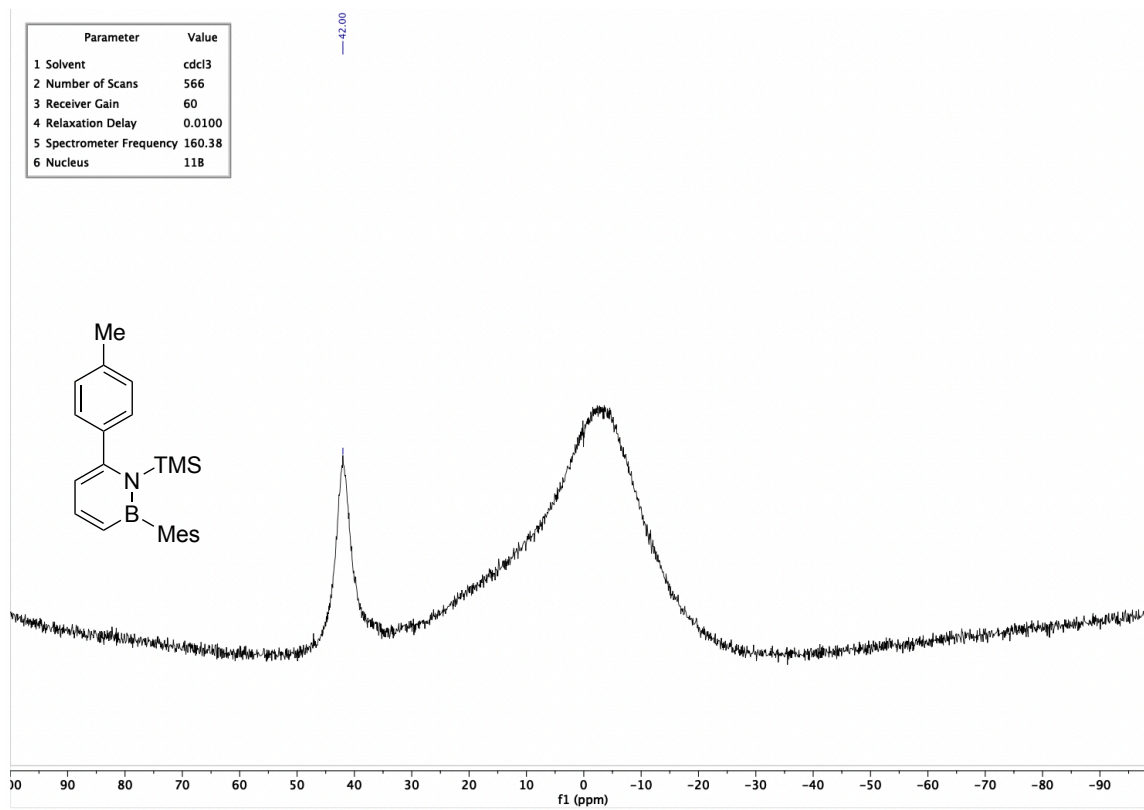


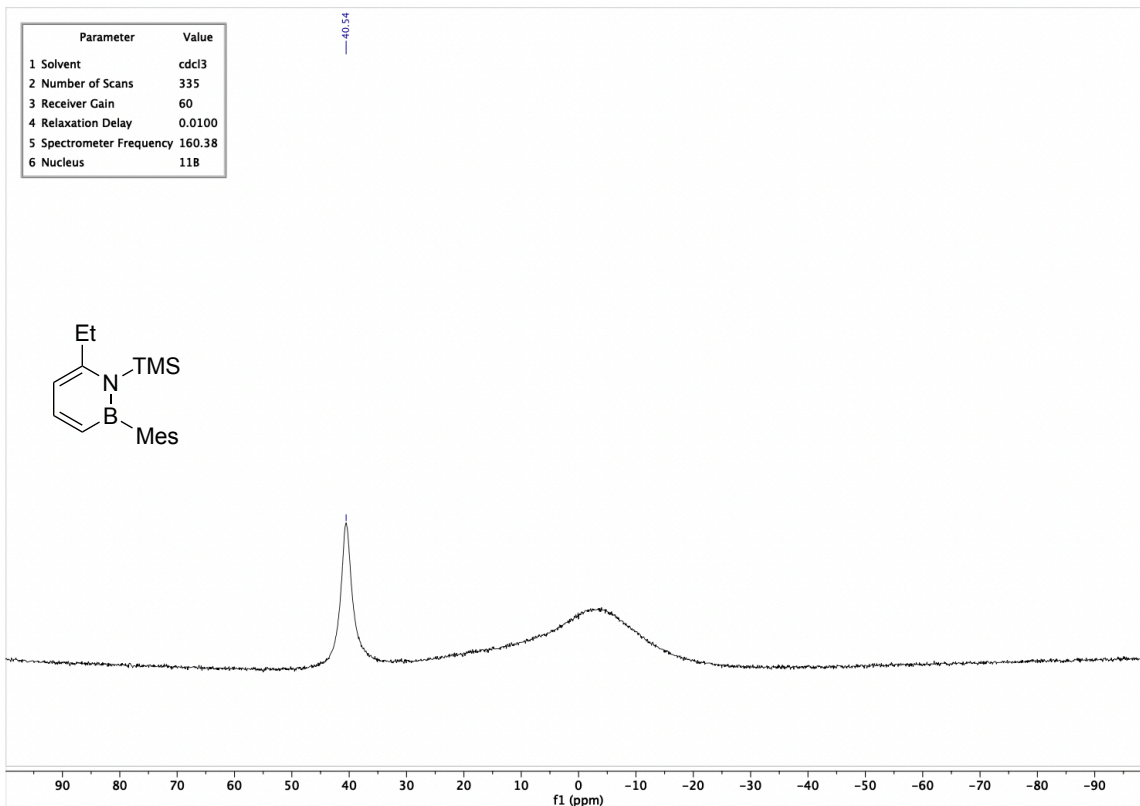
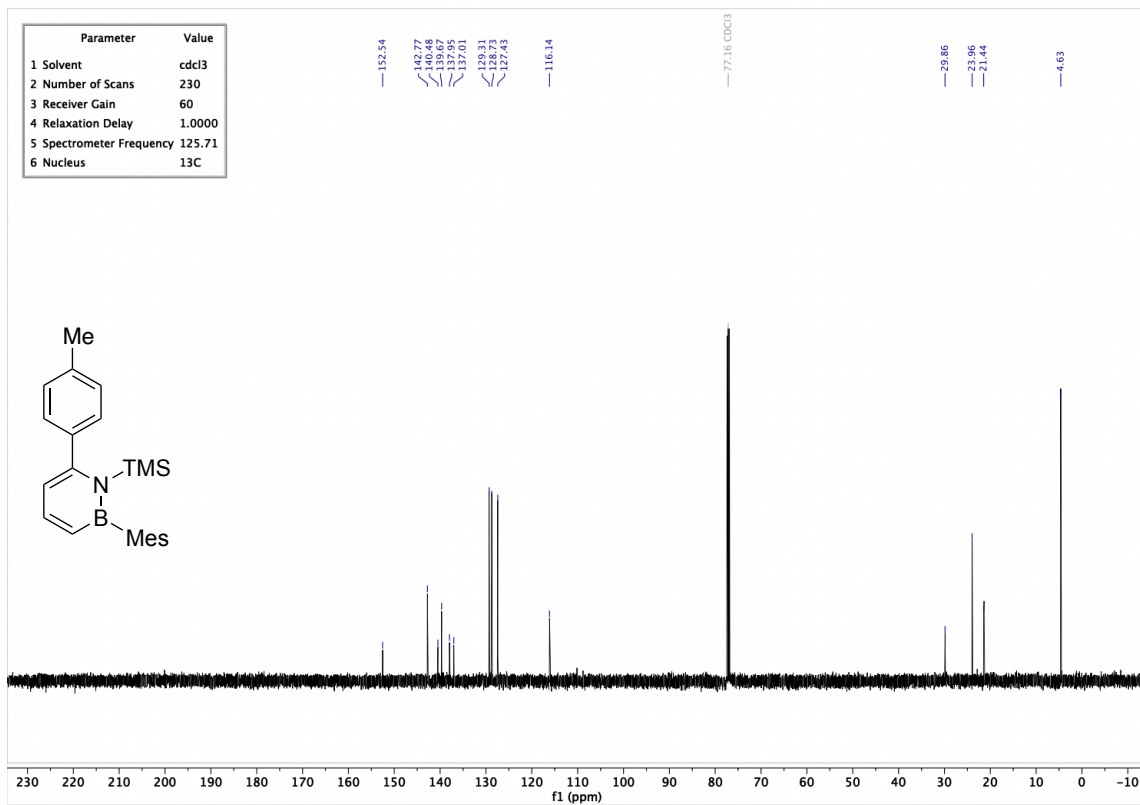


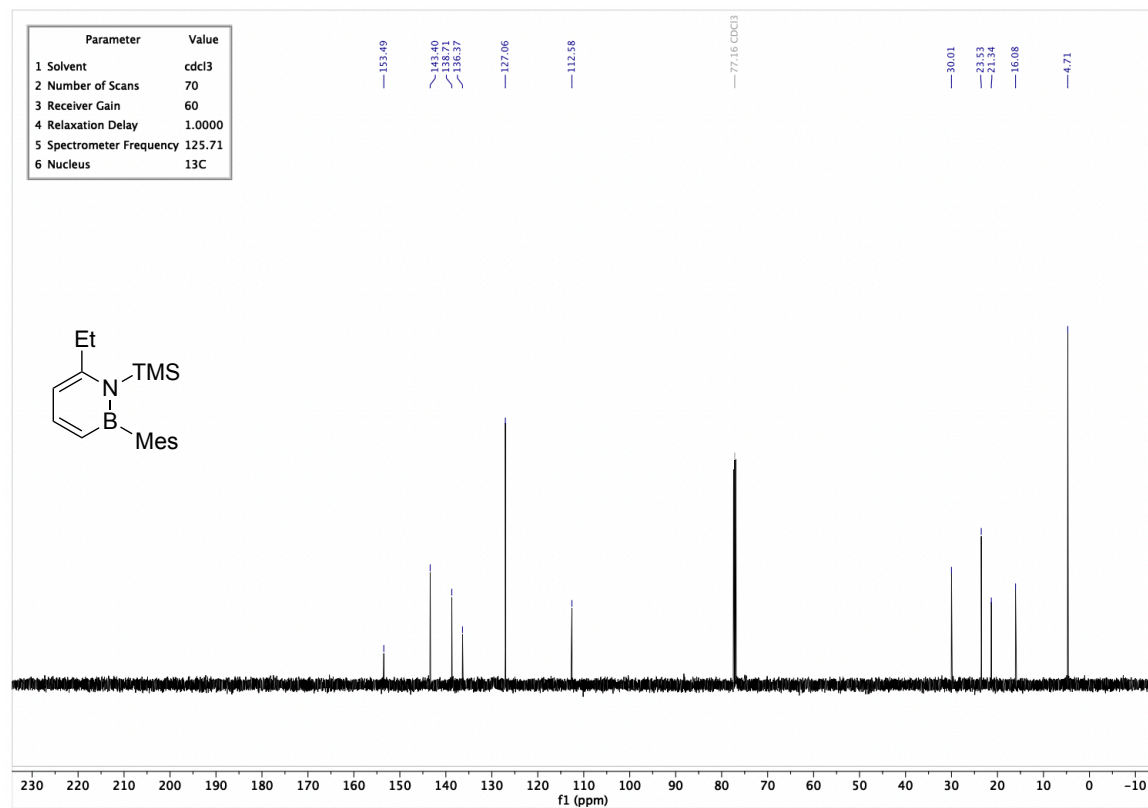
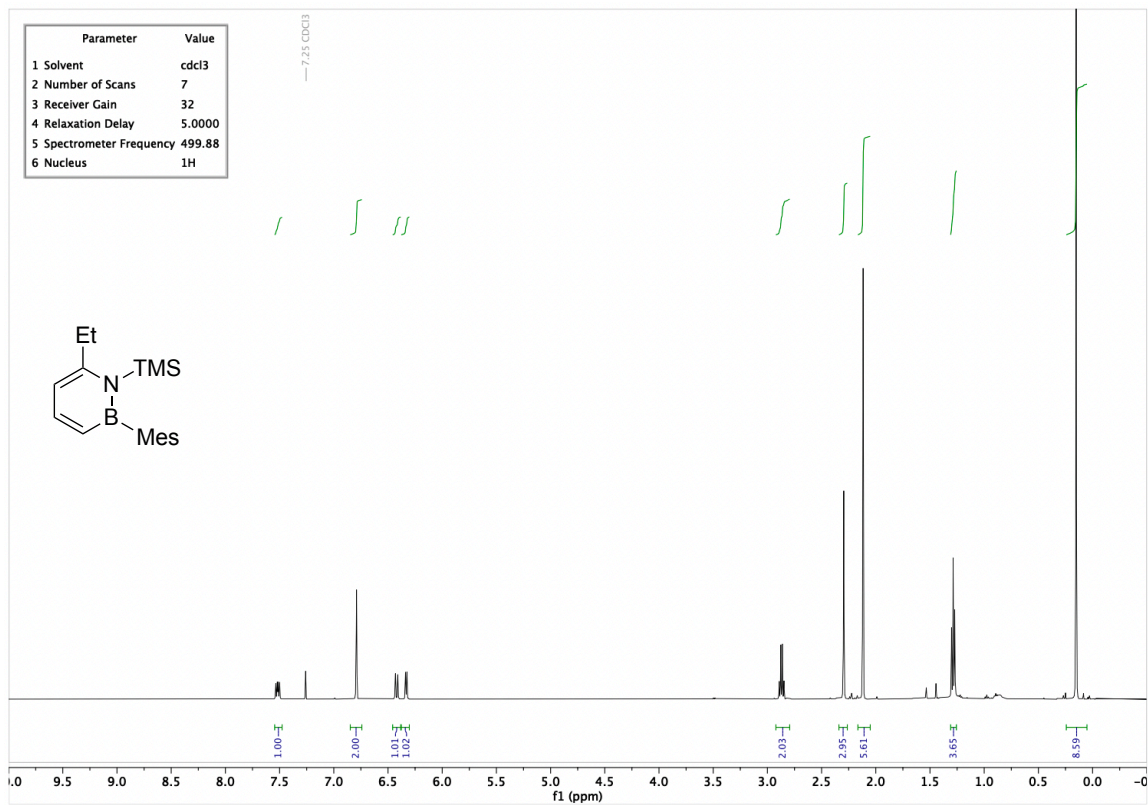


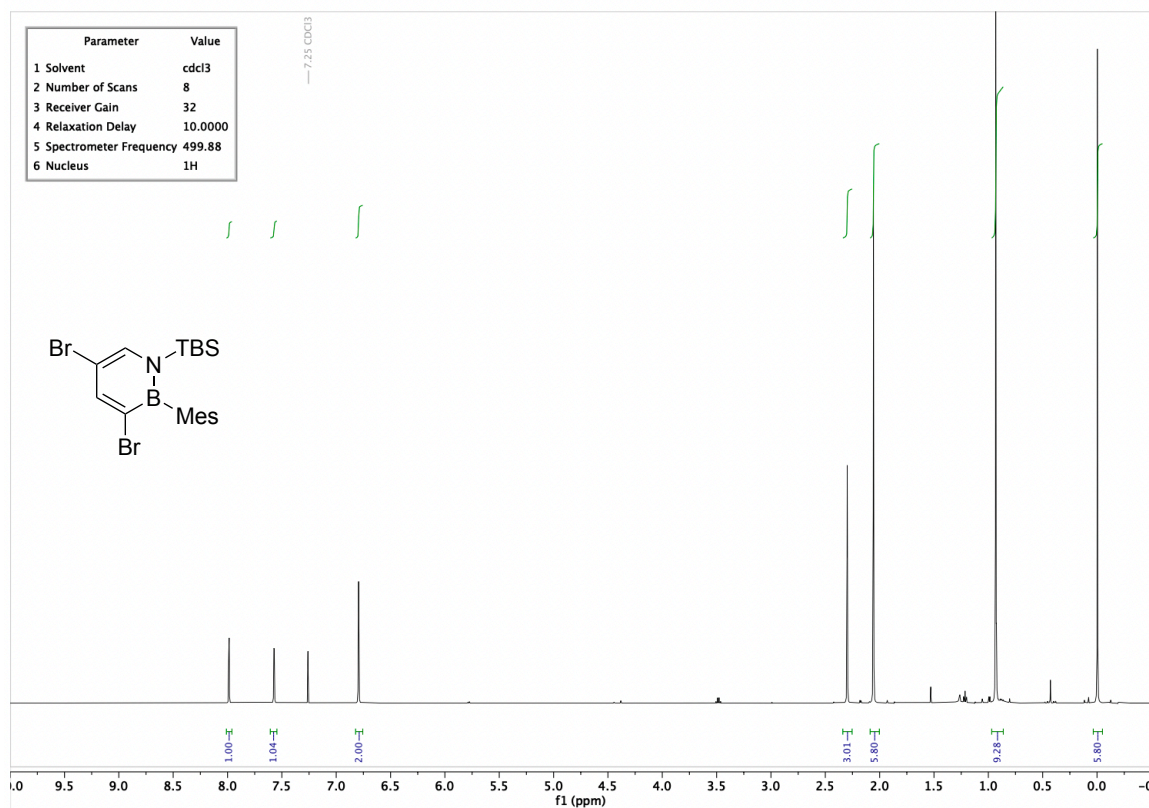
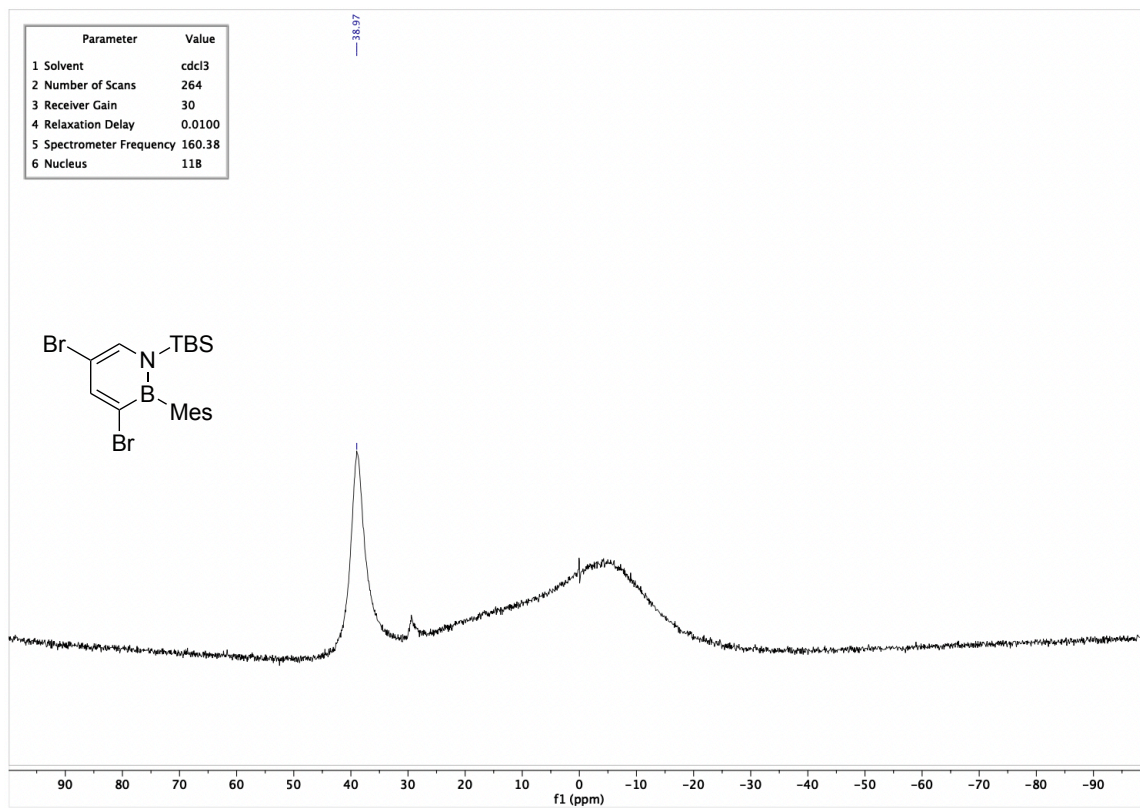


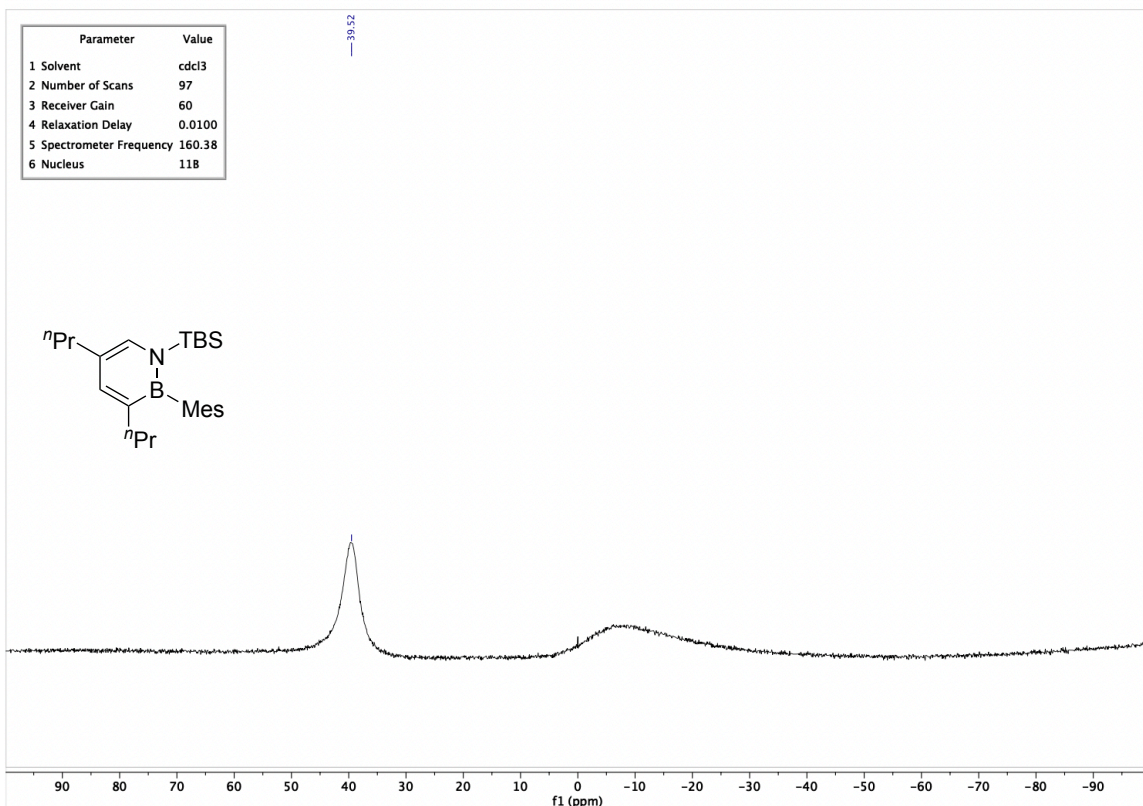
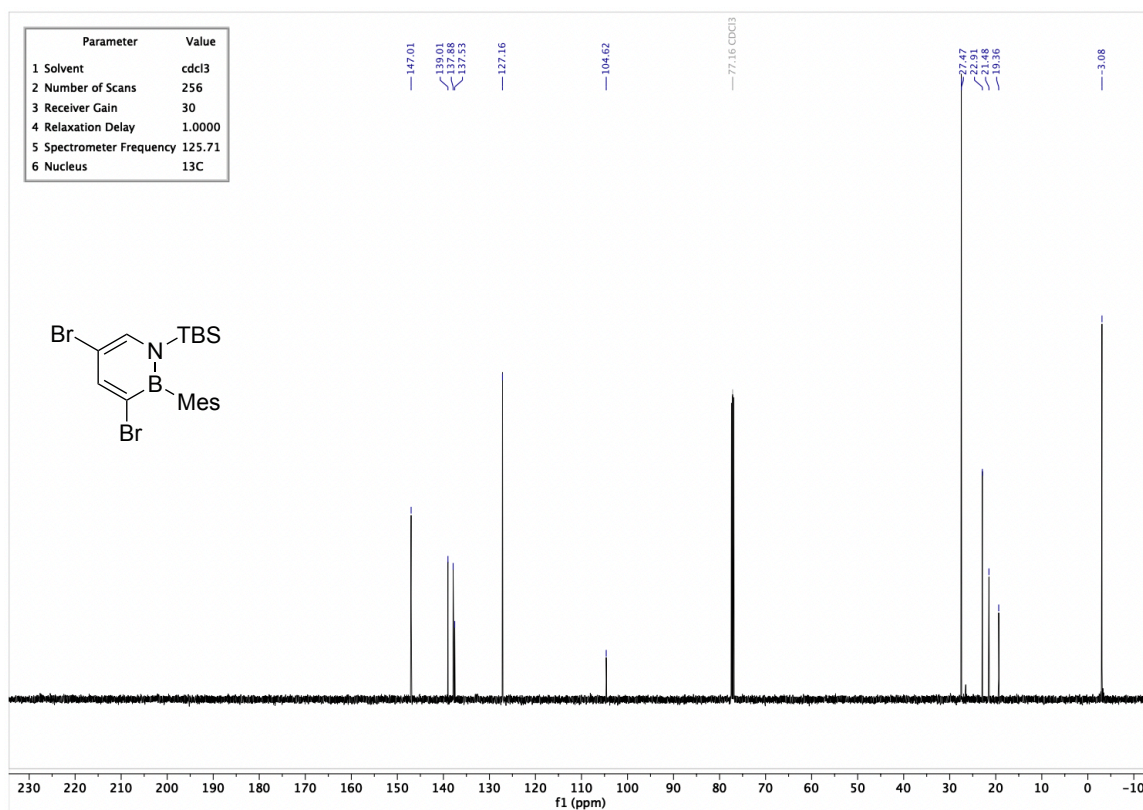


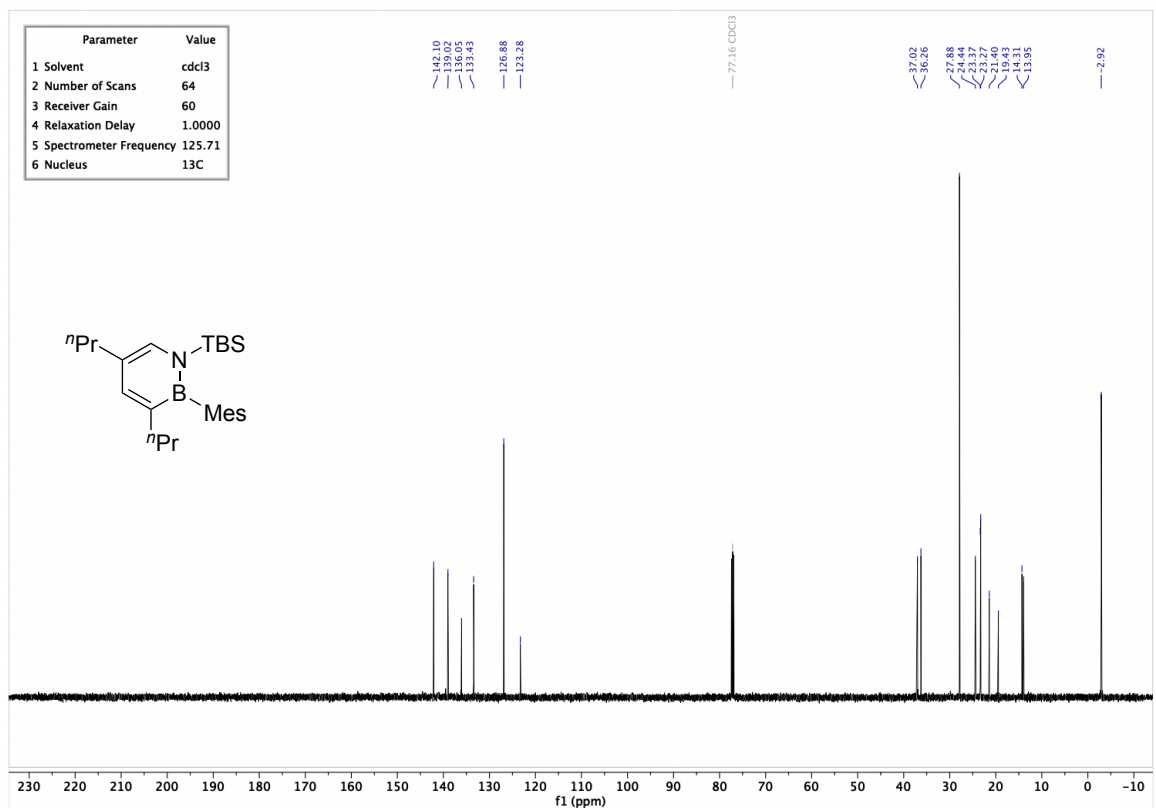
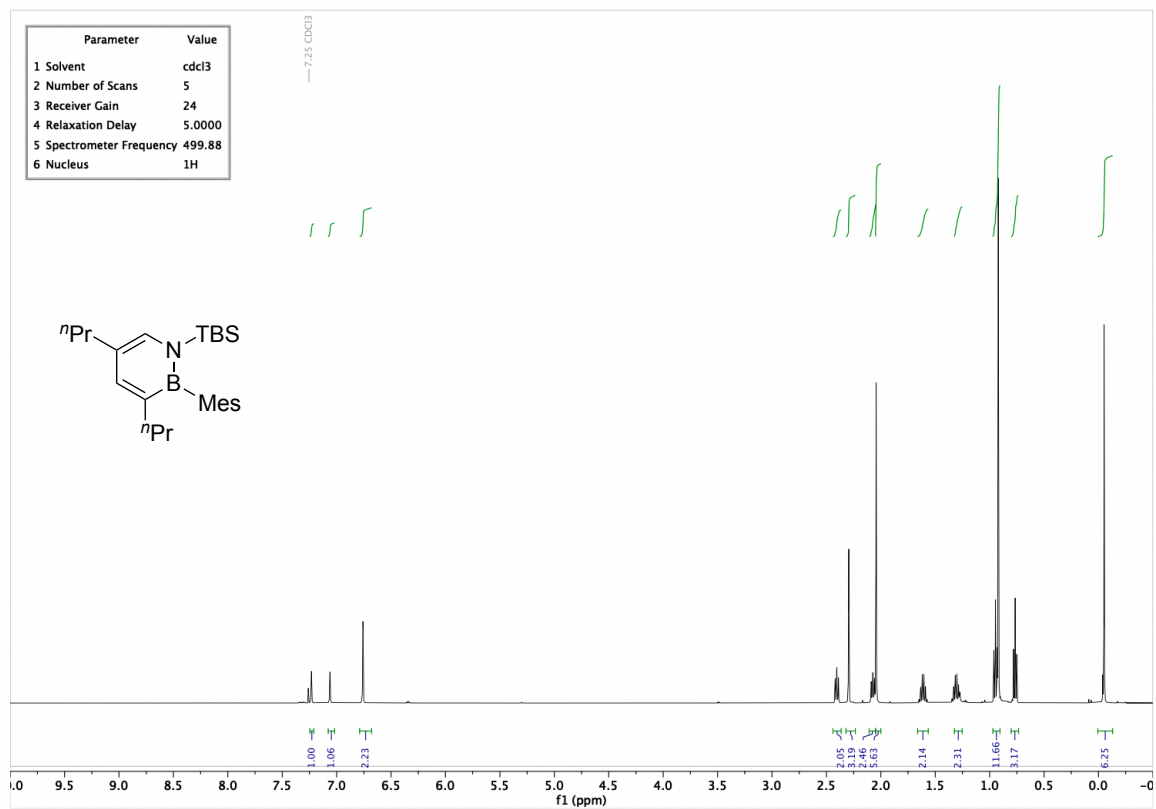


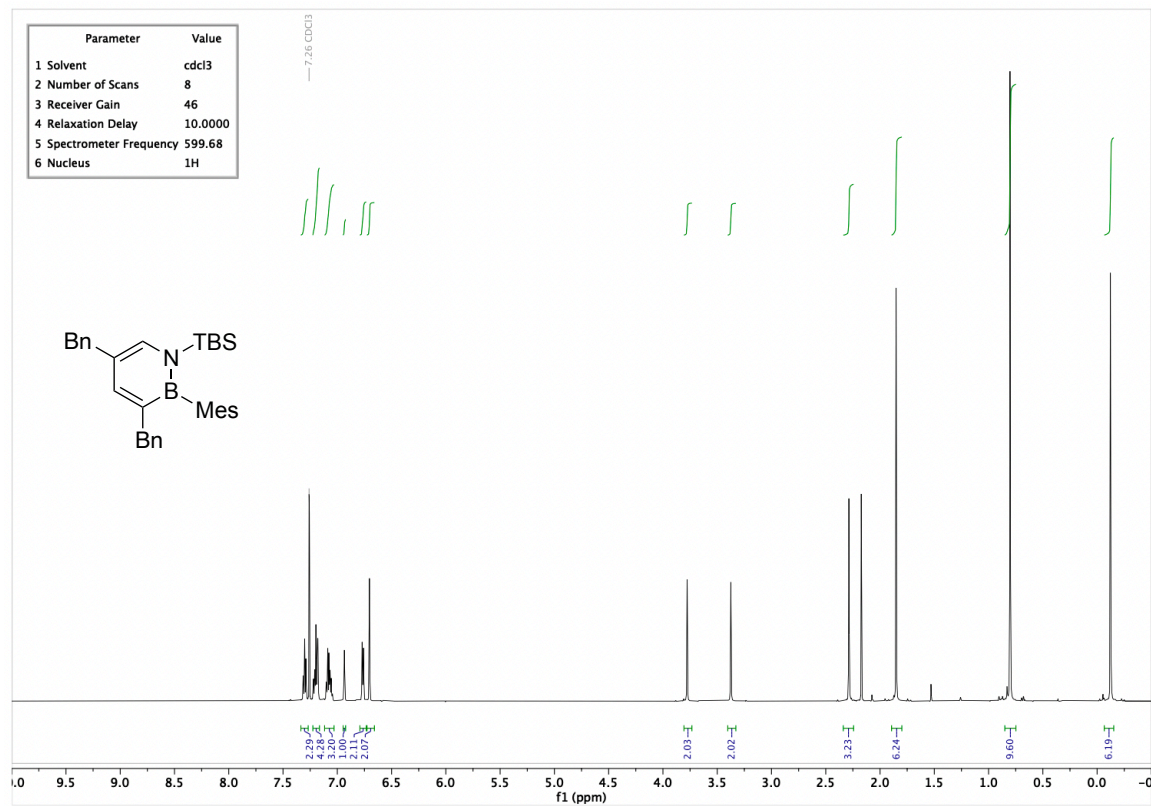
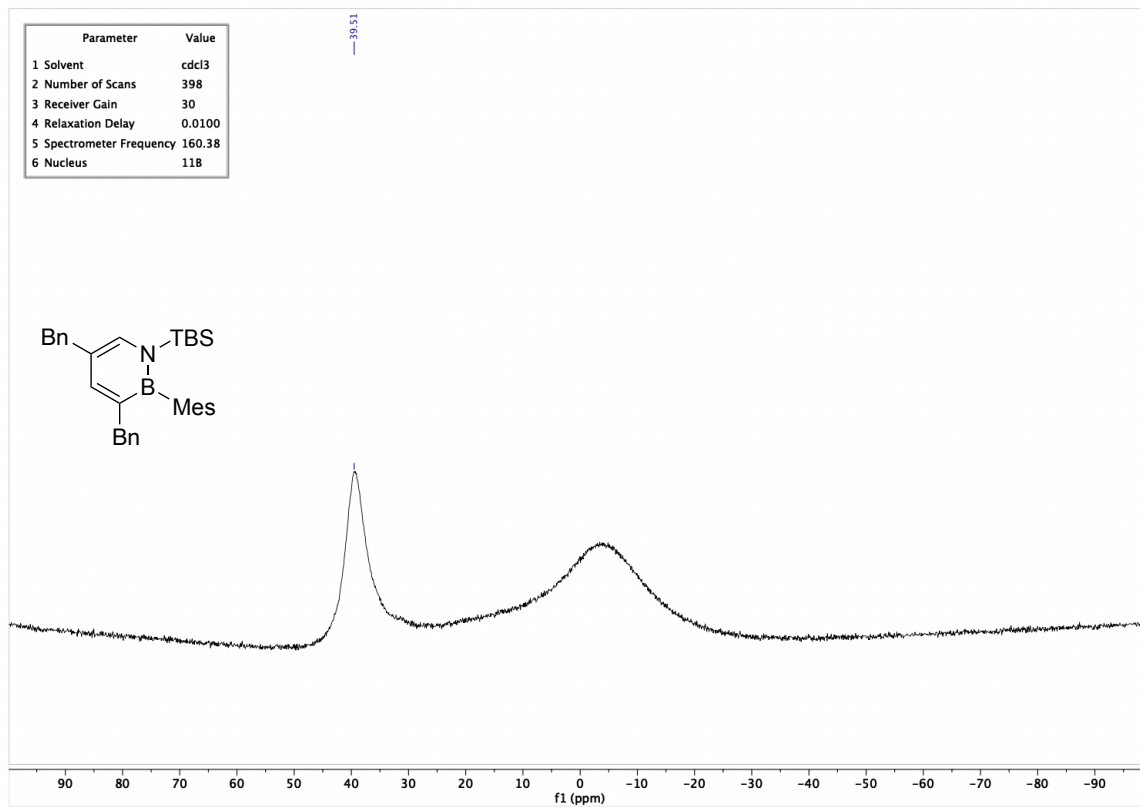


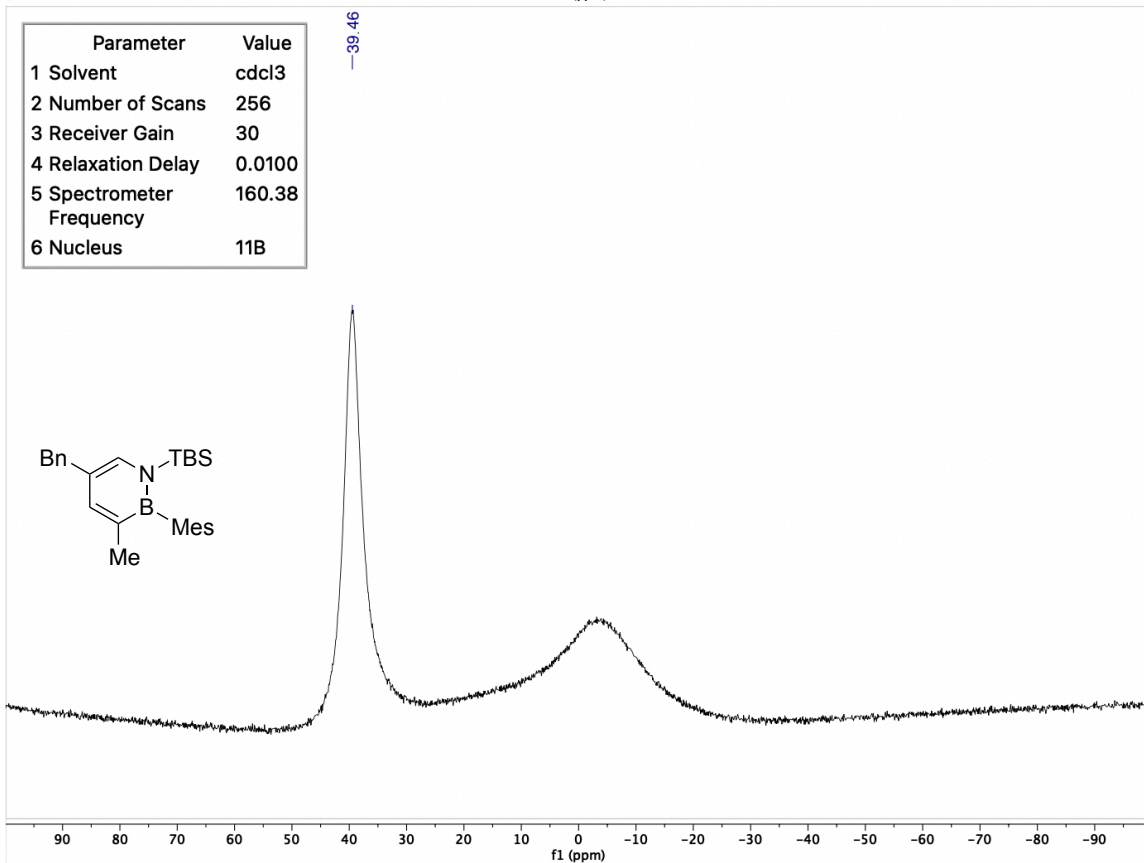
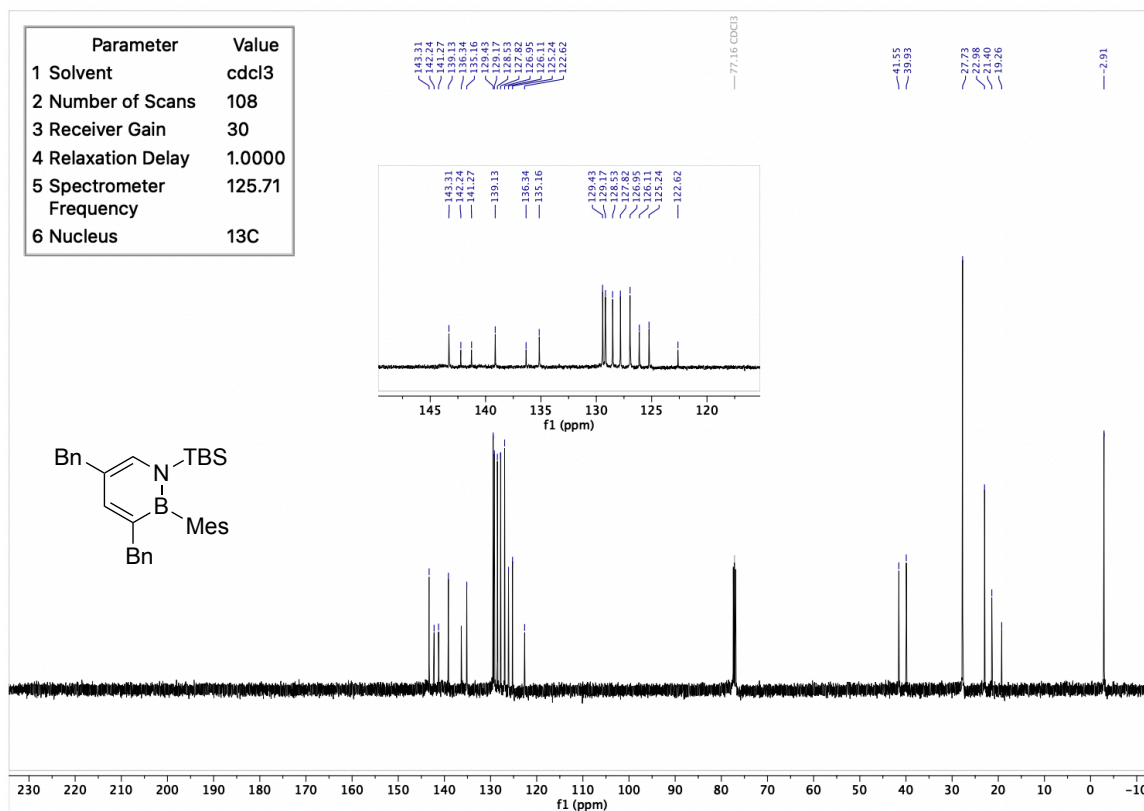


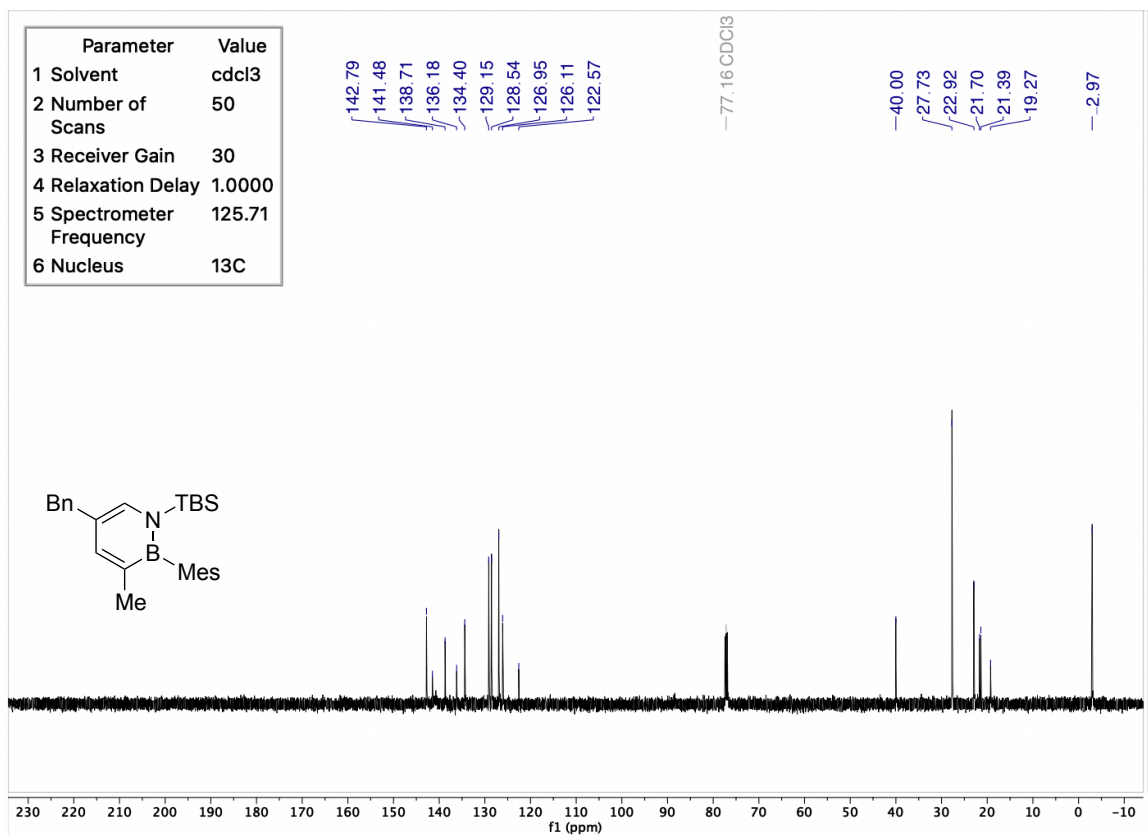
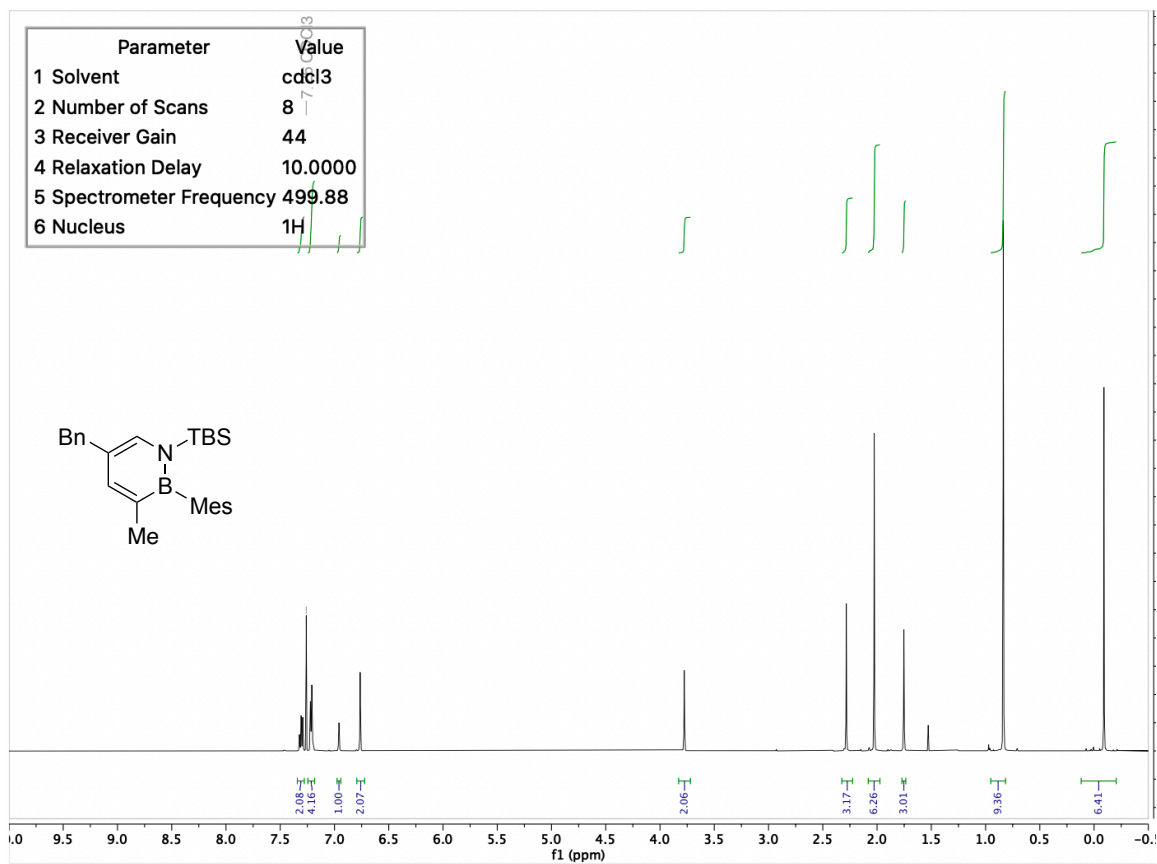


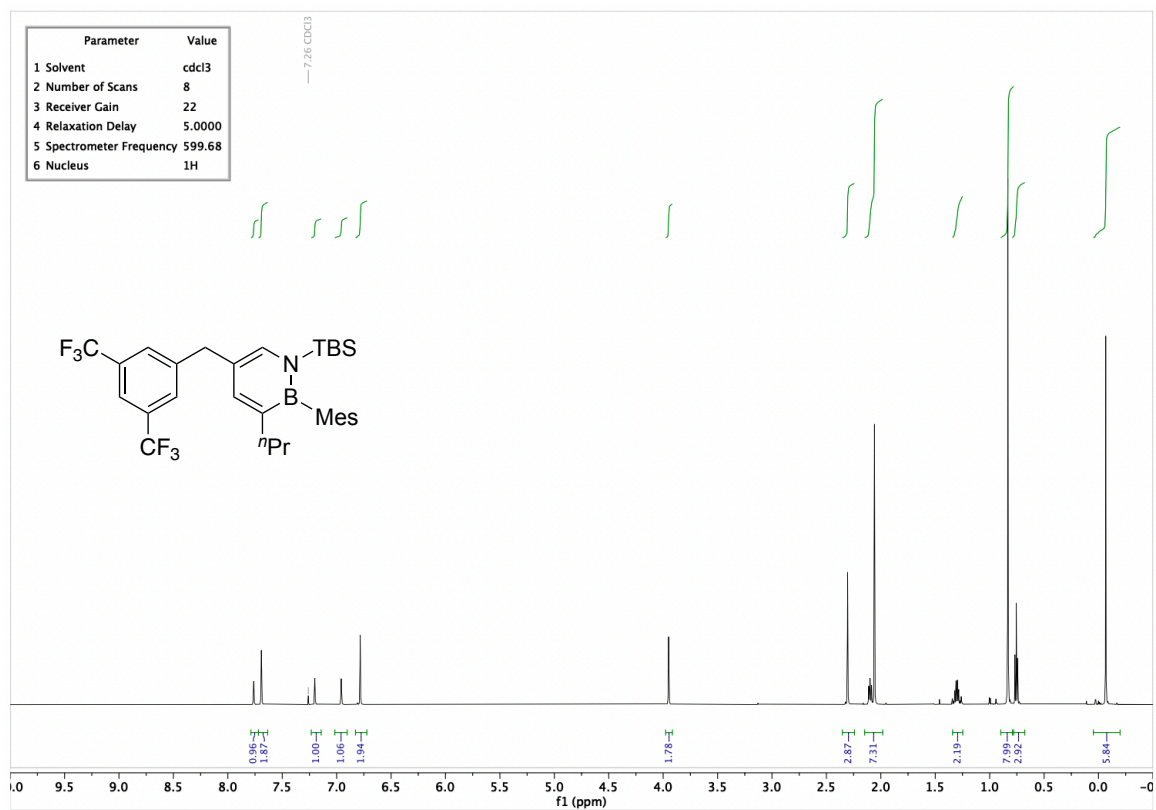
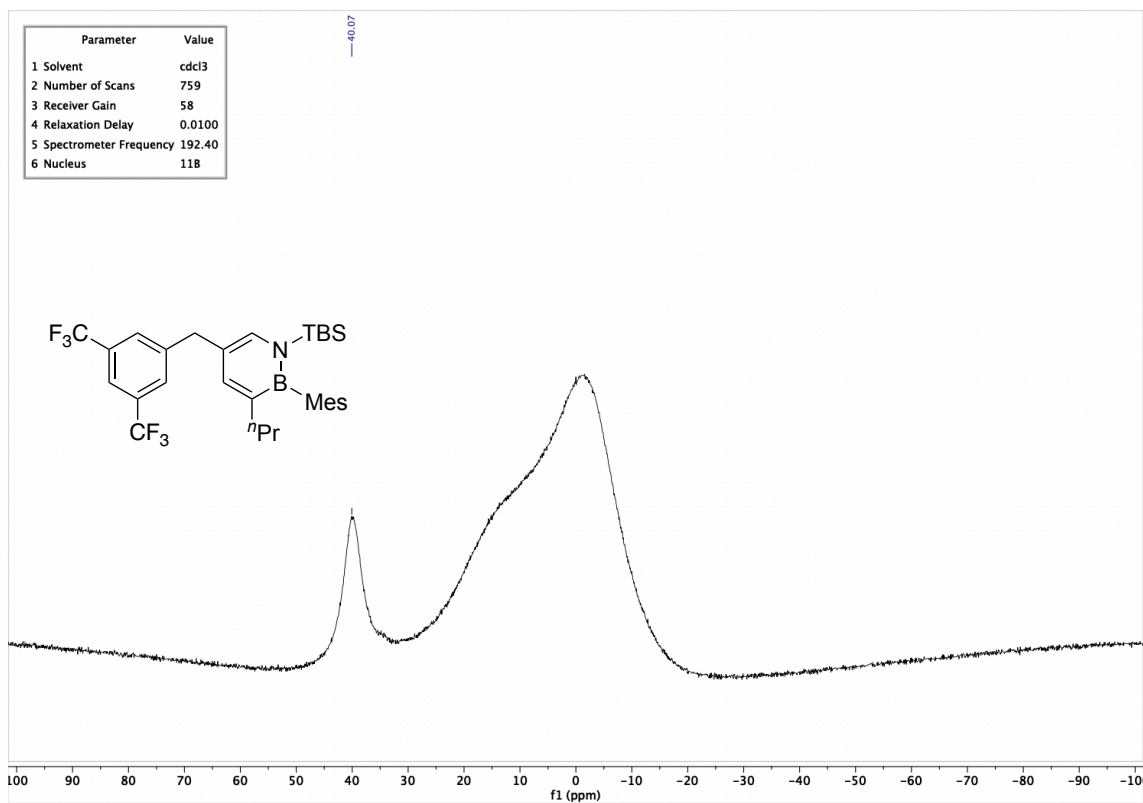


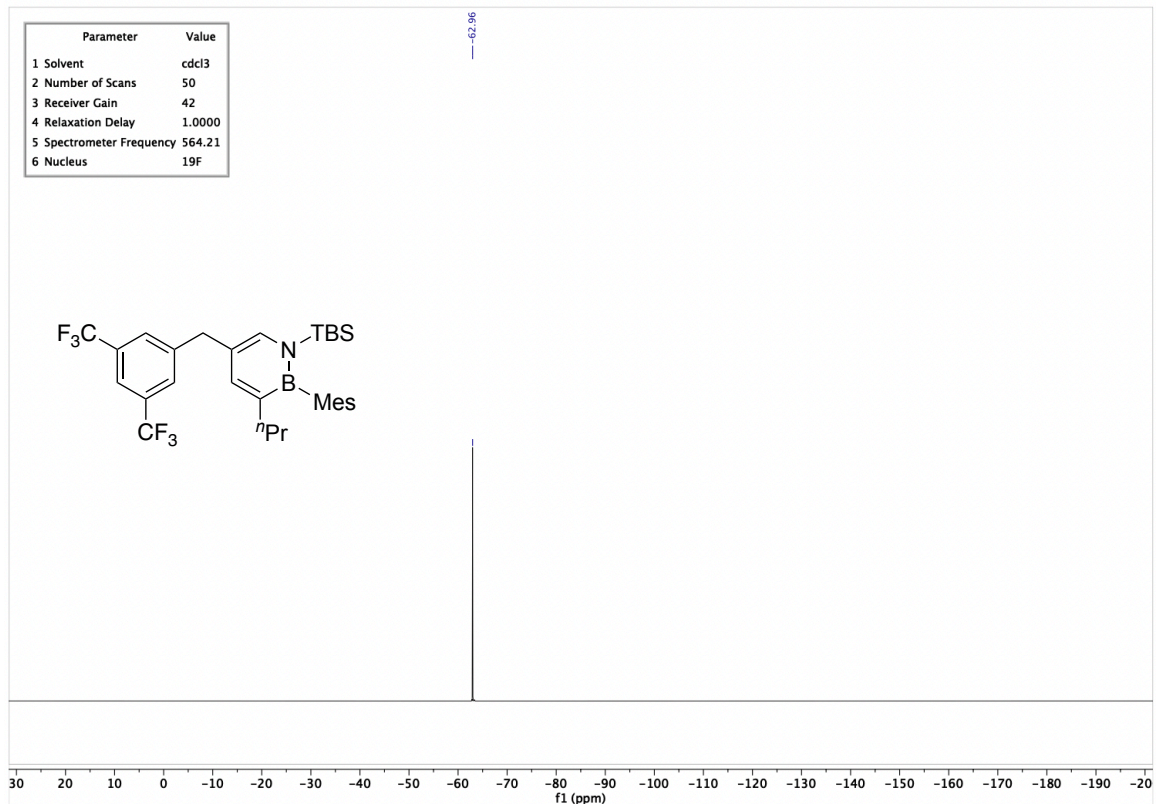
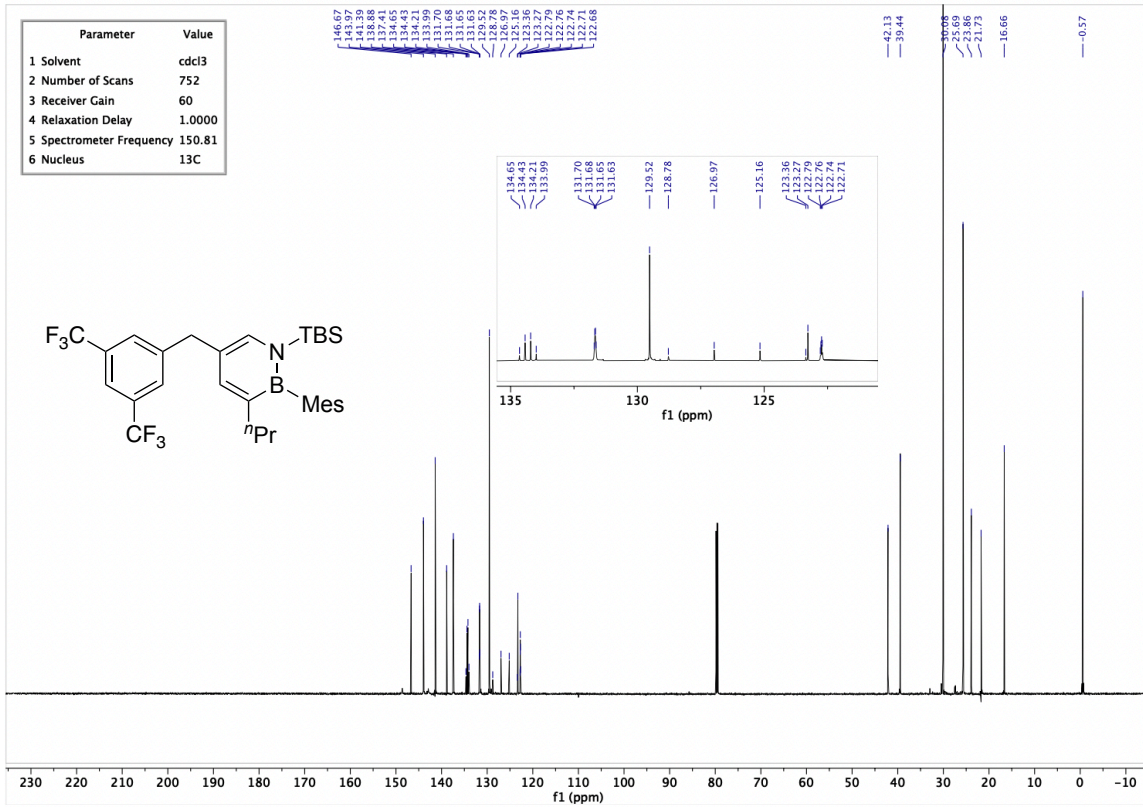


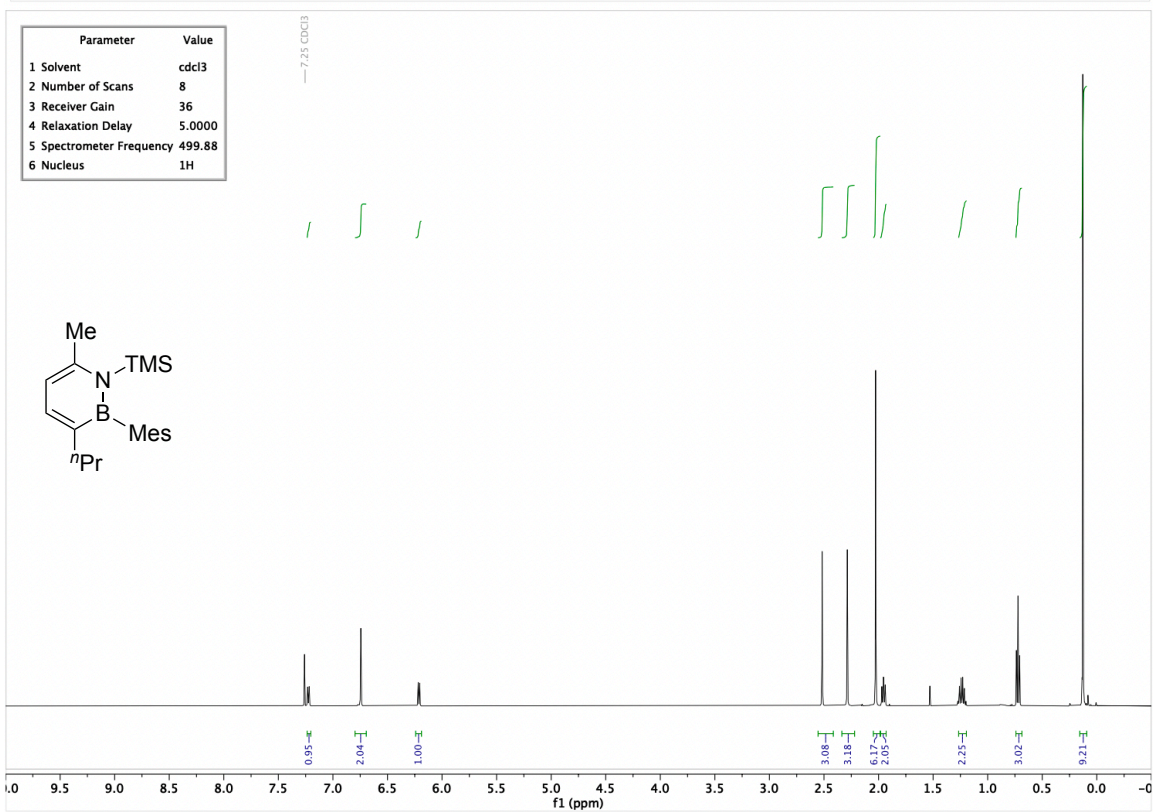
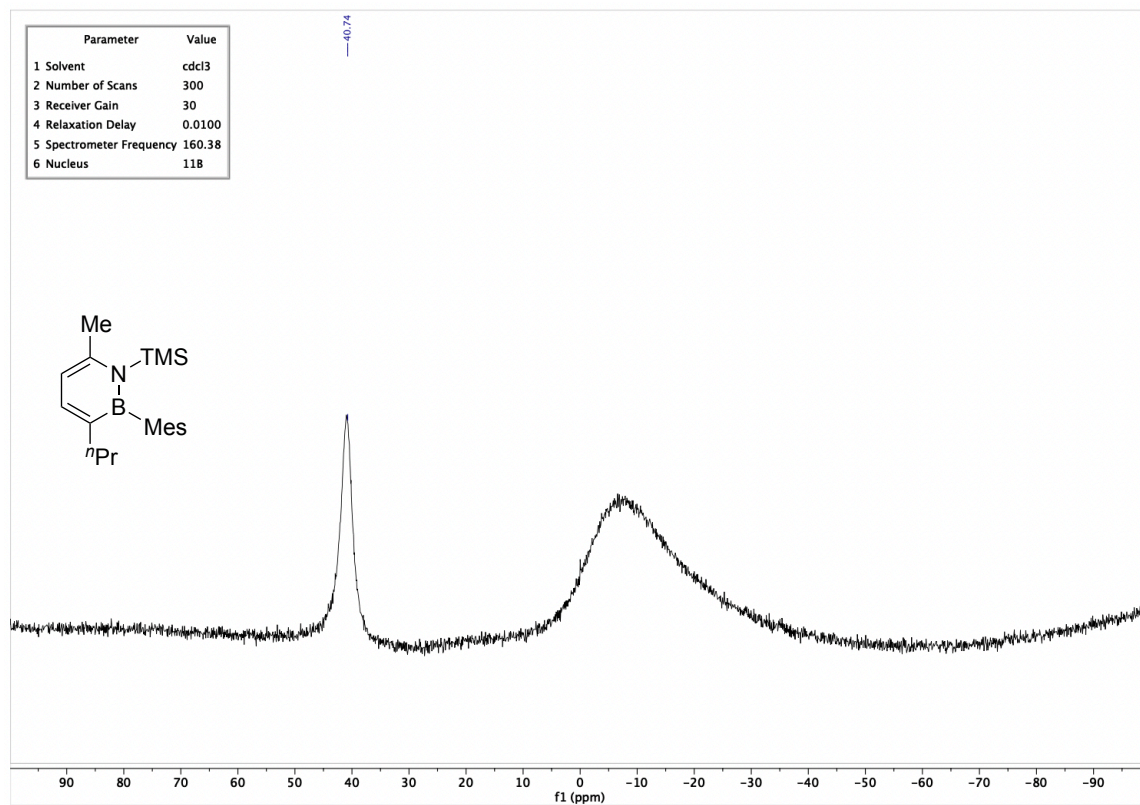


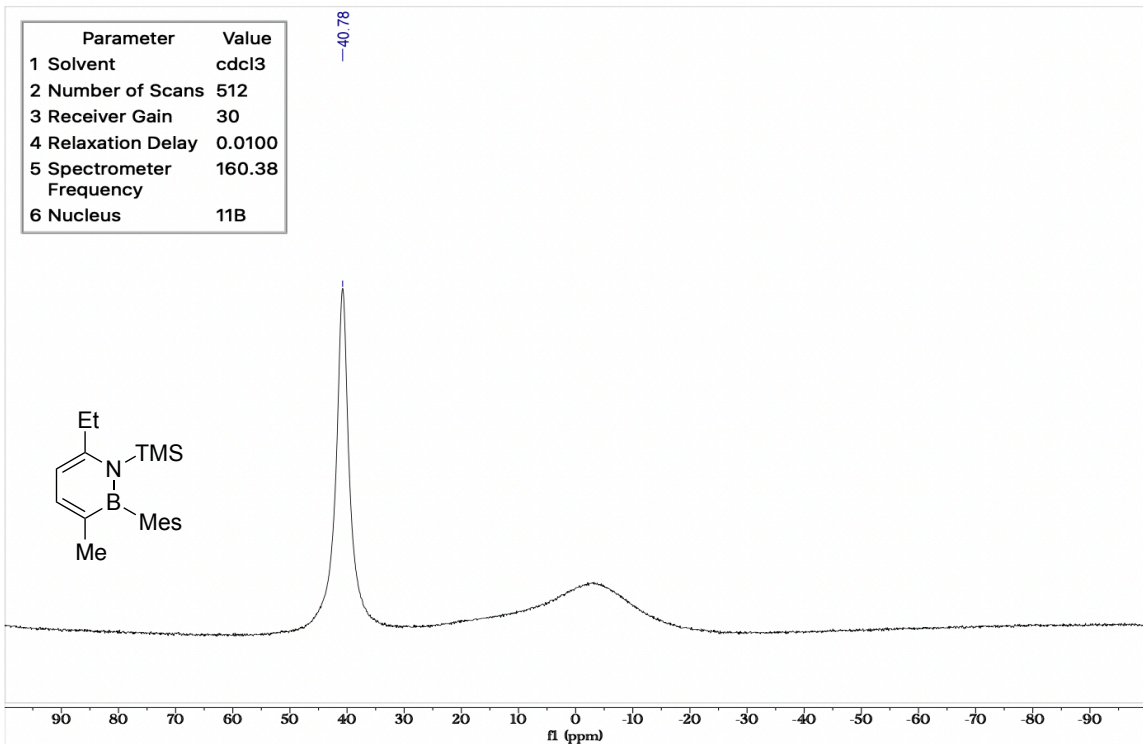
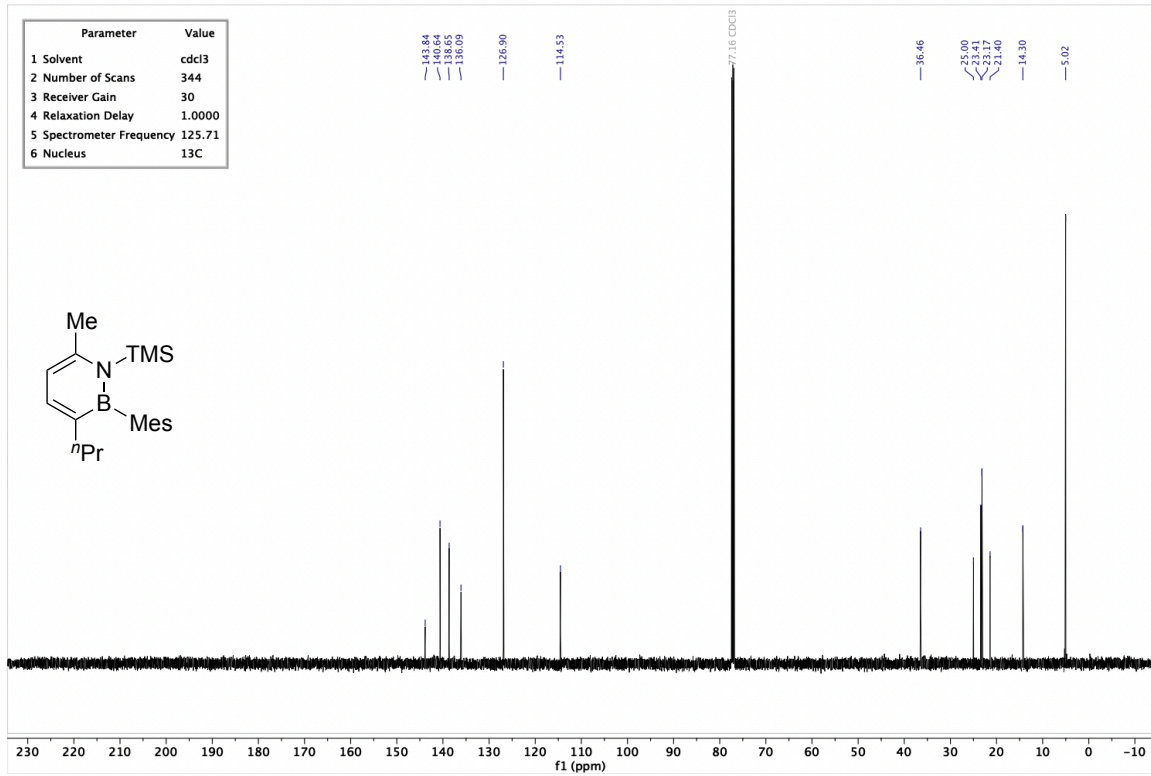


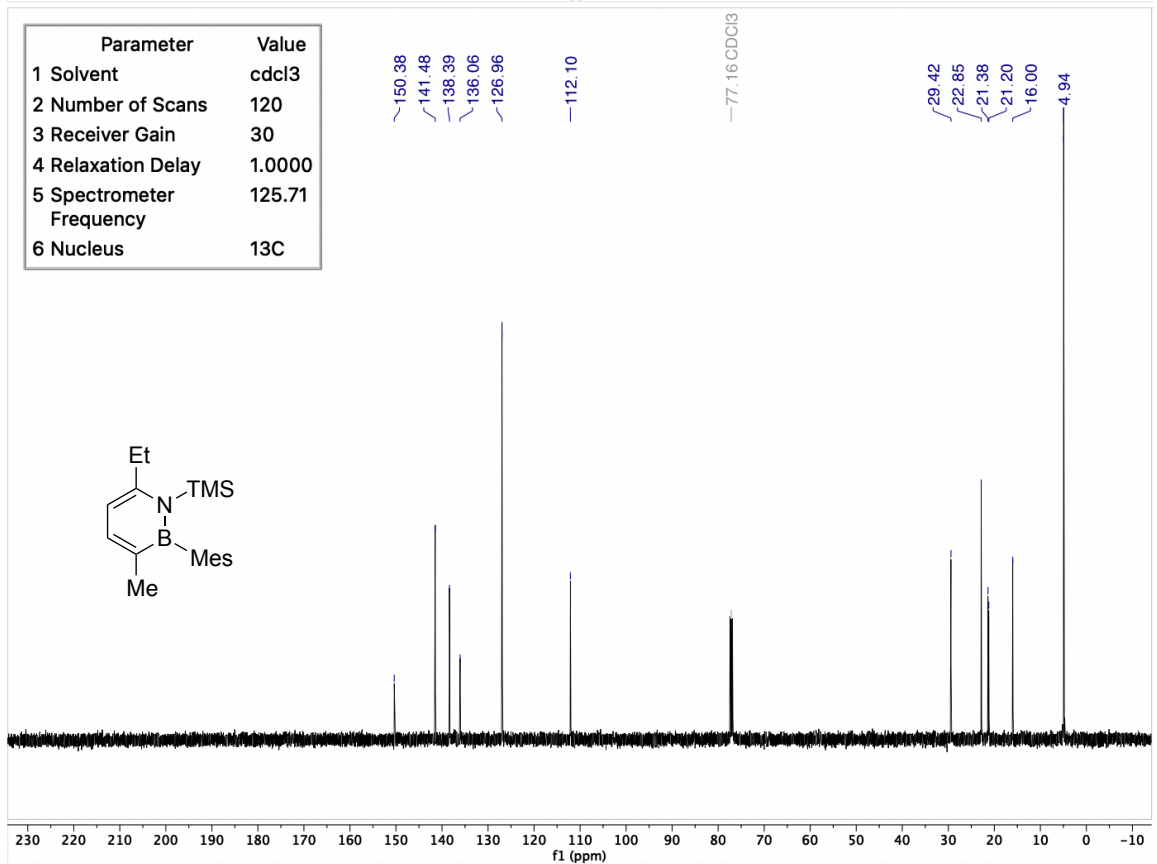
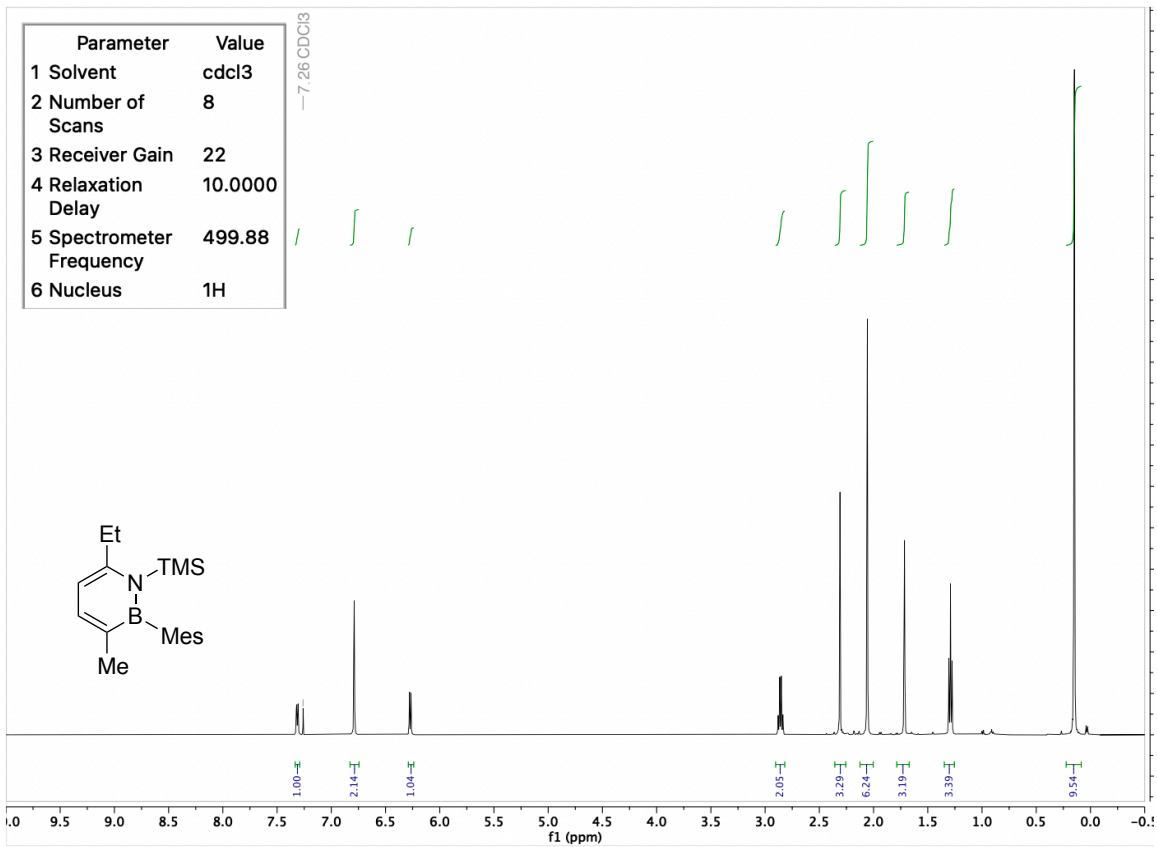


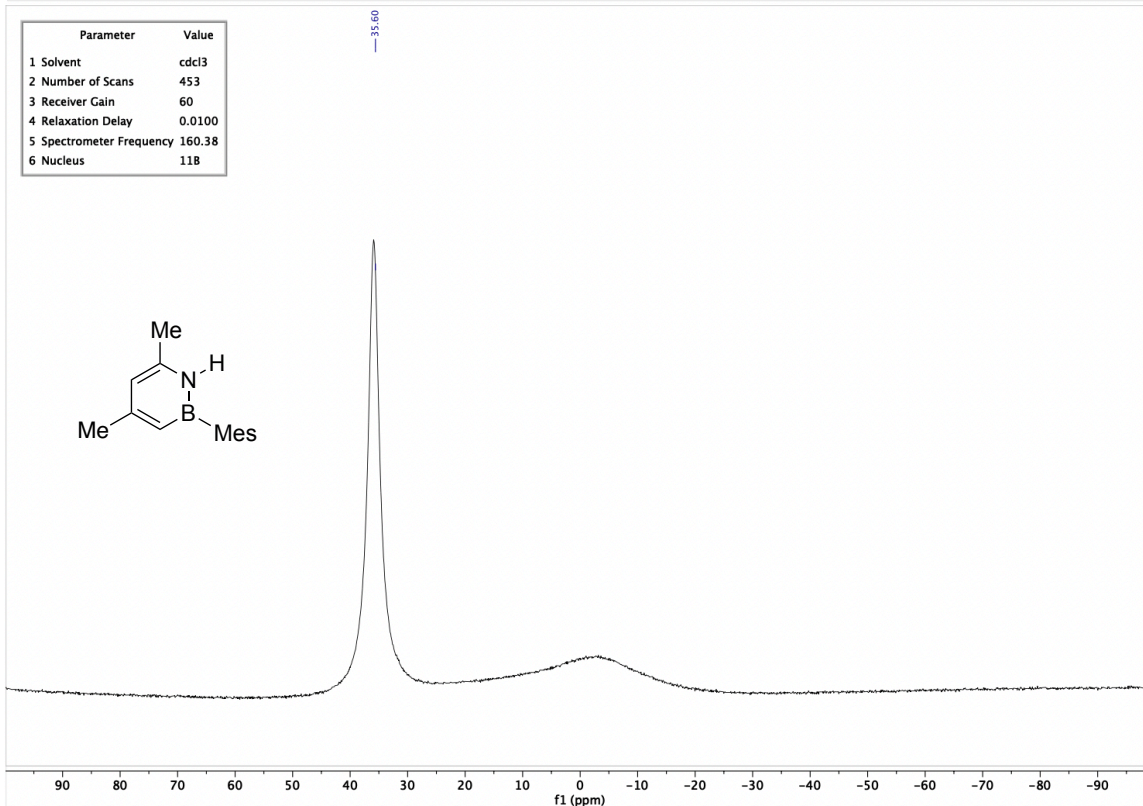
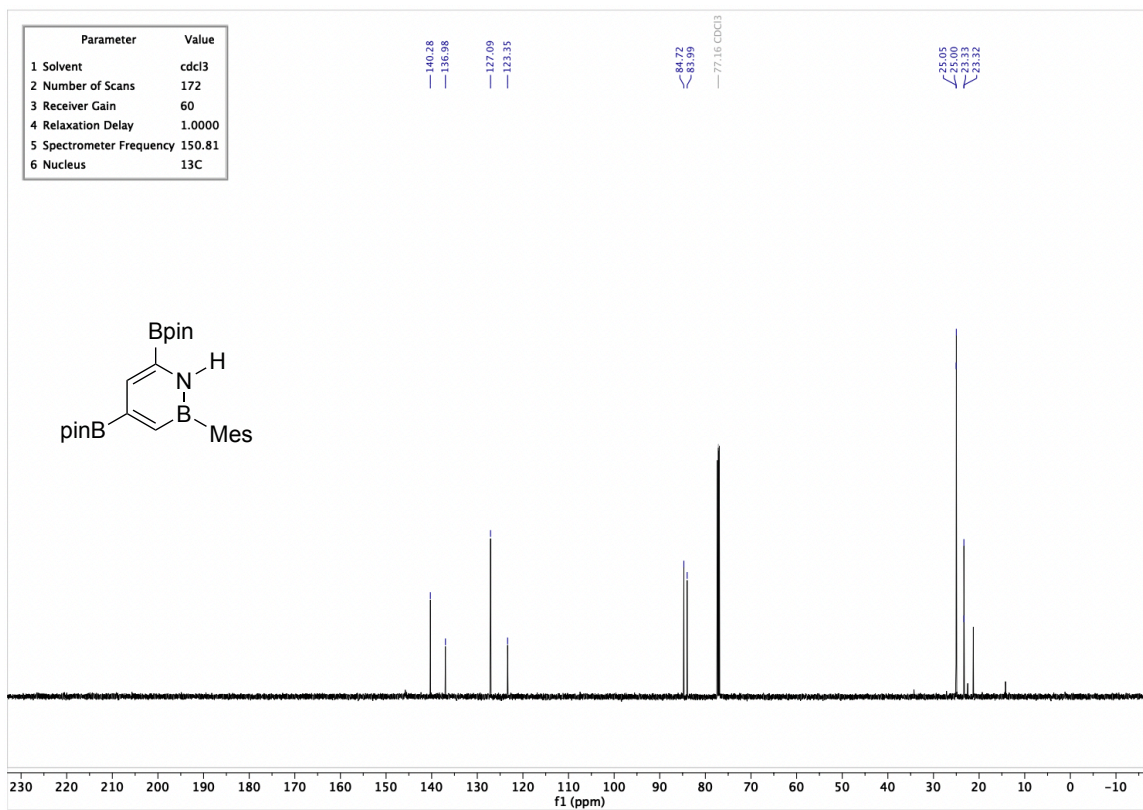


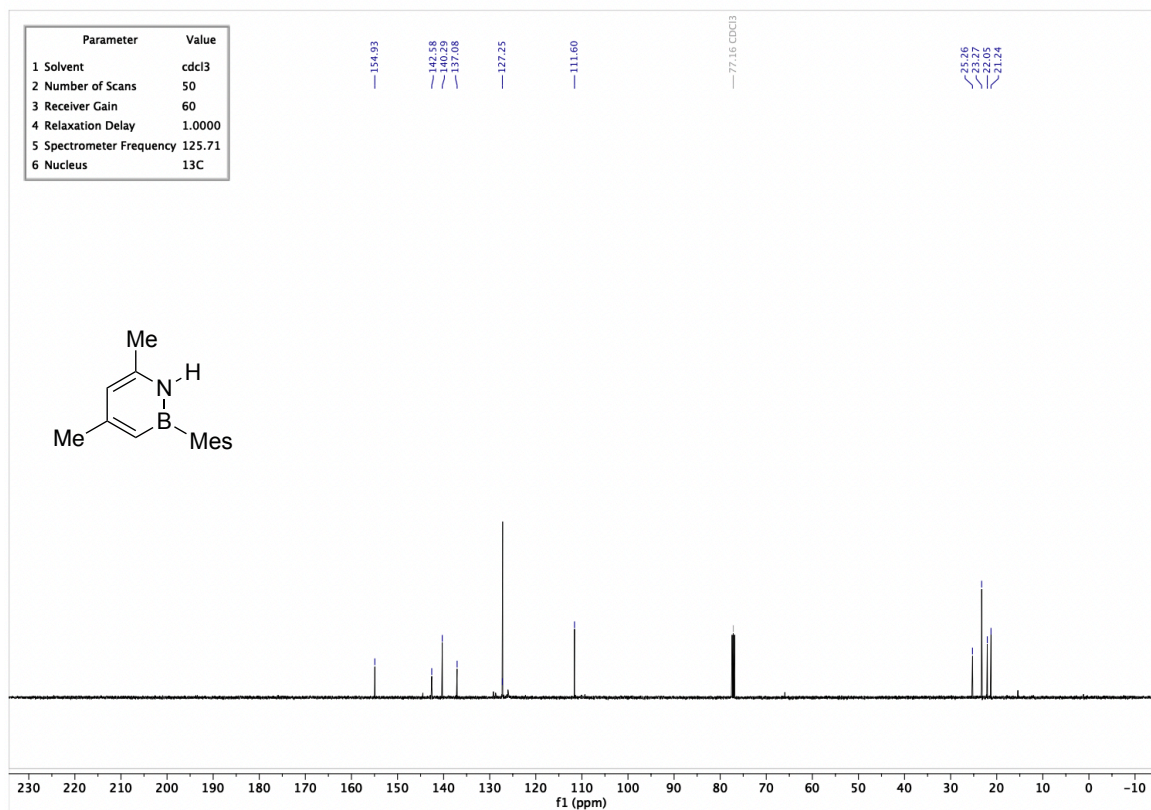
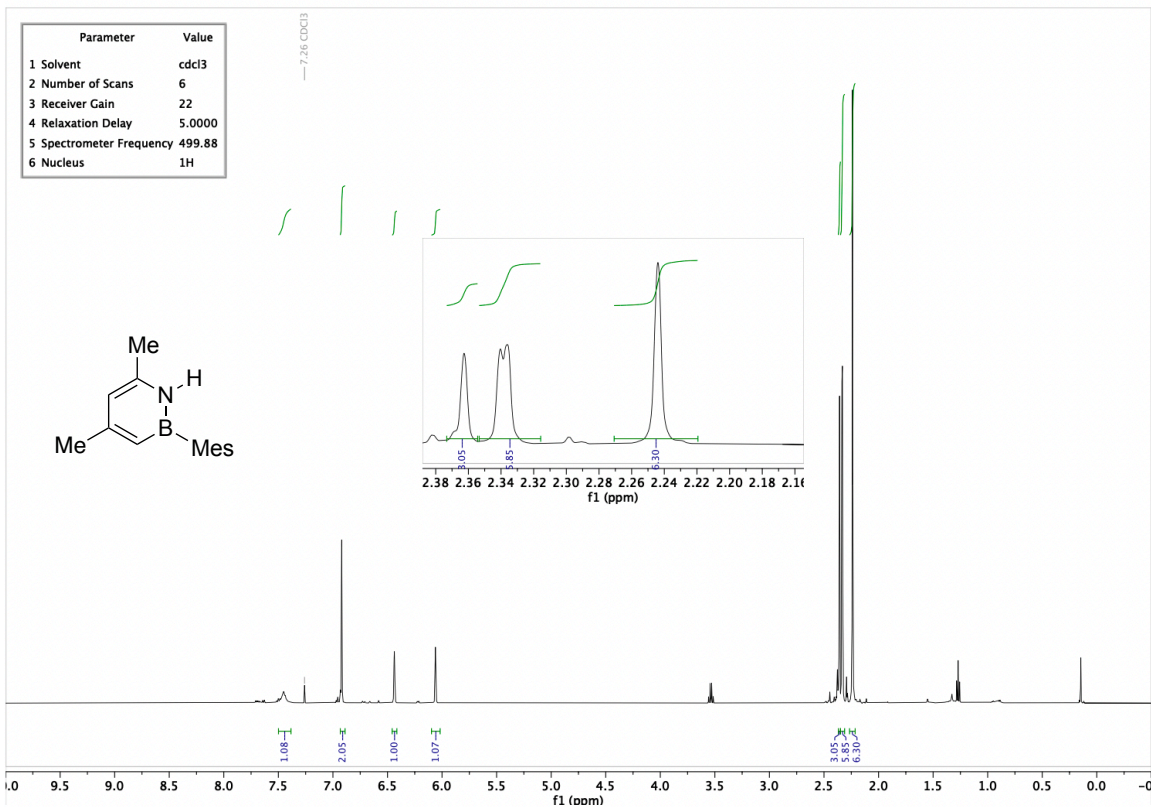


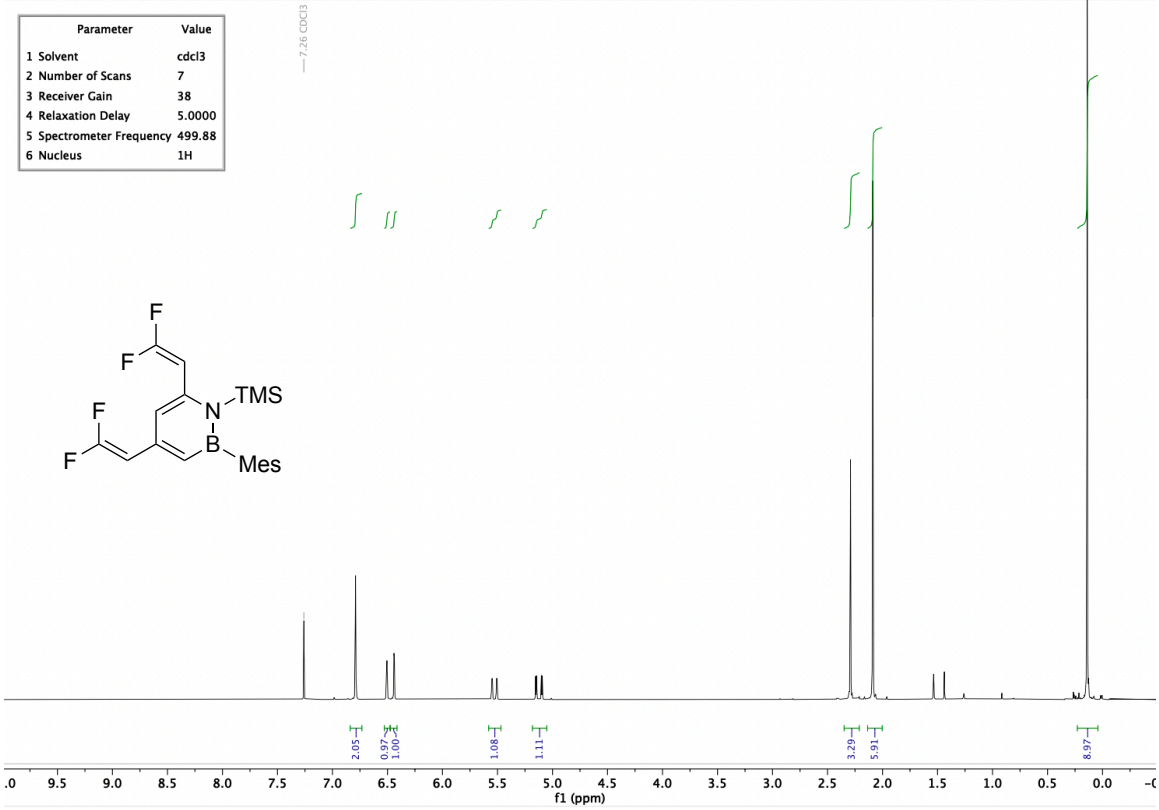
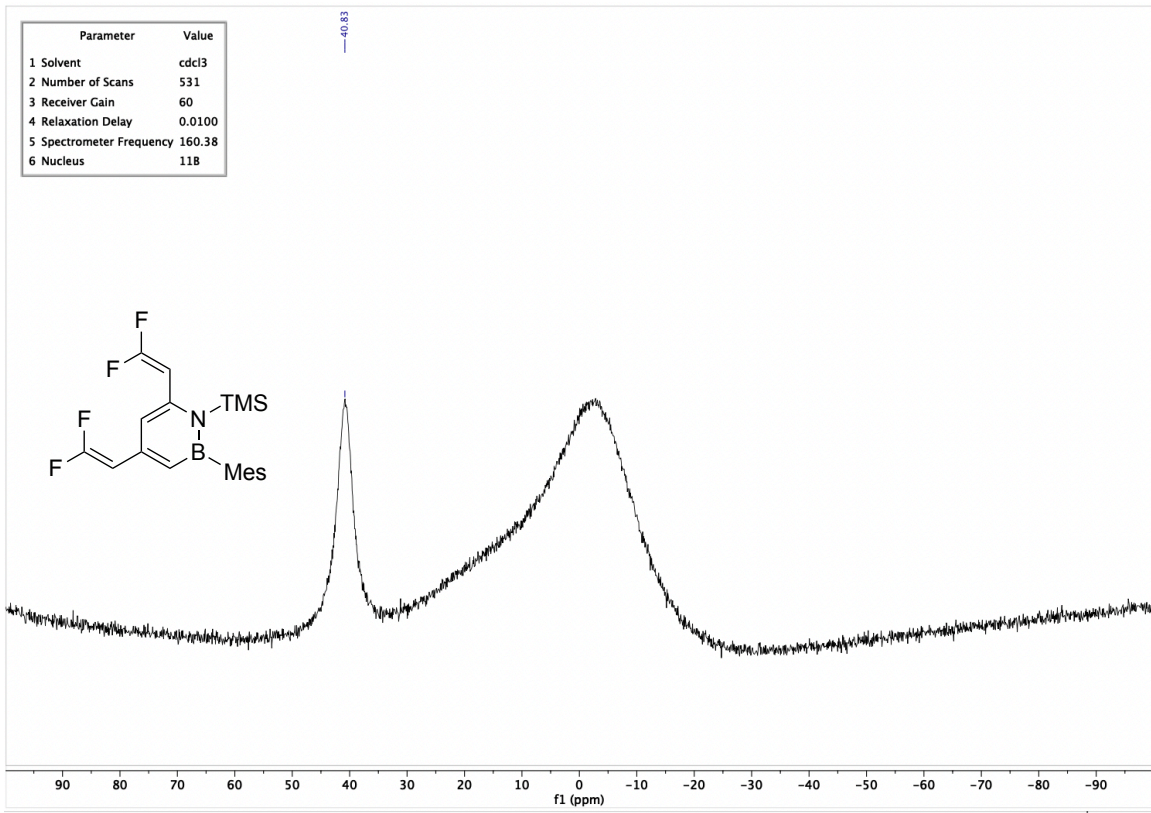


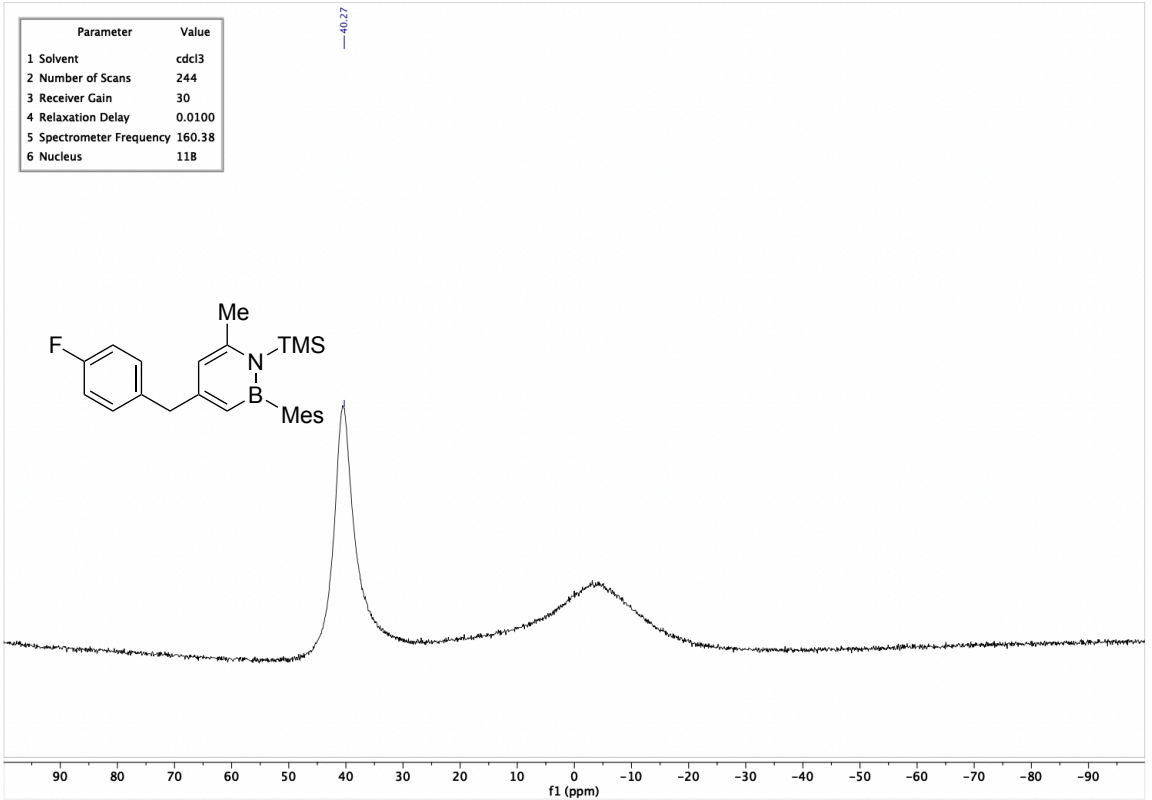
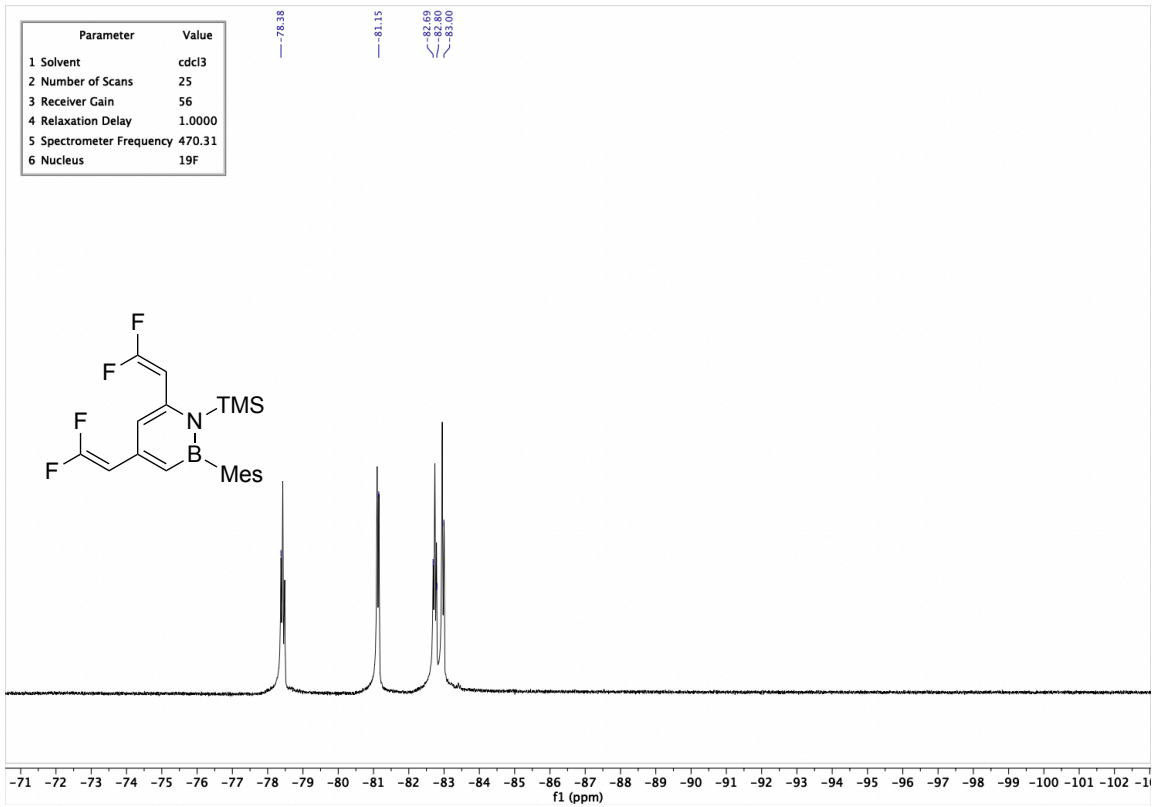


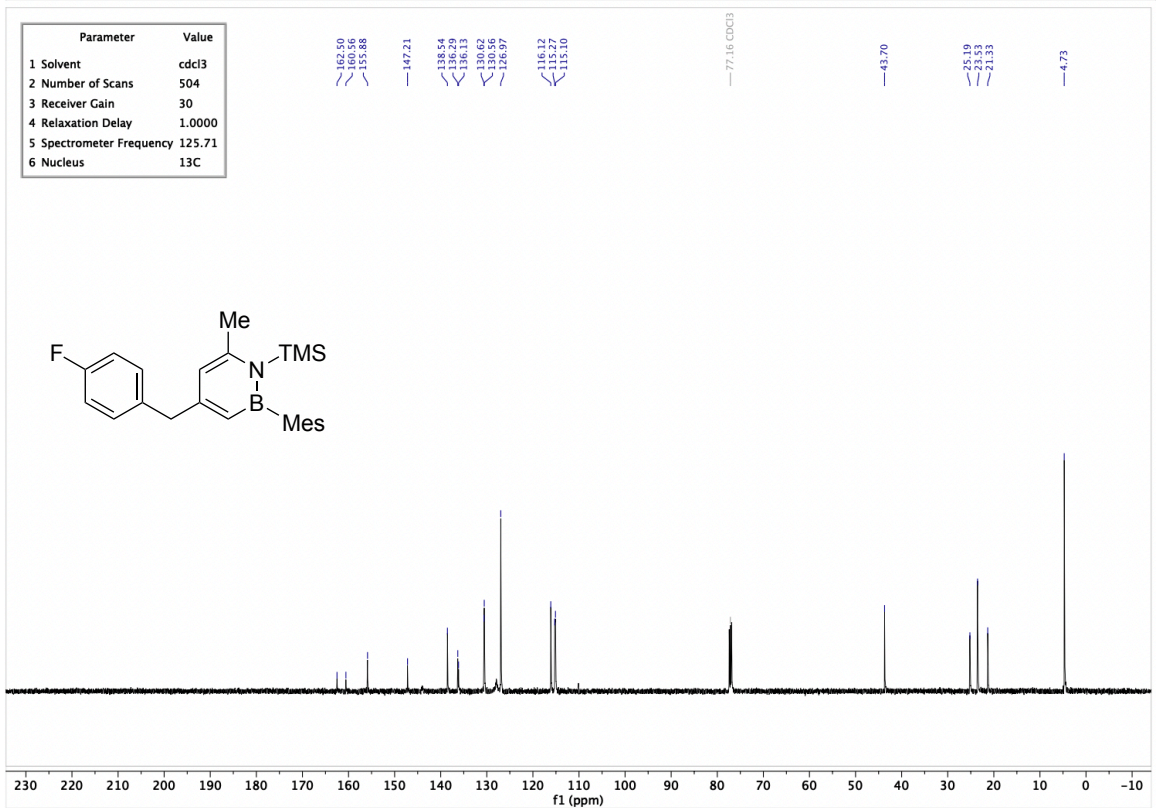
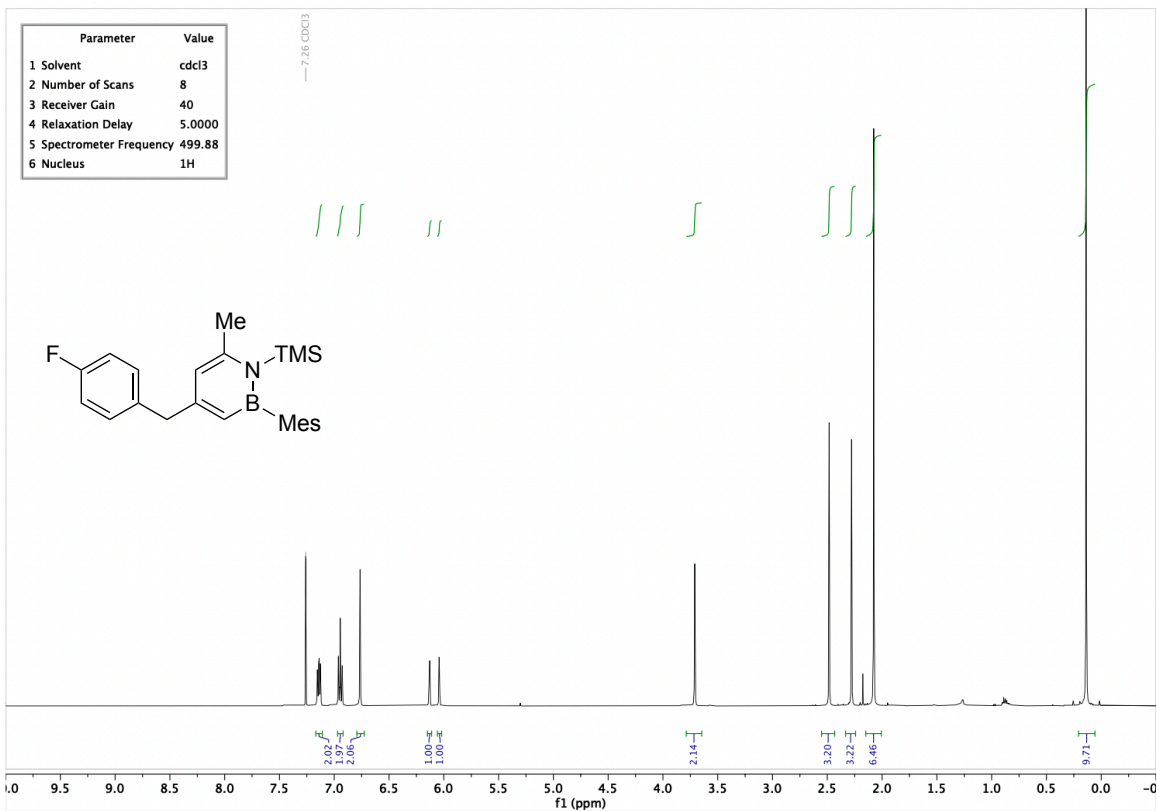


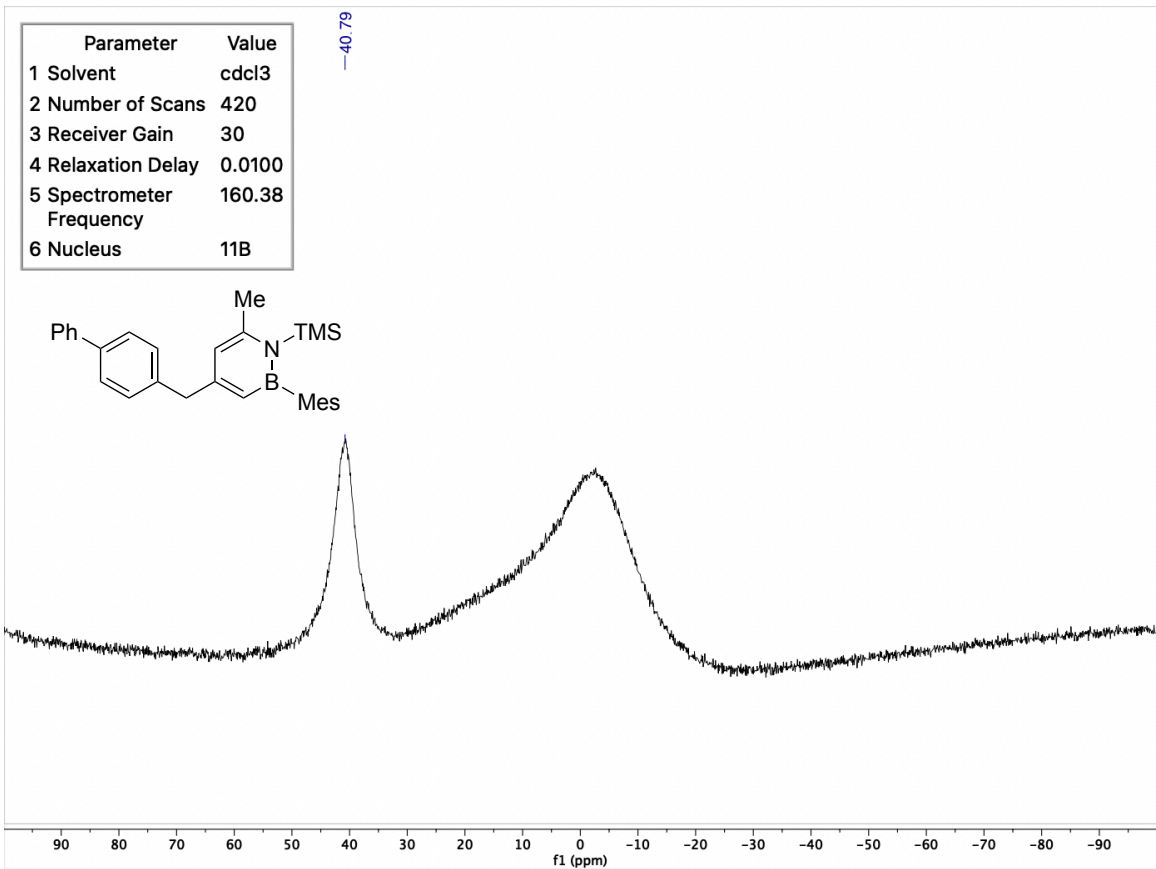
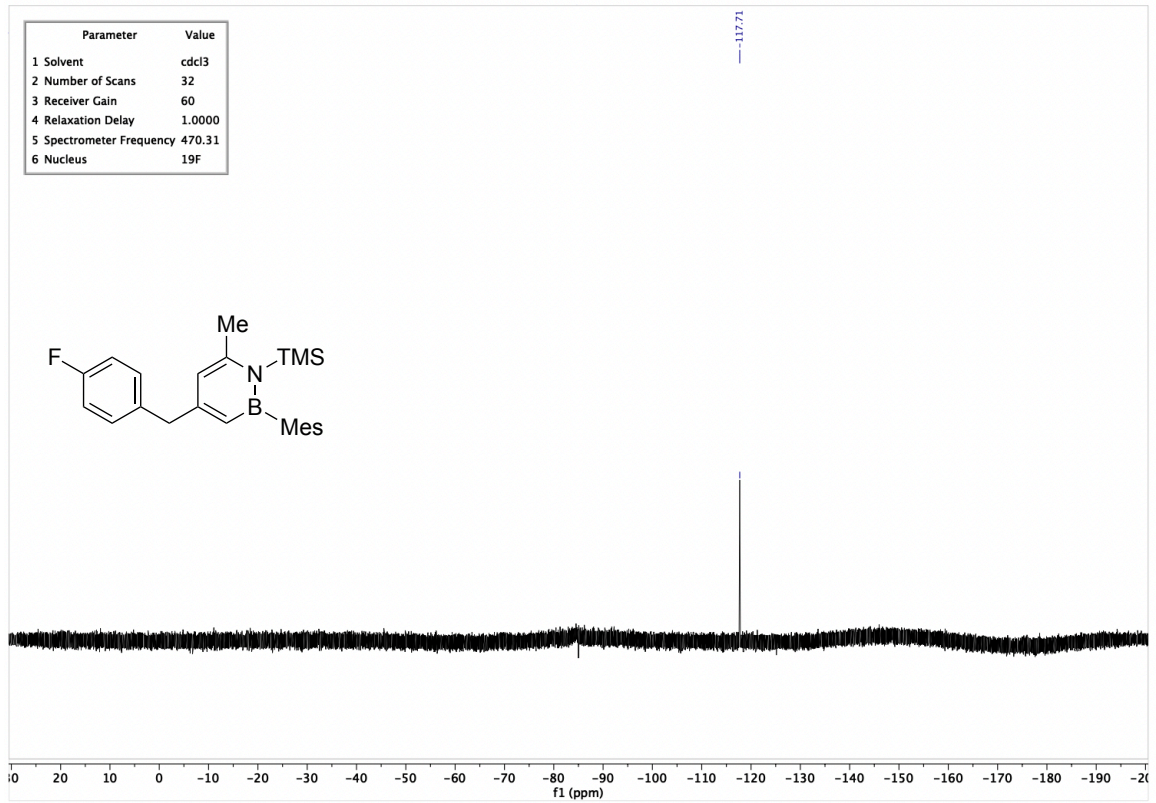


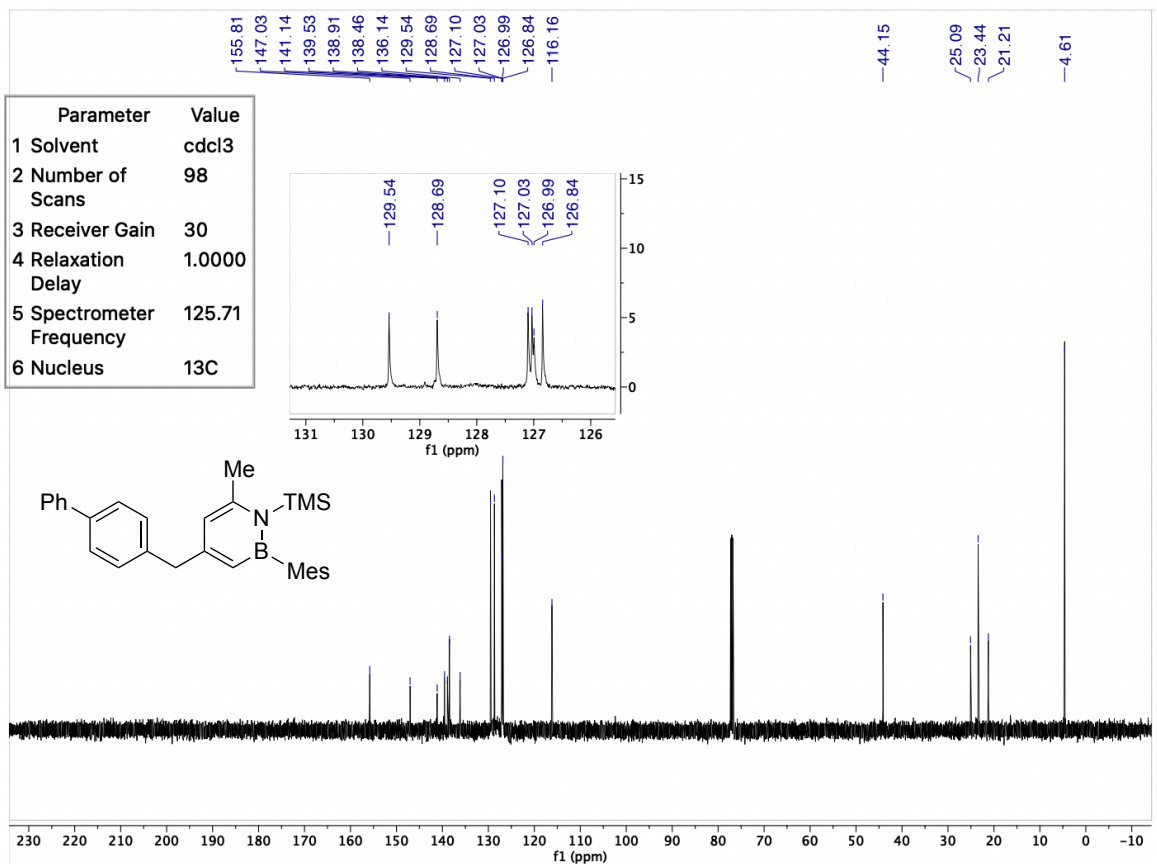
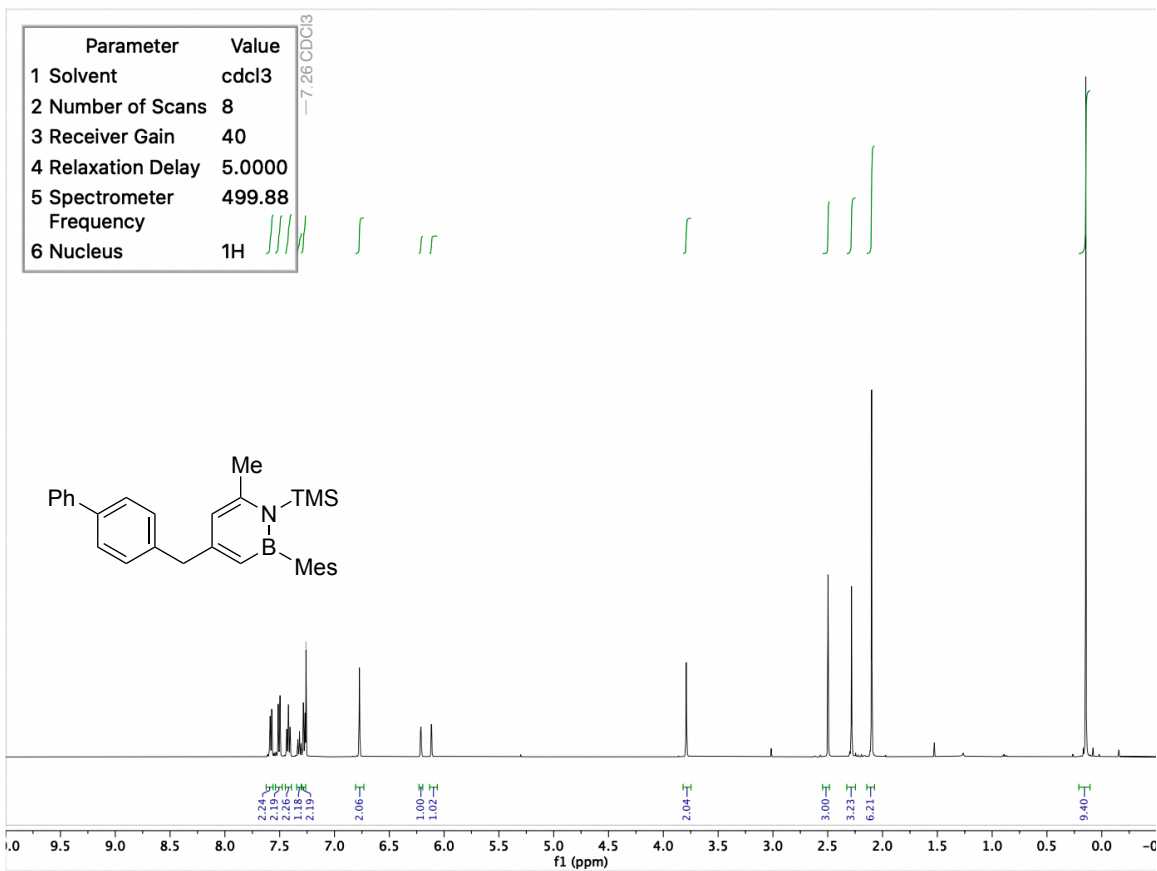


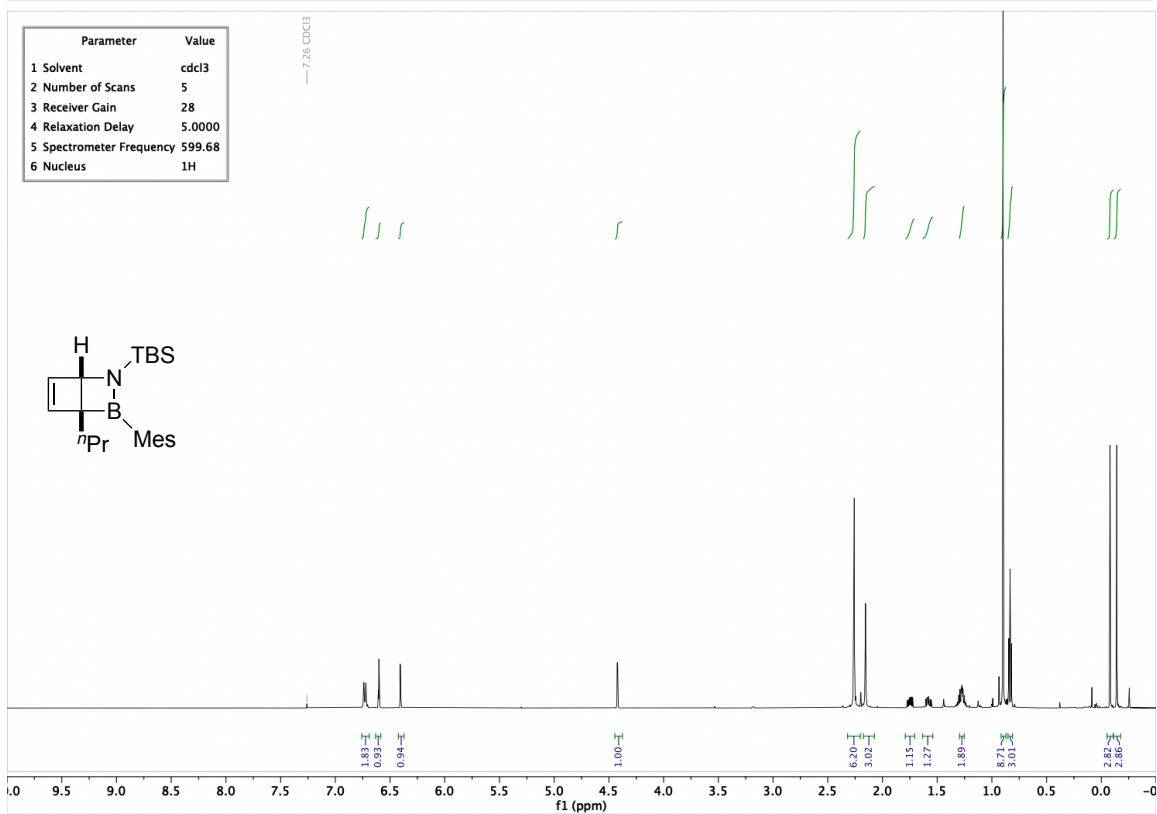
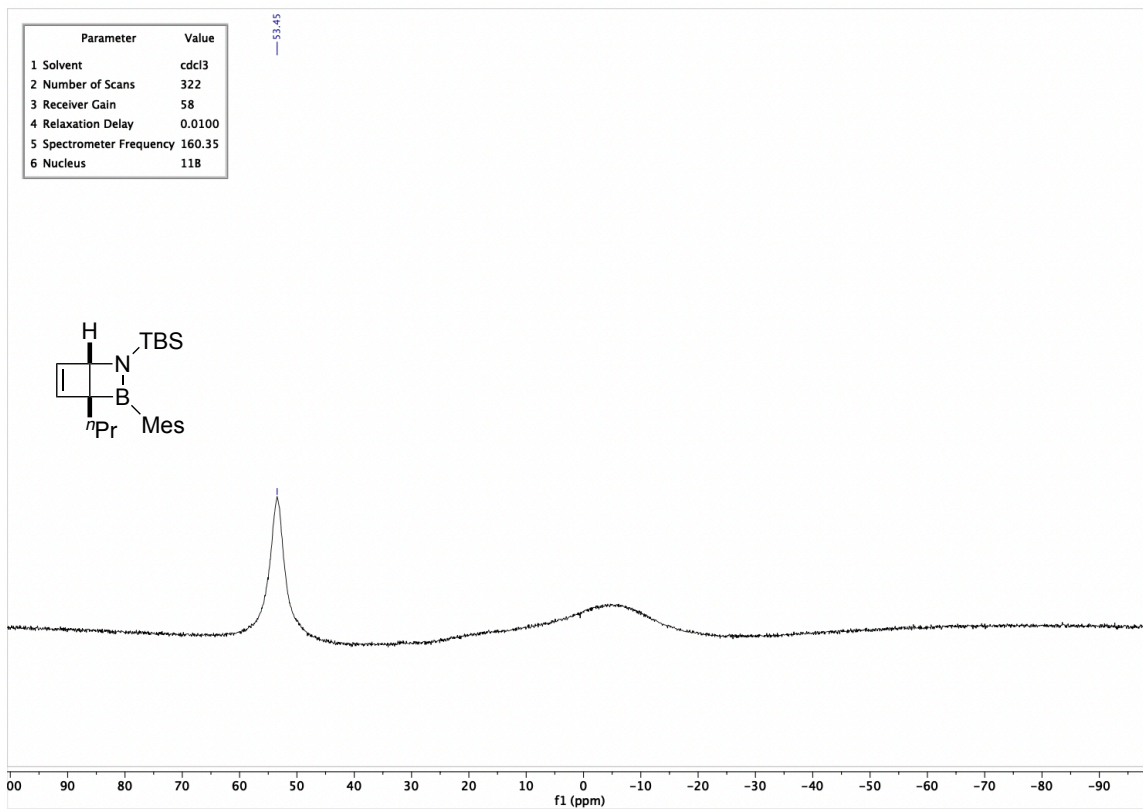


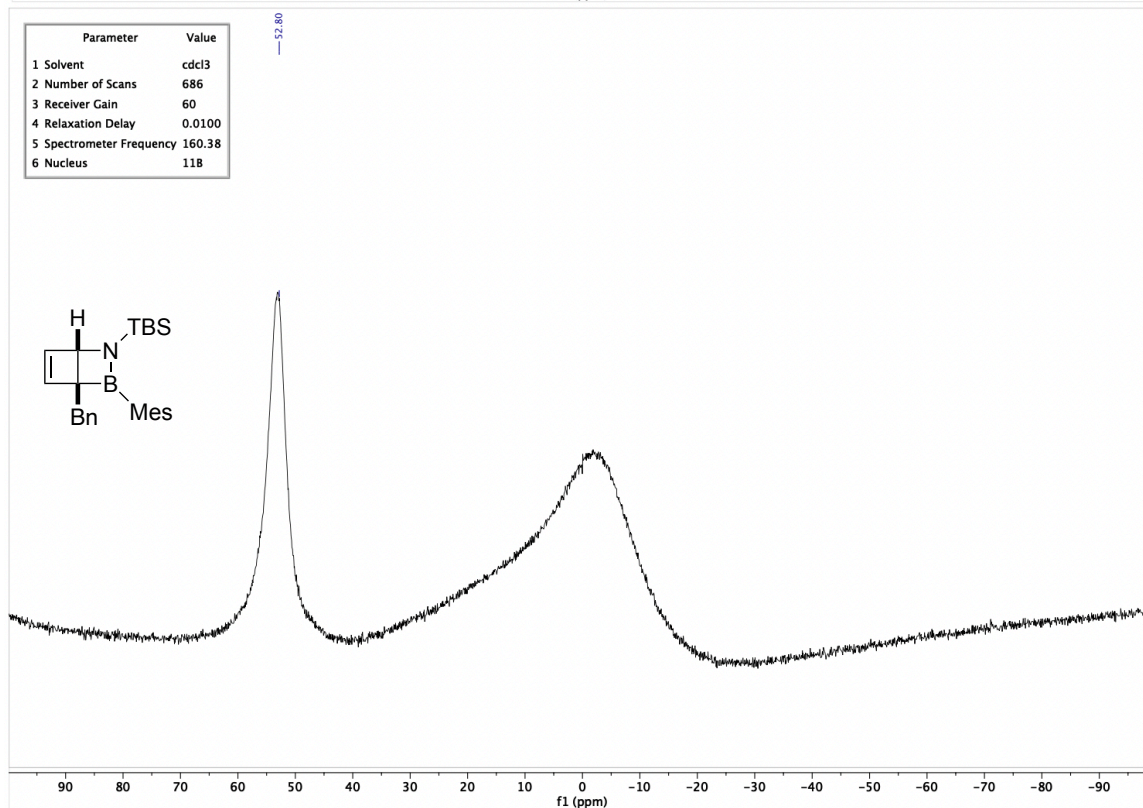
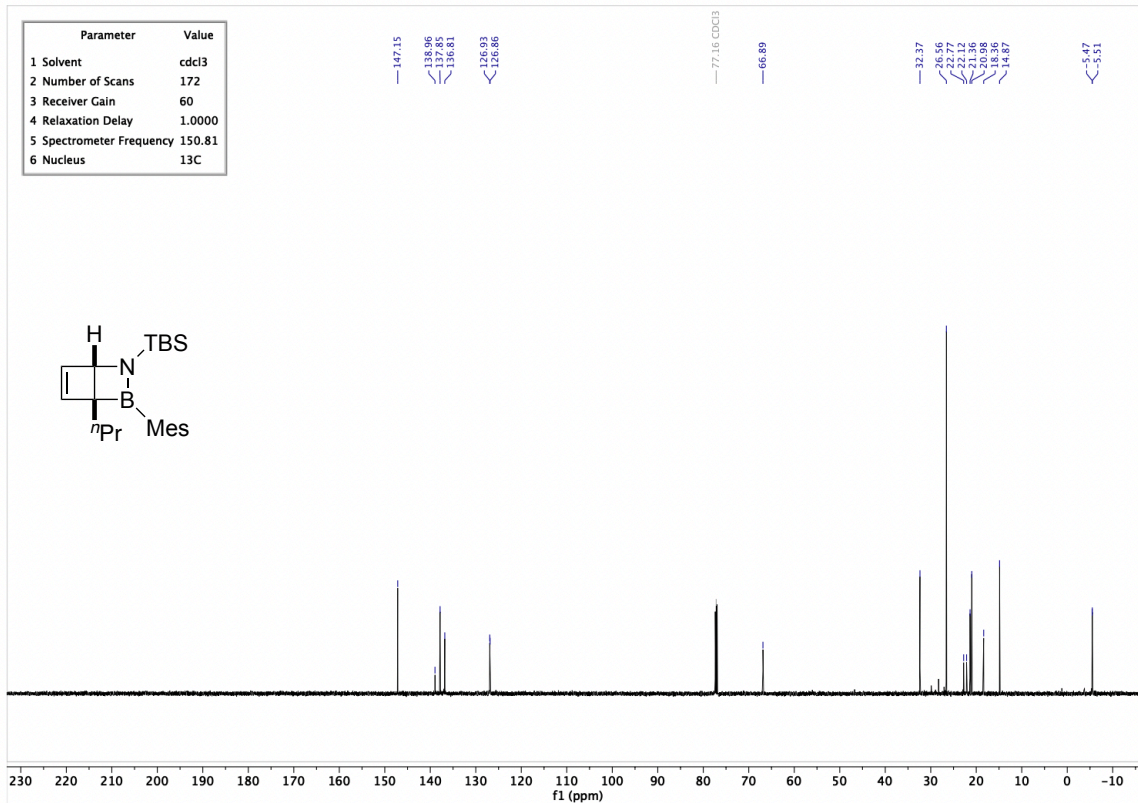


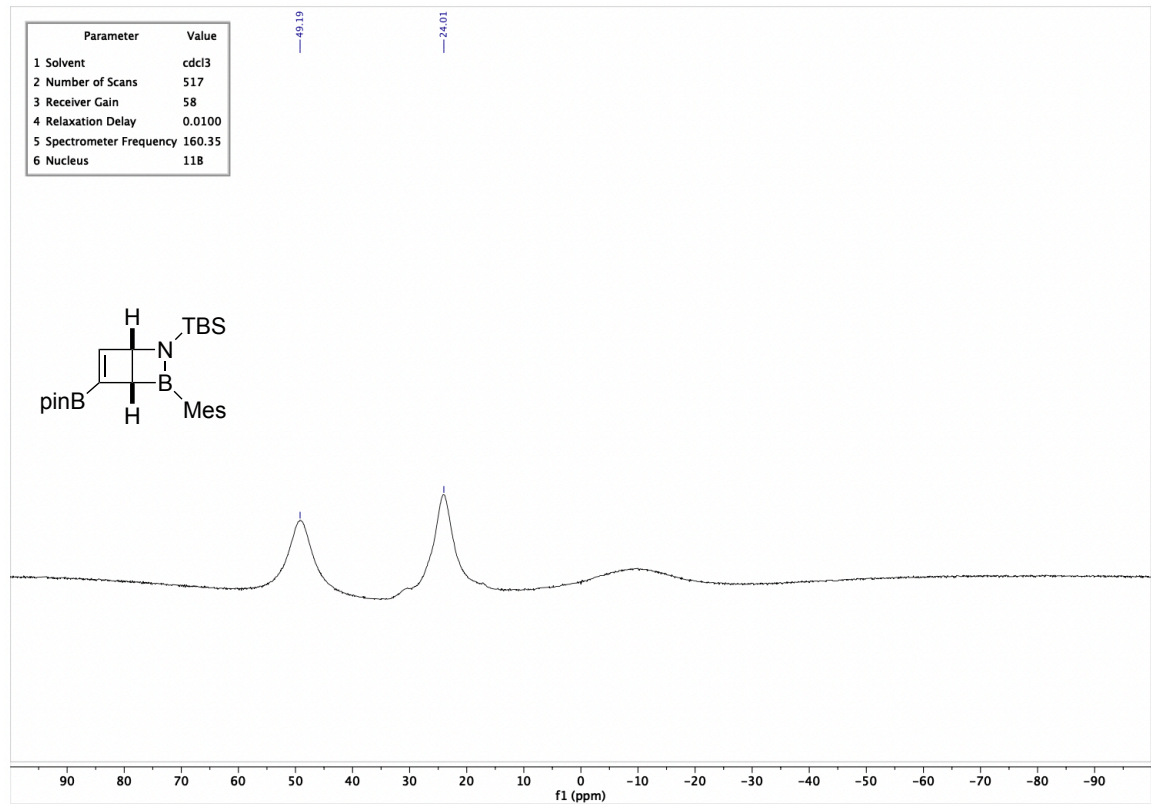
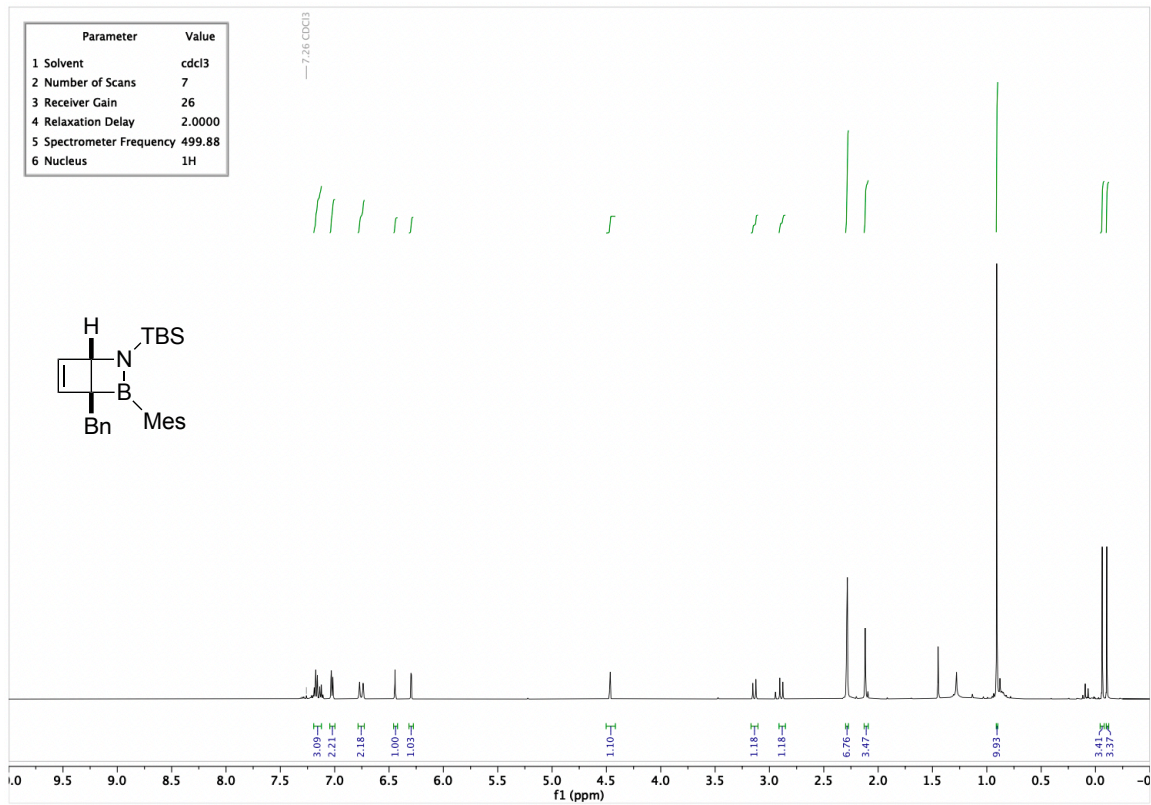


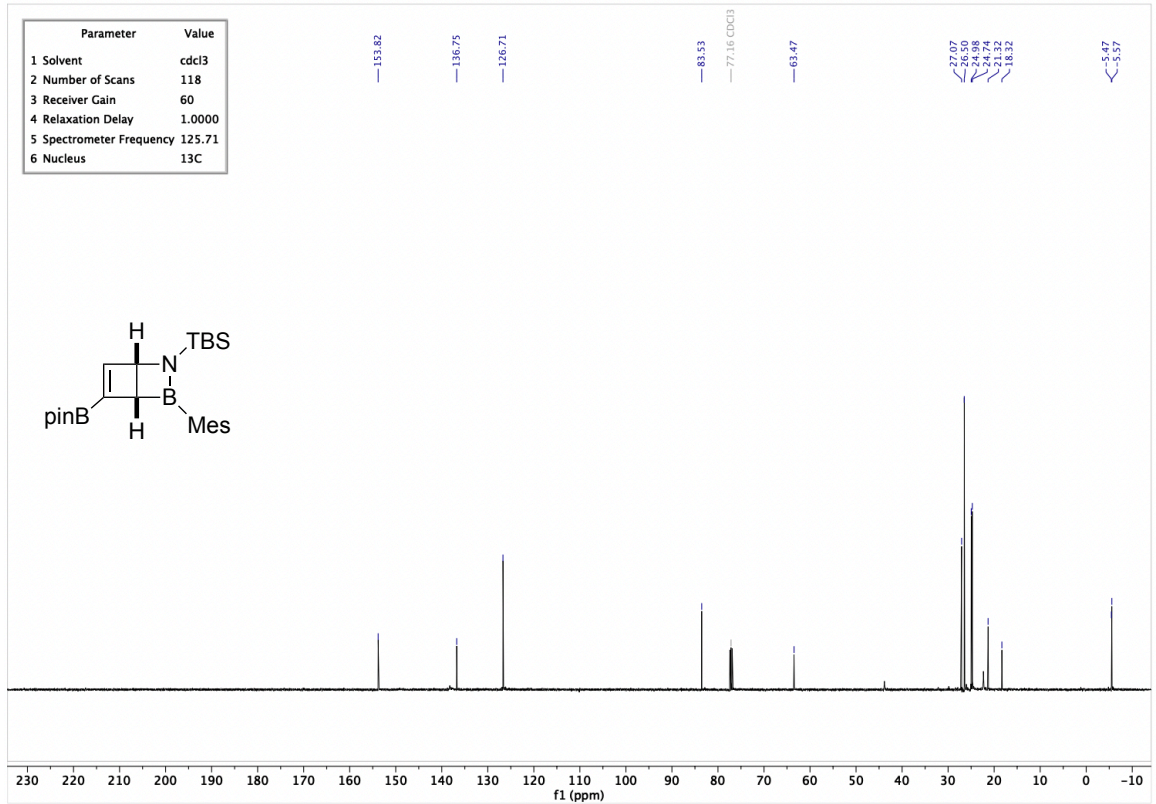
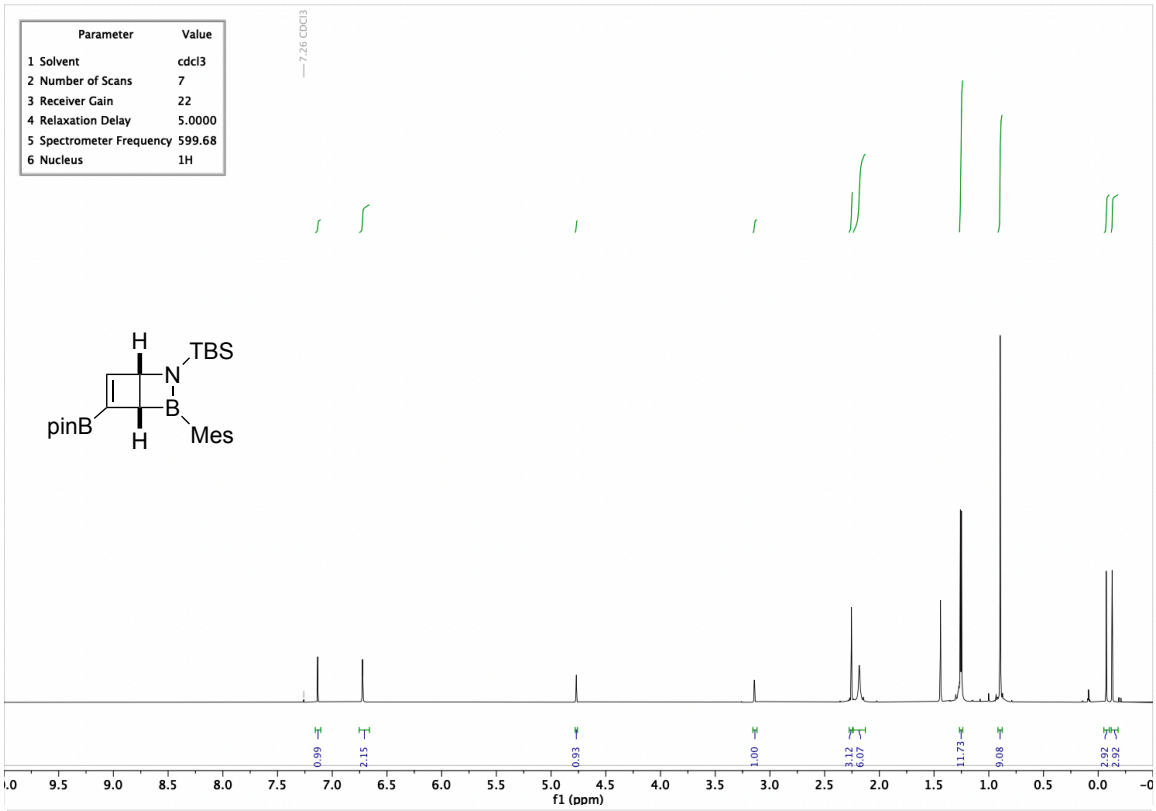


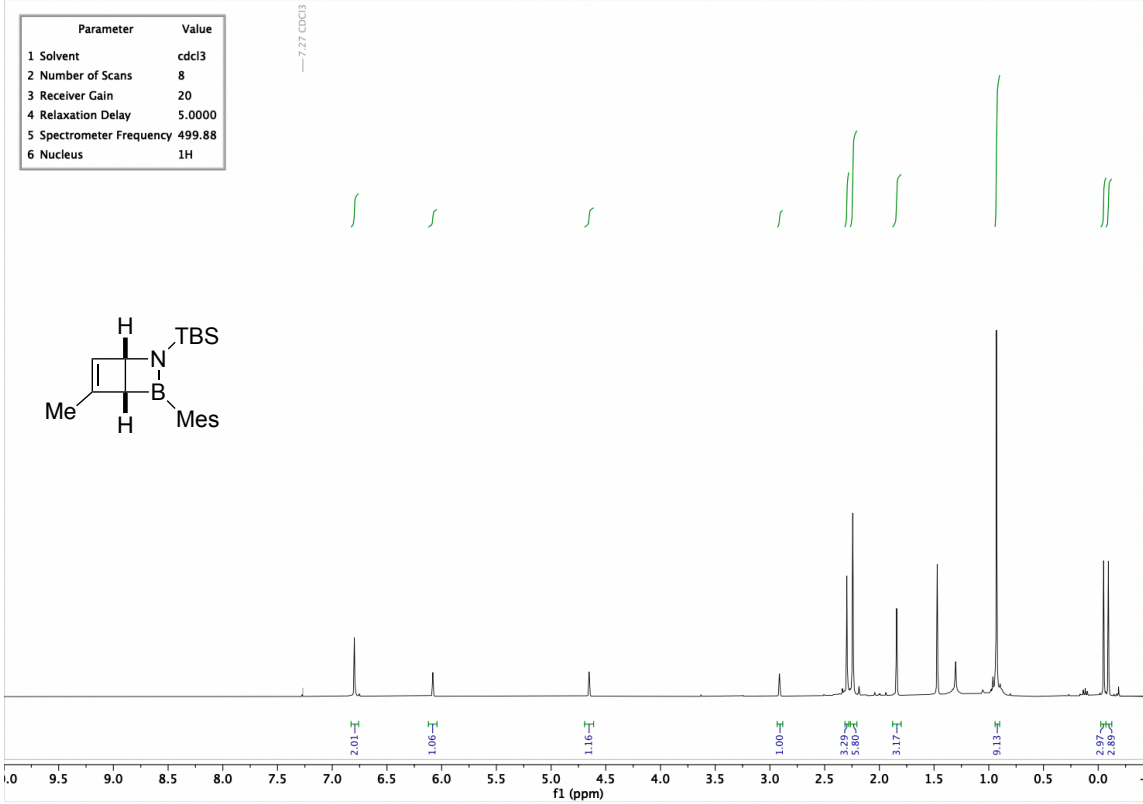
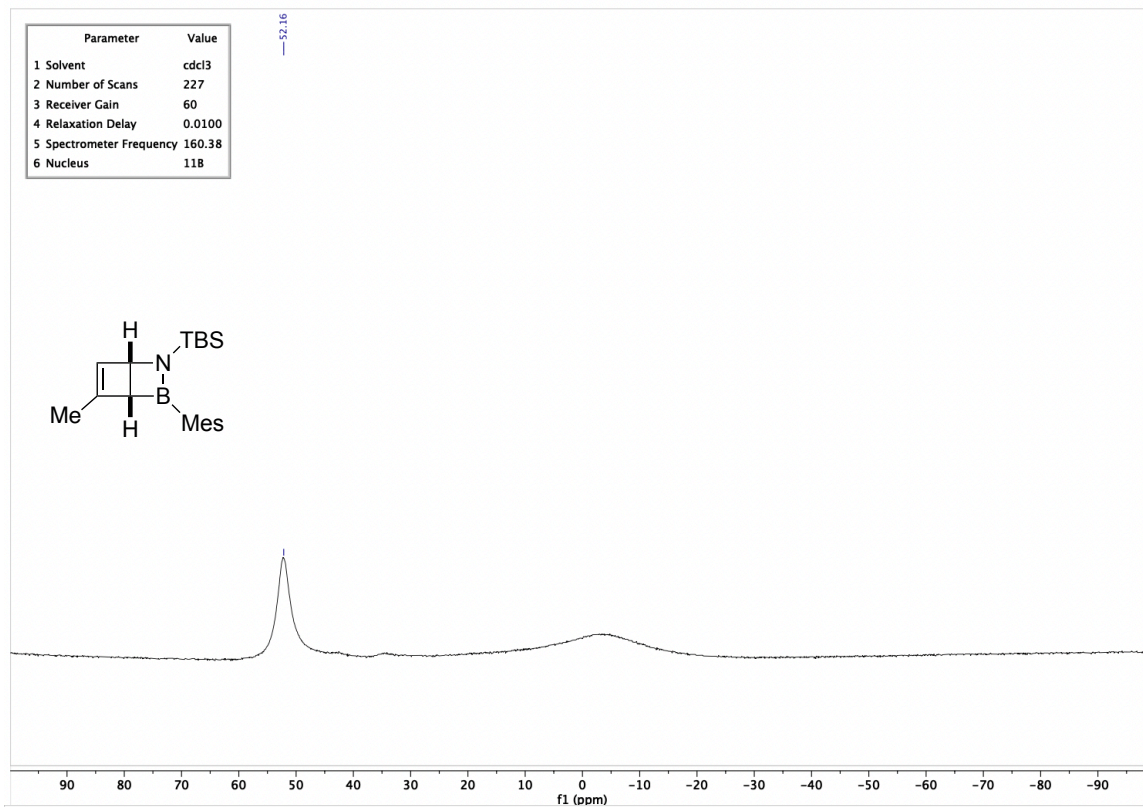


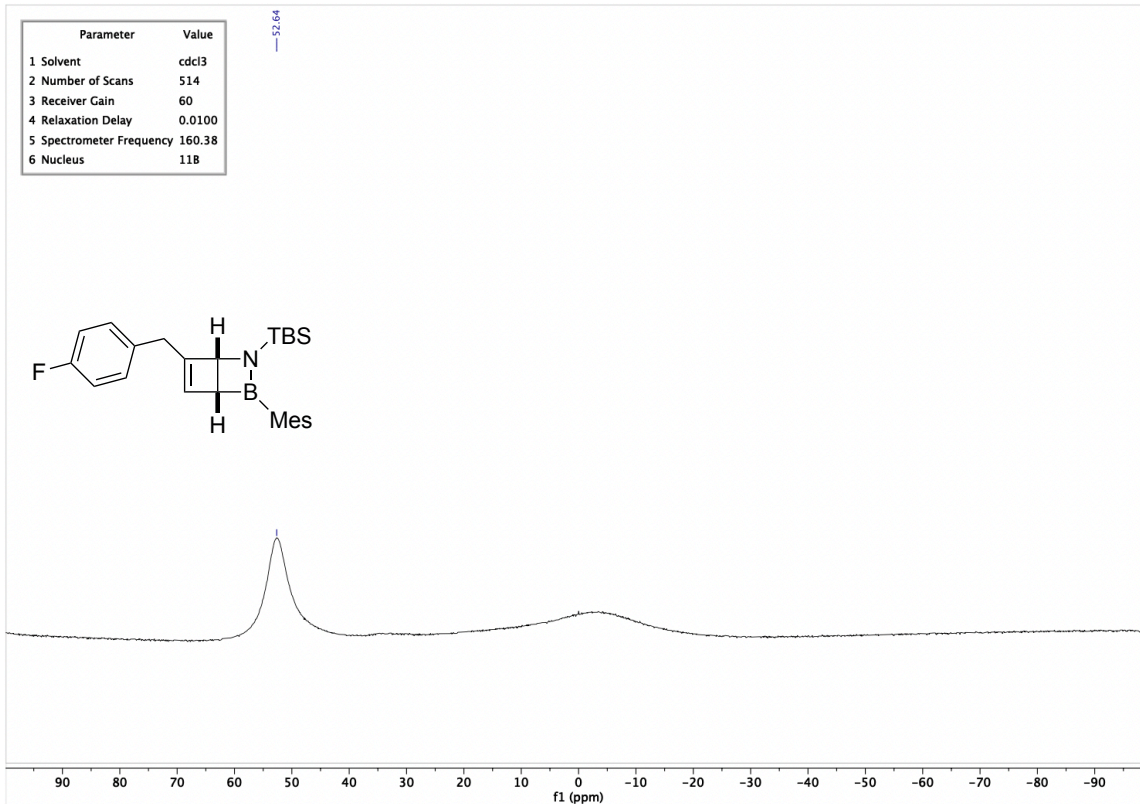
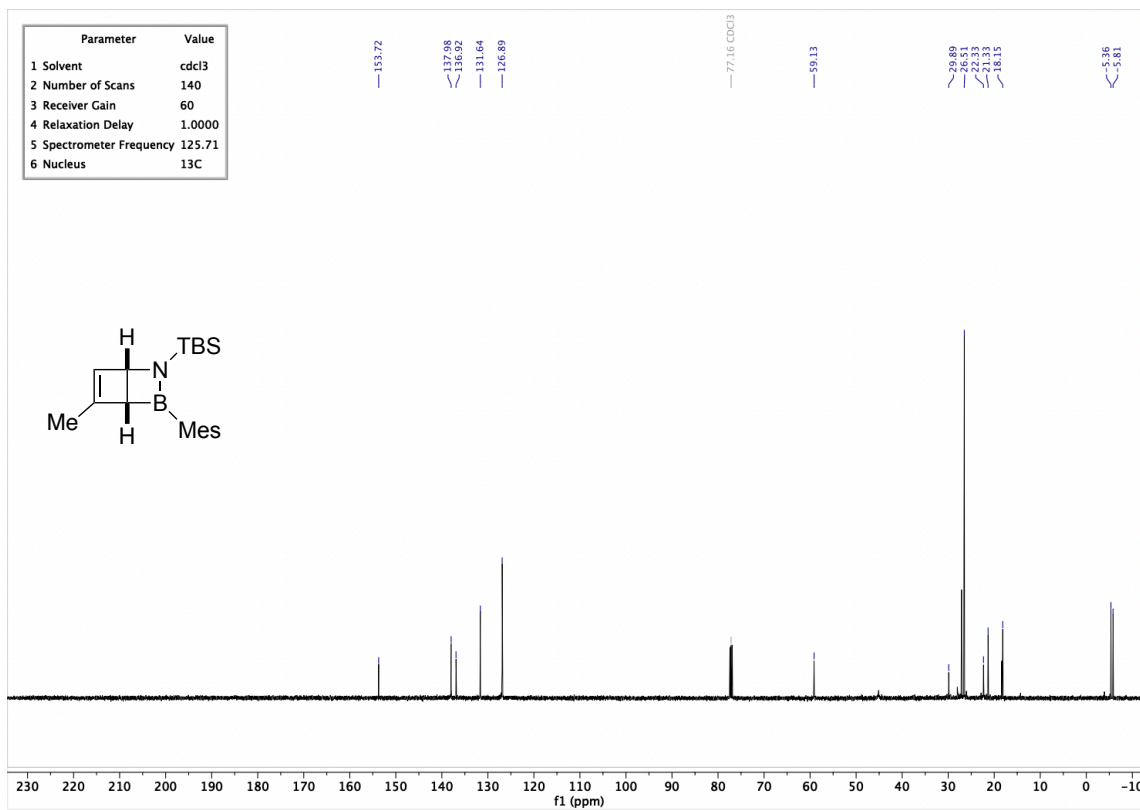


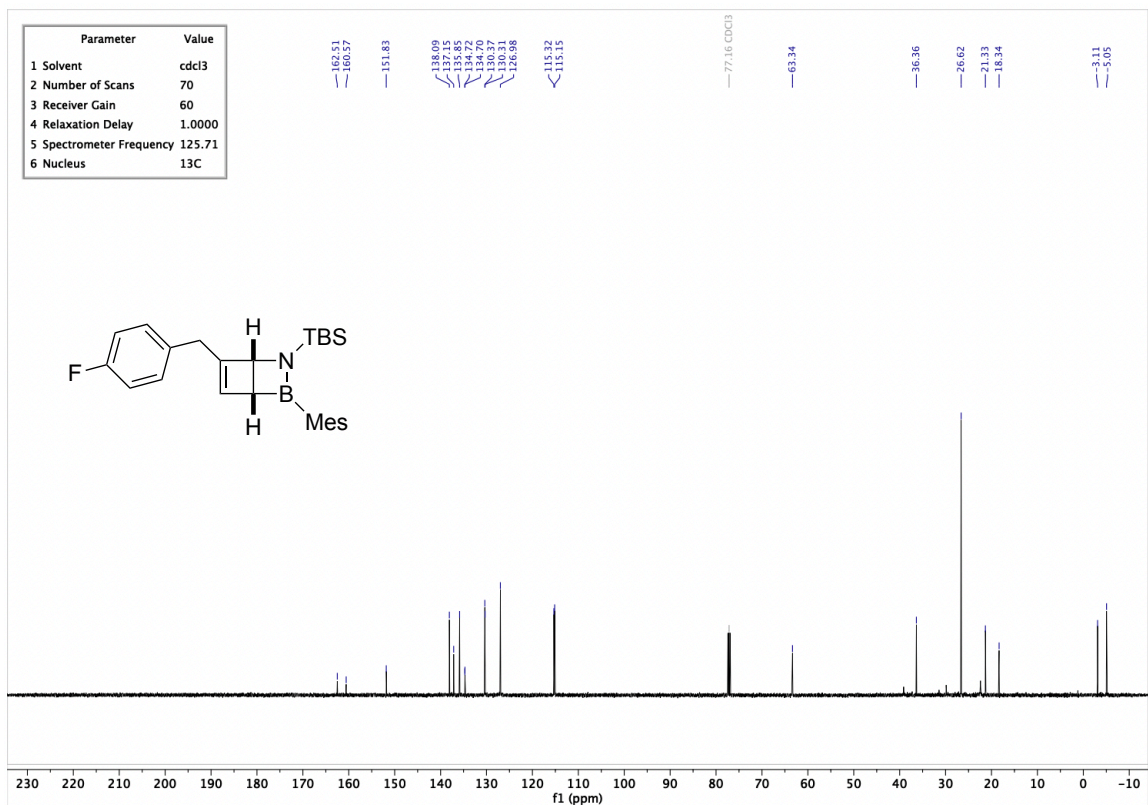
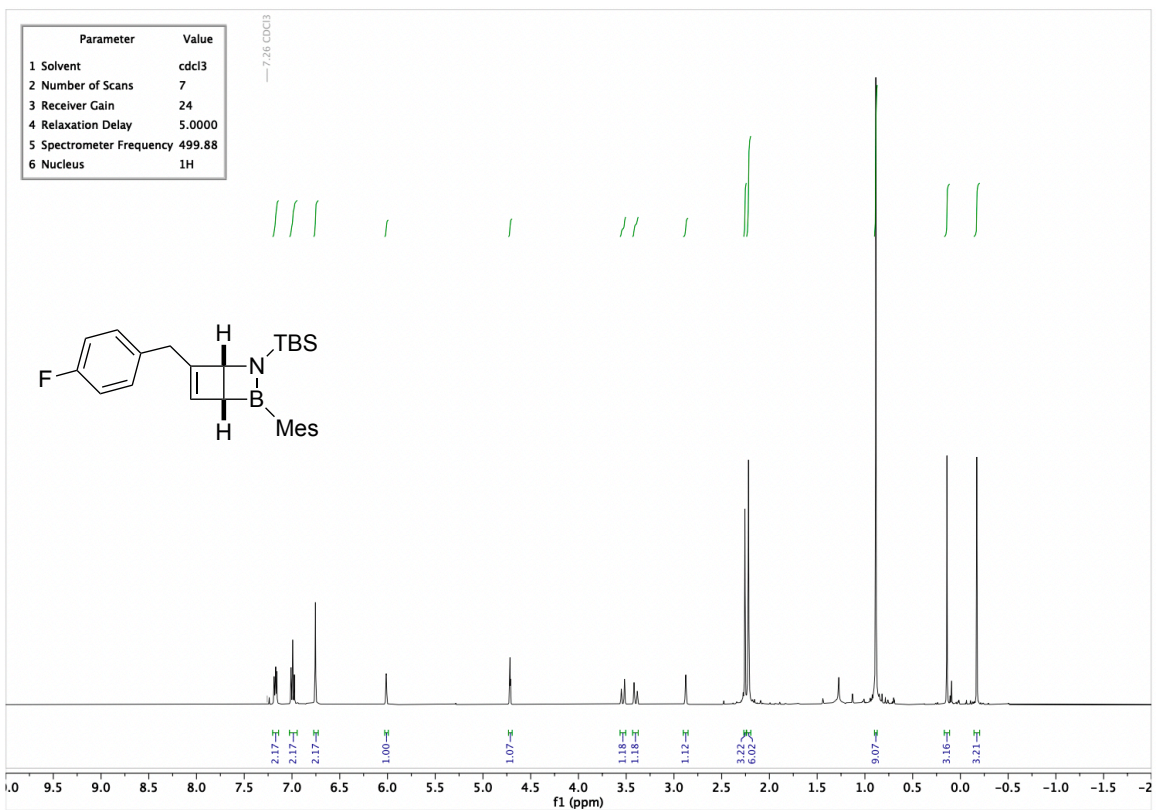


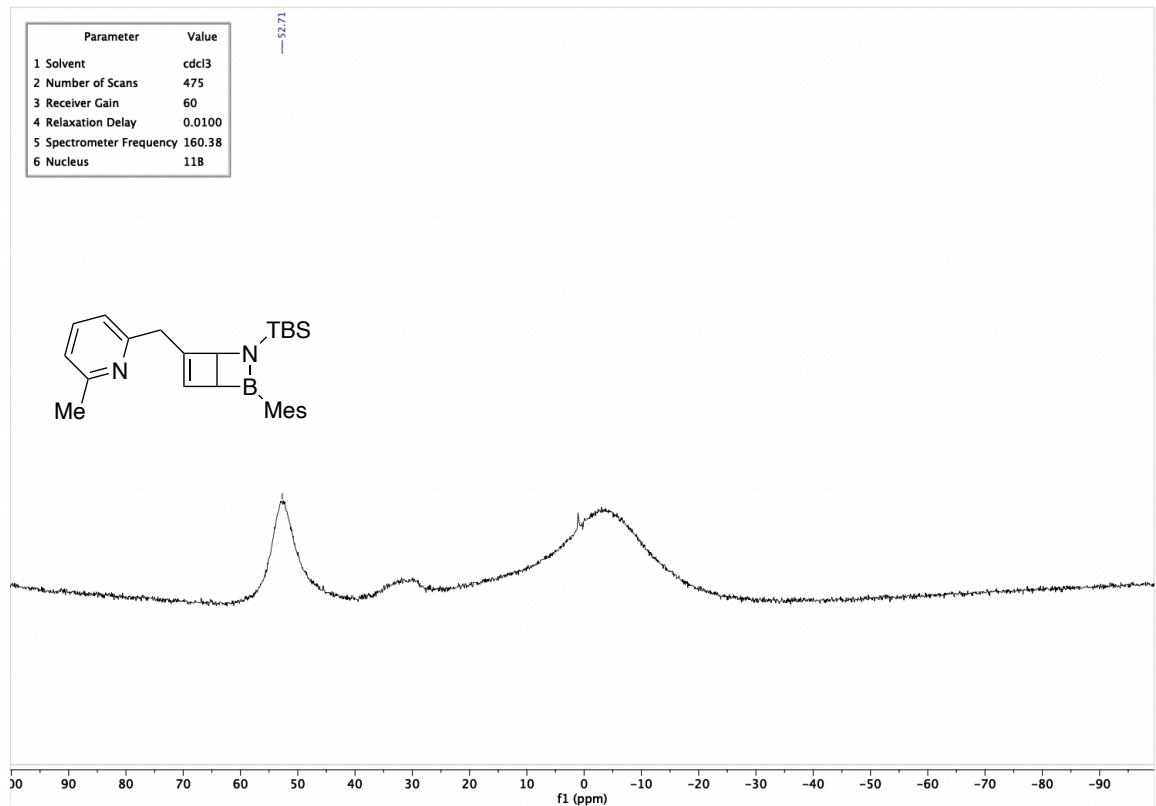
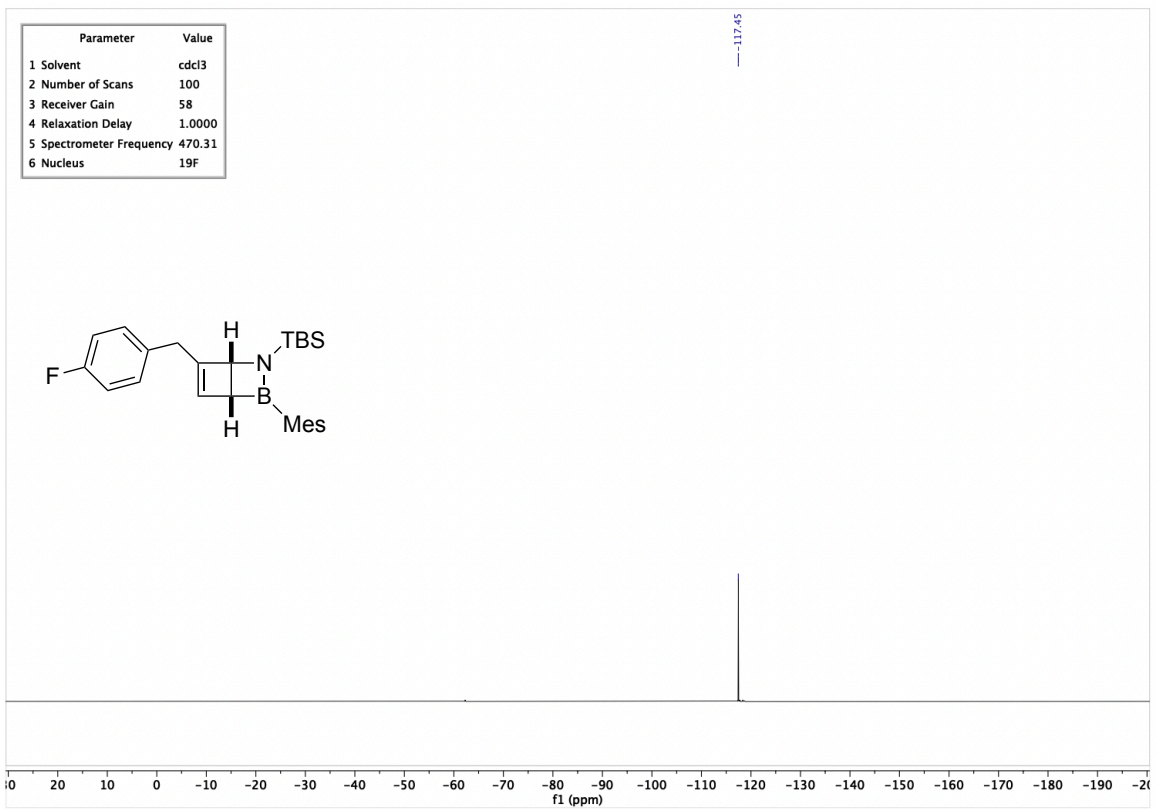


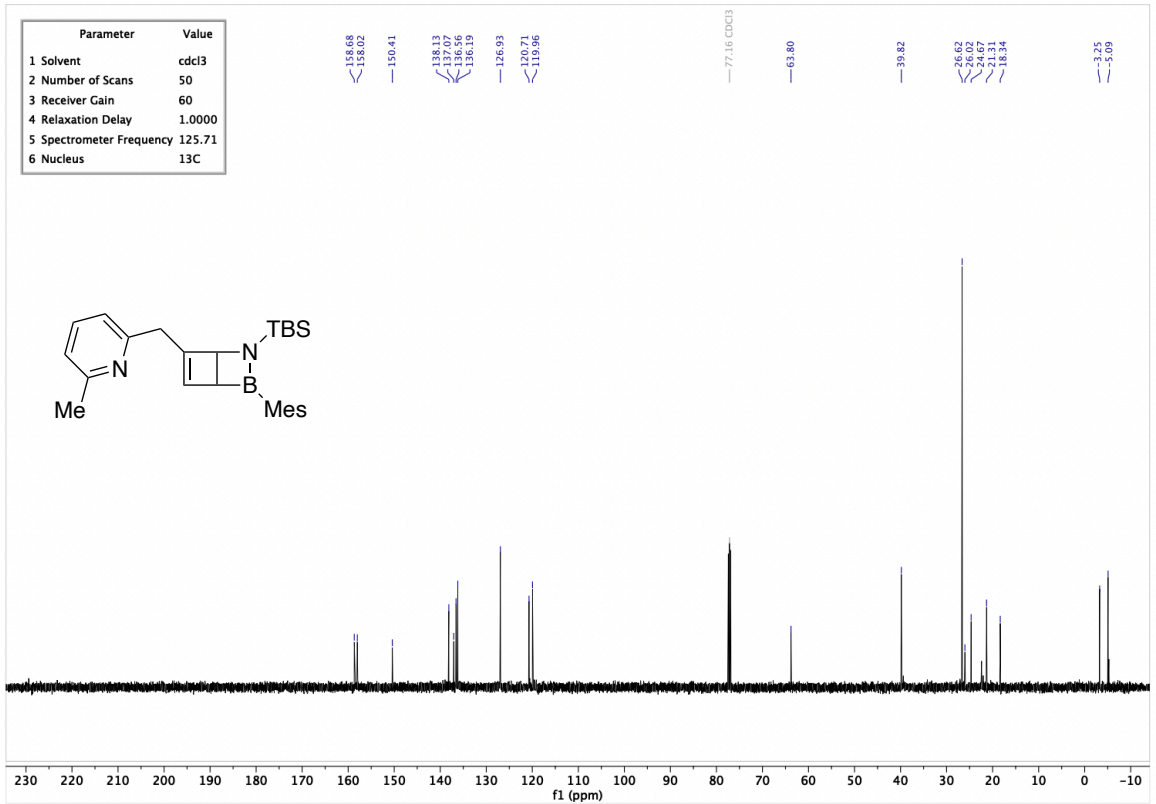
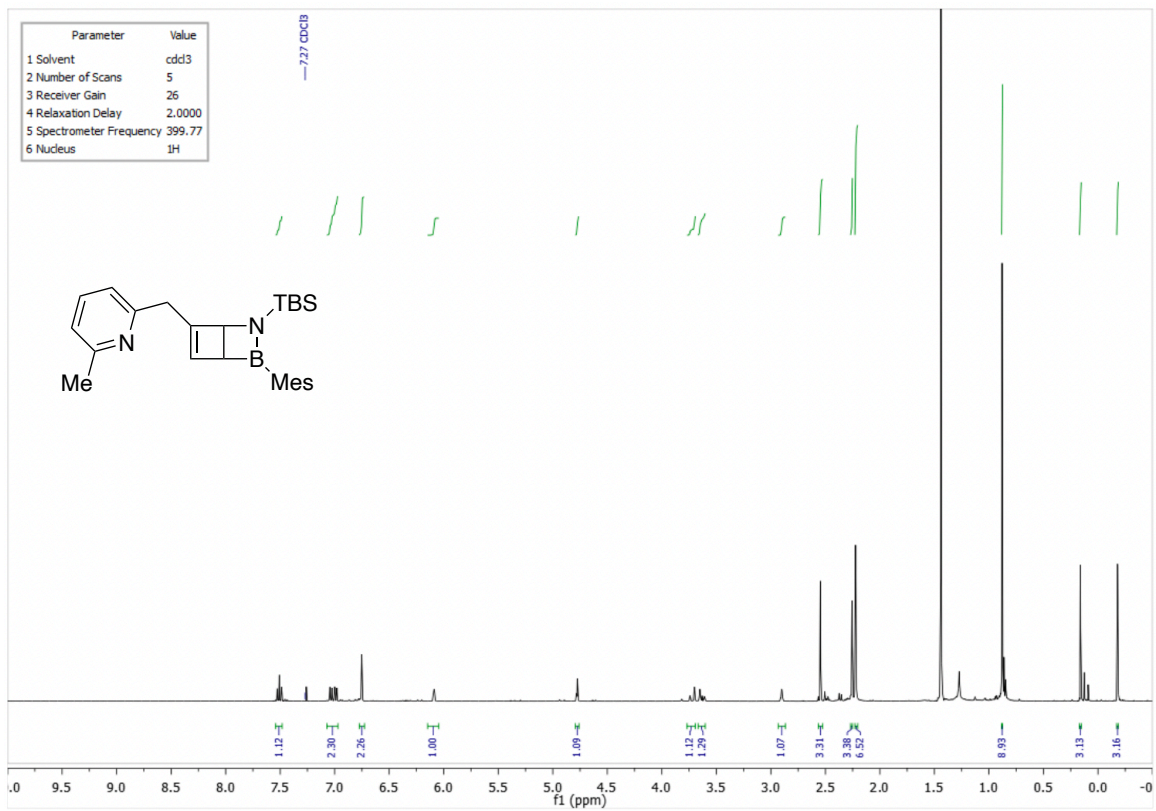


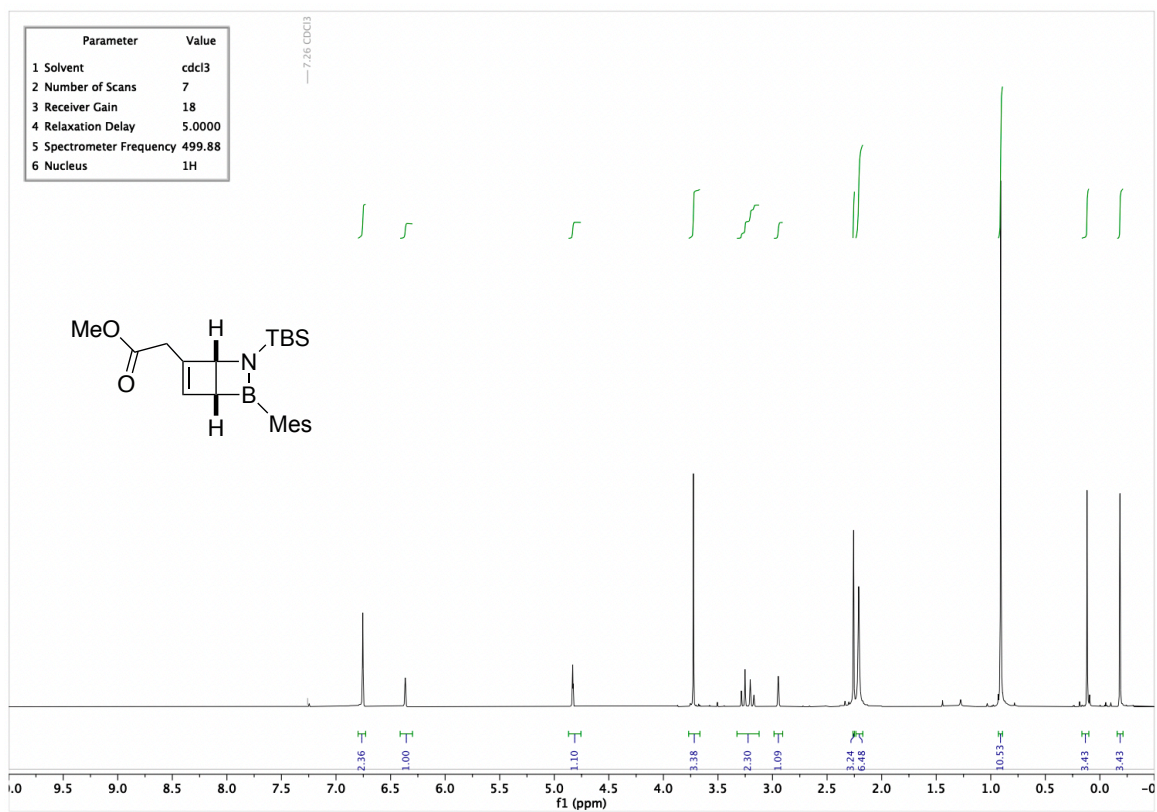
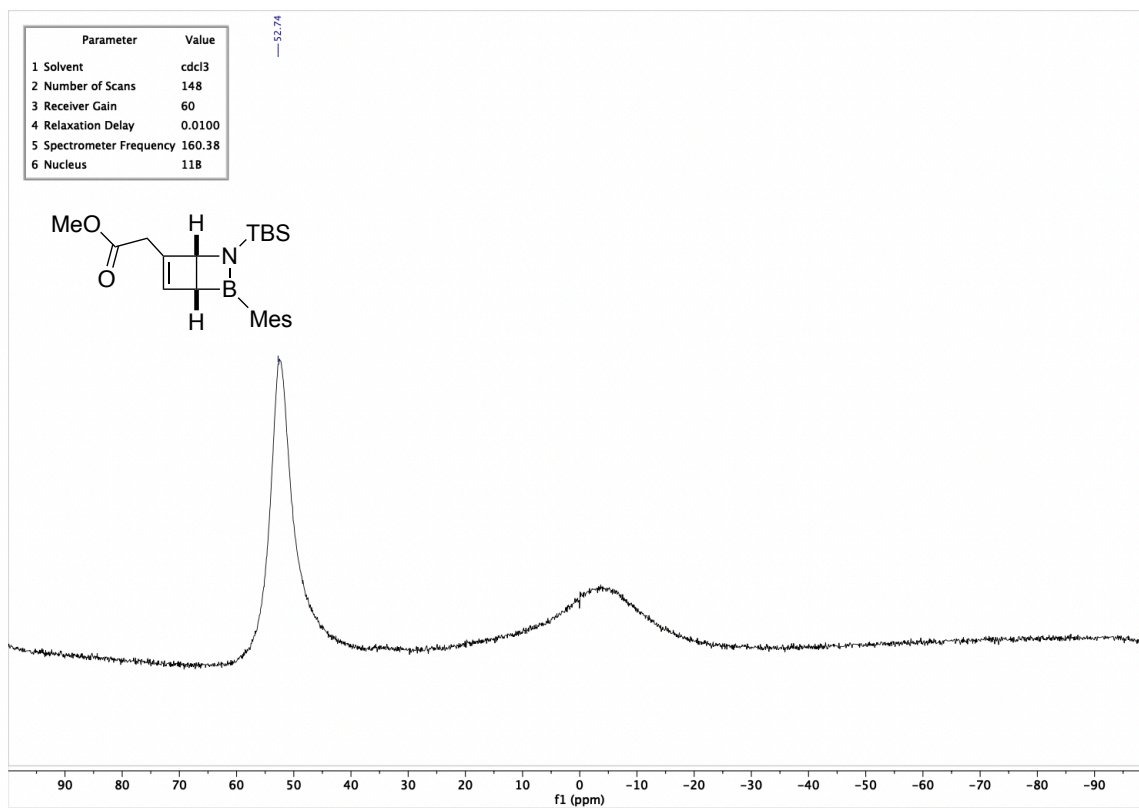


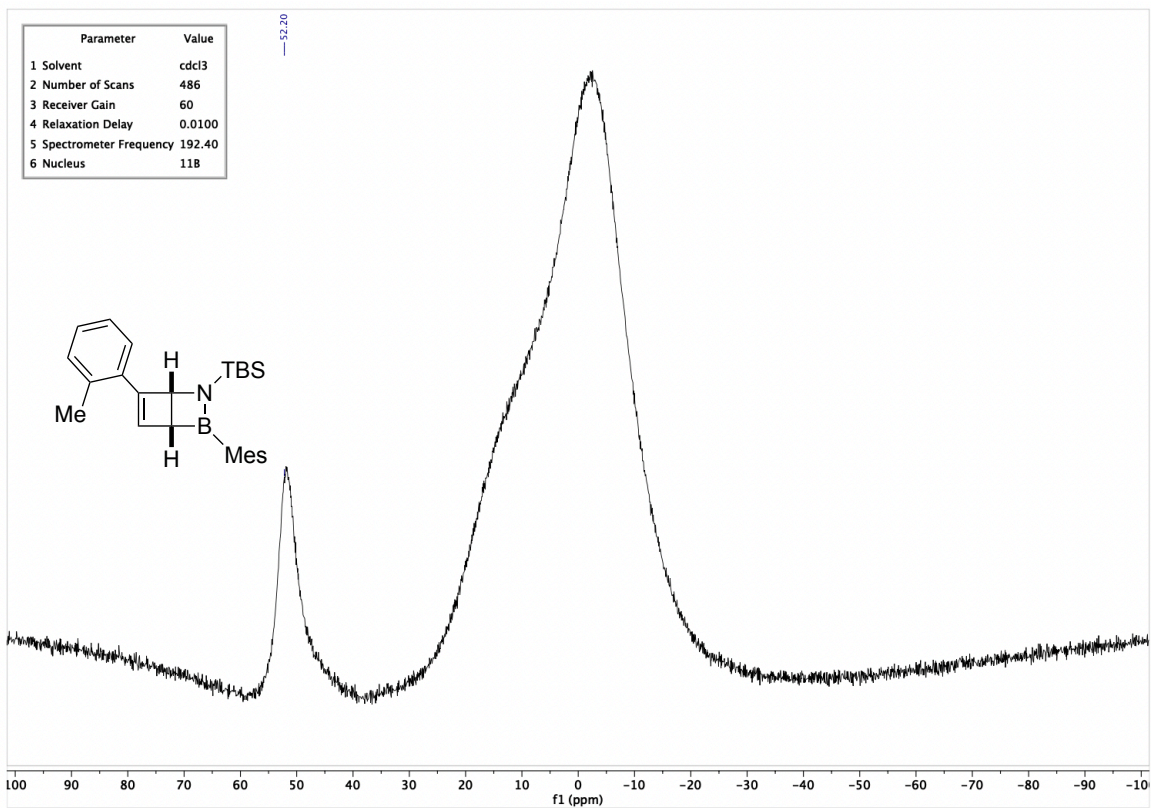
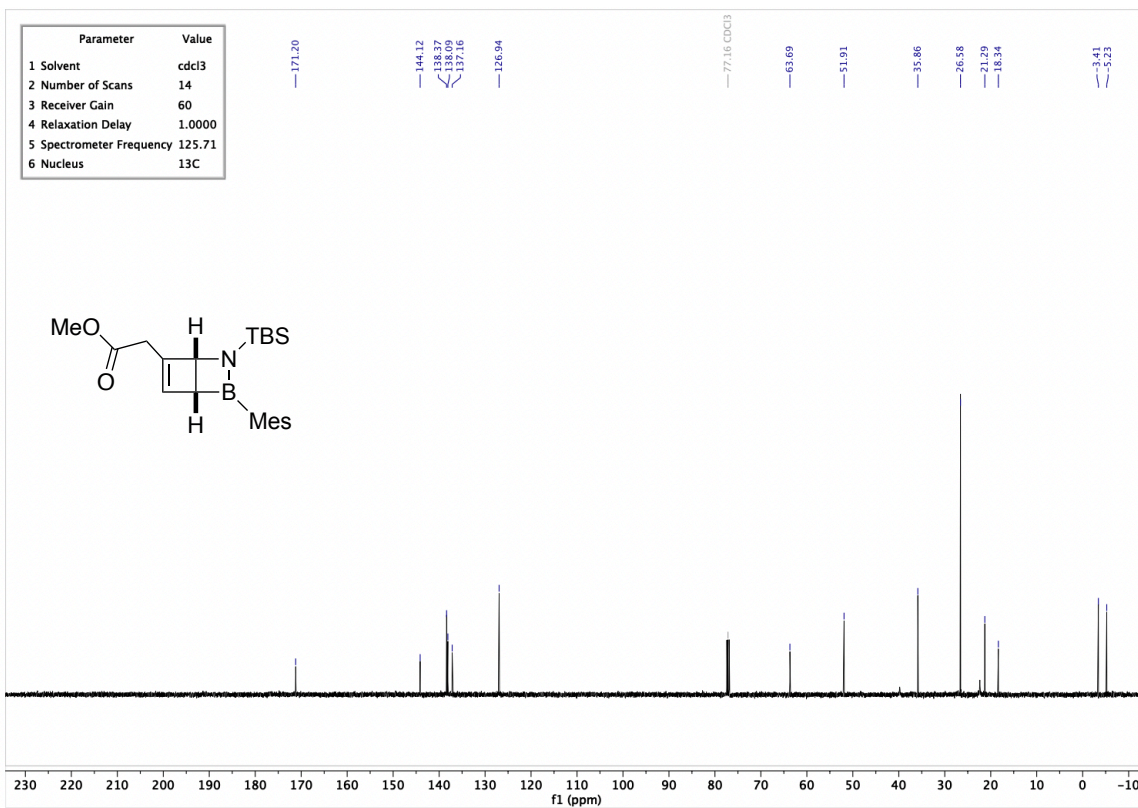


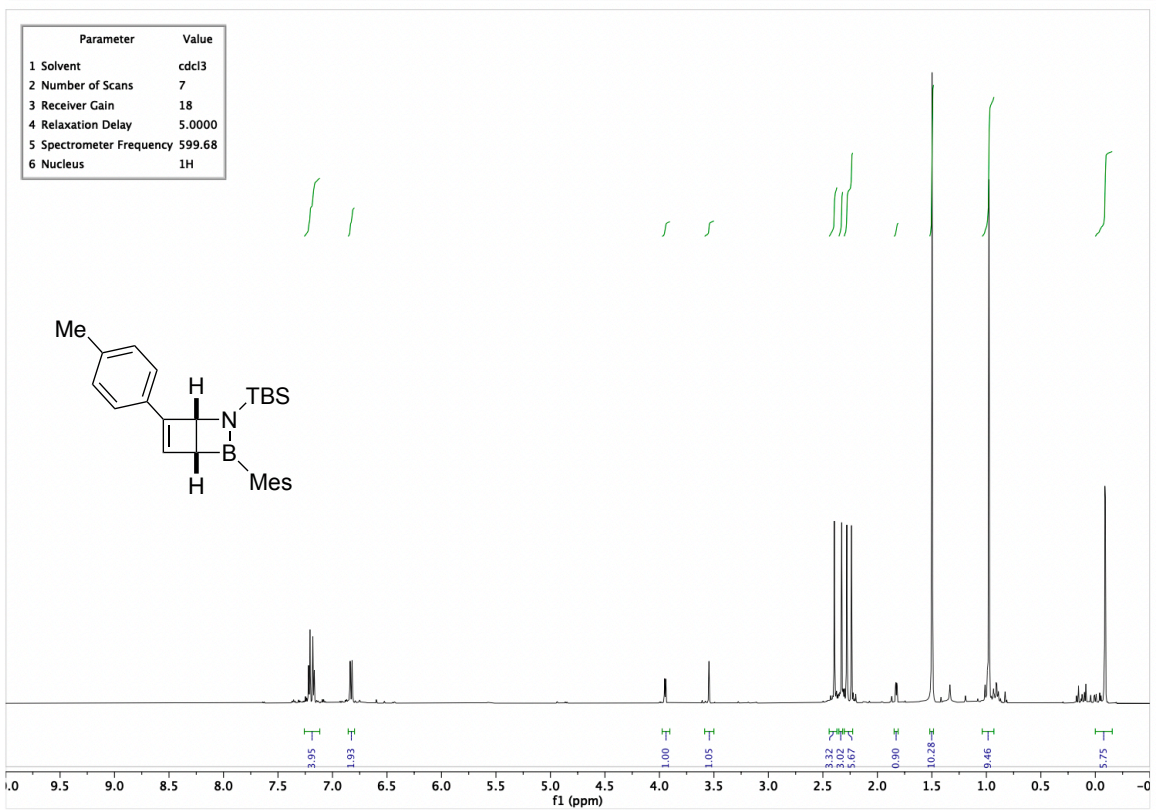
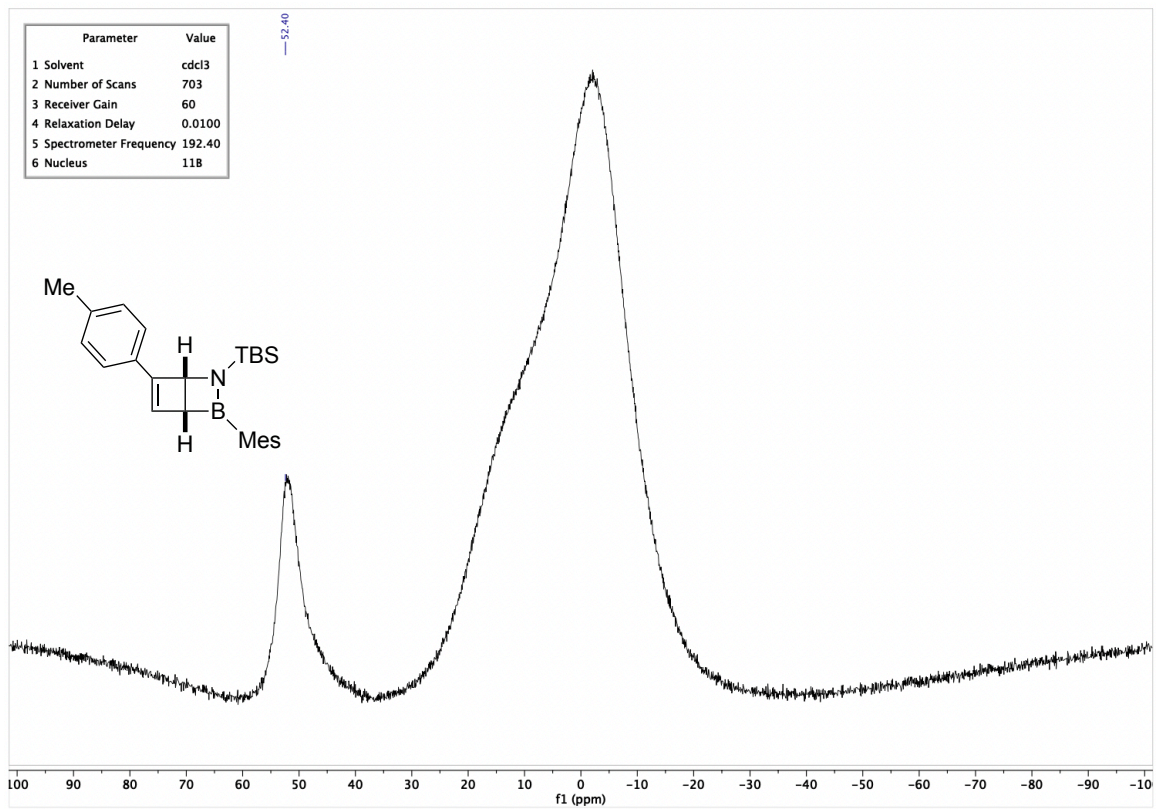


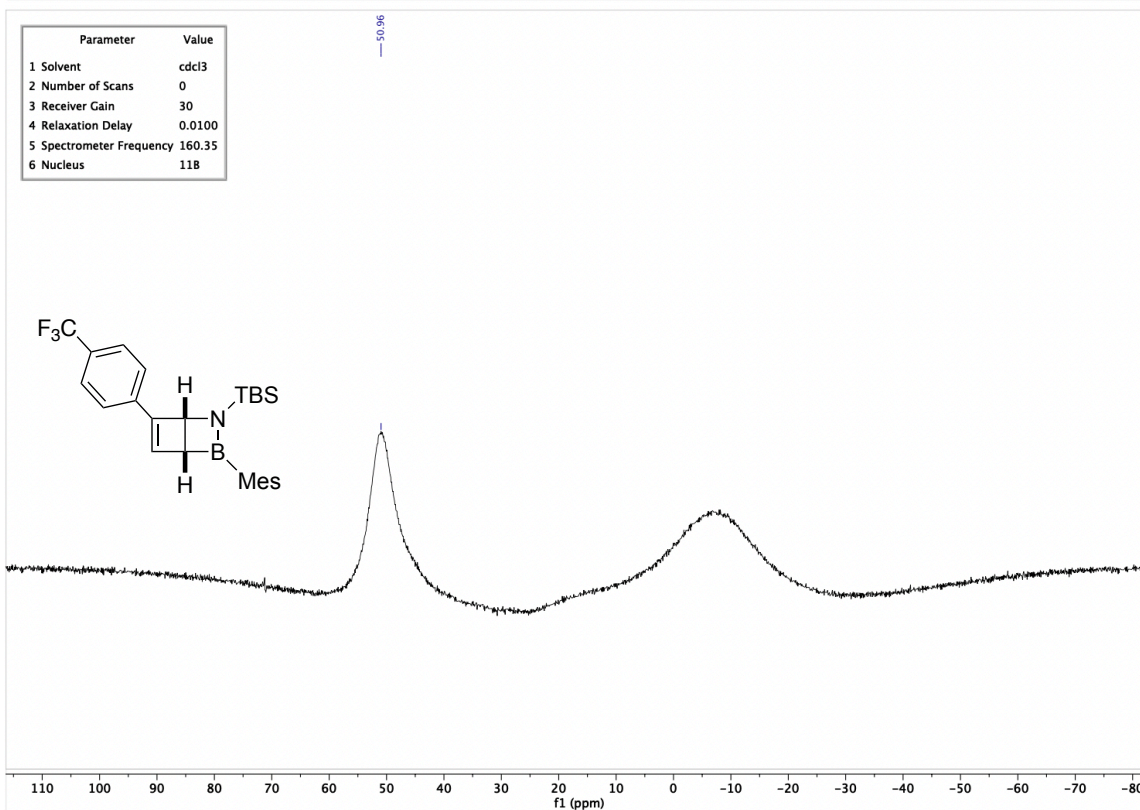
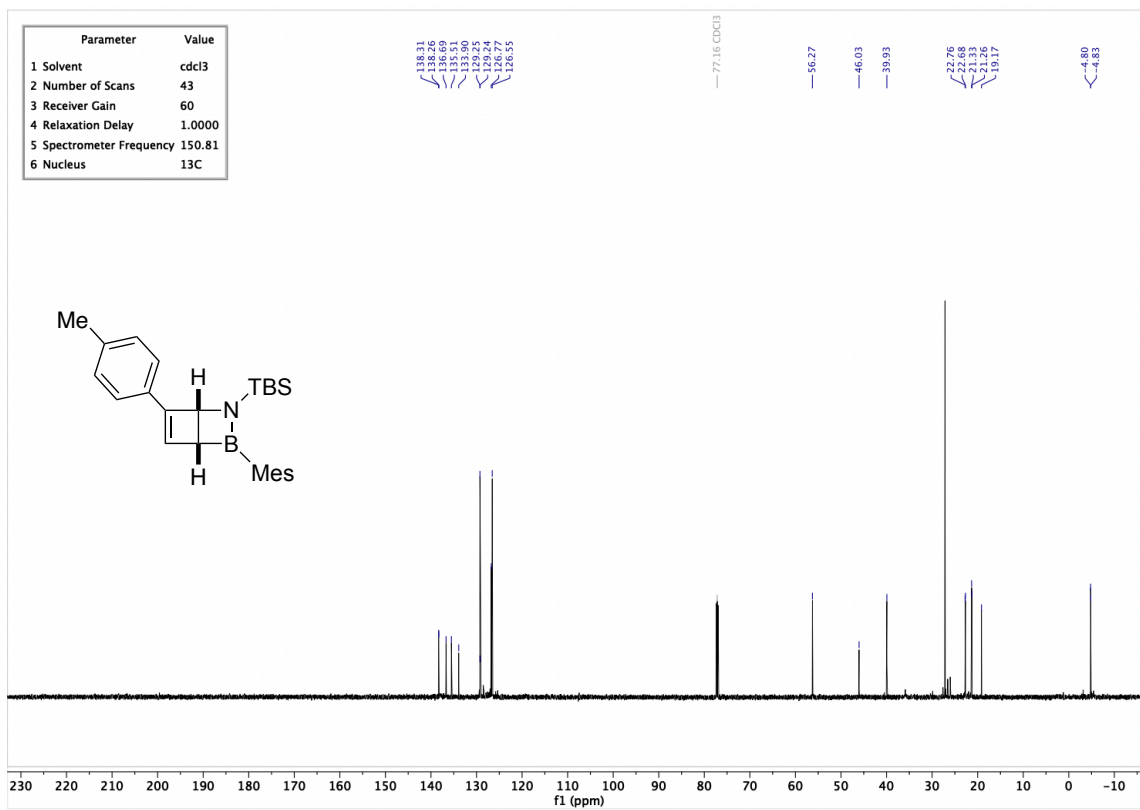


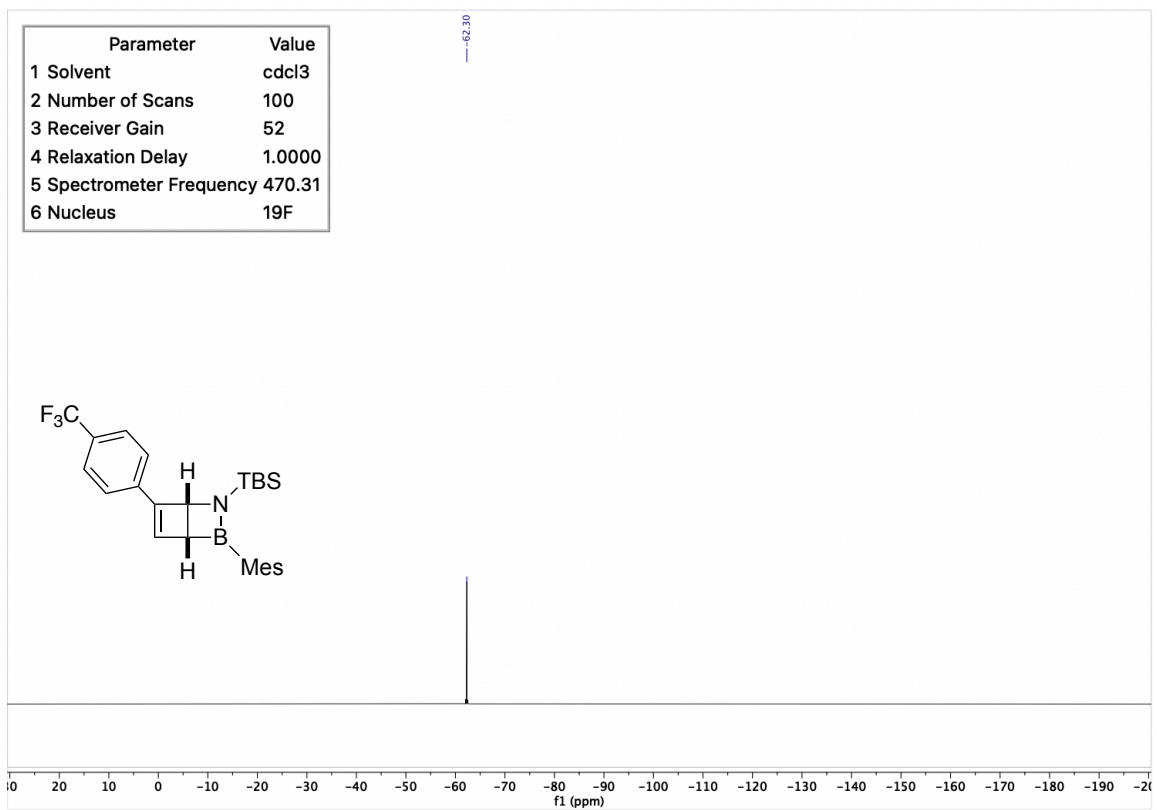
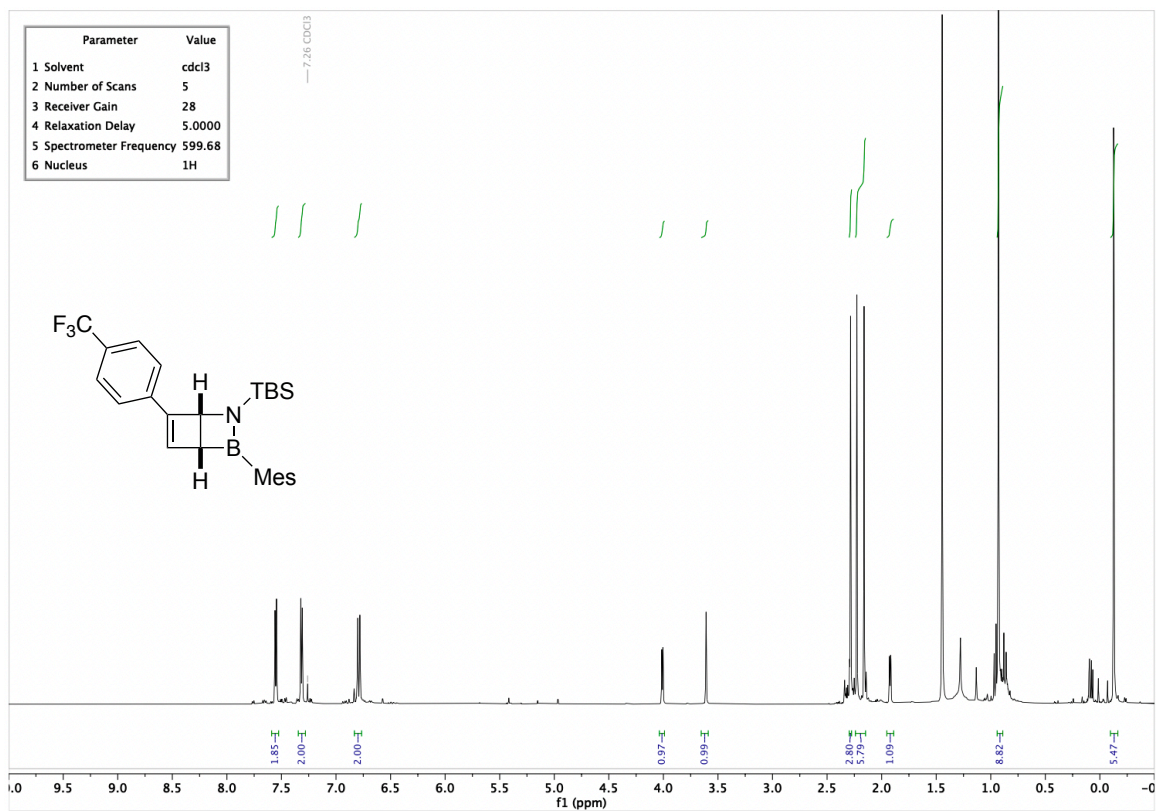


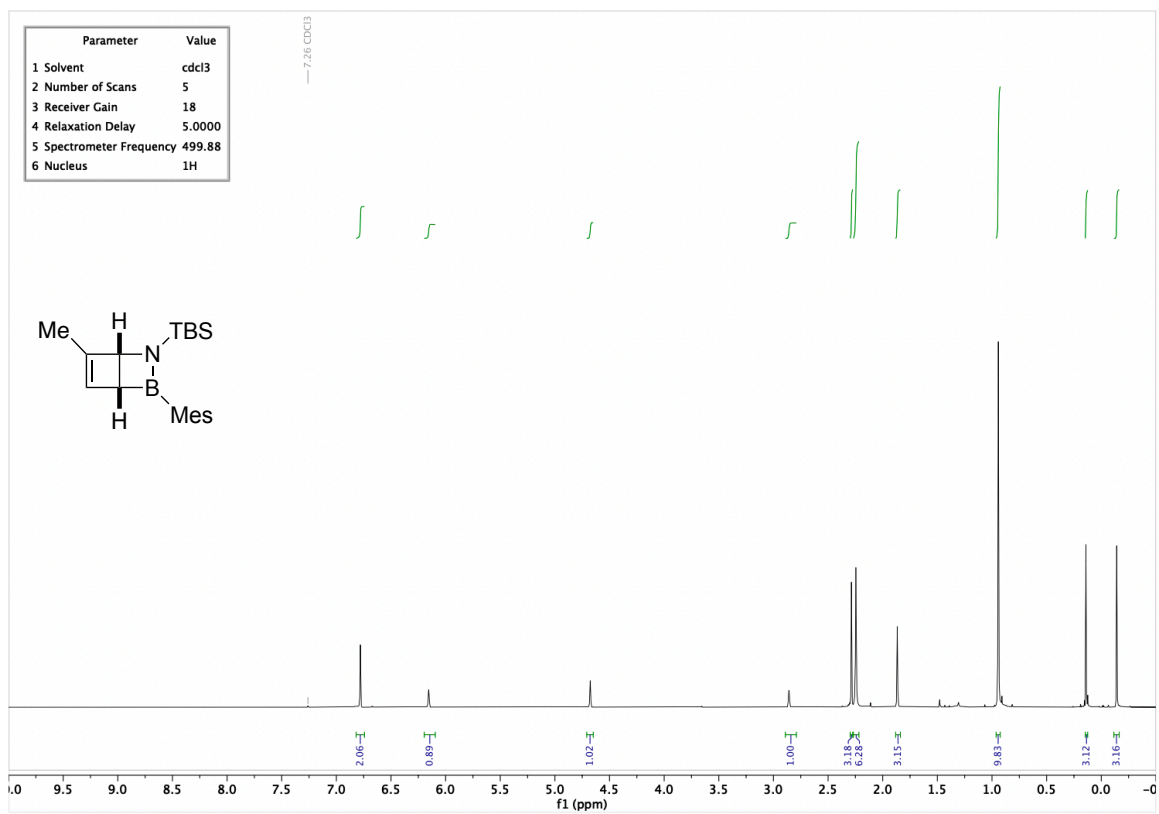
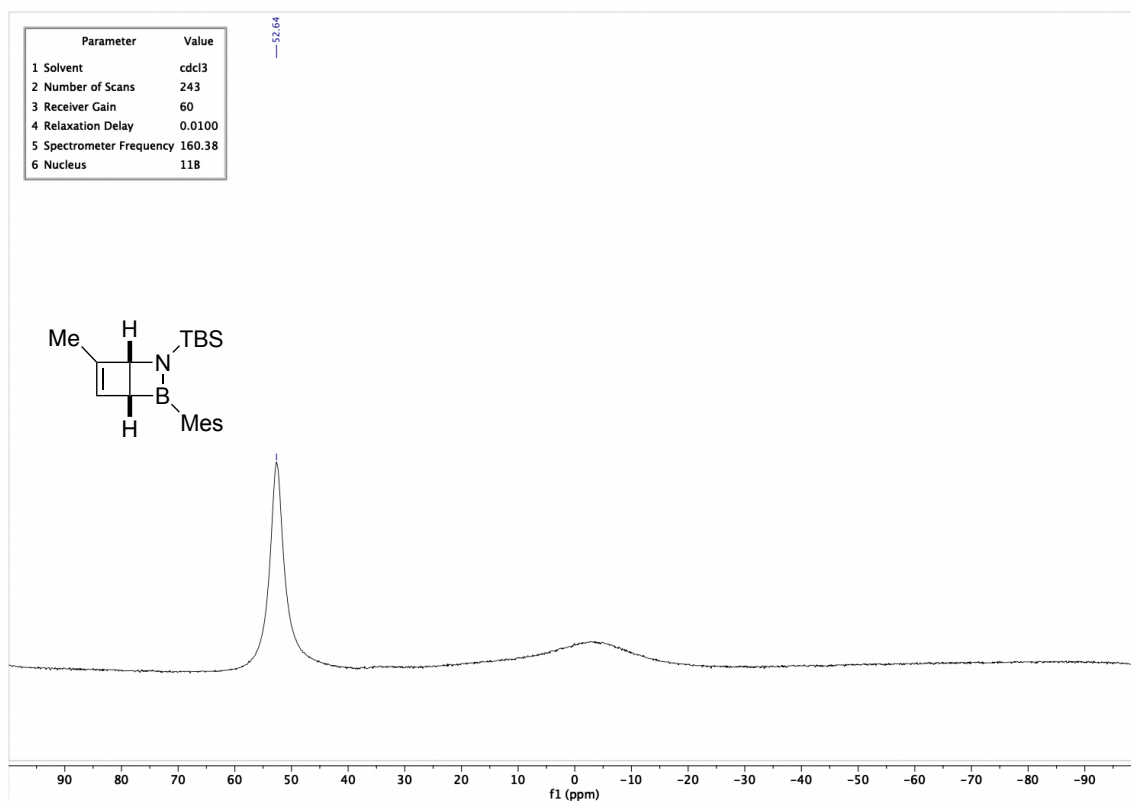


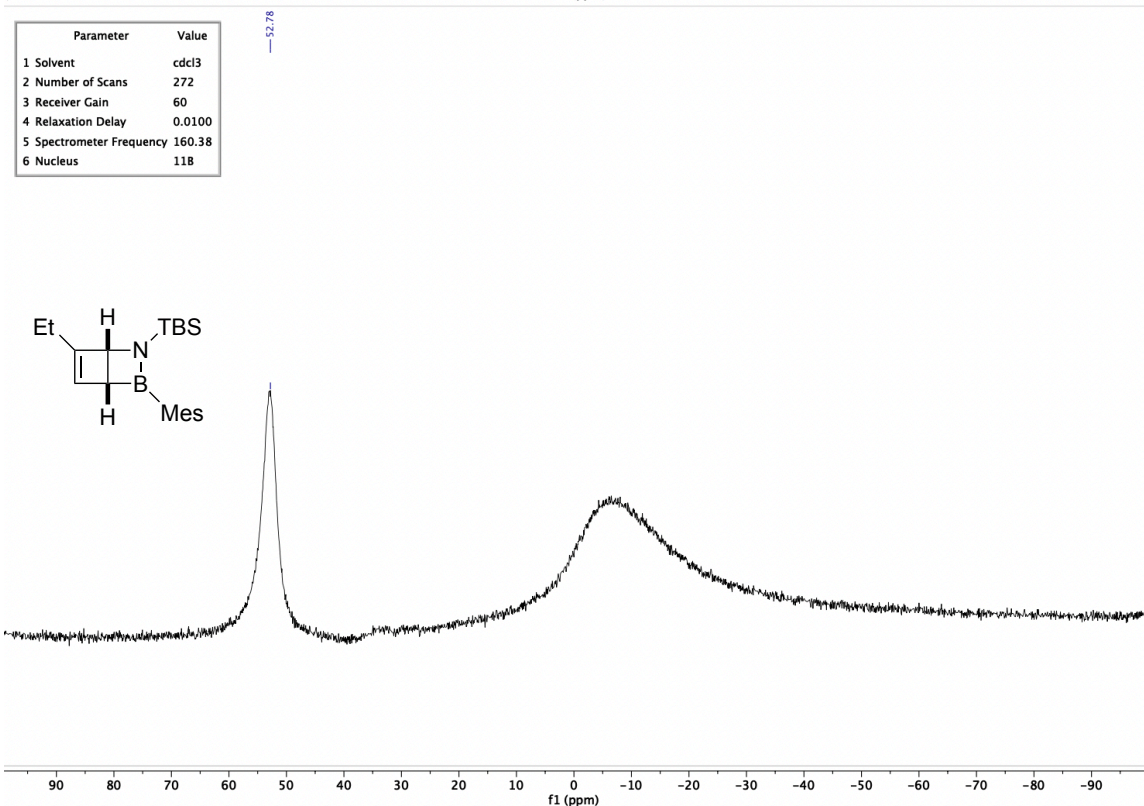
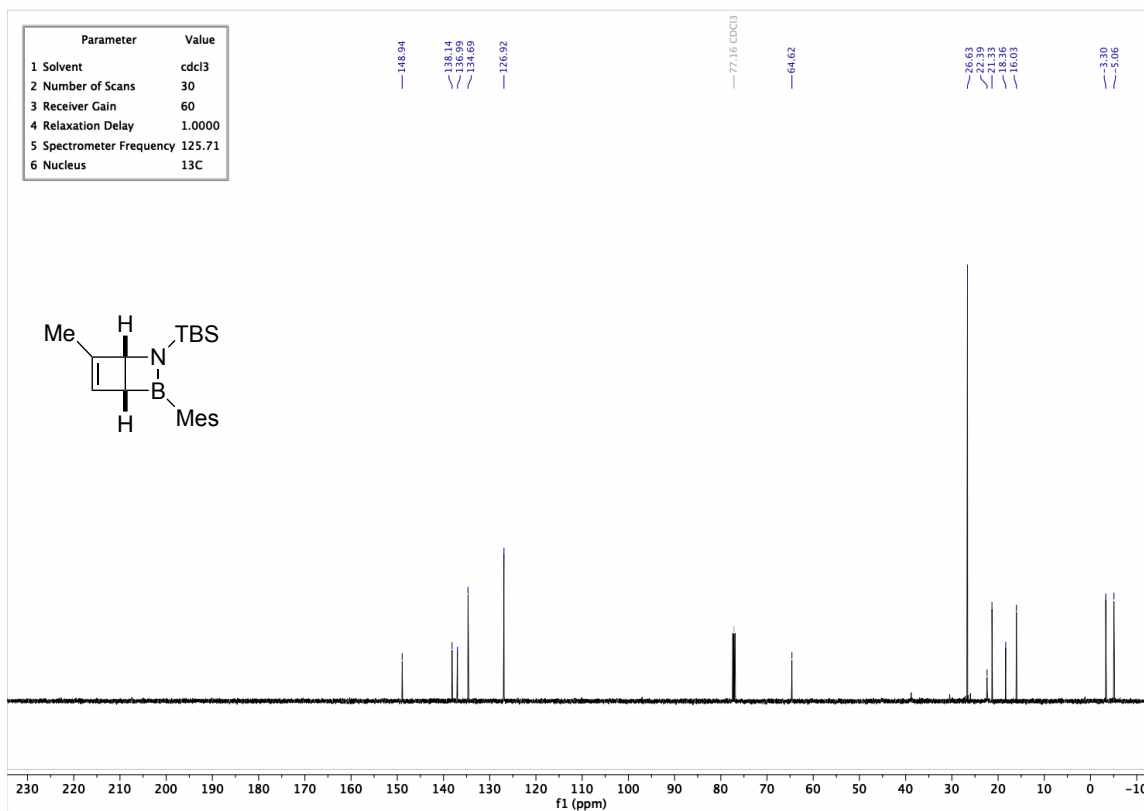


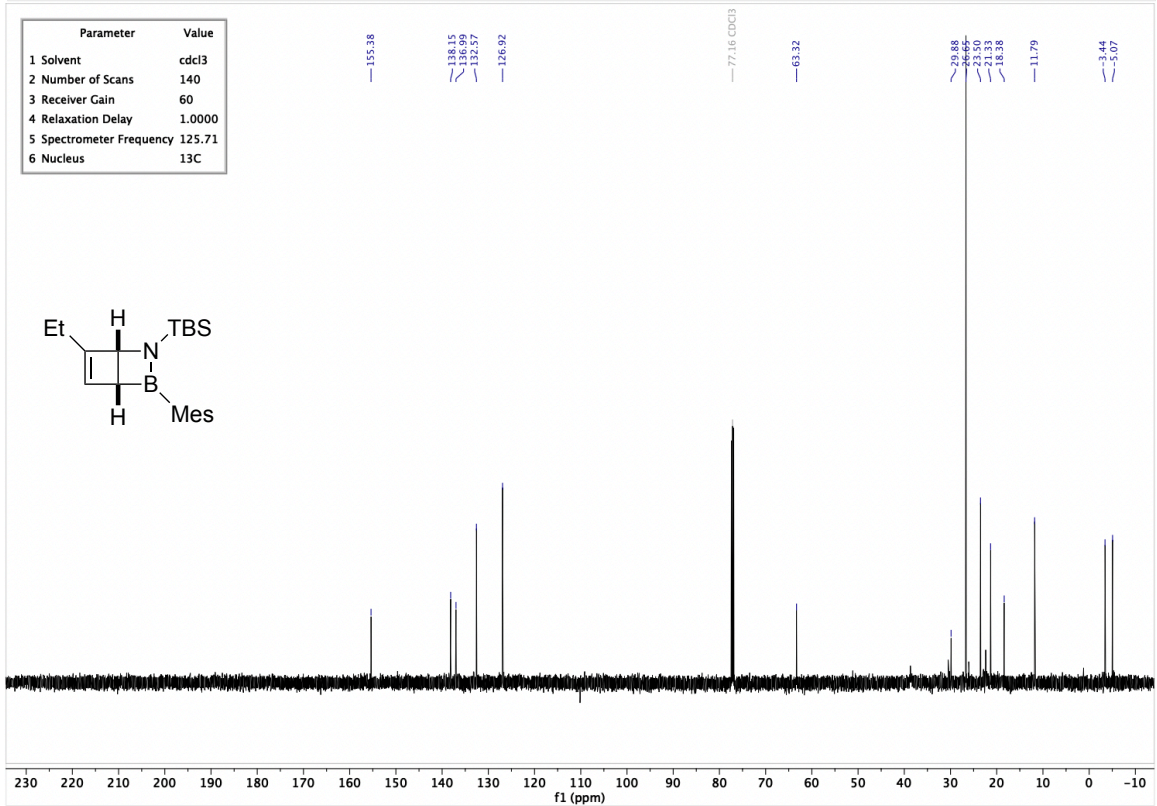
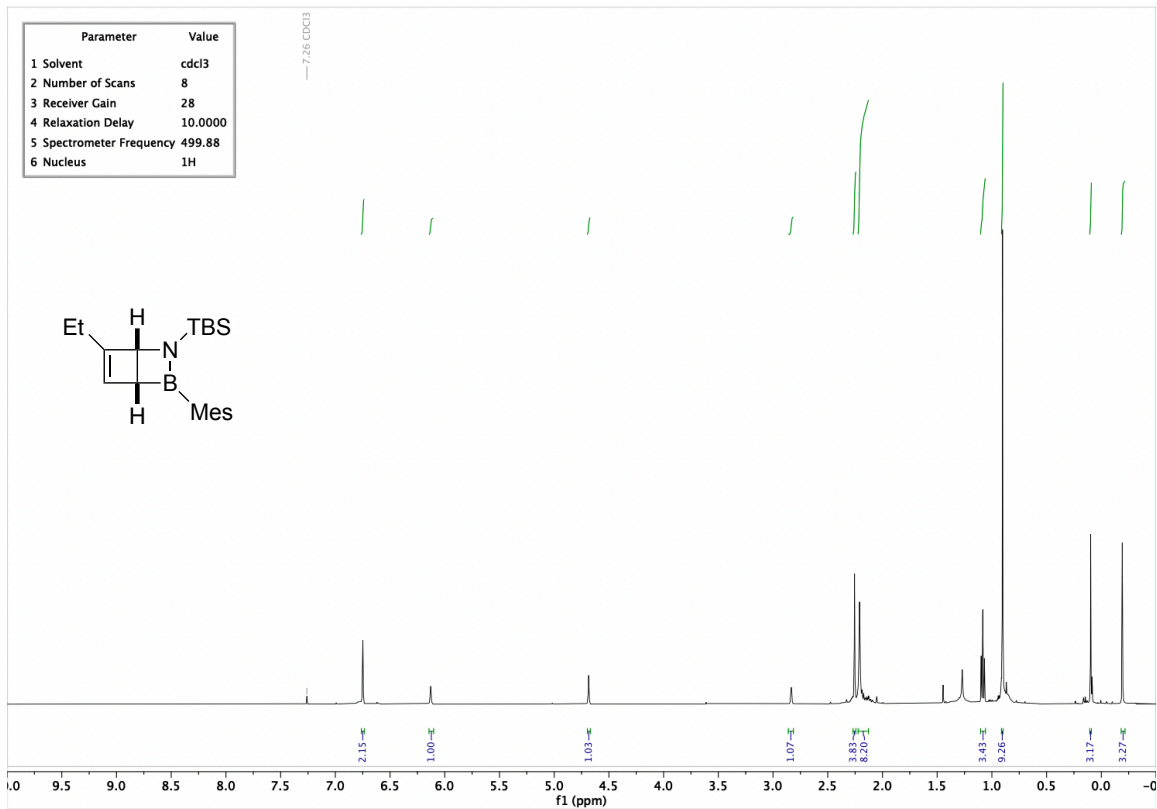


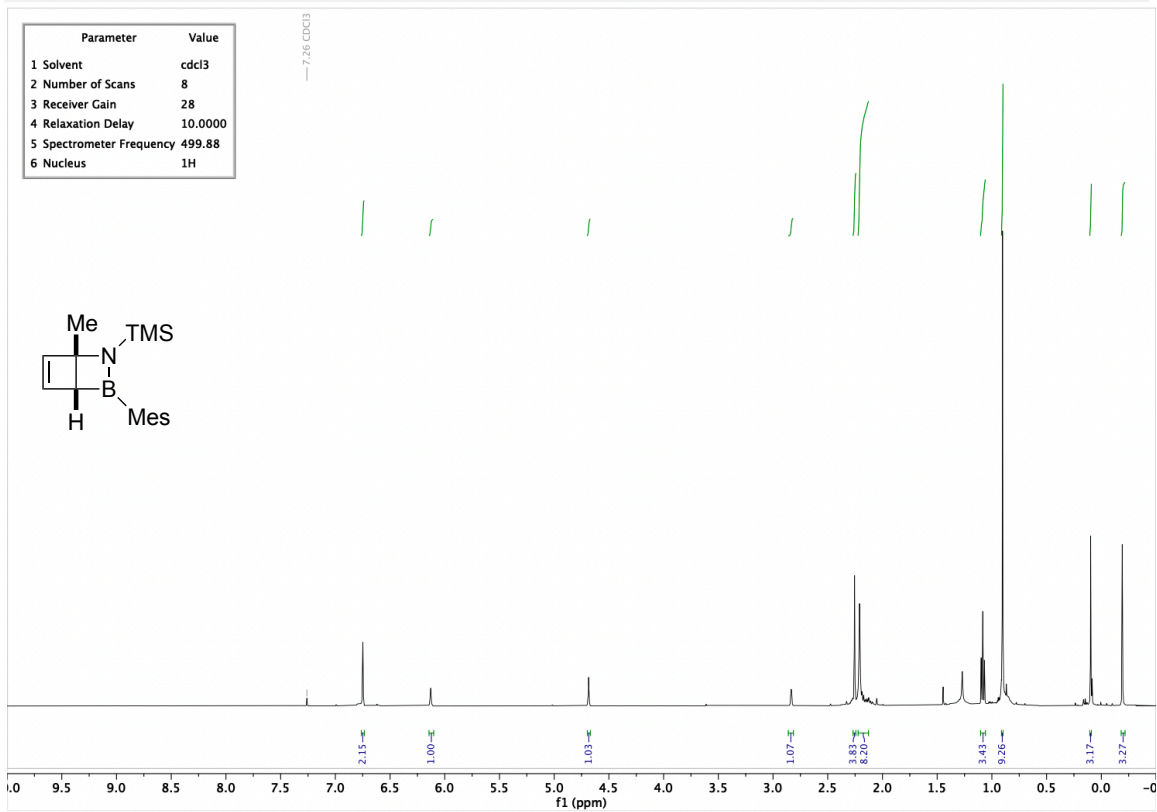
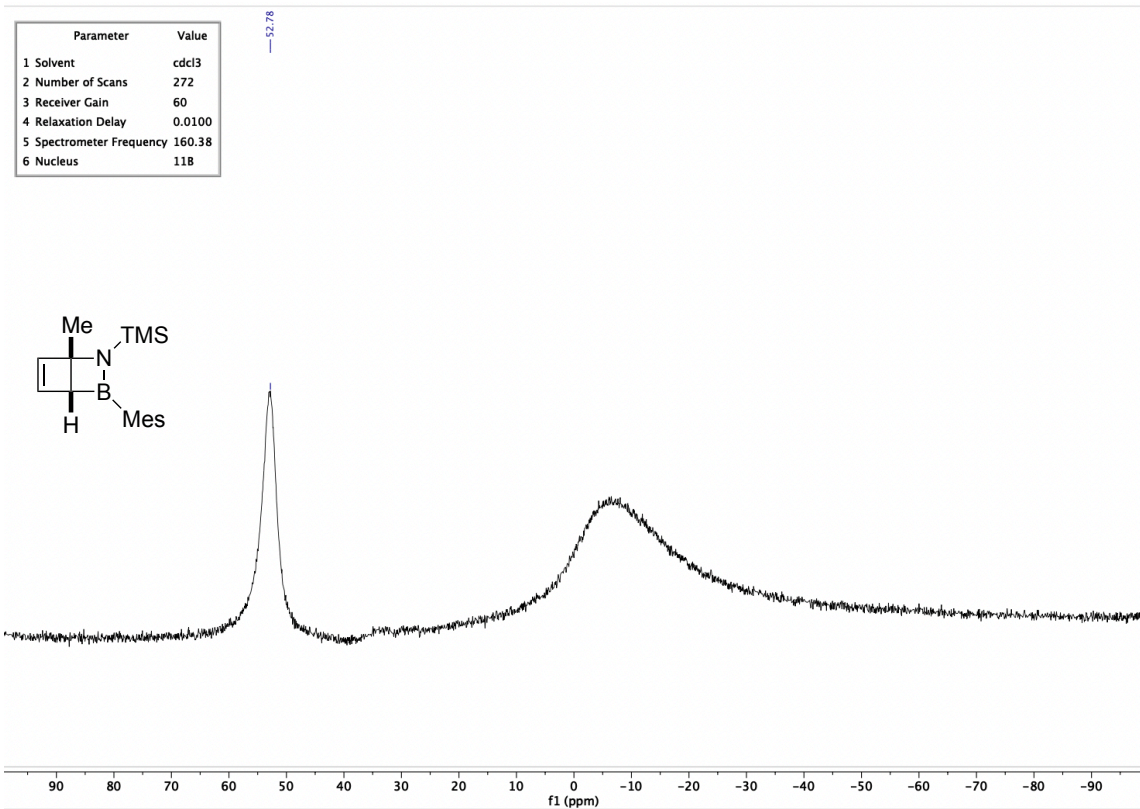


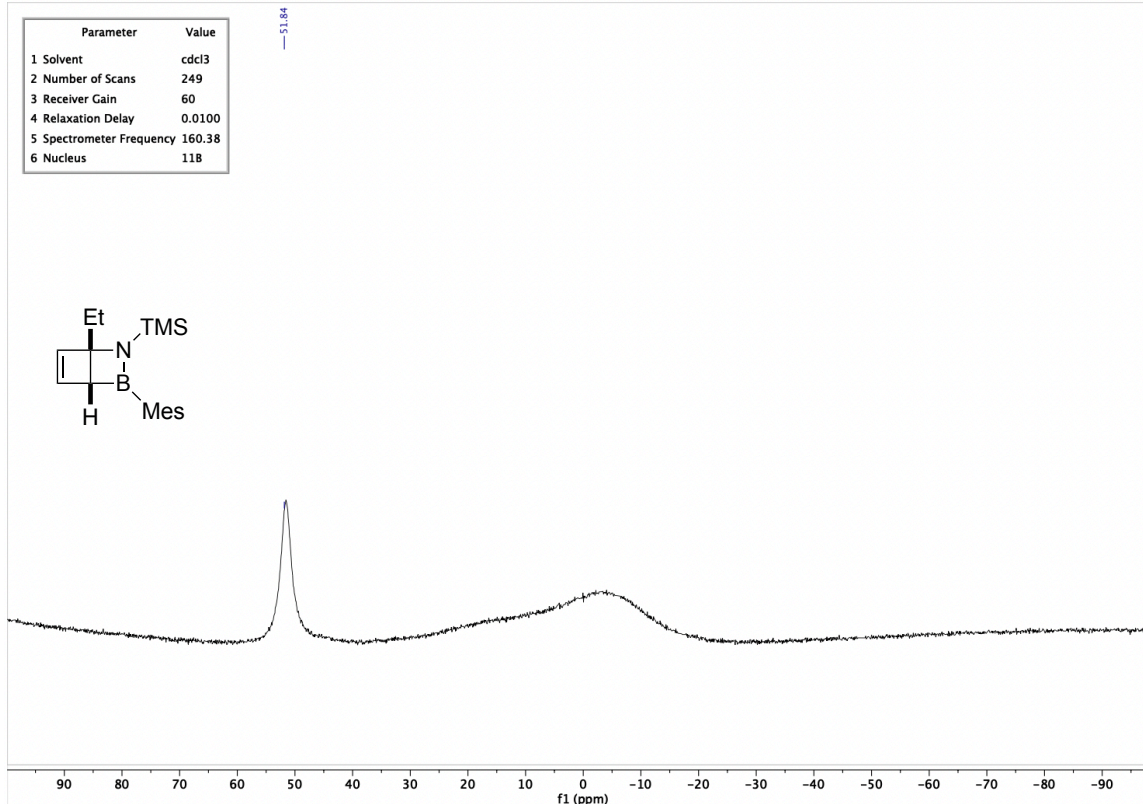
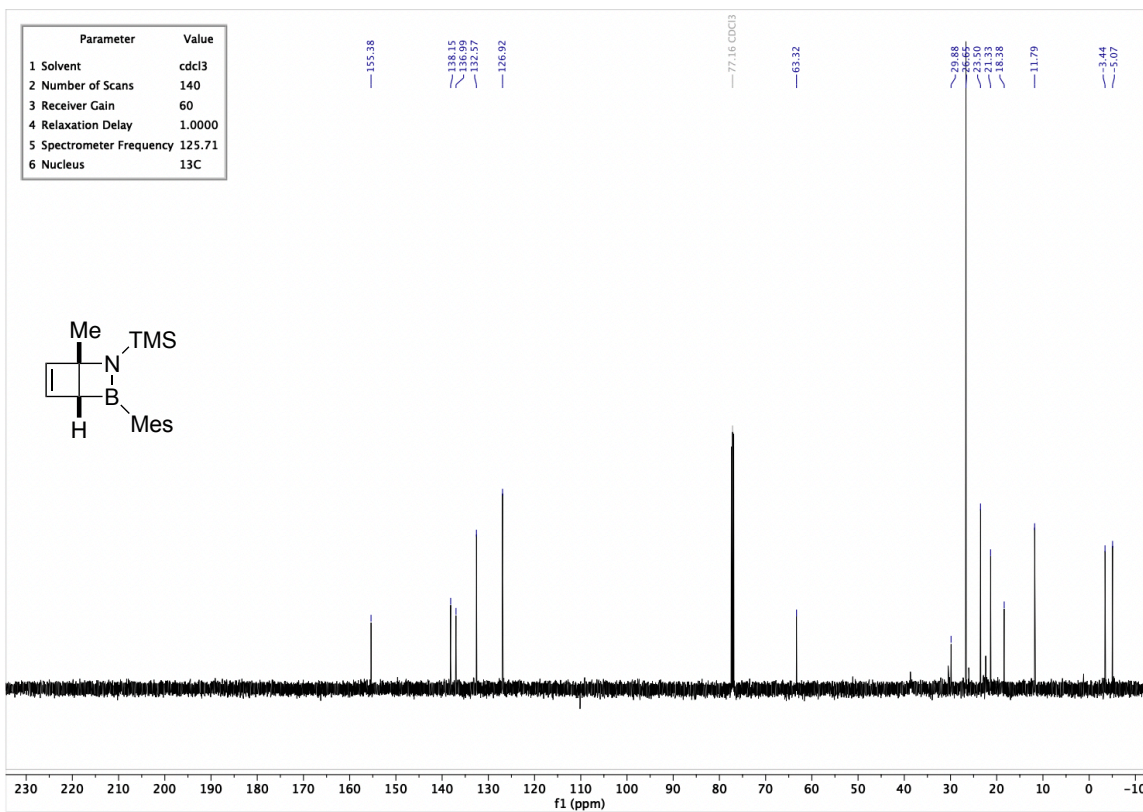


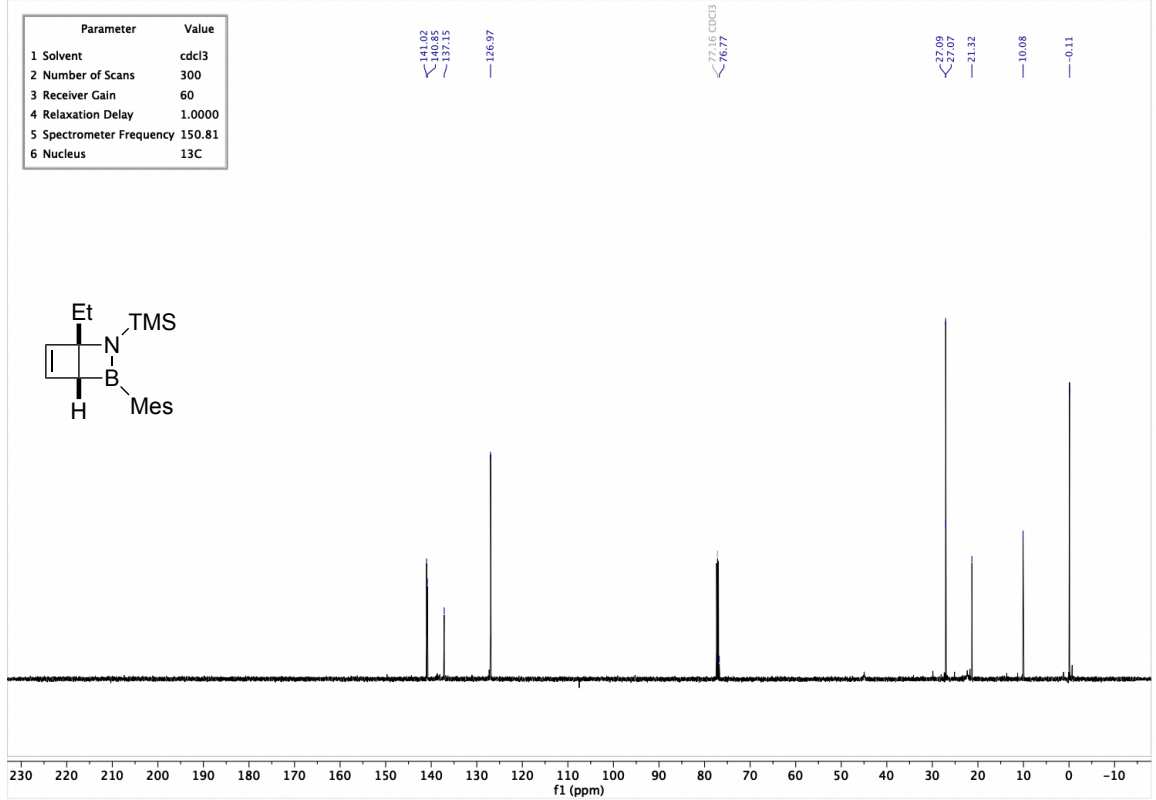
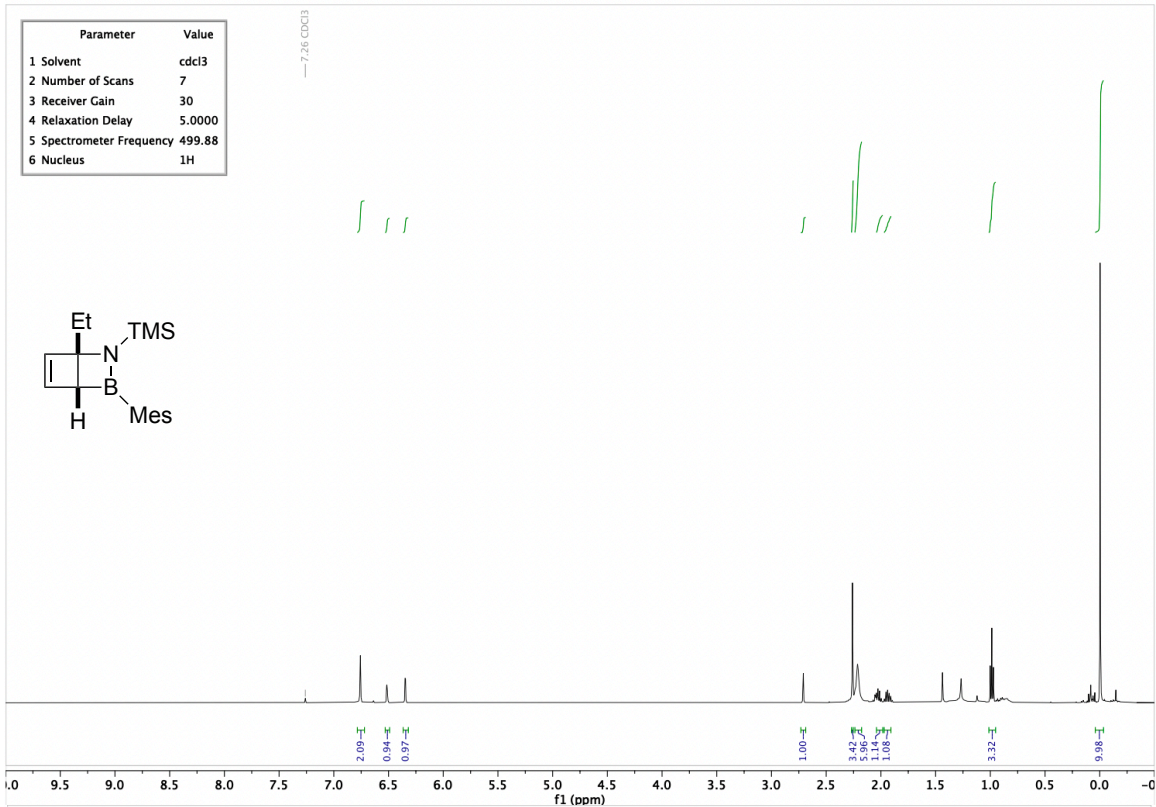


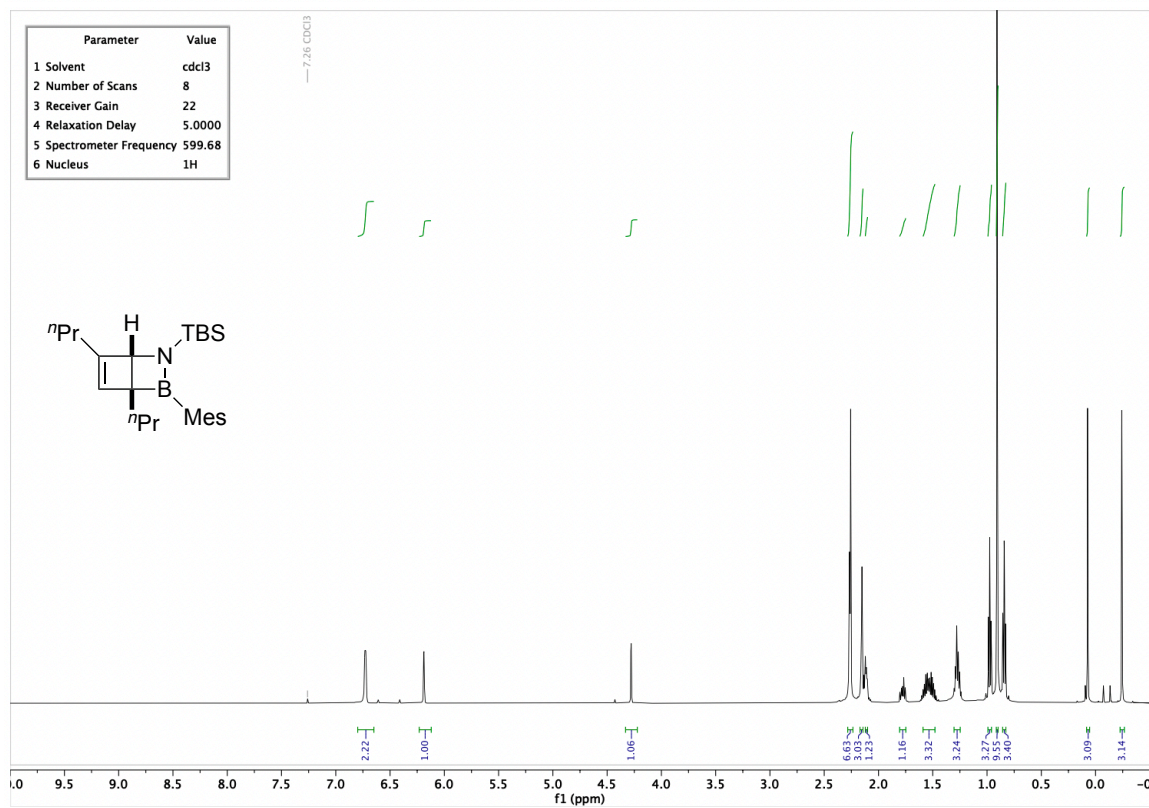
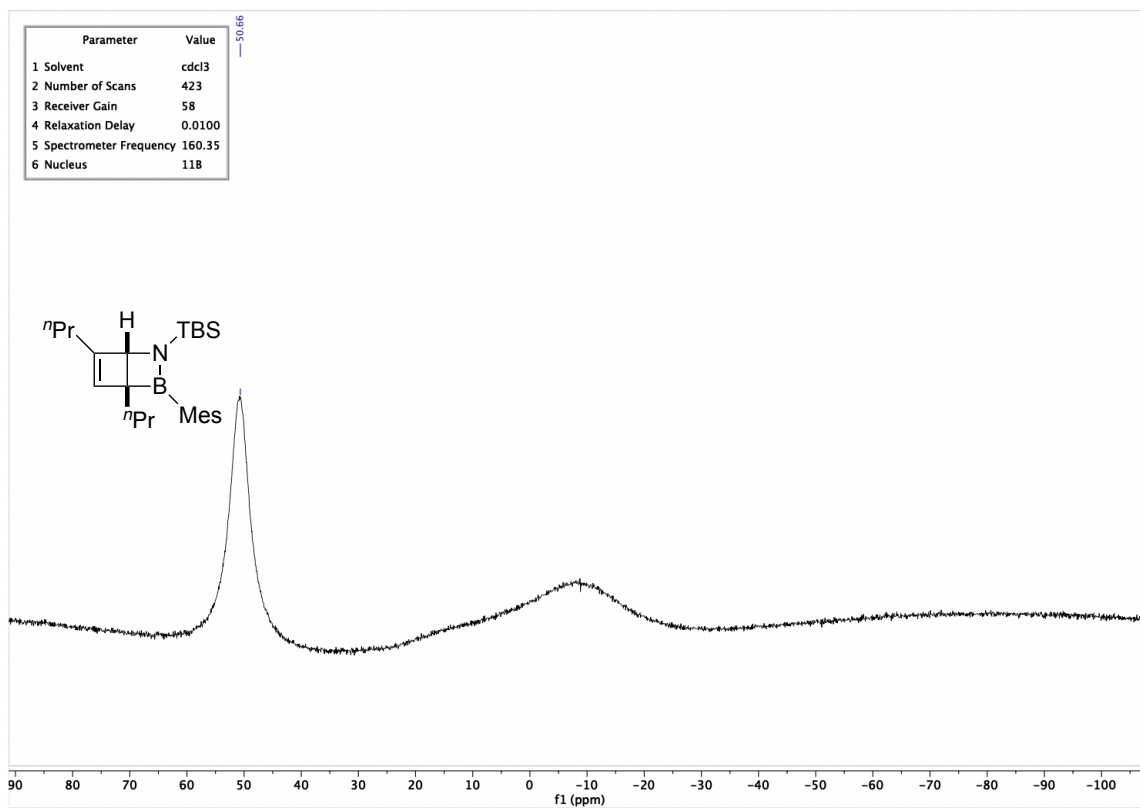


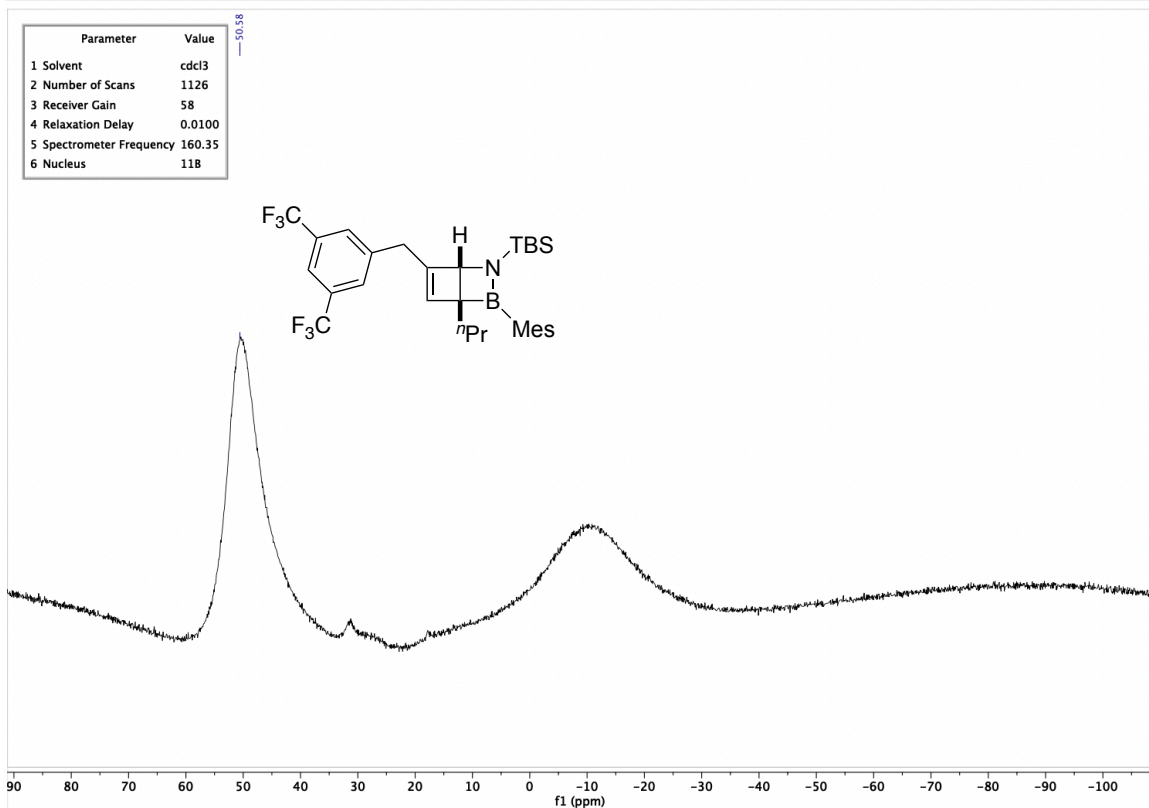
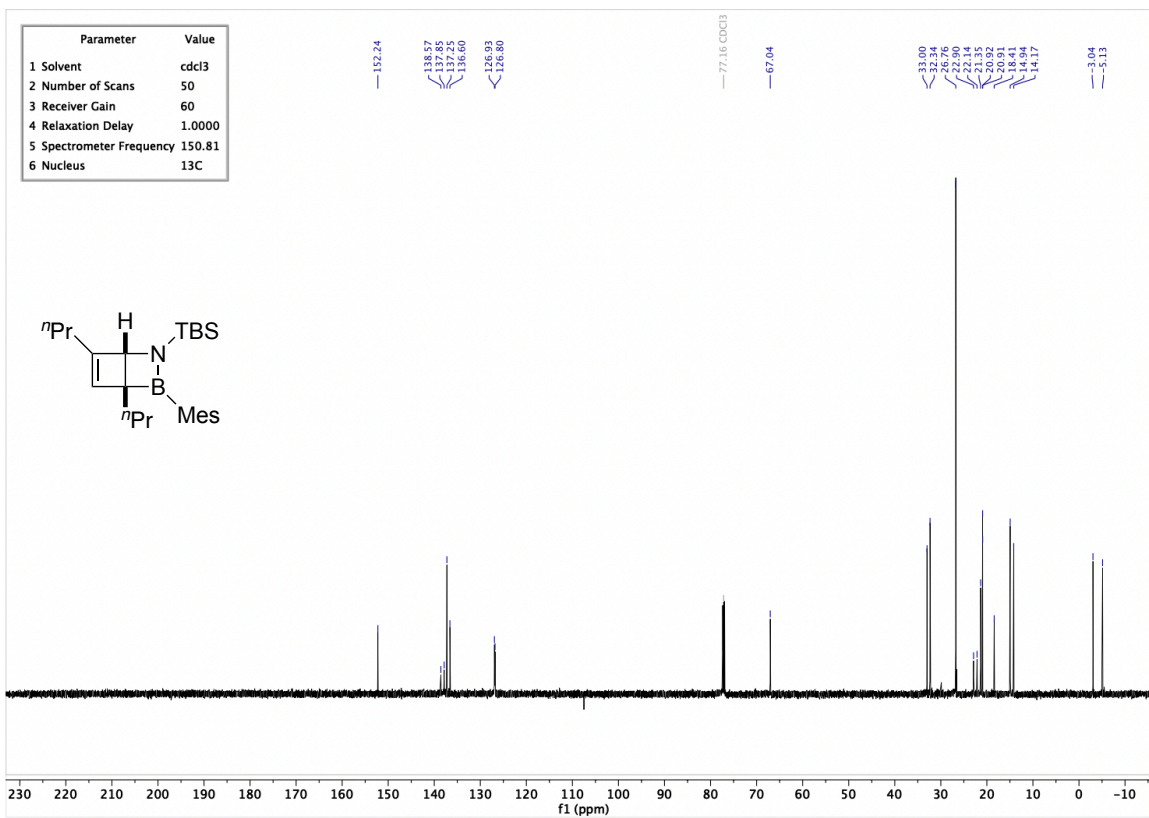


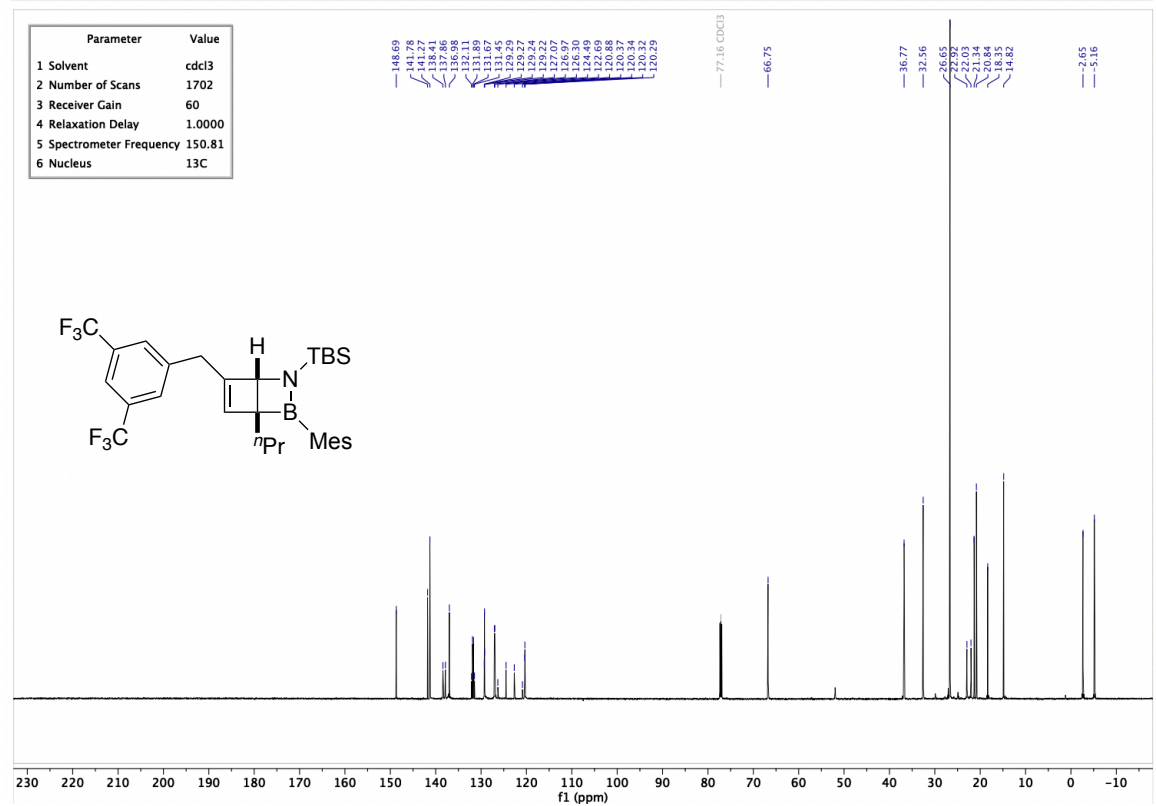
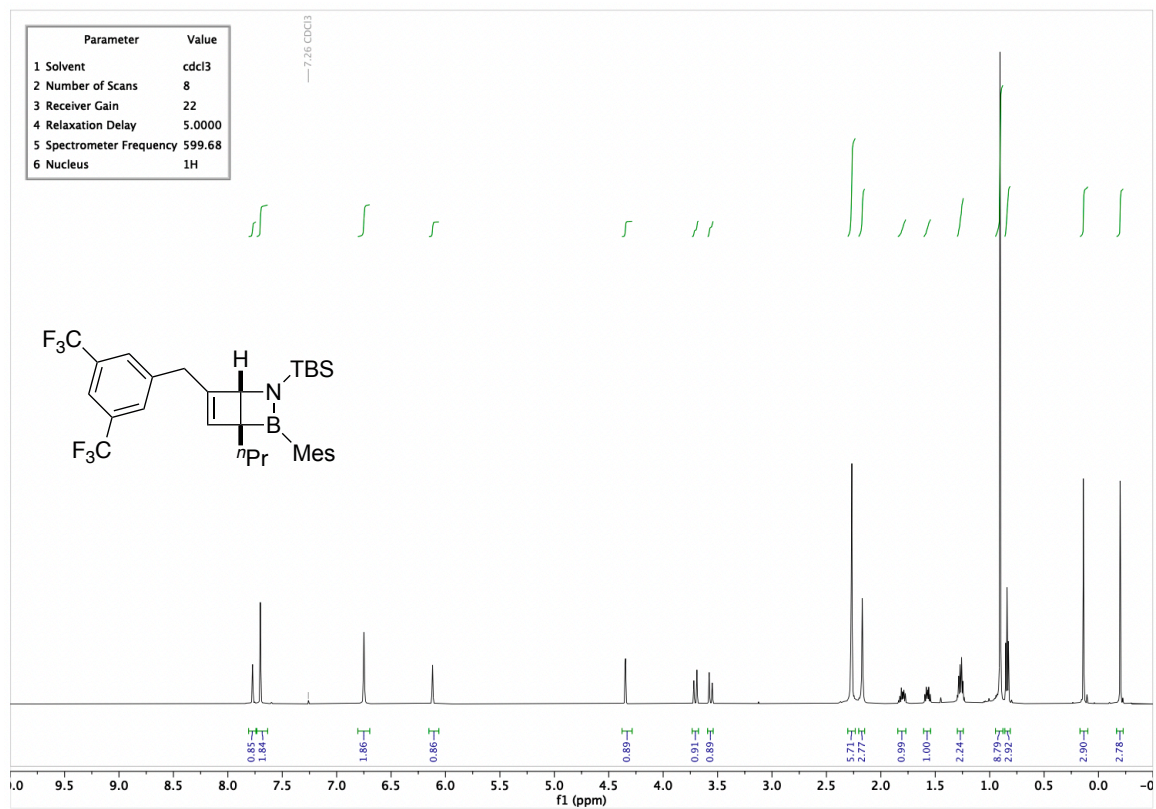




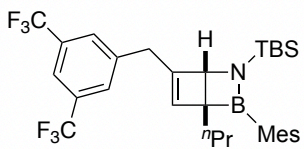




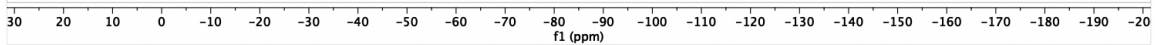




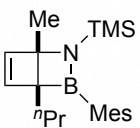
Parameter	Value
1 Solvent	cdcl3
2 Number of Scans	50
3 Receiver Gain	40
4 Relaxation Delay	1.0000
5 Spectrometer Frequency	564.21
6 Nucleus	19F



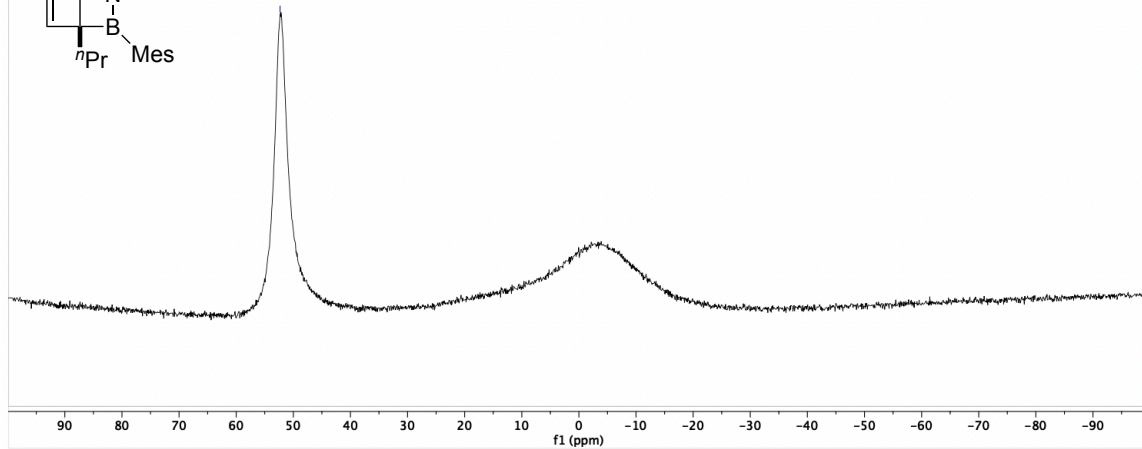
-62.74

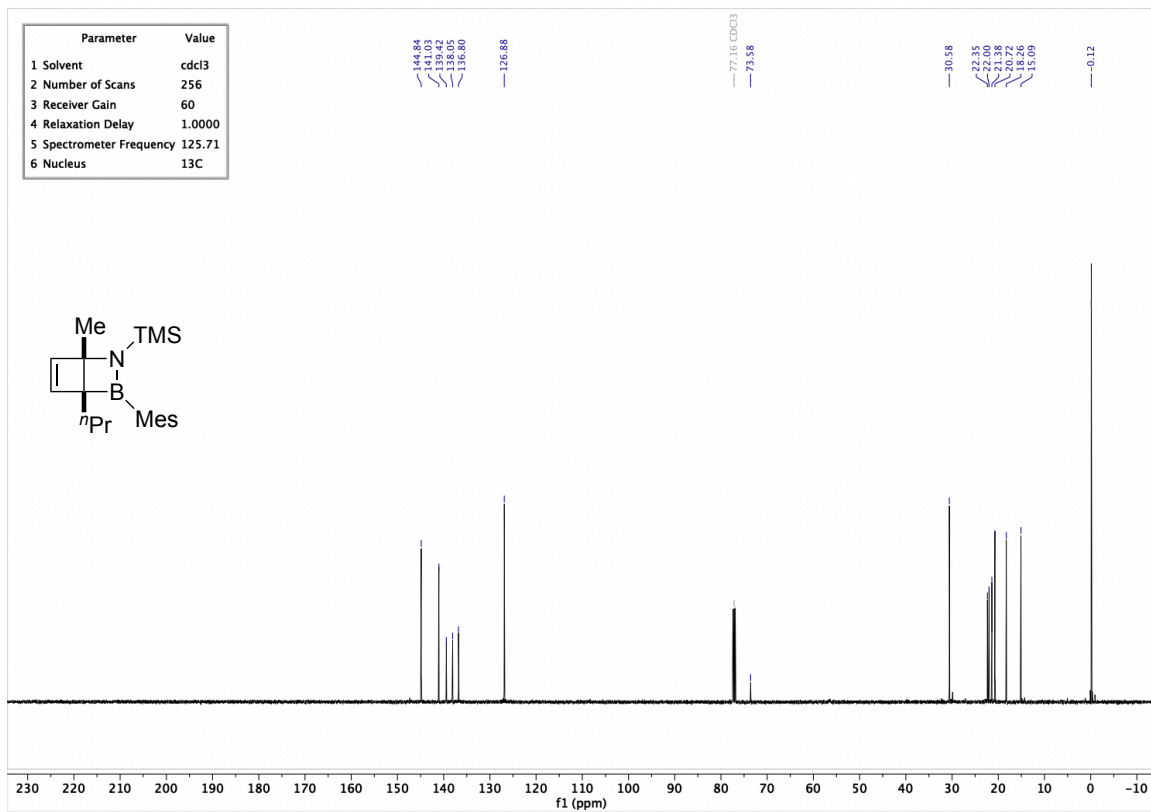
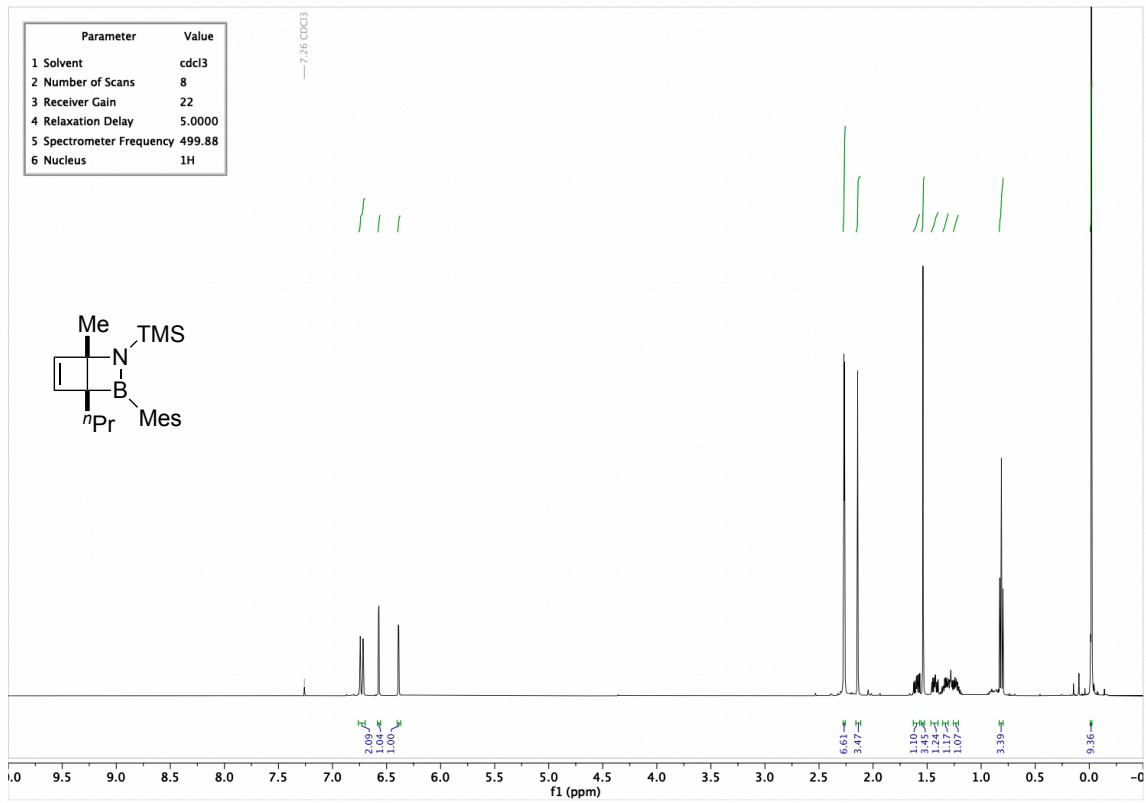


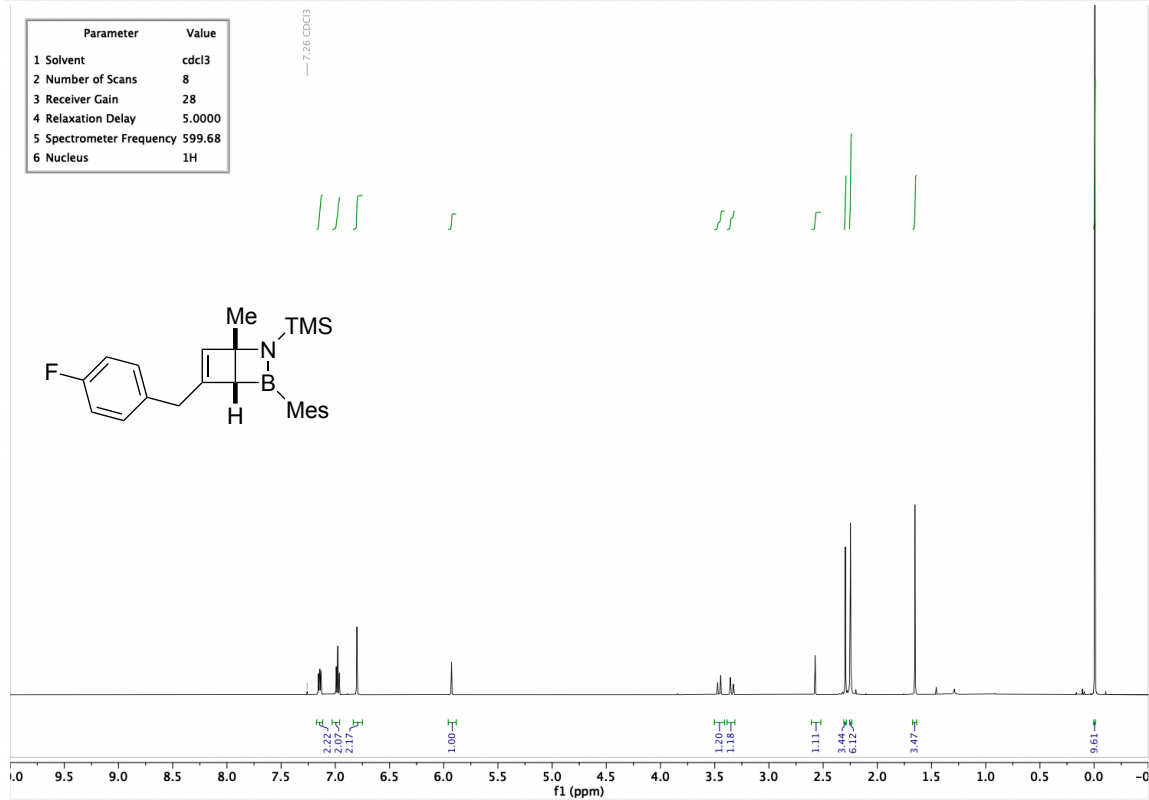
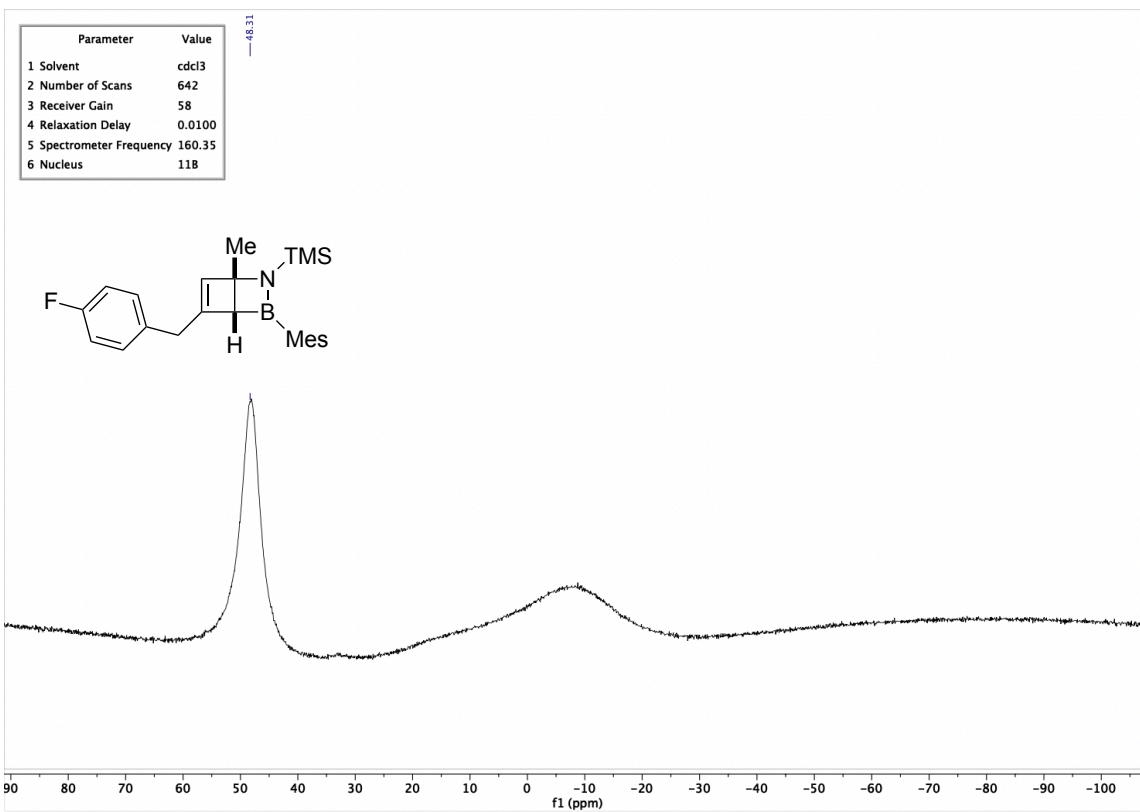
Parameter	Value
1 Solvent	cdcl3
2 Number of Scans	117
3 Receiver Gain	60
4 Relaxation Delay	0.0100
5 Spectrometer Frequency	160.38
6 Nucleus	11B

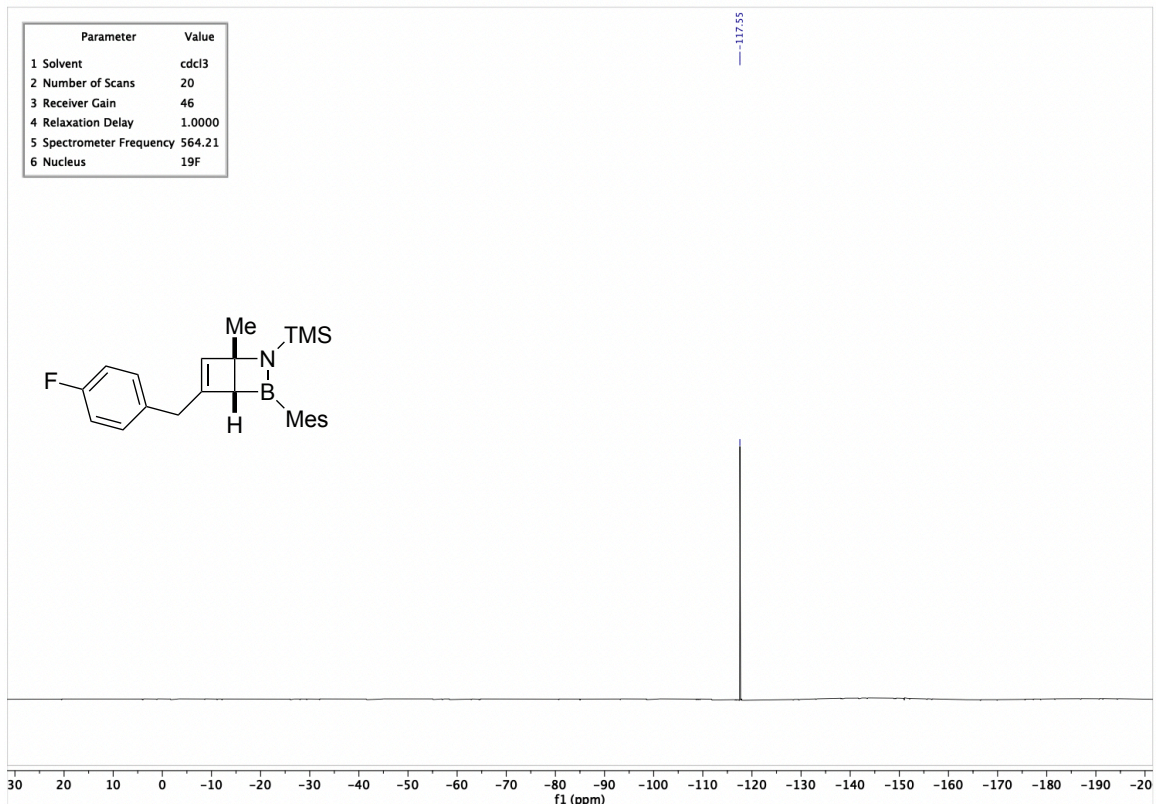
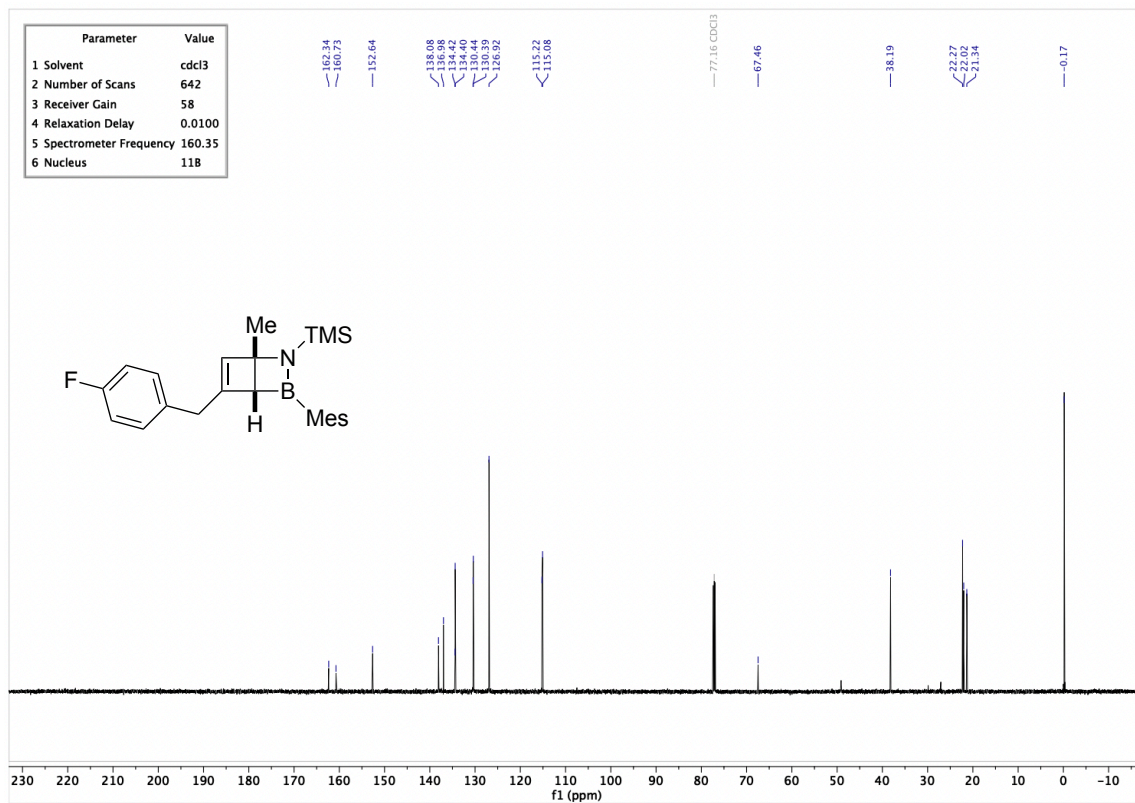


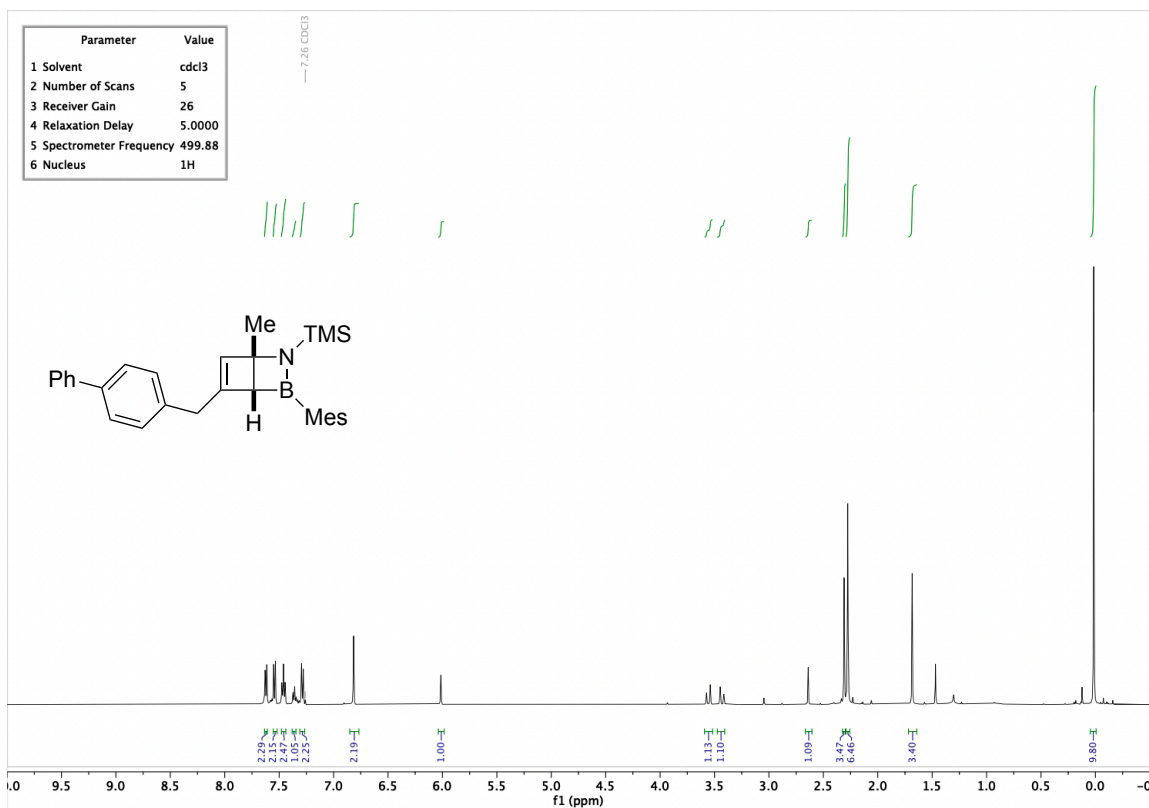
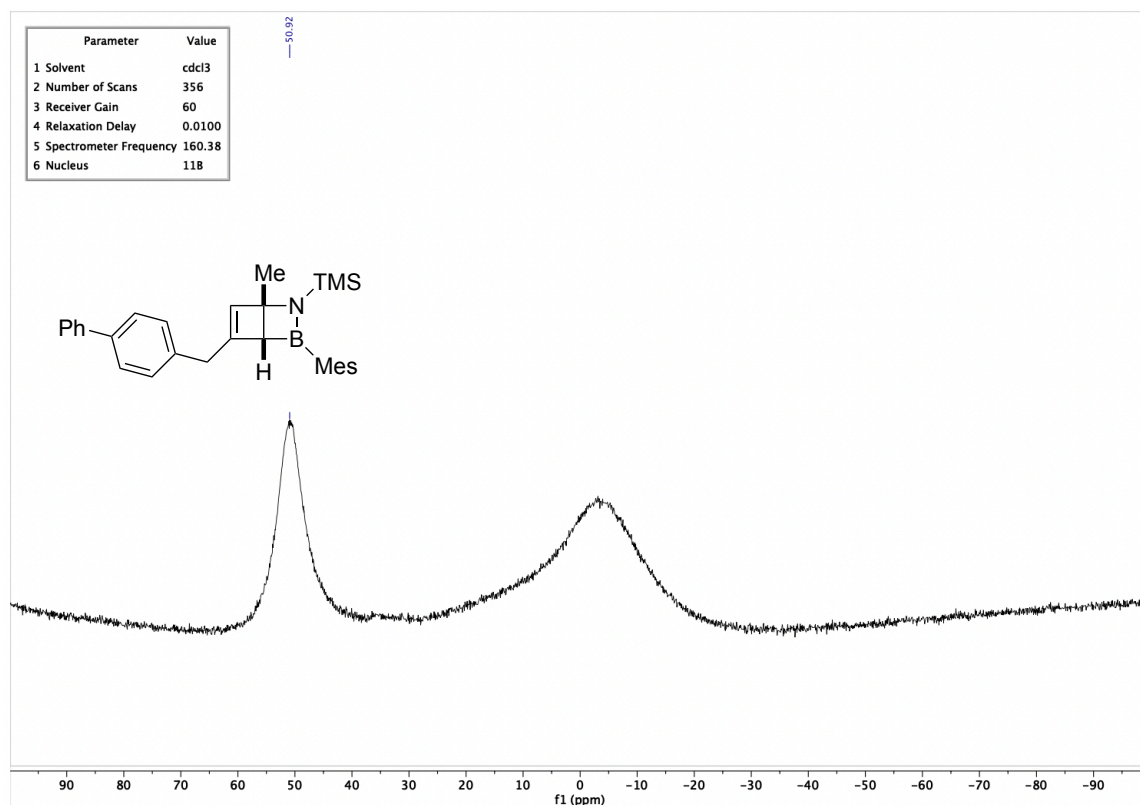
-52.32

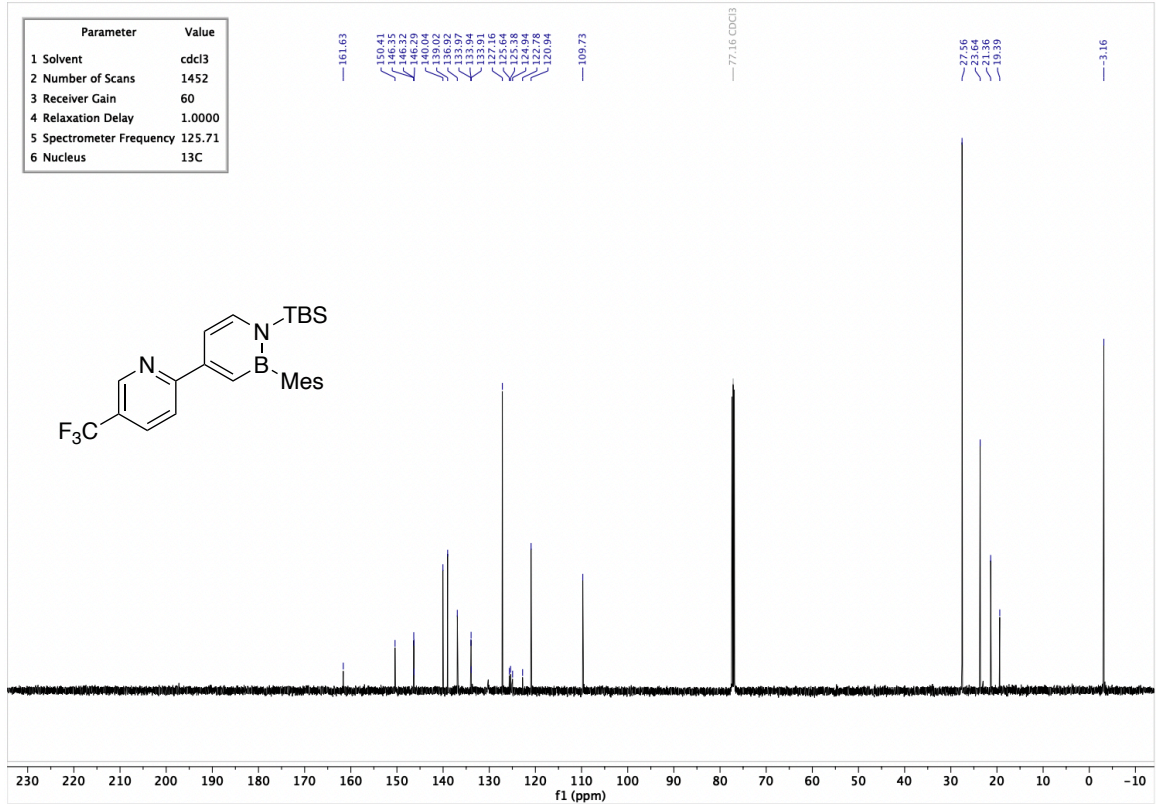
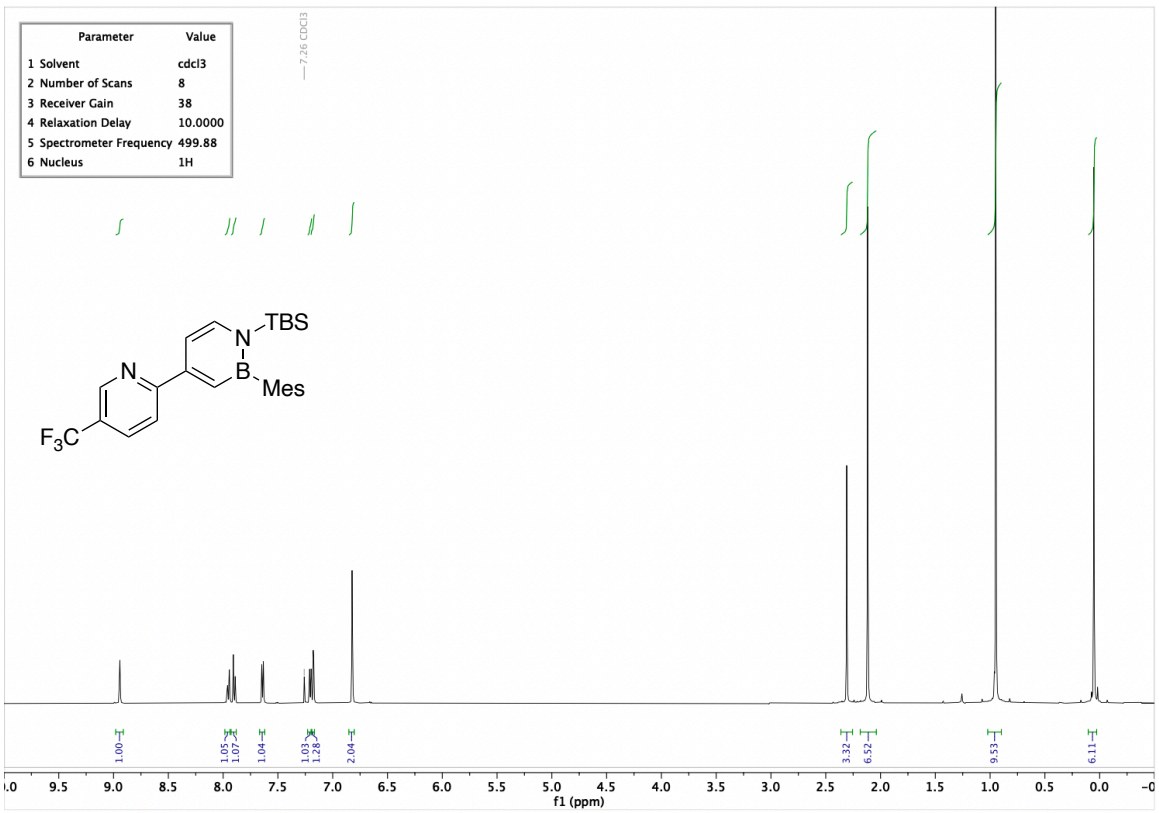


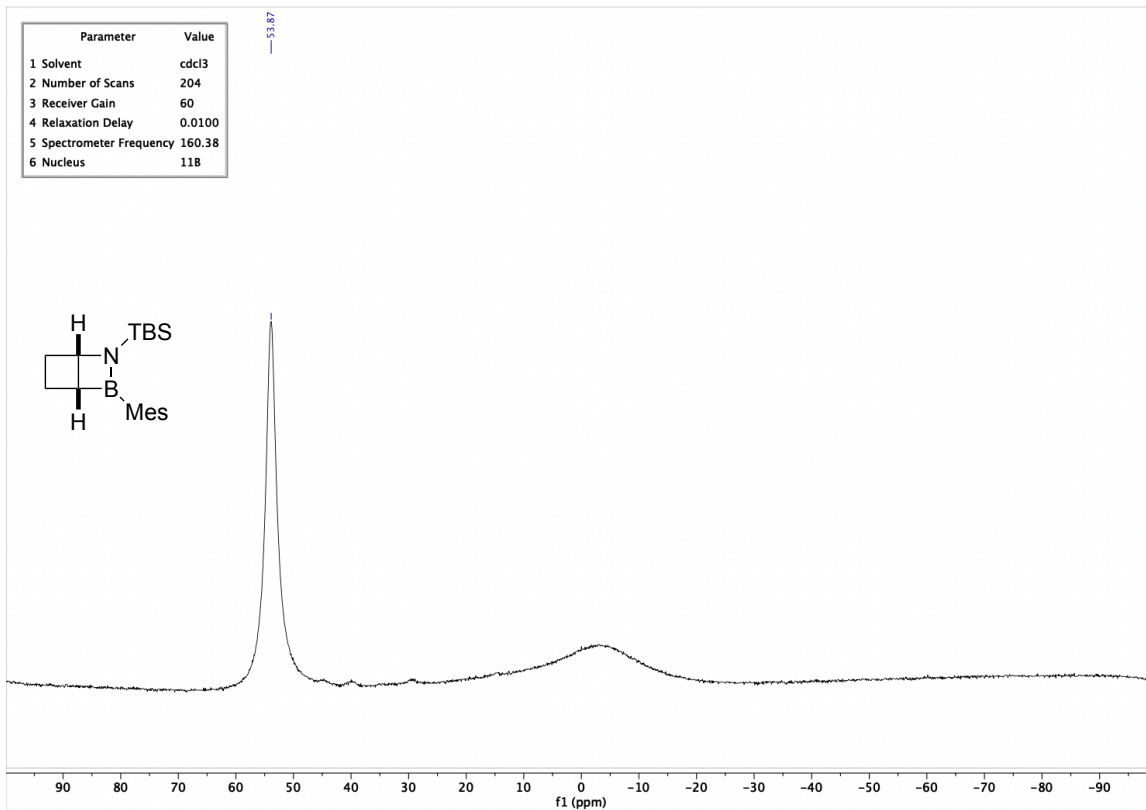
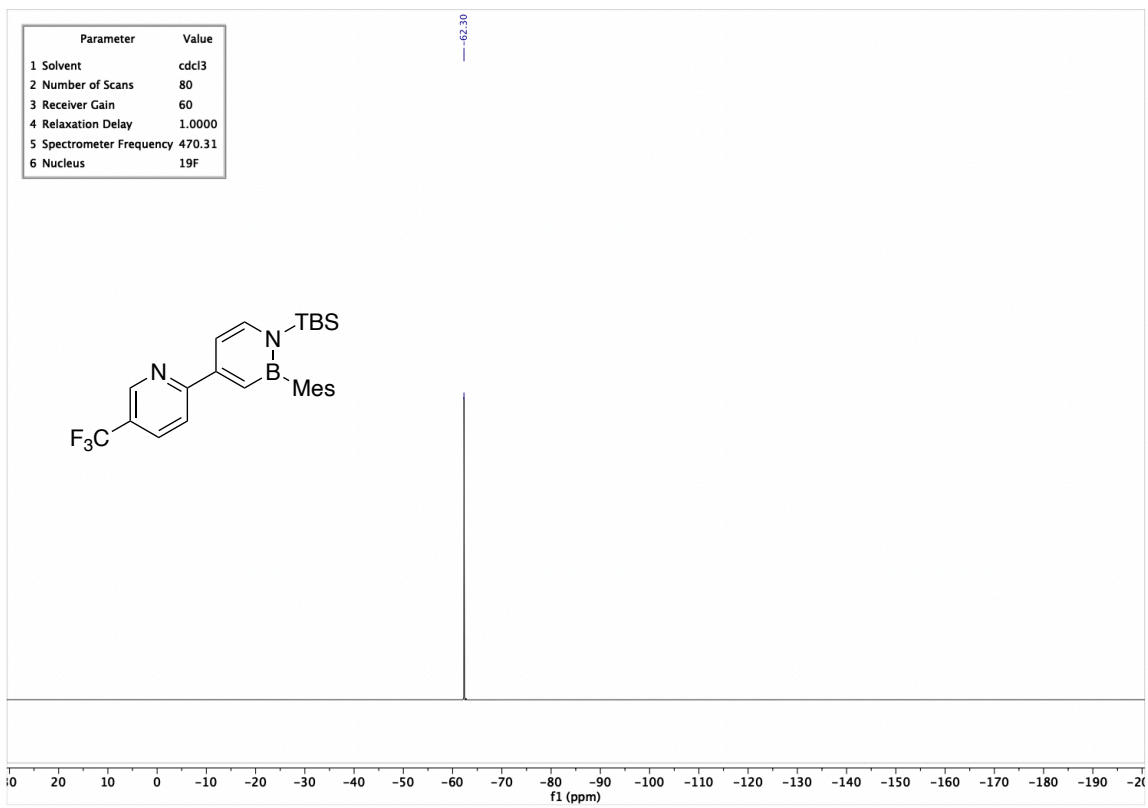


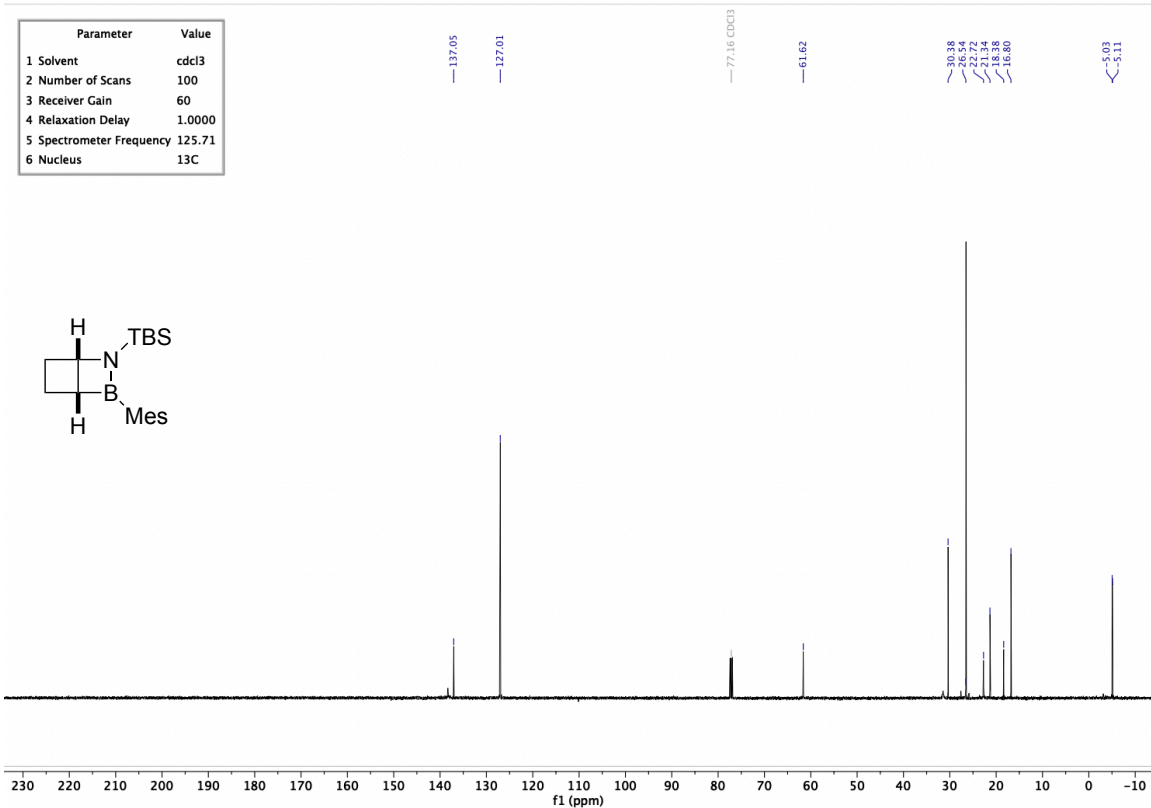
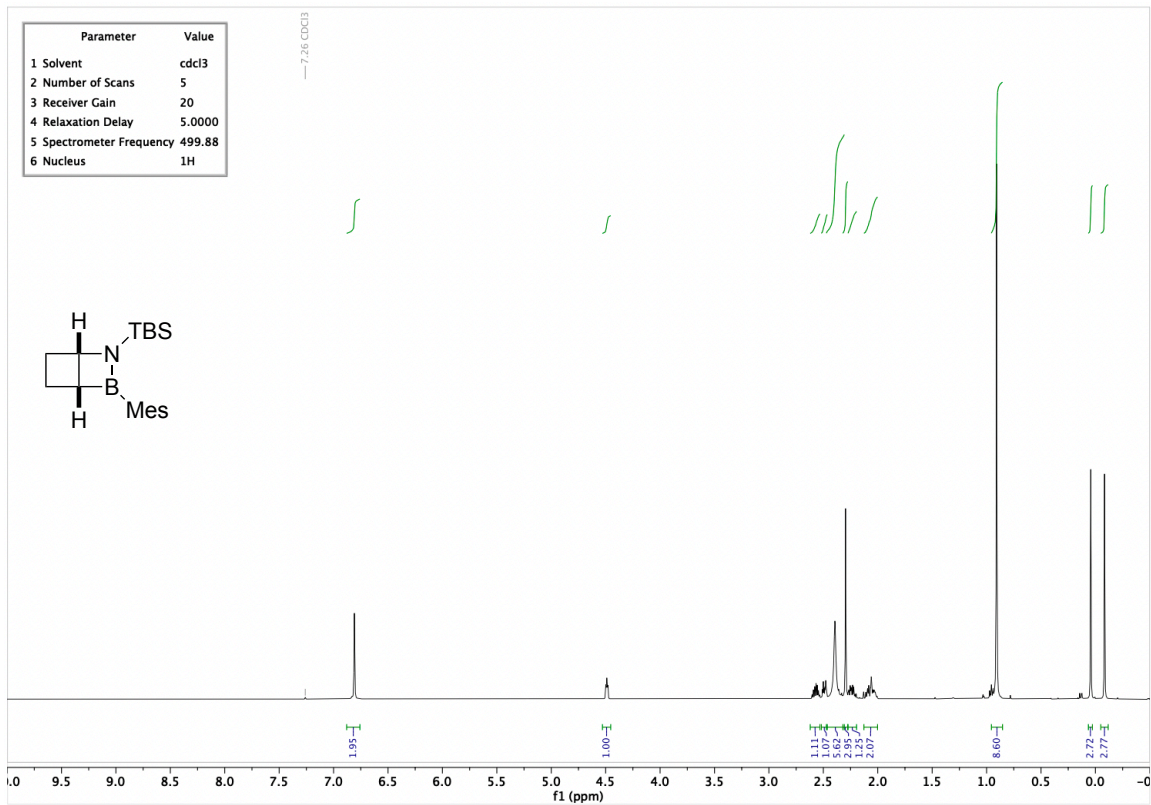


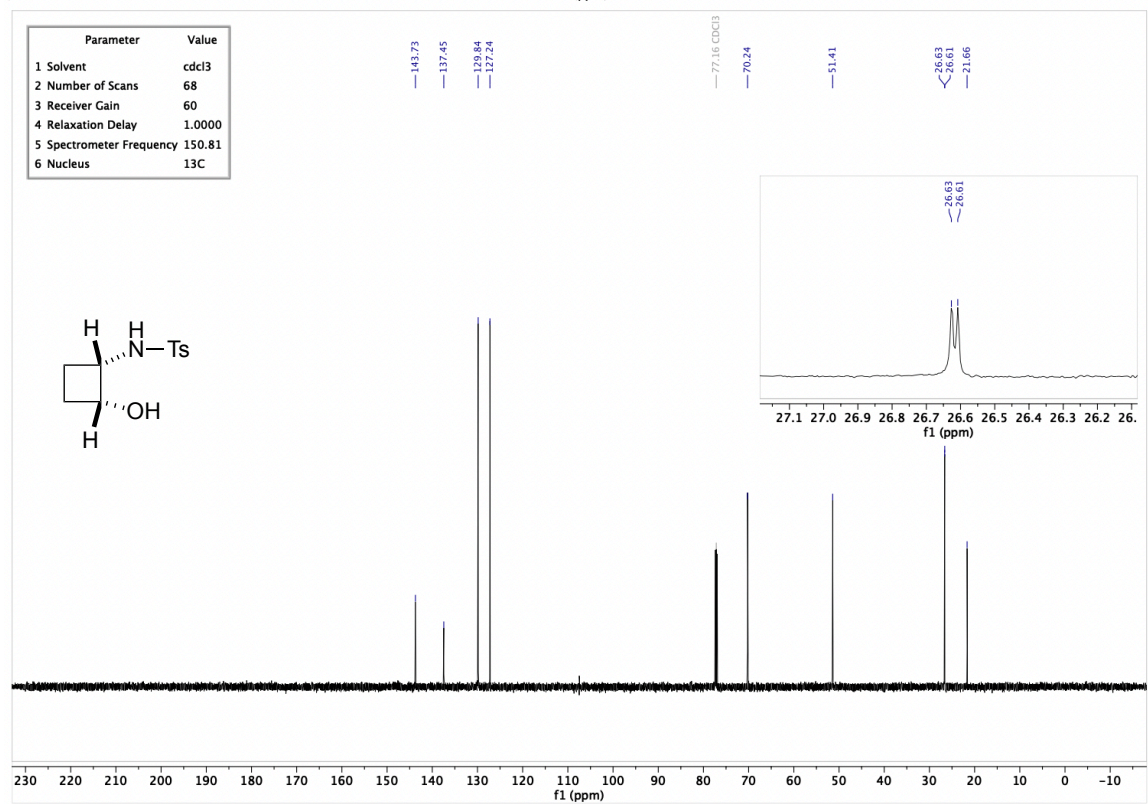
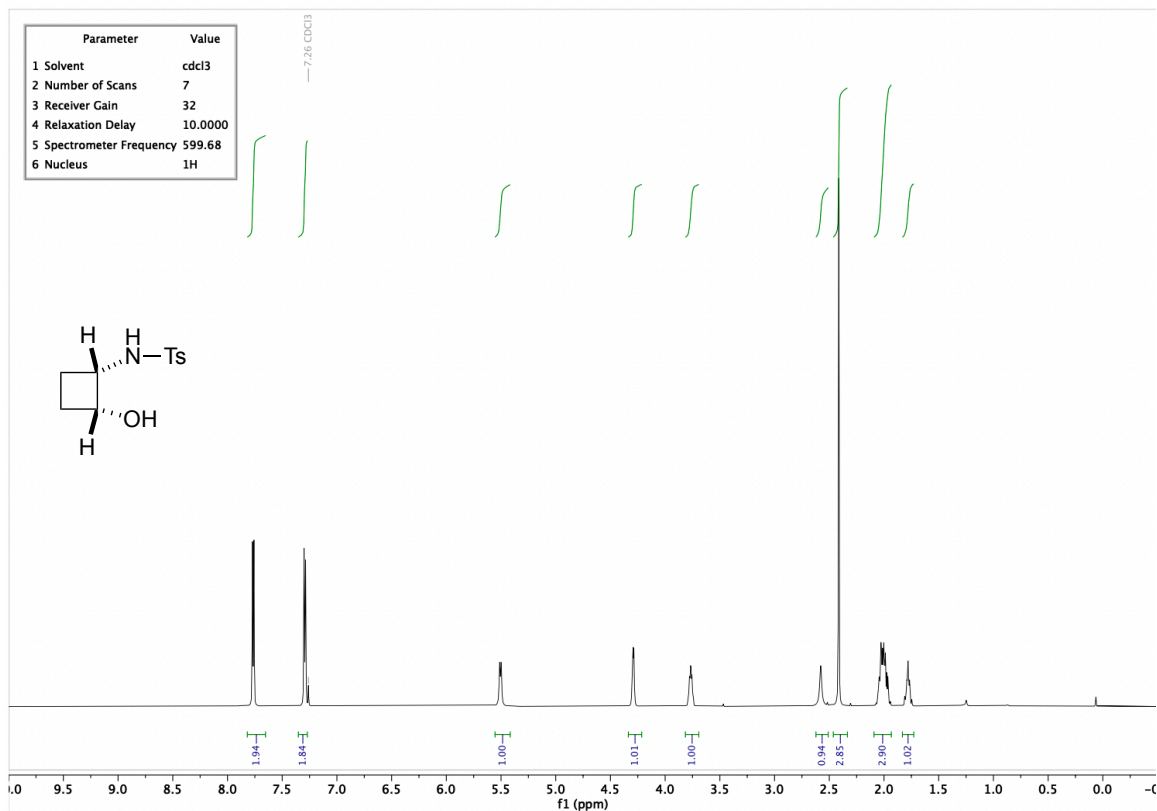


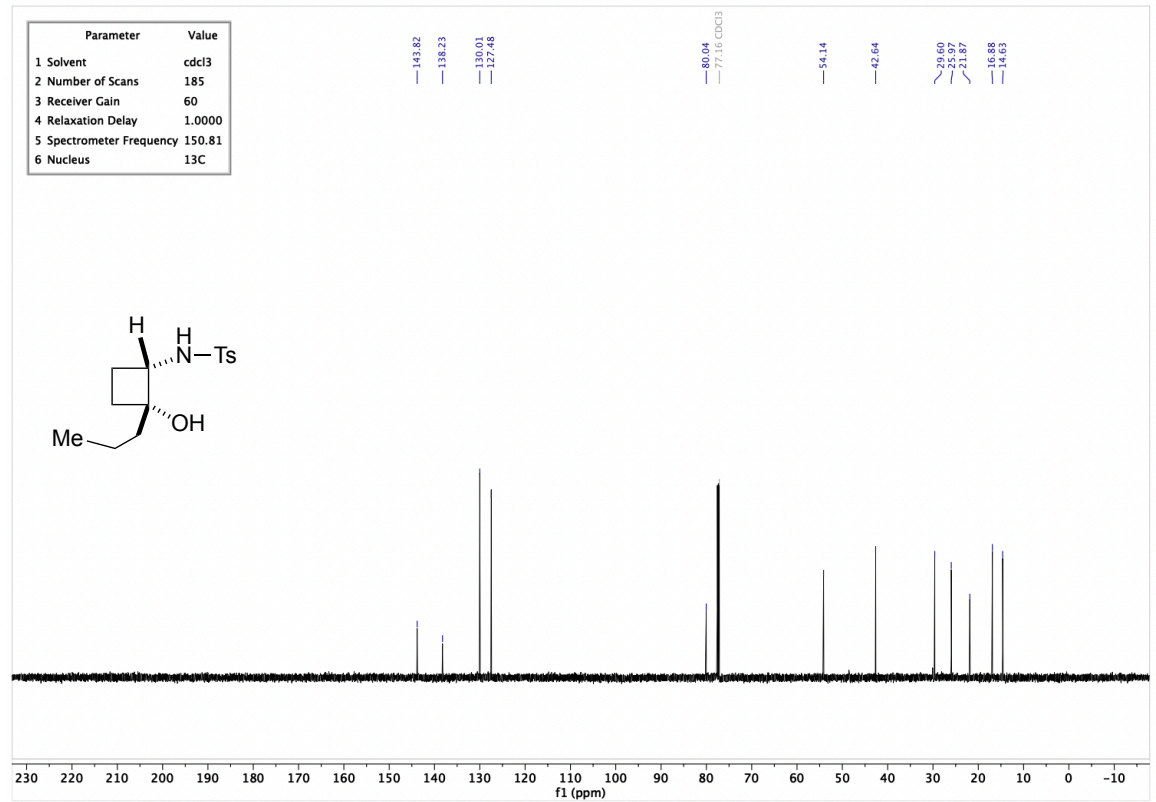
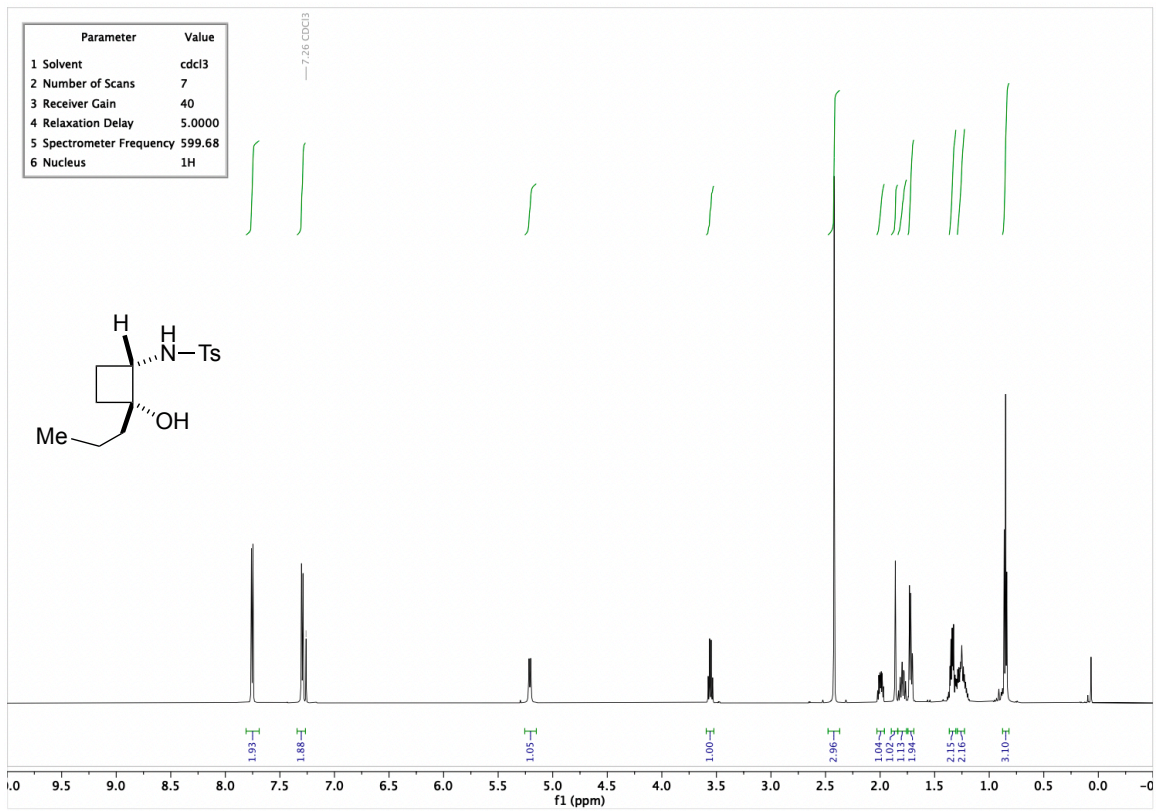


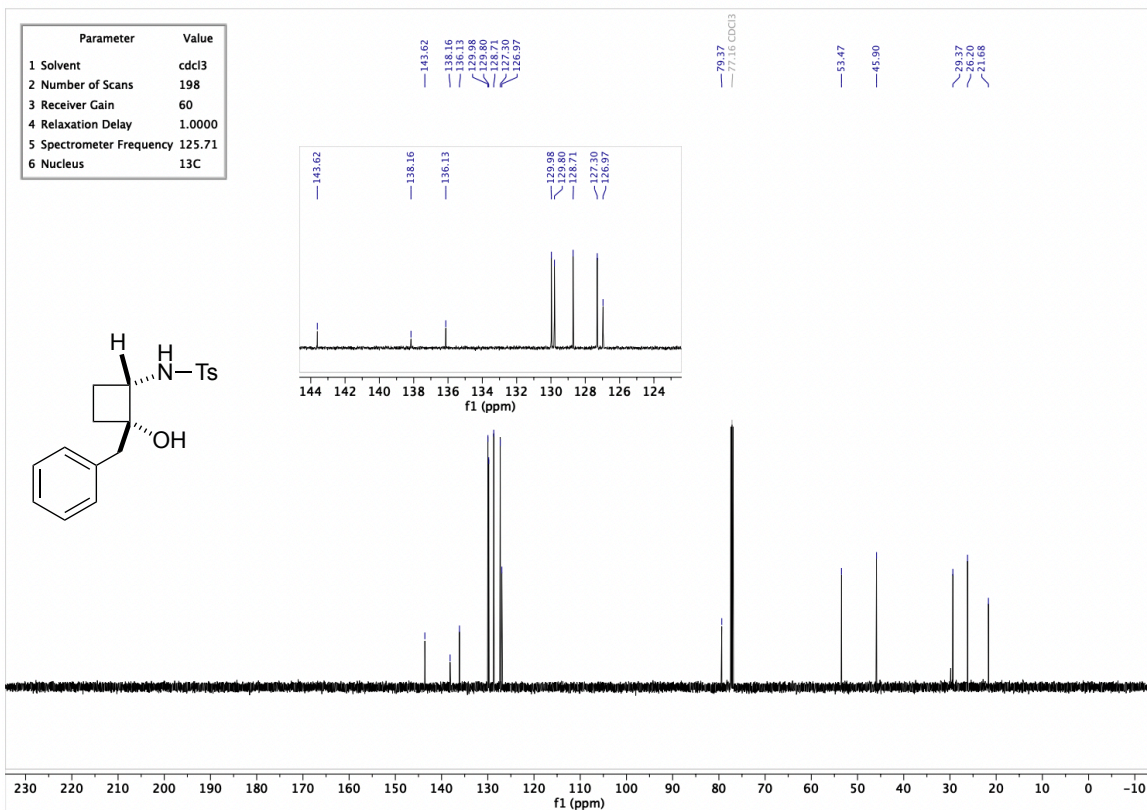
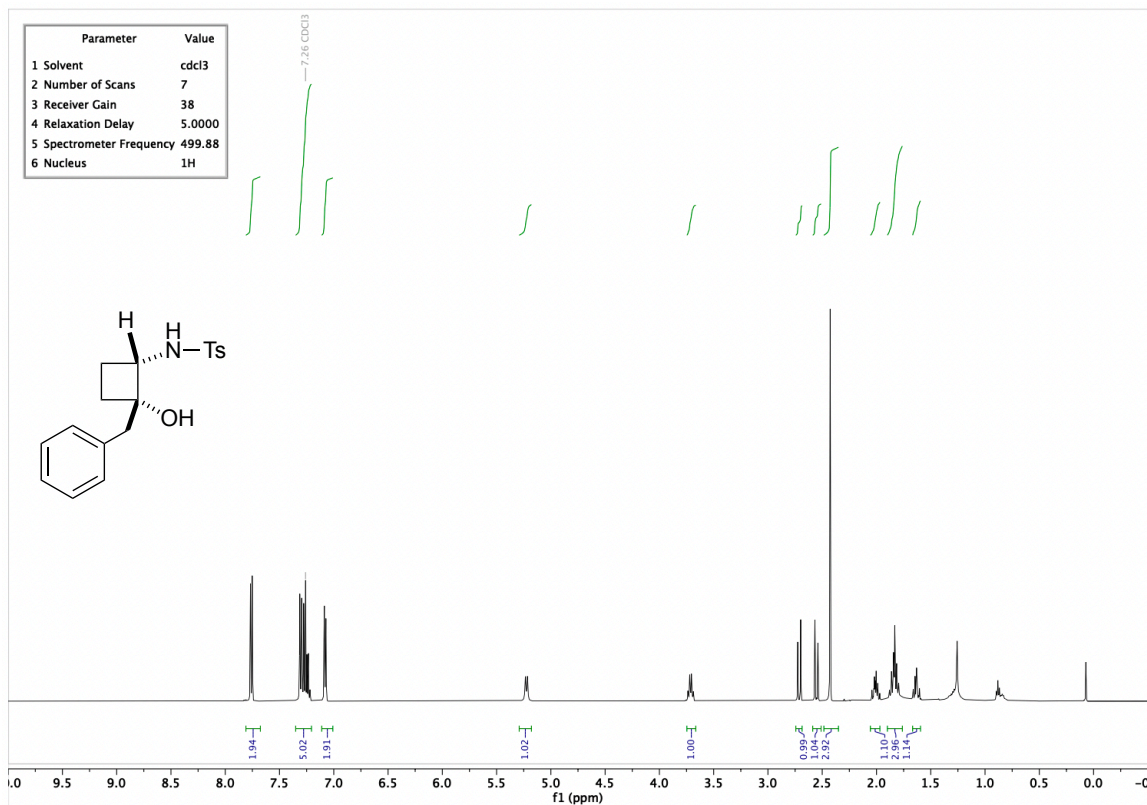


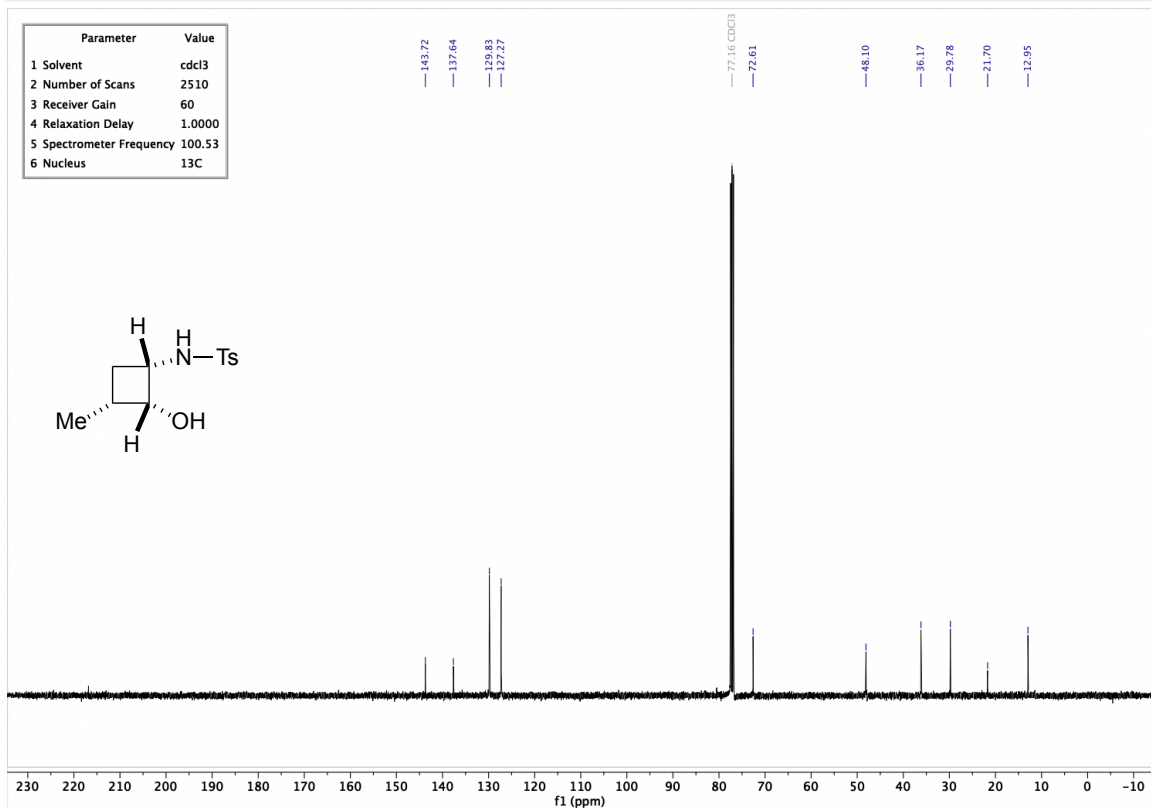
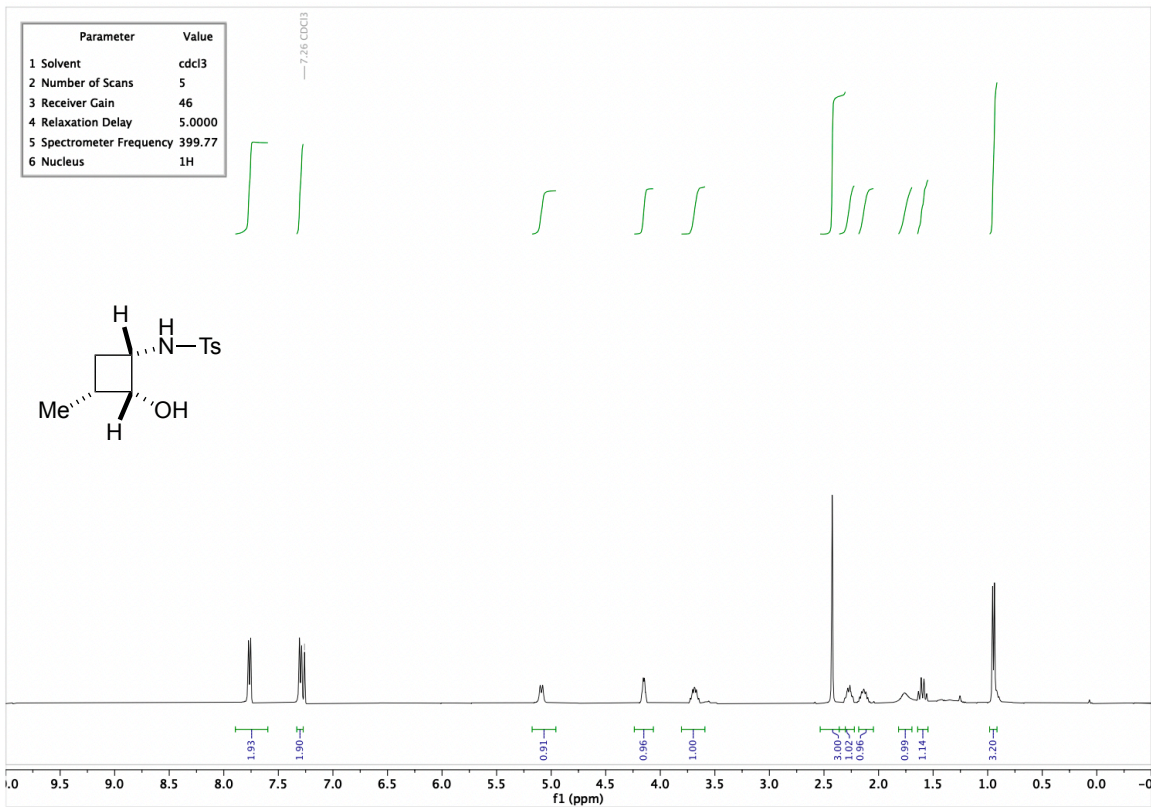


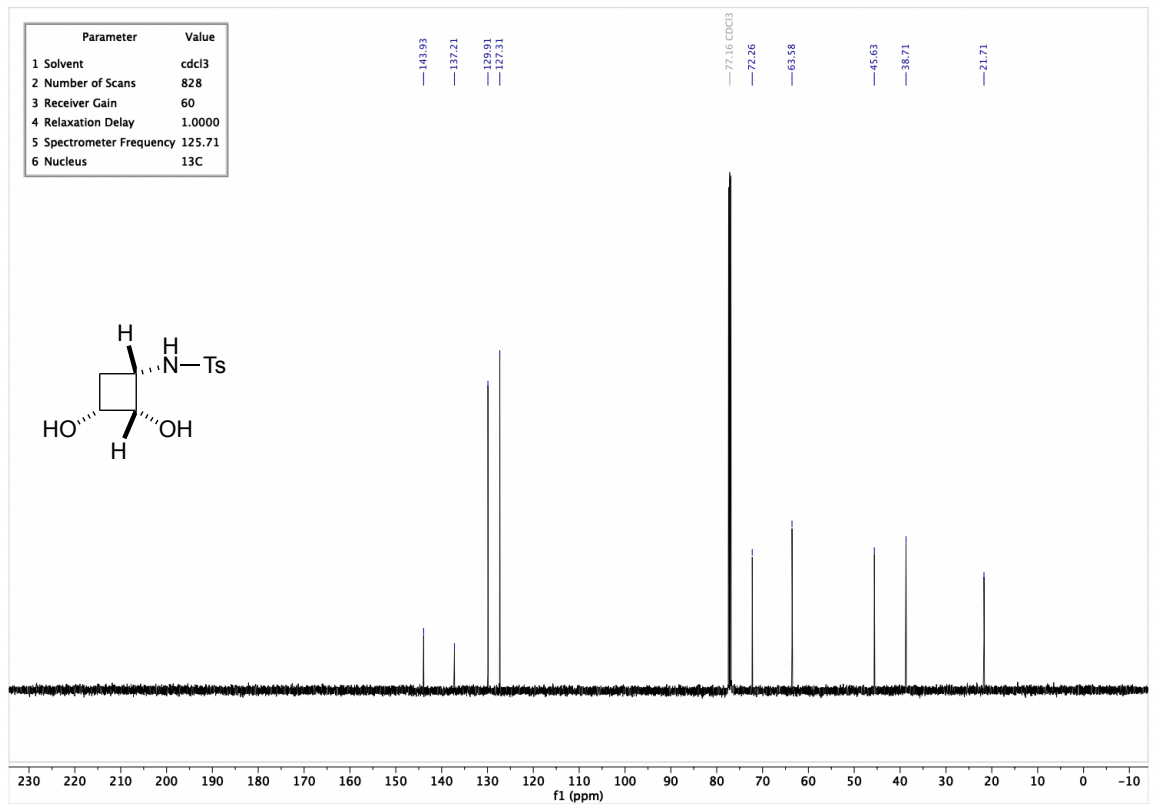
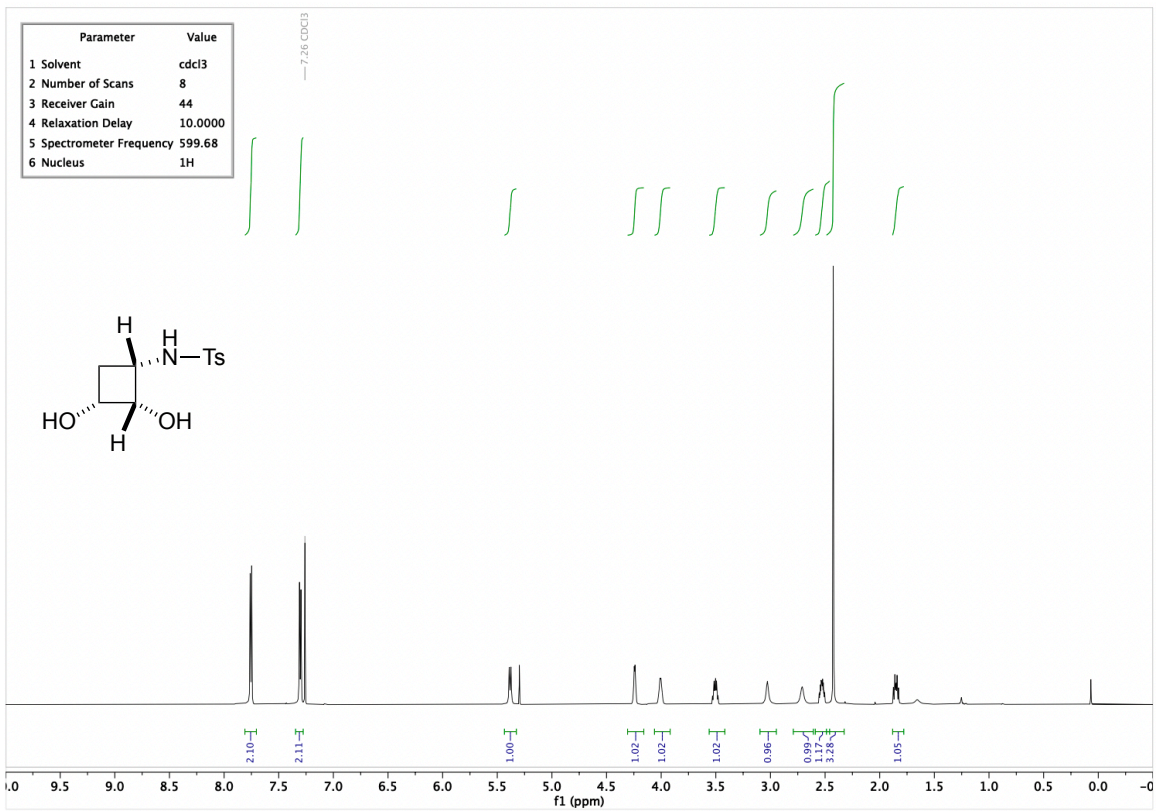


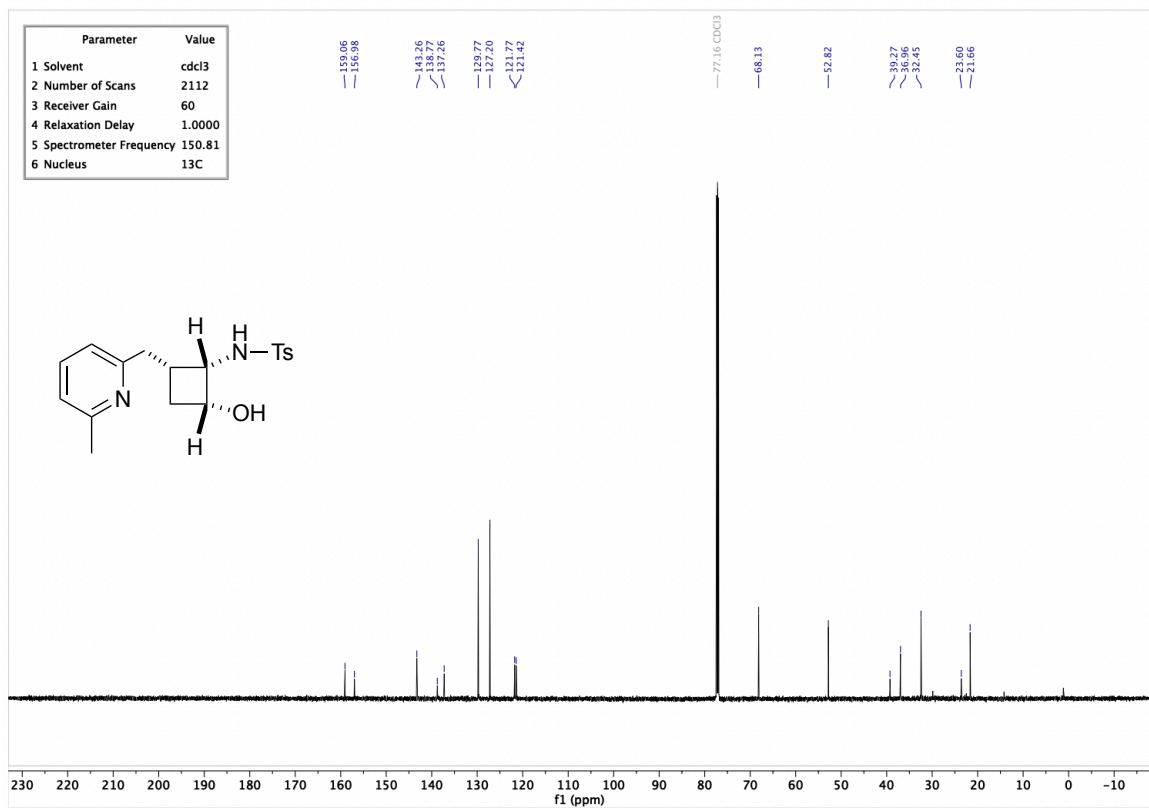
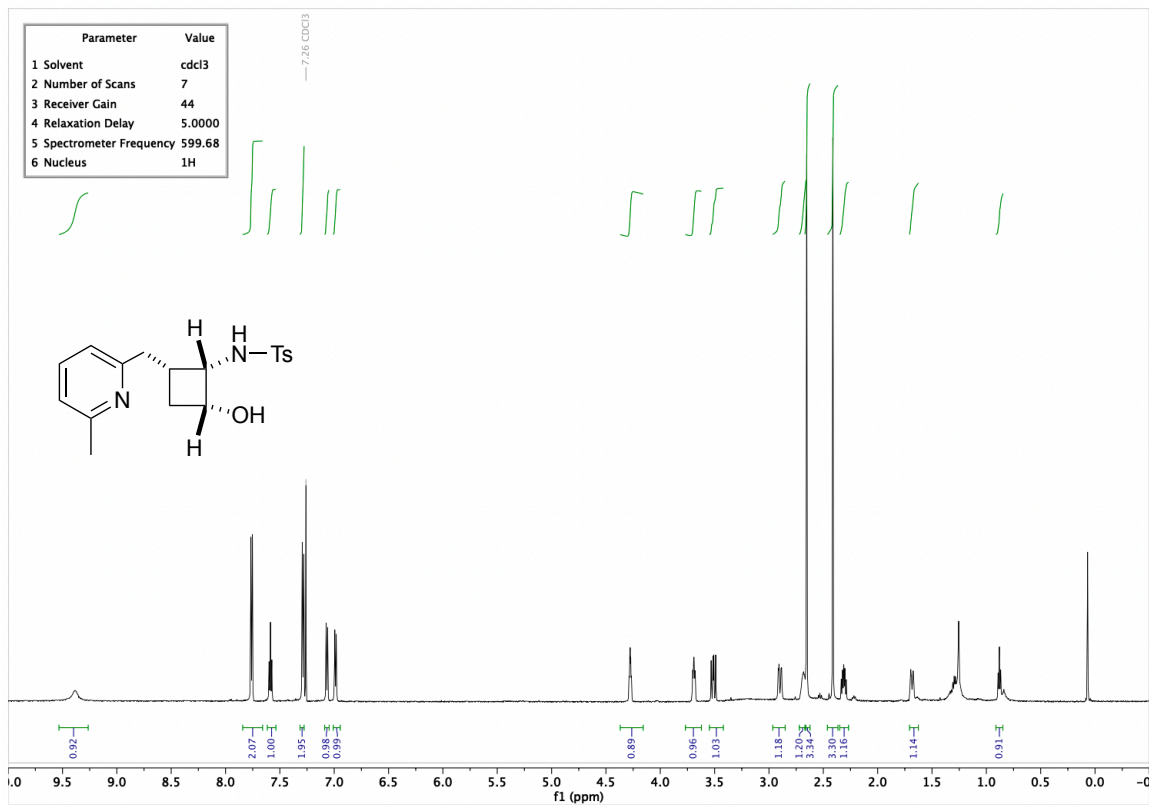


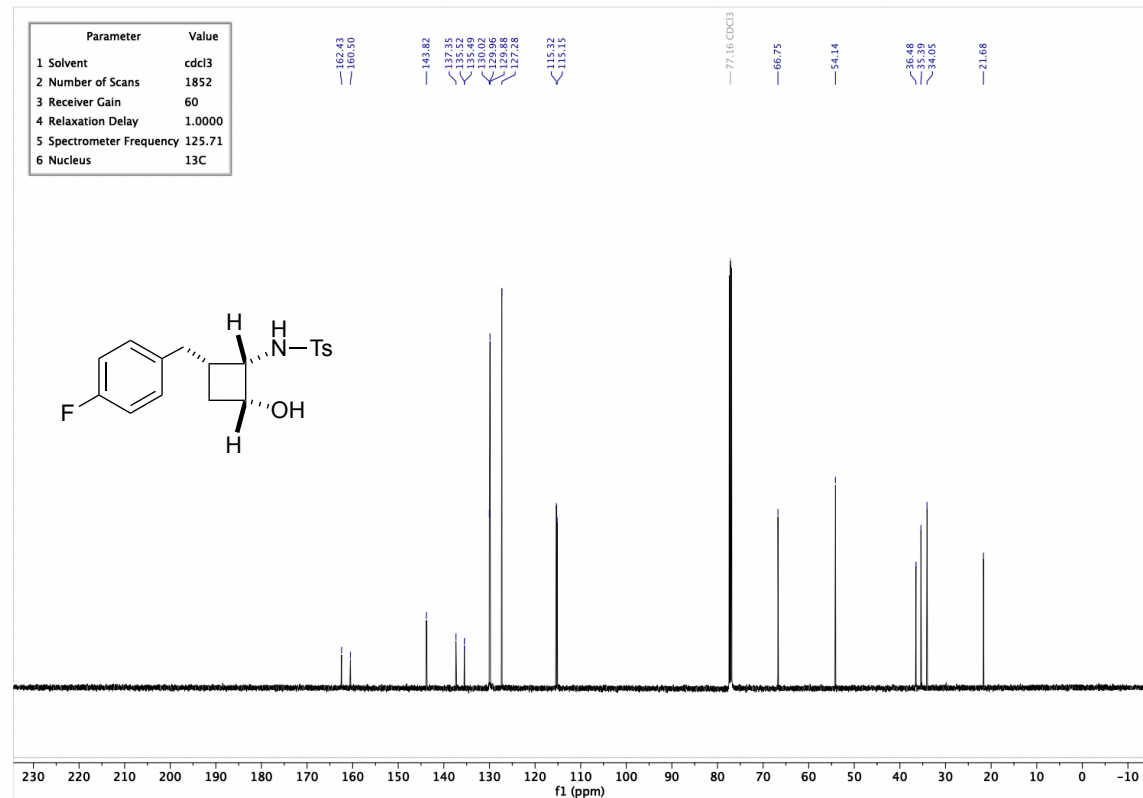
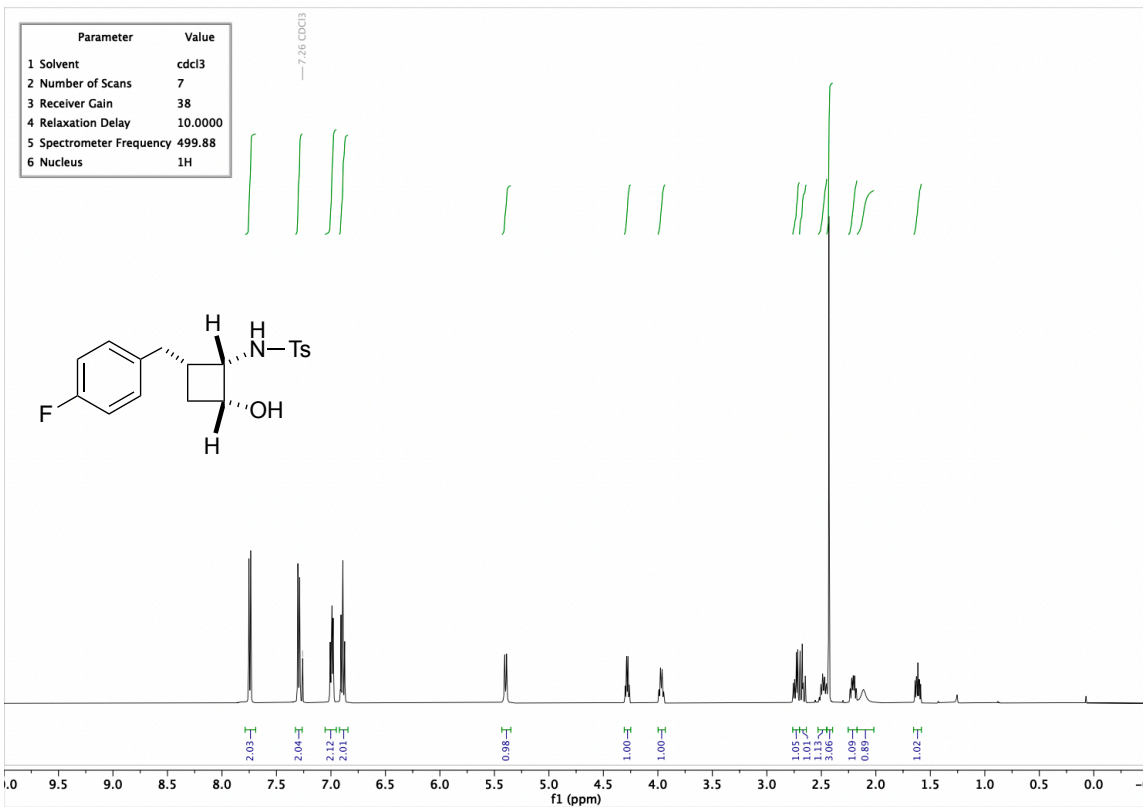


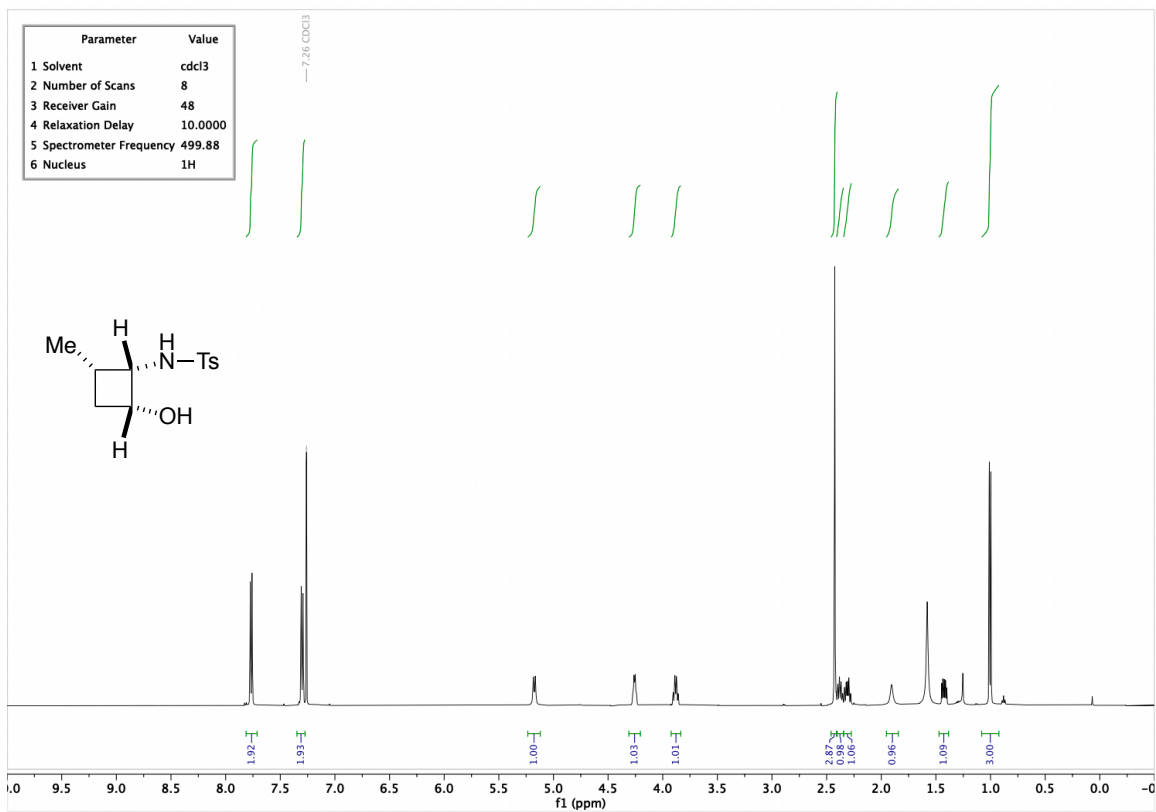
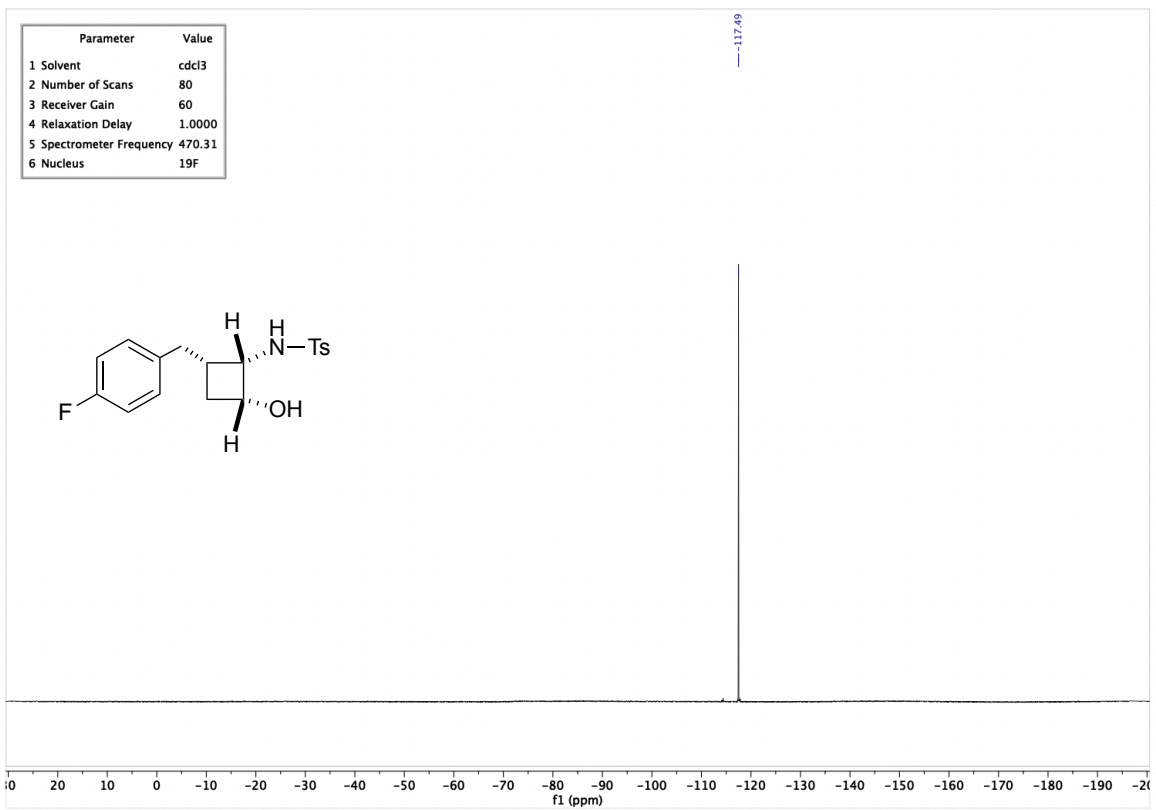


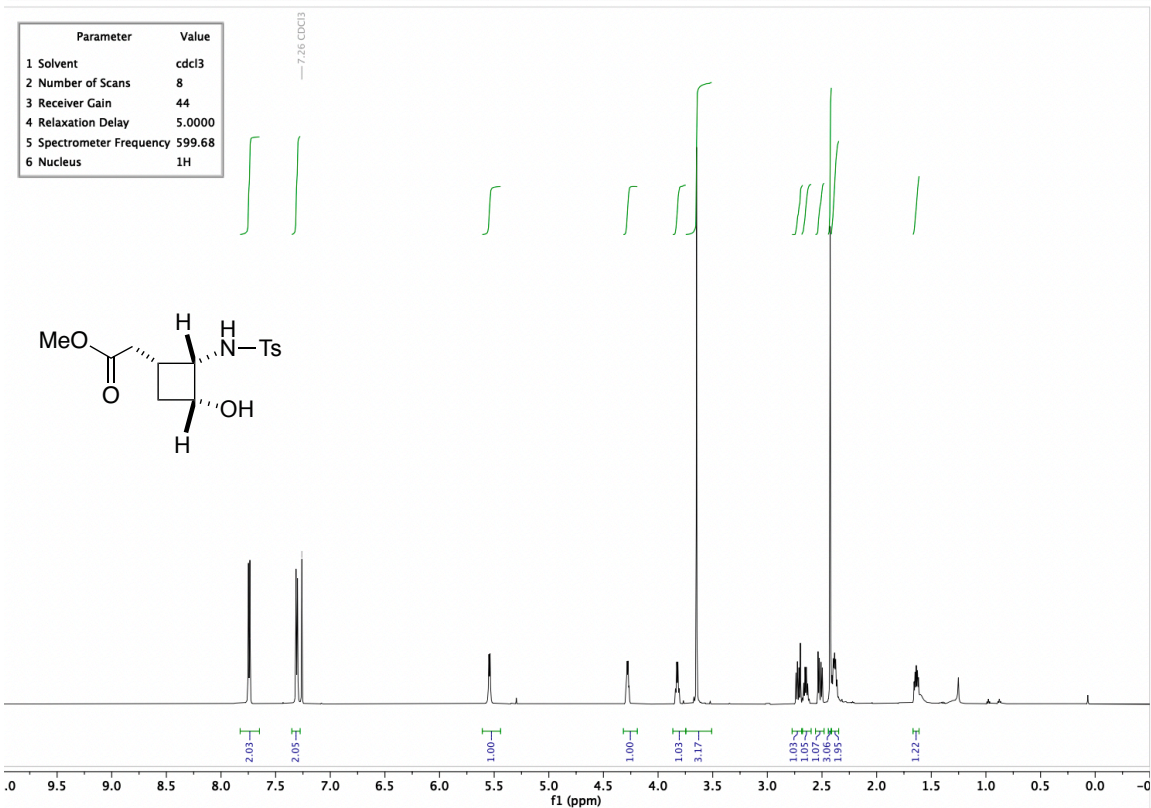
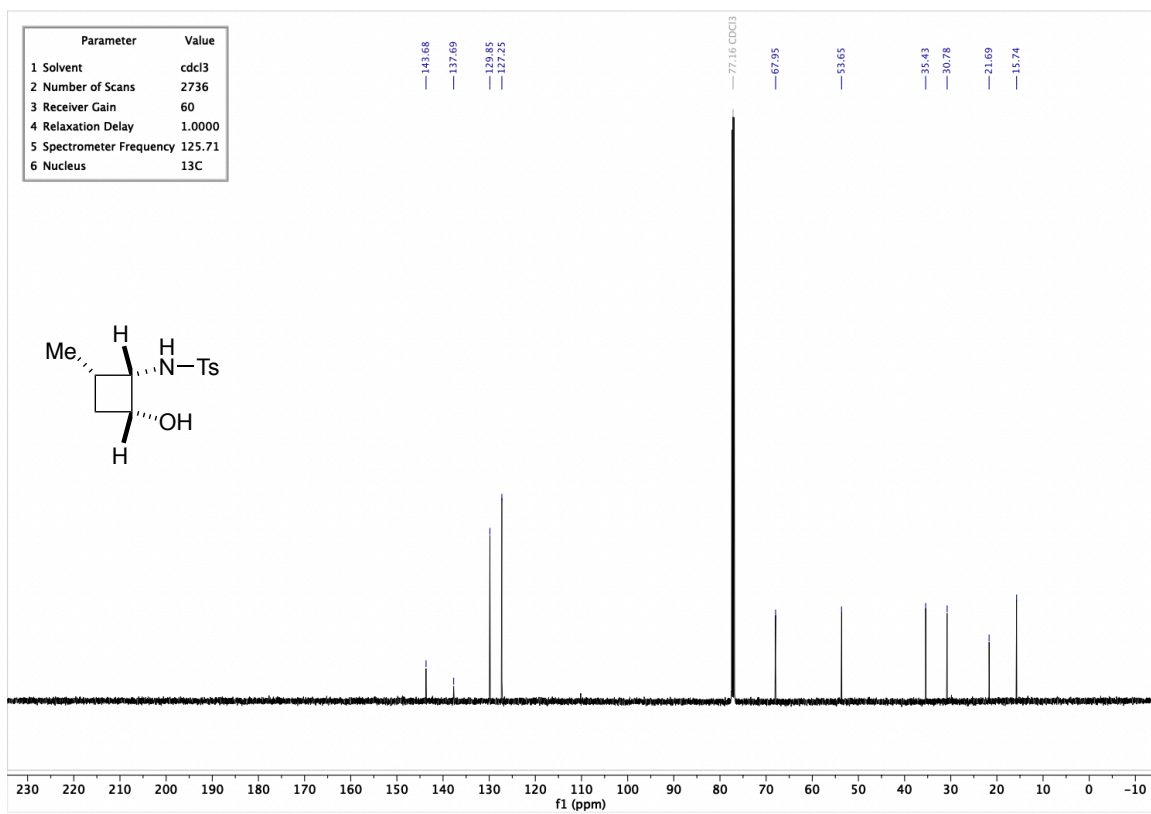


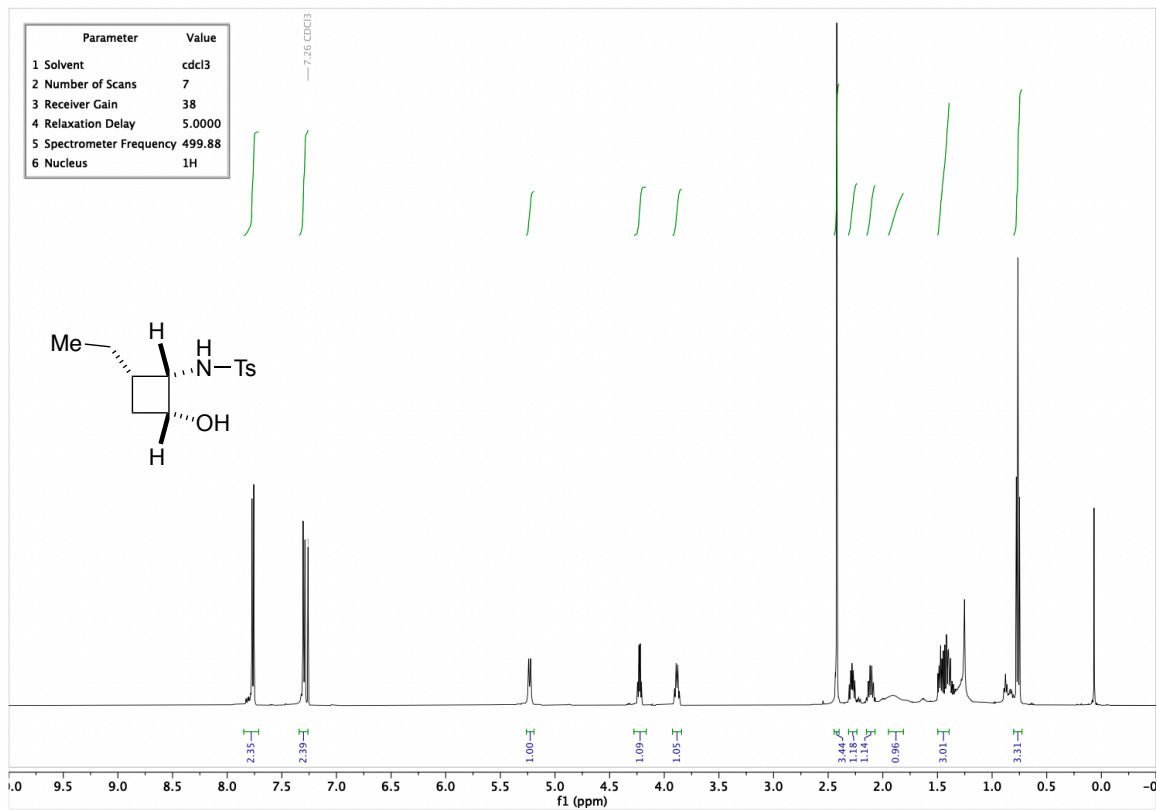
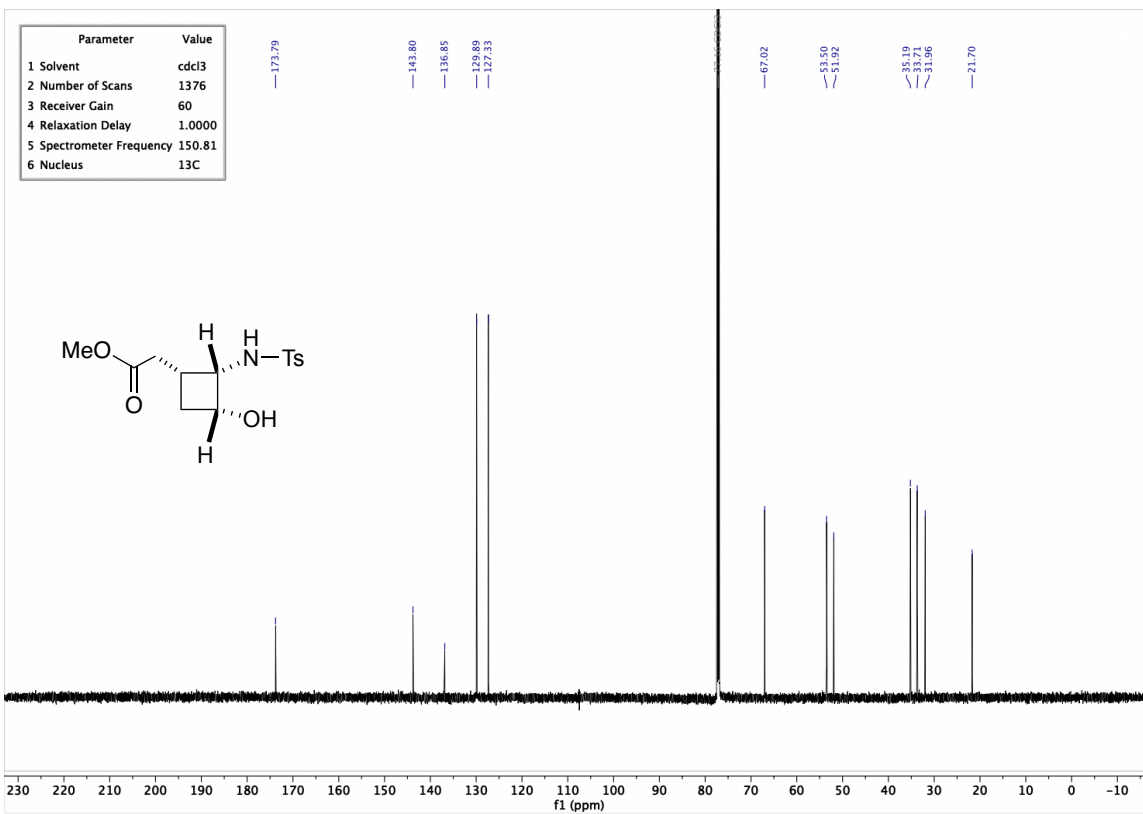


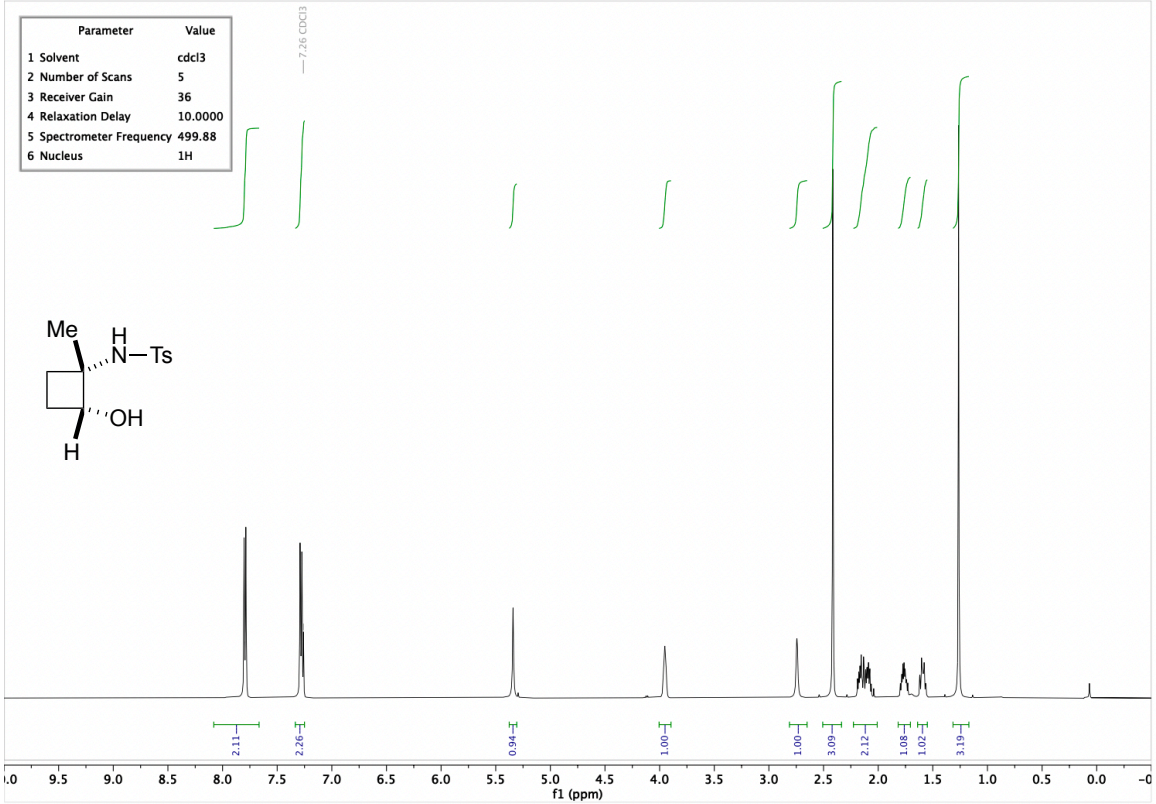
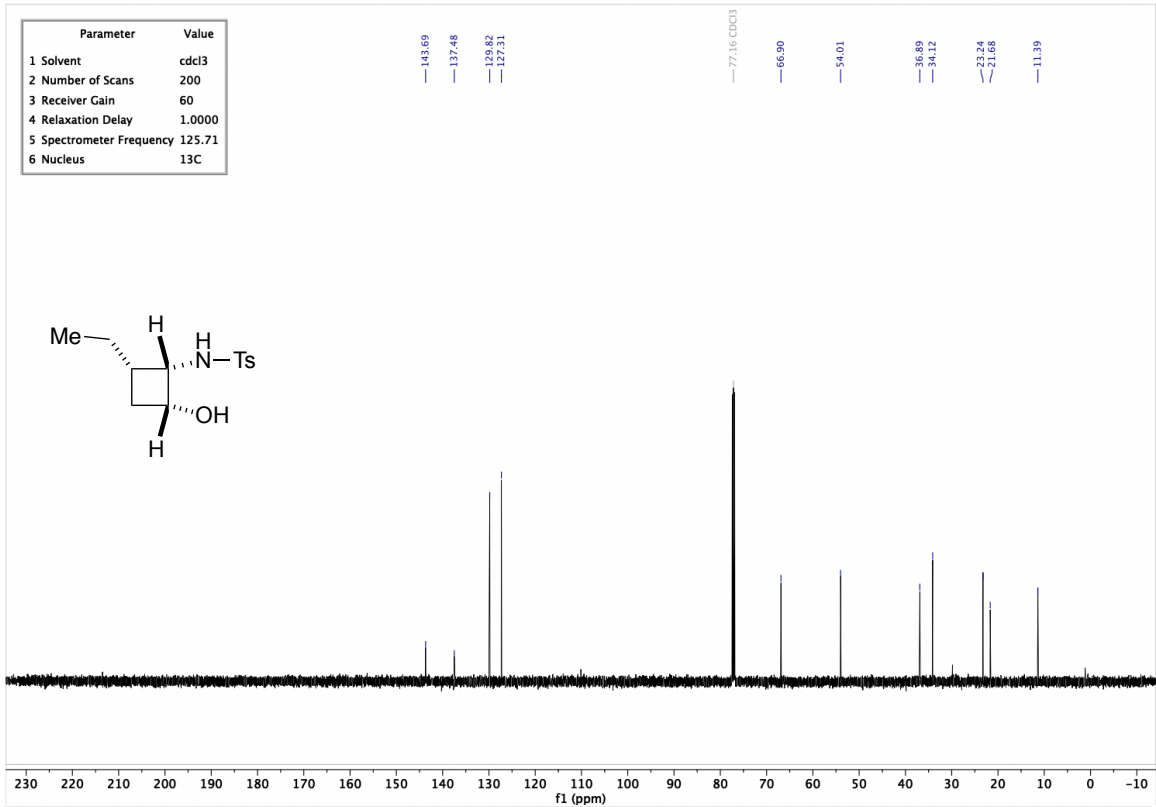


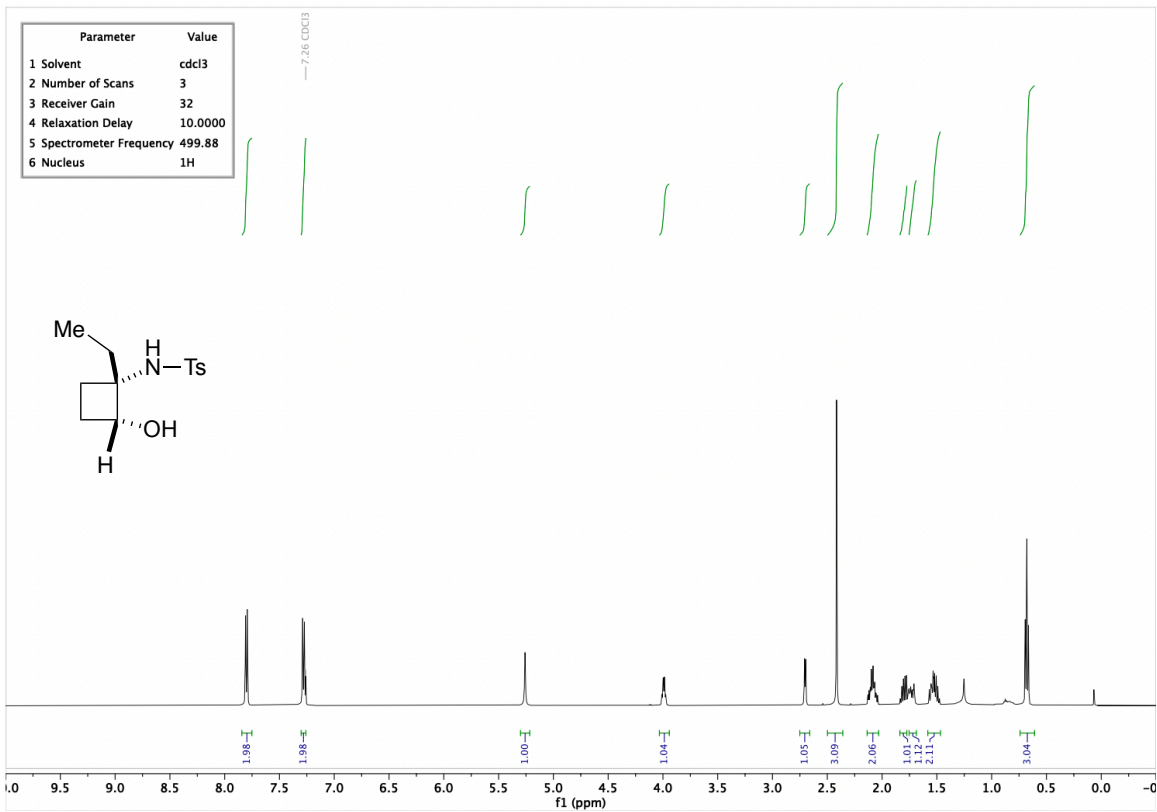
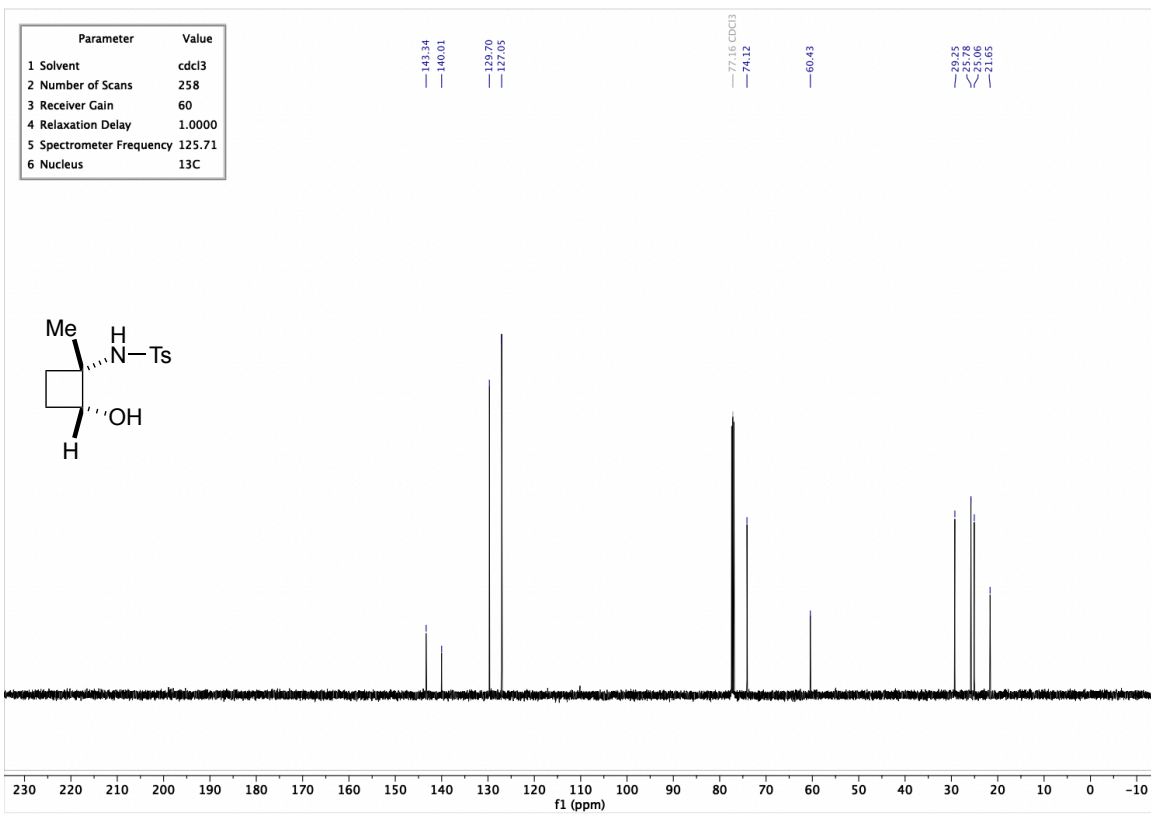


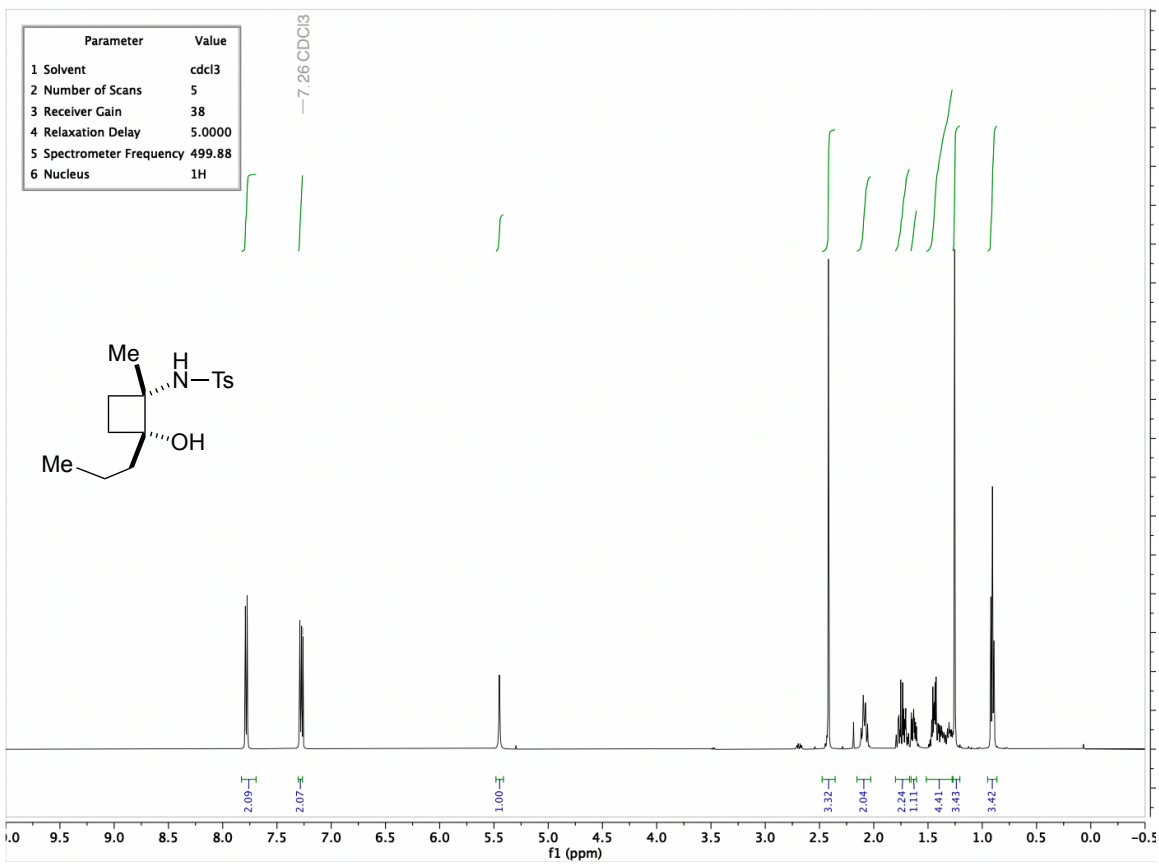
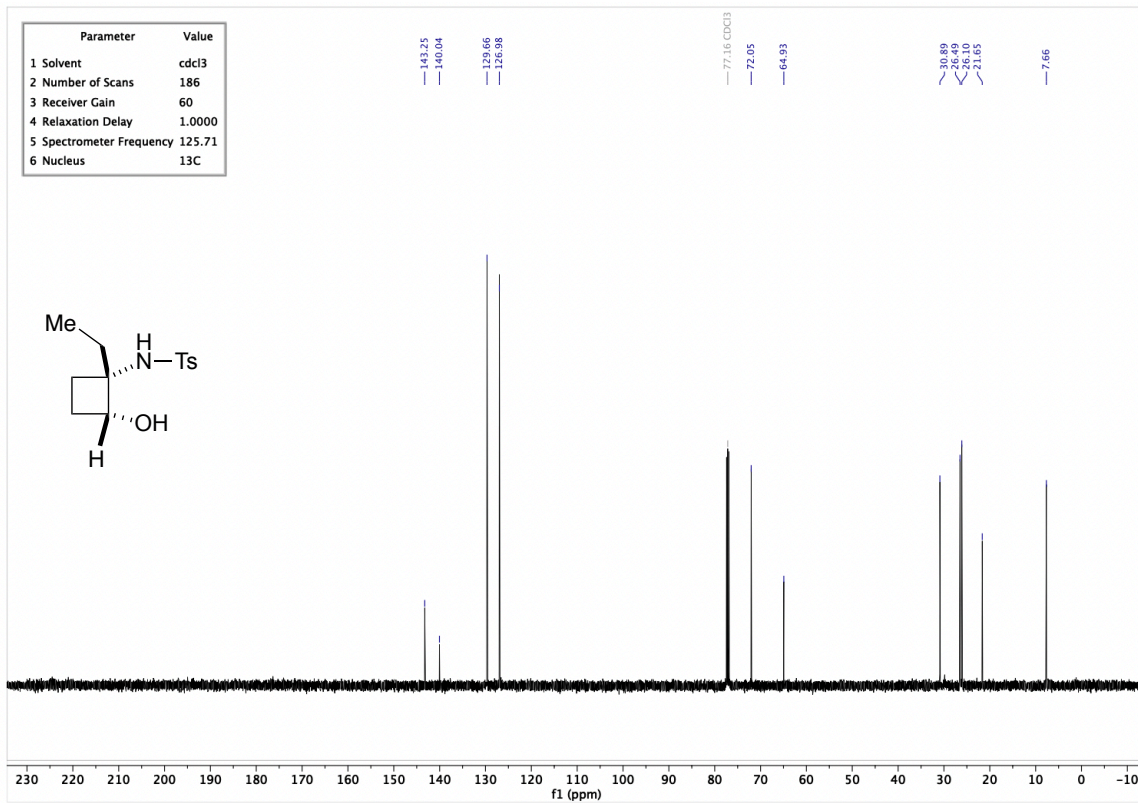


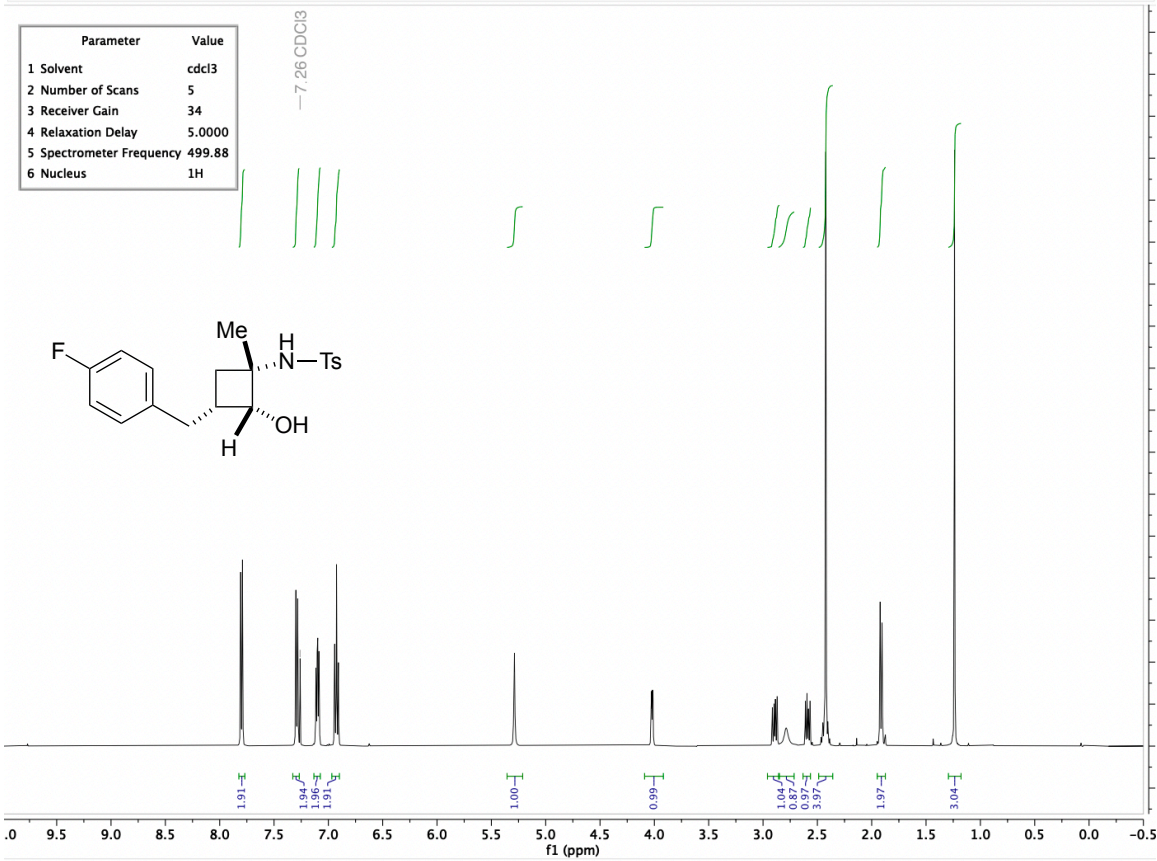
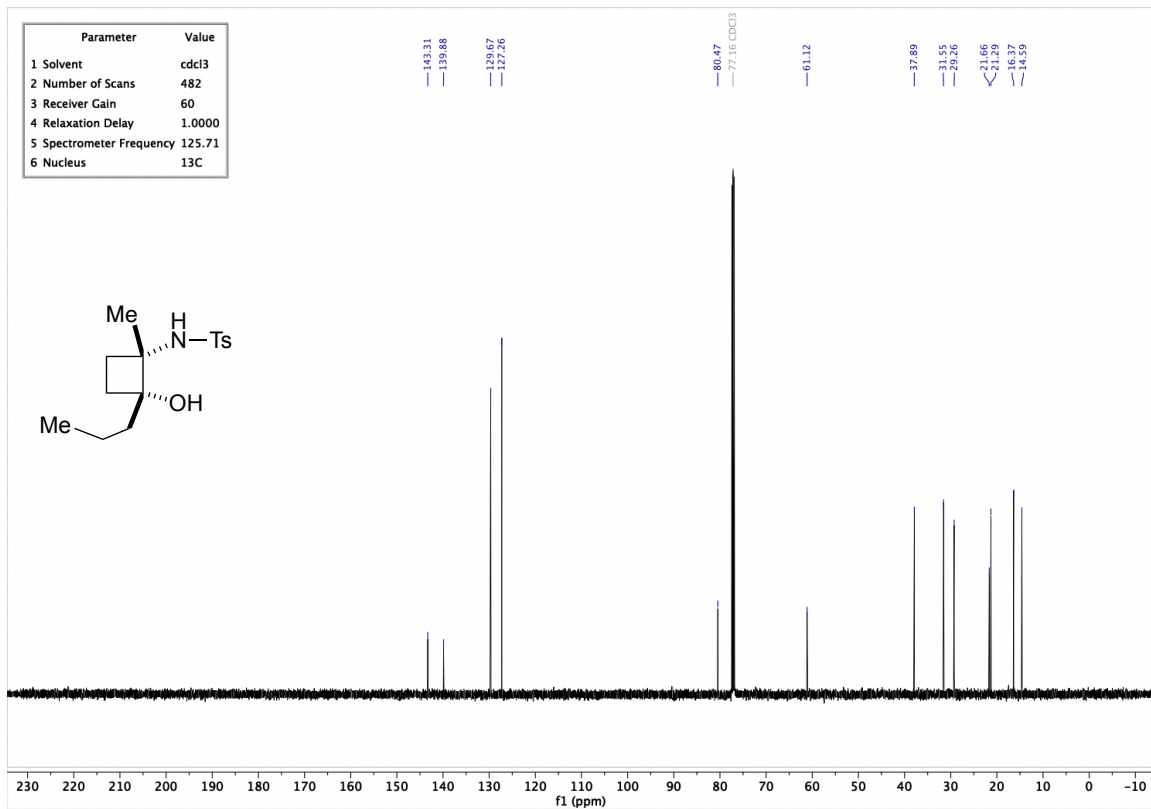


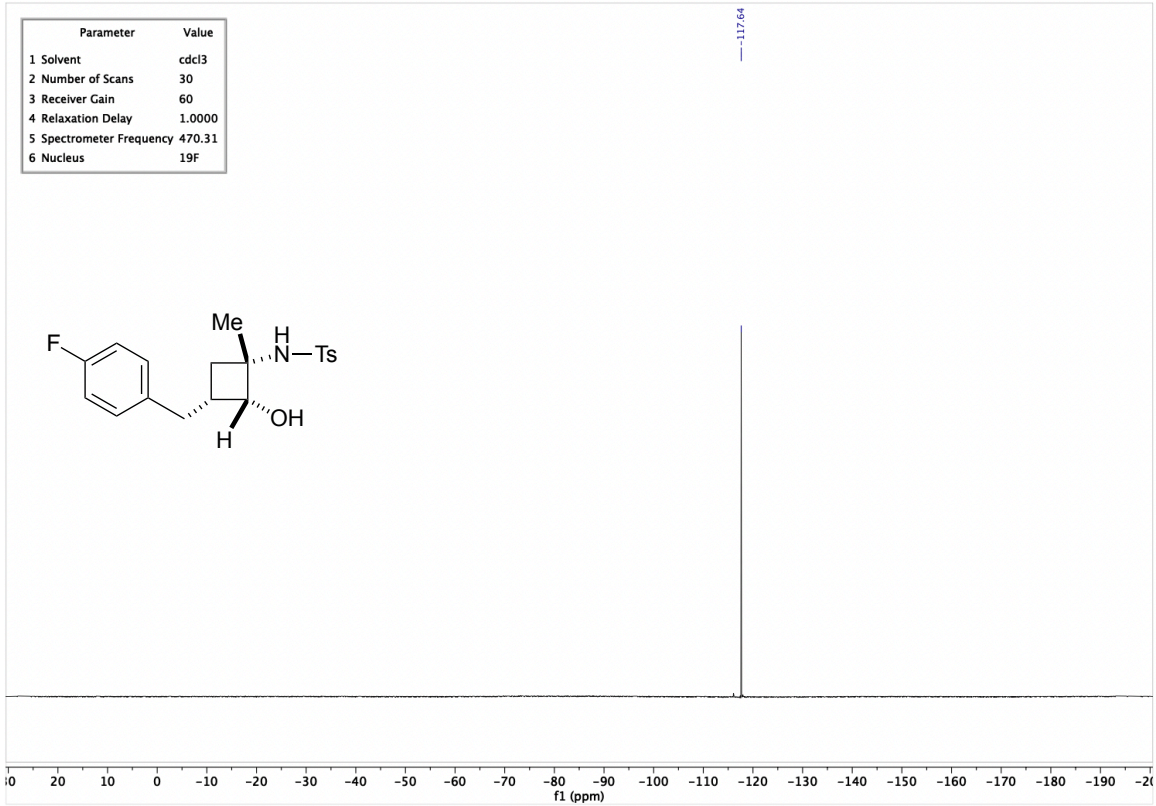
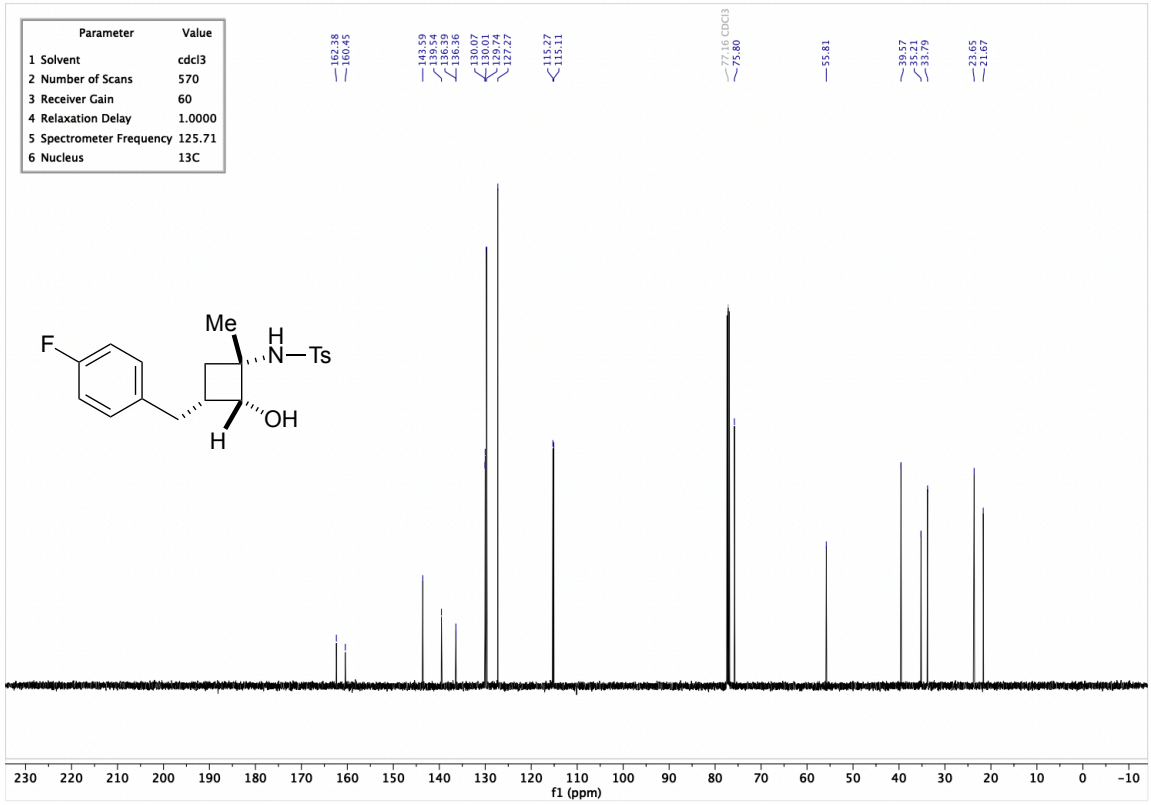


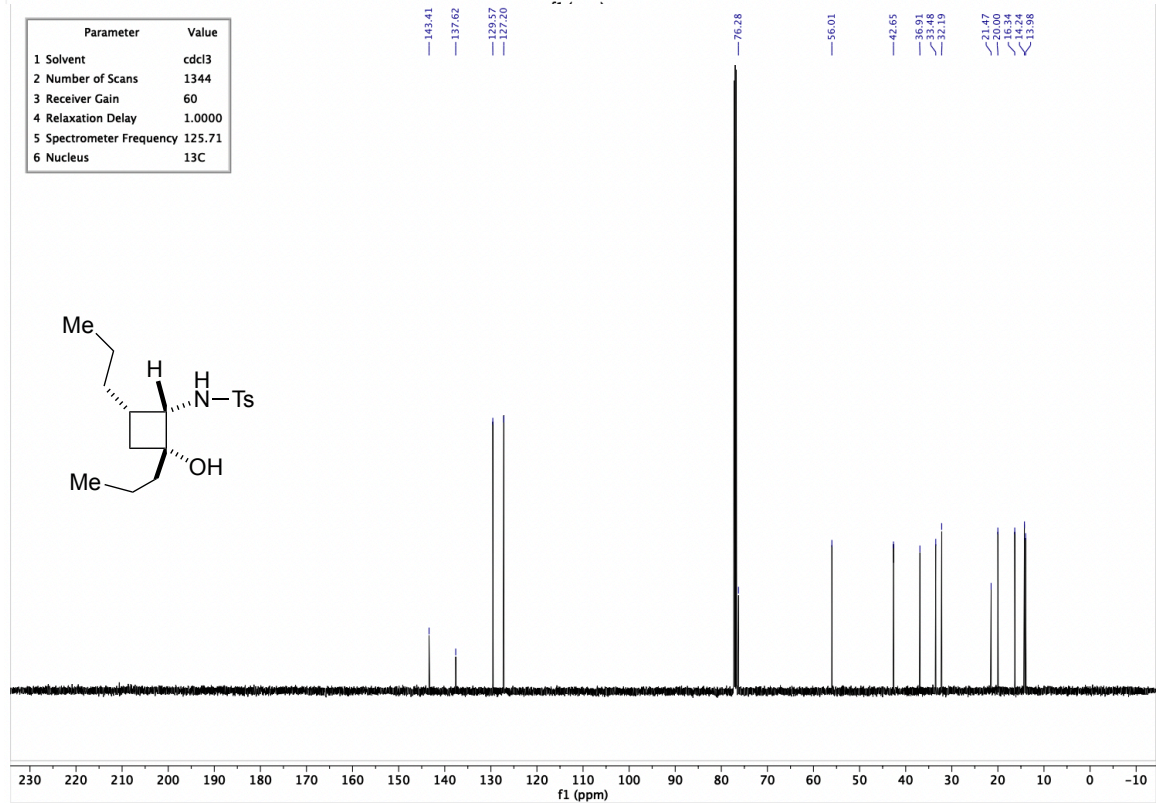
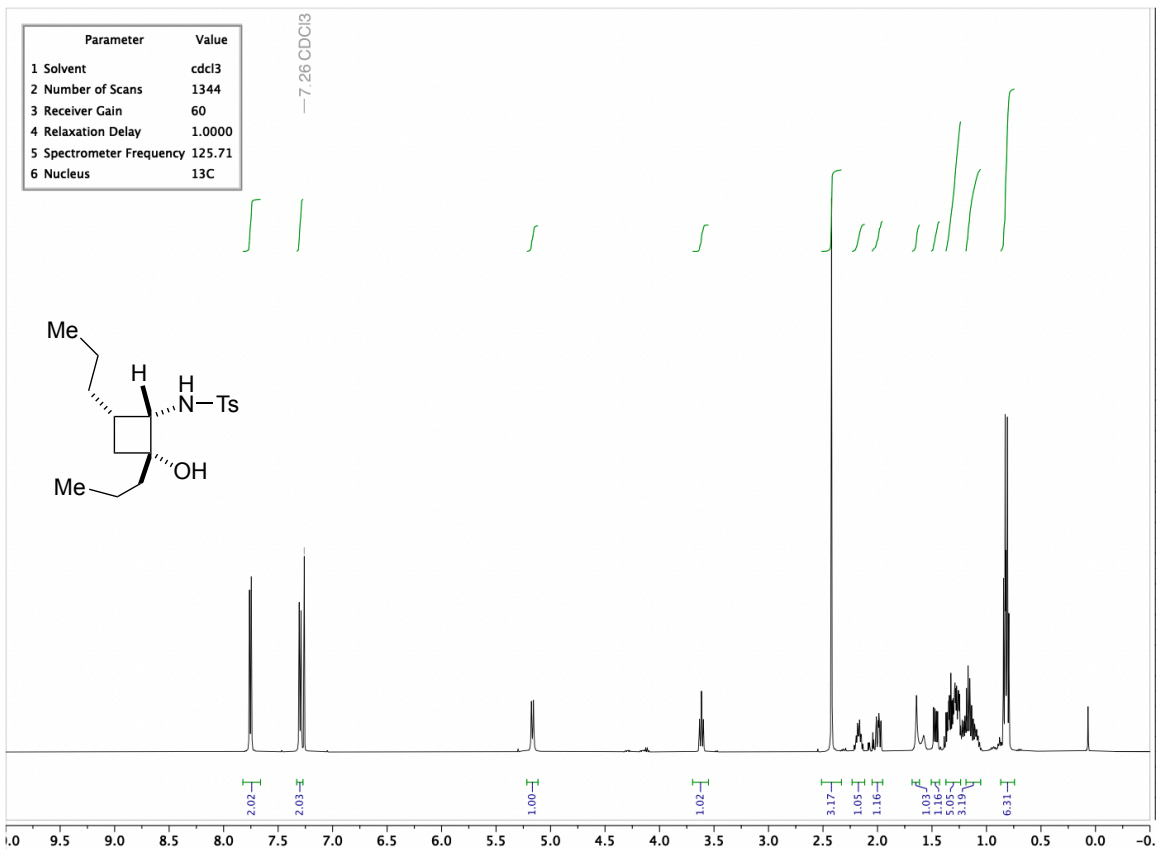


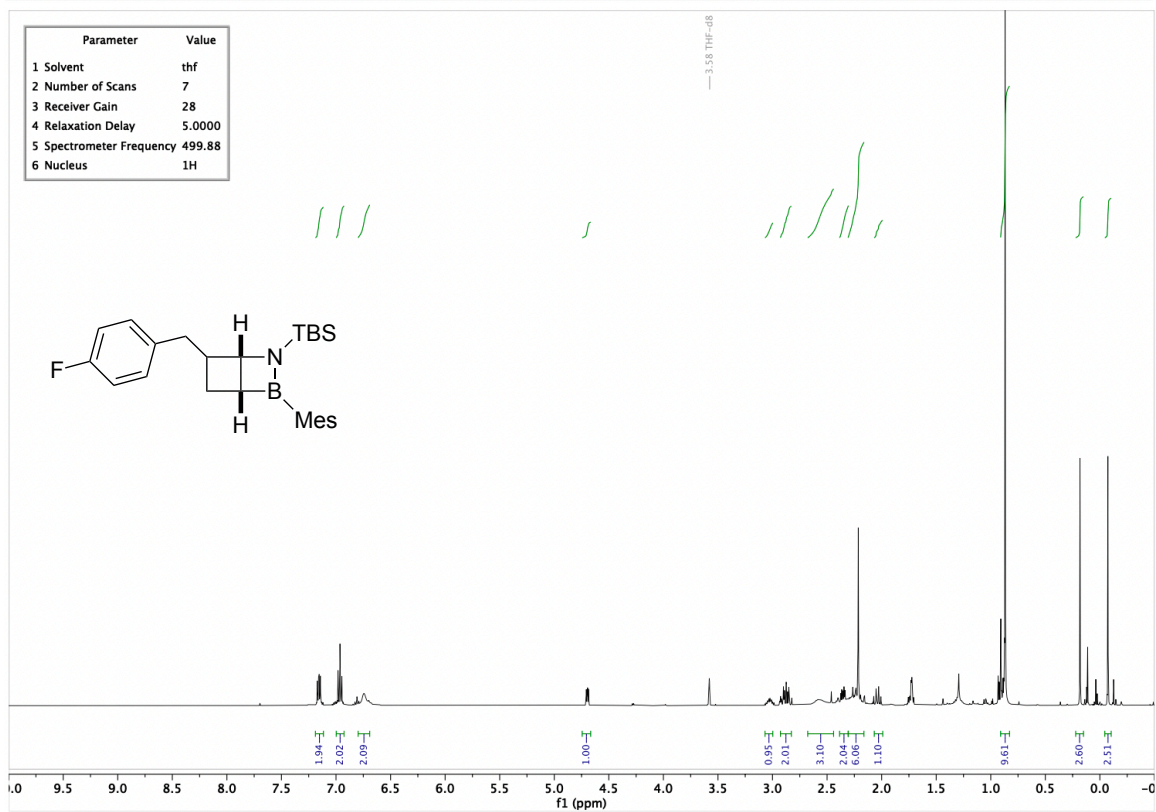
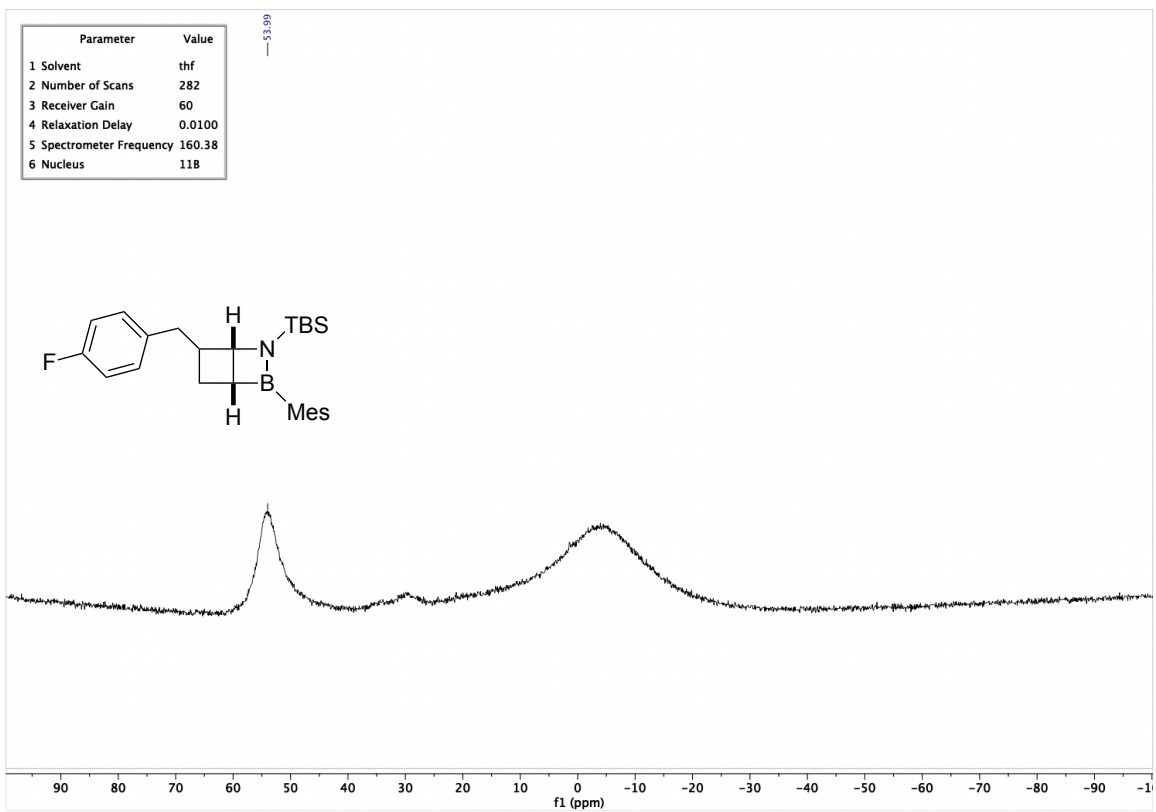


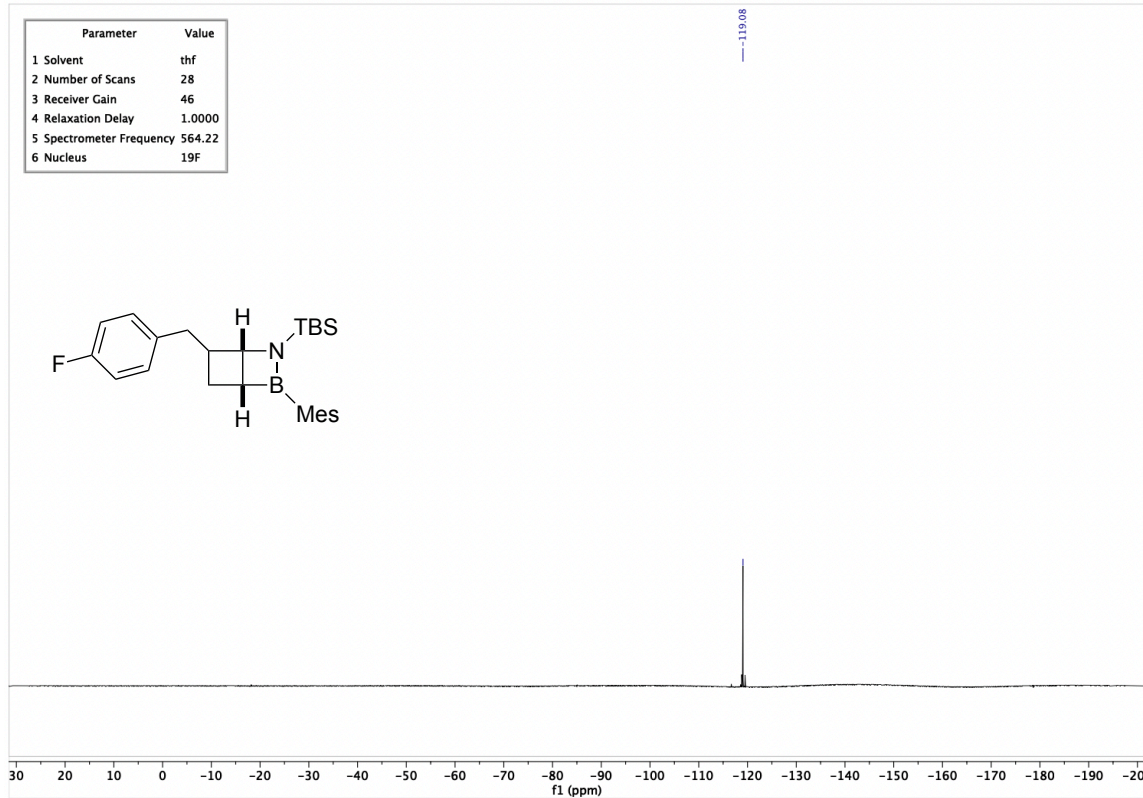
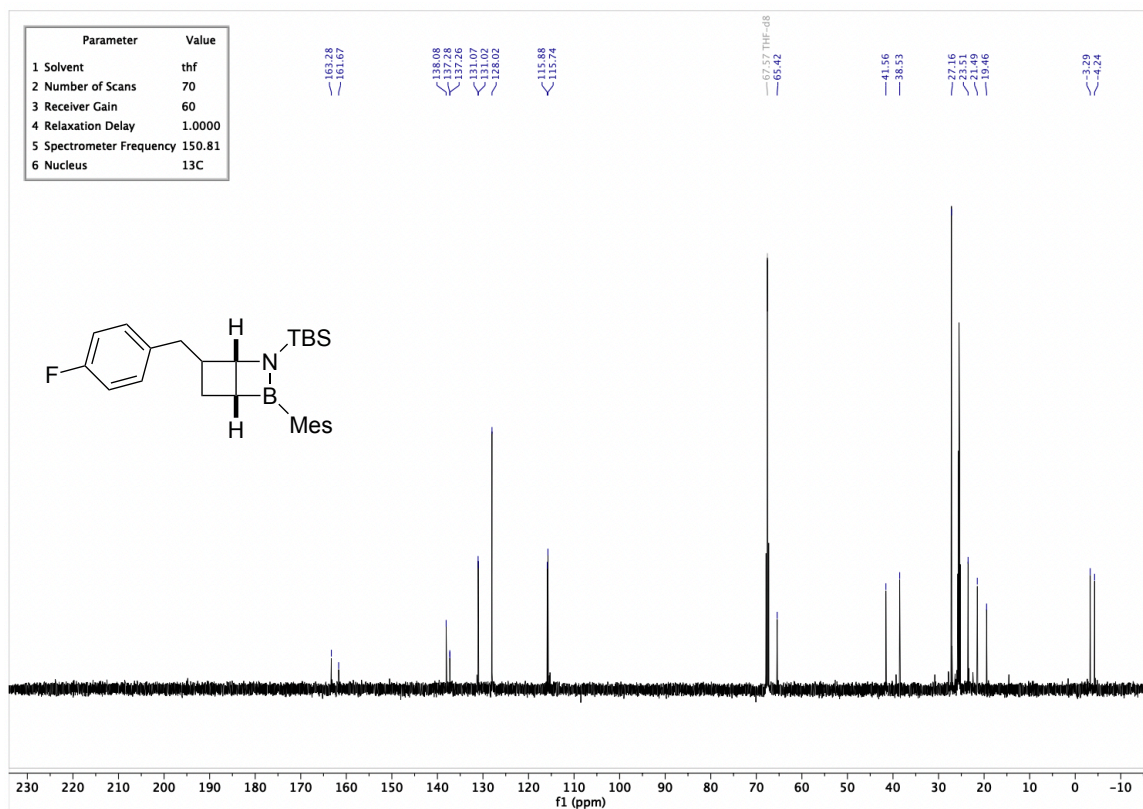


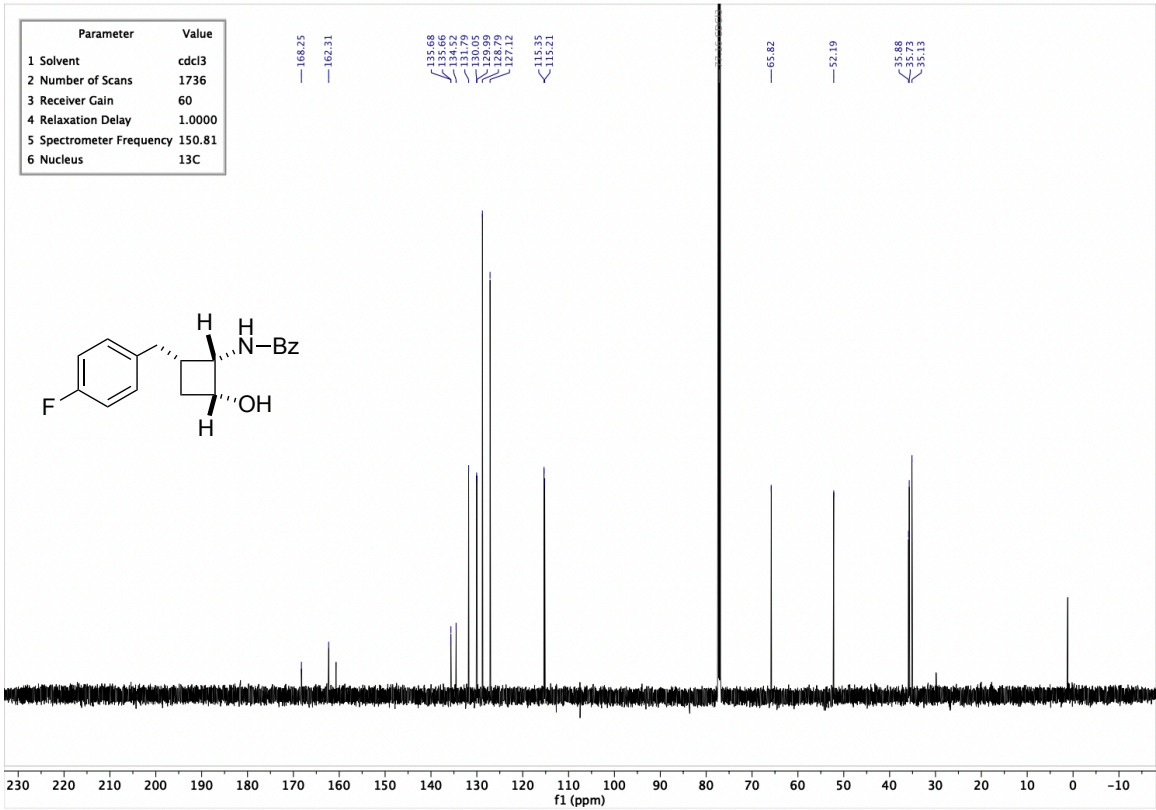
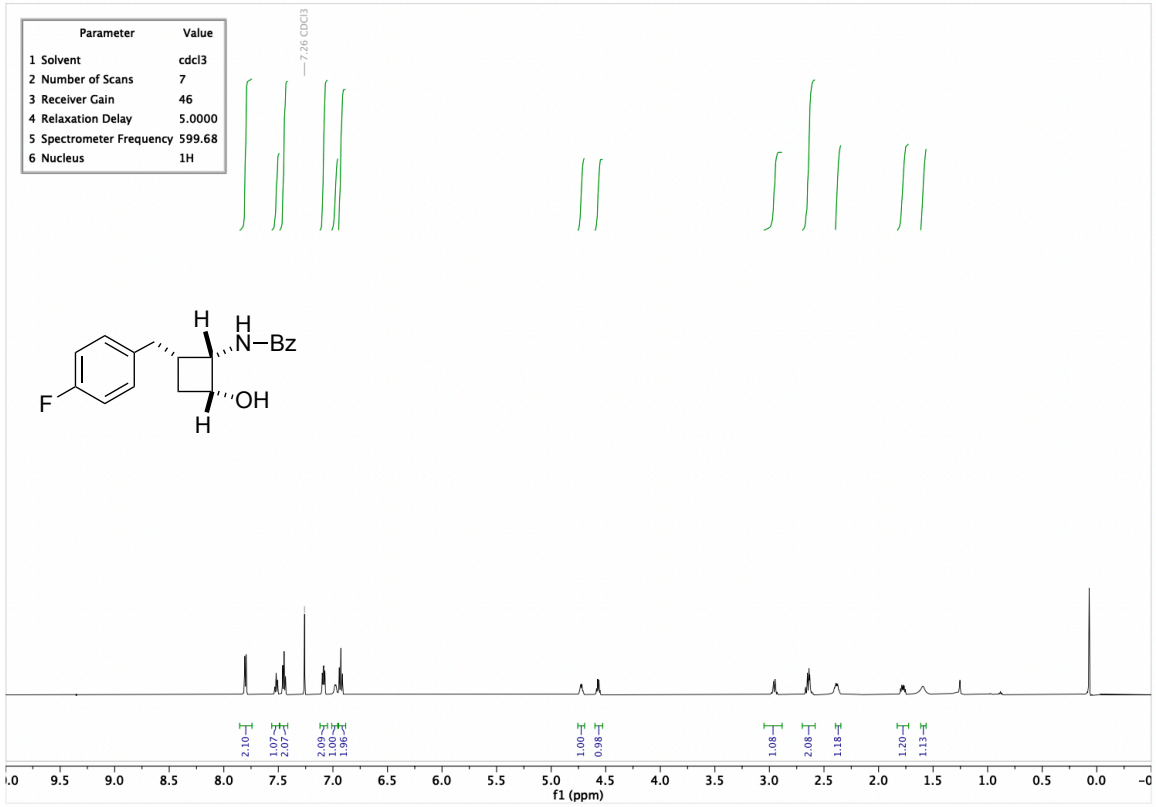






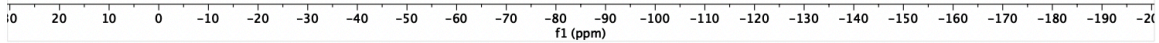
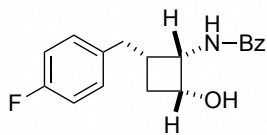




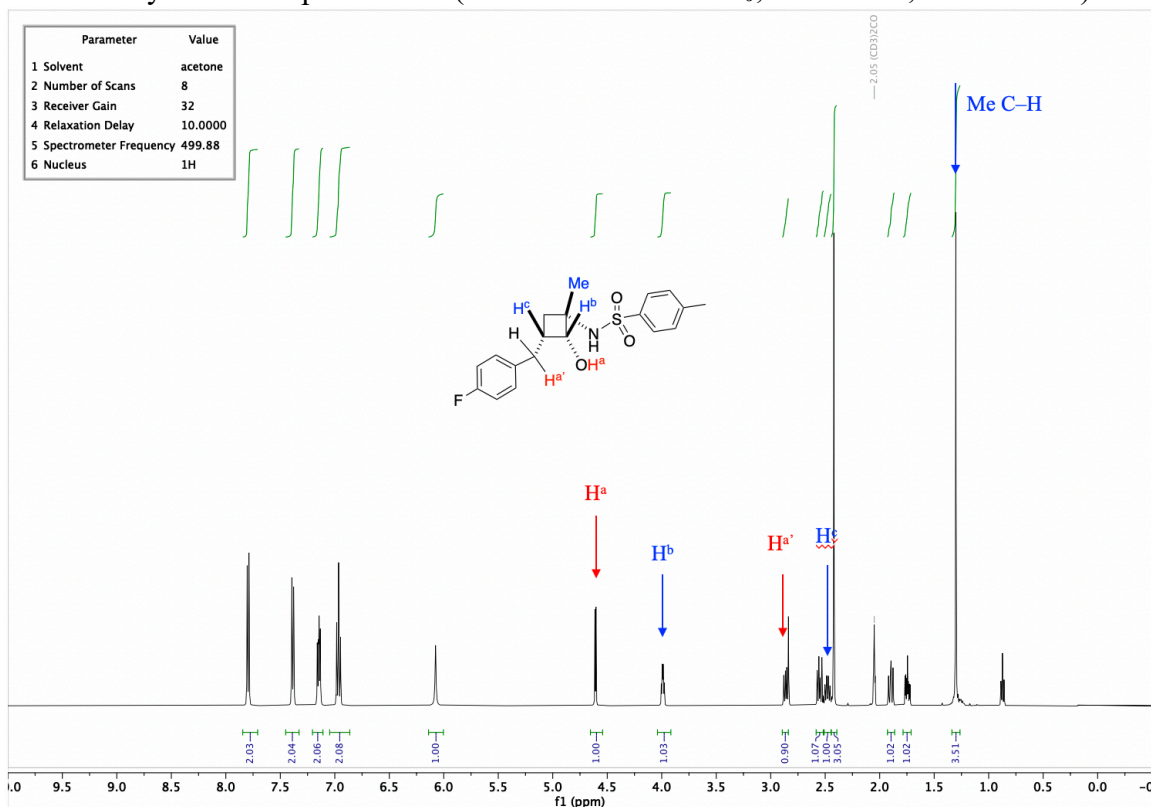


Parameter	Value
1 Solvent	cdcl3
2 Number of Scans	40
3 Receiver Gain	60
4 Relaxation Delay	1.0000
5 Spectrometer Frequency	470.31
6 Nucleus	19F

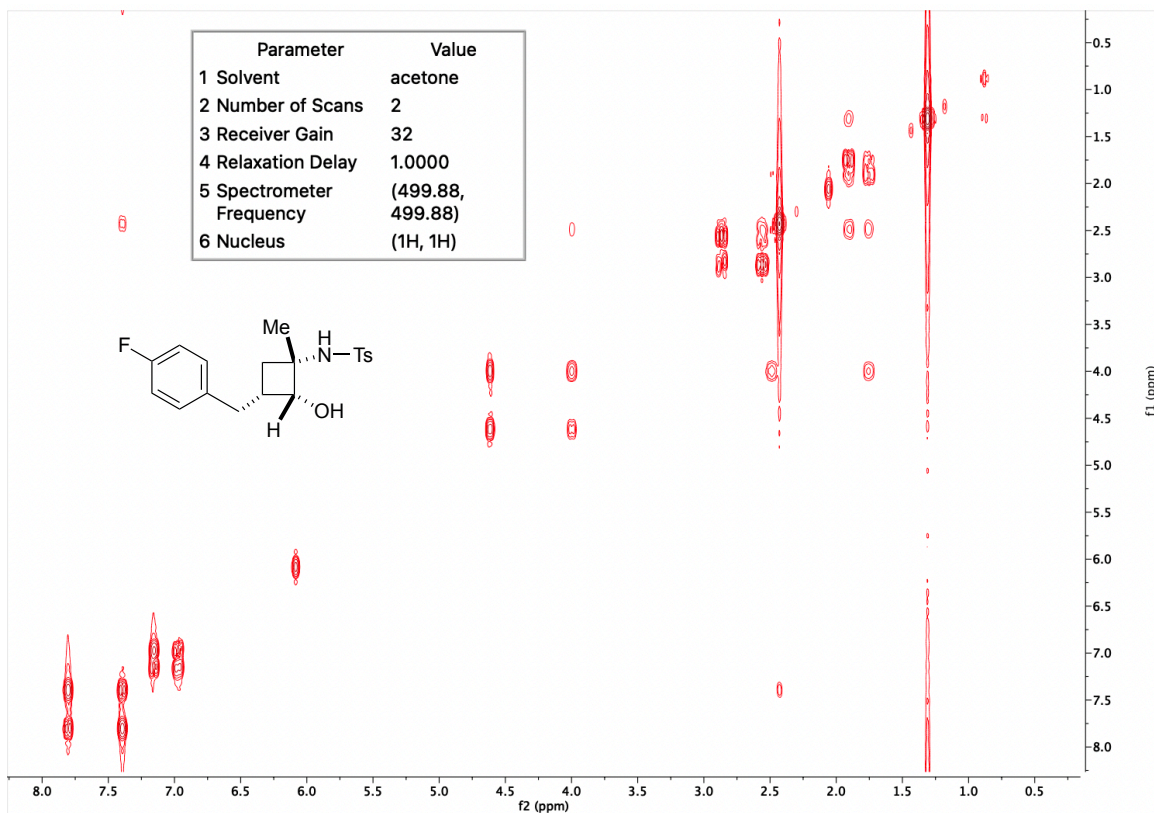
-117.55



NMR Analysis of Compound 2.92 (¹H NMR in acetone-d₆; 1D-COSY; 2D-NOESY)



1D-COSY



2D-NOESY

